

N 69 18309

NASA CR 99901

NATIONAL AERONAUTICS AND SPACE ADMINISTRATION

CASE FILE
COPY

Technical Report 32-1264

Surveyor VII Mission Report

Part I. Mission Description and Performance

Prepared by the Surveyor Project Staff

JET PROPULSION LABORATORY
CALIFORNIA INSTITUTE OF TECHNOLOGY
PASADENA, CALIFORNIA

February 15, 1969

NATIONAL AERONAUTICS AND SPACE ADMINISTRATION

Technical Report 32-1264

Surveyor VII Mission Report

Part I. Mission Description and Performance

Prepared by the Surveyor Project Staff

JET PROPULSION LABORATORY
CALIFORNIA INSTITUTE OF TECHNOLOGY
PASADENA, CALIFORNIA

February 15, 1969

TECHNICAL REPORT 32-1264

Copyright © 1969

Jet Propulsion Laboratory
California Institute of Technology

Prepared Under Contract No. NAS 7-100
National Aeronautics and Space Administration

Preface

The work described in this report was performed by the *Surveyor* Project of the Jet Propulsion Laboratory.

This three-part document constitutes the Project Mission Report on *Surveyor VII*, the seventh and last in a series of unmanned missions designed to soft-land on the moon and return data from the lunar surface.

Part I of this report consists of a technical description and a performance evaluation of the systems utilized in the *Surveyor VII* mission. Part I was compiled using contributions of many individuals in the major systems which support the Project, and is based on data evaluation prior to approximately March 1, 1968. Some of the information in this report was obtained from other published documents; a list of these documents is presented in a bibliography.

Part II of this report presents the scientific data derived from the mission and the results of scientific analyses which have been conducted. Part III consists of selected pictures from *Surveyor VII* and appropriate explanatory material.

Contents

I. Introduction and Summary	1
A. Surveyor Objectives	1
B. Project Description	3
C. Mission Summary	4
II. Space Vehicle Preparations and Launch Operations	13
A. Spacecraft Assembly and Testing	13
B. Launch Vehicle Combined Systems Testing at San Diego	14
C. Launch Operations at AFETR	14
D. Launch Phase Mission Analysis	19
III. Launch Vehicle System	21
A. <i>Atlas</i> Stage	21
B. <i>Centaur</i> Stage	22
C. Launch Vehicle/Spacecraft Interface	24
D. Vehicle Flight Sequence of Events	25
E. Performance	28
IV. Surveyor Spacecraft	33
A. Spacecraft System	33
B. Structures and Mechanisms	52
C. Thermal Control	59
D. Electrical Power	62
E. Propulsion	66
F. Flight Control	76
G. Radar	82
H. Telecommunications	91
I. Television	96
J. Soil Mechanics/Surface Sampler	101
K. Alpha Scattering Instrument	104
V. Tracking and Data System	117
A. Air Force Eastern Test Range	117

Contents (contd)

B. Manned Space Flight Network	125
C. Deep Space Network	127
VI. Mission Operations System	139
A. Functions and Organization	139
B. Mission Dependent Equipment	143
C. Mission Operations Chronology	146
VII. Flight Path and Events	167
A. Prelaunch	167
B. Launch Phase	168
C. Pre-midcourse Cruise Phase	168
D. Midcourse Maneuver Phase	173
E. Post-midcourse Cruise Phase	177
F. Terminal Phase	177
G. Landing Site	180
Appendix A. Surveyor VII Mission Events	181
Appendix B. Surveyor VII Spacecraft Configuration	197
Appendix C. Surveyor VII Spacecraft Content of Telemetry Modes	201
Appendix D. Surveyor VII Spacecraft Temperature Histories	205
Glossary	222
Bibliography	225

Tables

II-1. Major Surveyor VII operations at Cape Kennedy	15
II-2. Surveyor VII countdown time summary	19
III-1. Atlas propellant residuals	29
III-2. Centaur usable propellant residuals	30
IV-1. Surveyor VII spacecraft telemetry summary	38
IV-2. Surveyor engineering instrumentation	40
IV-3. Notable differences between Surveyors VI and VII.	41

Contents (contd)

Tables (contd)

IV-4. Surveyor spacecraft subsystem and system reliability estimates as presented at consent-to-launch meetings	43
IV-5. Final reliability figures for Surveyor subsystems and systems	43
IV-6. Boost phase accelerations: Surveyor VII vs Surveyor VI	48
IV-7. Predicted and actual terminal descent events	50
IV-8. Predicted and actual values of terminal descent parameters	50
IV-9. Shock absorber forces and times of footpad impacts for lunar landing	54
IV-10. Thermal compartment component installation	56
IV-11. Pyrotechnic devices	59
IV-12. Electrical power performance during transit	64
IV-13. Comparison of predicted and actual thrust commands for midcourse phase and case separation phase of terminal descent	67
IV-14. Surveyor VII propulsion system temperature ranges during transit and first lunar day	72
IV-15. Vernier propulsion system temperatures during the lunar day	72
IV-16. Postlanding vernier propulsion system anomalies	73
IV-17. Flight control modes	77
IV-18. Surveyor VII star map analysis	79
IV-19. Typical signal processing parameter values	96
IV-20. Summary of SM/SS operating time and response to commands	103
IV-21. Characteristics of alpha scattering instrument data channels	111
IV-22. Engineering parameters telemetered from alpha scattering instrument	112
IV-23. Data accumulation time summary	115
V-1. AFETR configuration for Surveyor VII mission	120
V-2. Atlas/Centaur Mark Event readouts	124
V-3. GSFC network configuration	125
V-4. DSN tracking and telemetry data requirements	128
V-5. Characteristics for S-band tracking systems	129
VI-1. CDC mission-dependent equipment support of Surveyor VII at DSIF stations	144
VI-2. Reported Surveyor VII command, TV, and alpha scattering activity before shutdown for first lunar night	144
VII-1. Surveyor VII encounter conditions based on selected pre-midcourse orbit determinations	172

Contents (contd)

Tables (contd)

VII-2. Midcourse maneuver alternatives.	177
VII-3. <i>Surveyor VII</i> encounter conditions based on selected post-midcourse orbit determinations	178
VII-4. Injection and terminal conditions for pre- and post-midcourse trajectories . . .	179
A-1. Mission flight events	182
A-2. Lunar operations	189

Figures

I-1. Earth-moon trajectory and major events	5
I-2. Mosaic of <i>Surveyor VII</i> pictures showing rugged lunar terrain strewn with rocks. Boulder in foreground is 2 ft across and casts a 4-ft-long shadow (Catalog 7-SE-22)	9
I-3. Lunar sites of soft-landed <i>Surveyor</i> spacecraft	11
II-1. Liftoff of <i>Atlas/Centaur</i> AC-15 with SC-7 from Launch Complex 36A	18
II-2. Final <i>Surveyor VII</i> launch window design for January 1968	19
III-1. <i>Atlas</i> (SLV-3C)/ <i>Centaur</i> / <i>Surveyor</i> space vehicle configuration	22
III-2. <i>Surveyor/Centaur</i> interface configuration	24
III-3. Launch phase nominal events	26
III-4. <i>Centaur</i> clockwise roll attitude relative to local vertical	29
IV-1. <i>Surveyor</i> spacecraft (SC-7) in cruise mode	34
IV-2. Simplified spacecraft functional block diagram (SC-7).	35
IV-3. <i>Surveyor</i> spacecraft system reliability estimates	42
IV-4. Terminal descent nominal events	44
IV-5. Main retro burn profile (typical)	45
IV-6. Range-velocity "descent contour"	46
IV-7. <i>Surveyor VII</i> touchdown orientation	51
IV-8. Landing leg assembly	53
IV-9. Loads on spacecraft shock absorber during landing	54
IV-10. Antenna/solar panel configuration	55
IV-11. Thermal switch	58
IV-12. Thermal design	61
IV-13. Functional diagram of <i>Surveyor VII</i> electrical power subsystem	63

Contents (contd)

Figures (contd)

IV-14. Calculated battery energy profile during transit	65
IV-15. Typical postlanding regulated current requirements	65
IV-16. Typical postlanding solar panel current and power output	66
IV-17. First lunar day battery temperature and energy level	66
IV-18. Vernier propulsion system schematic	68
IV-19. Vernier propulsion system installation	69
IV-20. Helium tank assembly	70
IV-21. Vernier engine thrust chamber assembly	71
IV-22. <i>Surveyor VII</i> propulsion system temperature ranges during transit and first lunar day	72
IV-23. Main retrorocket motor	74
IV-24. Main retro motor thrust vs time	75
IV-25. Simplified flight control functional diagram	76
IV-26. Gas-jet attitude control system	77
IV-27. <i>Surveyor VII</i> descent profile	81
IV-28. Altitude marking radar functional diagram	82
IV-29. Altitude marking radar AGC	83
IV-30. Simplified RADVS functional block diagram	84
IV-31. RADVS beam orientation	85
IV-32. Reflectivity of RADVS beams during terminal descent	87
IV-33. Slant range vs time during terminal descent	89
IV-34. X-component of velocity V_x during terminal descent	89
IV-35. Y-component of velocity V_y during terminal descent	90
IV-36. Z-component of velocity V_z during terminal descent	90
IV-37. Radio subsystem block diagram	91
IV-38. Receiver A/Omniantenna A total received power during transit	93
IV-39. Receiver A/Omniantenna B total received power during transit	93
IV-40. DSIF received power during transit	94
IV-41. Simplified signal processing functional block diagram	95
IV-42. <i>Surveyor VII</i> television camera	97
IV-43. Simplified television camera functional block diagram	98

Contents (contd)

Figures (contd)

IV-44. TV photometric/colorimetric reference chart	99
IV-45. SM/SS operating envelope and permissible region for redeployment of ASI sensor head	101
IV-46. Surveyor VII spacecraft in postlanded configuration	102
IV-47. SM/SS temperature profile and period of operation	104
IV-48. SM/SS redeploying ASI sensor head to second sample site (January 21, 1968, 11:44:53 GMT)	105
IV-49. Location of SM/SS operations and ASI samples	106
IV-50. Mosaic of Surveyor VII pictures showing area of SM/SS operations prior to conducting tests (Photograph P-8511)	107
IV-51. Mosaic of Surveyor VII pictures showing area of SM/SS operations after conducting tests (Photograph 211-2612B)	107
IV-52. ASI components	108
IV-53. View of bottom of ASI sensor head	109
IV-54. Diagrammatic view of sensor head illustrating functional operation	110
IV-55. ASI deployment mechanism	112
IV-56. SM/SS forcing the sensor head against the helium tank preparatory to applying downward force to free it (January 12, 1968, 06:57:30 GMT)	114
V-1. Planned up-range TDS coverage for the Surveyor VII mission	118
V-2. Planned near-earth TDS coverage for January 7, 1968	119
V-3. AFETR C-band radar coverage	121
V-4. AFETR VHF telemetry coverage	122
V-5. AFETR S-band telemetry coverage	123
V-6. MSFN VHF and S-band telemetry coverage	126
V-7. MSFN C-band radar coverage	126
V-8. DSS 71 antenna, Cape Kennedy, Florida	127
V-9. DSIF station view periods and command activity: transit phase	130
V-10. DSS received signal levels during transit	131
V-11. DSIF station tracking periods and reported command activity: postlanding (first lunar day)	133
V-12. DSN/GCS communications links for the Surveyor VII mission	135
V-13. General configuration of SFOF Data Processing System	137
VI-1. Organization of the MOS during the Surveyor VII mission	141
VI-2. Surveyor VII telemetry bit rate/mode profile	149

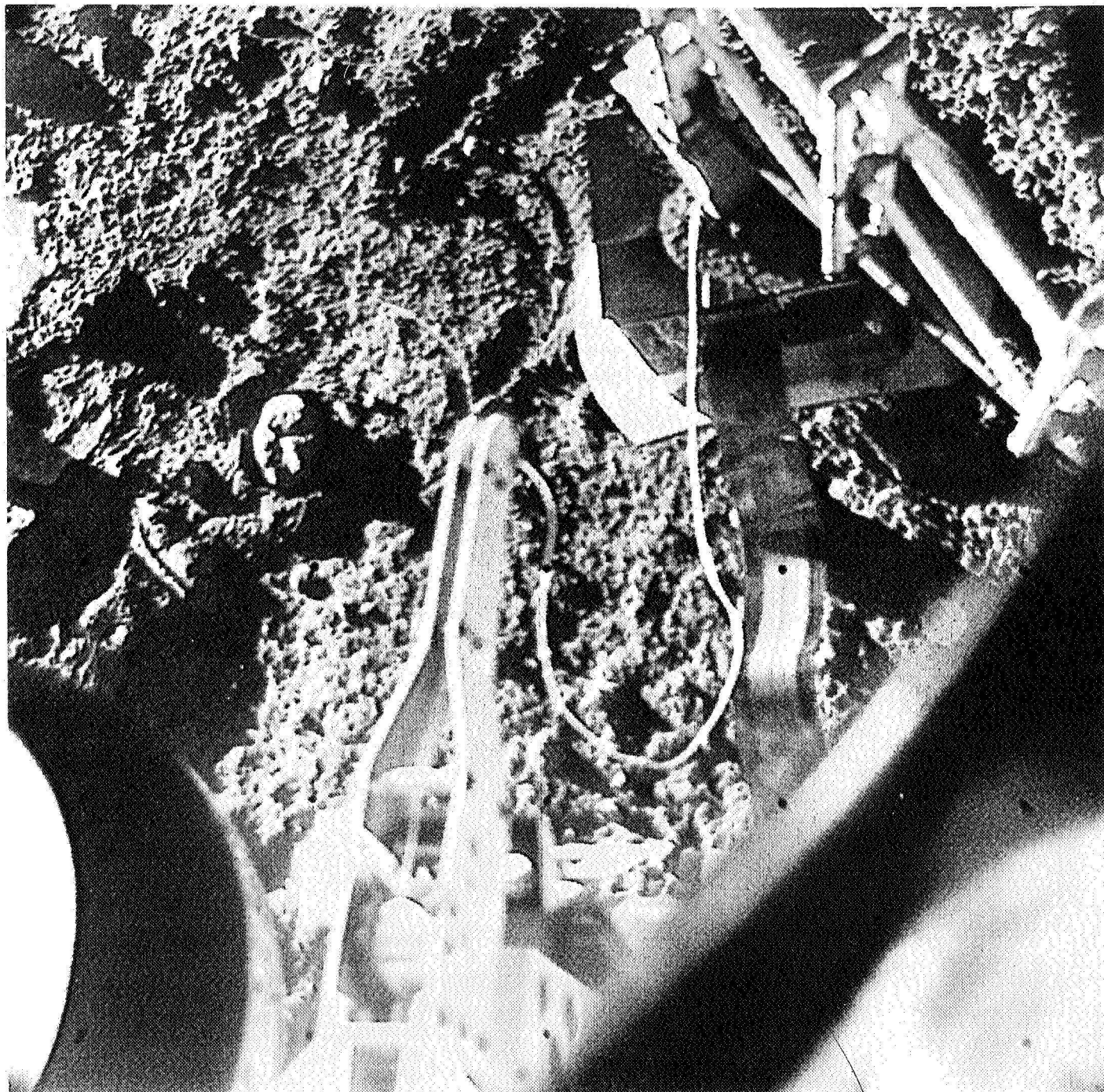
Contents (contd)

Figures (contd)

VI-3. Key spacecraft thermal and power parameters controlled during first lunar night operations before shutdown	163
VII-1. <i>Surveyor</i> and <i>Centaur</i> trajectories in earth's equatorial plane	169
VII-2. <i>Surveyor VII</i> earth track	170
VII-3. Computed <i>Surveyor VII</i> pre-midcourse unbraked impact locations	171
VII-4. <i>Surveyor VII</i> landing location	174
VII-5. Midcourse correction capability contours (for a correction 20 hr after injection)	175
VII-6. Effect of noncritical component of midcourse velocity correction on terminal descent parameters	176
D-1. Landing gear transit temperatures	206
D-2. Compartment A transit temperatures	207
D-3. Compartment B transit temperatures	208
D-4. Vernier propulsion system transit temperatures	209
D-5. Main retro motor transit temperatures	210
D-6. Radar and flight control transit temperatures	211
D-7. Solar panel and planar array transit temperatures	212
D-8. ASI and SM/SS transit temperatures	212
D-9. Electrical power subsystem postlanding temperatures	213
D-10. Vernier propulsion subsystem postlanding temperatures	215
D-11. Scientific instruments, postlanding temperatures	218

Abstract

Surveyor VII, the last in a series of seven unmanned spacecraft designed to soft-land on the moon and return engineering and scientific data, was launched from Cape Kennedy, Florida, on January 7, 1968. All established objectives for the mission were achieved. Following a nominal lunar transit phase, a completely successful soft landing was achieved on the ejecta or flow blanket north of the crater Tycho in the lunar highlands at 40.92°S latitude and 11.45°W longitude. *Surveyor VII* performed extensive operations and experiments before shutdown after sunset of the first lunar day and also was operated for a considerable period of time during the second lunar day. A large quantity of high-quality television pictures were obtained from the rock-strewn surface on which the spacecraft landed. In addition, other new information was obtained, including data on the chemical composition of the lunar surface from operation of an alpha scattering instrument and data on the physical properties of the lunar surface from operation of a soil mechanics/surface sampler. This was the first mission on which both these instruments were carried. The surface sampler was used to overcome a problem with deployment of the alpha scattering instrument and also to redeploy it on the lunar surface.



**Surface sampler redeploying the alpha scattering instrument to third sample location
(Photograph received January 22, 1968, 11:21:12 GMT)**

I. Introduction and Summary

Surveyor VII was launched by *Atlas/Centaur* AC-15 from Cape Kennedy, Florida, at 06:30:00.545 GMT on January 7, 1968. After a 22.4-min coast in parking orbit, the spacecraft was very accurately injected into a lunar transfer trajectory. Transit phase performance was excellent, including the precise execution of a 11.08-m/sec midcourse correction and the performance of a completely successful terminal descent and soft landing. Touchdown occurred at 01:05:37.62 GMT, January 10, 1968, on the Tycho ejecta or flow blanket in the lunar highlands at 40.92°S latitude and 11.45°W longitude.*

Very extensive postlanding operations were conducted on this, the last *Surveyor* mission. Along with results obtained from the television camera and other spacecraft engineering instrumentation, abundant data was received from the alpha scattering instrument (ASI) and soil mechanism/surface sampler (SM/SS), this being the first time both these instruments were carried on the same mission. Difficulty was encountered in deployment of the alpha scattering instrument. However, the surface sampler was utilized as a "mechanical hand" to overcome this problem as well as to redeploy the alpha scattering instrument on the lunar surface. *Surveyor VII* was operated until about 80 hr after sunset of the first lunar day. The spacecraft also responded to reawakening commands during the second lunar day and, although the spacecraft

*Site based on correlation of *Surveyor* and *Lunar Orbiter* pictures.

power system was crippled, operations were sustained for an additional 8 earth days.

Surveyor VII satisfied all of the mission objectives and provided unique data on a lunar highland site for comparison with data received from previous *Surveyor* missions which had soft-landed on maria sites.

A. Surveyor Objectives

The *Surveyor* Project was conducted to explore the moon with unmanned, automated soft-landing spacecraft which were equipped to respond to earth commands and transmit back scientific and engineering data from the lunar surface.

1. Overall Project Objectives

The overall objectives of the *Surveyor* Project were:

- (1) To accomplish successful soft landings on the moon as demonstrated by operations of the spacecraft subsequent to landing.
- (2) To provide basic data in support of *Apollo*.
- (3) To perform operations on the lunar surface which will contribute new scientific knowledge about the moon and provide further information in support of *Apollo*.

2. Results of Previous Surveyor Missions

Surveyor I was launched on May 30, 1966, and soft-landed near the western end of the *Apollo* zone of interest at 2.45°S latitude and 43.21°W longitude (based on *Lunar Orbiter III* data). Operations on the lunar surface were highly successful. In addition to a wide variety of other types of lunar surface data, over 11,000 television pictures were received in the course of operations during the first two lunar days. *Surveyor I* exhibited a remarkable capability to survive eight lunar day and night cycles involving temperature extremes of +250 and -250°F.

Surveyor II was launched on September 20, 1966, and achieved a nominal mission until execution of the mid-course velocity correction. One of the three vernier engines did not fire, causing the spacecraft to tumble. Attempts to stabilize the spacecraft by repeatedly firing the verniers were unsuccessful. When nearly all the spacecraft battery energy had been consumed prior to lunar encounter, the mission was terminated shortly after firing of the main retro motor 45 hr after launch. A thorough investigation was made by a specially appointed Failure Review Board. Although a precise failure mode could not be established, oxidizer clogging was the most probable failure mode. A number of recommendations were made to assure against a similar failure and to provide better diagnostic data on future missions.

Surveyor III was launched on April 17, 1967, and achieved a successful soft landing, although the spacecraft lifted off twice after initial touchdown before finally coming to rest. Based on correlation with *Lunar Orbiter III* photographs, the *Surveyor III* landing site has been located in the Ocean of Storms at 2.94°S latitude and 23.34°W longitude, about 625 km east of the *Surveyor I* landing site. Important new data was obtained as a result of extensive postlanding operations with a soil mechanics/surface sampler instrument, the television camera, and other spacecraft equipment. The lunar surface characteristics determined by *Surveyor III* confirmed the findings of *Surveyor I* and indicated the suitability of an additional site for *Apollo*, which will utilize final descent and landing system technology similar to that of *Surveyor*.

Surveyor IV was launched on July 14, 1967, and achieved a very nominal mission until the spacecraft radio signal was abruptly lost on July 16, 1967, about 2½ min before expected soft landing. The loss of signal occurred during the main retro phase just 1.4 sec before

predicted retro motor burnout, when the spacecraft was about 49,000 ft above the lunar surface and traveling 1070 ft/sec. Exhaustive attempts to reestablish telecommunications with *Surveyor IV* through July 18, 1967, were unsuccessful. A formally appointed Technical Review Board conducted a detailed examination of the *Surveyor IV* mission, but was unable to find evidence of any single or multiple cause for the failure.

Surveyor V was launched on September 8, 1967. A helium leak developed during midcourse correction and persisted although several additional vernier engine firings were made in an attempt to correct the problem. Nevertheless, a completely successful soft landing was achieved as the result of an intensive and resourceful effort by a special Hughes Aircraft Company (HAC)/JPL task force team, which assembled during the flight and redesigned the terminal descent sequence by taking full advantage of the inherent flexibility in the basic spacecraft design. In addition to an abundance of television and other data obtained by extensive postlanding operation of the spacecraft, important new data was obtained with an alpha scattering instrument and soil magnet for use in determining the chemical composition and magnetic properties of the lunar surface. Data was also obtained for the first time on the lunar surface erosion effects of firing the vernier rocket engines after landing. The *Surveyor V* results supported and extended the findings of *Surveyors I* and *III* to provide additional assurance of the suitability of the *Surveyor* landing sites for *Apollo*.

Surveyor VI was launched on November 7, 1967. After a very nominal transit phase, the spacecraft soft-landed on a relatively level surface in the Central Bay at 0.47°N latitude and 1.38°W longitude. Spacecraft performance throughout the lunar day was excellent, permitting very extensive operations on the lunar surface. Abundant data was obtained from the alpha scattering instrument, television camera, soil magnet, and other spacecraft instrumentation. In addition, a unique experiment was conducted wherein the spacecraft performed a hop to a new location about 8 ft from the original landing site.

3. Surveyor VII Mission Objectives

The *Surveyor VII* mission objectives established before launch were as follows:

- (1) Perform a soft landing on the moon.
- (2) Obtain postlanding television pictures of the lunar surface.

- (3) Determine the relative abundance of the chemical elements in the lunar soil by operation of the alpha scattering instrument.
- (4) Manipulate the lunar material with the soil mechanics/surface sampler (SM/SS) in view of the television camera.
- (5) Obtain touchdown dynamics data.
- (6) Obtain thermal and radar reflectivity data on the lunar surface.

Surveyor VII satisfied all the mission objectives. Whereas the previous successful *Surveyor* spacecraft returned data from lunar mare sites to fulfill obligations in support of the *Apollo* Program, *Surveyor VII* returned desired data from a specially selected site in the lunar highlands.

B. Project Description

The *Surveyor* Project was managed by the Jet Propulsion Laboratory for the NASA Office of Space Science and Applications. The Project was supported by four major administrative and functional elements or systems: Launch Vehicle System, Spacecraft System, Tracking and Data System (TDS), and Mission Operations System (MOS). In addition to overall project management, JPL was assigned the management responsibility for the Spacecraft, Tracking and Data Acquisition, and Mission Operations Systems. NASA/Lewis Research Center (LeRC) was assigned responsibility for the *Atlas/Centaur* launch vehicle system.

1. Launch Vehicle System

Atlas/Centaur launch vehicle development began as an Advanced Research Projects Agency program for synchronous-orbit missions. In 1958, General Dynamics/Convair was given the contract to modify the *Atlas* first stage and develop the *Centaur* upper stage; Pratt & Whitney was given the contract to develop the high-impulse LH₂/LO₂ engines for the *Centaur* stage.

The Kennedy Space Center, Unmanned Launch Operations branch, working with LeRC, was assigned the *Centaur* launch operations responsibility. The *Centaur* vehicle utilizes Launch Complex 36, which consists of two launch pads (A and B) connected to a common blockhouse. The blockhouse has separate control consoles for each of the pads. Pad 36A was utilized for the *Surveyor VII* mission.

The launch of *Atlas/Centaur* AC-15 on the *Surveyor VII* mission was the seventh operational flight of an *Atlas/Centaur* vehicle, all of which have been very successful. This was the fourth *Surveyor* mission to utilize the "parking orbit" mode of ascent, wherein the *Centaur* stage burns twice. The first burn injects the vehicle into a temporary parking orbit with a nominal altitude of 90 nm. After a coast period of up to 25 min, the *Centaur* reignites and provides the additional impulse necessary to achieve a lunar intercept trajectory. The parking orbit ascent mode permits launching for all values of lunar declinations. This allows the design of launch periods which are compatible with favorable postlanding lunar lighting. In contrast, the *Surveyor* direct ascent missions (*Surveyors I, II, and IV*) could utilize only those days (about 8 per month) for which the lunar declination was less than approximately -14° .

Surveyor VII was the third mission to utilize the *Atlas* SLV-3C booster, which was uprated from the previous LV-3C configuration by incorporating a 51-in. extension of the tank section, to provide greater propellant capacity, and by increasing the engine thrust levels sufficiently to maintain adequate liftoff acceleration.

2. Spacecraft System

Design, fabrication, and test operations of the *Surveyor* spacecraft were performed by Hughes Aircraft Company under the technical direction of JPL.

Surveyor is a fully attitude-stabilized spacecraft designed to receive and execute a wide variety of earth commands, as well as perform certain automatic functions including the critical terminal descent and soft-landing sequences. Overall spacecraft dimensions and weight of 2200 to 2300 lb were established in accordance with the *Atlas/Centaur* vehicle capabilities. *Surveyor* has made significant new contributions to spacecraft technology through the development of new and advanced subsystems required for successful soft landing on the lunar surface. New features which were employed to execute the complex terminal phase of flight include: a solid-propellant main retro motor, throttlable vernier engines (also used for midcourse velocity correction), extremely sensitive velocity- and altitude-sensing radars, and an automatic closed-loop guidance and control system. The demonstration of these devices on *Surveyor* missions is a direct benefit to the *Apollo* program, which will employ similar techniques.

All *Surveyor* spacecraft carried a survey television camera and engineering instrumentation for obtaining

in-flight and postlanding data. As an additional scientific instrument, *Surveyors III* and *IV* carried a soil mechanics/surface sampler device to provide data based on picking, digging, and handling of lunar surface material. A magnet was also attached to one of the spacecraft footpads for missions beginning with *Surveyor IV* to determine magnetic properties of the soil. On *Surveyors V* and *VI*, an alpha scattering instrument (ASI) was substituted for the SM/SS device to obtain data from which a chemical analysis of the lunar surface material could be made. *Surveyor VII* carried both the SM/SS and ASI as well as additional magnets attached to a second footpad and the SM/SS.

3. Tracking and Data System

The TDS provided the tracking and communications link between the spacecraft and the Mission Operations System. For *Surveyor* missions, the TDS used the facilities of (1) the Air Force Eastern Test Range (AFETR) for tracking and telemetry of the spacecraft and vehicle during the launch phase, (2) the Deep Space Network (DSN) for processing and computing, and (3) the Manned Space Flight Network (MSFN) and the World-Wide Communications Network (NASCOM), both of which are operated by Goddard Space Flight Center (GSFC).

The critical flight maneuvers and most television operations on *Surveyor* missions were commanded and recorded by the Deep Space Station at Goldstone, California (DSS 11), during its view periods. Other stations which provided prime support for the *Surveyor VII* mission were DSS 42, near Canberra, Australia, and DSS 61, near Madrid, Spain. During postlanding operations on the *Surveyor VII* mission, DSS 42 and DSS 61 also obtained many television pictures, an abundance of alpha scattering data, and other engineering and scientific data. Additional support, on a limited basis, was provided by DSS 71 (Cape Kennedy) during prelaunch and launch phase, DSS 51 at Johannesburg, South Africa, which provided initial one-way acquisition and coverage during the transit phase, DSS 14 (with a 210-ft antenna at Goldstone) to provide telemetry data during touchdown and to back up DSS 11 during the critical flight phases (midcourse correction and terminal descent).

4. Mission Operations System

The Mission Operations System essentially controlled the spacecraft from launch through termination of the mission. In carrying out this function, the MOS con-

stantly evaluated the spacecraft performance and prepared and issued appropriate commands. The MOS was supported in its activities by the TDS as well as with special hardware provided exclusively by the *Surveyor* project and referred to as mission-dependent equipment. Included in this category are the Command and Data Handling Consoles installed at each of the prime DSIF stations and at DSS 71, the Television Ground Data Handling System (TV-GDHS) installed at DSS 11 (TV-11), and the Space Flight Operations Facility (SFOF) (TV-1), and other special display equipment.

C. Mission Summary

Surveyor VII was launched on January 7, 1968, the first day of the selected launch period, from Launch Pad 36A at Cape Kennedy with the *Atlas/Centaur* AC-15 vehicle. Liftoff ($L + 00:00$) occurred at 06:30:00.545 GMT, less than 1 sec after the revised opening of the launch window, which had been delayed during the countdown to achieve improved downrange tracking coverage. Very satisfactory launch phase performance was achieved. Following *Atlas* powered flight on a 103-deg flight azimuth, the *Centaur* first burn injected the spacecraft into a parking orbit with an altitude close to the nominal 90 nm. After a 22.4-min coast period, the *Centaur* was reignited and injected the spacecraft into a lunar transfer trajectory. The injection was very accurate, with the estimated uncorrected impact point only 77 km from the prelaunch target point (4.95°S latitude and 3.88°E longitude).

The earth-moon trajectory and major events are depicted in Fig. I-1. Following spacecraft separation, the *Centaur* performed a required retro maneuver sequence to provide increased separation distance from the spacecraft and to miss the moon. After separation, the spacecraft properly executed the automatic antenna/solar panel positioning and sun acquisition sequences. These sequences established the desired attitude of the spacecraft roll axis and insured an adequate supply of solar energy during the coast period.

Tracking and telemetry data received in one-way lock by stations of the AFETR and MSFN confirmed a normal mission during the near-earth portion of flight. As planned, DSS 42 was the first station to establish two-way lock and exercise control of the spacecraft by command. Thereafter, the DSIF stations received and recorded all desired spacecraft data and transmitted necessary earth commands. Nearly continuous two-way

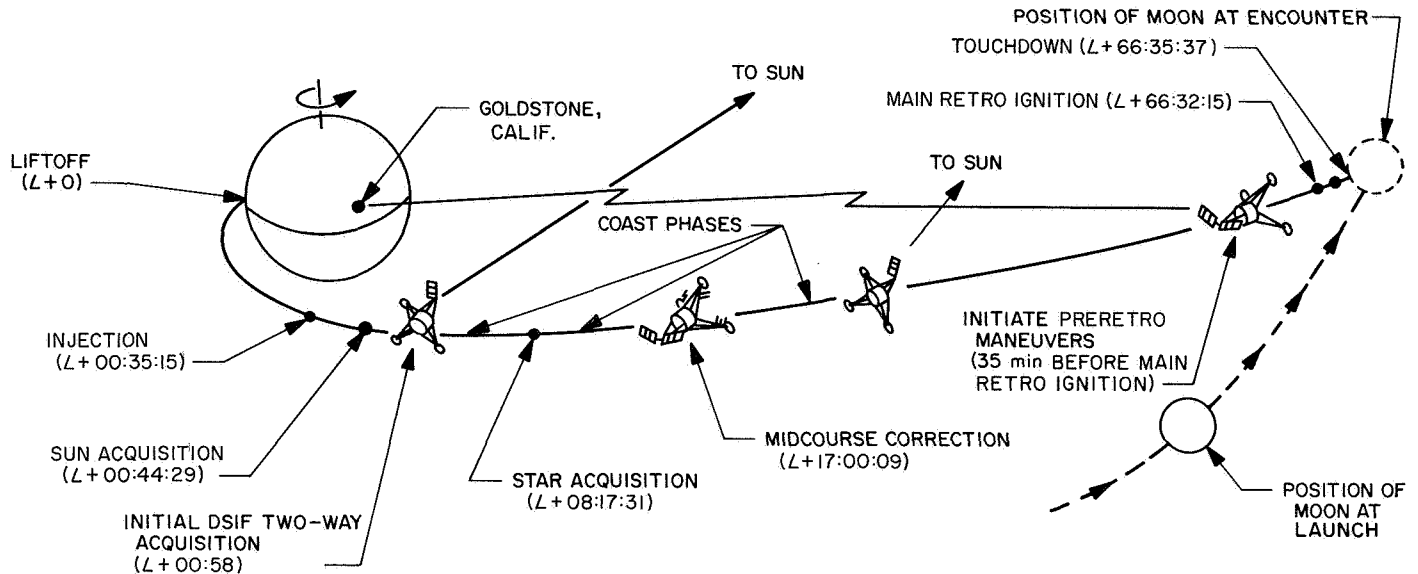


Fig. I-1. Earth-moon trajectory and major events

coverage of the transit phase was provided, including two-way tracking coverage during the midcourse correction. Extensive use was made of doppler resolver data on this mission to effectively reduce the standard deviation of the doppler data to about $\frac{1}{4}$ the value without the resolver.

Spacecraft lock-on with the star Canopus was achieved about 8 hr after liftoff following a spacecraft roll maneuver, during which the Canopus sensor provided data for a star map. During the roll maneuver, it was noted that the Canopus tracker sensitivity was such that a usable lock-on signal would not be provided. Therefore, lock-on was achieved by sending a command from earth when Canopus was in the field of view. This mode of initial acquisition was a planned option and presented no difficulty, the Canopus tracker maintaining lock-on after initial establishment. Canopus lock-on provided 3-axes attitude reference, which is required before the midcourse and terminal maneuvers can be executed.

The landing site finally selected for *Surveyor VII* was on the Tycho ejecta or flow blanket at 40.87°S latitude and 11.37°W longitude. This required a midcourse correction of 11.08 m/sec, which was executed during the first "pass" over DSS 11, Goldstone, about 17 hr after liftoff. A roll-yaw maneuver sequence was performed in preparation for the velocity correction. To execute the correction, the vernier engines were fired for 11.35 sec. Shortly after the velocity correction, the spacecraft was returned to coast orientation, with sun and Canopus lock

achieved by execution of the reverse roll maneuver. Because of the magnitude of the required midcourse correction and since the desired landing site was only 10 km in radius, it was expected that a second midcourse correction would be necessary. The second correction would have been performed during the second Goldstone pass. However, the first midcourse correction resulted in a miss of only 1.7 km from the selected aim point, obviating the second correction.

Spacecraft system performance during the coast phases was excellent, with no anomalies occurring. Many gyro drift checks were conducted to accurately determine the drift rates, which were below the 1.0 deg/hr specification value. Because the drift rates were small, compensation of the midcourse and terminal maneuvers for them was waived.

In preparation for terminal descent, a roll-yaw-roll maneuver combination was executed, beginning about 35 min before retro ignition, to properly align the retro-rocket nozzle in the direction of the velocity vector. Following the attitude orientation maneuver and other preparations commanded from earth, the actual terminal descent sequence was performed completely automatically by the spacecraft.

The terminal descent sequence began with a *mark* signal from the spacecraft altitude marking radar (AMR) when the spacecraft was 60 miles slant range from the lunar surface. After a timed delay of 2.8 sec, which had

been preset in the flight control programmer by earth command, the three liquid-propellant vernier engines ignited, followed (after an additional 1.1-sec delay) by ignition of the solid-propellant main retro motor. Performance of the spacecraft through all phases of the descent was very satisfactory, with all events occurring close to the predicted times. The total time of descent from vernier engine ignition until touchdown was 202.9 sec.

The main retro motor provided 8000 to 10,000 lb thrust for about 40 sec, with the vernier engines maintaining the spacecraft in an inertially fixed attitude. Following retro case ejection, which occurred 12 sec after main retro burnout, the radar altimeter and doppler velocity sensor (RADVS) became operational and differentially throttled the vernier engines to point the spacecraft longitudinal axis along the flight path while maintaining a total thrust level of about 0.9 lunar *g*. When the spacecraft reached 464 ft/sec velocity and 20,246 ft slant range, approximately equal to conditions specified by a "descent contour" that had been programmed in the spacecraft before launch, the RADVS controlled the spacecraft to closely follow the velocity/slant-range contour down to the 14-ft altitude mark. At this point the vernier engines were cut off, causing the spacecraft to free-fall to the lunar surface.

The spacecraft touched down at 01:05:37.62 GMT on January 10, 1968, with a velocity of about 12 ft/sec. A completely successful soft landing was achieved on a relatively flat, level surface. The spacecraft missed hitting any of the large rocks and boulders which litter the area (Fig. I-2), including one large rock very near Footpad 2. All three legs contacted the surface within a time span of approximately 1/20 sec.

The *Surveyor VII* landing site has been identified on *Lunar Orbiter* high-resolution photographs by correlation of features appearing on *Surveyor VII* television frames. This has permitted accurate determination of the site location on the Tycho ejecta or flow blanket at 40.92°S latitude and 11.45°W longitude. The *Surveyor VII* site is indicated in Fig. I-3 together with landing sites of previous *Surveyor* missions. With the successful soft landing of *Surveyor VII*, five *Surveyor* spacecraft have been successfully soft-landed at selected sites on the moon.

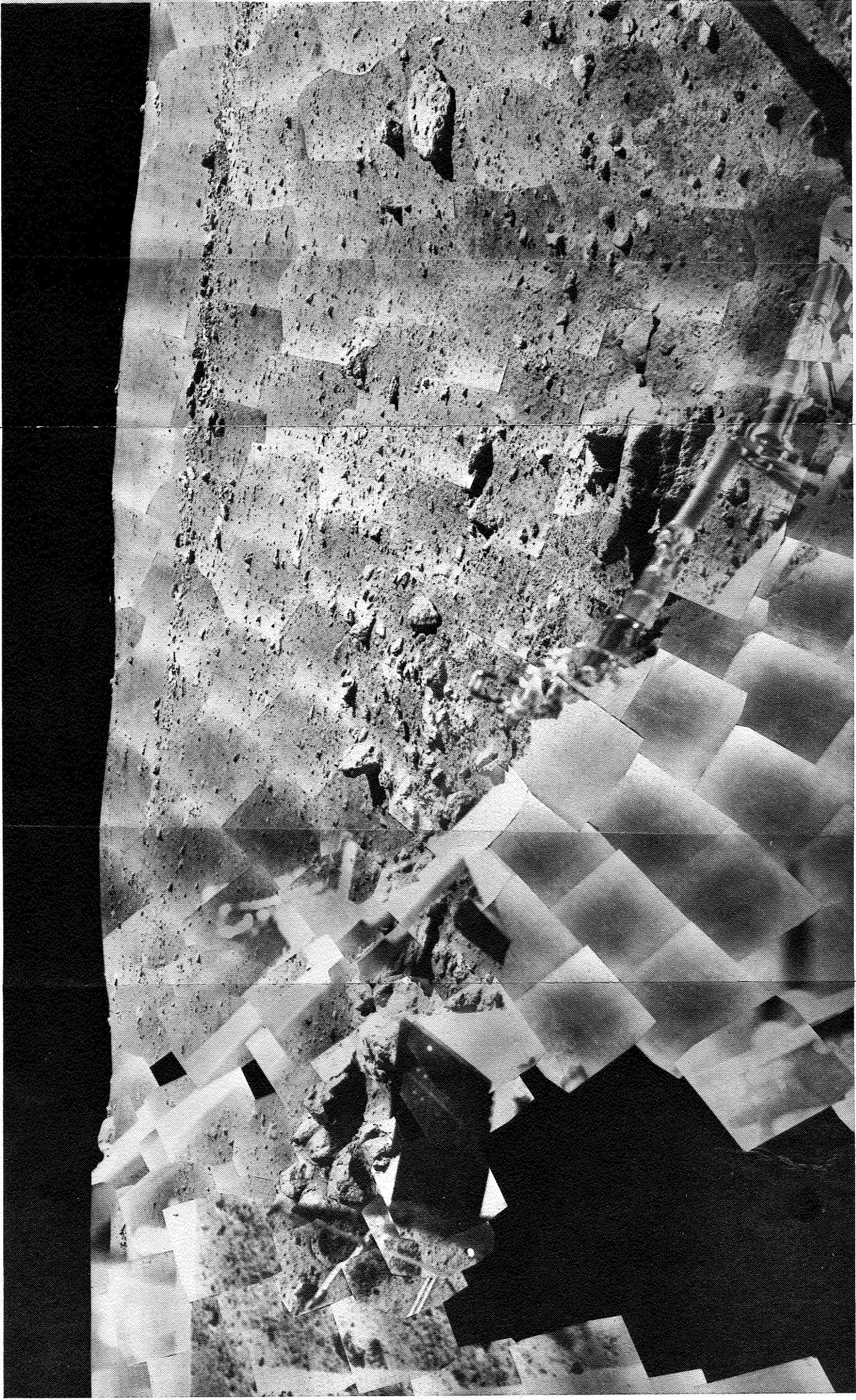
Communication had been maintained with the *Surveyor VII* spacecraft throughout the terminal descent and landing sequence, making it possible to immediately proceed with postlanding operations. Landing occurred

approximately 35 hr after local sunrise, and the initial assessment of postlanding telemetry data indicated the spacecraft condition to be excellent. Very extensive operations were conducted on the lunar surface.

The first television picture (in 200-line mode) was taken about 41 min after touchdown. A total of 14 good-quality 200-line television pictures were obtained before the spacecraft was reconfigured for transmission of 600-line pictures. The 600-line mode required positioning of the solar panel to receive maximum solar power and precise pointing of the planar array toward the earth to provide maximum signal strength. This reconfiguration was accomplished smoothly in less than 1 hr, permitting many pictures to be taken in the 600-line mode before the end of the Goldstone touchdown view period, when it was necessary to transfer to DSS 42 at Canberra, Australia.

Extensive television operations were conducted during each DSIF pass until after sunset. Even during the hot lunar noon period, it was possible to operate the camera at a partial duty cycle by adjusting the antenna/solar panel positioner (A/SPP) to shade the camera and one of the main electronics compartments. Although most of the *Surveyor VII* television pictures were obtained during Goldstone view periods, when the special TV Ground Data Handling System could be used to relay the pictures from Goldstone to the SFOF for evaluation in real-time, DSS 42 and DSS 61 (near Madrid, Spain) participated actively in television operations. *Surveyor VII* obtained a total of over 20,000 pictures, which were of high quality. This performance reflects the significant improvements incorporated in the camera for the *Surveyor VI* and *VII* missions.

The *Surveyor VII* television sequences included (1) a large number of wide- and narrow-angle panoramas of the lunar surface out to the horizon, (2) pictures of stars to aid in spacecraft attitude determination, (3) images obtained with different polarized filters, (4) images obtained with different focus settings to provide a means of determining the distance of objects from the cameras, (5) pictures of the visible parts of the spacecraft, (6) pictures showing disturbances of the lunar soil resulting from landing, (7) pictures showing the amount of material adhering to the bar magnets, and (8) a postsunset sequence lasting about 16 hr that included star and solar corona observations and earthshine pictures. Other unique television operations conducted on this mission were: frequent, unobstructed, narrow-angle views of the earth



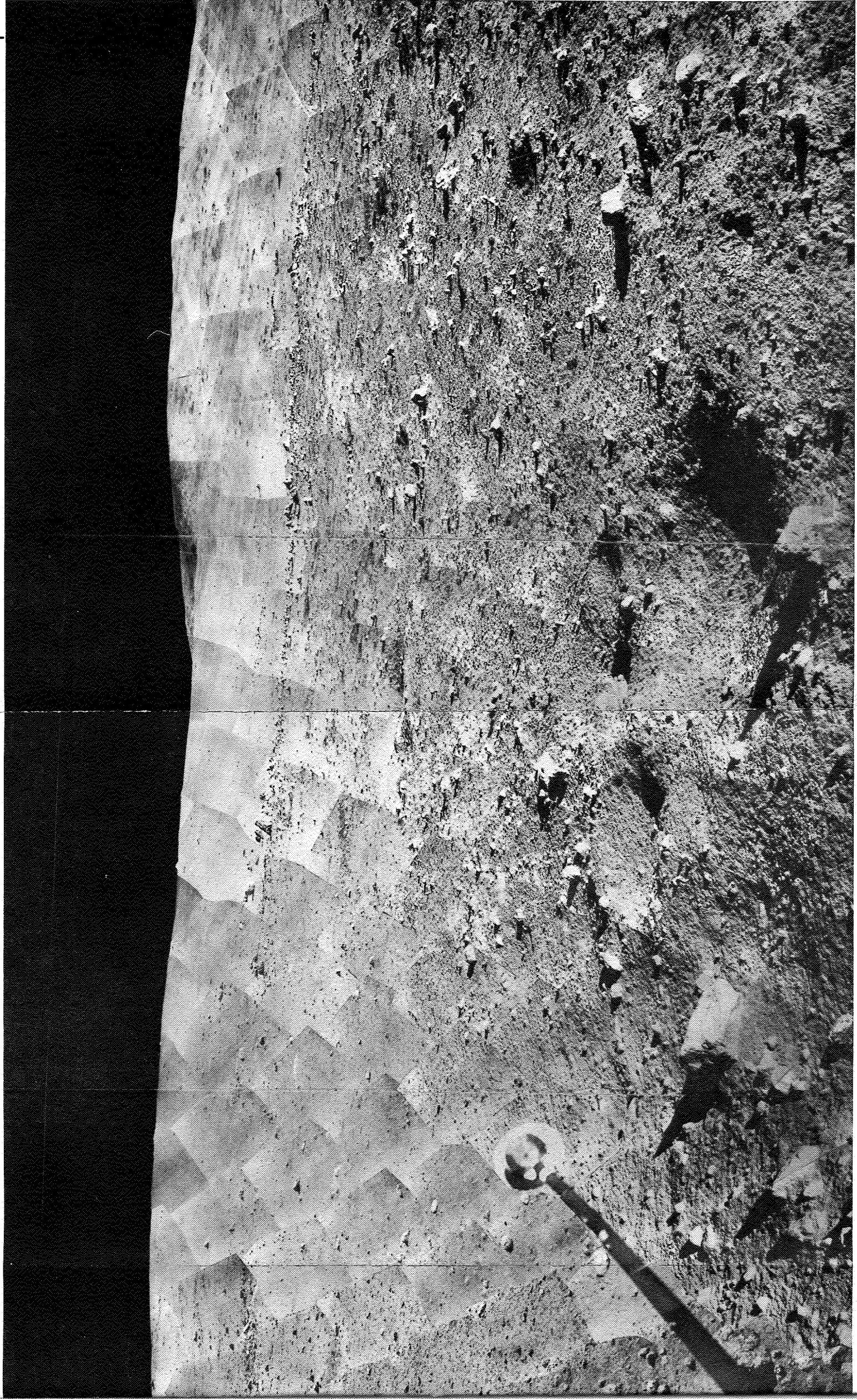
+5°—
0°—
-5°—
-10°—
-15°—
-20°—
-25°—
-30°—
-35°—

1a

w↑

2a

N ↑



— +5°

— 0°

— -5°

— -10°

— -15°

— -20°

— -25°

— -30°

— -35°

/

E ↑



+5°—

0°—

-3°—

-10°—

-15°—

-20°—

-25°—

-30°—

-35°—

2

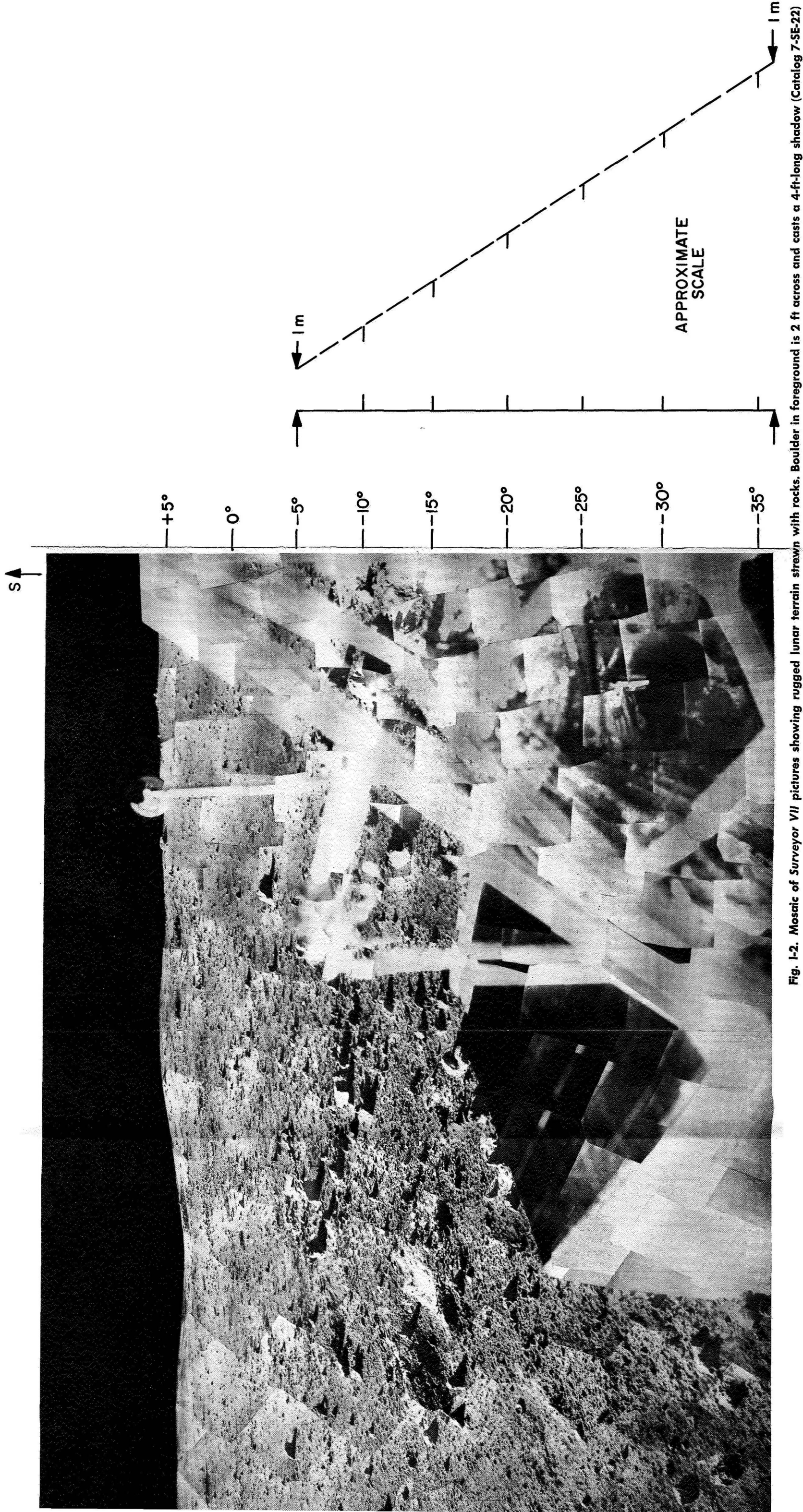


Fig. 1-2. Mosaic of Surveyor VII pictures showing rugged lunar terrain strewn with rocks. Boulder in foreground is 2 ft across and casts a 4-ft-long shadow (Catalog 7-SE-22)

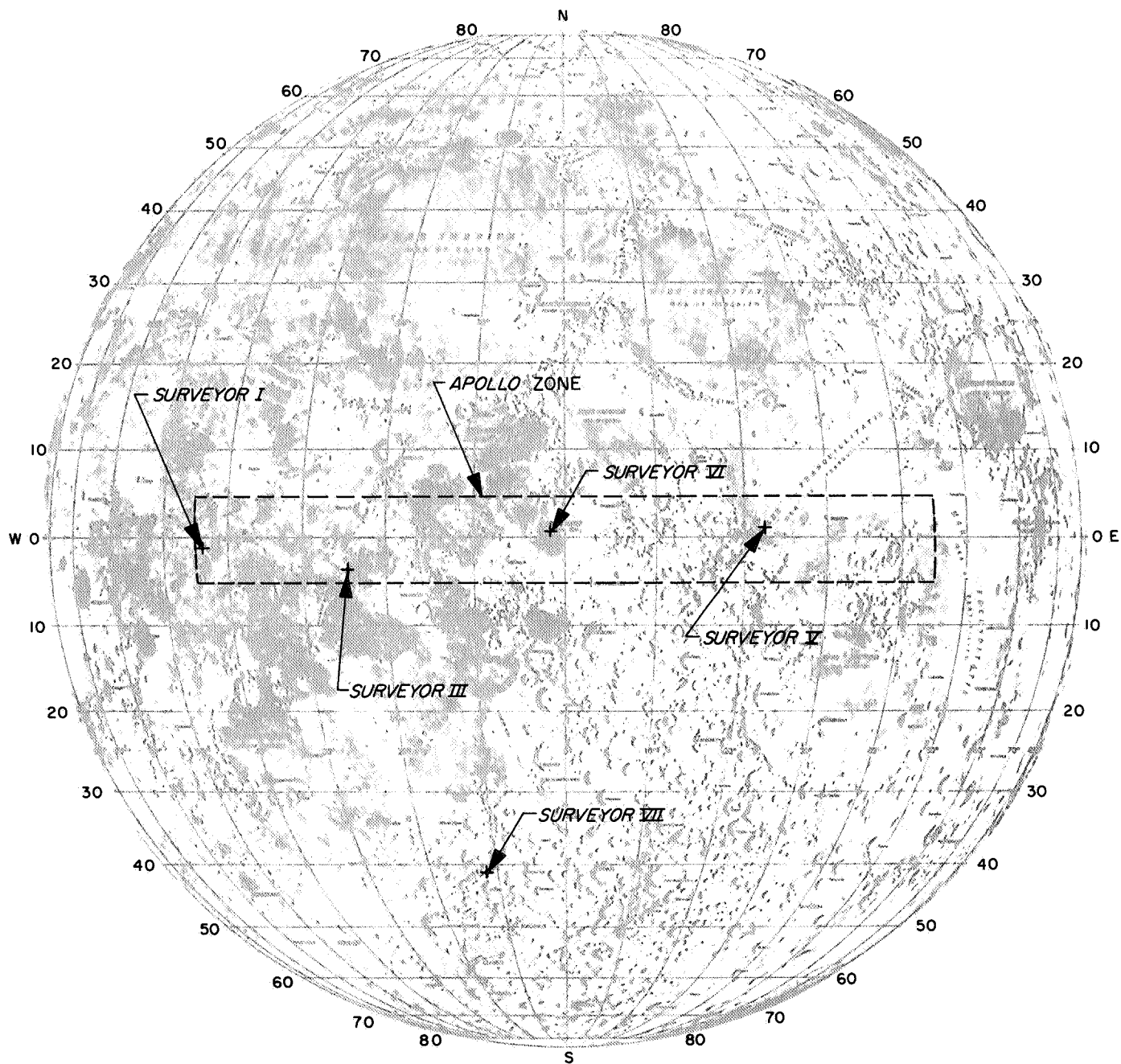


Fig. I-3. Lunar sites of soft-landed Surveyor spacecraft

with and without polarizing filters (made possible by the location of the landing site about 40 deg off the lunar equator); stereoscopic views using an auxiliary mirror mounted on the antenna/solar panel mast; observations of particle accumulation on seven specially located "dust" mirrors; pictures of the SM/SS operations, including the coordinated use of the SM/SS to free the ASI sensor head when it failed to deploy to the surface (see below) and to redeploy it on the surface. Television operations also included observation of laser beams transmitted from earth.

Many television pictures were repeated during the lunar day to obtain views under different lighting conditions, and a series of frames was obtained toward the end of the lunar day showing the progression of shadows cast by the spacecraft and lunar surface features.

The alpha scattering instrument was also operated extensively to provide desired data for chemical analysis of the lunar surface material. However, difficulty was encountered during initial deployment to the lunar surface, which delayed the ASI surface operations. The sensor head was designed for deployment to the surface in a two-step operation. Prior to deployment, calibration data was obtained in the stowed position with the sensor head in contact with a standard sample. In the first step of deployment, the instrument was released to a position about 22 in. above the lunar surface, where background radiation was detected. When the second step was commanded to deploy the sensor head on the surface, the mechanism jammed. Fortunately, the surface sampler was also carried on this mission and, when other means failed to release the ASI sensor head, it was finally freed and pushed to the surface by carefully coordinated commanding of the SM/SS. The SM/SS was also used to redeploy the sensor head, enabling the ASI to obtain data for three different samples of surface material: undisturbed surface material, a lunar rock, and an area that had been trenched extensively with the SM/SS. Because the alpha scattering experiment had been delayed due to the failure to deploy, sufficient data for a chemical analysis of the third sample was not obtained until *Surveyor VII* operations were resumed on the second lunar day.

Operation of the SM/SS had been scheduled to begin after deployment of the ASI sensor head to the lunar surface. However, as a result of the ASI deployment problem, some SM/SS operations were conducted prior to deployment of the ASI. SM/SS performance was ex-

cellent. Operations performed included the following basic experiments: 16 bearing tests, the digging of seven trenches (single or multipass), two impact tests, and the moving or handling of four rocks. Operation of the surface sampler was guided almost entirely by television pictures taken at selected intervals between stepping commands. For this reason, surface sampler operations were conducted during Goldstone view periods when the TV-GDHS could be utilized for real-time "monitoring" of the instrument at the SFOF in Pasadena. Data from the surface sampler experiments consisted primarily of the television pictures obtained. Measurement of SM/SS motor currents compared against prelaunch calibration were also a means of deducing strength and density of lunar surface material.

Spacecraft engineering data was received frequently throughout the lunar day to enable repeated assessment of the spacecraft condition. In addition, two-way doppler tracking data was obtained whenever possible, using the resolver doppler counter.

The latitude of the *Surveyor VII* site made it more difficult or impossible to shade certain spacecraft components by means of the solar panel or planar array. Nevertheless, by careful scheduling of operations and experiments, a high level of activity was possible most of the time.

First lunar day operations were continued almost 80 hr after sunset, with intermittent standby periods, until 14:12 GMT, January 26, when the spacecraft was shutdown.

During the second lunar day, *Surveyor VII* responded to the first turn-on command at 19:00 GMT, on February 12. Telemetry indicated serious degradation of the battery (several shorted cells and loss of pressurization), precluding heavy loading of the power system. Despite this problem, the spacecraft was operated for more than 8 earth days. During this period, additional pictures were taken in 200-line mode (600-line mode was inoperable), including pictures of lunar surface areas newly revealed as a result of an 8-deg tilt of the spacecraft caused by the collapse of leg 1 shock absorber. Highest priority was given to the alpha scattering experiment, and over 20 hr of good alpha data was obtained (the proton detector system was inoperable) utilizing solar panel current. SM/SS operations were limited to a brief but successful test of the extension stepping capability of the instrument. Final loss of the spacecraft carrier signal occurred at 00:24 GMT, on February 21, 1968.

II. Space Vehicle Preparations and Launch Operations

The *Surveyor VII* spacecraft was assembled and flight-acceptance-tested at the Hughes Aircraft Company (HAC) facility, El Segundo, California. After completion of these tests, the spacecraft was airlifted to the Air Force Eastern Test Range (AFETR), Cape Kennedy, arriving on November 6, 1967.

The *Atlas/Centaur* launch vehicle stages arrived at AFETR on October 18, and 22, 1967, respectively. Pre-launch assembly, checkout, and systems tests were performed successfully at AFETR, and launch was accomplished on January 7, 1968, at 06:30:00.545 GMT, 0.545 sec after the rescheduled opening of the launch window on the first day of the launch period.

A. Spacecraft Assembly and Testing

Tests and operations on the spacecraft were conducted by a test team and data analysis team which worked with the spacecraft throughout the period from the beginning of testing until launch. The test equipment used to control and monitor the spacecraft performance at all test facilities includes (1) a system test equipment assem-

bly (STEA) containing equipment for testing each of the spacecraft subsystems, (2) a command and data handling console (CDC) similar to units located at the DSIF stations (see Section VI-B) for receiving telemetry and TV data and sending commands, and (3) a computer data system (CDS) for automatic monitoring of telemetry during spacecraft testing.

The *Surveyor VII* spacecraft (SC-7) began system testing on May 16, 1967, and passed through the following test phases:

1. Spacecraft Ambient Testing

The ambient test phase consists of initial system checkout (ISCO) and mission sequence tests. During ISCO, each subsystem is first tested for subsystem performance and then is tested for compatibility and calibration with the other spacecraft subsystems. Initial system operational verification is demonstrated by a system readiness test (SRT). Removal of spacecraft components for use on SC-5 and SC-6 resulted in the delay of some ISCO testing until an available time during the mission sequence test period.

The mission sequence (MS) tests are performed to obtain system performance characteristics of the spacecraft under ambient conditions and in the electromagnetic (EM) environment expected on the launch pad and in the flight prior to separation from the *Centaur*. Mission Sequences 1 and 2 are compressed (32-hr) mission runs without the expected EM environment. Mission Sequence 3 is a full (68-hr) mission with plugs out and the expected launch EM environment. This test phase was completed on July 31, 1967.

2. Solar-Thermal-Vacuum (STV) Testing

The STV test sequences are conducted to verify proper spacecraft performance in simulated missions at various solar intensities and a vacuum environment. During STV tests, and in the vibration tests which follow, the propellant tanks are loaded with "referee" fluids to simulate flight weight and thermal characteristics.

Preparation for SC-7 STV testing began on August 1, 1967. The first test in the solar vacuum chamber, a Phase A sequence conducted at 112% of nominal sun intensity (high sun), was aborted when Transmitter B and Receiver B malfunctioned. After replacement of the transmitter and receiver, and repair of a leak in the vacuum chamber, the test was rerun. During the rerun, the altitude marking radar (AMR) improperly generated a mark when it was enabled and poor-quality TV pictures were obtained.

The STV testing continued into a Phase B sequence conducted at 87% of nominal sun intensity without breaking vacuum in the chamber. Although no significant steps were eliminated, this test was shortened when, near the end of the sequence, the spacecraft battery exceeded its pressure alarm limit. Also, during the terminal descent portion of the Phase B sequence, the AMR again improperly generated a mark signal and the flight control system failed to turn on thrust phase power. The vacuum chamber was then opened for repair of the flight control sensor group (FCSC) and replacement of the AMR and flight TV camera. Another Phase A sequence was then successfully conducted, and preparations were begun for the vibration phase of system testing.

3. System Vibration Testing

Vibration tests are conducted in each of the three orthogonal axes of the spacecraft to verify spacecraft integrity and proper functional operation during and

after exposure to a simulated launch environment. During these tests, the spacecraft is placed in the launch configuration with the landing legs and omniantennas in the folded position. A vernier engine vibration (VEV) test is also conducted, with the vibration input at the vernier engine mounting points to simulate the vibration environment during the midcourse and terminal descent phases of flight. The spacecraft is checked functionally during each phase, and previbration and postvibration alignment checks are performed to verify that the spacecraft is not degraded by exposure to the vibration environment.

No problems were encountered during vibration testing of SC-7 in each of its three orthogonal axes. Prior to the VEV test, the repaired flight TV camera was reinstalled and the klystron power supply modulator (KPSM) was replaced. The new KPSM failed during checkout and caused damage to the signal data converter (SDC). After repair of the SDC and replacement of the KPSM, the spacecraft proceeded through the VEV testing with no significant problems. After transport preparations, the spacecraft was shipped by air to AFETR, arriving on November 6, 1967. The Combined Systems Test (CST) phase was eliminated from the *Surveyor VII* spacecraft operations because of schedule limitations.

B. Launch Vehicle Combined Systems Testing at San Diego

Following satisfactory completion of factory acceptance testing of each launch vehicle stage, the *Atlas* was installed in the Combined Systems Test Stand (CSTS) at San Diego on September 1, followed by the interstage adapter on September 5, and the *Centaur* on September 6. Test sequences in the CSTS culminated in a vehicle Flight Acceptance Composite Test (FACT) on October 6. Several hardware modifications and replacements were completed, and the NASA data review on October 10 and 11 determined the vehicle to be acceptable and ready for shipment to AFETR. The *Atlas* was shipped by air on October 17, followed by the nose fairing and interstage adapter on October 19, and the *Centaur* on October 21.

C. Launch Operations at AFETR

The major operations performed at AFETR for the launch vehicle and spacecraft are listed in Table II-1.

Table II-1. Major Surveyor VII operations at Cape Kennedy

Operation	Location	Date completed
AC-15 ^a erection (<i>Atlas</i> stage)	Launch Complex 36A	Oct 23, 1967
AC-15 erection (<i>Centaur</i> stage)	Launch Complex 36A	Oct 24
SC-7 ^b inspection, reassembly, and initial checkout	Building AO	Nov 12
SC-7 VPS functional test	Building AO	Nov 14
SC-7-PVT 4 and TV calibration	Building AO	Nov 18
SC-7 PVT 3	Building AO	Nov 20
SC-7 mate to adapter	Explosive Safe Facility (ESF)	Nov 24
SC-7 mate to <i>Centaur</i>	Launch Complex 36A	Nov 29
SC-7 spacecraft/DSS 71 compatibility test	Launch Complex 36A	Dec 1
AC-15/SC-7 J-FACT	Launch Complex 36A	Dec 1
SC-7 demate from <i>Centaur</i>	Launch Complex 36A	Dec 1
SC-7 decapsulation and demate from adapter	ESF	Dec 2
SC-7 initial alignment	ESF	Dec 5
SC-7 PVT 5 mission sequence	Building AO	Dec 9
SC-7 VPS high-pressure leak test	ESF	Dec 12
AC-15 flight control and propellant tanking integrated test (first)	Launch Complex 36A	Dec 14
AC-15 flight control and propellant tanking integrated test (second)	Launch Complex 36A	Dec 15
SC-7 VPS propellant loading and high-pressure leak test	ESF	Dec 16
SC-7 retro motor installation, and final weight, balance, and alignment	ESF	Dec 20
AC-15 FACT (without spacecraft)	Launch Complex 36A	Dec 21
SC-7 mate to adapter	ESF	Dec 22
AC-15 CRT	Launch Complex 36A	Dec 28
SC-7 PVT 6	ESF	Jan 2, 1968
SC-7 encapsulation and SRT	ESF	Jan 3
SC-7 final mate to <i>Centaur</i> and SRT	Launch Complex 36A	Jan 3
SC-7 commutator assessment and final SRT	Launch Complex 36A	Jan 6
<i>Surveyor VII</i> launch	Launch Complex 36A	Jan 7

^a*Atlas/Centaur* vehicle designation.
^b*Surveyor VII* spacecraft designation.

1. Initial Preparations

Receiving inspection and reassembly of the spacecraft at Building AO began on November 7, 1967, followed by a series of Performance Verification Tests (PVT 1, PVT 3, and PVT 4) and television calibrations to verify flight readiness of the spacecraft.

During PVT 1, spacecraft Receiver A was found to have shifted calibration. The receiver was removed from the spacecraft and returned to El Segundo for recalibration. After two spare receivers failed to perform prop-

erly, the original unit was later reinstalled. Also during this period, two leaking vernier propulsion system (VPS) fuel tanks were replaced and several pins in the FCSC Microdot connectors were replaced. Noise problems in the KPSM resulted in portions of PVT 3, including the closed-loop terminal descent and RADVS ranging tests, being deferred until after PVT 4, television calibration, and checkout of the soil mechanics/surface sampler. After replacement of the KPSM with another unit, which had been under repair at Ryan Aeronautical Company, the postponed portions of PVT 3 were satisfactorily performed. After the television camera vidicon was cleaned

at the conclusion of this series of PVT's, the plastic dust cover became lodged in the camera electronics, requiring shipment of the camera to El Segundo for disassembly and removal of the dust cover. Final camera alignment was postponed until after the Joint Flight Acceptance Composite Test (J-FACT) period.

The *Atlas* and *Centaur* stages of AC-15 were erected on launch pad 36A on October 23 and 24, respectively. All required launch vehicle operations preliminary to mating of the spacecraft and performance of the J-FACT were culminated with a successful guidance/autopilot (GAP) test on November 30.

2. Flight Acceptance Composite Tests and Launch Vehicle Propellant Tanking Test

Following initial testing at the Spacecraft Checkout Facility (SCF) in Building AO, the spacecraft was moved to the Explosive Safe Facility (ESF), where it was prepared for the J-FACT. The spacecraft was built up to flight configuration except for a dummy retromotor, non-flight shock absorbers, referee fluids instead of liquid propellants, leg and omniantenna deploy squibs in mufflers, and no flight calibration sources in the sensor head of the alpha scattering instrument. After the spacecraft was mated to the forward adapter, the helium and nitrogen tanks were pressurized, the spacecraft was encapsulated, and an SRT was performed on November 28.

The spacecraft was then transported to launch pad 36A and mated to the *Centaur* vehicle on November 29, 1967. After mating, an RF air-link optimization test, an SRT, and a practice countdown were performed independent of the launch vehicle to verify proper operation of the spacecraft and GSE. There were no anomalies. An integrated launch control test to check out the space vehicle countdown sequence was also performed on November 29. On November 30 and during the early morning of December 1, a compatibility test between the spacecraft and DSS 71, at Cape Kennedy, was performed with no significant problems.

The J-FACT was performed satisfactorily on December 1 with the spacecraft operating in the actual pre-launch environment. This test, involving all systems, covered launch through spacecraft separation and *Centaur* retro maneuver. Spacecraft/*Centaur* separation was simulated by manually disconnecting the adapter field joint electrical connector. The spacecraft temperature was maintained constant during the J-FACT period to

permit accurate pressure decay measurements of the vernier propulsion and attitude control systems.

During the J-FACT, between $T-120$ and $T-60$ min in the countdown, a launch vehicle electromechanical interference (EMI) test was conducted. The purpose of this test is to verify spacecraft electrical compatibility with the launch complex and vehicle propellant storage and handling systems in lieu of a cryogenic tanking operation. No spacecraft or launch vehicle anomalies were observed during performance of the EMI test. Except for an excessive leak in the spacecraft helium system, and intermittent operation of the *Atlas* gyro spin motor rotation detector (SMRD), no other significant spacecraft or launch vehicle anomalies were noted during the J-FACT period. The spacecraft was demated from the *Centaur* and returned to the ESF on December 1.

Following the J-FACT, several launch vehicle flight components were replaced or modified, including replacement of the liquid oxygen lines to the *Centaur* engines, removal of portions of the insulation panels to obtain proper clearance, and replacement of a *Centaur* umbilical adapter. Also, the *Atlas* flight gyro was replaced and a new *Atlas* arming device was installed. Satisfactory operation of these components was confirmed by appropriate retest in time to support the *Atlas/Centaur* flight control and propellant tanking integrated test conducted on December 14.

Although the launch vehicle was completely tanked on December 14, the test was unsatisfactory because of an excessive liquid hydrogen bulkhead pressure indication and a lower than normal liquid oxygen boiloff rate. Also, the liquid oxygen transfer system main dump valve did not open following completion of liquid oxygen tanking. The system was vented by opening the umbilical boom vent valve. After detanking, a leak which was discovered in the bulkhead was repaired, the dump valve was replaced, and a second tanking test was successfully performed on December 15.

The launch vehicle was then prepared for a Flight Acceptance Composite Test (FACT), without the spacecraft, to confirm satisfactory operation of all *Atlas/Centaur* ground and flight electrical systems. Preparations for this test included replacement of the *Centaur* guidance system and inverter, the *Atlas* range safety command arming device, and a transducer in the sustainer engine liquid oxygen pressure reference regulator.

The FACT, conducted on December 20, was considered satisfactory, although guidance optical acquisition was lost during the "hold-fire" test at $T-10$ sec in the count-down. This anomaly, which was probably due to a severe thunder and rain storm, required a hold of 2 min 35 sec to reacquire and would have necessitated *Centaur* propellant topping had it occurred during a launch attempt.

3. Final Flight Preparations

After return to the ESF following the J-FACT operations, the spacecraft was decapsulated, depressurized, and demated from the adapter. The flight helium and nitrogen pressure transducers were calibrated during depressurization. The nonflight items were removed and initial spacecraft alignment was completed. A leaking O-ring seal in the helium system, which was discovered during the J-FACT period, was also replaced at this time.

The spacecraft was then transported back to Building AO where a detailed mechanical inspection was performed. During this period, the postponed TV alignment was performed, and PVT 5, the final spacecraft system verification, was completed satisfactorily on December 9. The alpha scattering sensor head was removed from the spacecraft during the same period and flight sources were installed. The unit was calibrated in the unit area and installed on the spacecraft just prior to final encapsulation.

The spacecraft was then moved to the Propellant Loading Building (PLB) of the ESF. The vernier propulsion system (VPS) was loaded with referee fluids, and a high-pressure leak test was performed. The VPS pressure transducers were calibrated during depressurizing. The referee fluids were then down-loaded, the system vacuum-dried, and propellants were loaded aboard the spacecraft. A final high-pressure test was then performed to verify integrity of the propellant tanks.

The spacecraft was then moved to the assembly building in the ESF. Final weight, balance, and alignment were performed, and the spacecraft was mated to the retromotor. PVT 6 was performed in parallel with the alignment operations, and the spacecraft was mated to the forward adapter, after which the flight shock absorbers and pyrotechnic devices were installed, and the helium and nitrogen systems were pressurized for flight. A pressure decay test was then performed on the helium system to verify the helium leak rate after replacement of the O-ring seal. Although the leak rate was still high, it was within tolerance, and no further attempts were made to reduce the leakage rate.

After completion of the FACT on December 20, the launch vehicle system was prepared for the Composite Readiness Test (CRT), the last multiple systems test before launch. During this period, the *Atlas* propellant utilization (PU) system was replaced, the *Atlas* umbilical lanyards were changed from the LV type to the SLV configuration, and an umbilical solenoid was replaced and proper eject operation was verified. The launch readiness of the *Atlas/Centaur* electrical and RF systems was verified by the successful performance of the CRT on December 28.

After final inspection and cleaning were performed, the spacecraft was encapsulated within the nose fairing, and an SRT was completed on January 2, 1968. On January 3, the encapsulated spacecraft was transported to launch pad 36A, mated to the *Centaur*, and another spacecraft SRT was performed. Also on January 3, with the service tower in the launch position (removed), the spacecraft RF system was calibrated, the retro motor safe-and-arm check was completed, and a simulated countdown was performed.

4. Countdown and Launch

The final spacecraft SRT began at 17:25 GMT on January 6 at a countdown time of $T-680$ min. The spacecraft joined the launch vehicle countdown during the scheduled 60-min hold which started at $T-90$ min. As had been agreed upon earlier in the countdown, the 60-min hold was extended 35 min in order to delay opening of the window so that downrange tracking data coverage would be improved. The countdown was resumed at 05:50 GMT on January 7 and proceeded normally down to the scheduled 10-min hold at $T-5$ min. The countdown was resumed at 06:25 GMT and proceeded smoothly through liftoff (Fig. II-1), which occurred at 06:30:00.545 GMT, January 7, 1968, on a flight azimuth of 102.914 deg. The countdown included a total of 70 min of planned, built-in holds (the one of 60 min duration at $T-90$ min and the one of 10 min duration at $T-5$ min). As a result of the window opening being delayed by the 35-min extension of the $T-90$ min hold, a 102-min launch window was available on January 7, extending from 06:30 to 08:12 GMT. A countdown time summary is shown in Table II-2.

All vehicle systems performed satisfactorily throughout the powered phases of flight, and the spacecraft was accurately injected into a lunar transfer trajectory. Both *Centaur* burn periods were longer than predicted (by about 12.3 and 2.0 sec, respectively), but were within tolerance and had no detrimental effects on the mission.

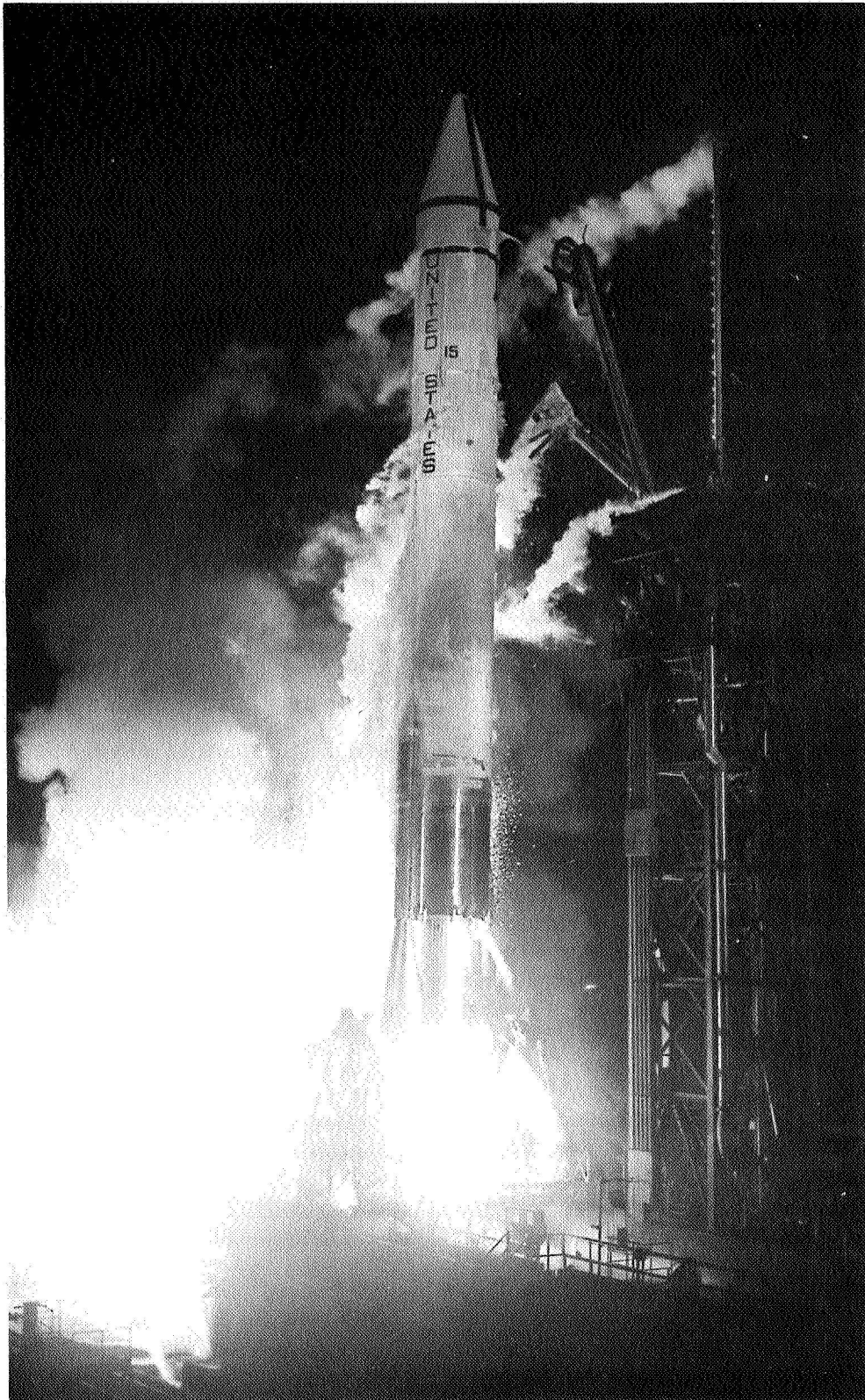


Fig. II-1. Liftoff of *Atlas/Centaur* AC-15 with SC-7 from Launch Complex 36A

Table II-2. Surveyor VII countdown time summary

Event	Countdown time, min	GMT, 1968
Started spacecraft SRT	T-680	Jan 6 17:25
Started launch vehicle countdown	T-335	23:10
Started 60-min built-in hold (BIH) ^a	T-90	Jan 7 03:15
End BIH; resumed countdown	T-90	04:50
Started 10-min BIH	T-5	06:15
Resumed countdown	T-5	06:25
Liftoff	T-0	06:30:00.545

^aAn option to extend the BIH an additional 35 min to ensure better down-range tracking data was exercised during the normal 60-min BIT at T-90 min.

Damage to Launch Complex 36A was moderate. The powered flight sequence of events and launch vehicle performance are described in Section III.

The atmospheric conditions during the launch were acceptable with unusually good visibility. Surface winds were 2 knots from 320 deg. Surface temperature was 64.5°F, with a relative humidity of 96% and a dewpoint of 64°F. Sea level atmospheric pressure was 30.32 in. of mercury. There was no cloud cover. The maximum expected wind shear parameter was 6 ft/sec per thousand feet of altitude occurring between 39,000 and 45,000 ft on an azimuth of approximately 260 deg from true north.

D. Launch Phase Mission Analysis

The *Surveyor VII* launch phase mission analysis activities during the prelaunch planning and countdown stages of the mission were devoted, for the most part, to launch constraint evaluations and launch window definitions. During the near-earth phase of the flight, the activities were centered about obtaining an early and continuing evaluation of the progress of the mission by monitoring information being gathered by each system of the *Surveyor* Project.

1. Prelaunch Planning Activities

The initial *Surveyor VII* launch windows for the January 1968 opportunity were derived from the results of the trajectory targeting effort, and were constrained by the maximum allowable launch azimuth corridor as defined by Range Safety and the maximum design parking orbit coast time capability of the launch vehicle (25 min).

These initial launch windows were considered as maximum windows and published in a launch constraints document for the *Surveyor VII* mission (see Bibliography). Also presented in this document are the preliminary best estimates of the launch window constraints due to the Tracking and Data System (TDS) near-earth coverage limitations. When the final near-earth support plans and commitments of the TDS were made available, so that the near-earth coverage capabilities and limitations could be identified, it was possible to establish the final launch windows for the mission.

The final planned launch windows are shown in Fig. II-2. The opening of these windows was constrained

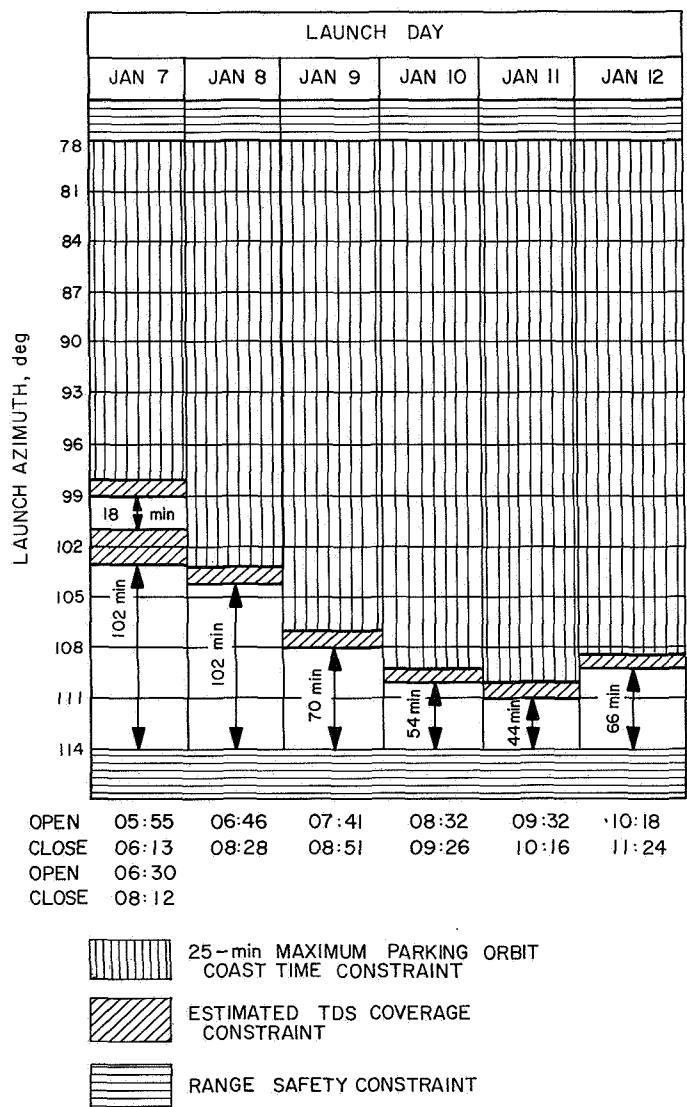


Fig. II-2. Final Surveyor VII launch window design for January 1968

by TDS coverage limitations, while the closing was dictated by the 115-deg azimuth restriction. The gap in the window on the first day also resulted from TDS coverage limitations.

There were only two AFETR range instrumentation ships available to support the *Surveyor VII* mission (as compared with the usual three). As a result, considerable effort was spent in attempting to optimize ship locations. For the first day of the launch period, January 7 (actual launch day), the opening launch azimuth was established at 99 deg in order to insure sufficient transfer orbit tracking coverage.

2. Countdown to Liftoff

The countdown on launch day (January 7) proceeded very smoothly. The Grand Turk radar was in the "red" for a while, but was considered as a backup to the Antigua radar, and therefore did not constitute a hold condition. It was back in the "green" by launch time. During the countdown, it was decided to delay the window opening by extending the scheduled hold at $T-90$ to launch on a flight of 103 deg rather than 99 deg. This decision was made because of the expected improved transfer orbit tracking coverage from the AFETR stations for the 103-deg azimuth. There were no unanticipated holds, and *Surveyor VII* liftoff occurred at the revised launch window opening.

3. Near-Earth Phase

The near-earth mission analysis was based on space vehicle Mark Events reported in near-real-time (see Sec-

tion V, Table V-2), the reported acquisition characteristics of the TDS stations, the reported space vehicle performance evaluations based on real-time telemetry data, the monitored powered flight trajectory characteristics, and the orbit determination calculations of the Real Time Computer System (RTCS) at Cape Kennedy.

The near-earth phase of the flight appeared to be completely nominal, with the launch vehicle performing exceedingly well. From information available during the period from liftoff through parking orbit injection, the normalcy of that portion of the flight was readily established.

The *Centaur* first burn was longer than expected by approximately 12 sec, but the parking orbit trajectory was nominal as determined from tracking data. The launch vehicle telemetry data retransmitted in real-time for the *Centaur* second-burn period indicated that the second-burn prestart ignition and cutoff events were nominal.

It was determined soon after injection that the *Surveyor VII* spacecraft was injected into a lunar impact trajectory based upon Pretoria tracking data. DSS 42 acquired the spacecraft at the nominally expected acquisition time, and the RTCS computed a transfer orbit based on the DSS 42 data. (Refer to Section VII for discussion of transfer orbit determination.) This orbit indicated a very nominal transfer trajectory. The spacecraft telemetry data received in real-time confirmed the spacecraft was performing normally.

III. Launch Vehicle System

Surveyor VII was launched very successfully by a General Dynamics/Convair *Atlas/Centaur* AC-15 launch vehicle. Liftoff occurred at 06:30:00.545 GMT on January 7, 1968, from Launch Complex 36A, AFETR, Cape Kennedy, Florida. Launch was via the indirect-ascent mode wherein the *Centaur* second stage coasted about 22.4 min in a near-circular parking orbit of about 90 nm altitude before reigniting and thrusting a second time to provide the desired injection conditions. Without a mid-course correction, it is estimated that the *Surveyor VII* spacecraft would have impacted the moon only 77 km (48 statute miles) from the prelaunch target point.

This was the seventh operational flight of an *Atlas/Centaur* vehicle, all of which have successfully launched *Surveyor* spacecraft. Four of these flights utilized the indirect-ascent mode. The other three utilized the direct ascent mode, which requires only one "burn" of the second stage to achieve injection.

The *Surveyor VII* mission was the third *Atlas/Centaur* flight to use the SLV-3C *Atlas*, which has a 51-in.-longer propellant tank section and increased thrust compared with the LV-3C *Atlas* previously used. The SLV-3C

Atlas/Centaur vehicle with the *Surveyor* spacecraft encapsulated in the nose fairing is 117 ft long and weighs about 325,000 lb at liftoff (2-in. rise). The basic diameter of the vehicle is a constant 10 ft from the aft end to the base of the conical section of the nose fairing. The configuration of the completely assembled vehicle is illustrated in Fig. III-1. Both the *Atlas* first stage and *Centaur* second stage utilize thin-wall, pressurized, main propellant tank sections of monocoque construction to provide primary structural integrity and support for all vehicle systems. The first and second stages are joined by an interstage adapter section of conventional sheet and stringer design. The clamshell nose fairing is constructed of laminated fiberglass over a fiberglass honeycomb core and attaches to the forward end of the *Centaur* cylindrical tank section.

A. *Atlas* Stage

The first stage of the *Atlas/Centaur* vehicle is a modified version of the *Atlas* used on many previous Air Force and NASA missions such as *Ranger* and *Mariner*. The SLV-3C *Atlas* utilizes an uprated Rocketdyne MA-5 propulsion system, which burns RP-1 kerosene and liquid

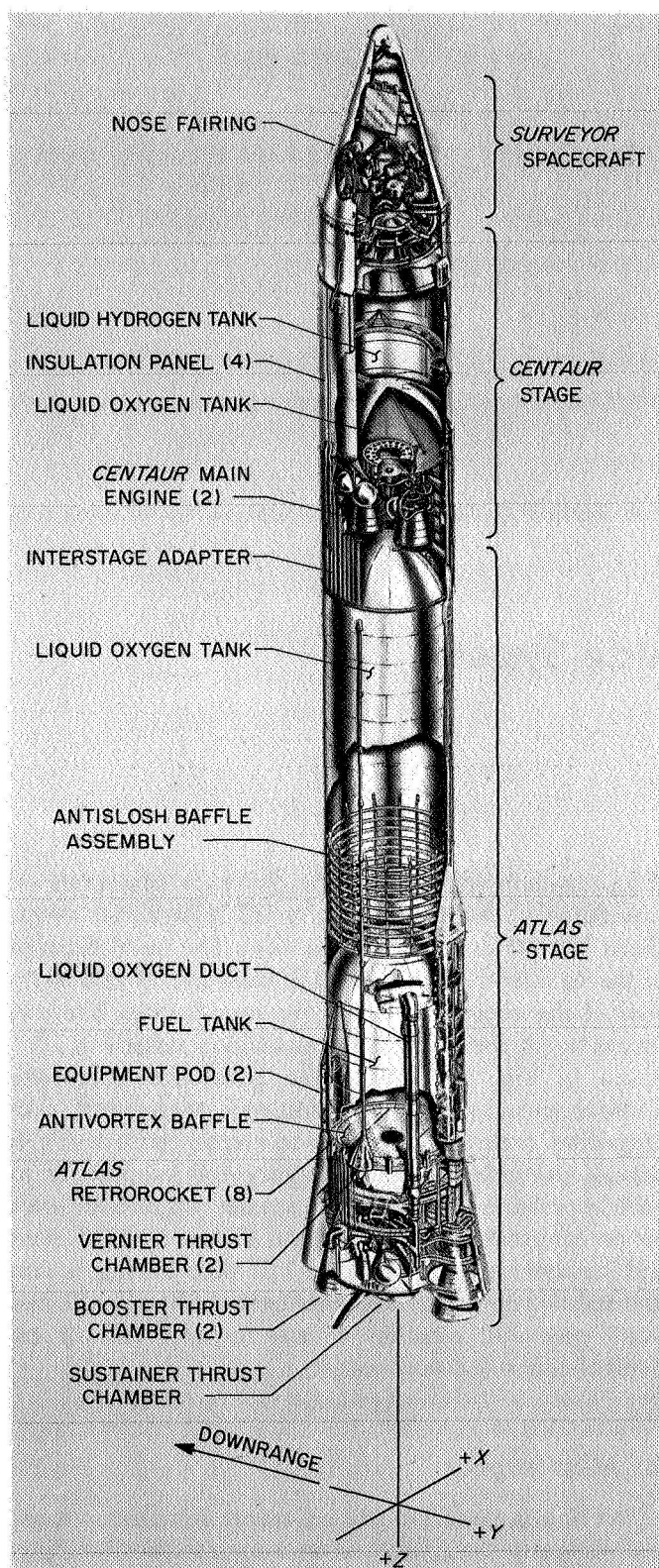


Fig. III-1. Atlas (SLV-3C)/Centaur/Surveyor space vehicle configuration

oxygen in each of its engines to provide a total liftoff thrust of approximately 395,000 lb. The individual sea-level thrust ratings of the engines are: two booster thrust chambers at 168,000 lb each, one sustainer engine at 58,000 lb, and two vernier engines at 670 lb each. The 51-in. extension of the SLV-3C *Atlas* tank section permits tanking of approximately 20,000 lb additional propellants.

The *Atlas* can be considered a 1½-stage vehicle because the "booster section," weighing 6000 lb and consisting of the two booster thrust chambers together with the booster turbopumps and other equipment located in the aft section, is jettisoned after about 2.6 min of flight. The sustainer and vernier engines continue to burn until propellant depletion. A mercury manometer propellant utilization system is used to control mixture ratio for the purpose of minimizing propellant residuals at *Atlas* sustainer engine cutoff.

Flight control of the first stage is accomplished by the *Atlas* autopilot, which contains displacement gyros for attitude reference, rate gyros for response damping, and a programmer to control flight sequencing until *Atlas*/*Centaur* separation. After booster jettison, the *Atlas* autopilot also is fed steering commands from the all-inertial guidance set located in the *Centaur* stage. Vehicle attitude and steering control are achieved by the coordinated gimbaling of the five thrust chambers in response to autopilot signals.

The AC-15 *Atlas* contained a single solid-state telemetry package for transmission of data over a VHF link of 229.9 MHz. The telemetry link utilized each of two antennas mounted on opposite sides of the vehicle at the forward ends of the equipment pods. Redundant range-safety command receivers and a single destructor unit are employed on the *Atlas* to provide the Range Safety Officer with means of terminating the flight by initiating engine cutoff, and/or destroying the vehicle.

B. Centaur Stage

The *Centaur* second stage is the first vehicle to utilize liquid hydrogen/liquid oxygen, high-specific-impulse propellants. The cryogenic propellants require special insulation to be used for the forward, aft, and intermediate bulkheads as well as the cylindrical walls of the tanks. The cylindrical tank section is thermally insulated by four jettisonable insulation panels having built-in fairings to accommodate antennas, conduits, and other

tank protrusions. Most of the *Centaur* electronic equipment packages are mounted on the forward tank bulkhead in a compartment which is air-conditioned prior to liftoff.

The *Centaur* is powered by two Pratt & Whitney constant-thrust engines rated at 15,000 lb thrust each in vacuum. Each engine can be gimballed to provide control in pitch, yaw, and roll. Propellant is fed from each of the tanks to the engines by boost pumps driven by hydrogen peroxide turbines. In addition, each engine contains integral "boot-strap" turbopumps driven by hydrogen propellant. Hydrogen propellant is also used for regenerative cooling of the thrust chambers. The AC-15 *Centaur* stage utilized RL10A-3-3 main engines, which were improved over those used on direct-ascent flights to provide for operation at lower NPSH (net positive suction head) and an increased specific impulse nominal rating of 444 sec.

A propellant utilization system is used on the *Centaur* stage to achieve minimum residual of one propellant at depletion of the other. The system controls the mixture ratio valves as a continuous function of propellant in the tanks by means of capacitive-type tank probes and an error ratio detector. The nominal oxygen/hydrogen mixture ratio is 5:1 by weight. Special design features were incorporated in the hydrogen tank design for parking orbit missions to insure propellant control during the coast phase. These include (1) an antiswirl/antislosh baffle located at the hydrogen level at the end of the first burn, (2) diffusers for energy dissipation at the tank inlets of propellant return and helium pressurization lines, and (3) special ducting to provide balanced thrust venting of the hydrogen tank.

The second stage utilizes a Minneapolis-Honeywell all-inertial guidance system containing a navigation computer which provides vehicle steering commands after jettison of the *Atlas* booster section. For windshear relief during the *Atlas* booster phase, the navigation computer may also be used to generate incremental pitch and yaw corrective signals to supplement the *Atlas* fixed pitch and yaw program. The incremental pitch and yaw programs are selected and fed into the navigational computer prior to launch based on measured wind conditions. The *Centaur* guidance signals are fed to the *Atlas* autopilot until *Atlas* sustainer engine cutoff and to the *Centaur* autopilot after *Centaur* main engine ignition. During flight, platform gyro drifts are compensated for analytically by the guidance system computer rather than by applying corrective gyro torquing signals.

The *Centaur* autopilot system provides the primary control functions required for vehicle stabilization during powered flight, execution of guidance system steering commands, and attitude orientation during parking orbit coast and following the powered phase of flight. In addition, the autopilot system employs an electromechanical programmer to control the sequence of programmed events during the *Centaur* phase of flight, including a series of commands required to be sent to the spacecraft prior to spacecraft separation. A dual-timer configuration is used to provide for the additional programmed events required on a parking orbit mission.

The *Centaur* reaction control system provides thrust to control the vehicle during parking orbit coast and after powered flight. For small corrections in yaw, pitch, and roll attitude control, the system utilizes six individually controlled, fixed-axes, constant-thrust, hydrogen peroxide reaction engines. These engines are mounted in clusters of three, 180 deg apart, near the periphery of the main propellant tanks just aft of the interstage adapter separation plane. Each cluster contains one 6-lb-thrust engine for pitch control and two 3.5-lb-thrust engines for yaw and roll control. In addition, four 50-lb-thrust and four 3-lb-thrust hydrogen peroxide engines are installed on the aft bulkhead, with thrust axes parallel to the vehicle axis.* These engines are used to provide axial acceleration for propellant control during parking orbit coast, to achieve initial separation of the *Centaur* from the spacecraft prior to retromaneuver blowdown, and for executing larger attitude corrections if necessary.

The *Centaur* stage utilizes a VHF telemetry system with a single antenna transmitting through the nose fairing cylindrical section on a frequency of 225.7 MHz. The telemetry system provides data from transducers located throughout the second stage and spacecraft interface area as well as a spacecraft composite signal from the spacecraft central signal processor.

Redundant range safety command receivers are employed on the *Centaur*, together with shaped-charge destruct units for the second stage and spacecraft. This provides the Range Safety Officer with means to terminate the flight by initiating *Centaur* main engine cutoff and destroying the vehicle and spacecraft retrorocket. The system can be safed by ground command, which is normally transmitted by the Range Safety Officer when the vehicle has reached orbital energy.

*The 3-lb-thrust engines were not installed for the direct-ascent missions.

A C-band tracking system is contained on the *Centaur* which includes a lightweight transponder, circulator, power divider, and two antennas located under the insulation panels. The C-band radar transponder provides real-time position and velocity data for the range safety instantaneous impact predictor as well as data for early orbit determination and postflight guidance and trajectory analysis.

C. Launch Vehicle/Spacecraft Interface

The general arrangement of the *Surveyor/Centaur* interface is illustrated in Fig. III-2. The spacecraft is completely encapsulated within a nose fairing/adapter system in the final assembly bay of the Explosive Safe Facility at AFETR prior to being moved to the launch pad. This encapsulation provides protection for the

spacecraft from the environment before launch as well as from aerodynamic loads and heating during ascent. An ablative-type coating (Thermolag) is applied over the nose fairing, *Centaur* insulation panels and interstage adapter to provide added thermal protection.

The spacecraft is first attached to the forward section of a two-piece, conical adapter system of aluminum sheet and stringer design by means of three latch mechanisms, each containing a dual-squib pin puller. The following equipment is located on the forward adapter: three separation spring assemblies, each containing a linear potentiometer for monitoring separation; a 52-pin electrical connector with a pyrotechnic separation mechanism; three pedestals for the spacecraft-mounted separation sensing and arming devices; a shaped-charge destruct assembly directed toward the spacecraft retro-motor; a diaphragm to provide a thermal seal and to

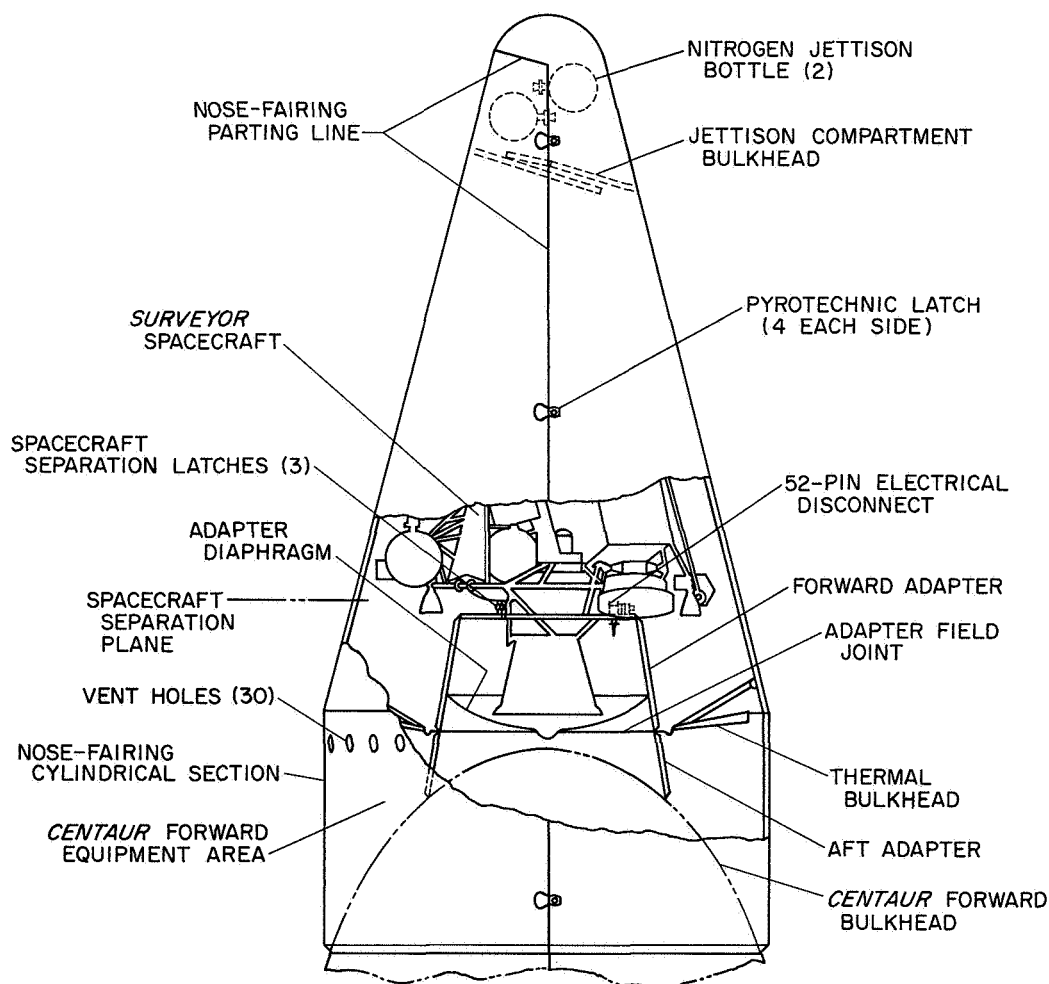


Fig. III-2. *Surveyor/Centaur* interface configuration

prevent contamination from passing to the spacecraft compartment from the *Centaur* forward equipment compartment; and accelerometers for monitoring vibration at the separation plane. Three high-frequency accelerometers were installed on the spacecraft adapter for this mission. As on the two previous *Surveyor* missions (AC-13 and AC-14), two high-frequency accelerometers were located on the *Centaur* side of the separation plane just below the spacecraft attachment ring of the forward adapter section. One of these accelerometers was mounted in the radial direction near spacecraft Leg 1 attach point; the other was mounted in the longitudinal direction near Leg 3 attach point. The outputs of both accelerometers were telemetered continuously.

On AC-15 an additional high-frequency accelerometer was installed just below the spacecraft attachment ring, mounted tangentially in the XY plane 90 deg counterclockwise from the radial accelerometer, looking aft. Data from the tangential accelerometer was transmitted via the *Atlas* telemetry system until *Atlas/Centaur* separation. On flights prior to AC-13, one accelerometer had been mounted differently in a radial direction on the adapter, and four accelerometers had been installed on the spacecraft side of the separation plane.

The low-drag nose fairing is an RF-transparent, clamshell configuration consisting of four sections fabricated of laminated fiberglass cloth faces and honeycomb fiberglass core material. Two half-cone forward sections are brought together over the spacecraft mounted on the forward adapter. An annular thermal bulkhead between the adapter and base of the conical section completes encapsulation of the spacecraft.

The encapsulated assembly is mated to the *Centaur* with the forward adapter section attaching to the aft adapter section at a flange field joint requiring 72 bolts. The conical portion of the nose fairing is bolted to the cylindrical portion of the fairing, the two halves of which are attached to the forward end of the *Centaur* tank around the equipment compartment prior to mating of the spacecraft. Doors in the cylindrical sections provide access to the adapter field joint. The electrical leads from the forward adapter are carried through three field connectors and routed across the aft adapter to the *Centaur* umbilical connectors and to the *Centaur* programmer and telemetry units.

Special distribution ducts are built into the nose fairing and forward adapter to provide air conditioning of the spacecraft cavity after encapsulation and until liftoff. Seals are provided at the joints to prevent shroud leak-

age except out through vent holes in the cylindrical section. Prior to launch, the shroud cavity is monitored for possible spacecraft propellant leakage by means of a toxic gas detector tube which disconnects at liftoff. Tubes are also inserted into each of the vernier engine combustion chambers to permit nitrogen purging for humidity control and leak detection until manual removal before the service tower is rolled away. The spacecraft alpha scattering instrument is also purged by means of a tube which disconnects at liftoff.

The entire nose fairing is designed to be ejected by separation of two clamshell pieces, each consisting of a conical and cylindrical section. Four pyrotechnic pin-puller latches are used on each side of the nose fairing to carry the tension loads between the fairing halves. Nose fairing loads are transmitted to the *Centaur* tank through a bolted joint, which also attaches to the forward end of the *Centaur* insulation panels and contains a flexible linear shaped charge for insulation panel and nose fairing separation. A nitrogen bottle is mounted in each half of the nose fairing near the forward end to supply gas for cold gas jets to force the panels apart. Hinge fittings are located at the base of each fairing half to control ejection, which occurs under vehicle acceleration of approximately 1 g during the *Atlas* sustainer phase of flight.

D. Vehicle Flight Sequence of Events

All vehicle flight events occurred satisfactorily. As has occurred on all previous *Surveyor* missions, the *Centaur* burned longer than expected but well within allowable limits. Predicted and actual times for the vehicle flight sequences of events are included in Table A-1 of Appendix A. Figure III-3 illustrates the major nominal events. The times reported in near-real-time for Mark Events are listed in Section V, Table V-2. Following is a brief description of the vehicle flight sequence of events, with all times referenced to liftoff (2-in. rise) unless otherwise noted. (Refer to Section II-B for a description of the countdown.)

1. *Atlas* Booster Phase of Flight

Hypergolic ignition of all five *Atlas* engines was initiated 2 sec before liftoff. Vehicle liftoff occurred at 06:30:00.545 GMT on January 7, 1968, only 0.545 sec after the revised window opening time on the first day of the launch period. (The window opening had been delayed during the countdown to improve transfer orbit tracking coverage by the downrange AFETR stations.)



Fig. III-3. Launch phase nominal events

The launcher mechanism is designed to begin a controlled release of the vehicle when all engines have reached nearly full thrust. At 2 sec after liftoff, the vehicle began a 13-sec programmed roll from the fixed launcher azimuth setting of 105 deg to a planned launch azimuth of 102.914 deg. The programmed pitchover of the vehicle began 15 sec after liftoff and lasted until booster engine cutoff (BECO), by which time the vehicle had pitched over 72 deg. Incremental pitch (Code 101) and yaw (Code 6) program signals from the *Centaur* navigational computer were used. These pitch and yaw programs had been selected on the basis of prelaunch wind analysis.

The vehicle reached Mach 1 at 64 sec and maximum aerodynamic loading occurred at 78 sec. During the booster phase of flight, the booster engines were gimballed for pitch, yaw, and roll control, and the vernier engines were active in roll control only, while the sustainer engine was centered.

At 152.4 sec, BECO was initiated by a signal from the *Centaur* guidance system when vehicle acceleration equalled 5.73 g (expected value: 5.7 ± 0.08 g). At 3 sec after BECO, with the booster and sustainer engines centered, the booster section was jettisoned by release of pneumatically operated latches. Events beginning with BECO occur later on SLV-3C *Atlas* flights because of the increased propellant tank capacity.

2. *Atlas* Sustainer Phase of Flight

At BECO + 8 sec, the *Centaur* guidance system was enabled to provide steering commands for the *Atlas* sustainer phase of flight. During this phase the sustainer engine was gimballed for pitch and yaw control, while the verniers were active in roll. *Centaur* guidance commanded an additional 8 deg of pitchover, resulting in a total vehicle pitchover of about 80 deg by the end of the sustainer phase. The *Centaur* insulation panels were jettisoned by firing shaped charges at 197.1 sec at an altitude of approximately 54.7 nm, where the aerodynamic heating rate was rapidly decreasing. At 226.4 sec, squibs were fired to unlatch the clamshell nose fairing, which was jettisoned 0.5 sec later by means of nitrogen gas thruster jets activated by pyrotechnic valves.

Other programmed events which occurred during the sustainer phase of flight were (1) the unlocking of the *Centaur* hydrogen tank vent valve to permit venting as required to relieve hydrogen boiloff pressure, (2) starting of the *Centaur* boost pumps about 46.3 sec prior to *Centaur* first main engine start (MES 1), and (3) locking

of the *Centaur* oxidizer tank vent valve followed by "burp" pressurization of the tank.

Sustainer and vernier engine cutoff (SECO and VECO) occurred at 248.7 sec as a result of oxidizer depletion, which was the predicted cutoff mode. Shutdown began with an exponential thrust decay phase of about 1-sec duration due to low oxidizer inlet pressure to the turbopump and resulting loss in turbopump performance. Then, final fast shutdown by propellant valve closure was initiated by actuation of a switch when fuel manifold pressure dropped to 650 ± 50 psi. Also, at the SECO event, the *Centaur* hydrogen tank vent valve was locked and the tank was burp-pressurized for a duration of one second.

Separation of the *Atlas* from the *Centaur* occurred 1.9 sec after SECO by firing of shaped charges at the forward end of the interstage adapter. This was followed by ignition of eight retrorockets located at the aft end of the *Atlas* tank section to back the *Atlas*, together with the interstage adapter, away from the *Centaur*.

3. *Centaur* First Burn Phase of Flight

The *Centaur* prestart sequence for providing chill-down of the propulsion system was initiated 8 sec before first ignition of the *Centaur* main engines (MES 1). MES 1 was commanded 11.5 sec after SECO, at 260.2 sec. *Centaur* guidance was reenabled 4 sec after MES 1 to provide steering commands during the *Centaur* first burn. The guidance system continued to command vehicle pitchover and, by the end of the first burn, total vehicle pitchover was about 98 deg from the liftoff vertical. Main engine cutoff (MECO 1) was commanded by guidance at 593.1 sec, when sufficient impulse had been delivered for injection into the desired parking orbit. *Centaur* first-burn duration was 332.9 sec, or about 12.3 sec longer than predicted for the actual launch conditions.

4. *Centaur* Coast Phase of Flight

Coincident with MECO 1, two of the 50-lb-thrust hydrogen peroxide engines were turned on and provided a low level of axial acceleration to overcome transient disturbances to the propellants caused by main engine shutdown. After 76 sec, the 50-lb engines were turned off and two of the 3-lb axial engines were turned on to retain the propellants at the proper location in the tanks. During the parking orbit coast period, the hydrogen peroxide engines also were enabled for attitude control,

and pitchover of the vehicle was continued to maintain alignment of the vehicle longitudinal axis approximately with the parking orbit flight path.

The required parking orbit coast time varies with actual liftoff time. For this flight, the coast period (MECO 1 to MES 2) lasted for 1346.2 sec (22.4 min). The *Centaur* stage can support coast periods of from 116 sec to 25 min in duration. Initial occurrence of hydrogen tank venting during the coast period was observed 695 sec after MECO 1. Intermittent venting continued until vent valve closure at the start of pressurization for second burn.

At 40 sec before the end of the coast period, the 3-lb engines were turned off and two of the 50-lb engines turned on again until MES 2 to insure propellant control during the events preceding ignition, which included "burp" pressurization of the propellant tanks, starting of the boost pumps 28 sec before MES 2, and initiation of the prestart (chilldown) sequence 17 sec before MES 2.

5. *Centaur* Second Burn Phase of Flight Through Spacecraft Separation

Second main engine start occurred at 1939.3 sec, followed 4 sec later by *guidance enable* for second burn steering control. After a burn time of 115.6 sec, when sufficient velocity had been attained, the *Centaur* engines were shut down by guidance commanded at 2054.9 sec. *Centaur* second burn duration was about 2.0 sec longer than expected. At main engine cutoff, the hydrogen peroxide engines were enabled again for attitude stabilization.

During the 60.4-sec period between MECO 2 and spacecraft separation, the following signals were transmitted to the spacecraft from the *Centaur* programmer: *extend spacecraft landing gear*, *unlock spacecraft omniantennas*, and *turn on spacecraft transmitter high power*. An arming signal also was provided by the *Centaur* during this period to enable the spacecraft to act on the preseparation commands.

The *Centaur* commanded separation of the spacecraft electrical disconnect 5.5 sec nominal before spacecraft separation, which was initiated at 2115.3 sec. The *Centaur* attitude-control engines were disabled for 5 sec during spacecraft separation in order to minimize vehicle turning moments.

6. *Centaur* Retro Maneuver Phase of Flight

At 5 sec after spacecraft separation, the *Centaur* began a turnaround maneuver using the attitude-control engines to point the aft end of the stage in the direction of the flight path. About 40 sec after beginning the turn, which required approximately 110 sec to complete, two of the 50-lb-thrust hydrogen peroxide engines were fired for a period of 20 sec while the *Centaur* continued the turn. This provided initial lateral separation of the *Centaur* from the spacecraft. About 240 sec after spacecraft separation, the propellant blowdown phase of the *Centaur* retro maneuver was initiated by opening the hydrogen and oxygen prestart (chilldown) valves. Oxygen was vented through the engine nozzles while hydrogen discharged directly through the chilldown valves. The oxygen tank pressure remained relatively constant, indicating that liquid oxygen remained in the tank throughout the blowdown. At 111 sec from start of blowdown, the fuel tank pressure decay rate increased, indicating that most of the liquid hydrogen had been expelled at that time.

Coincident with termination of propellant blowdown, a hydrogen peroxide depletion experiment was initiated by firing two of the 50-lb engines. Hydrogen peroxide depletion was indicated about 48.5 sec after start of the experiment. After 100 sec, the hydrogen peroxide experiment was concluded by energizing the *Centaur* power changeover switch at 2705.3 sec, which turned off all power except telemetry and the C-band beacon.

E. Performance

The *Atlas/Centaur* AC-15 vehicle performance was completely satisfactory, providing injection into the desired parking orbit followed by successful restart and very accurate injection of the *Surveyor VII* spacecraft into the prescribed lunar transfer trajectory.

1. Guidance and Flight Control

Autopilot performance was satisfactory throughout the flight, with proper initiation of programmed events and control of vehicle stability. Vehicle disturbances were at or below expected levels and similar to the previous SLV-3C flights. During the *Atlas* phase of flight, the vehicle was easily controlled after *Atlas* autopilot activation at 42-in. motion. Vehicle stability was also satisfactorily maintained during the *Centaur* phase of flight.

The guidance system performed well throughout the flight. A near-circular parking orbit was achieved, having an apogee of 90 nm and a perigee of 86 nm. The spacecraft was injected on a lunar transfer trajectory which would have resulted in an uncorrected impact only 77 km from the prelaunch target point. (Refer to Section VII for a presentation of vehicle guidance accuracy results in terms of equivalent midcourse velocity correction.)

The guidance system provided the programmed incremental pitch and yaw signals during booster phase, and all guidance system discrete commands including BECO, SECO backup, MECO 1, and MECO 2 were generated as planned. Each time guidance was enabled, the initial attitude errors (maximum 5 deg nose left and 6 deg nose up at BECO + 8 sec) were quickly nulled, after which vehicle attitude errors remained small during each of the respective closed-loop steering phases of flight.

The *Centaur* reaction control system performed properly, providing required vehicle attitude control during the coast and retro maneuver phases, the necessary low-level axial thrust for propellant management while in parking orbit, and initial lateral separation from the spacecraft after injection. Disturbing torques occurred as expected owing to boost pump exhaust, main engine chilldown venting, and exhaust impingement from the axially mounted hydrogen peroxide engines. Although the yaw disturbance increased almost to the 3σ dispersion level during second main engine prestart, it was well within the control capability of the attitude control system. For this flight, temperature sensors added in the *Centaur* engine compartment provided useful data on the impingement effects of hydrogen peroxide engine exhaust products.

During the *Centaur* phase of flight, the vehicle is rate-stabilized in roll rather than roll-position-stabilized. Vehicle roll attitude during the *Centaur* powered phase of flight is presented in Fig. III-4.

2. Propulsion and Propellant Utilization

Atlas propulsion system performance was satisfactory. Normal sustainer cutoff characteristics were exhibited following oxidizer depletion, which had been predicted.

Performance of the *Atlas* propellant utilization (PU) system was also satisfactory. The predicted *Atlas* residuals (propellant above pump) are compared in Table III-1,

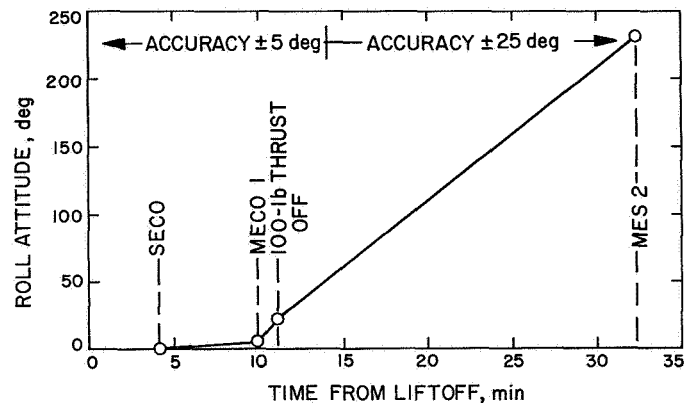


Fig. III-4. *Centaur* clockwise roll attitude relative to local vertical

with values computed from flight data assuming nominal flow rates from port uncovering times until actual SECO.

The *Centaur* propulsion system performed well during both burn periods. Both burns were longer than predicted (by about 12.3 and 2.0 sec, respectively). The thrust chamber pressure of both engines was about 8 psi lower than expected. The indicated low thrust level would account for about 6.9 sec of the longer burn time. The cause of the remainder of the burn time is not known at this time; however, the *Centaur* has also burned for a period longer than expected on each of the previous *Surveyor* missions and, in each case, about 4 to 7 sec of the additional burn time is unexplained.

Table III-1. *Atlas* propellant residuals, lb

Residuals	Actual	Predicted
Oxidizer	453	246
Fuel	247	223

The turbine inlet pressure and speed data of the fuel and oxidizer boost pumps exhibited trends after MES 2 which are indicative of gas flow through the hydrogen peroxide catalyst beds. A similar anomaly was observed during the second burns of the previous parking orbit missions, but the effect on main engine performance has been negligible.

The *Centaur* PU system also performed very well during both burn periods. The predicted and preliminary actual *Centaur* usable residuals after MECO 1 and MECO 2 are compared in Table III-2.

Table III-2. Centaur usable propellant residuals, lb

Usable residuals	Actual	Predicted
MECO 1		
Oxidizer	7133	7202
Fuel	1564	1440
MECO 2		
Oxidizer	513	545
Fuel	147	129

Based on a nominal mixture ratio of 5.0:1, the usable residuals would have provided 9.1 sec additional burn time before theoretical oxidizer depletion, with an ultimate fuel residual of approximately 46 lb. Comparing this to the predicted value of 20 lb residual hydrogen indicates a *Centaur* PU system error of 26 lb excess hydrogen.

3. Pneumatic, Hydraulic, and Electrical Power Systems

Operation of the *Atlas* pneumatic system, including the programmed tank pressurization and pneumatic control functions, was properly accomplished throughout the flight. Both *Centaur* propellant tanks were maintained at satisfactory levels during all phases of flight, with expected occurrences of the "burp" pressurizations and hydrogen tank venting. The size of the oxygen tank pressurization line orifice had been increased for this flight to provide increased tank pressure and thereby an increased margin of net positive suction head at MES 2. The oxygen tank pressure increase as a result of burp pressurization was 3 psi, or approximately double the increase on previous flights.

Performance of the vehicle hydraulic and electrical power systems was satisfactory throughout the flight. There were no unexpected power demands or transients, although it was noted that the *Centaur* inverter voltages were generally higher than on previous flights.

4. Telemetry, Tracking, and Range Safety Command

The *Atlas* and *Centaur* instrumentation and telemetry systems functioned well, with only a few measurement anomalies. A total of 131 *Atlas* and 162 *Centaur* measurements were telemetered on this flight. Continuous *Atlas/Centaur* data was obtained until about 4 min after parking orbit injection, when a 6½-min coverage gap occurred. Thereafter, continuous data was again ob-

tained except for periods of noisy data occurring from before MECO 2 until shortly after spacecraft separation. The noisy data was due to the vehicle attitude and the resulting look angle of the Pretoria (South Africa) receiving station, which caused the receiving antenna to be looking into a null region of the vehicle antenna.

The *Centaur* C-band radar apparently operated normally, although an evaluation of the system can only be made on the basis of received tracking data and station operator logs, because the airborne system is not instrumented. Refer to Section V for a description of tracking and telemetry data coverage.

The *Atlas* and *Centaur* range safety command systems performed satisfactorily. About 17 sec after parking orbit injection (MECO 1), a range safety command to disable the destruct systems was sent and properly executed.

5. Vehicle Loads and Environment

Vehicle loads and thermal environment were within expected ranges throughout the flight. Maximum axial accelerations were 5.73 g at BECO during the booster phase and 1.76 g just before SECO during the sustainer phase. Longitudinal oscillations during launch were normal, reaching a maximum (0.54-g peak-to-peak at 6 Hz) at 0.7 sec and being damped out by 20 sec.

The three high-frequency accelerometers located on the forward spacecraft adapter indicated expected steady-state vibration levels during the flight which agreed well with similar measurements of previous flights. The radially oriented accelerometer indicated a maximum steady-state value during launch of 2.2 g (rms) concentrated between 450 and 570 Hz. The maximum longitudinal steady-state level indicated during launch was 1.3 g (rms), with predominant frequencies at 160, 310, and 450 Hz. The maximum tangential vibration was 0.9 g (rms) during launch, with predominant frequencies at 160, 280, and 340 Hz. Low-level, short-duration transients were recorded throughout the launch phase; they are believed to be due to a combination of dynamic and thermal loads in the area of the *Centaur* forward bulkhead and adapter structure. (Also see Section IV-A for a discussion of launch phase vibration environment.)

The *Surveyor* compartment thermal and pressure environments were normal throughout flight. The ambient

temperature within the compartment was 84°F at liftoff and gradually decreased to 72°F by $L + 76$ sec as a result of expansion during ascent. The ambient pressure decayed characteristically to essentially zero prior to nose fairing jettison.

6. Separation and Retro Maneuver Systems

All vehicle separation systems functioned normally. Booster section jettison occurred as planned, with resulting vehicle rates and high-frequency accelerometer data comparable to previous flights.

Satisfactory insulation panel jettison was confirmed by normal transient effects on vehicle rates, axial acceleration, vibration, etc. The times of 35-deg rotation of the four insulation panels during jettison are provided by a breakwire at one hinge arm of each panel. Average panel rotational rates to the 35-deg position, derived from the breakwire instrumentation, were from 77 to 87 deg/sec. These values are consistent with rates determined on previous flights.

Normal separation of the nose fairing was verified by indications of 3-deg rotation from disconnect wires which are incorporated in the pullaway electrical connectors of each fairing half. The spacecraft compartment pressure

remained at zero throughout nose fairing jettison, with no pressure surge at thruster bottle discharge.

Atlas/Centaur separation occurred as planned. Displacement data obtained with respect to time is in close agreement with expected values and indicates successful *Atlas* retro rocket operation. There was no indication of contact between stages as the *Atlas* cleared the *Centaur*.

Spacecraft separation occurred successfully. Because the telemetry data is noisy for this period of time, it is not possible to determine the precise times for first motion and full extension of the separation springs. Data from the extensometers (linear potentiometers) does indicate similarity of the spring extension slopes, and the magnitude of the *Centaur* rates following separation also indicates a smooth, well-controlled separation.

All phases of the *Centaur* retro maneuver were executed as planned. Five hours after spacecraft separation, the *Centaur/Surveyor* separation distance was computed to be about 1425 km, which is well in excess of the required minimum distance of 336 km at that time. The *Centaur* closest approach to the moon was computed to be approximately 19,635 km and occurred at about 13:19 GMT on January 10, 1968.

IV. Surveyor Spacecraft

The basic objectives of the *Surveyor VII* mission were: (1) to accomplish a soft landing on the moon at a site outside the Apollo zone of interest (an ultimate choice of 40.87°S latitude and 11.37°W longitude was made, requiring, as a result, an oblique approach angle of 36°); (2) to obtain postlanding television pictures of the lunar surface; (3) to ascertain lunar surface mechanical properties through manipulations of the soil mechanics/surface sampler; (4) to determine the chemical elements and their relative abundance on the lunar surface, utilizing the alpha scattering instrument; and (5) to obtain data on radar reflectivity, thermal characteristics, touchdown dynamics, magnetic properties and other measurements of the lunar surface through use of spacecraft equipment.

Surveyor VII met all of its objectives. Liftoff occurred at 06:30:00.545 GMT on January 7, 1968. Spacecraft performance was normal, including execution of the planned midcourse correction. Accuracy of this correction was precise enough to eliminate the necessity of performing a planned second midcourse correction. A completely successful soft landing was achieved, with the spacecraft performing very close to predicted parameters throughout the descent. Touchdown occurred at 01:05:37.61 GMT on January 10, 1968. The spacecraft soft-landed on the ejecta or flow blanket of the crater Tycho, at 40.92°S

latitude and 11.45°W longitude, approximately 1.7 km (1.1 miles) from the desired landing site.

After landing, the spacecraft performed extensive operations, including the acquisition of an abundance of useful alpha scattering data and a wide variety of good-quality television pictures (over 21,000 were received before camera shutdown after sunset of the first lunar day). Other scientific and engineering tests and experiments were also successfully performed.

The spacecraft survived the lunar night and again responded to commands to provide additional television pictures and other data on the second lunar day.

A. Spacecraft System

In the *Surveyor* spacecraft design, the primary objective was to maximize the probability of successful spacecraft operation within the basic limitations imposed by launch vehicle capabilities, the extent of knowledge of transit and lunar environments, and the current technological state of the art. In keeping with this primary objective, design policies were established which (1) minimized spacecraft complexity by placing responsibility for mission control and decision-making on earth-based

equipment and personnel wherever possible, (2) provided for the capability of transmitting a large number of different data channels from the spacecraft, (3) provided for spacecraft control by means of a large number of individual commands from earth, and (4) made all subsystems as autonomous as practicable.

Figure IV-1 illustrates the *Surveyor* spacecraft in the cruise mode and identifies many of the major components. A simplified functional block diagram of the

spacecraft system is shown in Fig. IV-2. The spacecraft design is discussed briefly in this section and in greater detail in the subsystem sections which follow. A detailed configuration drawing of the spacecraft is contained in Appendix B.

1. Spacecraft Coordinate System

The spacecraft coordinate system is an orthogonal, right-handed Cartesian system. It is shown in Fig. IV-1

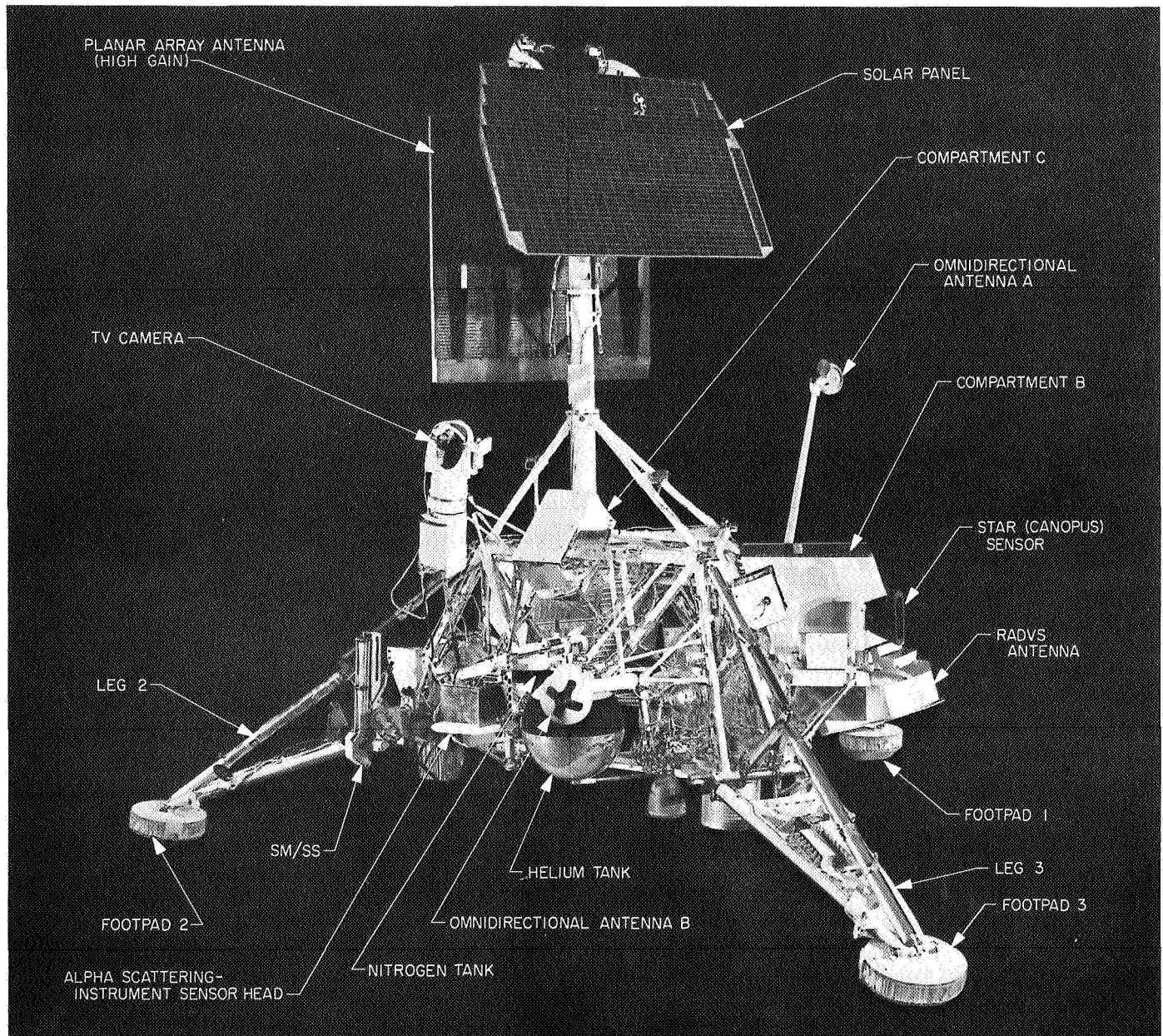


Fig. IV-1. *Surveyor* spacecraft (SC-7) in cruise mode

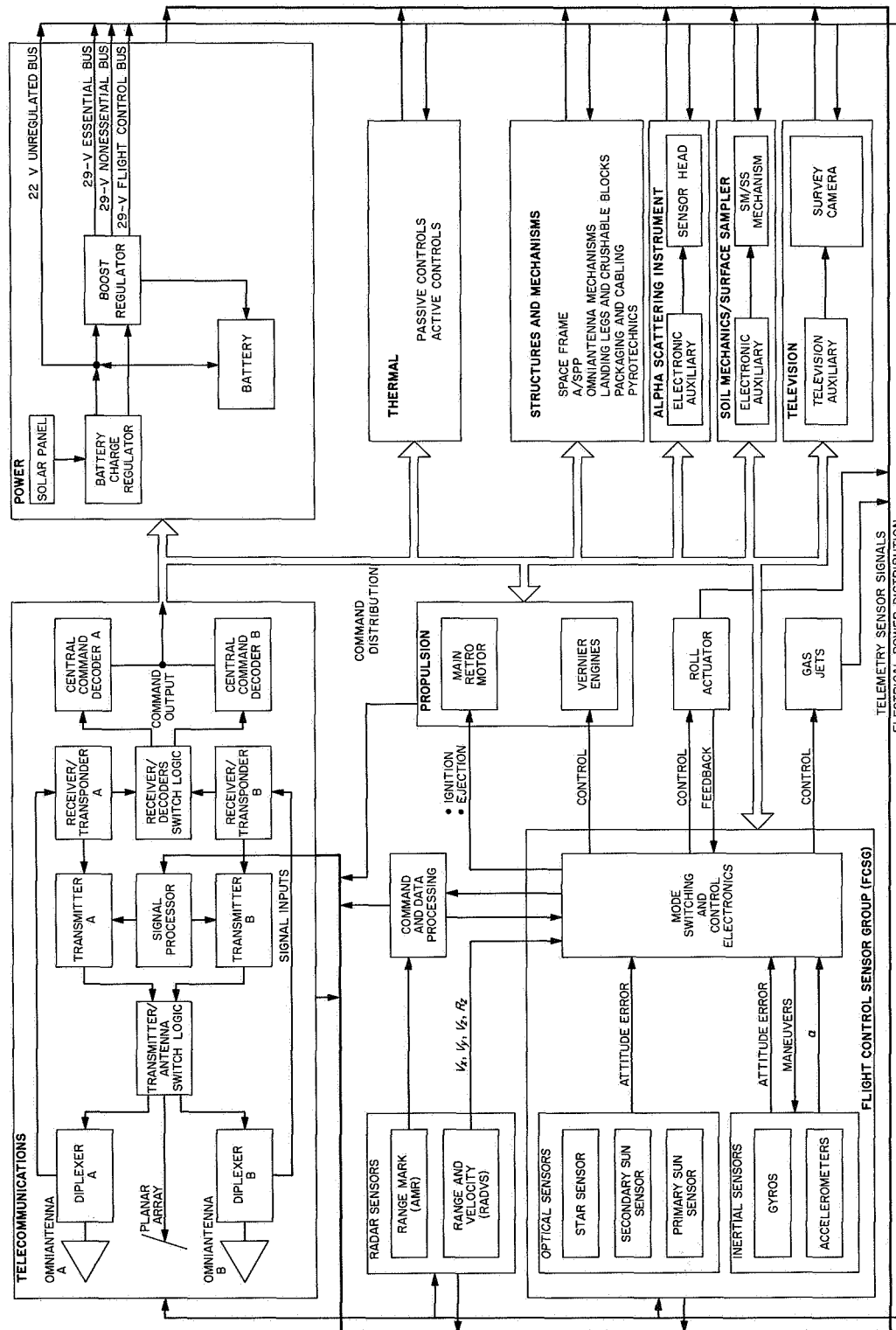


Fig. IV-2. Simplified spacecraft functional block diagram (SC-7)

as related to the physical configuration of the spacecraft. During normal cruise flight, the minus Z axis points in the direction of the sun, the minus X axis is aligned with the star Canopus, and Leg 1 lies in the Y-Z plane.

Vernier engine thrusting during the midcourse correction maneuver occurs along the minus Z axis, which has been pointed in some computer-optimized, trajectory-correcting direction.

Retro motor thrusting occurs during the terminal descent maneuver along the minus Z axis, which has been pointed in opposition to the spacecraft's velocity vector at time of ignition.

Reference directions for the spacecraft motions about the orthogonal axes prior to thrusting during these maneuvers are also shown in Fig. IV-1.

2. Spacecraft Mass Properties

The *Surveyor VII* spacecraft weighed 2289.2 lb at separation of the spacecraft from the *Centaur* and 674 lb at touchdown. To obtain stability over a wide range of conditions based upon landing site assumptions and the approach angle requirement, the center of gravity is located low on the spaceframe and its permissible shift constrained by the attitude-stabilization capabilities of the flight control and vernier engine subsystems during retrorocket burning and ejection and vernier-controlled terminal descent.

3. Vehicle Structures and Mechanisms

The vehicle structures and mechanisms subsystem provides support, alignment, thermal protection, electrical interconnection, mechanical actuation, and touchdown stabilization for the spacecraft. The subsystem consists of the basic spaceframe, landing gear, crushable blocks, omnidirectional antenna mechanisms, antenna/solar panel positioner (A/SPP), pyrotechnic devices, electrical cabling, thermal compartments, and separation sensing and arming devices.

The spaceframe is the basic structure of the spacecraft and provides a rigid mount for all components of the spacecraft and mounting surfaces and attachments for connecting to the *Centaur*. The tripodic landing gear and crushable blocks stabilize the spacecraft and absorb impact energy during touchdown. The omnidirectional antenna mechanisms provide for omniantenna deployment. The A/SPP supports and positions (around four

independent axes) the planar array antenna and solar panel. The pyrotechnic devices mechanically actuate mechanisms, switches, and valves. The electrical cabling interconnects the spacecraft subsystems and components. The thermal compartments provide thermal control for temperature-sensitive components. The separation-sensing and arming devices insure that certain critical squib-firing circuits will remain disabled until after *Centaur* separation.

4. Thermal Control

Thermal control of equipment over the extreme temperature range of the lunar surface (+260 to -250°F) is accomplished by techniques representing the latest state of the art in the design of lightweight spacecraft. Included are "passive" controls such as superinsulation of electronic compartments and special surface finishes to achieve optimum absorption and emission characteristics, "active" heater systems, and "semiactive" thermal switches.

5. Electrical Power

Surveyor VII utilized the same high-efficiency electrical power subsystem as that incorporated on *Surveyors V* and *VI*. Electrical power for the spacecraft is supplied by a solar panel and a sealed, rechargeable silver-zinc battery. Power regulation and distribution are provided by a battery charge regulator (BCR) and a boost regulator (BR). The BCR provides solar panel switching functions and battery charge control. The battery is connected to the unregulated bus, which distributes power to spacecraft loads not requiring regulation. The unregulated bus voltage is converted by the BR to supply spacecraft loads requiring regulated power. The BR contains: (1) a preregulator that provides power for the spacecraft "essential" loads, (2) an overload trip circuit regulator that controls power for "nonessential" loads, (3) a flight control regulator that provides power for flight control loads, and (4) a shunt regulator that converts excess solar panel power for battery charging. The solar panel can be connected either to the unregulated bus or directly to the preregulator output bus, in which mode the power system operates most efficiently.

6. Propulsion

The propulsion subsystem consists of three bipropellant vernier engines and associated hardware and a single solid-propellant retrorocket motor. The purpose of the propulsion system is to provide the spacecraft with a trajectory-correcting force vector during the midcourse

correction maneuver and a velocity-retarding force vector during terminal descent to the lunar surface. The propulsion subsystem performs these functions in response to flight control subsystem preprogrammed sequences, initiated by DSIF station command, and sensor outputs.

The three vernier engines also provide attitude stabilization during main retrorocket burning and attitude and velocity vector control during the remainder of terminal descent after the retro motor is ejected. Vernier Engine 1 can be swiveled to provide a thrust vector component about the roll axis. Engines 2 and 3 are stationary and provide thrust parallel to the roll axis. The thrust of each engine can be differentially throttled over a range of 30 to 104 lb to provide attitude control in pitch and yaw.

The solid-propellant retro motor is utilized to remove the major portion of the spacecraft approach velocity during terminal descent. It has a partially submerged nozzle to minimize overall length. The motor provides a thrust of 8000 to 10,000 lb for a duration of about 41 sec.

7. Flight Control

The flight control subsystem provides for spacecraft attitude stability during transit and vernier engine control during midcourse correction and terminal descent. It includes the following spacecraft elements: flight control sensor group (FCSG), attitude control jets, attitude control gas supply, and Vernier Engine 1 roll actuator.

The FCSG contains inertial (gyros), optical (Canopus sensor, acquisition sun sensor, primary sun sensor), and acceleration sensors and flight control electronics. The outputs of these sensors and the radar subsystem are utilized by analog electronics to provide commands for operation of attitude gas jets and the spacecraft vernier and main retro propulsion systems. The flight control subsystem requires ground commands for the initiation and control of various functions.

The celestial sensors allow the spacecraft to be locked to a specific orientation defined by the vectors from the spacecraft to the sun and the star Canopus and the angle between them. Initial search for and acquisition of the sun is accomplished by the acquisition sun sensor. The primary sun sensor then maintains the orientation with the sun line.

Integrating gyros are used to maintain spacecraft orientation inertially during vernier or retro motor thrusting or when the celestial references are not available. Accelerometers measure the thrust levels of the

spacecraft propulsion system during midcourse correction and terminal descent phases.

A pair of attitude jets is located on each of the three legs of the spacecraft. The attitude jets provide for angular rate stabilization after spacecraft separation from the *Centaur*, attitude orientation for sun and Canopus acquisition, attitude control during coast phases, and attitude orientation for midcourse correction and terminal descent. The attitude control gas supply provides nitrogen under regulated pressure from a supply tank to the attitude jets.

The three vernier engines are controlled by the flight control subsystem signals to provide variable thrust over a wide range. Also, signals to the vernier roll actuator provide roll control by tilting the thrust axis of Vernier Engine 1 during thrust phases of flight.

8. Radar

Two radar systems are employed by the *Surveyor* spacecraft. An altitude marking radar (AMR) provides a *mark* signal to initiate the main retro sequence. In addition, a radar altimeter and doppler velocity sensor (RADVS) functions with the flight control subsystem to provide three-axis velocity, range, and altitude *mark* signals for flight control during the main retro and vernier phases of terminal descent. The RADVS consists of a doppler velocity sensor, which computes velocity along each of the spacecraft X, Y, and Z axes, and a radar altimeter, which computes slant range from 50,000 ft to 14 ft and generates *1000-ft mark* and *14-ft mark* signals.

9. Telecommunications

The spacecraft telecommunications subsystem provides for (1) receiving and processing commands from earth, (2) providing angle tracking and one- or two-way doppler data for orbit determination, and (3) processing and transmitting spacecraft telemetry data.

Continuous command capability is assured by two identical receivers, which remain on throughout the life of the spacecraft and operate in conjunction with two omniantennas and two command decoders. Logic circuits determine the interconnecting redundant arrangement used at any one time.

Operation of a receiver in conjunction with a transmitter through a transponder interconnection provides a

phase-coherent system for doppler tracking of the spacecraft during transit and after touchdown. Two identical transponder interconnections (Receiver/Transponder A and Receiver/Transponder B) are provided for redundancy. Transmitter B with Receiver/Transponder B is the transponder system normally operated during transit, but other combinations are commandable from earth.

Data signals from transducers located throughout the spacecraft are received and prepared for telemetry transmission by signal-processing equipment which performs commutation, analog-to-digital conversion, and pulse-code and amplitude-to-frequency modulation functions. Most of the data signals are divided into six groups (commutator modes) for commutation by two commutators located within the telecommunications signal processor. (An additional commutator is located within the television auxiliary for processing television frame identification data.) The content of each commutator mode has been selected to provide essential data during particular phases of the mission (refer to Table IV-1 and Appendix C). Other signals such as strain gage and gyro

speed data, which is required continuously over brief intervals, are applied directly to subcarrier oscillators.

Summing amplifiers are used to combine the output of any one commutator mode with continuous data. The composite signal from the signal processor, or television data from the television auxiliary, is sent over one of the two spacecraft transmitters. The commutators can be operated at five different rates (4400, 1100, 550, 137.5, and 17.2 bits/sec) and the transmitters at two different power levels (10 W or 100 mW). In addition, switching permits each of the transmitters to be operated at either the high- or low-power level with any one of the three spacecraft antennas (two omniantennas and a planar array). The planar array (high-gain antenna) is utilized for efficient transmission of wideband telemetry information.

Selection of data mode, data rate, transmitter power, and transmitter-antenna combination is made by earth command. A data rate is selected for each mission phase which will provide sufficient signal strength at the DSIF

Table IV-1. Surveyor VII spacecraft telemetry summary

Data mode or type	Method of transmission	Data rate	Number of signals		Signals emphasized	Primary use
			Analog	Digital		
1	PCM/FM/PM	All	42	40	Flight control, propulsion	Canopus acquisition midcourse maneuver
2	PCM/FM/PM	All	80	59	Flight control, propulsion, AMR, RADVS	Transit interrogations, backup for main retro phase
3	PCM/FM/PM	All	21	40	Inertial guidance, AMR, RADVS, vernier engines	Backup for vernier descent phase
4	PCM/FM/PM	All	75	29	Temperatures, power status, telecommunications	Transit interrogations, lunar operations
5	PCM/FM/PM	All	108	50	Flight control, power status, temperature	Midcourse and terminal attitude maneuvers, launch and primary cruise data, lunar interrogations
6	PCM/FM/PM	All	47	74	Flight control, power status, AMR, RADVS, vernier engine conditions	Terminal descent thrust phase
7	PCM/FM	4400 bits/sec	13		TV survey camera	TV camera interrogation, TV camera operation
Strain gages	FM/PM	Continuous analog	3		Strain gages	Touchdown force on spacecraft legs
Gyro speed	FM/PM	50 Hz continuous	3		Inertial guidance unit	Verify gyro sync

station to maintain the telemetry error rate within satisfactory limits.

10. Television

The television subsystem includes a survey camera and a television auxiliary for final decoding of commands and processing of video and frame identification data for transmission by either of the spacecraft transmitters.

The survey camera is designed to provide photographs of the lunar surface panorama, portions of the spacecraft, and the lunar sky. Photographs may be obtained in either of two modes: a 200-line mode for relatively slow (61.8 sec/frame) transmission over an omniantenna or a 600-line mode for a more efficient and rapid (3.6 sec/frame) transmission over the planar array.

Except for additional black thermal paint on the inside of the mirror assembly hood to better protect the mirror mounted in the camera turret from stray light reflections, the camera is the same as that carried aboard *Surveyor VI*. The vidicon picture tube axis subtends an angle of about 16 deg with the spacecraft Z axis. The vidicon tube is pointed upward toward a mirror mounted in the camera hood. The mirror together with the hood can be rotated 370 deg, and the mirror can be tilted in steps for horizontal and vertical scanning, respectively. Special auxiliary viewing mirrors are mounted on the spacecraft frame to provide picture acquisition of areas of interest under the spacecraft. *Surveyor VII* also was equipped with a stereo viewing mirror to permit viewing of the same area from a different angle and several small dust particle mirrors to show the amount of adhering dust as a result of touchdown or posttouchdown firing of the vernier engines.

The camera can be focused over a range from 4 ft to infinity and can be "zoomed" to obtain photos in narrow-angle (6.4 deg) or wide-angle (25.4 deg) field of view. A lens iris provides a stop range from $f/4$ to $f/22$. The camera is equipped with a focal plane shutter which normally provides an exposure time of 150 msec but can be commanded to remain open for time exposures. A sensing device, attached to the shutter, will keep it shut if the light level is too strong. The same device automatically controls the iris setting. This device can be overridden by command from earth. On the *Surveyor VI* and *VII* cameras, a filter wheel assembly between the lens and mirror contained one clear and three polarized filters.

11. Alpha Scattering Instrument

An alpha scattering instrument (ASI) was included in the spacecraft system for the *Surveyor VII* mission. This instrument contains a radioactive source of alpha particles, the interaction of which with the lunar surface material produces back-scattering of alpha and proton particles. Detectors are used to determine the characteristics of the back-scattering from which the relative abundance of chemical elements can be determined. The instrument consists of a sensor head, a deployment mechanism, and associated electronics contained in a thermally insulated compartment. During transit to the moon, the sensor head is held in a stowed position, where it is in contact with a standard sample. Following an initial calibration period after landing, the sensor head is deployed—first to a position above the lunar surface where it obtains data on background radiation, and then to a position where it rests on the lunar surface to obtain lunar back-scattering data. An electronics auxiliary provides command decoding, signal processing, power management, and the interface with the rest of the spacecraft.

12. Soil Mechanics/Surface Sampler (SM/SS)

The SM/SS instrument carried on *Surveyor VII* consists of an electromechanical mechanism (lazy tongs and scoop) and an electronics auxiliary with the necessary supporting structure and interconnecting wire harnesses. The mechanism is actuated by ground command to pick, scrape, dig, or trench the lunar surface. The scoop can be extended 64 in. from its stowed position, moved 54 deg vertically and 112 deg radially by means of the lazy tongs. The results of SM/SS operations are obtained primarily through TV pictures. The only telemetry data obtained on the instrument itself are current measurements of the four drive motors. From these measurements, approximate force information can be derived.

Surveyor VII carried an SM/SS functionally identical to that carried by *Surveyors III* and *IV*. Its mounting to the spaceframe, however, was rotated 30 deg in the direction of Pad 3, to permit handling of the alpha scattering sensor head. Two horseshoe magnets were recessed into the back side of the door on the scoop.

13. Engineering Instrumentation

Transducers are located throughout the spacecraft system primarily to provide performance data that is sent to the DSIF stations by the telecommunication subsystem. Some of the transducers also provide data useful in

Table IV-2. Surveyor engineering instrumentation

Measurement	Subsystem location									
	Structures, mechanisms, and thermal control	Electrical power	Propulsion	Flight control	Radar	Telecommunications		ASI and SM/SS	TV	Total
						Signal processing	Radio and command decoding			
Temperature	29	4	18	9	6		2	5	4	77
Pressure		1	3	1						5
Position (potentiometers)	7								6	13
Position (switches)	11	2		35	15	4	8		4	79
Current		13						1		14
Voltage		5		14	7		6	4		36
Strain	3		3							6
Acceleration				1						1
Gyro speed				3						3
Power (RF)							2			2
Optical				9						9
Calibration				1		10			1	12
Totals	50	25	24	73	28	14	18	10	15	257

deriving knowledge of certain characteristics of the lunar surface. In most cases the transducers and associated signal conditioning are a physically integral part of the subsystem whose performance is being monitored. All the instrumentation signals provided for the *Surveyor VII* spacecraft are summarized in Table IV-2.

All of the temperature transducers are resistance-type units, except for two microdiode bridge amplifier assemblies used in the television subsystem. The voltage and position measurements consist mainly of signals from the command and control circuits. A strain gage is mounted on each of the vernier engine brackets to measure thrust and on each of the three landing leg shock absorbers to monitor touchdown dynamics.

The flight control accelerometer is mounted on the retromotor case to verify motor ignition and provide gross retromotor performance data.

Additional discussion of instrumentation is included with the individual subsystem descriptions.

14. Design Changes

Table IV-3 presents a summary of notable differences in design between the *Surveyor VI* and *VII* spacecraft.

15. Spacecraft Reliability

The prelaunch reliability estimate presented at the consent-to-launch meeting for the *Surveyor VII* spacecraft was 0.65 at 50% confidence level and assuming successful injection. The *Surveyor VII* spacecraft system reliability estimates vs systems test experience are shown graphically in Fig. IV-3. Table IV-4 lists the reliability estimates for SC-7 as presented at the consent-to-launch meetings. Table IV-5 sets forth the final reliability figures for SC-7. For comparison purposes, SC-1 through SC-6 quantities are also given in the figure and both tables. The primary source of data for these reliability estimates is the time and cycle information experienced by the spacecraft control items during systems tests. Tests and flight data from previous spacecraft was included in reliability predictions for subsequent spacecraft if there were no significant control item design differences.

The principal cause of the predicted drop in reliability for SC-7 resulted from an anomaly which occurred during the preparation for a solar-thermal-vacuum exposure test. Application by the ground support equipment of gyro preheat power produced a greater than full-scale (pegged) reading on the 3-A ammeter monitoring gyro preheat current. Extensive troubleshooting and analyses

Table IV-3. Notable differences between Surveyors VI and VII: changes incorporated on Surveyor VII

Item	Description
Soil mechanics/surface sampler	The SM/SS was functionally identical to those mounted on <i>Surveyors III</i> and <i>IV</i> , but modified to contain two horseshoe magnets which were recessed into the back side of the door of the scoop. Mounting to the spacecraft frame was rotated 30 deg, in the direction of footpad 3, to permit handling of the alpha scattering sensor head after its deployment
Dust mirrors	Seven special 0.5-in. hexagonal mirrors were mounted at specified locations to detect adhering lunar dust dispersed during touchdown or posttouchdown vernier engine firing
Special viewing mirror	A special viewing mirror was mounted on the lower portion of the A/SPP mast to obtain stereoscopic photographs of a portion of the lunar surface within the SM/SS operational area
Television camera	Black paint was applied to certain internal surfaces of the mirror assembly hood to prevent excessive glare
Footpad magnet	A magnet/control-bar assembly was mounted to Leg 3 footpad in addition to the one on Leg 2 footpad
Thermal control and heater assembly (TC&HA)	The Compartment A TC&HA was changed to one whose set point was 20°F instead of 50°F to improve lunar night survivability
Vernier propulsion	Vernier engines containing helium filters were installed. The filters minimize contamination of the solenoid-operated valves
Photo chart	A photometric chart was installed on Omnantenna A
Retro motor	A higher-impulse retro motor was used

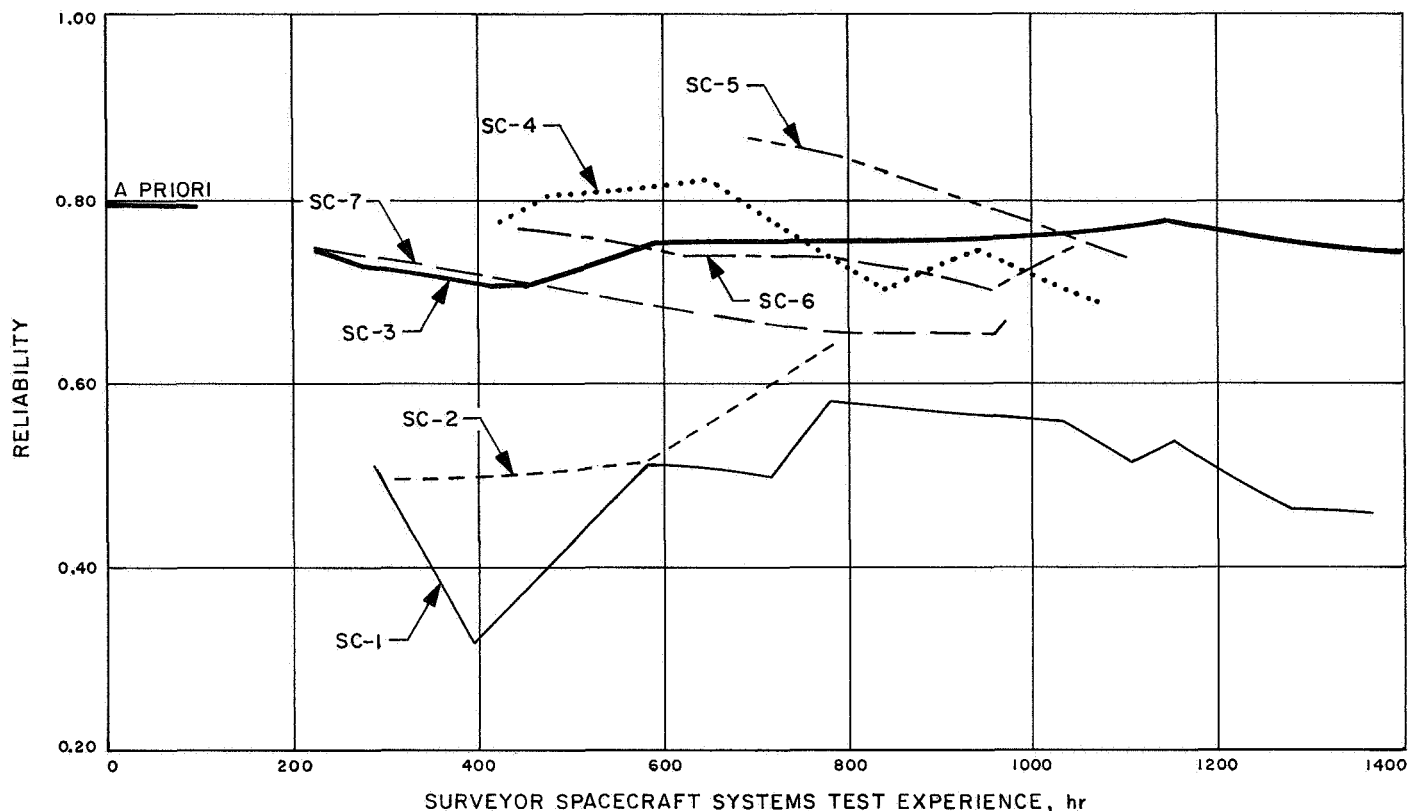


Fig. IV-3. Surveyor spacecraft system reliability estimates

on both the spacecraft and test equipment failed to uncover the source of the problem. Efforts to duplicate the problem also failed.

16. Functional Description of Spacecraft Automatic Flight Sequences

The *Surveyor* spacecraft system has been designed for automatic operation in the following flight sequences:

a. Solar panel deployment and sun acquisition. Immediately upon separation from the *Centaur*, the spacecraft automatically deploys the solar panel to the transit position in a two-step sequence. First, the solar panel axis of the A/SPP is unlocked and the solar panel is rotated 85 deg from the stowed position to an orientation normal to the spacecraft Z axis. When this position is reached, the solar panel axis is locked and the roll axis is unlocked. The antenna/solar panel combination is then rotated 60 deg about the roll axis and finally locked in the transit position.

Also upon separation from the *Centaur*, the angular rates of motion about the spacecraft's three axes are

sensed by the gyros, which then automatically control the actuation of the cold gas jets in nulling these rates to within deadband limits of ± 0.1 deg/sec. This rate-nulling is allowed 51 sec, after which time the sun acquisition sequence is initiated. First, a minus-roll maneuver is started that permits the sun to be acquired by the acquisition sun sensor, which has a 10-deg-wide by 196-deg-fan-shaped field of view centered about the spacecraft minus X axis. Upon initial sun acquisition, the roll is stopped and a positive yaw maneuver is initiated to permit the narrow-angle field-of-view primary sun sensor to acquire and lock onto the sun. A secondary sun sensor is mounted on the solar panel to provide a means for sun acquisition by DSS command if the automatic sequence fails and to aid posttouchdown lunar operations in solar panel positioning.

Upon completion of the solar panel deployment and sun acquisition sequences, the spacecraft coasts with its roll axis (and the active face of the solar panel) held positioned toward the sun by maintaining the sun within the field of view of the center cell of the primary sun sensor. The other axes are held inertially fixed by means of the roll gyro.

Table IV-4. Surveyor spacecraft subsystem and system reliability estimates as presented at consent-to-launch meetings

	Spacecraft						
	SC-1	SC-2	SC-3	SC-4	SC-5	SC-6	SC-7
Subsystem							
Telecommunications	0.926	0.941	0.965	0.920	0.987	0.989	0.991
Vehicle and mechanisms	0.816	0.865	0.905	0.910	0.850	0.820	0.884
Propulsion	0.991	0.991	0.967	0.945	0.945	0.934	0.928
Electrical power	0.870	0.938	0.932	0.952	0.985	0.986	0.975
Flight controls	0.953	0.930	0.970	0.937	0.944	0.939	0.921
Systems interaction factor	0.737	0.930	0.959	0.964	~1.000	~1.000	0.895
Overall spacecraft system	0.457	0.655	0.732	0.681	0.738	0.702	0.655

Table IV-5. Final reliability figures for Surveyor subsystems and systems (includes all applicable data)

	Spacecraft						
	SC-1	SC-2	SC-3	SC-4	SC-5	SC-6	SC-7
Subsystem							
Telecommunications	0.925	0.944	0.965	0.929	0.987	0.991	0.992
Vehicle and mechanisms	0.816	0.868	0.907	0.854	0.853	0.880	0.899
Propulsion	0.991	0.991	0.968	0.947	0.934	0.927	0.927
Electrical power	0.869	0.958	0.935	0.953	0.985	0.988	0.977
Flight controls	0.952	0.889	0.971	0.931	0.945	0.940	0.922
Systems interaction factor	0.736	0.949	0.967	0.978	0.986	1.000	0.904
Overall spacecraft system	0.456	0.658	0.745	0.653	0.722	0.751	0.674

b. Canopus acquisition. Some time after sun acquisition, a roll maneuver is initiated by DSS command for star mapping and Canopus acquisition. As the spacecraft rolls about its Z axis, the Canopus sensor provides intensity signals of objects which pass through its field of view and have intensities within the sensitivity range of the sensor. Comparing a map constructed from these signals and a map based on predictions permits identification of Canopus from among the other signals. After sufficient spacecraft roll to permit Canopus identification, automatic Canopus acquisition is normally commanded by the DSS to permit the spacecraft to lock on Canopus automatically the next time Canopus passes through the sensor field of view. Canopus acquisition together with sun lock establishes the three-axis attitude reference upon which the midcourse and terminal maneuvers are based.

c. Midcourse velocity correction. The spacecraft executes each of the required trajectory-correcting attitude maneuvers (roll, pitch, or yaw) computed at the Space Flight Operations Facility (SFOF) and commanded via a Deep Space Station. The spacecraft automatically terminates each maneuver when the magnitude of the maneuver (previously transmitted by DSS command and stored in the flight control programmer) has been accomplished. Each maneuver (roll, pitch, or yaw) must be accomplished serially since the flight control programmer can store only one magnitude at a time and can only apply it to rotation about one axis at a time.

The magnitude of the vernier engines thrust time for required velocity correction is also transmitted to the

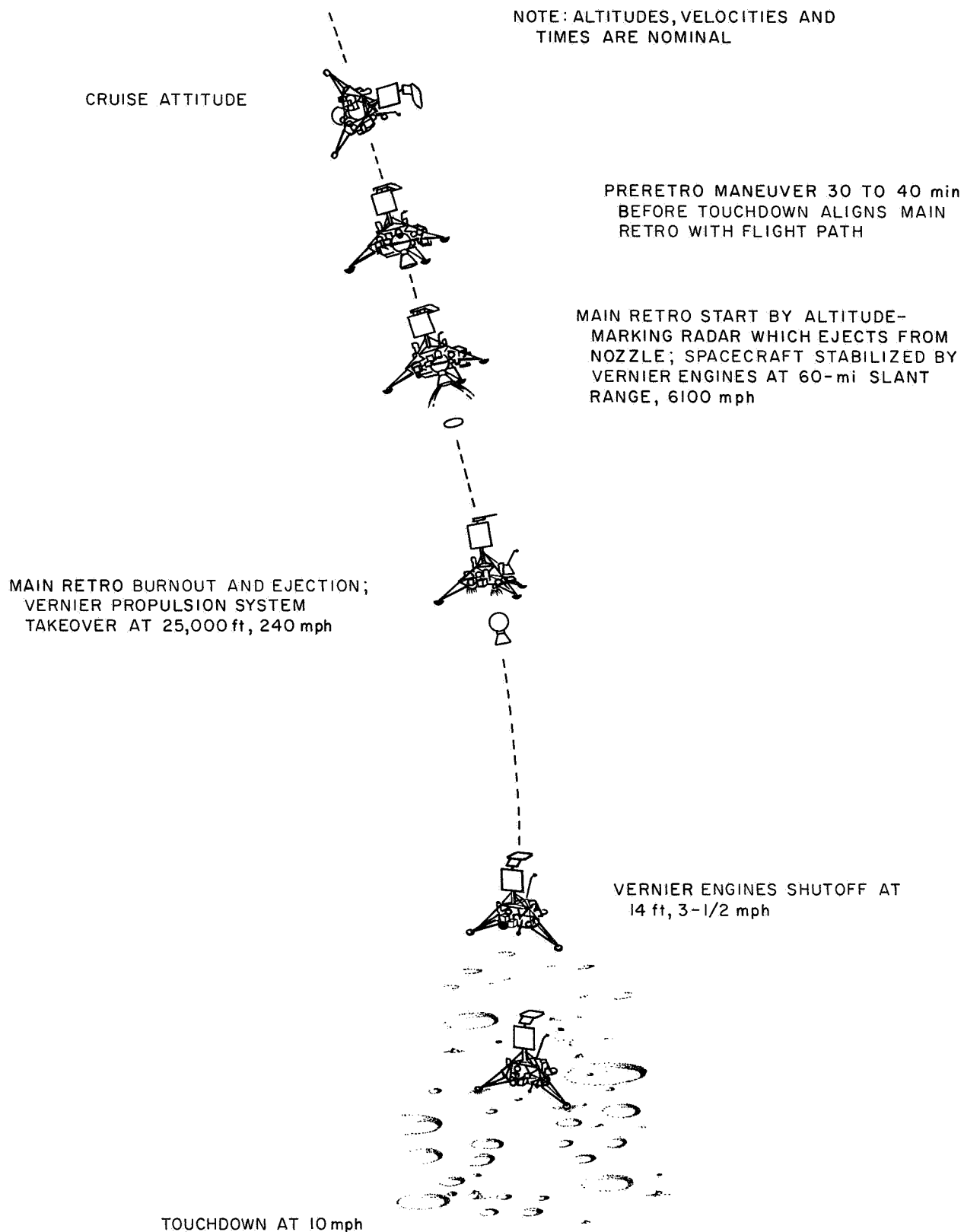


Fig. IV-4. Terminal descent nominal events

spacecraft, verified, and stored by the flight control subsystem. During the thrusting phase, the three vernier engines provide a constant spacecraft acceleration of about 0.1 earth g until cutoff, which occurs automatically when the stored magnitude of thrust time has been accomplished. Also during thrusting, the vernier engines are differentially throttled, and the roll actuator is controlled in order to maintain attitude stabilization.

d. Terminal descent sequence. Terminal descent begins with the spacecraft executing, by DSIF command, certain SFOF computer-required maneuvers (roll, pitch, or yaw) (Fig. IV-4) such that (1) the expected direction of the retro motor's thrust vector will be aligned in opposition to the spacecraft velocity vector, (2) the spacecraft roll attitude will provide the most desirable landed orientation for lunar operations, and (3) RADVS and telecommunications descent constraints are not violated. Following completion of the attitude maneuvers, the AMR is activated. It has been preset to generate a *mark* signal when the slant range to the lunar surface is 60 ± 1 miles. A backup signal, delayed a short interval after the AMR *mark* should occur, is transmitted from the DSIF station to the spacecraft in the event the AMR *mark* is not generated. The ignition of the vernier engines and the ignition of the retro motor, a fixed 1.1 sec later, are delayed from the AMR *mark* by some SFOF computer-optimized amount which had been transmitted to and stored by the spacecraft after the completion of the attitude orientation maneuvers.

During the firing of the retro motor (Fig. IV-5), the spacecraft attitude is inertially stabilized by differentially throttling the vernier engines while maintaining their total thrust at either a 150- or 200-lb level. The retro motor burns at essentially constant thrust (8000 to 10,000 lb) for about 40 sec, after which the thrust starts to decay. This tailoff (decay) is detected by an inertia switch which increases the total thrust of the vernier engines to the high level (312 lb) and initiates, after a time delay of about 12 sec, ejection of the expended retro motor. At this point the spacecraft lunar-related velocity is less than 10% (100 to 700 ft/sec) of its preretro-motor-ignition value. Its lunar altitude ranges between 10,000 and 50,000 ft.

About 2 sec after separation of the retro motor, the thrust of the vernier engines is reduced and controlled to produce a constant spacecraft acceleration toward the lunar surface of 0.1 lunar g , as measured by the Z-axis-oriented accelerometer. The spacecraft attitude remains inertially stabilized until the doppler velocity sensor locks onto the lunar surface. The composite thrust axis of the vernier engines is then aligned and maintained in opposition to the spacecraft velocity vector as computed by the RADVS. Under these conditions, the spacecraft performs a "gravity turn" such that the vernier engine composite thrust vector, the spacecraft plus Z axis and the spacecraft velocity vector come into coincidence with the local lunar gravity vector.

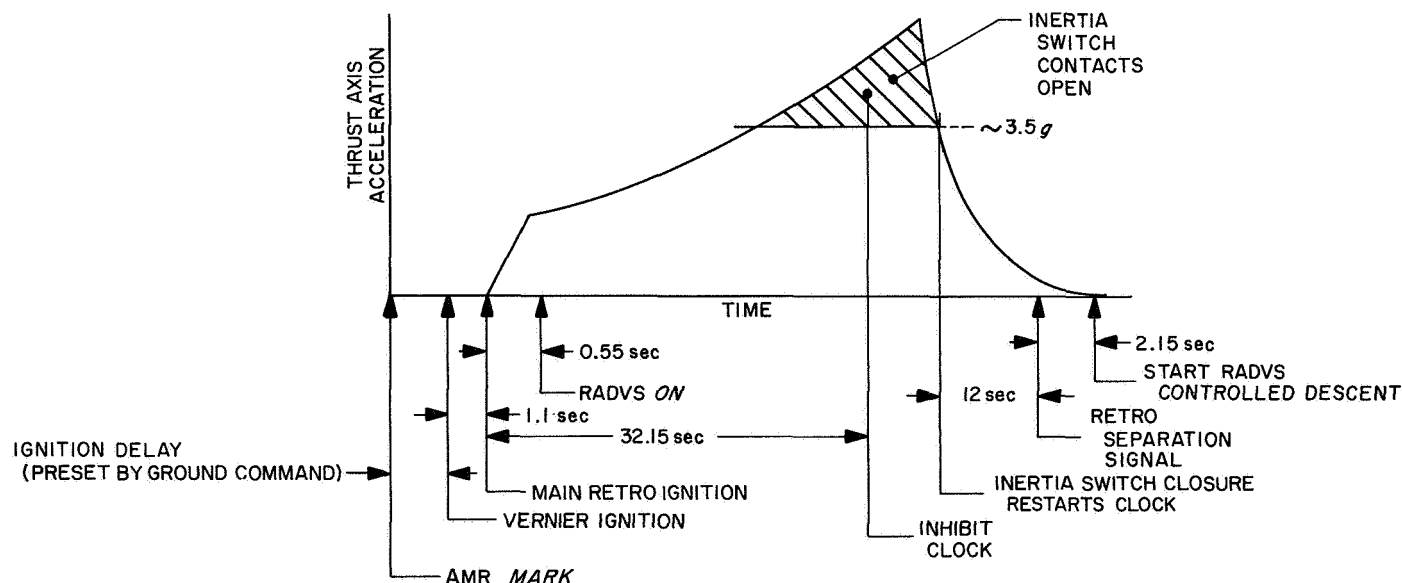


Fig. IV-5. Main retro burn profile (typical)

The vehicle accelerates at 0.1 lunar g until the radars determine that the "descent contour" has been reached (Fig. IV-6). This contour corresponds, in the vertical case, to descent at a constant deceleration. The vernier thrust is controlled such that the vehicle follows the descent contour until shortly before touchdown, when a constant-velocity (5-ft/sec) descent is programmed from 40 to 14 ft. At this point, a 14-ft mark is generated by the RADVS which turns off the engines, resulting in a free-fall acceleration to, and touchdown at, approximately 13 ft/sec.

RADVS operational limitations constrain the retro motor burnout conditions. Nonlinear operation of the doppler velocity sensor for slant ranges above 50,000 ft and velocities above 700 ft/sec requires that retro motor

burnout be constrained accordingly. The altimeter upper limit is between 30,000 and 40,000 ft, depending on velocity. These constraints are illustrated in the range-velocity plane of Fig. IV-6.

The allowable retro motor burnout region is further restricted by the maximum thrust capability of the vernier engine system. To accurately control the final descent, the minimum thrust must be less than the least possible landed weight (lunar gravity) of the vehicle. The result is a minimum thrust of 90 lb. This in turn constrains the maximum vernier thrust to 312 lb because of the limited range of throttle control possible.

Descent at the maximum thrust to touchdown defines a curve in the range-velocity plane below which retro motor burnout cannot be allowed to occur. Actually, since the vernier engines are also used for attitude stabilization by differential thrust control, it is necessary to allow some margin from the maximum thrust level. Furthermore, since it is more convenient to sense deceleration than thrust, the vernier-engine-controlled portion (following retro motor ejection) of terminal descent is performed at nearly constant deceleration rather than at constant thrust. Therefore, maximum thrust is only utilized at the start of the vernier-engine-controlled portion of terminal descent.

The maximum spacecraft deceleration defines a parabola in the range-velocity plane. For vertical descents at least, this curve defines the minimum altitude (range) at which retro motor burnout is permitted to occur in order to achieve a soft landing. This parabola is indicated in Fig. IV-6. (For ease of spacecraft mechanization, the parabola is approximated by a descent contour consisting of straight-line segments.)

Retro motor burnout must occur sufficiently above the descent contour to allow time to align the thrust axis with the velocity vector before the trajectory intersects the contour. Thus a "nominal burnout locus" (also shown in Fig. IV-6) is established which allows for altitude dispersions plus an alignment time, which depends on the maximum angle between the flight path and roll (Z) axis at burnout. The allowable burnout region having been defined, the size of the retro motor and ignition altitude are determined such that burnout will occur within that region.

In order to establish the maximum propellant requirements for the vernier system, it is necessary to consider dispersions in retro motor burnout conditions as well as

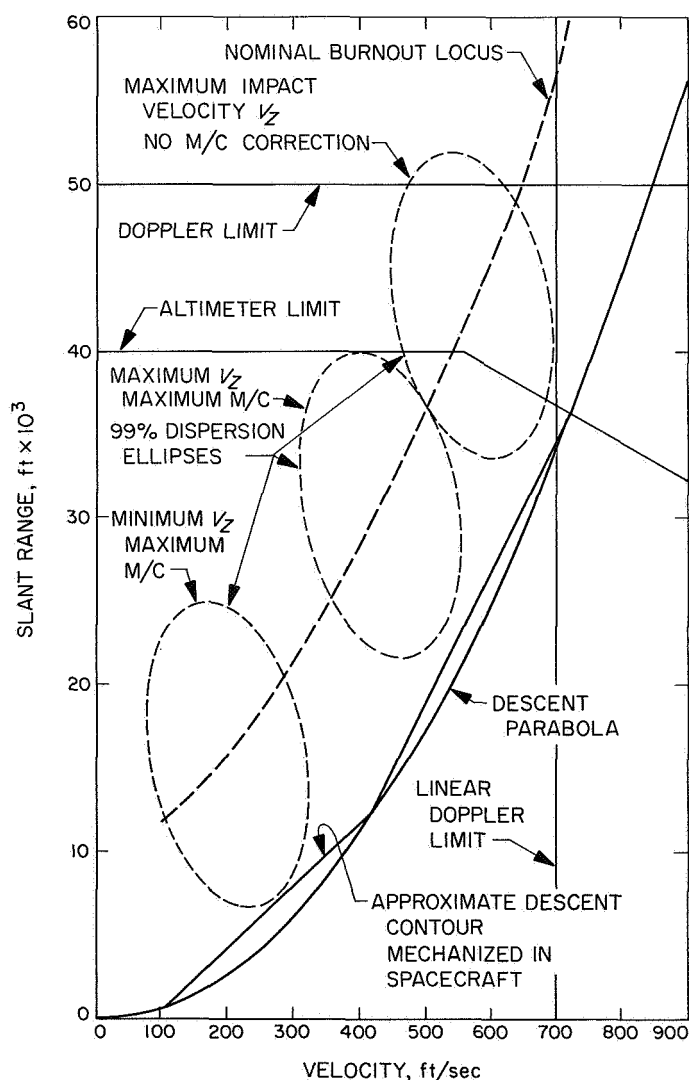


Fig. IV-6. Range-velocity "descent contour"

midcourse maneuver fuel expenditures. The principal sources of retro motor burnout velocity dispersion are the imperfect alignment of the vehicle prior to retro motor ignition and the variability of the total impulse. In the case of a vertical descent, these variations cause dispersions of the type shown in Fig. IV-6, where the ellipses define a region within which burnout will occur with probability 0.99. The design chosen provides enough fuel so that, given a maximum midcourse correction, the probability of running out of fuel is less than 0.01.

The spacecraft landing gear is designed to withstand a horizontal component of the landing velocity as well as the vertical component. The horizontal component of the landing velocity is zero in the case of perfect control. However, dispersions arise primarily because of the following two factors:

- (1) Measurement error in the doppler system resulting in a velocity error normal to the thrust axis.
- (2) Nonvertical attitude due to (a) termination of the "gravity turn" at a finite velocity, and (b) attitude control system noise sources.

Since the attitude at the beginning of the constant-velocity portion of the terminal descent (40 to 14 ft) is under inertial control (rather than RADVS control), these errors give rise to a significant horizontal component of velocity at touchdown.

17. Spacecraft System Performance

A summary of *Surveyor VII* spacecraft system performance is presented below by mission phases. Also refer to Sections IV-B through IV-K for spacecraft subsystem performance; Section VI-C presents a chronology of mission operations.

a. Countdown and launch phase performance. *Surveyor VII* performed flawlessly during an extended prelaunch countdown. Though originally scheduled for launch at 05:55 GMT, a delay of 35 min was authorized early in the countdown in order to improve downrange tracking coverage.

Liftoff occurred at 06:30:00.545 GMT on January 7, 1968, with the spacecraft in the standard launch configuration (transmitter low power on, legs and omniantennas folded, solar panel and planar array stowed and locked, etc.).

During the boost-through-separation phase of launch, the *Surveyor VII* spacecraft was subjected to acoustically and mechanically induced random vibrations, linear accelerations associated with transient responses to flight events (pitch, roll, and yaw) of the launch vehicle and shock spectra associated with squib firing. The *Surveyor VII* interface vibration instrumentation consisted of three high-frequency accelerometers located on the *Centaur*/spacecraft adapter immediately below the spacecraft attachment points. One accelerometer was oriented in a longitudinal direction (parallel to the spacecraft Z axis) at the Leg 3 attachment point and the other in the radial direction (perpendicular to the Z axis) at the Leg 1 attachment point. The third accelerometer, not included on previous missions, was mounted in the same direction as the radial accelerometer, but 90 deg counterclockwise from it looking aft, to provide tangential vibration data at the spacecraft attachment ring. The dynamic environment as indicated by the accelerometers was as anticipated. The radial and longitudinal accelerometer data is depicted in Table IV-6.

The spacecraft properly executed all preseparation events initiated by the *Centaur* programmer, including extending the landing legs, deploying the omniantennas, and switching Transmitter B to high power. Spacecraft separation from the *Centaur* was also accomplished in a normal manner.

b. Postseparation through star acquisition performance. The automatic solar panel deployment and A/SPP roll-axis rotation sequence was initiated by *Centaur*/spacecraft separation and occurred normally. The solar panel was unlocked and required about 325 sec to step through 85 deg and lock in its transit position. Upon locking of the solar panel, the A/SPP roll axis was unlocked; about 230 sec was required for the A/SPP to step +60 deg and lock in its transit position.

Centaur/spacecraft separation also enabled the attitude control subsystem cold gas jets. The small angular rates which had been imparted to the spacecraft upon separation from the *Centaur* were nulled by the attitude control system in less than 46 sec. After the 51-sec built-in time delay from electrical disconnection from the *Centaur*, the sun acquisition sequence was initiated beginning with a negative roll turn through 224 deg. This turn was automatically terminated upon illumination of the acquisition sun sensor. Then followed a positive yaw turn through 37 deg, resulting in the illumination of the primary sun sensor center cell and termination of the sun acquisition sequence.

**Table IV-6. Boost phase accelerations:
Surveyor VII vs Surveyor VI**

Event	Accelerometer output (0-to-peak g unless noted)			
	Radial accelerometer		Longitudinal accelerometer	
	Surveyor VI	Surveyor VII	Surveyor VI	Surveyor VII
Liftoff	2.26 rms	1.80 rms	1.21 rms	1.04 rms
Maximum aerodynamic loading	0.71 rms	0.83 rms	0.55 rms	0.62 rms
BECO	1.4	<1.0	4.5	3.6
Insulation panel jettison	>10	>10	>10	>10
Nose fairing separation	2.5	5.1	4.1	>10
SECO	1.5	<1.0	3.0	<1.0
Atlas/Centaur separation	>10	>10	>10	>10
MES 1	<1.0	<1.0	<1.0	<1.0
MECO 1	1.0	1.2	2.8	3.1
MES 2	<1.0	<1.0	<1.0	<1.0
MECO 2	2.7	2.3	4.5	4.1
Landing leg extension	7.0	N/A	>10	N/A
Landing leg lock	3.5	N/A	5.6	N/A
Omniantenna deployment	2.9	2.9	7.2	>10
N/A = not available.				

DSS 42 established two-way telecommunications at about $L + 58$ min, and an assessment of spacecraft telemetry indicated all systems to be normal. The spacecraft responded correctly to a sequence of earth commands which placed it in the cruise configuration, the transmitter operating in low-power at 1100 bits/sec.

The *cruise mode on* command was delayed from the scheduled time in the standard sequence of events by 2 min, 10 sec due to a high-intensity signal in the Canopus sensor (probably earth). This delay eliminated the possibility of locking on to this high-intensity signal, a condition which would have resulted in unnecessary cold gas expenditure and additional commanding to break the lock later in the flight.

Star mapping was command-initiated on schedule at approximately $L + 8$ hr. Canopus was easily identified

after rolling $+269$ deg. Other objects shown by the map included several lesser-magnitude stars, the earth, the moon, and the Milky Way.

Automatic Canopus lock-on (acquisition) did not occur as anticipated because the star's illumination intensity exceeded the upper threshold of the Canopus sensing circuit. As a result, it was necessary to command *sun mode on* from earth, which inhibited any further positive roll turning, and *manual lock on*, which forced the acquisition of this celestial reference. Subsequent analysis has not revealed any definitive cause for the lack of automatic acquisition of the star.

c. Midcourse (trajectory correction) maneuver performance. Because of the anticipated late selection of the exact landing site from several candidate sites under consideration, the launch vehicle was targeted to a compromise point with selenographic coordinates of 4.95°S and 3.88°E . The injection accuracy resulted in only a 77-km (48-mile) miss from the initial target. This fact, together with a final landing site selection of the Tycho ejecta blanket (40.87°S , 11.37°W) and other descent constraints, dictated two potential corrections at about $L + 17$ hr and $L + 48$ hr. The first correction called for a negative ($-$) 3.1-deg roll turn, a positive ($+$) 117.1-deg yaw turn, and a thrust of 11.35 sec by the vernier engines.

As on previous spacecraft, attempts were made at the initiation of each of the turns to minimize the error contribution associated with the cruise-oriented, optical limit-cycle deadband.

The commands to start each of the turns were transmitted by the DSIF station in anticipation (based on gyro error observation) of a limit cycle null (zero pointing error) for the turn axis under consideration. This "leading" of the null was necessary because of the earth-to-spacecraft signal transit time. The success with which this was accomplished can be seen from the fact that only -0.055 deg of roll error existed at the start of the roll turn, and only $+0.110$ deg of pitch and -0.135 deg of yaw existed at the start of the yaw turn.

The midcourse (trajectory correction) maneuver was flawlessly performed by the spacecraft; real-time data showed a roll of -3.15 deg, a yaw of 117.1 deg and a thrust duration of 11.36 sec. Further, post-midcourse trajectory analysis from tracking data revealed that the maneuver had been so accurate that a second correction was not needed.

In the process of returning to the cruise orientation after midcourse by reverse yaw and roll turns, it was found that the reverse roll turn was not necessary, Canopus already being in the sensor's field of view. Consequently, *cruise mode on* and *manual lock on* were transmitted to the spacecraft, commanding it to assume the celestial-oriented cruise configuration. The latter command transmission was necessary because of the conditions, previously mentioned, which nullified automatic Canopus acquisition.

d. Coast phase (cruise) performance. During the approximately 56-hr cruise portion of the flight (8 hr before and 48 hr after midcourse correction), the spacecraft performed normally. Deviations from the standard flight sequence of operations included additional gyro drift checks (nine instead of the scheduled four) and complete engineering data assessments (engineering interrogations). The former were performed so that more confidence could be attributed to the gyro drift values supplied for compensation of the preretro (terminal) maneuvers, the latter to provide additional thermal data in preparation for the anticipated second midcourse correction.

Other idiosyncrasies noted during the cruise portion of flight were associated with solar panel switch tripping (turning off and removing the solar panel from the power subsystem) and receiver/decoder indexing (cycling through the four different receiver/decoder combinations). The tripping of the solar panel switch, a normal functioning of an overvoltage protection circuit, occurred when cyclic operation of various heaters resulted in minimum battery loading during battery charging. Each tripping required the transmission of an earth command to turn the solar panel switch on again. Solar panel switch tripping occurred less frequently on this mission than on *Surveyor VI* because of the extra loading of the battery provided by the SM/SS heater.

The receiver/decoder indexing was brought about by the position of the earth with respect to the spacecraft during this flight and the uniqueness of the spacecraft physical configuration (payload including both the SM/SS and the ASI). As a result, Omnia antenna A possessed a deep signal null in its antenna reception pattern in the approximate direction of the spacecraft-to-earth position vector and, when the signal level into associated Receiver A dropped below a particular design threshold level, a reliability-enhancing mechanization indexed (changed) the receiver/decoder combination to be used for command processing.

Since the command threshold is above the indexing threshold, it became expedient to assure that all received commands were entering a decoder via the Omnia antenna B/Receiver B path. DSIF station interruption of command modulation was therefore employed throughout flight to force indexing to a proper receiver/decoder combination before any commands were sent.

e. Terminal maneuver and descent performance. Pre-maneuver thermal and power analysis yielded respective predictions of 42.78 sec of retro motor burn time and 74 A-hr of battery capacity remaining at touchdown. The final gyro drift rates supplied for compensation during the performance of the terminal maneuvers were +0.20, +0.65, and 0.00 deg/hr of pitch, roll, and yaw, respectively. These rates were adjudged to be so small, however, that compensation for them was waived.

The turns required were +80.5 deg of roll, followed by +96.1 deg of yaw, and finally -16.5 deg of roll. Commands for the first two maneuvers were transmitted to "lead" the spacecraft's respective limit cycle null points in the same manner as during midcourse maneuvering. The third maneuver did not require such care in initiation since it could not change the retro motor thrust vector established by the first two. The purpose of the -16.5 deg of roll was to orient the spacecraft in a preferred direction so that (1) radar control of the descent would have a higher probability of success (36-deg approach angle consideration), and (2) the A/SPP mast would cast a shadow 15 deg clockwise from the X axis, viewed from top of spacecraft, at touchdown (a post-landed operations consideration).

The first maneuver was initiated approximately 35 min before the scheduled retro motor ignition time. All turns were performed flawlessly. Subsequent preretro motor firing commands transmitted to the spacecraft were implemented, including the storage of a retro delay time (time from AMR mark signal generation to vernier engine ignition) of 2.775 sec.

Though a normally scheduled backup command (*emergency AMR mark* signal) was transmitted, telemetry confirmed that the automatic terminal descent sequence was initiated by the 60-mile AMR mark. Vernier engine ignition occurred 2.8 sec after the mark followed by retro motor ignition 1.1 sec later.

The remainder of the terminal descent - ejection of the AMR at retro motor ignition, RADVS turn-on, retro

motor burnout (after 43.2 sec) and ejection, vernier engine high-thrust operation, RADVS control of vernier engines, and descent contour acquisition (at 21,000 ft) and control to touchdown — occurred normally and very close to the anticipated event times (Table IV-7). No data was lost during the entire descent or during the final physical contact with the lunar surface. A comparison of predicted and actual terminal descent parameters is presented in Table IV-8.

f. Touchdown performance. In the process of touching down, the footpad on Leg 1 was the first to contact the surface followed by the footpads on Legs 3 and 2, in that order and all within a period of 1/20 sec. The spacecraft rebounded slightly, 8 to 11 in. The vertical velocity component of the spacecraft at touchdown was 12.5 ft/sec. The landed weight was 674 lb.

Subsequent analysis placed touchdown at selenographic coordinates 40.92°S and 11.45°W on a slope of 3.2 deg and with the plus X axis of the spacecraft rotated 20.2 deg counterclockwise from lunar east (see Fig. IV-7).

Table IV-7. Predicted and actual terminal descent events (GMT January 10, 1968, at the spacecraft^a)

Event	Predicted ^b	Actual
AMR 60-mile mark	01:02:11.062	01:02:10.6
Vernier ignition	01:02:13.822	01:02:13.4
Main retro ignition	01:02:14.922	01:02:14.5
RADVS power on (warmup)		01:02:15
RADVS high voltage on		01:02:16
RODVS		01:02:48
Main retro burnout (3.5-g level)		01:02:57.7
Vernier high thrust		01:03:08
Retro case ejection signal ^c		01:03:09.7
Start RADVS control		01:03:11.8
RORA		01:03:16
Programmed descent segment acquisition		01:04:01.7
1000-ft mark		01:05:12.0
10-ft/sec mark		01:05:28.9
14-ft mark		01:05:35.0
Initial touchdown	01:05:26.350	01:05:36.32

^a1.297-sec RF delay time between spacecraft and DSIF stations.
^bBased upon final computer run. Only those parameters actually included on this run have been included herein.
^cExtrapolated from 3.5-g point due to data outage.

g. Posttouchdown performance. Surveyor VII lunar performance included approximately 317 hr of the first lunar day, 79¾ hr of the first lunar night, and 168 hr of the second lunar day. Its lunar performance differed in several ways from previous spacecraft. These differences can be generally classified as functions of:

- (1) Spacecraft configuration — alpha scattering instrument, SM/SS, additional mirrors, SM/SS magnets, and other components which resulted in more comprehensive lunar operations activity.
- (2) Spacecraft landed location on the lunar surface about 41°S latitude.
- (3) Anomalies and failures that arose during the spacecraft lunar lifetime.

When not being operated in support of anomaly investigation or correction, the spacecraft proceeded through usual routines to take pictures of the surrounding area and to analyze the composition and physical properties of the near surface. The extent to which the latter was

Table IV-8. Predicted and actual values of terminal descent parameters

Parameter	Predicted	Actual (best estimate)
Conditions at start of RADVS-controlled descent		
Altitude, ft	38,736	41,510
Velocity, ft/sec	477	452
Flight path angle with lunar vertical, deg	14.6	18.1
Programmed descent segment acquisition conditions		
Slant range, ft	22,000	20,246
Velocity, ft/sec	490	464
Vernier engine cutoff conditions		
Altitude, ft	13	12
Velocity, ft/sec	5	5
Flight path angle with lunar vertical, deg	0.02	0.03
Touchdown conditions		
Longitudinal velocity, ft/sec	12.6	12.4
Lateral velocity, ft/sec	0	0
Spacecraft weight, lb		674
Postlanding conditions		
Roll attitude (spacecraft +X-axis relative to lunar north), deg clockwise		290.2
Spacecraft tilt, deg		3.17

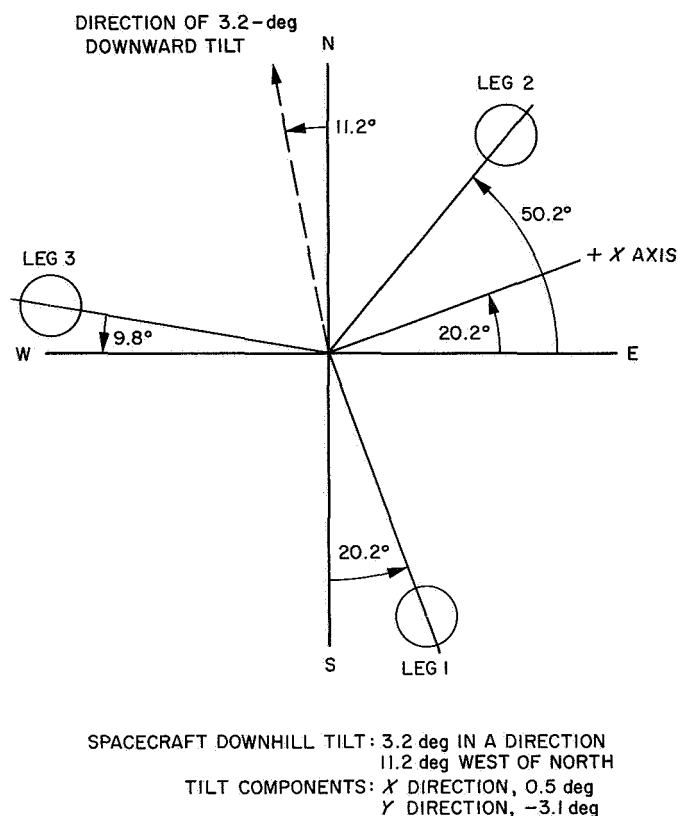


Fig. IV-7. Surveyor VII touchdown orientation

accomplished, however, exceeded previous spacecraft capabilities in that the SM/SS was employed to selectively position the ASI head. For the first time, alpha scattering measurements of a lunar rock sample and of a trenched-out area several inches deep were performed. Also, stereo pictures were obtained of the SM/SS operation with the aid of a flat (optically surfaced) mirror mounted on the A/SPP mast, and a dust dispersion assessment was made by taking pictures of seven small mirrored surfaces located on various portions of the spaceframe. Solar corona pictures were taken immediately following the first lunar day sunset, with television camera operation extending some 14 hr into the lunar night and resulting in exposure times of from 20 to 30 min.

In addition to these planned operations, the spacecraft also participated in a laser experiment whereby it successfully acquired television pictures of two earth-based laser beams aimed at the moon.

The location of the spacecraft on the moon (41°S) produced unique thermal control problems during the lunar day. The maximum elevation angle that the sun reached

during the day was approximately 53 deg. Shading of the ASI head with the solar panel or planar array was impossible, and shading of the helium check and relief valves, TV camera, and Compartments A and C was performed where possible on a tradeoff basis. During its inactive periods, the SM/SS was expediently positioned in such a way as to shade the ASI head.

The attainment of a major portion of the lunar performance objectives was seriously threatened soon after touchdown, when the ASI head would not deploy. Pre-deployment calibration, release, and background count data acquisition operations (a total of approximately 8 hr) were successful, but the sensor head would not lower to the lunar surface when commanded to do so. A/SPP stepping (to shake the head loose by vibration) and SM/SS tapping and nudging of the head failed to free its lowering mechanism.

Finally, some 55 hr after touchdown, the ASI head was forced to the lunar surface by various manipulations carried out with the SM/SS. Once deployed, the alpha scattering experiment yielded good-quality data.

This was the most significant anomaly which occurred during the first lunar day. Other minor anomalous occurrences had to do with spacecraft receiver fluctuations in the received signal strength and Transmitter A wide-band oscillator frequency drift. In the former case, the fluctuations resulted in nonresponse to some television operational commands. Subsequent repetitions of the same commands were successful. It is believed that the fluctuations were the result of multipath reflections of the incoming signal from surrounding topographical features. The latter anomalous performance was overcome by operating only with Transmitter B. Both of these anomalies were of a nuisance nature; their effect on the total mission was negligible.

A failure of the vernier engine fuel line 3 temperature sensor, P-25, occurred on January 14. Though negligible in effect on the remainder of the mission, this failure requires some mention owing to associated preflight history. The sensor had been suspect prior to flight because of an unexplainable small shift observed in the telemetry output. After extensive investigation it was decided to assume the risk of losing this data point rather than to risk damaging the fuel line by replacing the sensor.

Near the end of the first lunar day, fuel and oxidizer leaks precluded possibilities of either a static firing of

the vernier engines or a spacecraft hop to another location. Such possibilities were additionally compromised throughout the lunar day because of the high temperature of one of the vernier engines (a landed location/sun angle effect).

As the spacecraft entered the lunar night and temperatures started to drop, operations proceeded according to a preconceived plan generated to obtain as much scientific data as possible while still leaving the spacecraft in an optimum configuration for revival on the second lunar day. Performance was as expected; the only indicated failures were those of two thermal switches, which had failed to open by the time final shutdown was commanded, and possibly the locking mechanism on Leg 2, whose telemetry showed an appreciable sag.

Lunar sunset, based upon television pictures, occurred 2 hr earlier than anticipated. The standby configuration was first commanded some 16½ hr after sunset. Engineering interrogations, approximately every 2 hr, interrupted this standby status until final shutdown at 14:11 GMT on January 26, some 80 hr after sunset.

Seventeen days later, February 12, at 19:00 GMT *Surveyor VII* responded to the first revival attempt made on its second lunar day. An initial assessment of spacecraft status indicated a serious power problem (battery pressure under 2 lb), possibly the result of a cracked battery manifold. In addition, telemetry also indicated depletion of the helium supply (pressure under 50 lb) and collapse of Leg 1 (locking mechanism failure coupled with shock absorber fluid leakage).

Because of the condition of the battery (which also had several shorted cells besides low pressurization), an inordinate amount of the second lunar day's operations was spent in working around this power subsystem problem. Heavy loading of the subsystem could not be sustained. Science activities were limited to 45 200-line television pictures, one extension movement of the SM/SS, and 30 hr of alpha scattering data.

Spacecraft performance steadily deteriorated throughout the second lunar day. Temperatures associated with Compartment A (which contained the battery) were considerably higher than during the first lunar day.

Five days after revival (February 18, 2¾ days after lunar noon), the solar panel failed to step on command.

Each command attempt also resulted in loss of contact with the spacecraft. The battery had lost all load-carrying capability.

Spacecraft performance was intermittent from this point until final loss of spacecraft telemetry at the beginning of February 21, approximately one day before lunar sunset.

B. Structures and Mechanisms

The structure and mechanisms subsystem provides support, alignment, thermal protection, electrical interconnection, mechanical actuation, and touchdown shock absorption and vehicle stabilization for the spacecraft and its components. The subsystem includes the basic spaceframe, landing gear mechanism, crushable blocks, omnidirectional antenna mechanisms, antenna/solar panel positioner (A/SPP), pyrotechnic devices, electronic packaging and cabling, thermal compartments, thermal switches, and the separation sensing and arming device.

1. Spaceframe and Substructure

The spaceframe, constructed of thin-wall aluminum tubing, is the basic structure of the spacecraft. The landing legs and crushable blocks, the retrorocket engine, the *Centaur* interconnecting structure, the vernier engine brackets, and the A/SPP attach directly to the spaceframe. Substructures are used to provide attachment between the spaceframe and the following components: the thermal compartments, TV, alpha scattering instrument, RADVS antennas, omniantennas, flight control sensor group, attitude control nitrogen tank, and the vernier system helium tank.

During the *Surveyor VII* mission, there was no indication of any failures or anomalies attributable to structural malfunctions.

2. Landing Gear Subsystem

a. Configuration and functional description. The landing gear subsystem consists of three landing leg assemblies and three crushable honeycomb blocks attached to the spaceframe (Fig. IV-8). Each leg assembly is made up of a tubular inverted tripod structure with a shock absorber, an A-frame, a lock strut, and a honeycomb footpad.

During launch, the legs are folded for stowage under the shroud. Shortly before spacecraft separation, upon

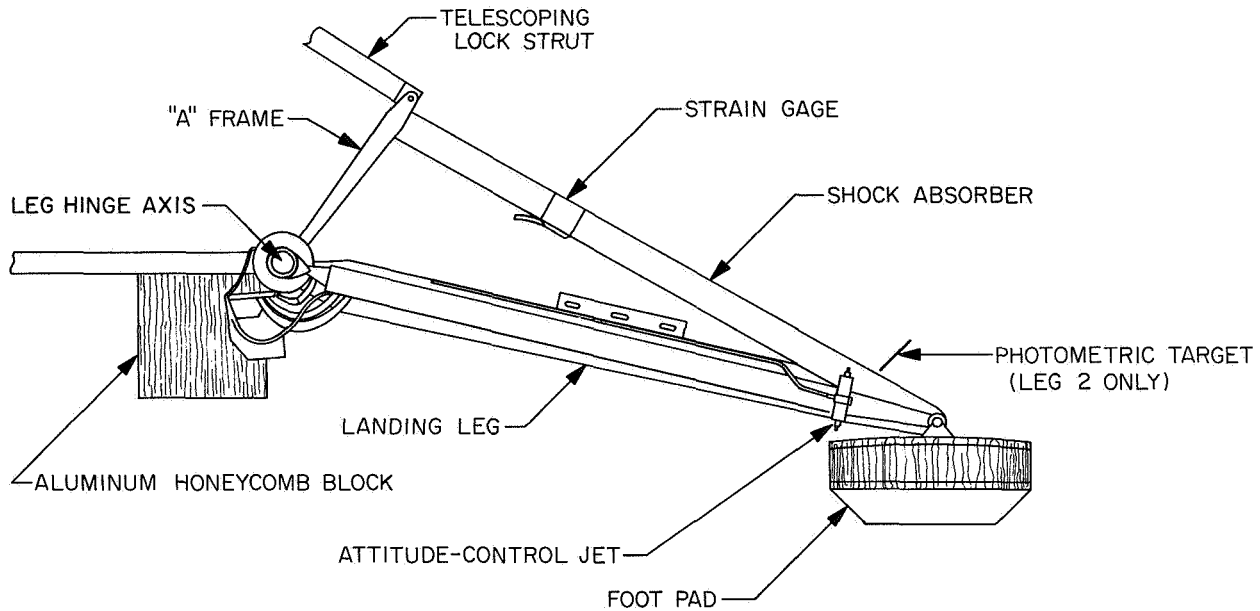


Fig. IV-8. Landing leg assembly

command from the *Centaur* programmer, the legs are released by squib-actuated pin pullers and deployed by leaf-type kickout springs located near the release pin pullers. Torsion springs at the hinge axes force the legs to the fully deployed positions, where they are automatically latched.

Upon landing, each leg pivots about its hinge axis while the landing loads are absorbed by compression of the upper member of the tripod, which is a combined shock absorber and spring assembly. These shock absorber columns are instrumented with strain gages. Axial loads measured by the strain gages are telemetered to provide continuous analog traces during the terminal descent and touchdown phase.

For vertical landings on hard, level surfaces at velocities in excess of about 8.5 ft/sec, the legs deflect sufficiently to cause the crushable blocks to contact the surface. Energy would then be further dissipated through penetration of the surface by the crushable blocks or by crushing of the blocks if the surface bearing pressure exceeds 40 psi. Crushing of the honeycomb footpads is not expected for landing velocities below 11.5 ft/sec or for surface bearing pressure less than about 10 psi.

Magnetic bars were attached to the side of Footpad 2 on *Surveyors V* and *VI*, and to Footpads 2 and 3 on *Surveyor VII* to detect the magnetic properties of the lunar surface material. The magnets were $2 \times \frac{1}{2} \times \frac{1}{8}$ -in.

bars made of Alnico V material. A control bar of non-magnetic material (Inconel X-750) was also attached with each magnet in view of the camera so that a comparison could be made of particle accumulation on the two bars. Refer to Part II of this report for a complete description of the soil magnet experiment.

b. Transit and lunar performance. The performance of the landing gear subsystem on the *Surveyor VII* mission was satisfactory. The legs were deployed in response to a command from the *Centaur* and latched into the landing positions.

Figure IV-9 shows the strain gage force histories of the three shock absorbers throughout the landing phase. The peak axial forces in the shock absorbers and times of initial impact of the footpads are given in Table IV-9. The forces are considered accurate within ± 80 lb, the times within ± 2 msec.

An evaluation of the data in Table IV-9, together with other engineering telemetry and postlanding video data, has resulted in the following reconstruction of events during the landing sequence: The 10-ft/sec descent velocity *mark* signal was generated 7.4 sec prior to initial ground contact when the spacecraft was at an altitude of 44 ± 4 ft. Immediately following this *mark*, the spacecraft was slowed to a constant descent velocity of 5.3 ± 0.5 ft/sec (nominal: 5.0 ± 1.5), which was maintained until the 14-ft altitude *mark* was generated

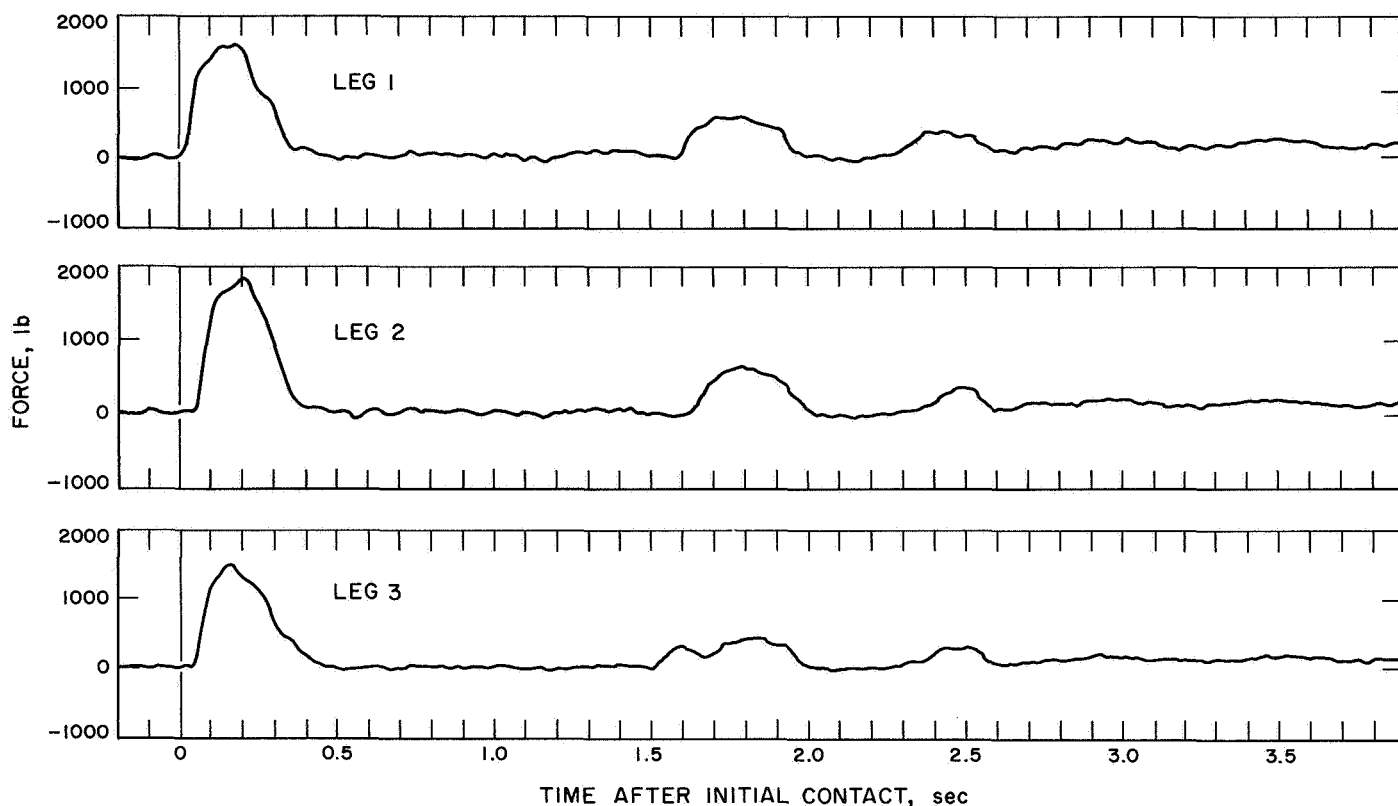


Fig. IV-9. Loads on spacecraft shock absorber during landing

1.3 sec before initial touchdown, at an altitude of 11.9 ± 1.0 ft (nominal: 13 ± 4.5). At this time, all three vernier engines were cut off, resulting in a free-fall period, during which time the spacecraft vertical velocity component increased to 12.4 ± 0.5 ft/sec (nominal: 12.6 ± 2.4) when Leg 1 first contacted the lunar surface. Angular spacecraft motions during the constant-velocity descent were very small. The following angular deflections were indicated between the reference attitude at the 10-ft/sec mark and the final resting position: pitch, -3.1 ± 0.1 deg; yaw, -1.7 ± 0.1 deg; roll, 0.0 ± 0.1 deg. The landed weight of *Surveyor VII* at the time of initial

lunar landing is estimated to have been 674 ± 0.5 lb (earth-weight).

The shock absorber force histories (Fig. IV-9) exhibit an initial high-force period of approximately 0.3-sec duration, followed by a 1.0- to 1.2-sec-long zero-force reading. This reading indicates that the spacecraft rebounded, raising the footpads by 8 to 11 in. from their initial impact positions.

The shock absorbers were not locked immediately after landing, in order to permit shock absorption capability for a possible postlanding spacecraft hop experiment. The leg shock absorber locking command was sent approximately 514 hr after touchdown at the end of the first lunar day; however, telemetry indicated appreciable sag of Legs 1 and 2.

Table IV-9. Shock absorber forces and times of footpad impacts for lunar landing

	Leg 1	Leg 2	Leg 3
Maximum shock absorber axial force, lb	1650	1760	1470
Time of initial footpad impact, GMT (January 10, 1968)	01:05:37.612	01:05:37.660	01:05:37.634

3. Omnidirectional Antennas

The omnidirectional antennas are mounted on the ends of folding fiberglass booms hinged to the space-frame. Squib-actuated pins retain the booms in the stowed position during launch and, by squib actuation, release the booms upon command from the *Centaur*

shortly before spacecraft separation. A leaf-type kickout spring located at the release pin on each omniantenna boom initiates movement. Torsion springs continue the movement to the fully deployed positions, where the booms are automatically locked. On *Surveyor VII*, as on *Surveyors V* and *VI*, Omniantenna B was painted black to reduce television picture glare. The paint had little effect on the thermal control of the spacecraft.

The omniantenna booms were extended by *Centaur* command, and both antennas were locked satisfactorily in the landing or transit position as indicated by telemetry.

4. Antenna and Solar Panel Positioner

The A/SPP supports and positions the high-gain planar array antenna and solar panel. The A/SPP has four axes of rotation: roll, polar, solar, and elevation (Fig. IV-10). Stepping motors rotate the axes in either direction in response to ground commands or during automatic deployment following *Centaur*/spacecraft separation. Once on the lunar surface, these four degrees of freedom allow the solar panel to track the sun, using only one stepper motor, while maintaining earth lock with the planar array. Each earth command gives approximately $1/8$ deg

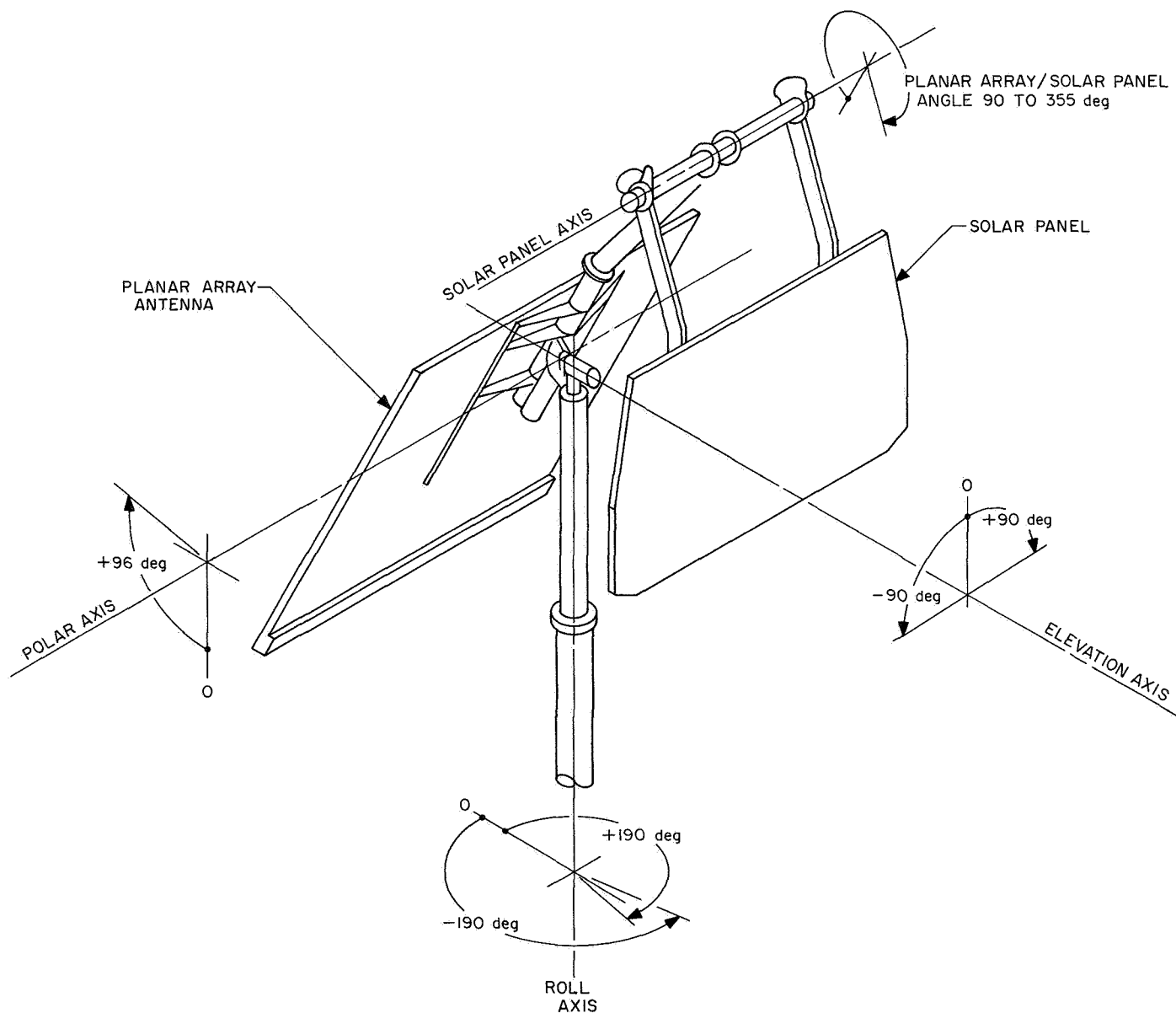


Fig. IV-10. Antenna/solar panel configuration

of rotation about the roll, solar, and elevation axes and approximately 1/15 deg about the polar axis.

The solar axis is locked with the solar panel in a vertical position for stowage in the nose fairing during launch. After spacecraft separation from the *Centaur*, the roll and solar axes are repositioned and locked such that the planar array is parallel to Leg 1 and the solar panel is perpendicular to the A/SPP. The A/SPP remains locked in this position until after touchdown, at which time the roll, solar, and elevation axes can be released in any order desired to reposition the A/SPP for solar panel acquisition of the sun and planar array acquisition of the earth. Following initial acquisition, the A/SPP is stepped periodically during the lunar day to maintain desired solar panel and planar array positioning relative to the sun and earth. Data from potentiometers on each axis can be used to determine spacecraft lunar orientation.

Surveyor VII used the same A/SPP configuration as *Surveyors V* and *VI*. The A/SPP was redesigned for *Surveyor V* to increase the structural and operational margins and to incorporate new high-torque stepping motors.

After the *Surveyor VII* spacecraft separated from the *Centaur*, the A/SPP operated as expected during the auto-deploy sequence, and the roll and solar axes relocked satisfactorily.

After touchdown, the following earth command sequence was used to acquire the sun and earth and to determine the spacecraft attitude. The roll-, elevation- and solar-axes pin pullers were fired. The elevation axis had to be unlocked and rotated to accommodate the *Surveyor VII* landing site in the southern latitude. A first attempt was made to acquire the earth by moving the roll, elevation, and polar axes and comparing the observed planar array antenna gain with the known antenna pattern. This initial attempt to acquire the earth and sun was successful and was accomplished in 40 min. The solar panel power and secondary sun sensor signals were used as a means of lock-on indication. The sun was acquired very close to its predicted position, indicating that the spacecraft was on a fairly level surface.

Later, after the initial sequence of 600-line TV pictures, the A/SPP was also used to make more accurate attitude determinations in the following manner. The A/SPP was stepped to obtain a precise sun sighting with

the secondary sun sensor. A precise earth sighting was obtained by stepping the planar array slowly through the earth position in two orthogonal A/SPP axes and observing potentiometer positions corresponding to maximum DSIF received signal strength. The potentiometer readings were then used in a computer program to obtain an accurate attitude determination.

Throughout the lunar day, the A/SPP stepping efficiency appeared to be 100%. During lunar noon, the temperature of the planar array reached a maximum of 214°F, which is 66° below the predicted maximum worst-case design condition. The number of degrees of movement of each axis at the end of the first lunar day (January 26, 1968) were: solar, 960; polar, 597; elevation, 353; and roll, 2175.

5. Thermal Compartments

Four thermal compartments (A, B, C and the SM/SS auxiliary) house the thermally sensitive spacecraft electronic equipment. Compartment C, which was added for *Surveyors V* and *VI*, was also used on *Surveyor VII* along with the SM/SS auxiliary; they are both insulated boxes with heaters that house the additional electronics needed to operate the alpha scattering instrument and the SM/SS. The main compartments, A and B, contain the components identified in Table IV-10. These components are arranged on thermal trays which distribute heat from the electronic components throughout the compartments.

Each main compartment contains a thermal control and heater assembly to maintain the temperature of the thermal tray above a specified temperature (above 40°F for Compartment A and above 0°F for Compartment B).

Table IV-10. Thermal compartment component installation

Compartment A	Compartment B
Receivers (2)	Central command decoder
Transmitters (2)	Boost regulator
Battery	Central signal processor
Battery charge regulator	Signal processing auxiliary
Engineering mechanisms auxiliary	Engineering signal processor
Television auxiliary	Low data rate auxiliary
Thermal control and heater assembly	Thermal control and heater assembly
Auxiliary battery control	Auxiliary engineering signal processor

The thermal control and heater assembly is capable of automatic operation, or may be turned on or off by earth command.

Each main compartment employs thermal switches (nine in Compartment A and six in Compartment B) which are capable of varying the thermal conductance between the inner compartment and the external radiating surface. The thermal switches maintain thermal tray temperature below $+125^{\circ}\text{F}$. Like the switches used on *Surveyors V* and *VI*, the switches used on *Surveyor VII* were set to open at $35 \pm 10^{\circ}\text{F}$.

An insulating blanket consisting of 75 sheets of 0.25-mil-thick aluminized Mylar is installed between the inner structure and the outer protective cover of each of the main compartments. The thermal blankets and protective covers for Compartments A and B, which were redesigned for *Surveyor V* to be made in two pieces, were also used on *Surveyor VII*. One piece covers the back and bottom of the compartments; the other piece covers the top, ends, and front. The redesign provides easier access to the electronic components during all phases of systems checkout and much simpler final compartment installation. The blanket for Compartment A, as redesigned, allows easier cable access into the electronics during STV tests.

6. Thermal Switch

The thermal switch is a thermal-mechanical device which varies the conductive path between an external radiation surface and the top of the equipment tray of each compartment (Fig. IV-11). The switch has two contact surfaces which are ground to within one wavelength (sodium light) of being optically flat. One surface is coated with a conforming substance to form an intimate contact with the mating surface. To reduce the contact sticking condition experienced on the *Surveyor I* and *III* missions, the coating surface, which consists of a room-temperature-curing (RTV) silicone compound, is vacuum-baked at 300°F to drive off the volatiles. The coating surface is also charged with molybdenum disulfide, which serves as a parting agent. These processes were employed in the hope that they would increase the opening reliability of the thermal switches significantly above that of the switches used on *Surveyors I* through *III*. Actuation of the thermal switch is accomplished by four bimetallic elements located at the base of the switch. These elements are connected mechanically to the top of the compartment so that switch actuation is controlled by compartment temperature.

The external radiator surface is such that it absorbs only 12% of the solar energy incident on it and radiates 74% of the heat energy conducted to its surface. When the switch is closed and the compartment is hot, the switch loses its heat energy to space. As the compartment gets cold, the switch contacts are designed to open about 0.020 in., thereby opening the heat-conductive path to the radiator and thus reducing the heat loss through the switch to almost zero. Four Compartment A and three Compartment B switches are instrumented with temperature sensors attached to the radiators. The temperature sensors provide an indication of switch actuation for those switches which are monitored.

On the *Surveyor VII* mission, the thermal switches were closed during flight and kept the electronics at or below the maximum allowable temperature at all times. All the thermal switches also remained closed during the lunar day after landing.

Based on a heat balance analysis made on each compartment and the telemetry data, it was determined that two of the nine thermal switches in Compartment A and none of the six switches on Compartment B were stuck closed as the spacecraft entered the lunar night. At spacecraft shutdown 80 hr after sunset, the two switches in Compartment A still remained closed. At least one additional switch which was open at shutdown had opened below the specified temperature range.

7. Pyrotechnic Devices

The pyrotechnic devices installed on *Surveyor VII* are listed in Table IV-11. All the squibs used in these devices are electrically initiated, hot-bridgewire, gas-generating devices. Qualification tests for flight squibs included demonstration of reliability at a firing current level of 4 or 4.5 A. "No fire" tests were conducted at a 1-A or 1-W level for 5 min. Electrical power required to initiate pyrotechnic devices is furnished by the spacecraft main battery. Power distribution is through 19.0- and 9.5-A constant-current generators in the engineering mechanism auxiliary (EMA).

All the taper pin assemblies associated with the A/SPP pin pullers were of the new design first incorporated on *Surveyor V*. They were all made heavier in conjunction with the A/SPP redesign in order to obtain a positive structural margin. The basic operating characteristics of the pin pullers were not changed, although the axial degree of freedom of the pins used to lock the solar axis during launch was limited to keep them from backing

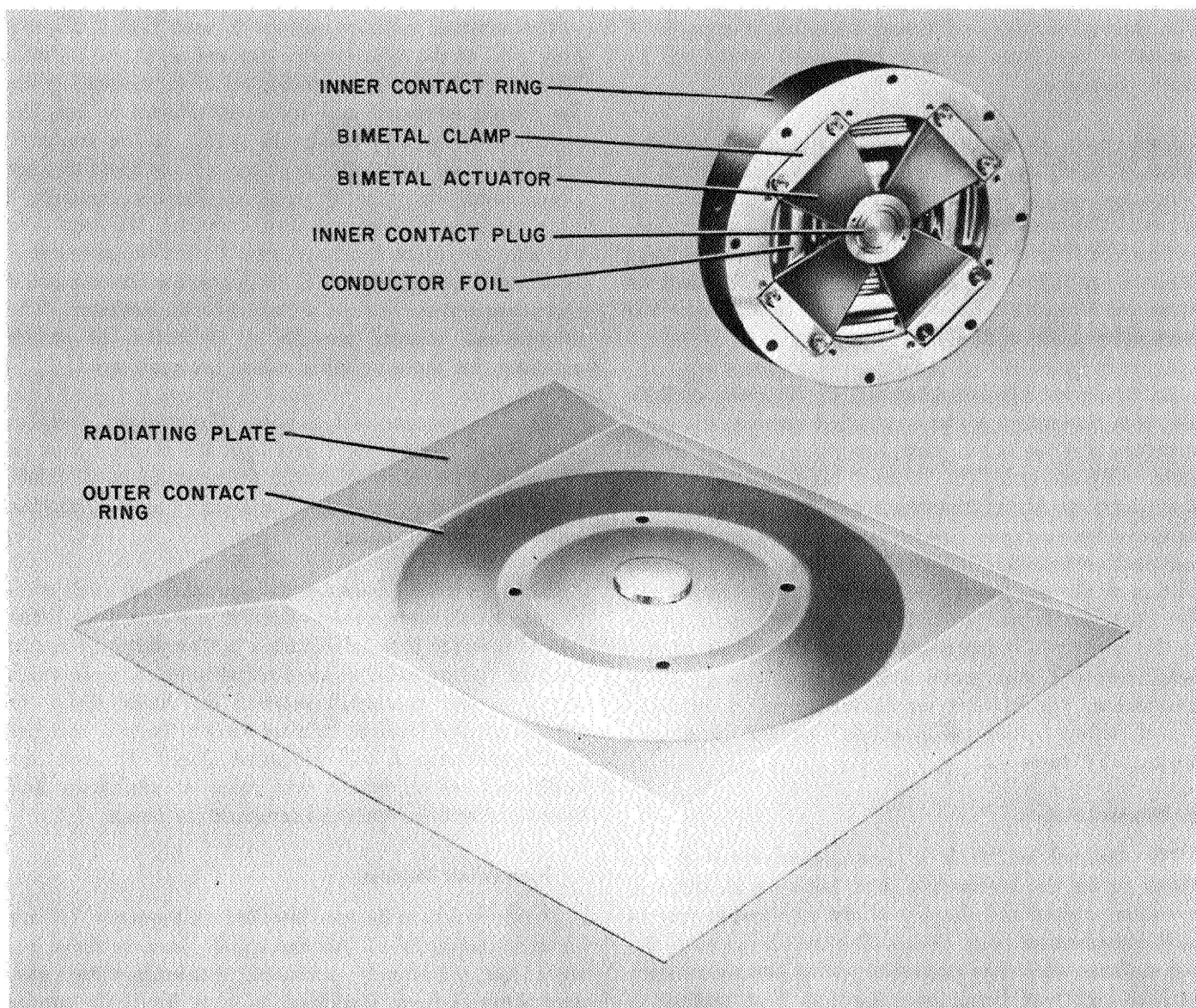


Fig. IV-11. Thermal switch

out due to vibration loads encountered during the launch phase of the flight.

All pyrotechnic devices functioned normally upon command. Mechanical operation of most of the squib-actuated locks, valves, switches, and pins are indicated on telemetry signals as part of the spacecraft engineering measurement data.

The shock absorber lock pins were not fired at the normal time (shortly after landing) in order to maintain the postlanding capability to fire the vernier engines. The command to fire the locks was transmitted about 40 hr

prior to lunar sunset. Telemetry received during the lunar night and the second lunar day indicated Legs 1 and 2 failed to lock.

8. Electronic Packaging and Cabling

The electronic assemblies provide mechanical support for electronic components in order to insure proper operation throughout the various environmental conditions to which they are exposed during a mission. The assemblies (or control items) are constructed utilizing sheet metal structure, sandwich-type etched circuit board chassis with two-sided circuitry, plated-through holes,

Table IV-11. Pyrotechnic devices

Type	Location and use	Quantity of devices	Quantity of squibs	Command source
Pin pullers	Lock and release Omnantennas A and B	2	2	Centaur programmer
Pin pullers	Lock and release landing legs	3	3	Centaur programmer
Pin pullers	Lock and release planar antenna and solar panel	7	7	Separation sensing and arming device and ground station
Pin puller	Lock and release Vernier Engine 1	1	1	DSIF station
Pin pullers	Alpha scatter unlatch and lower mechanism	2	2	DSIF station
Pin puller	SM/SS release mechanism	1	1	DSIF station
Separation nuts	Retrorocket attach and release	3	6	Flight control subsystem
Valve	Helium gas release and dump	1	2	DSIF station
Pyrotechnic switches	EMA Board 4, RADVS power on and off	4	4	DSIF station and flight control subsystem
Initiator squibs	Safe-and-arm assembly retro motor initiators	1	2	Flight control subsystem
Locking plungers	Landing leg, shock absorber locks	3	3	DSIF station
		28	33	

and/or bifurcated terminals. In general, each control item consists of only a single functional subsystem and is located either in or out of the three thermally controlled compartments, depending on the temperature sensitivity of the particular subsystem. Electrical interconnection is accomplished primarily through the main spacecraft harness. The cabling system utilizes lightweight, minimum-bulk, and abrasion-resistant wire which is constructed of extruded Teflon with a dip coating of modified polyamide.

C. Thermal Control

The thermal control subsystem is designed to provide acceptable thermal environments for all components during all phases of spacecraft operation.

1. Configuration and Functional Description

Spacecraft items with close temperature tolerances were grouped together in thermally controlled compartments. Those items with wide temperature tolerances were thermally decoupled from the compartments. The thermal design fits the "basic bus" concept in that the design was conceived to require minimum thermal design changes between missions. Monitoring of the performance of the spacecraft thermal design is provided by engineering temperature sensors which are distributed throughout the spacecraft. On the *Surveyor VII* space-

craft, 77 temperature sensors were located within the subsystems as follows:

Flight control	9
Mechanisms	3
Radar	6
Electrical power	4
Transmitters	2
Television	4
Vehicle structure	26
Propulsion	18
Alpha scattering instrument	2
Soil mechanics/surface sampler	3

The spacecraft thermal control subsystem is designed to function in the space environment, both in transit and on the lunar surface. Extremes in the environment as well as mission requirements on various components of the spacecraft have led to a variety of methods of thermal control. The spacecraft thermal control design is based upon the absorption, generation, conduction, and radiation of heat.

The radiative properties of the external surfaces of major items are controlled by using paints, by polishing,

and by using various other surface treatments. Reflecting mirrors are used to direct sunlight to certain components. In cases where the required radiative isolation cannot be achieved by surface finishes or treatments, the major item is covered with an insulating blanket composed of multiple-sheet aluminized Mylar. This type of thermal control is called "passive" control.

The major items whose survival or operating temperature requirements cannot be achieved by surface finishing or insulation alone use heaters that are located within the unit. These heaters can be operated by external command, thermostatic actuation, or both. The thermal control design of those units using auxiliary heaters also includes the use of surface finishing and insulating blankets to optimize heater effectiveness and to minimize the electrical energy required. Heaters are considered "active control."

Items of electronic equipment whose temperature requirements cannot be met by the above techniques are located in thermally controlled compartments. Each of the main compartments (A and B) is enclosed by a shell covering the bottom and four sides and contains a structural tray on which the electronic equipment is mounted. The top of each compartment is equipped with a number of temperature-actuated switches (nine in Compartment A and six in Compartment B). These switches, which are attached to the top of the tray, vary the thermal conductance between the tray and the outer radiator surfaces, thereby varying the heat-dissipation capability of the compartments. When the tray temperature increases, heat transfer across the switch increases. During the lunar night, the switch opens, decreasing the conductance between the tray and the radiators to a very low value in order to conserve heat. When dissipation of heat from the electronic equipment is not sufficient to maintain the required minimum tray temperature, a heater on the tray supplies the necessary heat. The switches are considered "semiactive."

Examples of units which are controlled by active, semi-active, or passive means are shown in Fig. IV-12.

2. Surveyor VII Performance

a. Transit phase. Surveyor VII did not experience any thermal anomalies during the transit phase of flight. Of the 75 temperature sensors monitored during transit, 70 were within 10°F of their predicted nominal steady-state

value. The remaining five were all within the allowable limits, and their characteristics were as follows:

Vernier Engine 3 (P-11). Engine 3 operated about 15°F above the nominal predicted before the midcourse maneuver and about 13 to 14°F above after the maneuver; the uncertainty for this prediction was $\pm 20^\circ\text{F}$.

Fuel line 3 (P-25). Fuel line 3 ran slightly warmer than the predicted heater-controlled bandwidth after midcourse.

SM/SS retraction motor (SS-14). The SM/SS motors had a steady-state temperature about 32°F above the predicted value. The band of uncertainty is $\pm 35^\circ\text{F}$. This was the first flight with these sensors; therefore, no refinement of the prediction band was possible.

SM/SS elevation drive motor (SS-15). The same behavior was exhibited by this sensor as by SS-14.

Compartment A radiator 2 (V-47). This switch opened during flight as it did on Surveyor V. It is possible that a 20° gradient could have existed across the switch at the time of opening, since this switch is in the shade of the solar panel in normal flight. If this was the case, the switch opening was not an anomaly. The equilibrium temperature of the radiator in the open position was -40°F .

Plots of transit temperatures for selected sensors are contained in Figs. D-1 through D-8 of Appendix D.

b. Postlanding phase. After Surveyor VII landed, the temperatures of most components were as expected. Five hours after landing, Engine 2 rose above 220°F. Since during the entire lunar day either Engine 2 or Engine 3 was above 220°F, the possibility of conducting a static firing or a spacecraft hop experiment was negated.

As the sun approached the lunar noon position, the science instruments exceeded their upper operating temperature limits, as expected. The TV camera was the only science instrument that could be shaded on Surveyor VII with either the solar panel or planar array. Shading of the TV camera around noon allowed its operation at a low duty cycle. (Compartment C could have been shaded with the panels, but the ASI sensor head could only be partially shaded with the SM/SS scoop.)

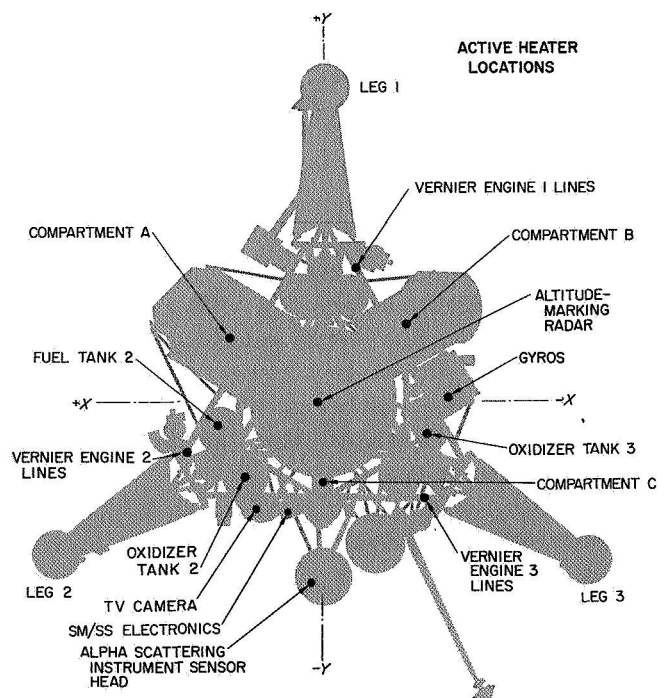
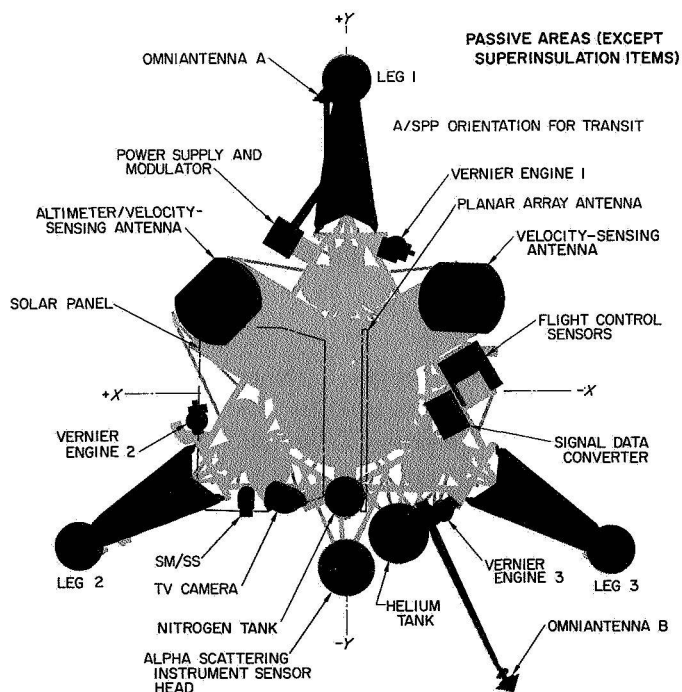
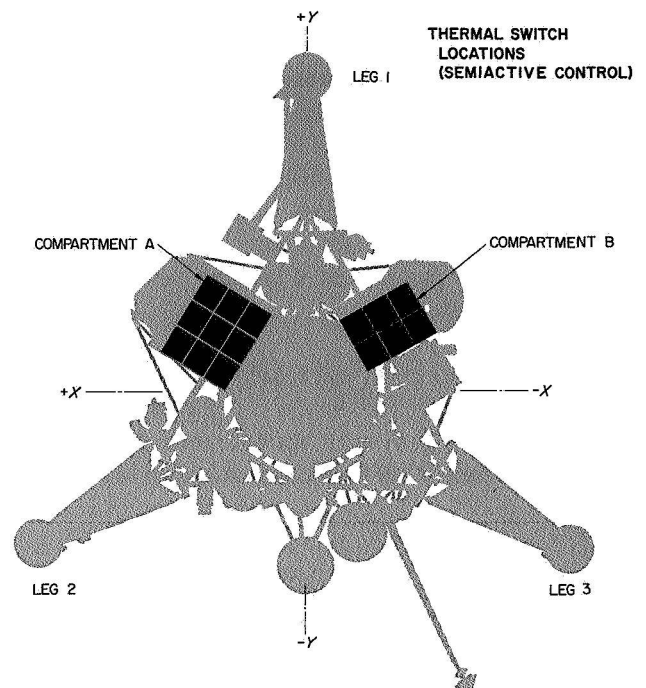
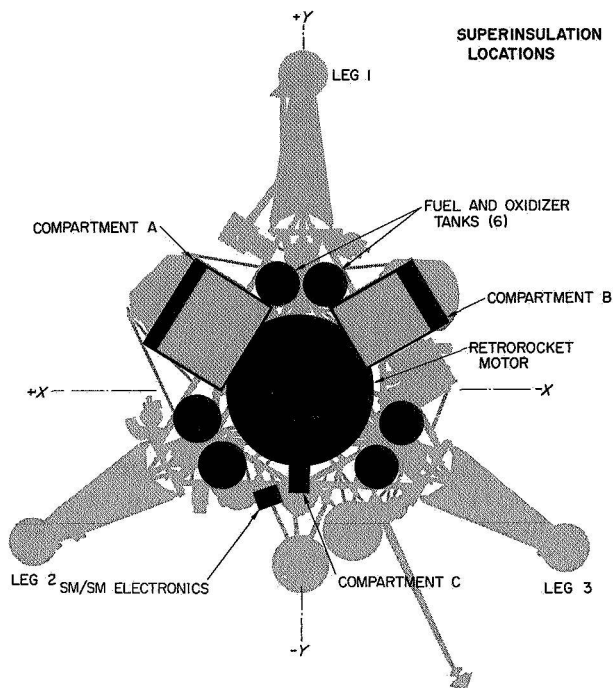


Fig. IV-12. Thermal design

Compartment A and B temperatures were within their operating limits throughout the first lunar day. The battery in Compartment A did not exceed 111°F due to the shading of the compartment. The helium check and relief valves were shaded during the latter part of the day in an attempt to minimize operational degradation. Two positions of the A/SPP gave good shading of the TV camera. The first position also shaded Compartment A. The second position shaded Compartment C and the check and relief valves. The first position was used until late in the lunar day, when it became desirable to warm up Compartment A.

The lunar sunset was approached with the spacecraft temperatures at desired levels. As the sun went down, spacecraft operations were started according to a pre-planned schedule. Compartments A and B were allowed to cool to 20°F and -15°F, respectively. The thermal switches started to open. At the last interrogation, power dissipation and cooling rates indicated that probably two thermal switches (one of which was instrumented) were stuck on Compartment A and none on Compartment B.

When *Surveyor VII* responded to commands on the second lunar day it was apparent that the battery had failed as indicated by its excessively high temperatures. Other temperatures were similar to those experienced on the first lunar day until communication was lost before the second sunset. Plots of selected postlanding temperatures for the first and second lunar day are contained in Figs. D-9 through D-11 of Appendix D.

D. Electrical Power

The electrical power subsystem was designed to store, convert, and distribute electrical energy. The power subsystem was redesigned (effective with the *Surveyor V* spacecraft) to provide better matching characteristics between power sources and power conditioning units and to introduce a number of improvements into the subsystem which increased the capability, reliability, and overall power performance.

1. Power Subsystem Description

A block diagram of the *Surveyor VII* power subsystem is shown in Fig. IV-13.

The spacecraft system derives its energy from two sources, a solar panel which converts solar radiation energy to electrical energy and one rechargeable battery, of 3650 W-hr nominal capacity.

Several improvements were made in the solar panel design for *Surveyor V* and later missions. Improved performance of the power subsystem resulted when a series-parallel solar cell arrangement was incorporated to obtain maximum power output at 30.5 ± 2 V during transit. In this arrangement, open-circuit voltage of the solar panel ranges from 65 V after sunrise on the lunar surface to 30 V at lunar noon. Flat-cell rather than shingle-cell mounting is used, thus providing more uniform bonding of the cells to the substrate for better performance over a wider temperature range.

The lower output voltage of the redesigned solar panel permits use of a simplified battery charge regulator (BCR) and switching of the solar panel directly to (1) the 30-V preregulated bus in the boost regulator (BR) during transit, or (2) the 22-V unregulated bus during lunar operations, when the temperature is higher and the solar panel voltage is lower. The power subsystem is in its most efficient mode of operation when the solar panel is connected to the 30-V preregulated bus. (This mode of operation was not possible in the previous design.) The unregulated bus is used for charging of the battery and for distribution of current from the BCR and battery to the unregulated spacecraft loads and the BR. The voltage on the unregulated bus can vary between 17.5 and 27.5 V with a nominal value of 22 V. The BCR also has an *off* mode in which the solar panel is left floating. The *off* mode can result from earth command or automatically if the battery voltage exceeds 27.3 V or battery pressure exceeds 65 psia. This automatic turnoff feature of the BCR can be enabled or disabled by earth command. In addition, the BCR houses the BCR output select logic that determines the position of the BCR output to BR preregulated bus or unregulated bus. The logic can be disabled by command.

The BR converter boosts the unregulated bus voltage, the output of which is used by the BR preregulator to supply 30 V to the preregulator bus. The essential loads are fed by the preregulated bus through series diodes which drop the preregulated bus voltage to the essential bus voltage of 29 V. The preregulator bus also feeds the flight control regulator and the nonessential regulator, which in turn feeds the flight control regulator and non-essential buses, respectively. These regulators can be turned on and off by earth commands. The nonessential regulator has a bypass mode which is used to connect the preregulated bus directly to the nonessential bus if the nonessential regulator fails.

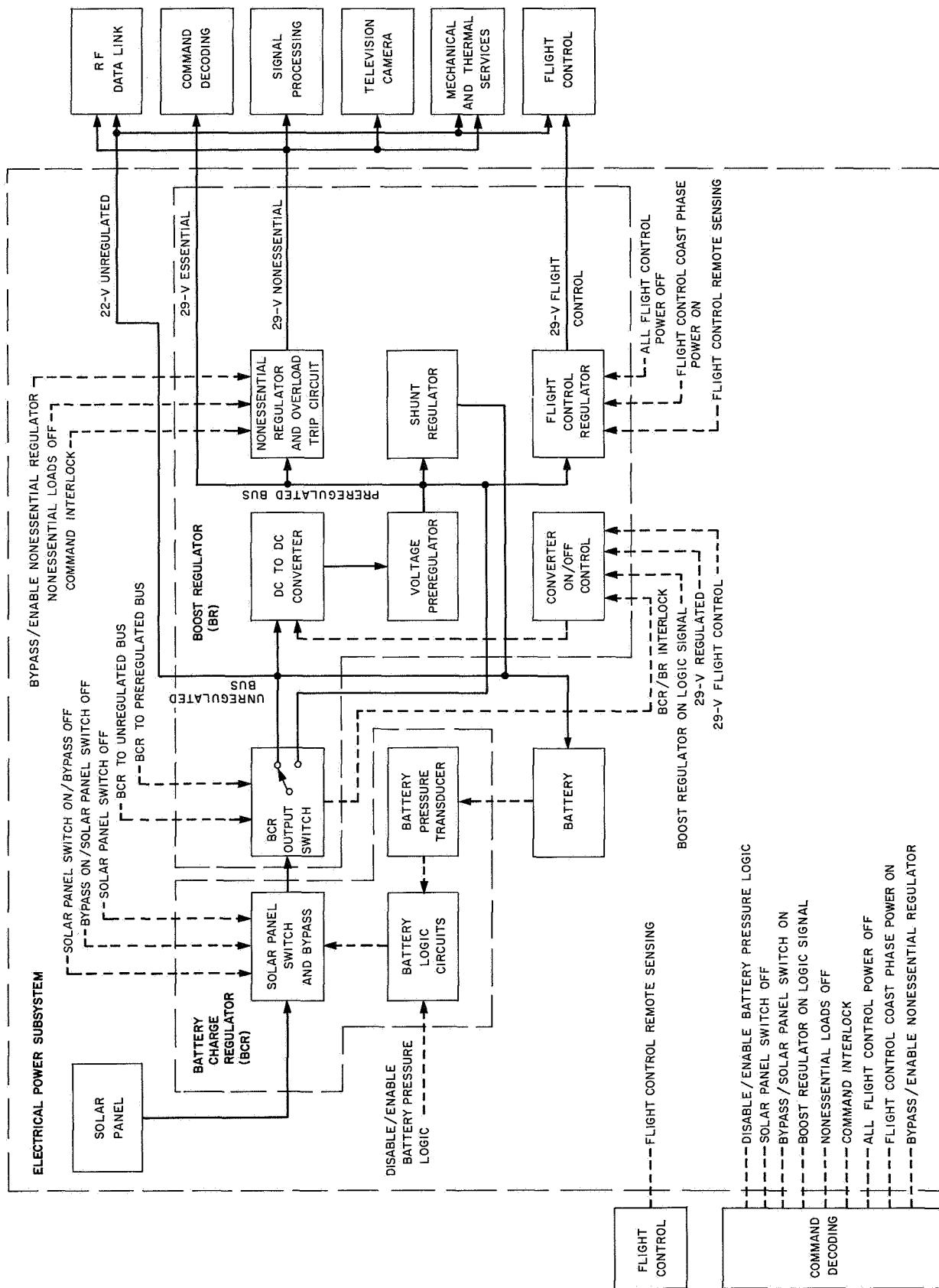


Fig. IV-13. Functional diagram of Surveyor VII electrical power subsystem

The BR operates at higher efficiency as a result of the simplified BCR. The higher efficiency is especially pronounced during transit because all the regulator current does not have to pass through the preregulator. In addition, a shunt regulator is connected between the pre-regulated bus and the battery to supply excess solar panel current to the battery and prevent excess solar panel voltage when the spacecraft current demands are low during transit. In the previous design, the shunt output was connected to battery ground so that no battery charging was possible. A relay to switch the BCR output to the preregulated bus or unregulated bus is housed in the unit.

In the redesigned power subsystem, the maximum battery storage capacity is 175 A-hr. The battery was expected to provide about 1000 W-hr during transit, the balance of the energy being supplied by the solar panel. Nominal expected battery energy remaining at touchdown is approximately 2450 W-hr.

2. Power Subsystem Performance

Performance of the electrical power subsystem was very satisfactory during the transit and postlanding phases of the *Surveyor VII* mission.

Expected and actual values of several power system parameters during the transit phase are presented in Table IV-12. The battery energy at liftoff was about 3625 W-hr (164 A-hr), which was the predicted nominal value. Following solar panel deployment after spacecraft separation and sun acquisition, solar panel voltage was 30.3 V with a current of 2.89 A. The BCR was connected to the preregulated bus and remained in that position until after touchdown. Solar panel output power was

about 5% above nominal, which can be attributed in part to greater-than-nominal solar intensity for the January 1968 launch period. The solar panel switch tripped out automatically due to high bus voltage about 6 hr after liftoff. About 20 min later, the *solar panel on* command was transmitted and the switch stayed on. During the next 5 hr, the switch tripped out five more times. This was normal operation of the BCR over-voltage-protection circuit resulting from battery charging during periods of minimum heater loads while the battery was nearly fully charged. This event had been predicted from results of spacecraft tests conducted in a solar-thermal-vacuum chamber.

Average solar panel current was 2.93 A at an average of 30.3 V during transit. Average BCR output current during the coast phase was 2.93 A compared to 2.60 A predicted. Although the BCR efficiency was not measured directly in flight, it was estimated to be close to the expected value of 94.6%. During high-power operation, the regulated loads were 3.9 A vs the predicted value of 3.3 A. The BR efficiencies of low- and high-power modes were 81% and 86%, respectively.

The average battery discharge current was 0.26 A during the first coast period; this was approximately 0.2 A lower than predicted owing to higher than anticipated solar panel output. Battery temperature averaged 79°F prior to midcourse, and battery pressure remained low, never exceeding 14.8 psia during the entire transit phase. The battery charge level followed the predicted profile closely, although the charge level remained slightly above predicted as illustrated in Fig. IV-14. Battery energy remaining at touchdown was estimated to be 2200 W-hr (102 A-hr).

After touchdown the power subsystem continued to perform satisfactorily. The two requirements imposed on the power system during lunar day operations were (1) supply the power required to support the engineering and scientific operations, and (2) recharge the battery to a fully charged condition prior to lunar sunset.

Typical spacecraft-regulated current requirements to support postlanding operations, including ASI, SM/SS, and TV camera operation are shown in Fig. IV-15.

Solar panel performance continued to be satisfactory throughout the lunar day. In addition to supplying power to the spacecraft for lunar operations, the solar panel was utilized to shade the compartments, the alpha

Table IV-12. Electrical power performance during transit

Parameter	Time period	Predicted	Actual
Battery energy, A-hr	Liftoff	165	164
	Touchdown	96	102
Average solar panel power, W	Coast phases	84	89
Average BCR output current, A	Coast phases	2.60	2.93
BCR efficiency, %	Coast phases	94.6	94.6
Regulated loads, A	High power	3.3	3.9
BR efficiency, %	Low power	80.5	81
	High power		86

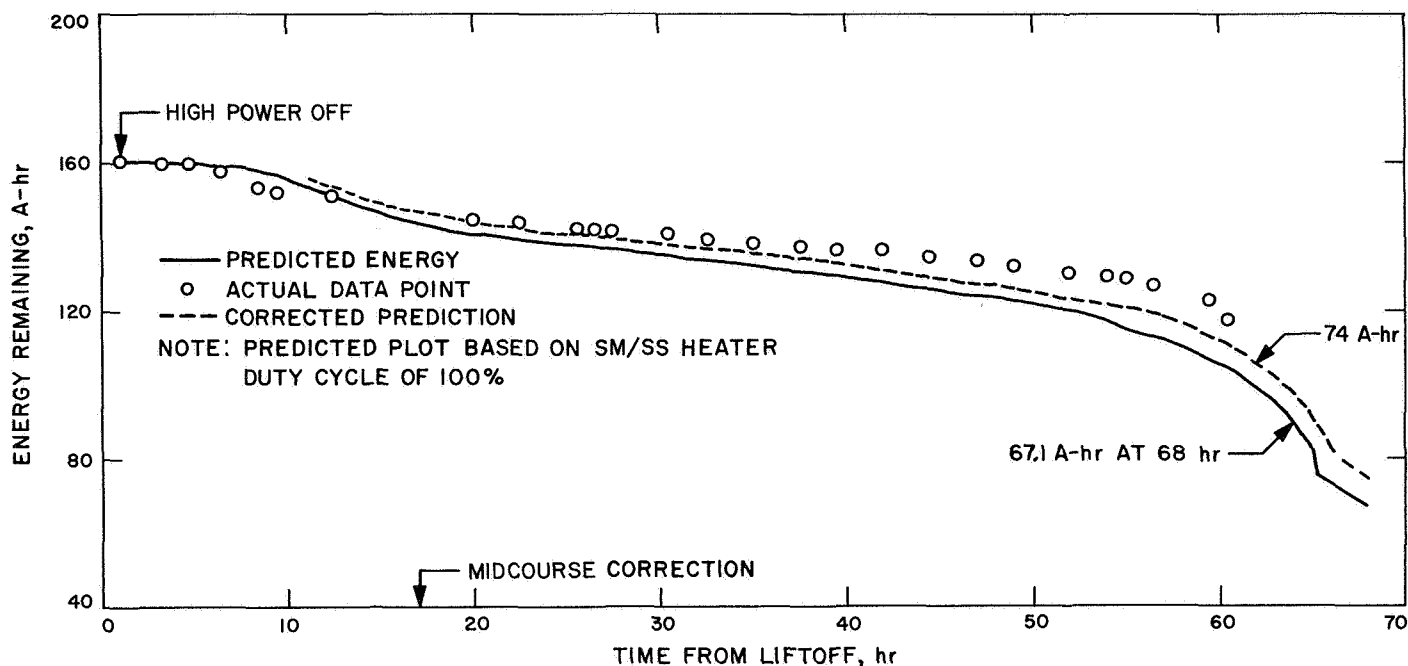


Fig. IV-14. Calculated battery energy profile during transit

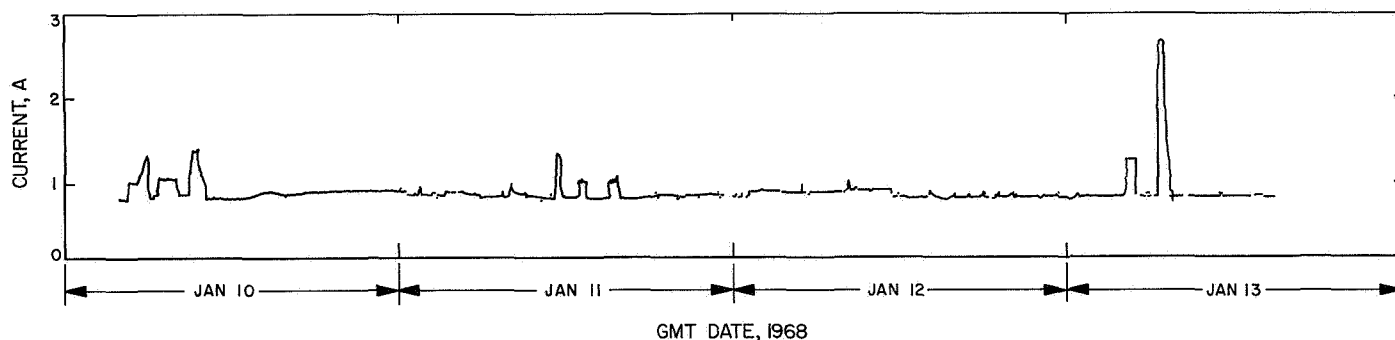


Fig. IV-15. Typical postlanding regulated current requirements

scattering electronics and sensor head, and the TV camera in order to provide a more comfortable environment. Figure IV-16 shows the solar panel voltage and current during a typical period of the lunar day. With about 62% charge remaining in the battery at touchdown, battery charging was not a major concern. The solar panel was never fully sun-oriented until the last 24 hours of the lunar day. The solar panel was positioned at all times approximately 15 to 45 deg ahead of the sun to prevent solar panel current from exceeding the desired battery charge rate, and to provide shading to the electronic compartment and TV camera.

Battery performance during the first lunar day is shown in Fig. IV-17. The battery reached a maximum charge of 173 A-hr just prior to sunset.

The prime consideration during lunar night operation was to spend the battery energy wisely in order to accomplish the following:

- (1) Maintain the battery temperature at $+20^{\circ}\text{F}$ as long as possible by dissipating power in compartment A until the battery was depleted to 45 A-hr. The 45-A-hr limit was determined from the results of lunar night survival tests. It represented (1) the energy storage level necessary to supply the spacecraft constant load requirements during cooldown and warmup of the battery to and from the temperature at which it would cease to provide power (zero-volt level), and (2) the minimum energy level necessary to prevent cell reversal.

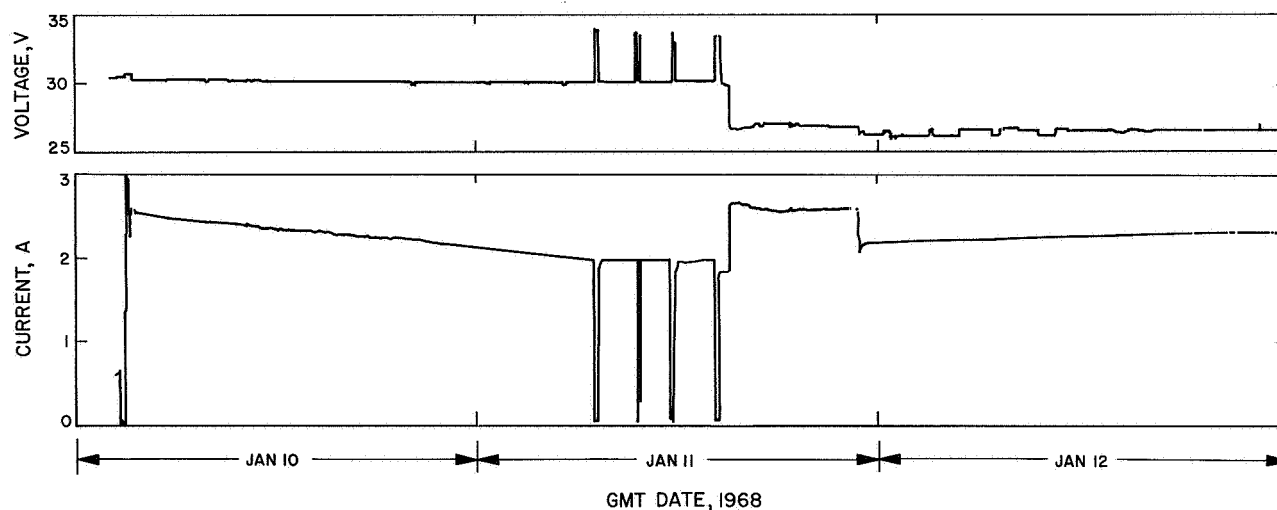


Fig. IV-16. Typical postlanding solar panel current and power output

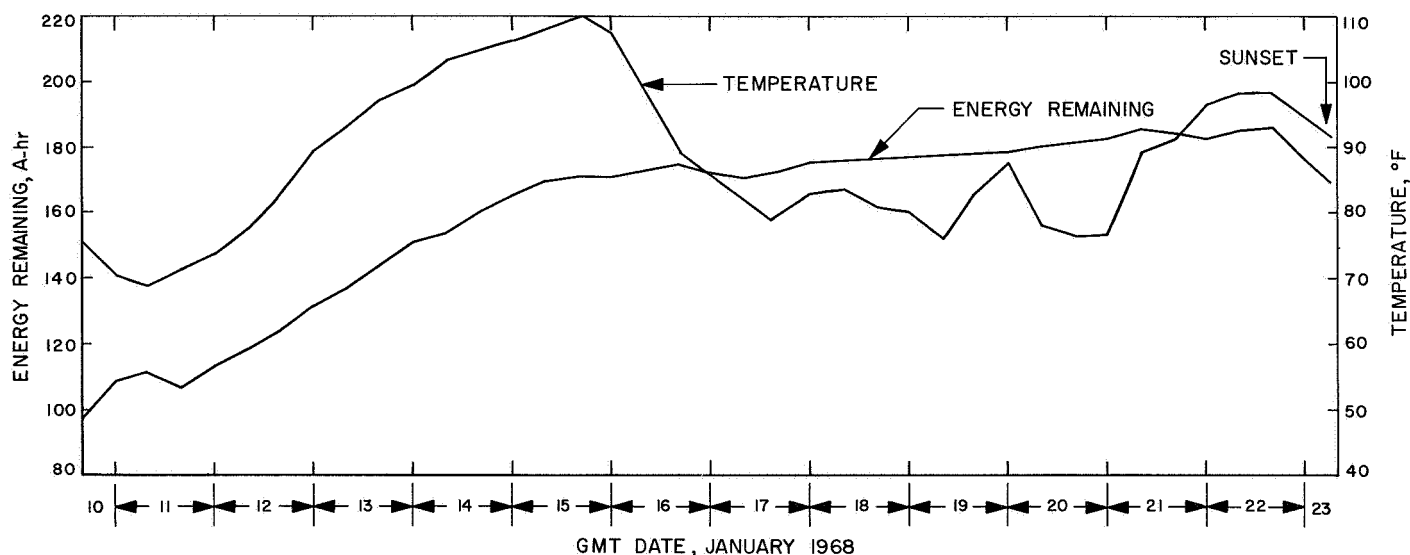


Fig. IV-17. First lunar day battery temperature and energy level

- (2) Prevent the battery temperature from dropping below -175°F . In tests performed at JPL, three batteries survived exposure to a simulated lunar night environment temperature of -175°F .

The spacecraft operated for about 79 hr after lunar sunset. The battery was expected to reach a minimum temperature of about $-250 \pm 30^{\circ}\text{F}$. The spacecraft responded and was operated during the second lunar day. However, the battery apparently sustained permanent damage. Battery temperature was high, indicating shorted cells, and battery pressure was low, possibly the result of a cracked manifold. Thus the power system could not support heavy loading.

E. Propulsion

The propulsion subsystem supplies thrust force during the midcourse correction and terminal descent phases of the mission. The propulsion subsystem consists of three vernier engines and a solid-propellant retrorocket motor. The propulsion subsystem responds to flight control subsystem preprogrammed sequences, sequences initiated by DSIF station command and sensor outputs.

1. Vernier Propulsion

The vernier propulsion subsystem supplies the thrust forces for the velocity vector correction portion of the

midcourse maneuver, attitude stabilization during retro-rocket motor burning, and attitude and velocity vector control during terminal descent after retro motor ejection from the spacecraft.

a. Vernier propulsion system description. The vernier propulsion system (VPS) consists of three thrust chamber assemblies and a propellant feed system, shown in the schematic of Fig. IV-18. The feed system is composed of three fuel tanks, three oxidizer tanks, a high-pressure helium tank, propellant lines, and valves for system arming, operation, and deactivation.

Fuel and oxidizer are contained in six tanks of equal volume, with one pair of tanks for each engine. Each tank contains a teflon expulsion bladder to permit complete and positive expulsion and to assure positive control under zero-g conditions. The oxidizer is nitrogen tetroxide (N_2O_4) with 10% by weight nitric oxide (NO) to depress the freezing point. The fuel is monomethyl hydrazine monohydrate ($MMH \cdot H_2O$). Fuel and oxidizer ignite hypergolically when mixed in the thrust chamber. The total minimum usable propellant load is 178.3 lb. The arrangement of the tanks on the spaceframe is illustrated in Fig. IV-19. Propellant freezing or overheating is prevented by a combination of active and passive thermal controls utilizing surface coatings, multilayered blankets, and electrical and solar heating. The propellant tanks are thermally isolated to insure that the spacecraft structure will not function as a heat source or heat sink.

Propellant tank pressurization is provided by the helium tank and high-pressure valves assembly (Fig. IV-20). The high-pressure helium is released to the propellant tanks by operation of a squib-actuated helium release valve. A single-stage regulator maintains the propellant tanks at a nominal working pressure of about 730 psi. Helium check and relief valves are located in a separate package on the spaceframe and are connected by a single line to the helium tank and high-pressure valve assembly. Filters at the inlet port of each relief valve assembly protect against contamination-induced leakage.

The check valves allow the flow of pressurizing helium to the propellant tanks but prevent the back flow of helium and propellant vapors from the propellant tanks to the pressure regulator or between fuel and oxidizer tanks. Helium relief valves protect the propellant tanks from excess pressure by venting helium from the system in the event of a helium pressure regulator malfunction.

The vernier engine thrust chambers (Fig. IV-21) are located near the hinge points of the three landing legs on the bottom of the main spaceframe. The moment arm of each engine is about 38 in. Engine 1 can be rotated ± 6 deg about an axis in the spacecraft XY plane for spacecraft roll (Z axis) control by means of a roll actuator which is unlocked by the same command that actuates the helium release valve. Engines 2 and 3 are not movable. The thrust of each engine, which is monitored by strain gages installed on each engine mounting bracket, can be throttled over a range of 30 to 104 lb. The specific impulse and mixture ratio vary slightly with engine thrust.

b. Vernier propulsion system performance. The *Surveyor VII* VPS performed normally throughout the entire transit phase, including midcourse correction and terminal descent. VPS parameters during launch and the pre-midcourse coast period were all well within their allowable limits. After completion of the pre-midcourse attitude change maneuvers, vernier propellant tank pressurization was commanded in accordance with the standard mission sequence by firing the helium release valve squib, allowing high-pressure helium gas into the inlet port of the helium pressure regulator. The regulator "locked-up" at 770 psia, which is well below the 838-psia relief valve cracking (venting) pressure. The propellant tank and helium tank pressures were stable and showed no signs of leakage.

A trajectory-correcting vernier engine firing time of 11.3-sec duration was executed on January 7 at 23:30:09 GMT. The VPS and the flight control subsystem successfully controlled the spacecraft attitude during this period. Table IV-13 shows the actual engine thrust levels compared with predicted levels. Note that the predicted

Table IV-13. Comparison of predicted and actual thrust commands for midcourse phase and case separation phase of terminal descent

Phase	Engine			Total thrust
	1	2	3	
Midcourse				
Predicted thrust, lb	78.5	78.5	73.0	230.0
Actual thrust, lb	79.0	79.2	73.6	231.8
Case separation phase of terminal descent				
Predicted thrust, lb	95.5	93.5	87.5	276.5
Actual thrust, lb	95.5	95.4	88.2	279.1

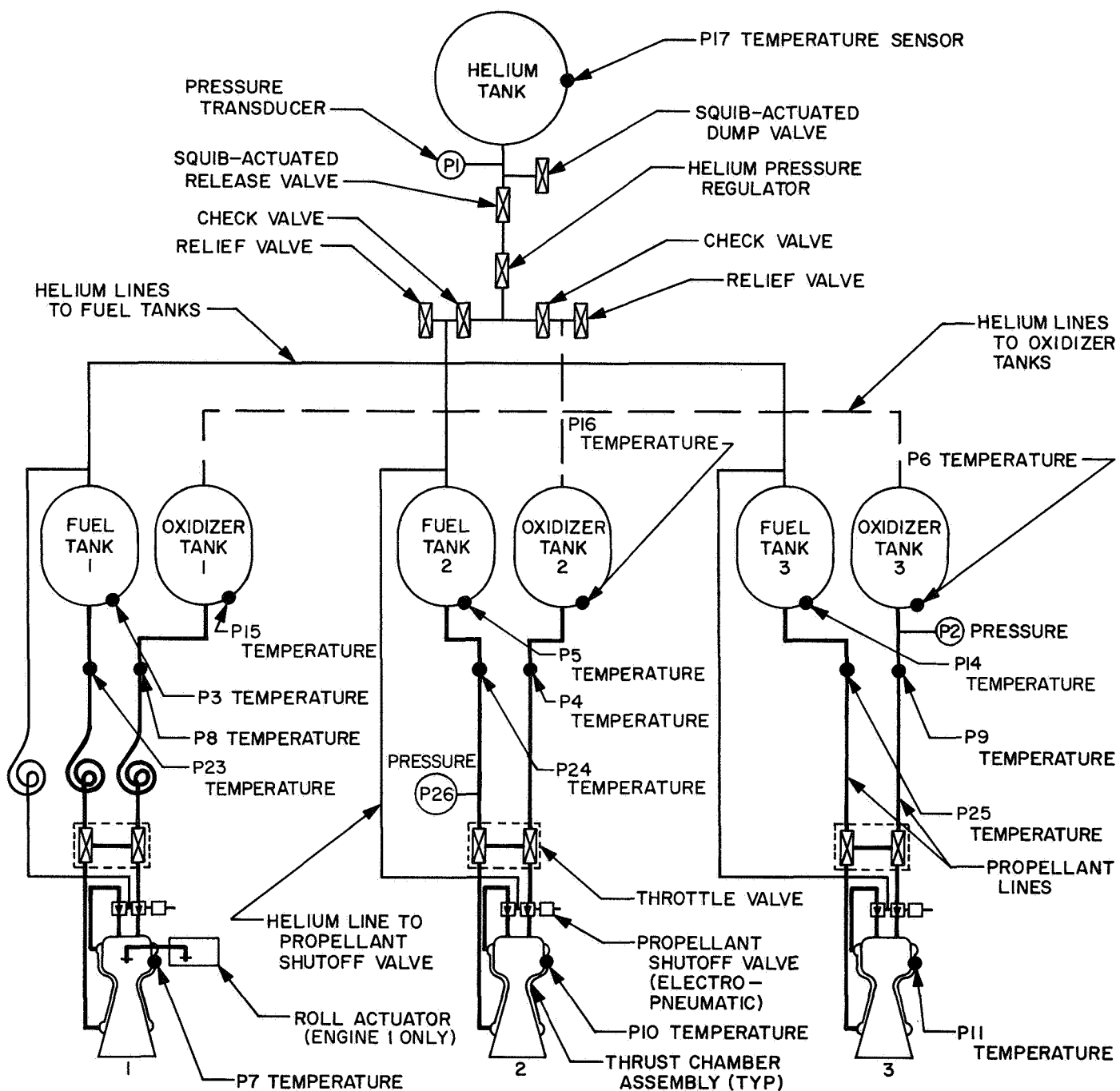


Fig. IV-18. Vernier propulsion system schematic

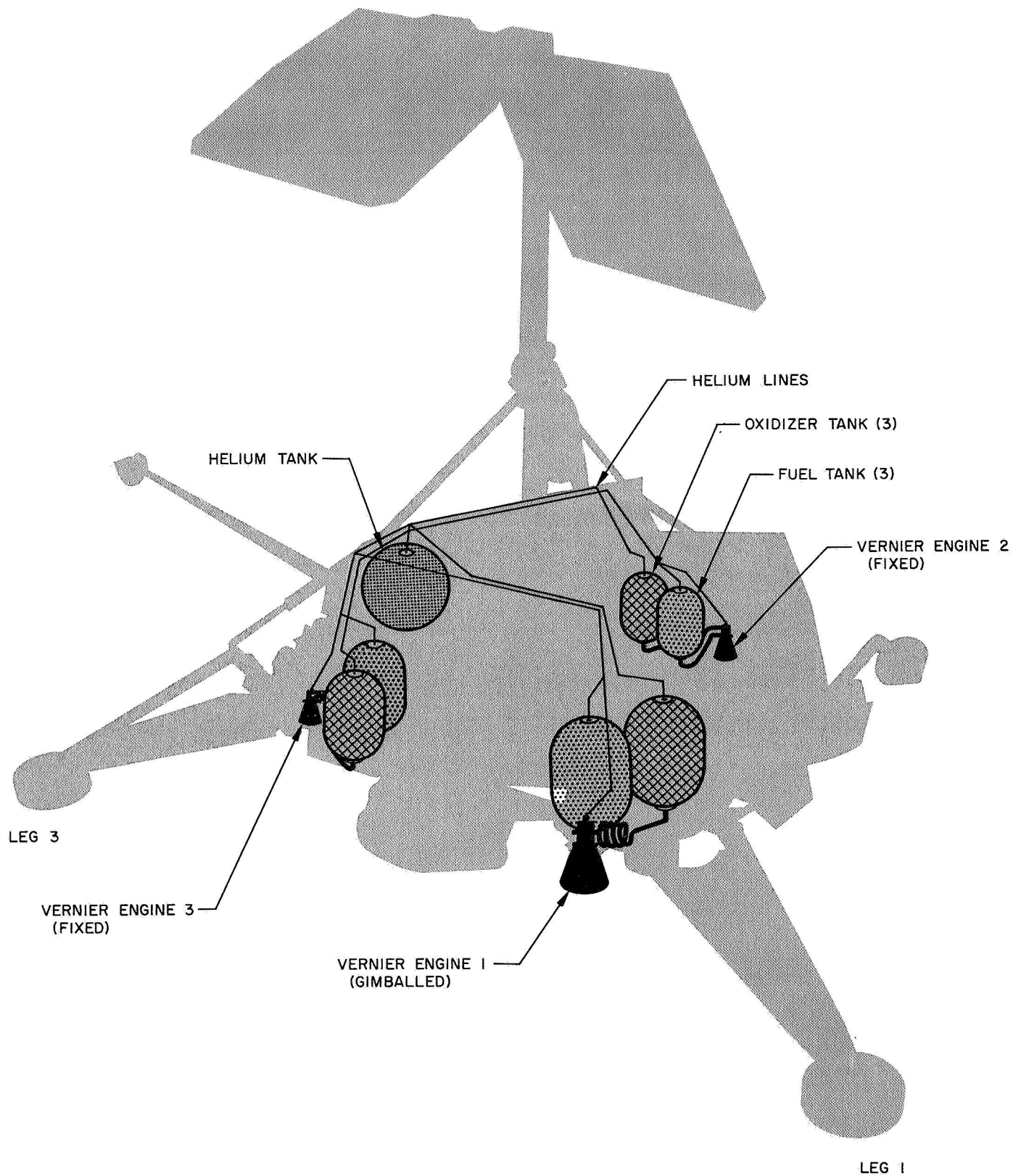


Fig. IV-19. Vernier propulsion system installation

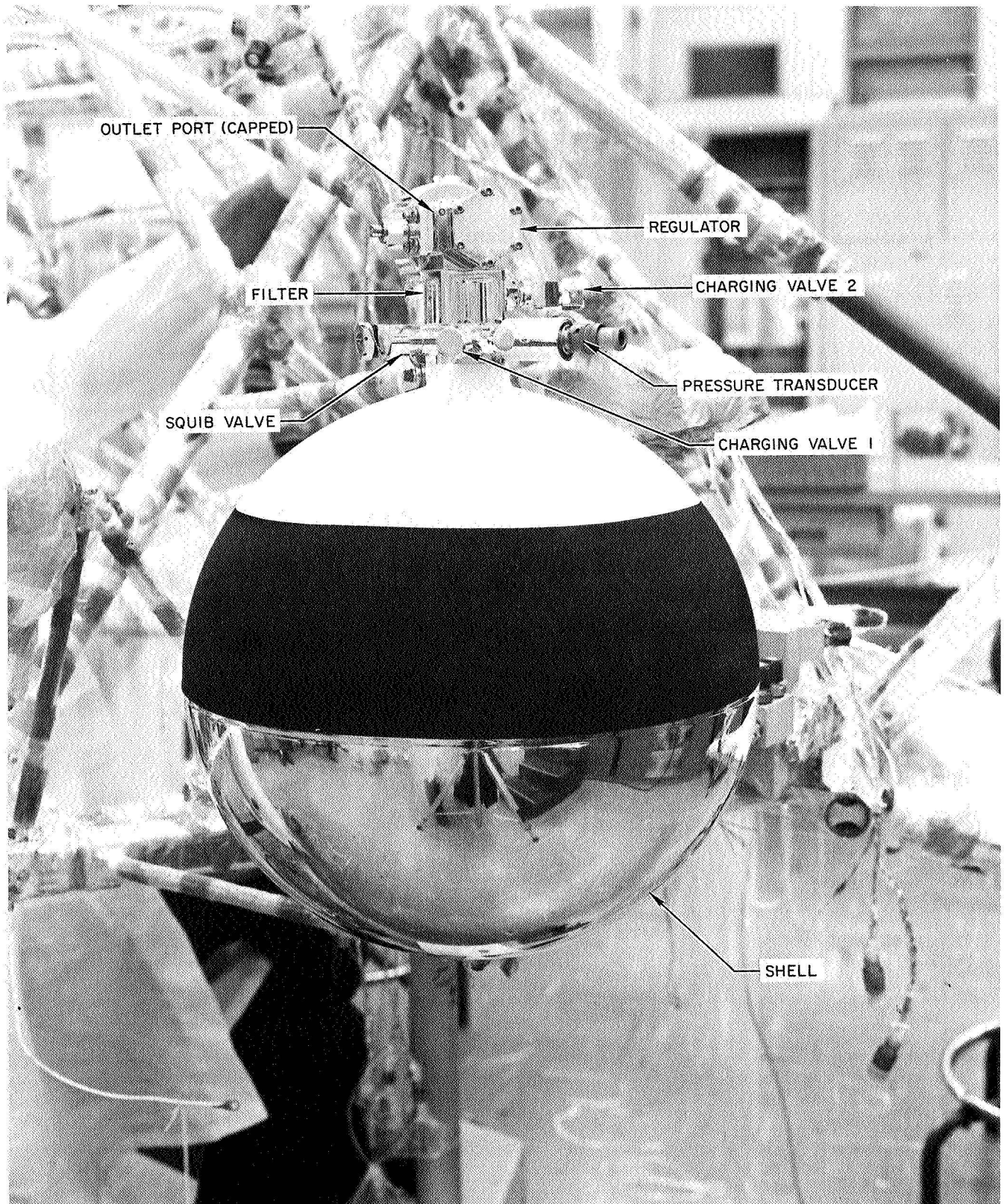


Fig. IV-20. Helium tank assembly

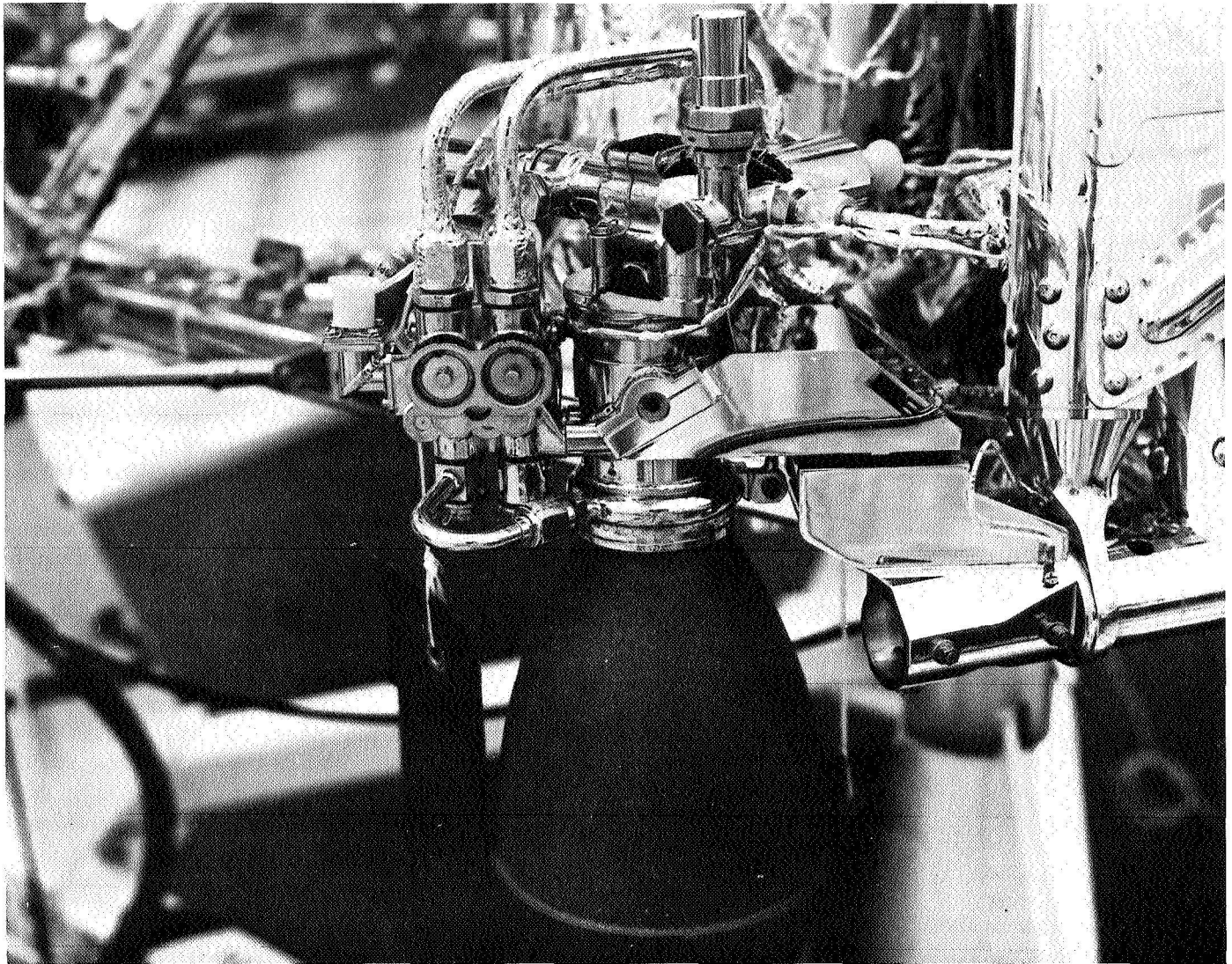


Fig. IV-21. Vernier engine thrust chamber assembly

and actual thrust commands agree within 2 lb. Engine shutoff at midcourse was very smooth, as shown by a maximum attitude perturbation of much less than 1 deg (10 deg is allowable). The calculated shutdown time dispersion between engines was less than 0.010 sec.

During the post-midcourse phase, VPS parameters continued to be normal and well within allowable limits. Figure IV-22 shows temperature extremes during the transit and lunar phases of the *Surveyor VII* mission.

Vernier ignition for terminal descent occurred at 01:02:15 GMT on January 10, followed 1.1 sec later by main retrorocket ignition. Both ignitions were very

smooth, as indicated by only small perturbations in the gyro angles. Differential throttling commands during the main retro phase indicated a total main retro disturbance moment less than 400 in.-lb. This is well below the 1800-in.-lb moment allowable. Vernier engine thrust commands and gyro angles were very smooth during the main retro burn phase and indicated stable spacecraft performance. Retro burnout and case separation also occurred smoothly. Radar-controlled descent after retro motor ejection was normal, and vernier engine cutoff occurred just above the surface. Propellant consumption data, presented in Table IV-14, showed that adequate amounts of propellant remained after landing to perform a posttouchdown vernier engine firing if one had been required.

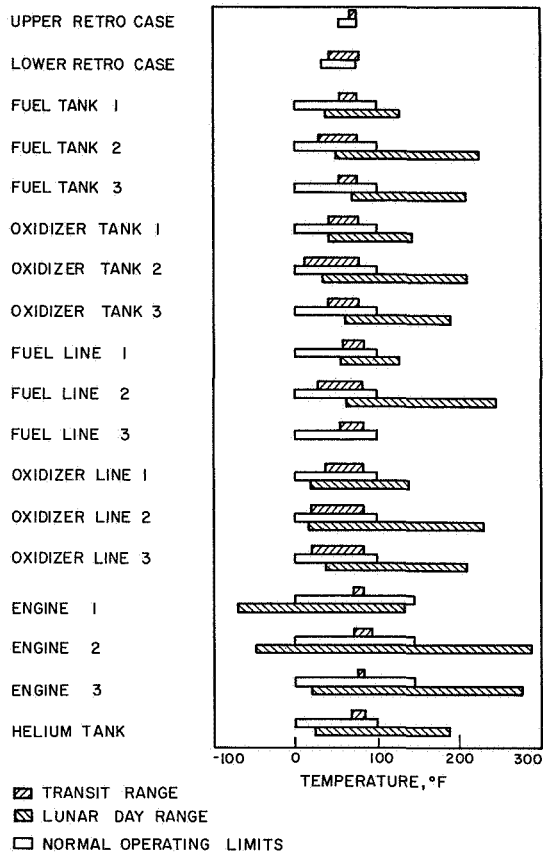


Fig. IV-22. Surveyor VII propulsion system temperature ranges during transit and first lunar day

Table IV-14. Vernier propellant usage, lb

	Total	Fuel	Oxidizer
Propellant loaded	183.83		
Unusable propellant	2.12		
Usable propellant	181.71	73.71	108.0
Used at midcourse	9.6	3.85	5.75
Remaining usable	172.11	69.86	102.25
Used at terminal	142.4	57.57	84.81
Remaining usable	29.71	12.29	17.44
Unusable propellant	2.12		
Total remaining after landing	31.83		

The latitude of the landing site, approximately 40°S, and the spacecraft landed orientation, negative Y axis of the spacecraft 22.5 deg west of north, resulted in high temperatures of propulsion subsystem components located on Legs 2 and 3. These engines, lines, and propellant tanks were subjected to nearly continuous solar heating throughout the lunar day. The southern latitude of the landing site also resulted in low sun elevations. This made it impossible to use the planar array and solar panel for shading the Leg 2 and 3 engines and propellant tanks and maintaining them at operational temperatures. This shading technique had been successfully used on Surveyor VI to extend the life of the propulsion system and to lower propulsion system temperatures, thus permitting a successful postlanding spacecraft hop experiment. Table IV-15 presents vernier propulsion system temperatures at different times through the lunar day.

During most of the lunar day, many of the vernier propulsion system components were at temperatures above their upper survival limits. This continued heating of the propellant tanks caused pressures in the fuel and oxidizer tanks to rise high enough to cycle the relief valves, thereby venting sufficient fuel and oxidizer to lower the pressure. During the first lunar day, the fuel relief valve cycled four times and the oxidizer relief valve cycled 12 times. After its twelfth cycle the oxidizer

Table IV-15. Vernier propulsion system temperatures (°F) during the lunar day

Time after touchdown, hr Time before sunset, hr	3 312	81 234	159 156	237 78	315 0
Leg 1 temperatures					
Engine	120	128	86	77	12
Oxidizer line	98	128	109	98	38
Fuel line	88	123	110	105	56
Oxidizer tank	71	136	133	120	64
Fuel tank	76	125	119	112	67
Leg 2 temperatures					
Engine	204	288	230	134	-42
Oxidizer line	106	220	222	166	56
Fuel line	98	230	228	164	66
Oxidizer tank	48	182	209	190	116
Fuel tank	61	204	219	174	96
Leg 3 temperatures					
Engine	56	133	233	272	199
Oxidizer line	60	135	177	210	138
Fuel line	—	—	—	—	—
Oxidizer tank	64	114	159	186	166
Fuel tank	71	104	181	208	170
Helium tank	32	169	190	170	110

relief valve leaked whenever it was exposed to direct sunlight. A list of the anomalies of the vernier propulsion system while on the lunar surface is presented in Table IV-16.

At 21:00 GMT on January 20, 55 hr prior to sunset, a fuel leak developed at Engine 2. This leak continued for more than 50 hr at a low rate and apparently terminated as sunset approached when decreasing engine temperature caused the fuel's viscosity to rise. At 02:00 on January 22, 29 hr after the Engine 2 fuel leak began, the oxidizer relief valve cycled and the oxidizer check

valve failed to open properly, causing a large difference (130 psi) between the oxidizer tank pressure and the regulator outlet pressure to exist. At 05:00 on January 23, 51 hr later, the oxidizer tank pressure came up to the regulated pressure (the check valve opened). It is hypothesized that these malfunctions of the oxidizer check and relief valves resulted from the high temperatures to which the system was exposed earlier in the lunar day.

At approximately 09:30 on January 23, 5½ hr after sunset, a leak developed on the pressurization side of the oxidizer system. This pressurant loss was probably due

Table IV-16. Postlanding vernier propulsion system anomalies

Event	GMT Day Hour	Telemetry indications	Probable point of failure and cause
Fuel leakage from Engine 2 (approx 1 lb)	Jan 20 21	Rapid 90°F negative change in Engine 2 temperature as fuel vaporizes and cools engine Elevated fuel line temperature as line is heated by warm propellant Analysis of pressure and temperature data indicates a loss of liquid fuel	Fuel poppet in Engine 2 shutoff valve. Seat degradation caused by high temperature exposure (288°F)
Oxidizer check valve stuck closed	Jan 21 07	Oxidizer pressure falls below the helium regulator pressure Correct regulator operation confirmed by fuel pressure data	Oxidizer check valve. Seat degradation caused by high temperature exposure
Reduced crack and reseal pressures of oxidizer relief valve	Jan 22 02	Rapid loss of 100-psi oxidizer pressure at a level less than the relief valve cracking pressure Relief valve had shown erratic behavior on January 14	Oxidizer relief valve seat coining and erosion caused by venting while at high temperature
Oxidizer check valve opened slightly and stuck closed again	Jan 22 18 and Jan 23 05	Rapid gain of 60 psi on oxidizer pressure Oxidizer pressure rose rapidly and stabilized at 760 psia	Oxidizer check valve seat degradation caused by high temperature exposure
Oxidizer relief valve leakage	Jan 23 09	Oxidizer pressure fell below its regulation level and continued dropping until data was lost Analysis of pressure and temperature data indicated a net loss of pressurant from the oxidizer side	Oxidizer relief valve seat coining and erosion caused by venting at high temperatures
Loss of liquid oxidizer from Oxidizer Tank 3 (approx 4 lb lost)	Jan 24 00	The general behavior of Oxidizer Tank 3 during postsunset cooldown indicated the tank liquid content to be approximately normal at sunset and that later the tank was nearly empty An increase in the temperature decay rate indicated a large reduction of tank thermal capacity Tank temperature profile during propellant freezing indicates little oxidizer remaining	Oxidizer Tank 3 liquid leakage probably at tank base O-ring seal. High temperatures cause severe chemical attack by oxidizer of Viton A O-ring material
Continuing gas side leak on the fuel side	After sunset	Analysis of fuel side pressure and temperature data indicated the continued loss of pressurant from the fuel side	Gas leakage through the Engine 2 fuel poppet in the shutoff valve following the depletion of propellant from fuel tank 2 noted above

to relief valve seat degradation during venting and high temperatures. From this time onward the oxidizer check valve also failed to operate properly.

At approximately 23:00 on January 23, 19 hr after sunset, an additional liquid oxidizer leak from Tank 3 developed.

In summary, the propellant system retained propellant and pressure for 260 hr after landing on the moon. Subsequent to this time the effects of high lunar temperatures resulted in propellant leaks from the parts of the subsystem associated with Legs 2 and 3 and in malfunctions of the oxidizer check and relief valves. The vernier propulsion system on *Surveyor VII* survived 32 hr longer than on any other spacecraft, this under temperature conditions more severe than observed on any previous *Surveyor* spacecraft.

2. Retrorocket Motor

The retrorocket motor performs the major portion of the deceleration of the spacecraft during terminal descent.

a. Retro motor description. The *Surveyor VII* retro motor was a spherical propellant unit with a partially submerged nozzle to minimize overall length (Fig. IV-23). Including its thermal insulating blankets, the motor weighed approximately 1445 lb, of which 1300 lb was propellant. The motor design utilizes a carboxyl/terminated polybutadiene composite-type propellant and conventional grain geometry.

The motor case is attached at three points on the main spaceframe near the landing leg hinges with explosive nuts for postburnout separation from the spacecraft. Friction clips around the nozzle flange provide attachment points for the altitude marking radar (AMR).

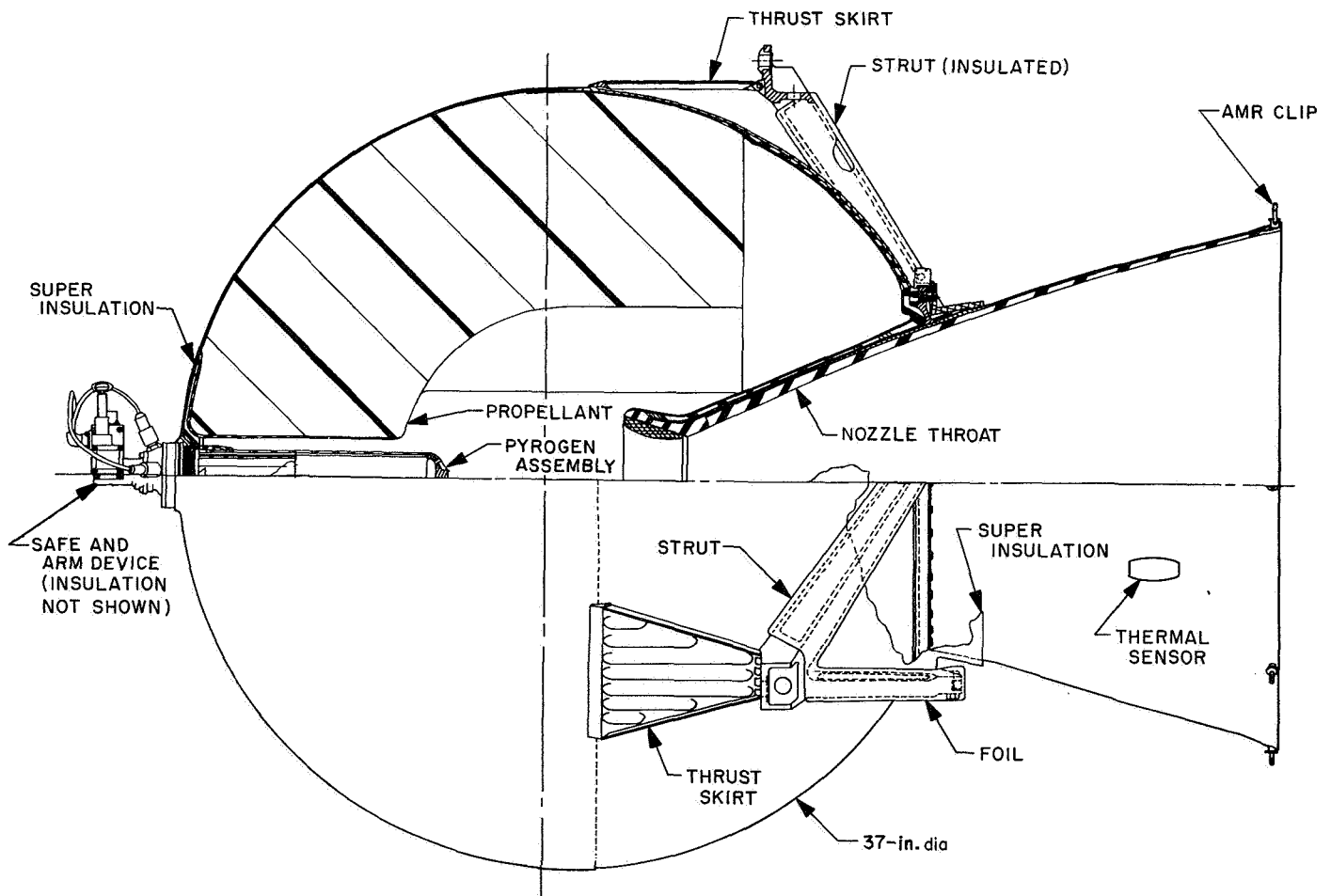


Fig. IV-23. Main retrorocket motor

The thermal control design of the retrorocket motor is completely passive, depending on its own thermal capacity and insulating blanket (21 layers of aluminized Mylar plus a cover of aluminized Teflon). The prelaunch temperature of the unit is $70 \pm 5^\circ\text{F}$. At terminal maneuver, when the motor is ignited, the propellant will have cooled to a thermal gradient with a bulk average temperature of about 50 to 55°F .

The AMR triggers the terminal maneuver sequence, during which retro motor firing is initiated. The retrorocket gas pressure then ejects the AMR. The motor operates at a thrust level of 8000 to 10,000 lb for approximately 42 sec at an average propellant temperature of 55°F .

b. Retro motor performance. Beginning at a uniform launch temperature of approximately 70°F , the retro

motor cooled at the predicted rate to a thermal gradient condition having a bulk average temperature of 54°F at the time of ignition. At this temperature, the predicted burn time to the 3500-lb thrust level (approximately 3.8-g level) at tailoff (burnout decay) was 42.78 sec. The post-flight doppler data analysis indicates an actual burn time of 42.74 sec to the 3500-lb thrust level, or a difference of 0.1%. Retro thrust vs time traces, reconstructed from both accelerometer and doppler data, are shown in Fig. IV-24. These compare very well with the predicted trace, which is also shown. The maximum thrust developed was 9200 lb, the same as the predicted value, while the total impulse delivered, based on analysis of velocity increment data, was approximately 0.2% higher than predicted.

The small variations in outputs of the gyros and inputs of the vernier engines indicated a stable spacecraft

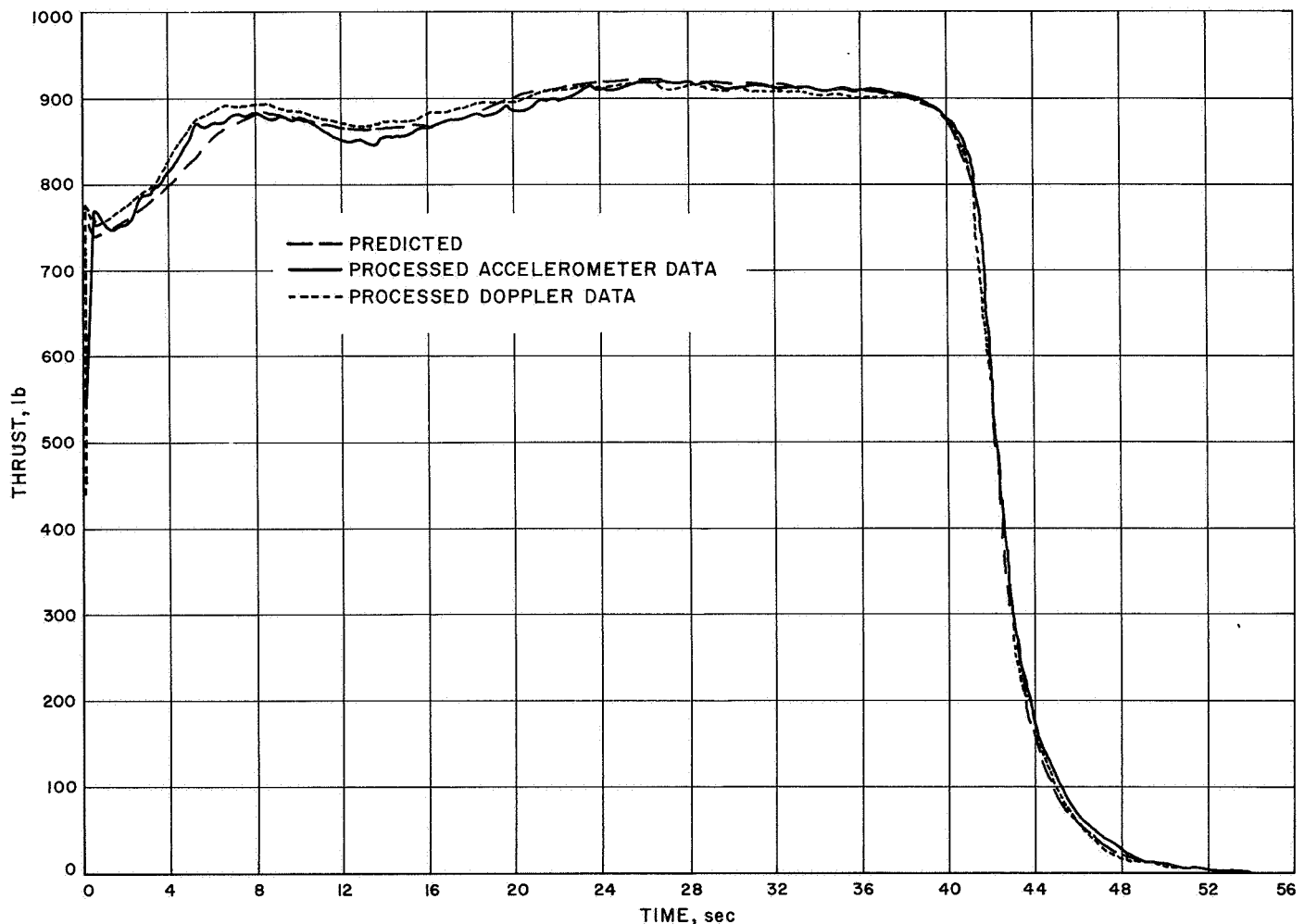


Fig. IV-24. Main retro motor thrust vs time

during the retro motor burn. Retro motor ignition produced a short-duration attitude torque of approximately 336 in.-lb and a roll torque of approximately 52 in.-lb. Following this ignition transient, the vernier engines operated nearly uniformly except for one short disturbance of 384 in.-lb approximately 39 sec after retro ignition. The maximum roll torque correction required after ignition was approximately 24 in.-lb. Assuming all this torque was produced by the main retro motor, the roll torque was well below the 90 in.-lb capability of the spacecraft attitude control system.

Separation and ejection of the retro motor resulted in little disturbance to the spacecraft flight attitude.

F. Flight Control

The flight control subsystem provides spacecraft velocity and attitude control during transit from the time of spacecraft separation from the *Centaur* vehicle to spacecraft touchdown on the lunar surface. The basic flight control functions include:

- (1) Attitude stabilization and orientation during transit.
- (2) Midcourse velocity correction based on ground commands.
- (3) Retro ignition and ejection and vernier descent control for soft-landing of the spacecraft.

1. Subsystem Description

The flight control subsystem consists of sensing elements, mode switching and control electronics, and vehicle control elements functionally arranged as shown in Fig. IV-25.

The principal references used by the spacecraft are inertial, celestial, and lunar; each is sensed respectively by inertial, optical, and radar sensors. The control electronics process the reference sensor outputs and earth-based commands to generate the necessary control signals for use by the vehicle control elements. The vehicle control elements consist of the attitude-control cold-gas-jet activation valves and gas supply system, the vernier engine throttlable thrust valves and controllable

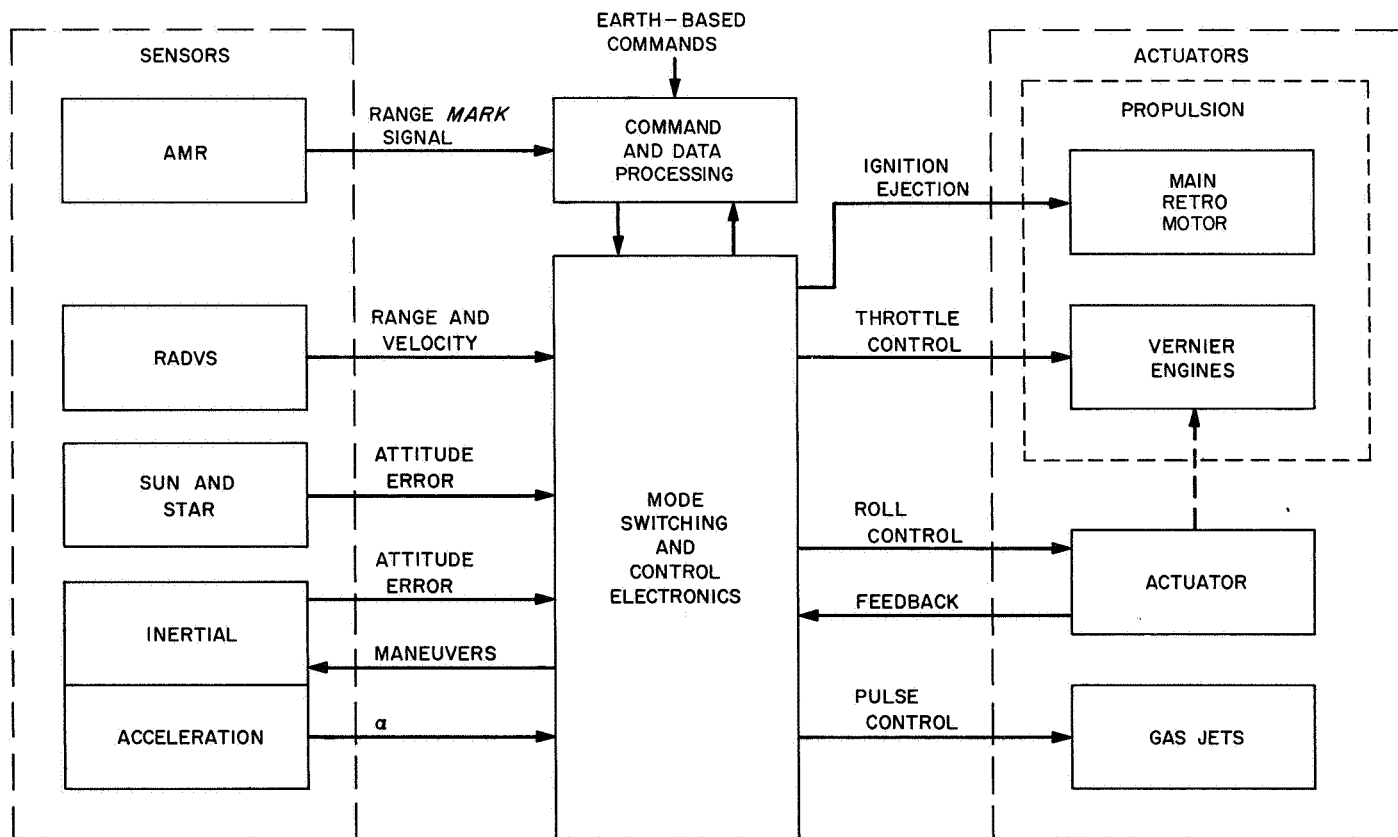


Fig. IV-25. Simplified flight control functional diagram

gimbal actuator, and the main retro igniter and retro case separation pyrotechnics.

The gas-jet attitude-control system is a cold gas system using nitrogen as a propellant. This system consists of a gas supply system and three pairs of solenoid-valve-operated gas jets interconnected with tubing (Fig. IV-26). The nitrogen supply tank is initially charged to a nominal pressure of 4600 psia. Pressure to the gas jets is controlled to 40 ± 2 psia by a regulator.

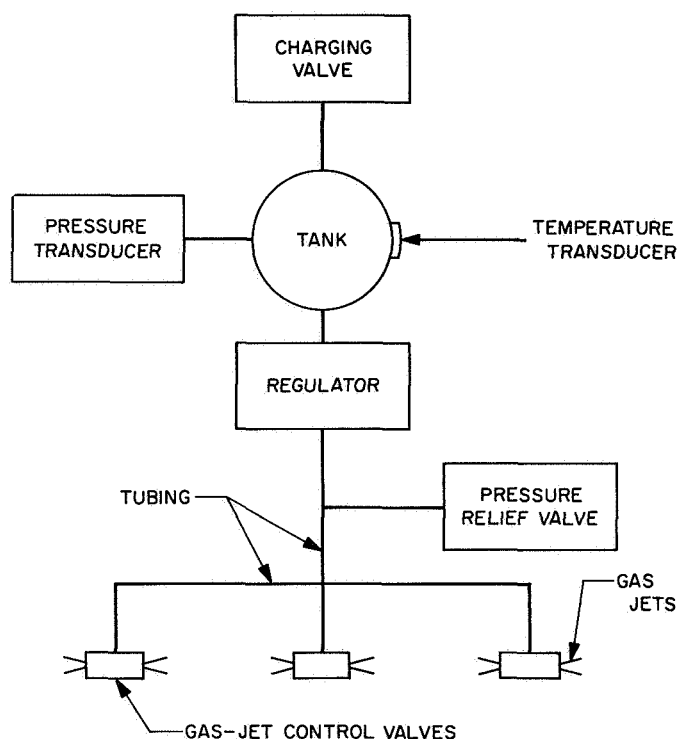


Fig. IV-26. Gas-jet attitude control system

Vehicle response in attitude, acceleration, and velocity is controlled as needed by various "control loops" throughout the coast and thrust phases of flight, as shown in Table IV-17. Upon separation of the spacecraft from the *Centaur*, stabilization of the spacecraft separation rates is achieved through activation of the gas jet system and use of rate feedback gyro control (rate mode). After rate capture, inertial mode is achieved by switching to position feedback gyro control.

Because of the long duration of the coast phase and the small unavoidable drift error of the gyros, celestial references are used to provide the desired attitude of the

Table IV-17. Flight control modes

Control loop	Flight phase	Modes	Remarks
Attitude control loop			
Pitch and yaw	Coast	Rate Inertial Celestial	Gas jet matrix signals
	Thrust	Inertial Lunar radar	Vernier engine matrix signals
Roll	Coast	Rate Inertial Celestial	Leg 1 gas jet signals
	Thrust	Inertial	Vernier Engine 1 gimbal command
Acceleration control loop			
Thrust axis	Thrust (mid-course) Thrust (terminal descent)	Inertial (with accelerometer) Inertial (with accelerometer)	Nominal 3.22 ft/sec ² Minimum 4.77 ft/sec ² Maximum 12.56 ft/sec ²
Velocity control loop			
Thrust axis	Thrust	Lunar radar	Command segment signals to 43-ft altitude Constant 5-ft/sec velocity signals to 13-ft altitude
Lateral axis	Thrust	Lunar radar	Lateral/angular conversion signals

spacecraft. Following a 51-sec delay after spacecraft electrical disconnect from the *Centaur*, a flight control timer automatically initiates the sun acquisition sequence by commanding a negative roll maneuver. The sun is first acquired by the acquisition sun sensor, which has a 10-deg-wide by 196-deg-fan-shaped field of view that includes the spacecraft Z axis and is centered about the minus X axis. The roll command is terminated after initial sun acquisition, and a positive yaw command is automatically initiated which allows the narrow-view primary sun sensor to acquire and lock-on the sun. A secondary sun sensor, mounted on the solar panel, provides a backup for manual acquisition of the sun if the automatic sequence fails.

Automatic Canopus acquisition and lock-on are normally achieved after initiation of a roll command from earth. This occurs because the Canopus sensor angle is preset with respect to the primary sun sensor prior to

launch for each mission. Star mapping for Canopus verification is achieved by commanding the spacecraft to roll while the spacecraft maintains sun lock.

The coast phase is performed with the spacecraft in the celestial-referenced mode except during initial rate-stabilization, midcourse and terminal descent maneuvers, and gyro drift checks, when inertial references (gyros) are used.

Midcourse velocity correction capability is provided by means of the vernier engine throttle valves, a precision timer, and an accurate acceleration sensing device. The difference between the command acceleration level and the output from the accelerometer provides an error signal which is used to command the throttle valves for the required thrust level. The timer controls the duration of vernier thrusting in accordance with a time interval preset by earth command.

The terminal maneuver descent sequence has been described in detail in Section IV-A-16. The flight control subsystem provides initial orientation of the main retro motor thrust vector and automatic sequencing after the lunar reference is first established by a signal from the AMR. Most of the approach velocity is removed by the solid-propellant retro motor during the initial phase of terminal descent. Spacecraft attitude during this phase is inertially stabilized using the gyros and differential throttling of the vernier engines.

During the vernier phase of descent, which follows main retro burnout and ejection, a sophisticated flight control technique is utilized that includes the use of radars to obtain range and velocities. The radar information is used by the flight control subsystem during the vernier phase of descent to compute longitudinal and lateral velocity commands for controlling the total vernier engine thrust to achieve the desired descent profile (approximately constant acceleration). The velocity data is applied to the attitude control loop to produce a near-gravity turn during descent by aligning the spacecraft thrust axis with the velocity vector.

2. Flight Control Performance

The flight control performed in an almost perfect manner during all phases of the last *Surveyor* mission. Only one anomaly was detected and it was of a non-critical nature. The anomaly prevented automatic Canopus lock and required the transmission from earth of a "manual lock" command to establish lock.

a. Launch phase. Adequate data was received at the SFOF from launch to approximately $L + 13$ min. However, there were losses of data at the following times:

$L + 27$ to $L + 32$ min

$L + 33$ to $L + 37$ min

The last period of data outage included spacecraft separation.

Most of the separation data relative to spacecraft attitude changes was lost and no estimate could be made of the separation-induced tipoff angular rates based on spacecraft gyro data. However, the rates were reduced to zero at the start of the sun acquisition sequence, which implied normal spacecraft/*Centaur* separation. As described in Section III-E-6, *Centaur* telemetry also indicated normal separation.

b. Sun acquisition. The sun acquisition sequence was automatically executed, resulting in primary sun sensor (center cell) lock-on. The acquisition sun sensor was illuminated after a negative roll of 224 deg. A positive yaw of 37 deg then established sun-lock. The sun acquisition sequence required about 8 min and 43 sec.

c. Canopus acquisition. Based on laboratory measurements of star intensities with a $1.0 \times$ Canopus sun channel gain for this particular sensor, it was estimated that, with an expected $1.10 \times$ Canopus gain, three stars, including Canopus, might be observed. In addition there existed the possibility that two pairs of close proximity stars might be observed as single, albeit erratic, stars.

The analog recorder traces of star angle and star intensity indicated four clearly distinguishable stars plus two wide, low-intensity signals and a 45-deg-wide high-intensity signal. The angular spacing of these signals compared with previously calculated star, earth, and moon angles permitted positive identification of Canopus, Alpha C Venaticorum, Mizar, the star groupings of Gamma U Minoris/Kochab and Caph/Shedar/Zeta Cassiopeiae plus the moon and the earth.

Table IV-18 indicates observed vs precalculated angles of objects plus telemetered intensity values. The roll angles were obtained by multiplying the incremental time from the start of roll by the average roll rate. The average roll rate was determined to be 0.502 deg/sec based on the time required to roll from the first peak value of Canopus intensity to the second peak value.

Table IV-18. Surveyor VII star map analysis (based on SFOF real-time data)

GMT (January 7, 1968)	Object (or event)	Roll angle, deg	Angle from Canopus, deg		Peak telemetered intensity, V
			Observed	Predicted	
14:24:06.9	(Start of roll)	0	-268.8	—	—
14:25:03.9	Particle 1	28.6	-240.2	—	1.12
14:25:29.1	Alpha C Venaticorum	41.3	-227.5	-227.3	0.67
14:26:03.6	Mizar and Particle 2	58.6	-210.2	-209.3	0.78
14:26:49.9	Gamma U Minoris/Kochab	81.8	-187.0	-188.2/ -187.4	0.64
14:28:27.4	Caph/Shedar/Zeta Cassiopeiae	130.8	-138.0	-142.3/ -138.2/ -135.8	0.72
14:30:02.4	Moon	178.5	-90.3	-90	0.74
14:33:02.4	Canopus	268.8	0	0	4.57
14:36:02.9	Earth	359.4	90.6	91	2.73
14:37:27.4	Alpha C Venaticorum	401.9	132.8	132.7	0.67
14:38:03.4	Mizar	419.9	151.1	150.7	0.77
14:38:46.5	Gamma U Minoris/Kochab	441.6	172.8	171.8/ 172.6	0.65
14:40:23.5	Caph/Shedar/Zeta Cassiopeiae	490.3	221.5	217.7/ 221.8/ 224.2	0.72
14:41:56.5	Moon	536.9	268.1	270	0.71
14:44:59.5	Canopus	628.8	0	0	4.59
14:45:00.3	(End of roll)	629.2	0.4	—	—
14:47:33.3	(Manual lock-on)	—	—	—	—
	Canopus, after acquisition	—	—	—	4.95

Since the Canopus lock-on signal did not appear when the spacecraft rolled past Canopus during the first revolution, it was decided to "manually" stop the roll maneuver when Canopus appeared in the sensor field of view during the second revolution, and then, after transient settling, to acquire Canopus by sending the manual lock-on command. At 14:45:00.3 GMT on January 7, telemetry signals indicated the end of roll when Canopus was 0.4 deg past the center of the field of view. At 007:14:47:32 GMT, the manual lock-on command was transmitted, and the star angle telemetry signal (FC-12) became the roll error telemetry signal which then nulled to within the roll optical deadband.

All star intensity values were greater than expected, leading to the conjecture that any or all of the following conditions prevailed:

- (1) Earth-based intensity measurements were too low owing to incorrect simulation of sun and/or star intensities.
- (2) The $0.8 \times$ Canopus sun filter installed for Surveyor VII was greater than 0.8.
- (3) The sun channel could have been partially blocked by a small particle, which would result in an apparent increase in the value of the sun filter.
- (4) Sun intensity was lower than predicted or star intensities were all higher than predicted.

Based on the experience of previous flights, wherein a fairly wide range of effective gains was observed, it is judged that several of the above conditions probably

combined to yield a sufficiently high effective gain, giving a star signal higher than the upper gate of the Canopus lock-on circuit.

d. Midcourse maneuvers and velocity correction. The maneuver combination selected to orient the spacecraft in the desired direction for the midcourse velocity correction consisted of a negative 3.1-deg roll maneuver, followed by a positive 117.1-deg yaw maneuver. The actual maneuver magnitudes were later verified as -3.15 deg of roll and $+117.008$ deg of yaw.

An attempt was made to reduce the optical mode limit-cycle contribution to the pointing error by initiating the attitude maneuvers at the respective limit-cycle null point. The following data indicates the optical errors that existed at the start of each maneuver:

$$\text{Roll} = -0.055 \text{ deg}$$

$$\text{Yaw} = +0.110 \text{ deg pitch} \\ -0.135 \text{ deg yaw}$$

The pre-midcourse attitude maneuver magnitudes were not corrected for gyro drift.

For the midcourse velocity correction, a quantity of 114 bits or 11.35 sec was entered into the magnitude register. Vernier engine ignition occurred at approximately 23:30:10.4 GMT on January 7. Ignition was smooth, with maximum pitch and yaw attitude changes of -0.08 and -0.20 deg, respectively. A burn time of 11.36 sec was verified.

The total indicated thrust based on the thrust commands of the vernier engines was approximately 231.8 lb, which compares to the expected level of 230 lb based on a separated spacecraft weight of 2289.23 lb.

Following the midcourse velocity correction, the reverse attitude maneuvers were commanded, resulting in reacquisition of the sun. The manual lock command had to be sent to obtain reacquisition of Canopus for reasons previously discussed.

e. Gyro drift measurements. Nine gyro drift checks were made during the flight. One was a check of roll axis only and eight were checks of drift about all three axes. Two gyro drift checks were made prior to the midcourse velocity correction. Based on the results of these tests, the following gyro drift rates were presented to SPAC for preretro attitude maneuver compensation:

$$\text{Roll} = +0.65 \text{ deg/hr}$$

$$\text{Pitch} = +0.2 \text{ deg/hr}$$

$$\text{Yaw} = 0.0 \text{ deg/hr}$$

The pitch and yaw gyro drift rates were so small that their effect on the attitude maneuvers required no compensation.

f. Nitrogen gas consumption. The calculated weight of the nitrogen contained in the attitude control system at launch was 4.60 lb, based on a telemetered tank pressure of 4726 psi and a tank temperature of 78.1°F . Prior to the terminal maneuvers, 4.20 lb of nitrogen remained in the nitrogen tanks, indicating a consumption of 0.40 lb up to that point in flight.

g. Terminal maneuvers and descent. As in the case of the pre-midcourse attitude maneuvers, an attempt was made to initiate the terminal maneuvers at the limit-cycle null points. The roll maneuver was initiated within approximately -0.08 deg of null, while the pitch and yaw optical errors at the start of yaw were $+0.12$ and $+0.03$ deg, respectively. The magnitudes of the maneuvers were verified to be $+80.49$ deg of roll, $+96.047$ deg of yaw and -16.644 deg of roll.

A total vernier thrust level of 201 ± 5 lb was selected for the main retro burn period. A vernier engine ignition delay of 2.775 sec (following AMR mark) was entered into the magnitude register. After *thrust phase power on* was commanded from earth and confirmed by the spacecraft, all terminal descent events beginning with generation of the AMR mark signal occurred automatically, as planned, at close to predicted times (refer to Table IV-7). A plot of slant range vs vertical velocity during terminal descent is presented in Fig. IV-27.

Peak attitude transients at vernier engine ignition were -0.23 deg roll, -0.08 deg pitch and -0.44 deg yaw. During main retro motor burn, the mean attitude errors were $+0.1$ deg roll, $+0.03$ deg pitch and -0.28 deg yaw. Peak roll actuator position at main retro motor ignition was $+0.43$ deg, while the mean value during main retro burn was -0.12 deg.

The changes in spacecraft attitude at touchdown were approximately -3.0 deg in pitch and -1.68 deg in yaw. *Thrust phase power off* was commanded and verified 36.7 sec after touchdown, and *flight control power off* was commanded and verified 63 sec after touchdown.

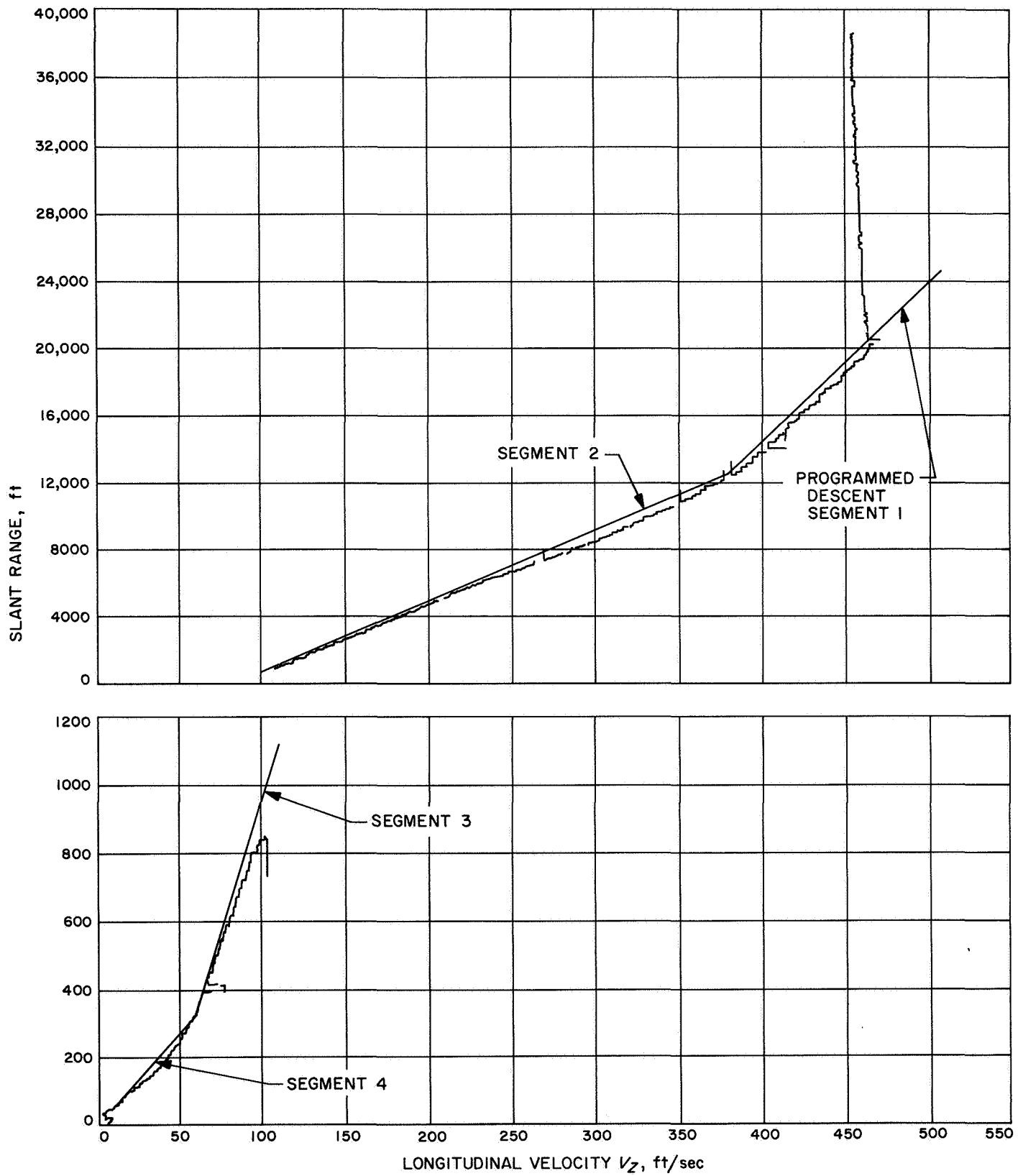


Fig. IV-27. Surveyor VII descent profile

G. Radar

Two radar devices, the altitude marking radar (AMR) and the radar altimeter and doppler velocity sensor (RADVS), are employed on the *Surveyor* spacecraft for use during the terminal descent phase.

1. Altitude Marking Radar

The AMR provides an altitude *mark* signal for automatic initiation of the spacecraft terminal descent sequence.

a. AMR description. The AMR (Fig. IV-28) is a conventional noncoherent radar employing a pulsed magnetron, single antenna, duplexed mixer, crystal-controlled solid-state local oscillator, wideband intermediate frequency (IF) amplifier, noncoherent detector, and video processing circuitry. Dynamic range is extended by automatic gain control (AGC) of the IF amplifier; AGC voltage is telemetered and provides an indication of received signal power. The video circuitry is of special design to provide the *mark* signal with high accuracy and reliability

at a slant range from the lunar surface that can be preset between 52 and 70 miles. Two fixed, adjacent range gates continuously examine the video signal. Their outputs are continuously summed and differenced. When the sum exceeds a fixed threshold and the difference simultaneously crosses zero with positive slope, the *mark* signal is generated. The sum threshold is set for an extremely low probability of marking on noise (*false mark*) throughout the operating time, while video integration plus a very substantial radar gain margin insure a high probability of marking successfully.

Two separate ground commands, whose timing is controlled, are required to fully activate the AMR. The first signal, called simply *AMR on*, commands on the primary power to the AMR, which includes all internal power except high voltage to the transmitter. The video signal is inhibited from reaching the marking circuits until the second command, thus eliminating any residual probability of false marking on noise during this warmup interval. The second signal, called *AMR enable*, commands on the transmitter high voltage and also removes the

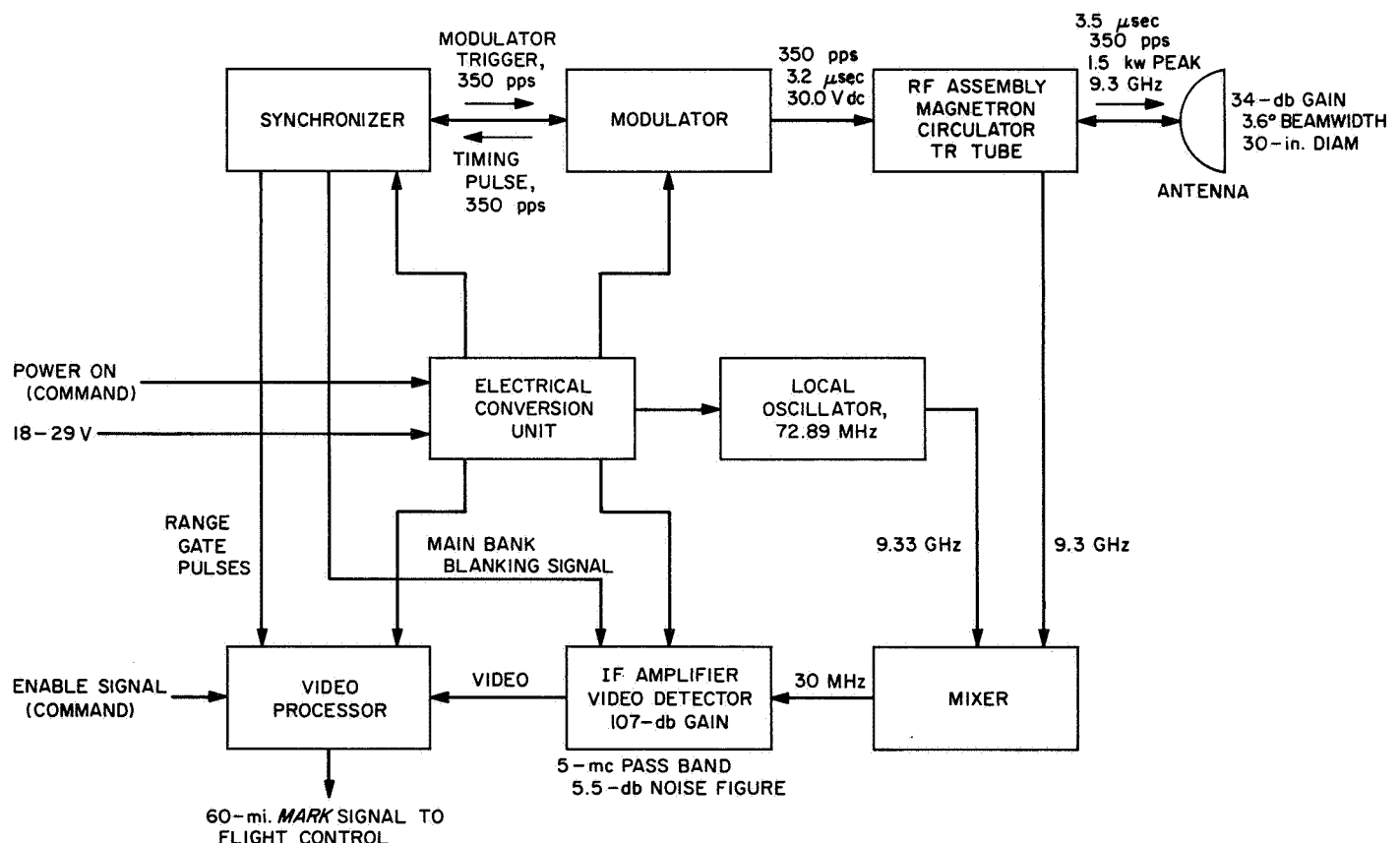


Fig. IV-28. Altitude marking radar functional diagram

video inhibit. This enabling function is timed not only for favorable thermal conditions at the expected marking time but also to preclude premature marking on second-round echoes at much longer ranges.

AMR signals which are telemetered include three digital signals and three analog signals plus analog temperature data. The three digital signals (R-1, R-11, FC-64) are confirmations of on-board discrete events; they confirm, respectively, that prime power has been applied (*AMR on*), that high voltage and video enabling have been applied (*AMR enable*), and that the self-generated slant range trigger (*AMR mark*) has occurred. The three analog signals (besides temperature) are magnetron current (R-12), AGC voltage level (R-14), and late gate detected video voltage level (R-29). The AGC not only confirms receiver response to RF return, but is also useful in evaluating terrain reflectivity. The magnetron current confirms pulsing of the magnetron after *enable*, and is useful primarily as a transmitter failure mode indication. The late gate signal, primarily a receiver failure mode indication, normally confirms presence of gated video signals rising quickly to a peak at the time of *mark* and decaying quickly thereafter.

The AMR mounts in the retrorocket nozzle and is retained by friction clasps around the nozzle flange, with spring washers between the AMR and the flange. When the retrorocket is ignited, the gas generated by the ignitor develops sufficient pressure to eject the AMR from the nozzle. The AMR draws 22-V dc power through a breakaway plug that also carries input commands, the output *mark* signal, and telemetry information.

b. AMR performance. On the *Surveyor VII* mission, the AMR functioned normally in all respects. The 60-mile *mark* was generated at the proper altitude. The *mark* then started the automatic terminal sequence.

The AMR AGC curve shown in Fig. IV-29 represents the signal power being received at the AMR feedhorn vs time to retro ignition. It can be seen that the received power increased smoothly and evenly as the spacecraft approached a slant range of 60 miles. At a return power level of -72.2 dbm the 60 mile *mark* was initiated. The return power at *mark* compares to within 6 dbm of the calculated signal return. The predicted return power for *mark* is -78.5 dbm. This signal level is based upon a pulse width of $23.6 \mu\text{sec}$ and an approach angle of 36° . AMR temperatures were as expected and compared favorably to those of previous missions. AMR temperatures are not telemetered during terminal descent, so

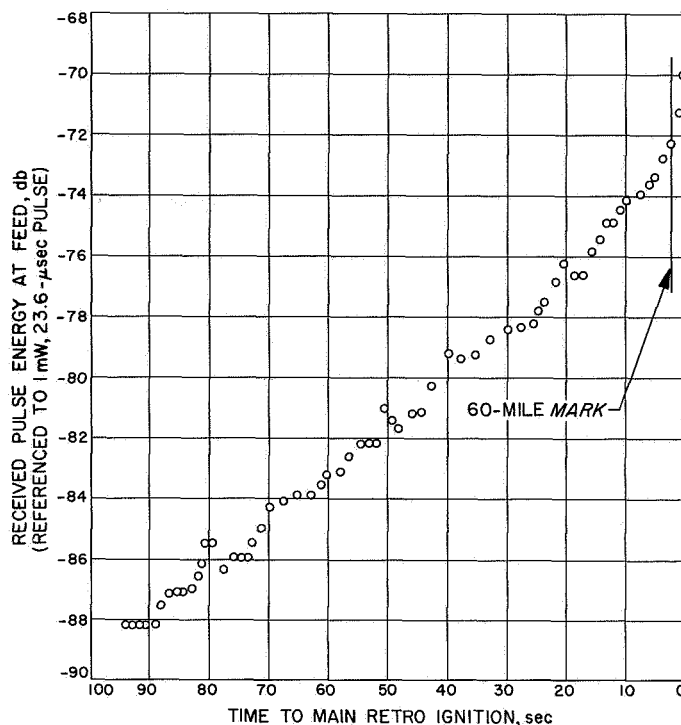


Fig. IV-29. Altitude marking radar AGC

that the last temperatures are those just prior to AMR *enable* and are given below:

Antenna edge (R-6) = -4°F

AMR electronics (R-7) = 11°F

2. Radar Altimeter and Doppler Velocity Sensor

The RADVS (Fig. IV-30) functions in the flight control subsystem to provide three-axis velocity, range, and altitude *mark* signals for flight control during the main retro and vernier phases of terminal descent. The RADVS consists of a doppler velocity sensor (DVS), which computes velocity along the spacecraft X, Y, and Z axes, and a radar altimeter (RA), which computes slant range from 40,000 to 14 ft and generates 1000-ft and 14-ft *mark* signals. The RADVS comprises five assemblies: (1) klystron power supply/modulator (KPSM), which contains the RA and DVS klystrons, klystron power supplies, and altimeter modulator, (2) altimeter/velocity sensor antenna, which contains beams 1 and 4 transmitting and receiving antennas and preamplifiers, (3) velocity sensing antenna, which contains beams 2 and 3 transmitting antennas and preamplifiers, (4) RADVS signal data converter (SDC), which consists of the electronics to convert doppler shift signals into dc analog signals, and (5) interconnecting waveguide. The RADVS is turned on at

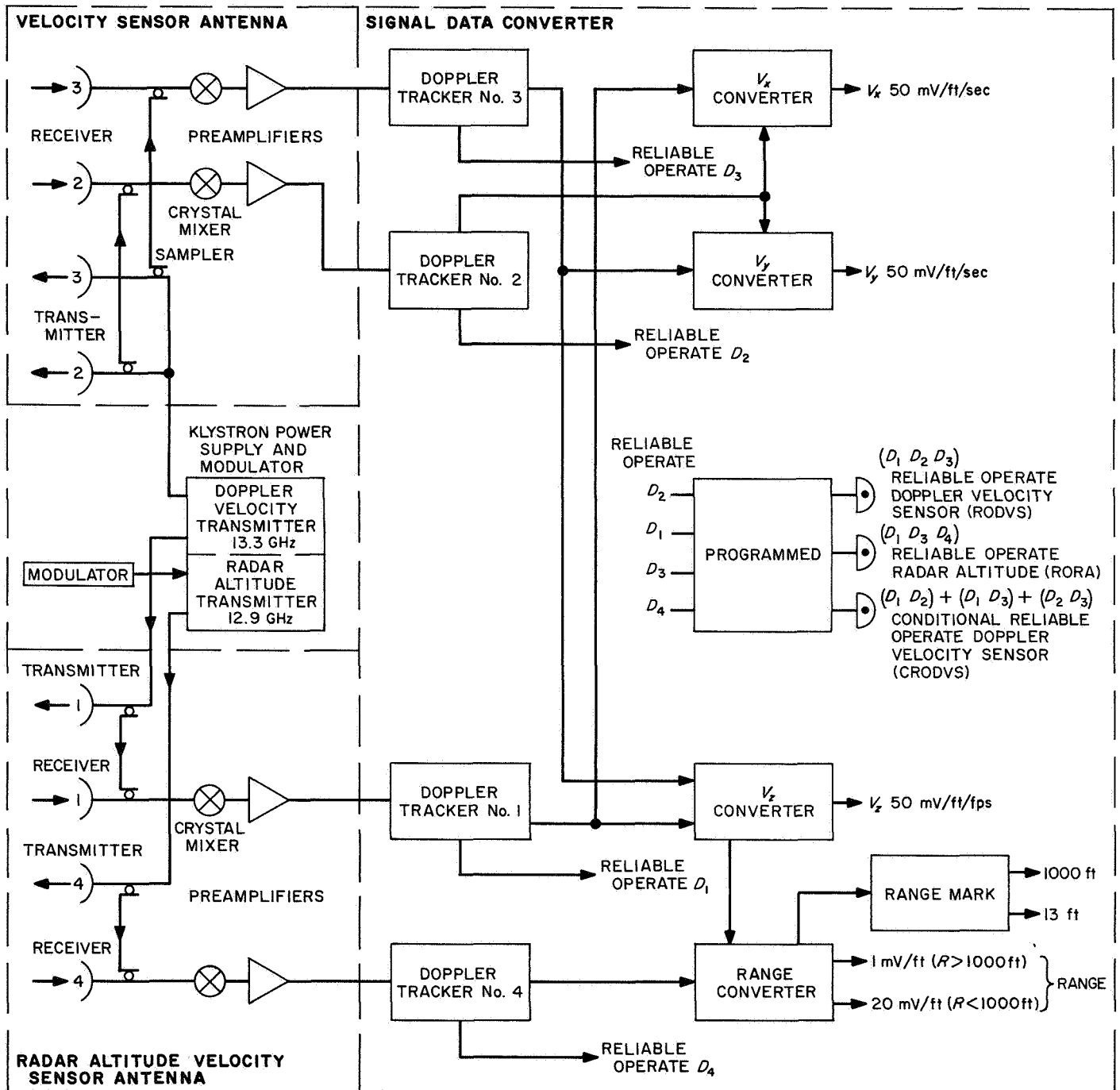


Fig. IV-30. Simplified RADVS functional block diagram

about 50 miles above the lunar surface and is turned off at about 14 ft.

a. Doppler velocity sensor description. The doppler velocity sensor (DVS) operates on the principle that a reflected signal has a doppler frequency shift proportional to the approaching velocity. The reflected signal frequency is higher than the transmitted frequency for the closing condition. Three beams directed toward the lunar surface enable velocities in an orthogonal coordinate system to be determined. The RADVS beam orientation is shown in Fig. IV-31.

The KPSM provides an unmodulated DVS klystron output at a frequency of 13.3 GHz. This output is fed equally to the DVS 1, DVS 2, and DVS 3 antennas. The RADVS velocity sensor antenna unit and the altimeter velocity sensor antenna unit provide both transmitting and receiving antennas for all three beams. The reflected signals are mixed with a small portion of the transmitted frequency at two points $\frac{3}{4}$ wavelength apart for phase

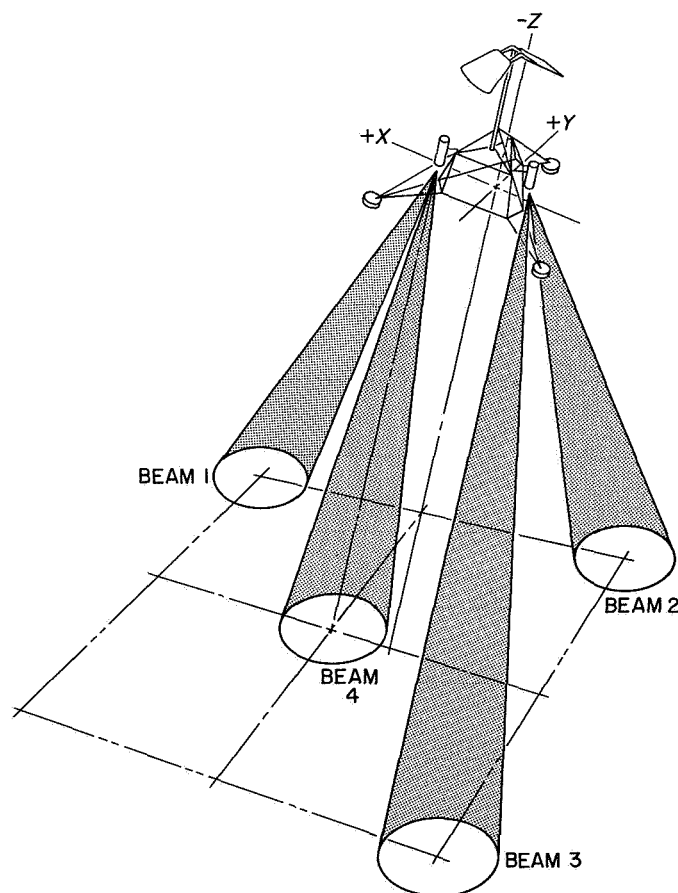


Fig. IV-31. RADVS beam orientation

determination, detected, and amplified by variable-gain amplifiers providing 40, 65, or 90 db of amplification, depending on received signal strength. The preamp output signals consist of two doppler frequencies, shifted by $\frac{3}{4}$ transmitted wavelength, and preamp gain-state signals for each beam. The signals are routed to the trackers in the RADVS signal data converter.

The D1 through D3 trackers in the signal data converter are similar in their operation. Each provides an output which is 600 kHz plus the doppler frequency for approaching doppler shifts. If no doppler signal is present, the tracker will operate in search mode, scanning frequencies between 82 kHz and 800 Hz before retro burnout, or between 22 kHz and 800 Hz after retro burnout. When a doppler shift is obtained, the tracker will operate as described above and initiate a lock-on signal. The tracker also determines amplitude of the reflected signal and routes this information to the signal processing electronics for telemetry.

The velocity converter combines tracker output signals D_1 through D_3 to obtain dc analog signals corresponding to the spacecraft X, Y, and Z velocities; $D_1 + D_3$ is also sent to the altimeter converter to compute range.

Reliability and reference circuits produce a *reliable operate doppler velocity sensor* (RODVS) signal if D_1 through D_3 lock-on signals are present beginning about 3 sec after main retro burnout. The RODVS signal is routed to the flight control electronics and to the signal processing electronics telemetry. The system is designed to produce a *conditional reliable operate doppler velocity sensor* (CRODVS) signal if only one or two, rather than all three, of the DVS beams are in lock. If the CRODVS signal occurs, the spacecraft will steer into the un-locked beam(s) to achieve lock-on of all beams and generation of RODVS. For *Surveyor IV* and later missions, the period of time that CRODVS was enabled has been extended to the 1000-ft mark to facilitate landings at increased approach angles. On earlier missions, CRODVS was disabled 1 sec after the three velocity trackers had achieved lock. When CRODVS is inhibited, the spacecraft switches to inertial attitude hold if beam lock is lost. Availability of CRODVS to 1000-ft altitude allows spacecraft maneuvering to reacquire lock, thus assuring greater probability of maintaining the programmed descent profile.

Cross-coupled sidelobe logic (CCSL) is provided in the signal data converter to protect against false lock-on by a tracker of a sidelobe from another beam. The logic compares amplitude and frequencies between beams and

breaks lock if the amplitude and bandwidth characteristics indicate that a cross-coupled sidelobe is being tracked. Prior to *Surveyor IV*, spacecraft had CCSLL provisions only for beams 2 and 3. Later spacecraft have been provided with CCSLL between beams 1, 2, and 3. Also, on the later spacecraft, the CCSLL has been disabled below 1000-ft altitude because the CCSLL is most effective at higher altitudes and may produce erroneous outputs near the lunar surface.

b. Radar altimeter description. Slant range is determined by measuring the reflection time delay between the transmitted and received signals. The transmitted signal is frequency-modulated at a changing rate so that return signals can be identified.

The RF signal is radiated, and the reflected signal is received by the altimeter/velocity sensor antenna. The received signal is mixed with two samples of transmitted energy $\frac{3}{4}$ wavelength apart, detected, and amplified by 40, 60, or 80 db in the altimeter preamp, depending on signal strength. The signals produced are difference frequencies resulting from the time lag between transmitted and received signals of a known shift rate, coupled with an additional doppler frequency shift because of the spacecraft velocity.

The altimeter tracker in the signal data converter accepts doppler shift signals and gain-state signals from the altimeter/velocity sensor antenna and converts these into a signal which is 600 kHz plus the range frequency plus the doppler frequency. This signal is routed to the altimeter converter for range dc analog signal generation.

The range mark, reliability, and reference circuits produce the 1000-ft *mark* signal and the 14-ft *mark* signal from the *range* signal generated by the altimeter converter where the doppler velocity V_z is subtracted giving the true range.

The *range mark* and *reliable operate radar altitude* (RORA) signals are routed to flight control electronics. The signals are used to rescale the *range* signal, for vernier engine shutoff and to indicate whether or not the *range* signal is reliable. The RORA signal is also routed to signal processing for transmission to DSIF.

c. RADVS performance. RADVS performance for the *Surveyor VII* mission is considered nominal. The RADVS system was turned on approximately 5 sec after the AMR *mark* (which initiated the automatic terminal se-

quence). Approximately 22 sec after RADVS primary power was applied, the radar transmitters were turned on through internal RADVS circuits.

Reflectivity of the RADVS beams is shown in Fig. IV-32. The predicted signal return power levels for a vertical spacecraft approach are plotted for the DVS beams. The predicted signal power levels for the DVS beams closely match the actual data. In all previous missions (*Surveyors I, III, V, VI*) the DVS return power average was lower when compared to the predicted return.

As can be seen, the predicted return radar power for *Surveyor VII* was approximately 3 db lower than the actual data of beams 1 and 3. For beam 2 the predicted is approximately 2 db higher. The overall match of actual spacecraft data to the predicted power levels is considered good. One possible reason for the increase of signal return power on this mission could be related to the increased roughness of the lunar surface at the *Surveyor VII* landing site compared with the relatively smooth landing sites of the other spacecraft. The roughness of terrain would cause an increase of signal energy return paths (multipath effect) which could have caused an average power increase. The reflectivity curve of beam 4 compares closely to data of previous spacecraft in signal level and gain state position vs time to touchdown. The IF amplifier saturation of the DVS beams just prior to touchdown (last 6 sec) is the expected nominal performance.

The spacecraft range vs time to touchdown is shown in Fig. IV-33. The range decreased smoothly from 40,000 ft to touchdown. Figures IV-34 through IV-36 are plots of the velocity components along each of the three spacecraft axes during terminal descent. The velocity beam trackers (beams 1, 2, and 3) and the altimeter (beam 4) locked onto the reflected signal prior to retro burnout. The data indicates that the altimeter tracker locked onto the return signal above 40,000 ft (Fig. IV-33) and was in saturation at 147 sec to touchdown. At the approximate time of retro ejection, beams 1 and 4 lost lock. Both beams regained lock within 3.5 sec after retro ejection. Tracker unlocks at retro ejection were noted on previous missions and the unlocks on the *Surveyor VII* mission in all probability were due to the retro motor case passing through the radar beams. Because of the inertially fixed attitude of the spacecraft prior to RADVS control, the X and Y velocity components increased to about -124 and -65 ft/sec, respectively. After initiation of RADVS control, these velocity components were removed in about 3 sec.

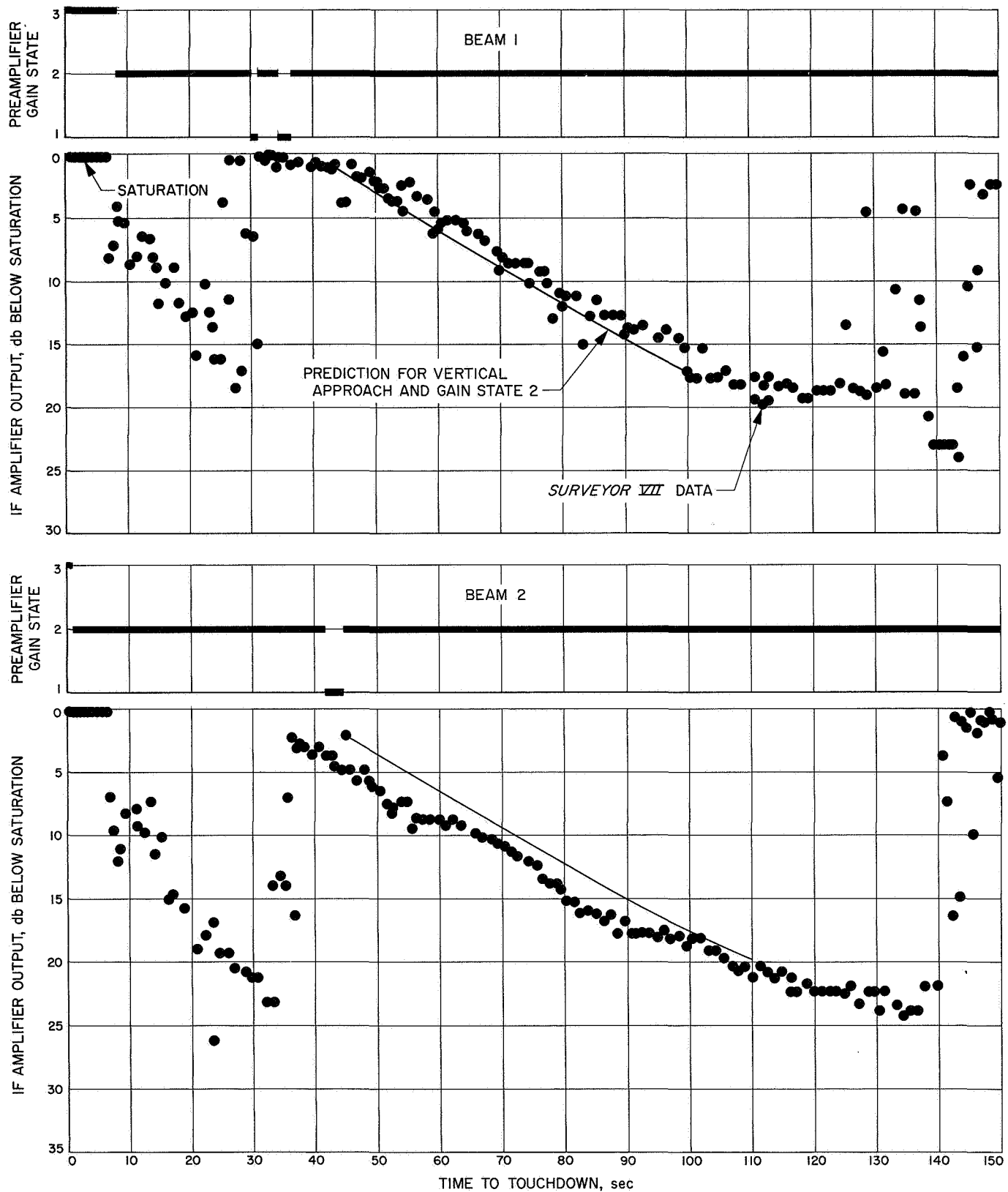


Fig. IV-32. Reflectivity of RADVS beams during terminal descent

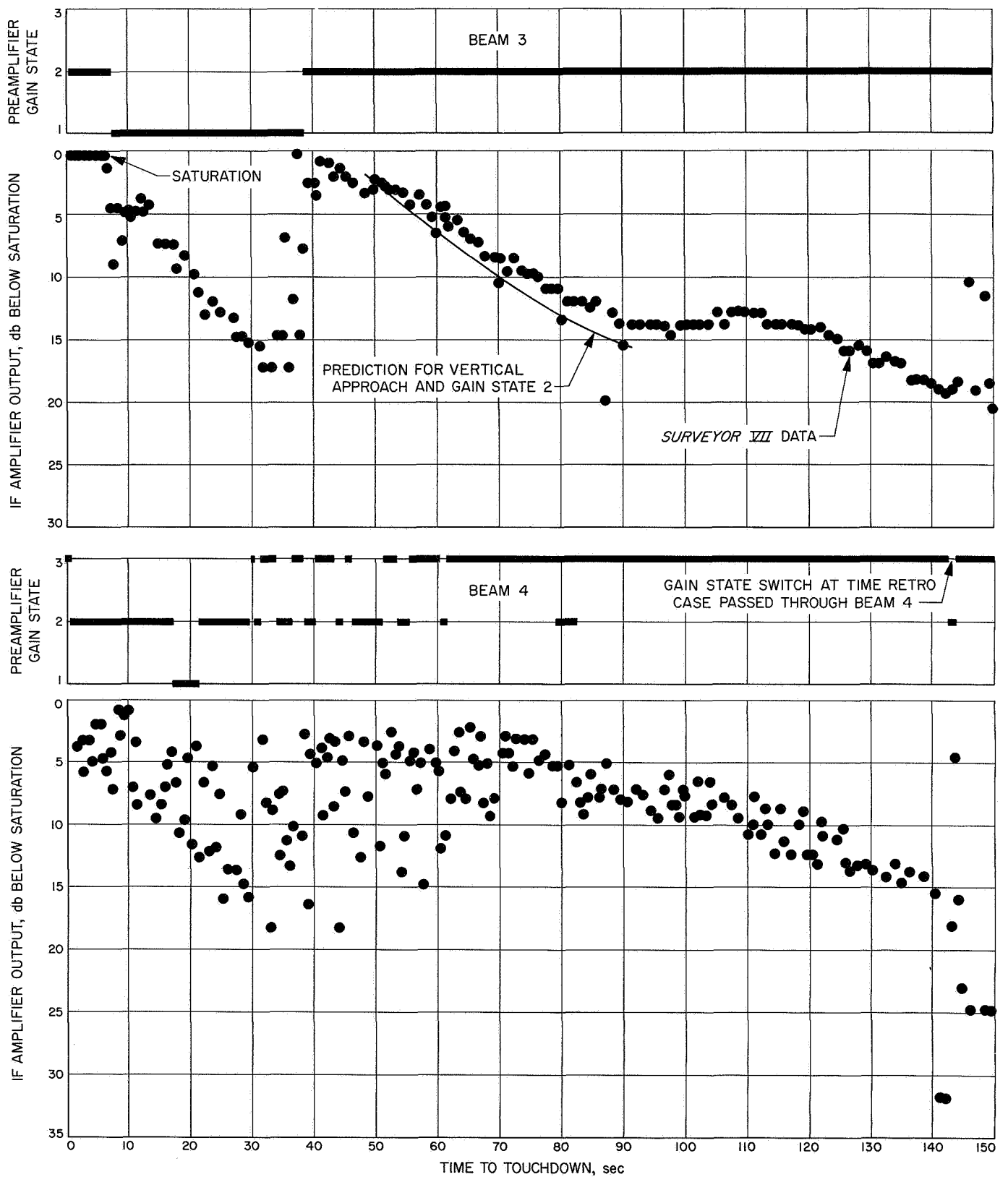


Fig. IV-32 (contd)

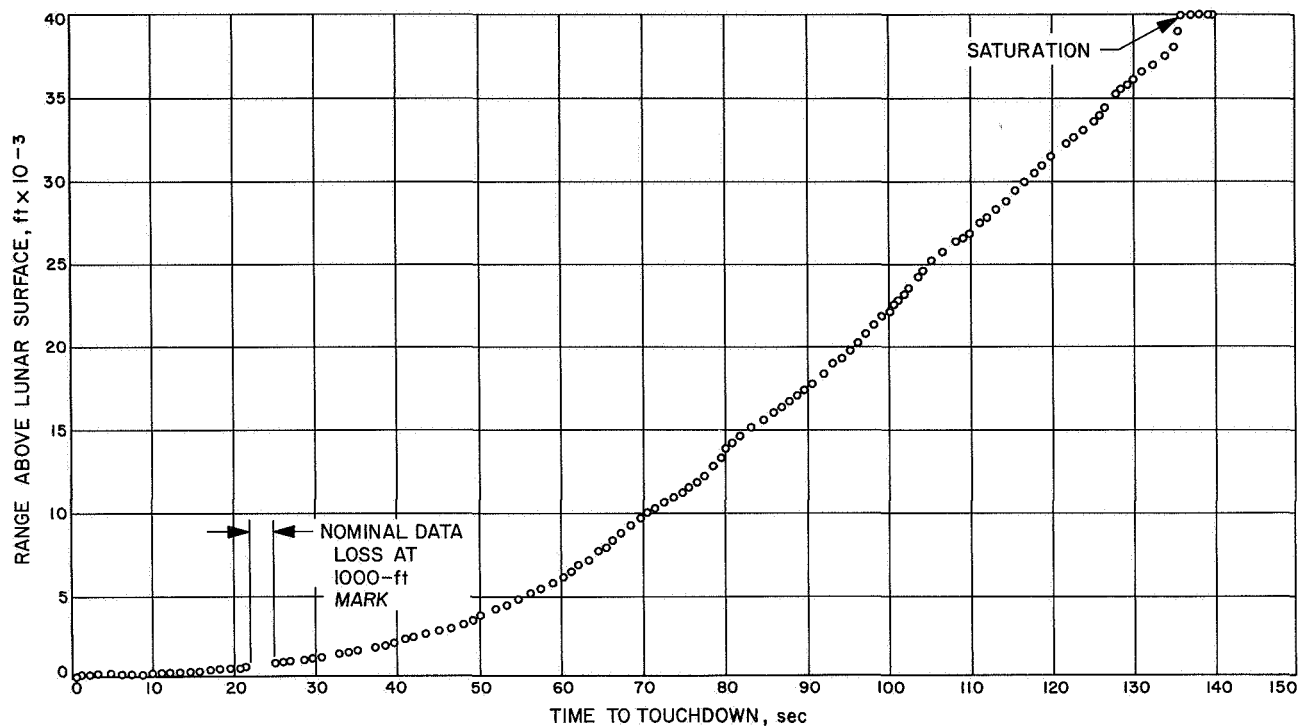


Fig. IV-33. Slant range vs time during terminal descent

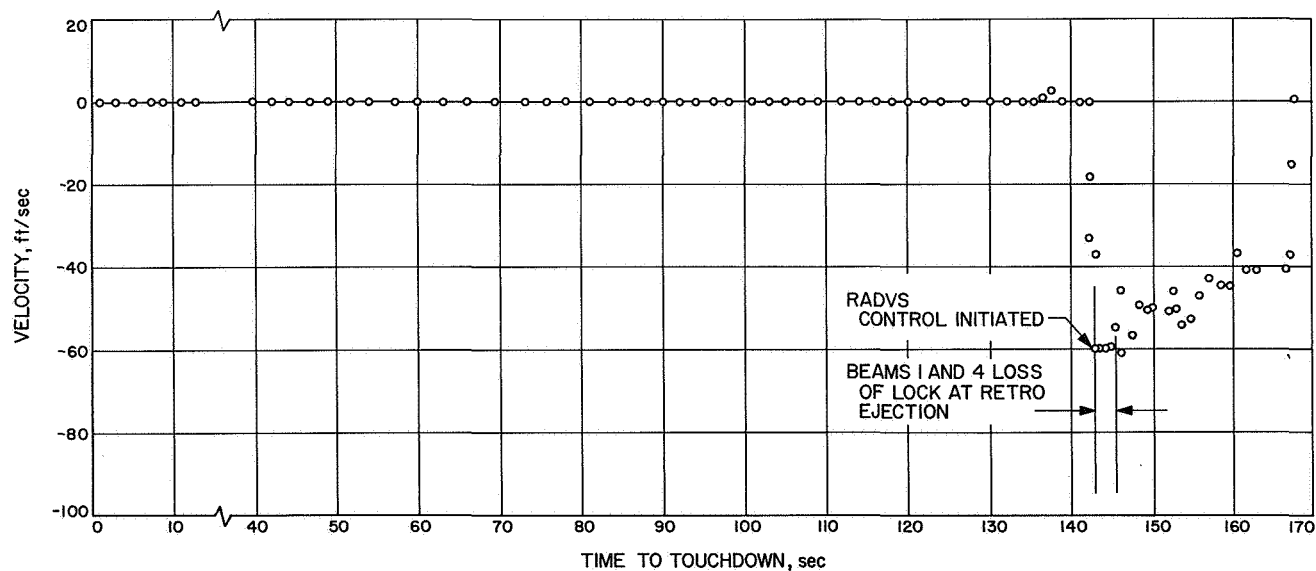


Fig. IV-34. X-component of velocity V_x during terminal descent

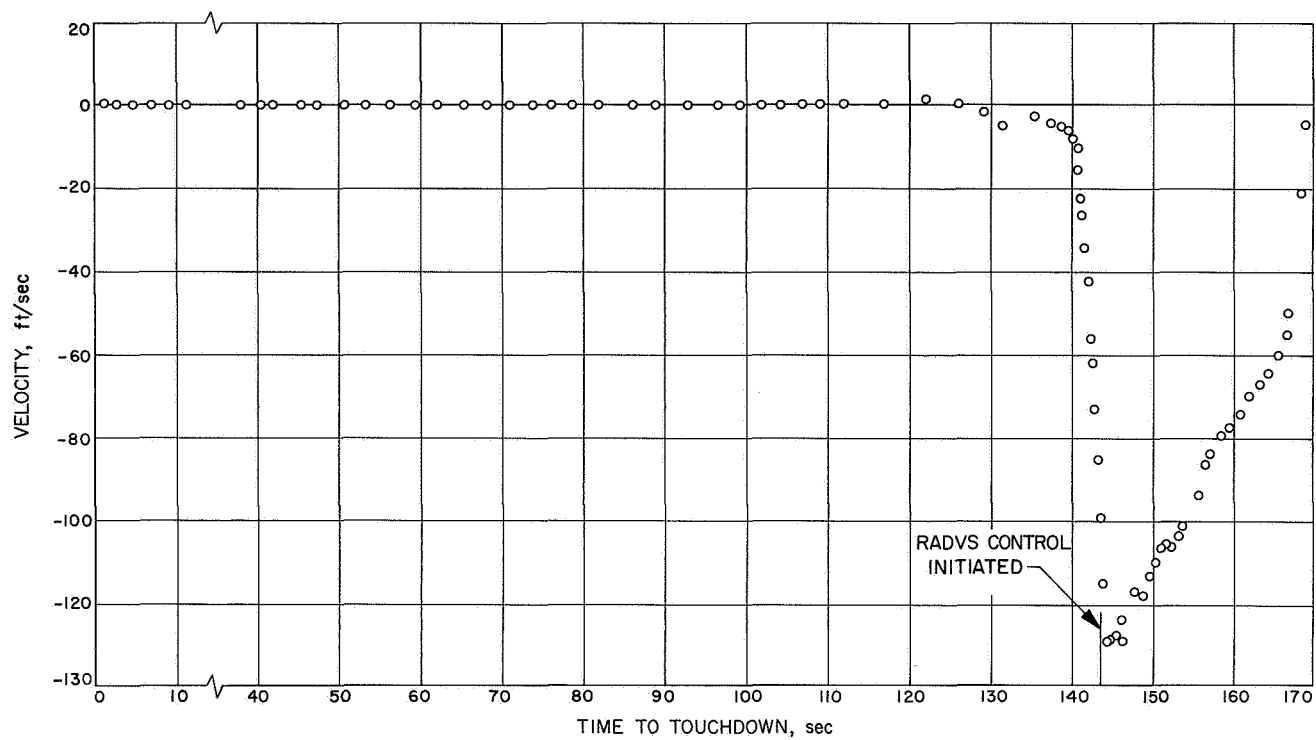


Fig. IV-35. Y-component of velocity V_Y during terminal descent

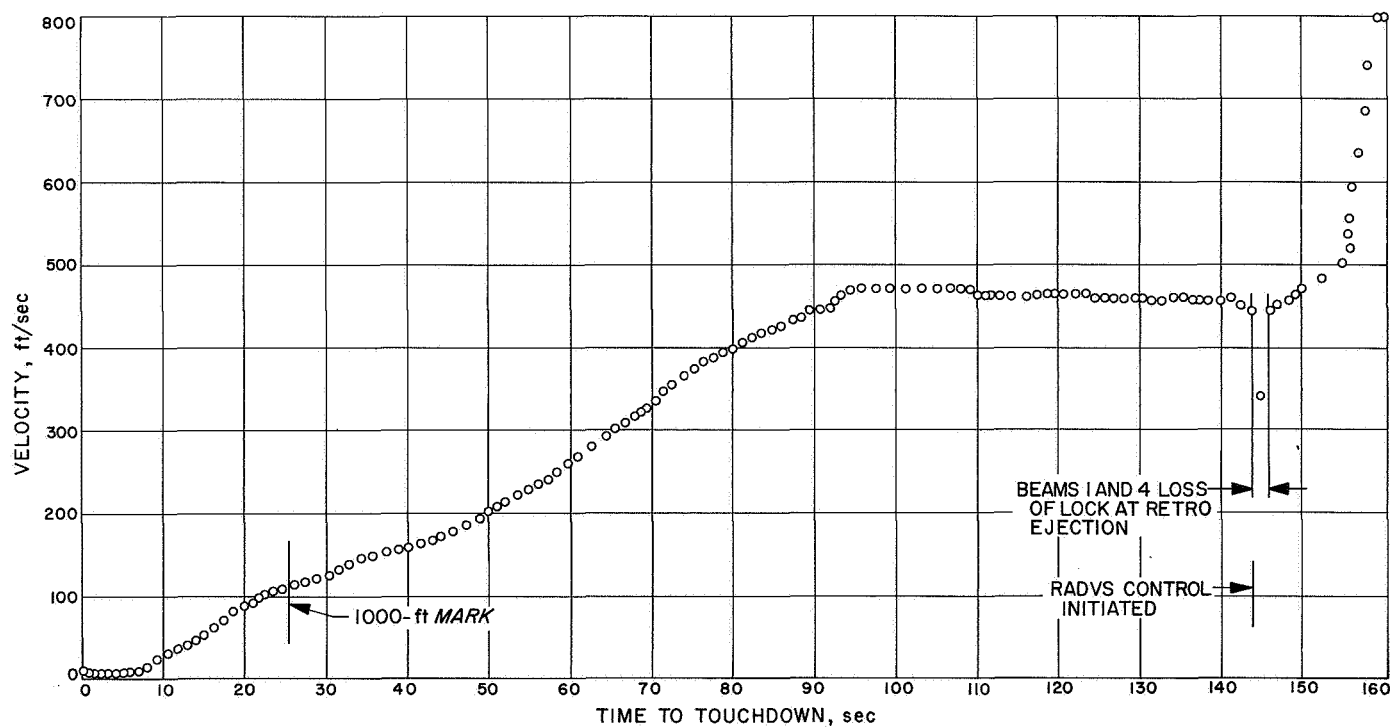


Fig. IV-36. Z-component of velocity V_Z during terminal descent

H. Telecommunications

The *Surveyor* telecommunications subsystem contains radio, signal processing, and command decoding equipment to provide (1) a method of telemetering information to the earth, (2) the capability of receiving and processing commands to the spacecraft, and (3) angle-tracking one- or two-way doppler for orbit determination.

1. Radio Subsystem

The radio subsystem utilized on the *Surveyor* spacecraft is shown schematically in Fig. IV-37. Dual receivers, transmitters, and antennas were originally meant to provide redundancy for added reliability. As presently mechanized, this is not completely true owing to switching limitations. Each receiver is permanently connected to its corresponding antenna and transmitter. The transmitters, which are capable of operation in two different power modes (100-mW low power, and 10-W high power), can each be commanded to transmit through any of the three antennas. The *Surveyor* radio system operates at S-band, 2295-MHz down-link, and 2113-MHz up-link.

a. Receivers. Both receivers are identical, crystal-controlled, double-conversion units, which operate continuously as they cannot be commanded off. Each unit is capable of operation in an automatic frequency control (AFC) mode, or an automatic phase control (APC) mode. The receivers provide two necessary spacecraft functions: the detection and processing of commands from the ground stations for spacecraft control (AFC and APC modes), and the phase-coherent spacecraft-to-earth signal required for doppler tracking (APC mode).

b. Transmitters. Transmitters A and B are identical units which provide the spacecraft-to-earth link for telemetry and doppler tracking information. The transmitters are commanded on, one at a time, from the ground stations. Each unit contains two crystal-controlled oscillators, wideband for TV and scientific information, narrowband for engineering data. Either unit can be commanded on at will, and, in addition, can operate from the receiver voltage-controlled oscillator (transponder mode) when coherent signals are required for two-way doppler tracking. The transmitters may be commanded to operate through any one of the spacecraft

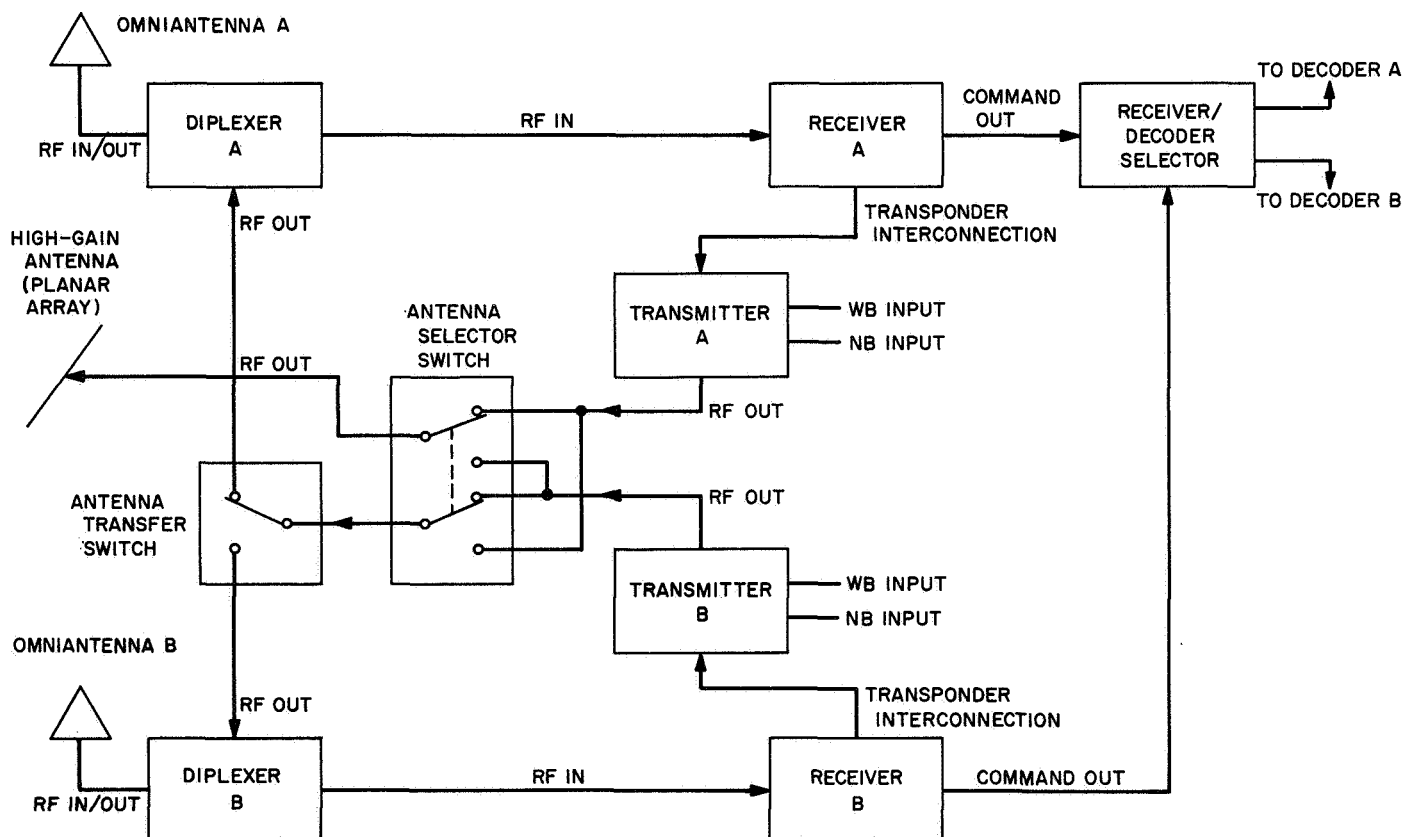


Fig. IV-37. Radio subsystem block diagram

antennas as desired, and both are capable of providing either 100 mW or 10 W of output power.

c. Transponders. Two identical transponder interconnections permit each transmitter to be operated, on command, in a transponder mode. In the transponder mode, a transmitter is operated with the corresponding receiver voltage-controlled oscillator to provide coherent signals when two-way doppler tracking data is required.

d. Antennas. Three antennas are utilized on the *Surveyor* spacecraft. Two antennas are omnidirectional units which provide receive-transmit capability for the spacecraft. The third antenna is a high-gain, 27-db directional planar array used for transmission only of wide-band information.

e. Radio subsystem performance. The radio subsystem performed well during the *Surveyor VII* mission, with no indications of abnormal behavior. The spacecraft transmitter went to the high-power mode upon command from the *Centaur* vehicle shortly before spacecraft separation. The spacecraft was acquired by DSS 42, Tidbinbilla, approximately 50 min after liftoff, and the transmitter was then commanded to low-power operation.

Canopus acquisition was accomplished about 8½ hr after liftoff.

Receiver A/Omniantenna A performance for the flight is plotted in Fig. IV-38. Available predictions for the performance of this unit were grossly in error. Predictions were invalidated by the addition of the ASI and the SM/SS. These instruments were expected to disturb previously obtained antenna patterns for Omniantenna A; however, time and expense did not warrant performing new antenna pattern measurements. Signal variations for Receiver A/Omniantenna A varied widely throughout the mission, and this variation is believed to have been caused by the distortion of the antenna patterns. This belief is somewhat confirmed by the fact that during gyro drift checks the signal levels would increase and decrease as the orientation of the spacecraft changed. These changes would remove the spacecraft antenna from a critical null position to a more favorable radiation point. Available predictions for Receiver A/Omniantenna A are, therefore, not plotted in Fig. IV-38.

Receiver B/Omniantenna B performance for the flight is plotted in Fig. IV-39. Prior to Canopus acquisition, the predicted signal strength is not expected to be valid

and deviations between predicted and measured signal strength are of no concern. After Canopus acquisition, the receiver signal strength varied as much as 5 db from predicted levels, but in general remained 1 to 2 db below predictions. Variations in actual to predicted levels have occurred in previous missions and are attributed in part to antenna patterns and look angles. The received signal strength remained well above the command threshold level of -114 dbm, and no difficulty in commanding the spacecraft was experienced during the entire transit phase to the moon.

A plot of down-link signal strength is shown in Fig. IV-40. Again predictions furnished for comparison between actual and measured signal levels were found to be in error. Down-link signal strengths compare favorably with those of previous missions. For the purpose of clarity the furnished down-link predicted signal strengths have been omitted from Fig. IV-40.

2. Signal Processing Subsystem

The *Surveyor* signal processing subsystem accepts, encodes, and prepares for transmission voltages, currents, and resistance changes corresponding to various spacecraft parameters such as events, voltages, temperatures, accelerations, etc.

The signal processor employs both pulse-code modulation and amplitude-to-frequency modulation telemetry techniques to encode spacecraft signals for frequency- or phase-modulating the spacecraft transmitters and for recovery of these signals by the ground telemetry equipment. A simplified block diagram of the signal processor is shown in Fig. IV-41.

The input signals to the signal processor are derived from various voltage or current pickoff points within the other subsystems as well as from standard telemetry transducing devices such as strain gages, accelerometers, temperature transducers, and pressure transducers. These signals generally are conditioned to standard ranges by the originating subsystem so that a minimum amount of signal conditioning is required by the signal processor.

As illustrated in Fig. IV-41, some of the signal inputs are commutated to the input of the analog-to-digital converter (ADC) while others are applied directly to sub-carrier oscillators. The measurements applied directly are accelerometer and strain gage measurements which require continuous monitoring over the short intervals in which they are active.

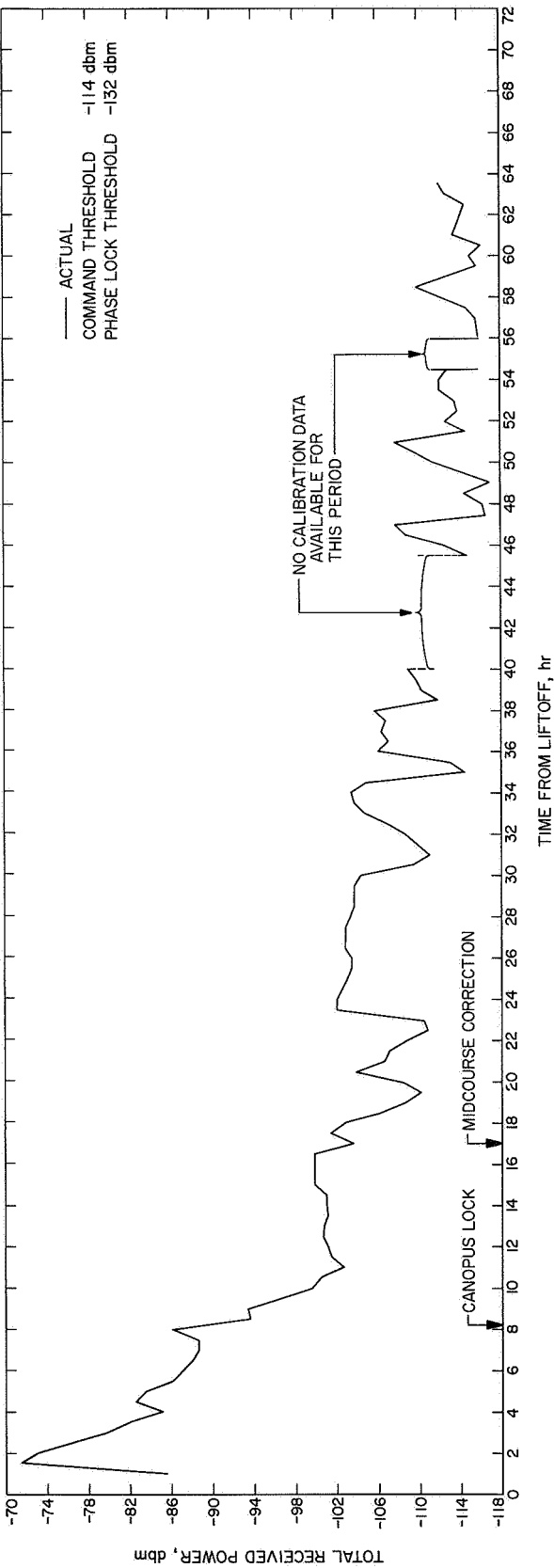


Fig. IV-38. Receiver A/Omniantenna A total received power during transit

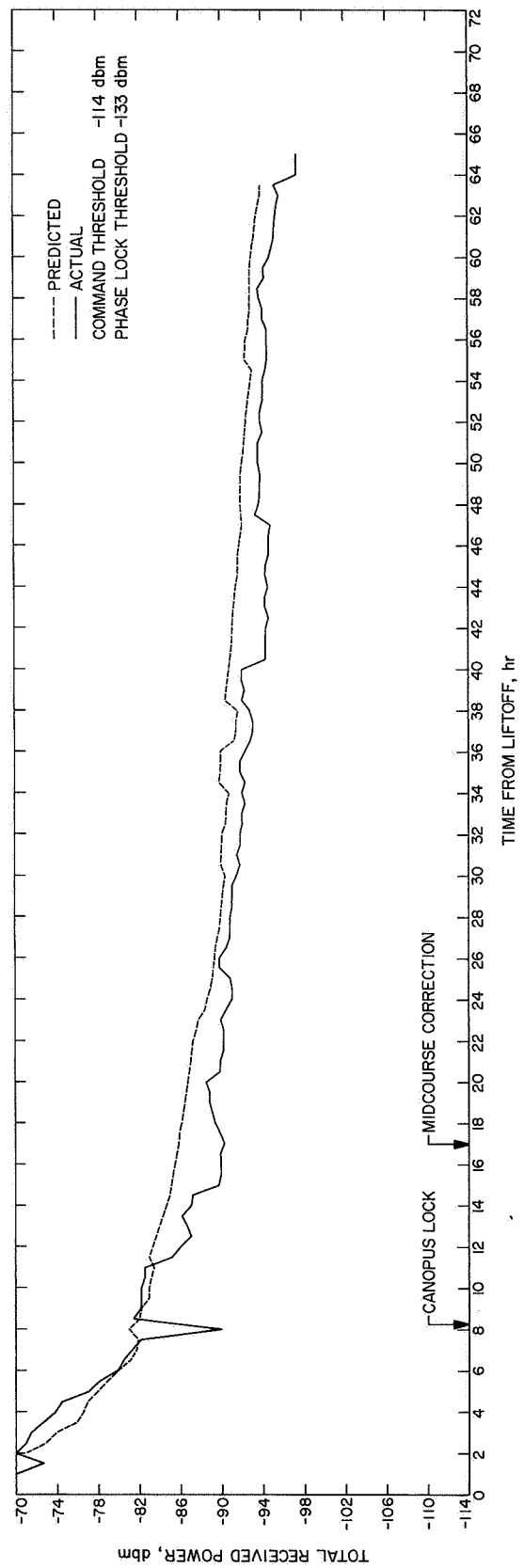


Fig. IV-39. Receiver B/Omniantenna B total received power during transit

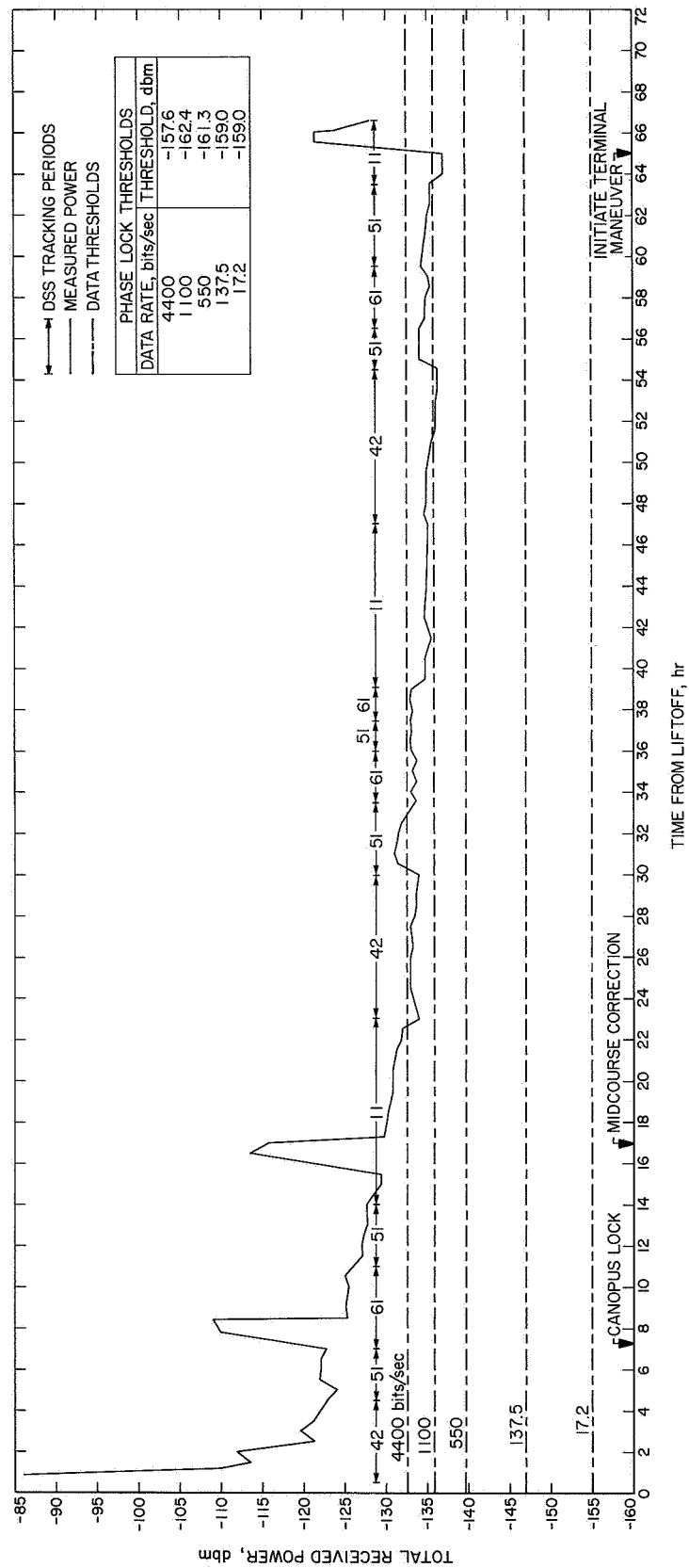


Fig. IV-40. DSIF received power during transit

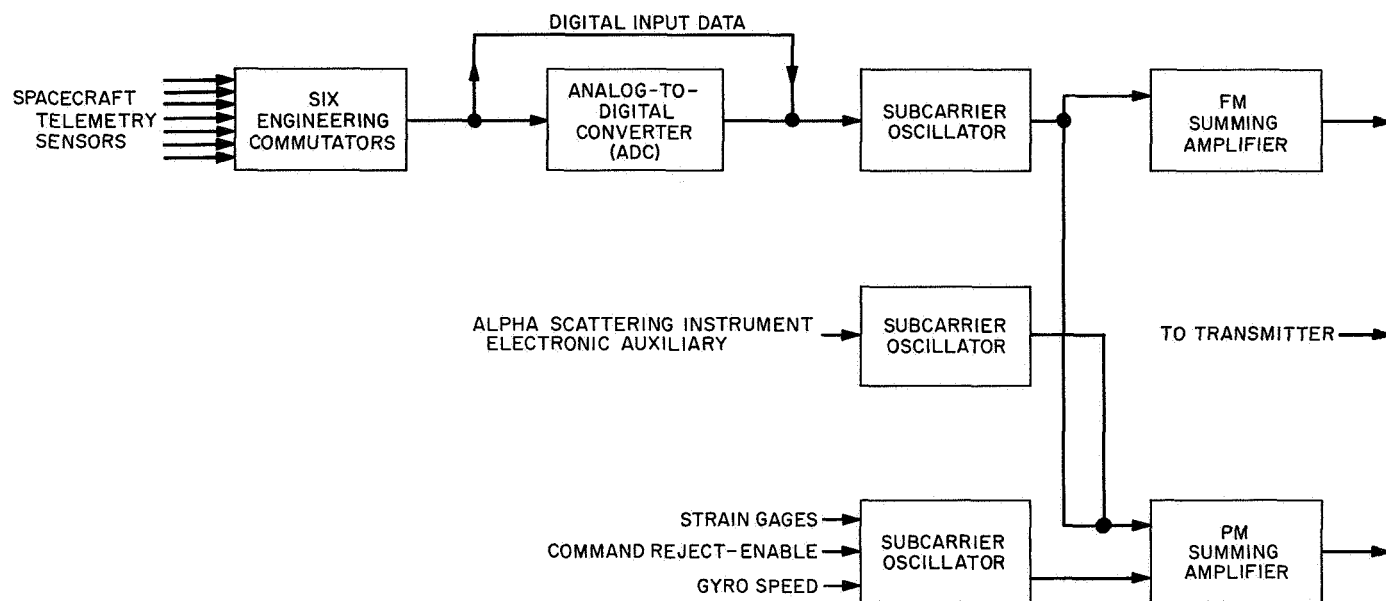


Fig. IV-41. Simplified signal processing functional block diagram

The commutators apply the majority of telemetry input signals to the ADC, where they are converted to a digital word. Binary measurements such as switch closures or contents of a digital register already exist in digital form and are therefore routed around the ADC. In these cases, the commutator supplies an inhibit signal to the ADC and, by sampling, assembles the digital input information into 10-bit digital words. The commutators are comprised of transistor switches and logic circuits which select the sequence and number of switch closures. There are six engineering commutator configurations (or modes) used to satisfy the telemetry requirements for the different phases of the mission and one TV commutator configuration located in the TV auxiliary.

The ADC generates an 11-bit digital word for each input signal applied to it. Ten bits of the word describe the voltage level of the input signal, and the eleventh bit position is used to introduce a bit for parity-checking by the ground telemetry equipment. The ADC also supplies commutator advance signals to the commutators at one of five different rates. These rates enable the signal processor to supply telemetry information at 4400, 1100, 550, 137.5, and 17.2 bits/sec. The bit rates and commutator modes are changed by ground commands.

The subcarrier oscillators are voltage-controlled oscillators used to provide frequency-multiplexing of the telemetry information. This technique is used to greatly increase the amount of information which is transmitted on the spacecraft carrier frequency.

The summing amplifiers sum the outputs of the subcarrier oscillators and apply the composite signal to the spacecraft transmitters. Two types of summing amplifiers are employed because of the transmitter's ability to transmit either a phase-modulated or a frequency-modulated signal.

The signal processing subsystem employs a high degree of redundancy to insure against loss of vital spacecraft data. Two ADC's, two independent commutators — the engineering signal processor (ESP) and auxiliary engineering signal processor (AESP) — and a wide selection of bit rates (each with the ADC driving a different subcarrier oscillator) provide a high reliability of the signal processing subsystem in performing its function.

From launch to touchdown, 166 commands effecting changes in the signal processor were received and properly executed by the signal processor. Table IV-19, shows representative prelaunch and in-flight values of the telemetered signal processing parameters. No signal processing anomalies were exhibited from launch to shutdown shortly after sunset.

3. Command Decoding Subsystem

From liftoff to touchdown on the moon, the *Surveyor VII* mission required a total of 335 earth commands. Seven of these were quantitative commands (QC's), which provided the spacecraft with the quantitative information

Table IV-19. Typical signal processing parameter values

Parameter	Prelaunch	Flight
ESP reference volts, V (mode 2)	4.865	4.865
ESP reference volts, V (mode 4)	4.885	4.885
ESP reference return, V	0.000	0.000
ESP unbalance current, μ A (mode 2)	-0.06717	-0.06717
ESP unbalance current, μ A (mode 4)	-0.06717	-0.06717
ESP full-scale current calibration, % error from nominal	-0.04873	0.04873
ESP midscale current calibration, % error from nominal	-0.1787	-0.1787
ESP zero-scale current calibration, % error from nominal	0.09537	0.09537
AESP full-scale current calibration, % error from nominal	0.02110	0.02110
AESP midscale current calibration, % error from nominal	0.2389	0.2389
AESP zero-scale current calibration, % error from nominal	0.1516	0.1516
AESP unbalance current, μ A	-2.197	-2.197
AESP reference volts, V	4.902	4.934

necessary for attitude and trajectory correction maneuvers; the other 328 were direct commands (DC's), which initiated single actions such as *extend omniantennas*, *AMR power on*, *A/D clock rate 1100 bits/sec*, etc.

These commands were received, detected, and decoded by one of the four receiver/central command decoder (CCD) combinations possible in the *Surveyor* command subsystem. The selection of the combination is accomplished by stopping the command information from modulating the up-link radio carrier for $\frac{1}{2}$ sec. Once the selection is made, the link must be kept locked up continuously by either sending serial command words or unaddressable command words (referred to as fill-ins) at the maximum command rate of 2 words/sec.

The command information is formed into a 24-bit Manchester-coded digital train and is transmitted in a PCM/FM/PM modulation scheme to the spacecraft. When picked up by the spacecraft omniantennas, the radio carrier wave is stripped of the command PCM information by two series FM discriminators and a Schmitt digitizer. This digital output is then decoded by the CCD for word sync, bit sync, the 5-bit address and its complement, and the 5-bit command and its complement (this

latter only for DC's, since the QC's contain 10 bits of information rather than 5 command bits and their complements). The CCD then compares the address with its complement and the command with its complement on a bit-by-bit basis. If the comparisons are satisfactory, the CCD then selects that one of the eight subsystem decoders (SSD's) having the decoded address bits as its address, applies power to its command matrix, and then selects that one of the 32 matrix inputs having the decoded command bits as its address to issue a 20-msec pulse which initiates the desired single action.

Those DC commands that are irreversible or extremely critical are interlocked with a unique command word. Ten of the DC's and all of the QC's are in this special category. None of these commands can be initiated if the interlock command word is not received immediately prior to the critical command.

The QC's, besides being interlocked, are also treated somewhat differently by the command subsystem. The only differences between the DC and QC are: (1) a unique address is assigned the QC words; (2) the QC word contains 10 bits of quantitative information in place of the 5 command and 5 command complement bits. Therefore, when this unique QC address is recognized, the CCD selects the flight control sensor group (FCSG) SSD and shifts the 10 bits of quantitative information into the FCSG magnitude register. Hence, the QC quantitative bits are loaded as they are decoded.

The command decoding subsystem performed properly throughout flight and through touchdown. No standard behavior was evidenced during lunar operations.

I. Television

The television subsystem is designed to obtain photographs of the lunar surface, lunar sky, and portions of the landed spacecraft. For missions beginning with *Surveyor III*, the subsystem has consisted of only a single television camera capable of panoramic viewing and a television auxiliary for processing commands and telemetry data.

The *Surveyor VII* television system provided pictures of excellent quality. Contributing to this was the improved camera system, which had been used for the first time on the *Surveyor VI* mission.

1. Survey Camera

Figure IV-42 illustrates the survey television camera, which differs in appearance from the cameras used before *Surveyor VI* because of a redesigned mirror hood assembly. The camera contains a mirror, filters, lens, shutter, vidicon, and the attendant electronic circuitry. Images can be obtained over a 360-deg panorama and over an elevation range from +40 deg above the plane normal to the camera Z axis to -60 deg below this same plane. The camera Z axis is inclined 16 deg from the spacecraft Z axis. Each picture, or frame, is imaged through an optical system onto a vidicon image sensor whose electron beam scans a photoconductive surface, thus producing an electrical output proportional to the conductivity changes resulting from the varying reception of photons from the subject. The camera is designed to accommodate scene luminance levels from approximately 0.008 ft-lamberts to 2600 ft-lamberts, employing various means of exposure control. Functionally, the camera provides a resolution capability of approximately 1 mm at 4 meters and can focus from 1.23 meters to infinity.

The mirror assembly contains a mirror supported at its minor axis by trunnions. This mirror is formed by vacuum-depositing a Kanogen surface on a beryllium blank, followed by a deposition of aluminum with an overcoat of silicon monoxide. The mirrored surface is flat over the entire surface to less than $\frac{1}{4}$ wavelength at $\lambda = 550 \text{ m}\mu$ and exhibits an average specular reflectivity in excess of 86%. The mirror is positioned by means of two drive mechanisms, one for azimuth and the other for elevation.

The mirror assembly also contains a four-section filter wheel. As redesigned for *Surveyors VI* and *VII*, three sections contain polarizing filters with polarization angles of 0, 45, and 90 deg, respectively, in a clockwise direction relative to the mirror elevation axis. The fourth section contains a neutral density filter element for nonpolarized observations. The neutral density filter transmission characteristic is selected such that the camera's response to nonpolarized light is identical to that of the polarizing filters (38%).

Camera operation is totally dependent upon reception of the proper commands from earth. Commandable operation allows each frame to be generated by shutter sequencing preceded by appropriate lens settings and mirror azimuth and elevation positioning to obtain selected views of the subject.

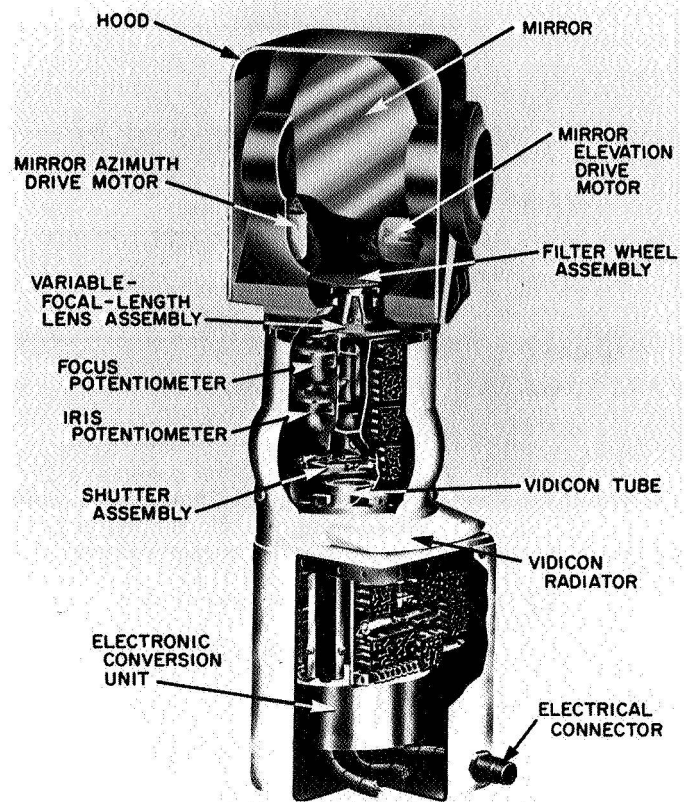


Fig. IV-42. *Surveyor VII* television camera

Figure IV-43 depicts a functional block diagram of the survey camera and television auxiliary. Commands for the camera are processed by the telecommunications command decoder, with further processing by the television auxiliary decoder. Identification signals, in analog form, from the camera are commutated by the television auxiliary, with analog-to-digital conversion being performed within the signal processing equipment of the telecommunications subsystem. The ID data in PCM form is mixed in proper time relationship with the video signal in the TV auxiliary and subsequently sent to the telecommunications system for transmission to earth.

The mirror assembly used on *Surveyors VI* and *VII* is a completely redesigned version of the mirror assembly used on all previous missions. The purpose of the redesign was to improve performance and reliability. Occasional failure to respond to azimuth or elevation stepping commands was corrected by increasing motor torque output and reliability, reducing frictional and inertial loading, and providing adjustable end stops. Pointing accuracy was improved. A labyrinth seal was added to reduce dust accumulation on optical surfaces when the mirror

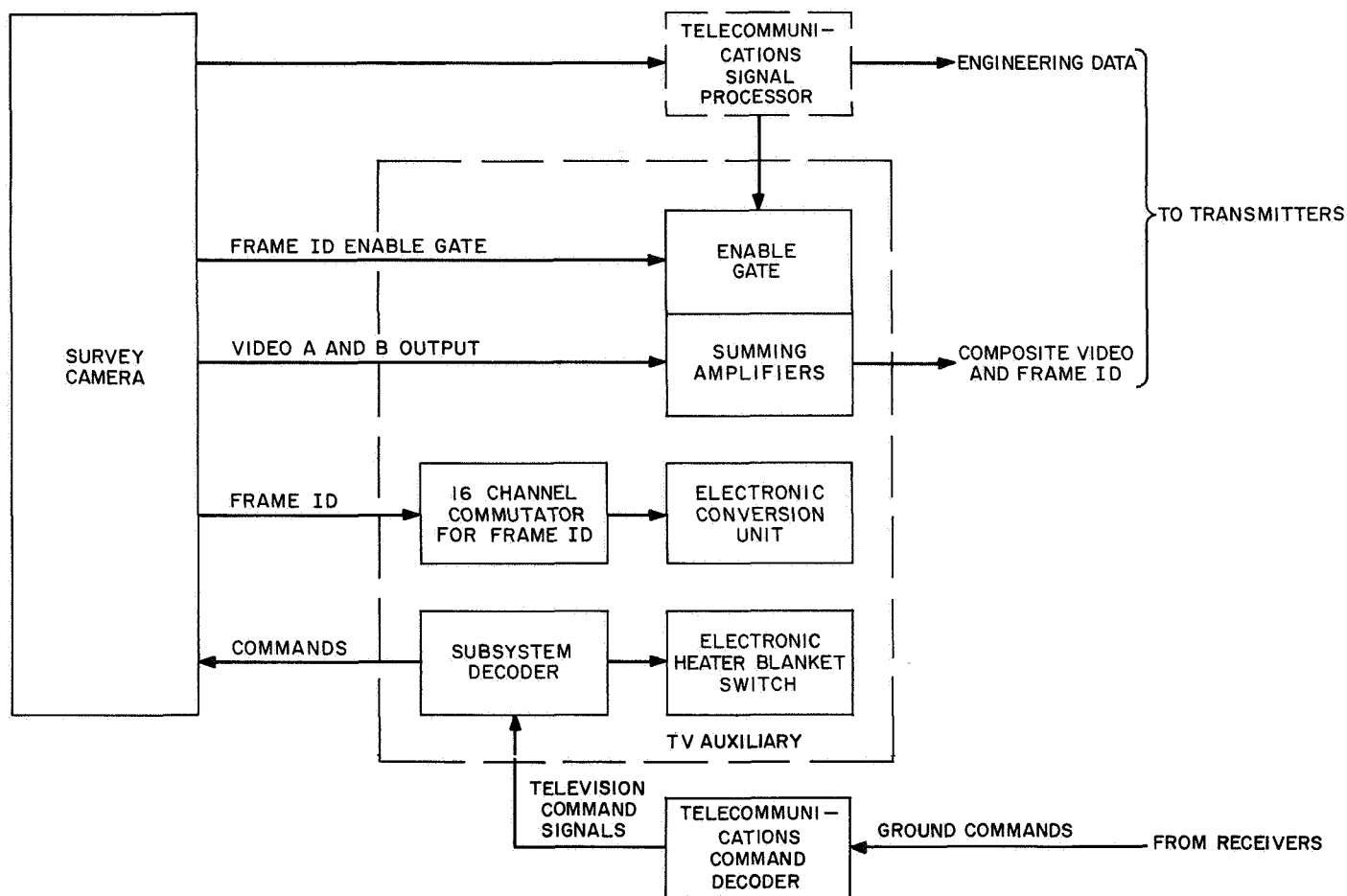


Fig. IV-43. Simplified television camera functional block diagram

is closed. The hood was extended at top and sides, and the front flange was painted black to reduce glare in pictures. On *Surveyor VII*, additional areas within the hood were painted black to further reduce glare susceptibility. Other design changes enabled removal of the hood or mirror assembly without requiring recalibration or requalification.

The optical formation of the image is performed by means of a variable-focal-length lens assembly placed between the vidicon image sensor and the mirror assembly. The lens is capable of providing a focal length of either 100 or 25 mm, which results in a field of view of approximately 6.43 or 25.3 deg, respectively. The aspect ratio was 1:1 on *Surveyor VII* rather than 1.1:1 as was the case on *Surveyor VI*. Special commanding can result in additional focal lengths between 25 and 100 mm. Additionally, the lens assembly may vary its optimum focus by means of a rotating focus cell from 1.23 meters to infinity, while an adjustable iris provides effective aper-

ture changes from $f/22$ to $f/4$. The redesigned camera used for *Surveyors VI* and *VII* provides $\frac{1}{2}$ - f -stop increments of adjustment compared to full- f -stop increments on the earlier camera. The aperture area increases by a factor of $\sqrt{2}$ for each $\frac{1}{2}$ - f -stop increment. While the most effective iris control is accomplished by means of command operation, a servo-type automatic iris is available to control the aperture area in proportion to the average scene luminance. As in the mirror assembly, potentiometers are geared to the iris, focal length, and focus elements to allow readout of these functions. A beam splitter, integral to the lens assembly, provides the necessary light sample (10% of incident light) for operation of the automatic iris.

Three modes of exposure control are afforded the camera by means of a mechanical focal plane shutter located between the lens assembly and the vidicon image sensor. In the *normal shutter* mode, upon earth command, the two shutter blades are sequentially driven

by solenoids across an aperture in the shutter base plate, with appropriate delay between blades. The time interval between the blade motions determines the exposure interval, which is nominally 150 msec.

In the second shutter mode (*open shutter mode*) the blades are positioned to leave the aperture open, thereby providing continuous light energy to the image sensor. This mode of operation is useful in the imaging of scenes exhibiting low luminance levels, including some of the brighter stars. The effective shutter time in this mode is 1.2 sec, nominally.

A third exposure mode, used for extremely low luminance levels such as stellar observations, lunar surface observation under earthshine illumination conditions, and faint solar corona observations, is referred to as the *integrate mode*. This mode is implemented by opening the shutter, turning off the vidicon electron beam, and then, after any desired exposure time, turning on the vidicon electron beam. Scene luminances on the order of 0.008 ft-lamberts are easily reproduced in this mode of operation, thereby permitting photographs under earthshine conditions. Detection of sixth-magnitude stars has been accomplished using this mode of operation with an exposure time of 5 min.

The transducing process of converting light energy from the object space to an equivalent electrical signal is accomplished by the vidicon tube. A reference mark is included in each corner of the scanned format, which provides, in the video signal, an electronic dark-current level of the scanned image.

In the normal, or *600-line* scan mode, the camera provides one frame every 3.6 sec. Each frame requires nominally 1 sec to be read from the vidicon and utilizes a bandwidth of approximately 220 kHz, requiring transmission over the high-gain (planar array) antenna in the high-power transmitter mode.

A second scan mode of operation provides one 200-line frame every 61.8 sec. Each 200-line frame requires 20 sec to complete the video transmission and utilizes a bandwidth of 1.2 kHz. This *200-line* mode is used for high-power transmission over either one of the omniantennas.

Integral to the spacecraft and within the viewing capability of the camera are two photometric/colorimetric reference charts (Fig. IV-44). These charts, one on Omniantenna B and the other adjacent to Footpad 3,

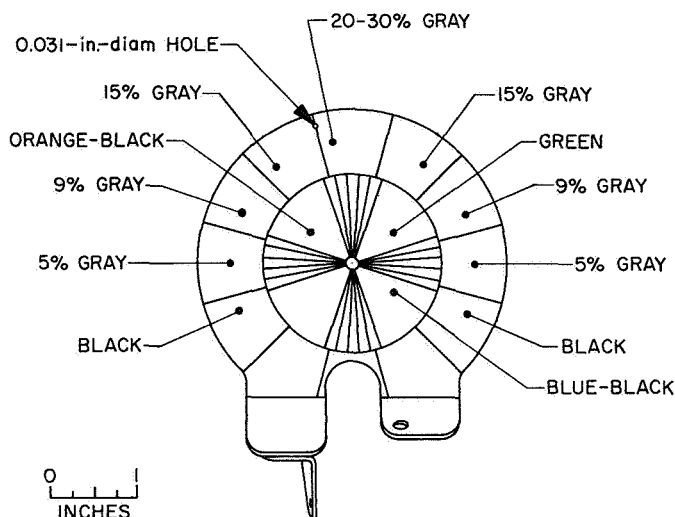


Fig. IV-44. TV photometric/colorimetric reference chart

are located such that the line of sight of the camera when viewing the chart is normal to the plane of the chart. The charts are identical, and each contains a series of 13 gray wedges arranged circumferentially around the chart. In addition, three color wedges, whose CIE chromaticity coordinates are known, are located radially from the chart center. A series of radial lines is incorporated to provide a gross estimate of camera resolution. Finally, the chart contains a centerpost which aids in determining the solar angles after lunar landing by means of the shadow information. Prior to launch, each chart is calibrated goniophotometrically to allow an estimation of postlanding camera dynamic range and to aid photometric data reduction.

The survey camera incorporates heaters to maintain proper thermal control and to provide a thermal environment in which the camera components operate. The heater elements are designed to provide a sustaining operating temperature during the lunar night if energized. These consume 36 W of power when activated. A minimum temperature of -20°F should be achieved prior to camera turn-on if operation is to be performed within known functional calibrations.

Three auxiliary mirrors were installed on the *Surveyor VII* spacecraft for viewing obstructed areas of interest beneath the spacecraft. The largest of these was mounted for viewing of the area beneath Vernier Engine 3 and Crush Block 3, the next largest was mounted for viewing the area beneath Vernier Engine 2 and Crush Block 2, and the smallest was mounted for viewing the alpha scattering instrument deployment area on the lunar surface.

An additional mirror was mounted on the spacecraft mast to permit the camera to view, effectively from an additional position, a portion of the area of the lunar surface upon which surface sampler operations were being conducted. The base-line separation provided stereoscopic sets of pictures for photogrammetric purposes.

Seven small "dust" mirrors were mounted at various locations in order to be mutually positioned within the line-of-sight of both the TV camera and an exhaust plume of one of the vernier engines. Their purpose was to present, as a function of the ratio of diffuse light scattering relative to the remaining specular reflectivity, a relative indication of each mirror's contamination by particle deposition or by erosion.

2. Performance Characteristics

A premission calibration was performed on the survey camera with the camera mounted on the spacecraft. Each calibration utilized the entire telecommunication system of the spacecraft, thereby including those factors of the modulator, transmitter, etc., which influence the overall image transfer characteristics. The calibration data, in FM form, was recorded on magnetic tape for playback through the ground support equipment (GSE) at Goldstone and Pasadena. Thus the final calibration data recorded on the real-time mission film and tape equipment provides a complete system calibration.

The parameters which were calibrated included light transfer characteristics, polarization response, sine wave response, erasure characteristics, automatic iris tracking, geometric linearity, and camera pointing accuracy. Data was taken in both 600- and 200-line scan modes and in normal shutter, open shutter, and integrate exposure modes. The calibration data shows that the *Surveyor VII* camera system has a 30% horizontal response at about 600 TV lines in the 600-line scan mode. The identical light transfer characteristics for the three polarizing filters and the neutral density filter provide the capability of taking a set of polarized pictures without the necessity of changing iris position. Reduction of polarimetric data is then independent of accuracy or repeatability limitations in iris control.

3. Mission Performance

Surveyor VII television camera performance was excellent in quality and quantity of pictures, as well as in the extent of operations which could be conducted unrestricted by camera problems. The camera performed

perfectly throughout the mission. Picture quality was excellent primarily because the camera characteristics exhibited good dynamic range. A contributing factor was that the optical surfaces remained clean because the redesigned mirror head assembly permitted the camera mirror to be fully closed during the transit phase.

During the first lunar day, in addition to DSS 11 operations, the camera was operated from DSS 42, Canberra, and to a lesser extent from DSS 61, Madrid, resulting in approximately 21,000 pictures being taken.

The *Surveyor VII* pictures include views of parts of the spacecraft, views of the area beneath the spacecraft using auxiliary mirrors, panoramic narrow- and wide-angle surveys of the lunar landscape in azimuth and elevation, photometric surveys of specially selected objects, stereoscopic views, star surveys, focus ranging sequences for mapping of the surrounding lunar surface, shadow progressions, views through different polarization filters, and a postsunset sequence lasting about 16 hr that included star and solar corona observations and earthshine pictures.

Because *Surveyor VII* landed at about 40°S latitude, it was the first of the seven spacecraft which could take frequent, unobstructed, narrow-angle views of the earth. Earth pictures, with and without polarizing filters were taken throughout the lunar day.

The camera was used to observe particle accumulation on the bar magnets and on the seven "dust" mirrors. It provided the visual aspect of the surface sampler experiment. It assisted in relocation and in ascertaining surface contact of the ASI. It was of particular value in interpreting the initial failure of the ASI to deploy and in guiding successful deployment by manipulation of the surface sampler.

The camera was also used to detect, for the first time, laser beams transmitted from the earth. Pictures of the earth were taken in which two laser beams can be seen. The beams, originating from argon ion lasers, were transmitted through telescopes at the JPL Table Mountain Observatory, in Wrightwood, California, and the Kitt Peak National Observatory, at Tucson, Arizona.

Operations attempted during the second lunar day were limited because of spacecraft power problems. Pictures in 600-line scan mode could not be transmitted in the normal way because high-power transmission was inoperative.

When 600-line pictures were commanded using low-power transmission, the received signal indicated a camera anomaly, which was possibly the absence of horizontal scan. However, camera performance in 200-line scan mode was normal, so this mode was used during whatever TV operations were permitted as determined by other spacecraft problems.

J. Soil Mechanics/Surface Sampler

The SM/SS is an electromechanical device which is remotely operated by earth-based command to pick, dig, scrape, trench, and handle lunar surface material. After the success of *Surveyor III* SM/SS operations, a decision was made to include the surface sampler on the *Surveyor VII* mission. The mounting attitude was modified

to provide a capability for the ASI sensor head relocation on the lunar surface. The area of permissible relocation of the sensor head can be seen in Fig. IV-45.

1. SM/SS Description

The SM/SS subsystem consists of a mechanism and an electronics auxiliary, with the necessary supporting substructure and interconnecting wire harnesses. The instrument mechanism is located below the survey television camera, between the ASI and Leg 2 as shown in Fig. IV-46. The mechanism has an extension/retraction arm which can also be pivoted in azimuth or elevation to permit operations within the surface area indicated in the figure. The arm is locked in the folded position until it is to be deployed after lunar landing, at which time it is unlocked by the firing of a squib. Attached to the end of

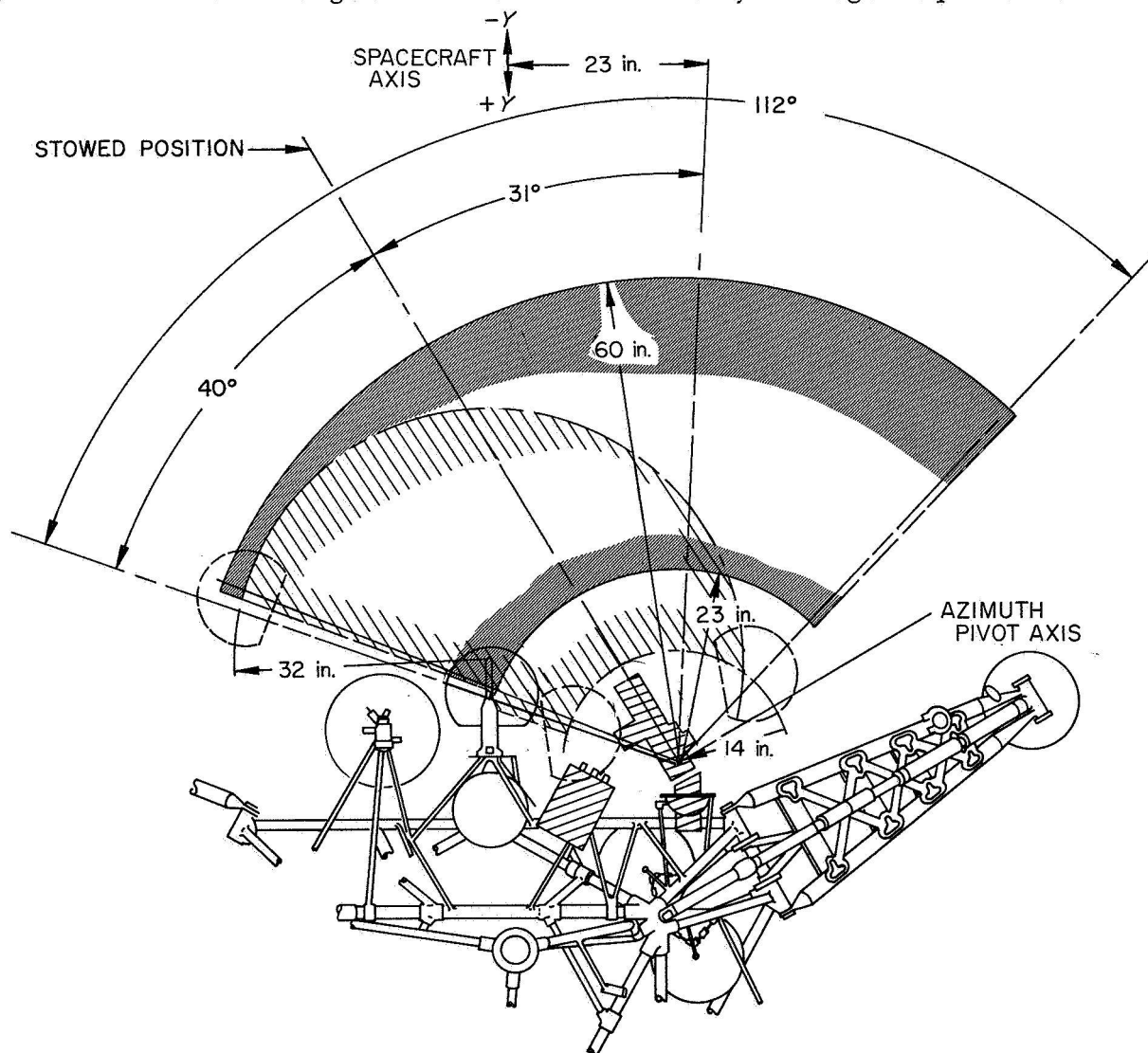


Fig. IV-45. SM/SS operating envelope and permissible region for redeployment of ASI sensor head

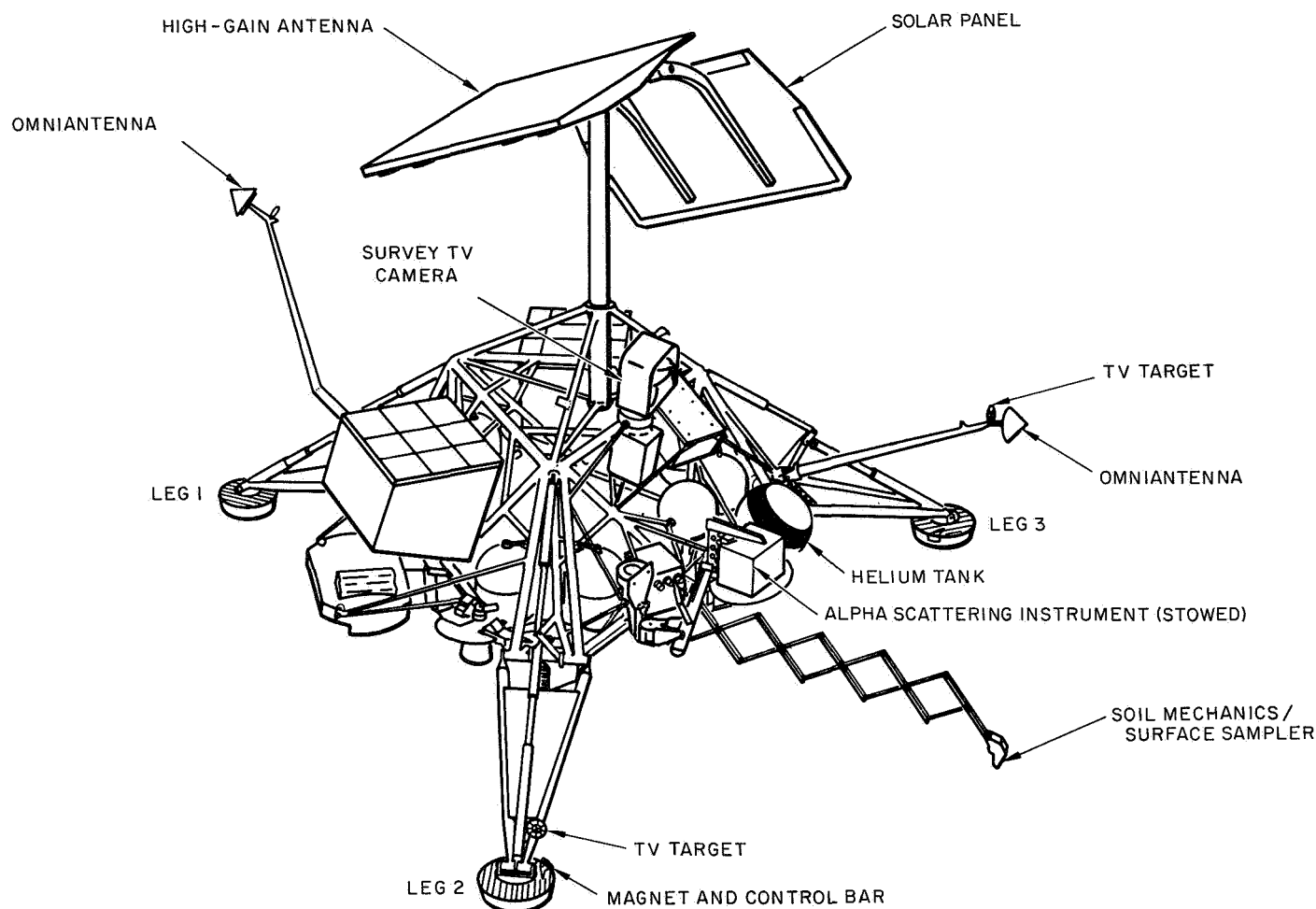


Fig. IV-46. Surveyor VII spacecraft in postlanded configuration

the arm is a scoop having a sharpened blade and a door. The scoop is capable of holding solid material up to about 1.25 in. (3.2 cm) in diameter and granular material up to about 6 in. (100 cm) in volume. A small bearing plate is attached to the scoop door to present a flat surface to the lunar surface when the door is closed. For the *Surveyor VII* mission, two small, rectangular horseshoe magnets were placed in the scoop door bearing plate.

Four electric motors are used to manipulate the SM/SS: one each for extension/retraction, azimuth, and elevation motions, and one located at the scoop to open or close the door. An electromechanical clutch can be operated by earth command to disengage the elevation drive train, allowing the scoop to be impelled downward by a pre-tensioned elevation torque spring to strike the lunar surface.

The electronics auxiliary provides command decoding, data buffering, power management, squib firing, and

switch control of the mechanism motors and clutch. Either a 2-sec or a 0.1-sec period of operation of any of the motors can be selected by earth command. The angle or distance through which the SM/SS moves by these commands depends on the motor involved, its condition, temperature, voltage, and the working load.

On *Surveyor VII*, the output of the motor current measuring amplifier was telemetered via five symmetrically spaced commutator frames and provided much-improved force data over previous spacecraft. Also, direct telemetry measurement of both the retraction and elevation motor temperatures provided for more accurate comparison of lunar data with preflight calibration information.

Since SM/SS direct instrumentation is limited to motor current, the primary means of obtaining SM/SS data is through the coordinated operation of the television camera, where television frames are commanded at selected intervals between SM/SS movements. Sequences and

priorities of SM/SS tests are therefore dependent upon viewing conditions, spacecraft shadow patterns, and the performance of the television system. The azimuth axes of the SM/SS mechanism and camera are not collinear; therefore, the television viewing angle of the scoop varies with scoop position.

A static bearing test is performed by exercising the extension and azimuth motions until the scoop is positioned above the desired surface point. Then the scoop is driven downward with the elevation motor until the desired penetration is achieved, or until the motor is stalled. The static test is normally performed with the scoop door closed to provide a flat surface for contact. However, an open scoop static test can also be carried out. As the SM/SS is extended, the angle that the scoop makes with the test surface varies. At contact with a smooth surface, the flat face of the scoop door is normal to the tangential elevation motion, when the arm is fully extended.

For an impact test, the scoop is also positioned first above the desired surface area. Then the elevation drive clutch is released, allowing the scoop to drop to the surface, accelerated by gravity and the elevation torque spring. Impact tests are also performed with the scoop door open or closed, as desired.

A trenching operation is performed by driving the scoop down into the surface with the door open, then drawing it toward the spacecraft by repeated commanding of the retraction motor. Material can be removed from the trench either by retracting the scoop until it is clear of the surface, forming a pile at the foot of the trench, or by closing the scoop and lifting the material out of the trench.

2. SM/SS Performance

During transit, the increased heater capacity (from 5.0 to 7.5 W) kept the SM/SS electronic auxiliary well within its operating limits. After touchdown, SM/SS operations were delayed to prevent disturbance of the ASI sample. Subsequent problems with the ASI deployment led to a turnon of the SM/SS.

Initial operations included firing of the pyrotechnic locking device to release the SM/SS from its stored position and a checkout of the arm drive mechanisms. Normal operation was achieved in all directions.

The SM/SS mechanism and auxiliary performed without a problem or failure throughout the mission; Fig. IV-47 shows the temperature profile and periods of operation. The total on-time and number of commands processed by the auxiliary are shown in Table IV-20.

Early in the first lunar day, the SM/SS was used to forcibly deploy the ASI to the lunar surface. Subsequent operations provided a second and third sample for ASI analysis. Fig. IV-48 shows the SM/SS moving the ASI during one of these redeployments.

During the course of the first lunar day, the SM/SS performed sixteen bearing tests, dug seven trenches, moved numerous rocks, and supported the ASI operation through redeployment and by providing shade for its thermal control surfaces. Figure IV-49 shows the location of the various operations, and Figs. IV-50 and IV-51 show the area of SM/SS operations before and after most of the surface tests were performed.

Table IV-20. Summary of SM/SS operating time and response to commands

	January 1968, GMT													Total
	11	12	13	14	15	16	17	18	19	20	21	22	23	
SM/SS power-on time (hr:min)	3:59	6:30	3:29	3:43	0:09	0:00	0:10	0:03	3:07	5:35	4:37	4:01	0:58	36:21
Commands addressed to SM/SS	806	1581	1499	2008	73	0	42	21	1364	2006	1289	1830	120	12,639
SM/SS functions performed	371	766	853	1190	38	0	18	9	989	1022	713	1017	61	6,956
SM/SS mechanism motions commanded	184	426	561	828	22	0	6	3	590	596	463	685	33	4,397

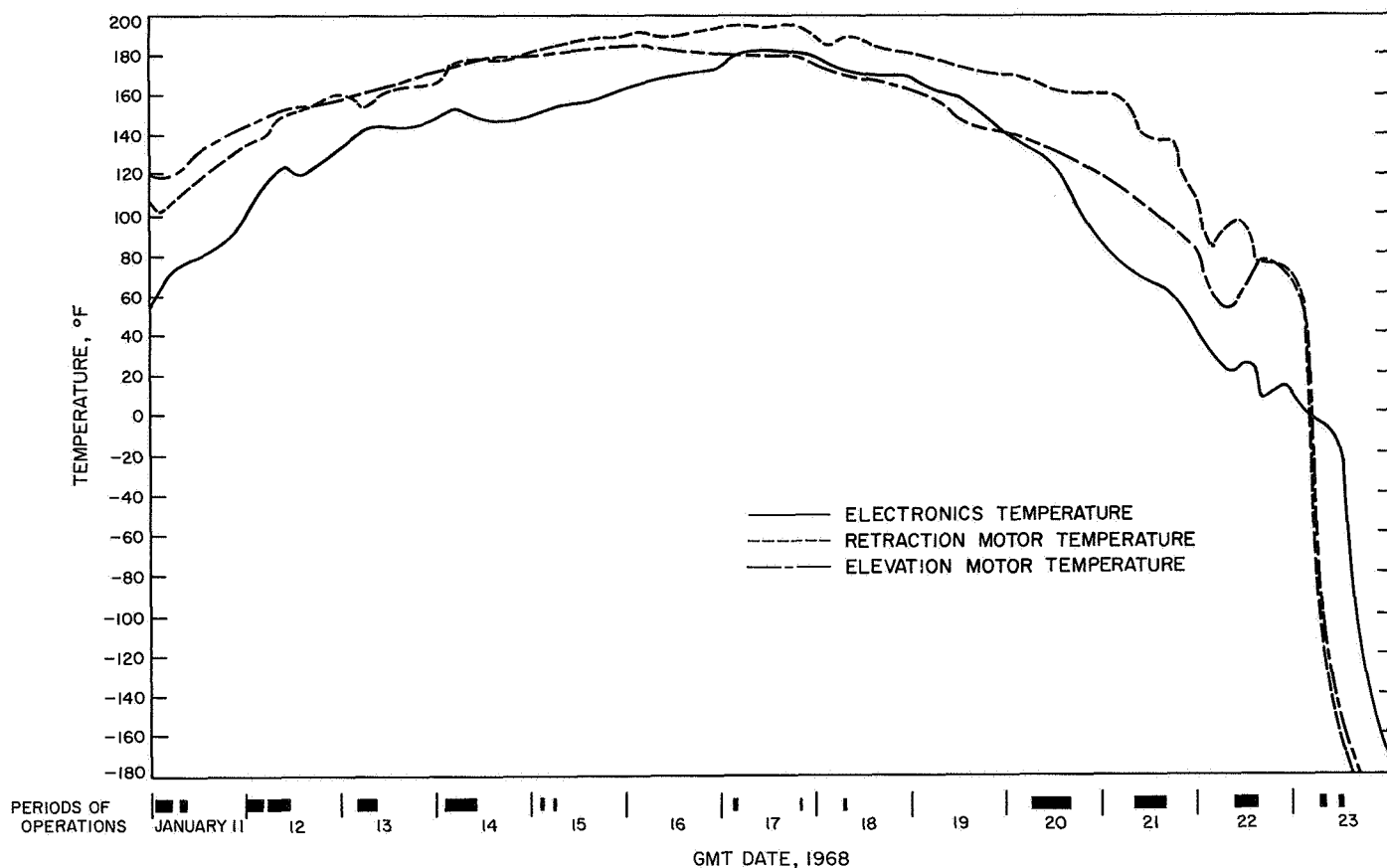


Fig. IV-47. SM/SS temperature profile and period of operation

The SM/SS subsystem was operated after sunset, and performed normally when the motors were at a temperature of approximately -167°F .

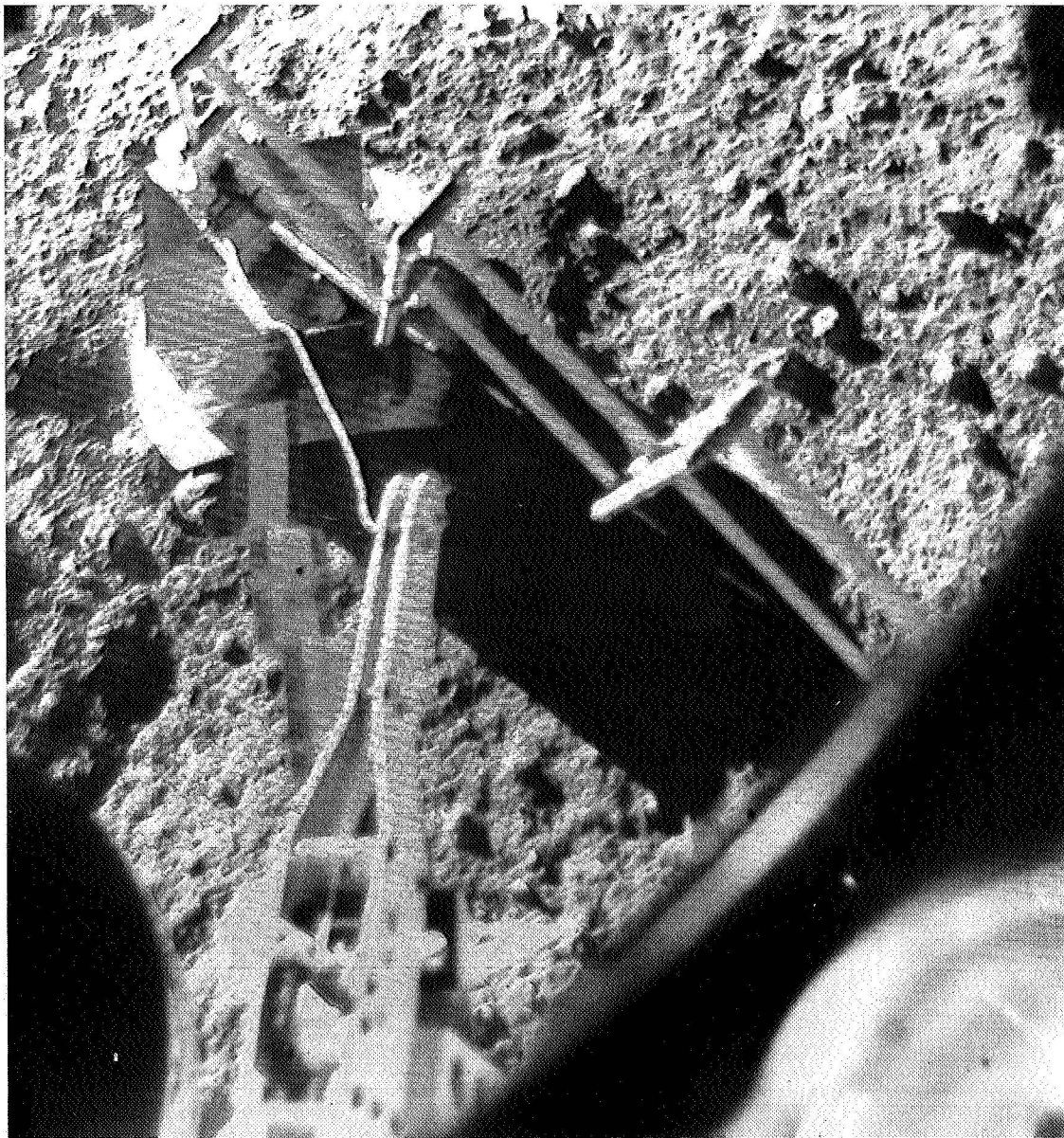
The scientific results and a detailed description of the operations are presented in Part II of this report.

K. Alpha Scattering Instrument

The alpha scattering technique of lunar surface chemical analysis takes advantage of the characteristic interactions of alpha particles with matter to provide information on the chemical composition. The energy spectra of the large-angle, elastically scattered alpha particles are characteristic of the nuclei doing the scattering. In addition, certain elements, when bombarded with alpha particles, produce protons, again with characteristic energy spectra. Consequently, these energy spectra and intensities of scattered alpha particles and protons can be used to determine the chemical composition of the material being exposed to the alpha particles.

The method has good resolution for the light elements found in rocks. (However, it can give only indirect information about hydrogen.) The resolution becomes poorer as the atomic weight increases (Fe, Co, and Ni cannot easily be resolved), even though the sensitivity is greater for heavy elements than for most light elements. The sensitivity for elements heavier than lithium is approximately 1 atomic percent.

The absence of an atmosphere on the moon makes practical the use, for such chemical analyses, of the relatively low-energy alpha particles from a radioactive source. $\text{Cm}^{242}(t_{1/2} = 163 \text{ days}, T_a = 6.11 \text{ MeV})$ is the nuclide used in the *Surveyor* instruments. The use of low-energy alpha particles, however, restricts the information obtained to that pertaining to the uppermost few microns of material. The method is thus one of *surface* chemical analysis. Moreover, using practical source intensities, the rate of analysis is rather slow. A relatively complete analysis requires about one day. In spite of these disadvantages, the use of a radioactive source makes possible a relatively simple and compact instrument for deployment directly onto the lunar surface.



**Fig. IV-48. SM/SS redeploying ASI sensor head to second sample site
(January 21, 1968, 11:44:53 GMT)**

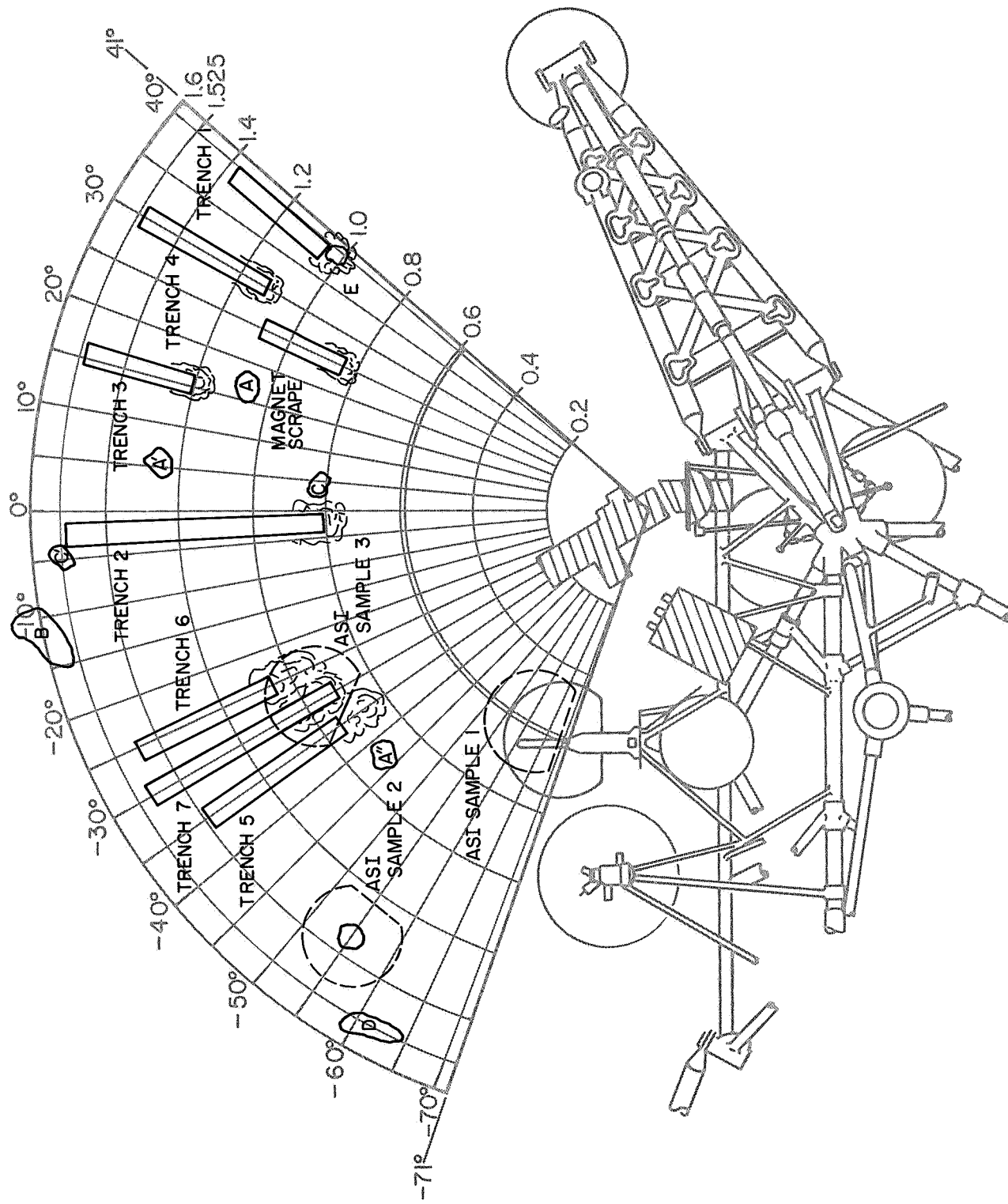


Fig. IV-49. Location of SM/SS operations and ASI samples

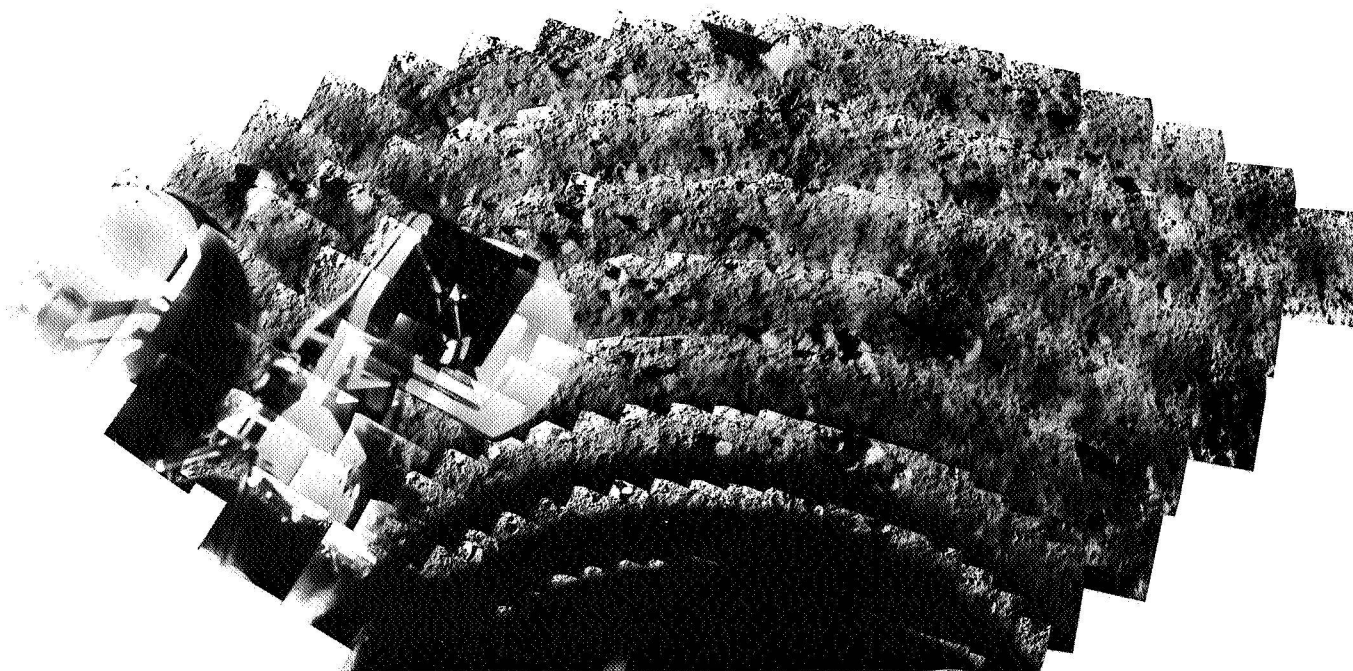


Fig. IV-50. Mosaic of Surveyor VII pictures showing area of SM/SS operations prior to conducting tests (Photograph P-8511)

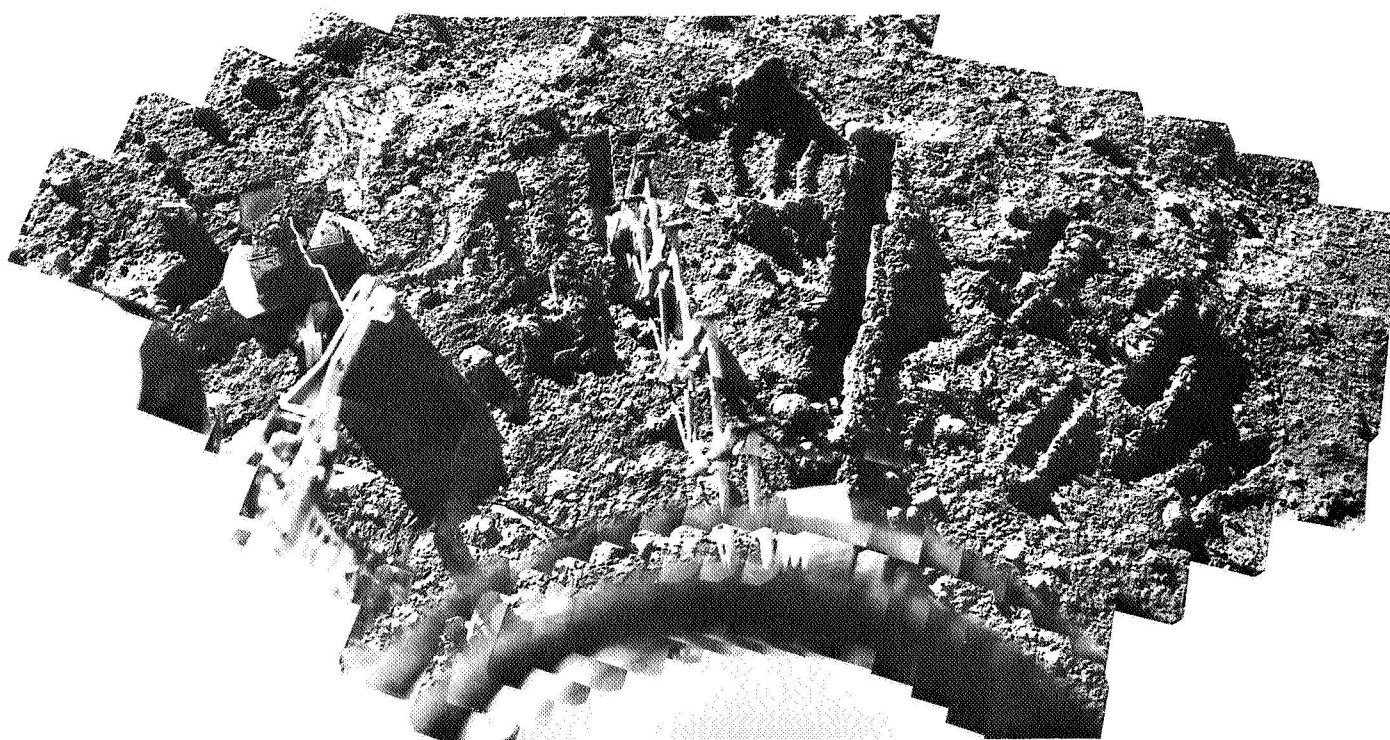


Fig. IV-51. Mosaic of Surveyor VII pictures showing area of SM/SS operations after conducting tests (Photograph 211-2612B)

1. Instrument Description

The ASI consists of a sensor head, which is deployed onto the lunar surface, and a digital electronics package located in a thermal compartment on the spacecraft. Associated equipment includes an electronic auxiliary, a deployment-mechanism/standard-sample assembly, and a thermally insulated electronics compartment. Figure IV-52 is a photograph of the instrument and its auxiliary hardware.

The ASI sensor head contains the radioactive sources which bombard the sample under analysis with a collimated stream of alpha particles through the circular opening in the bottom of the head. The alpha detectors

placed near the alpha sources register and measure the energy of alpha particles scattered almost directly backward from the sample. Similarly, four larger detectors perform the same function for protons produced by nuclear interaction of alpha particles with some of the light elements in the sample. After amplification and energy sorting, the signals from these detectors are converted to a form suitable for transmission to earth by digital electronic circuitry in one of the thermal compartments of the spacecraft.

In this mission, the instrument was modified from previous *Surveyor* instruments by the installation of a knob at the point on the top of the sensor head where the

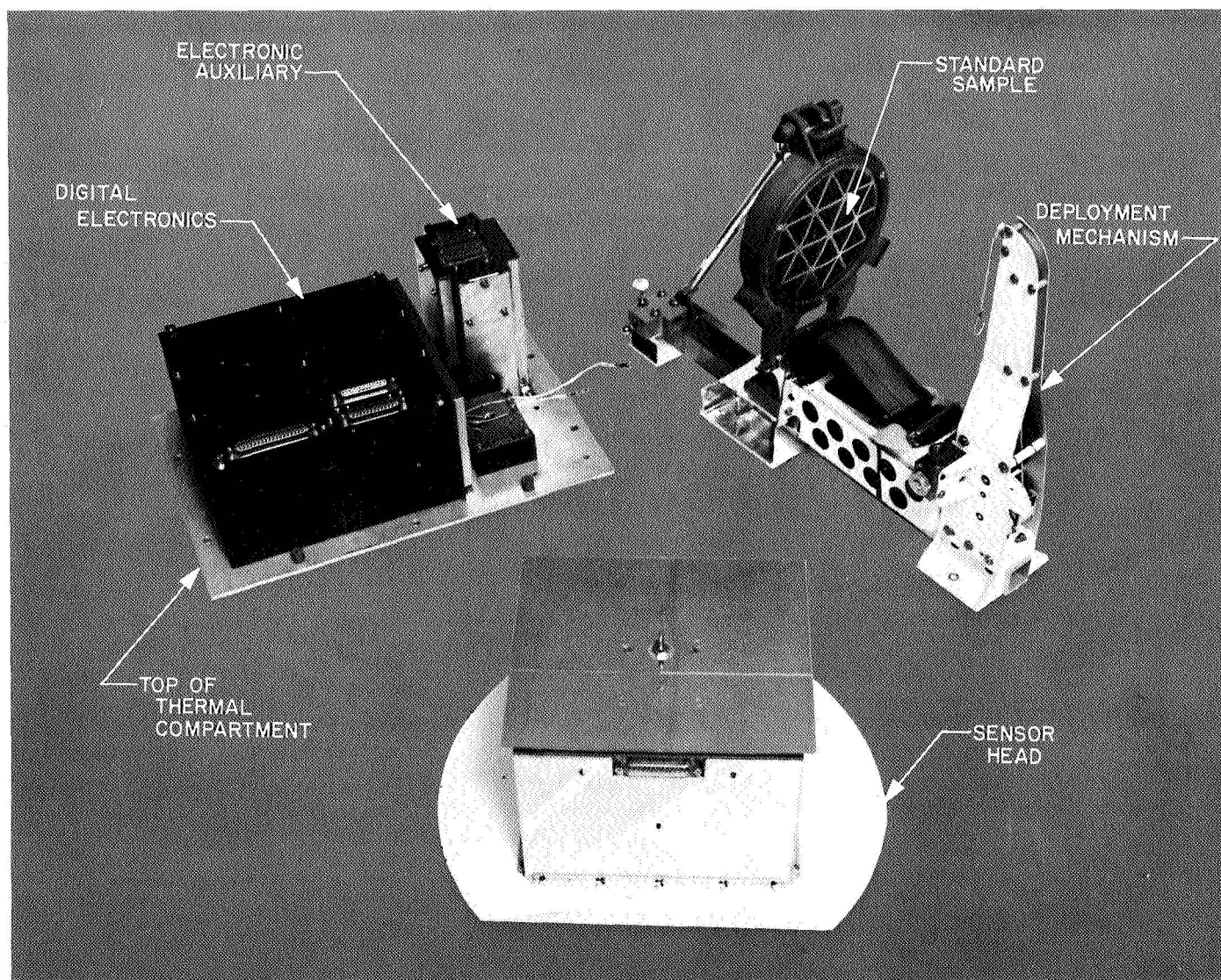


Fig. IV-52. ASI components

deployment cord is attached. This provided a handle for the surface sampler in moving the sensor head from one position to another on the moon.

The total weight of the alpha scattering equipment, including mechanical and electrical spacecraft-interface substructure and cabling, is 29 lb. Power dissipation is 2 W, increasing to 17 W when heaters in the sensor head and electronics compartment are both active.

a. Sensor head. The sensor head is primarily a box ($6\frac{3}{4} \times 6\frac{1}{2} \times 5\frac{1}{4}$ in. high), with a 12-in.-diameter plate

on the bottom. The main purpose of the plate is to minimize the probability of the box sinking appreciably into a possibly soft lunar surface. Figure IV-53 shows a bottom view of the sensor head. In the bottom of the sensor head is a sample port, $4\frac{1}{4}$ in. in diameter. Recessed $2\frac{3}{4}$ in. above this circular opening is a set of six curium-242 alpha sources, collimated in such a way that the alpha particles are directed through the opening. Across the face of each collimator is a thin, aluminum-oxide film to prevent recoils from the alpha source from reaching the sample area; a second film is mounted in front of each collimator for additional protection. Close to the

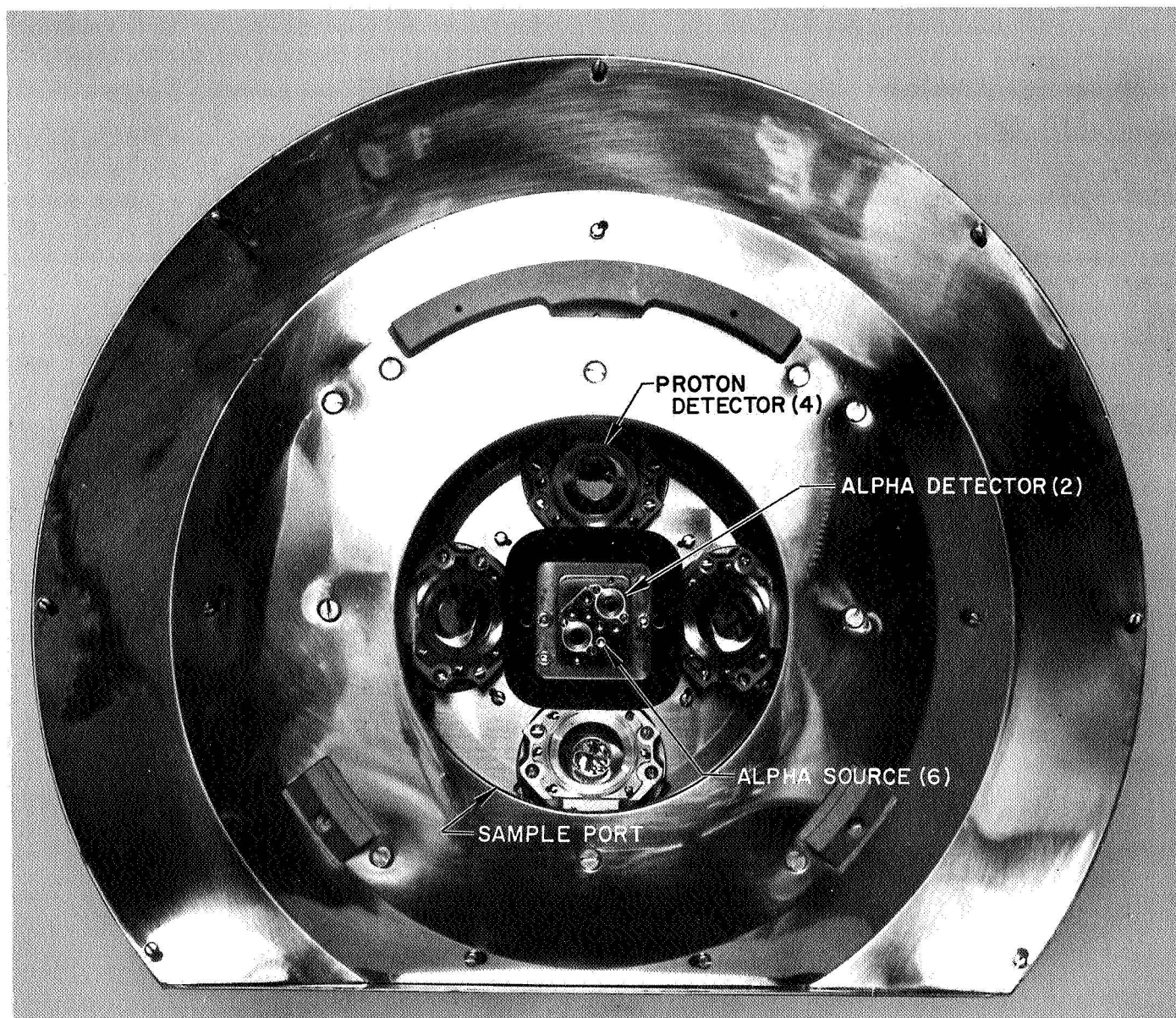


Fig. IV-53. View of bottom of ASI sensor head

alpha sources are two detectors arranged to detect alpha particles scattered back from the sample at an average angle of 174 deg from the original direction. These 0.031-in.² alpha detectors are of the silicon, surface-barrier type, with evaporated-gold front surface films. Thin films are mounted on collimation masks to protect the detectors from alpha contamination and excessive light.

The sensor head also contains four lithium-drifted silicon detectors (of approximately 0.155-in.² area each) designed to detect protons produced in the sample by the alpha particles. Gold foils, approximately 0.4-mil thick, prevent scattered alpha particles from reaching these detectors. Figure IV-54 is a diagrammatic side view of the sensor head, showing the configuration of sources, sample, and detectors.

Because the expected proton rates from the sample are low, and because these detectors are more sensitive to radiation from space, the proton detectors are backed by guard detectors. Most of the charged particles from space that strike a proton detector must first pass through the corresponding guard detector, whereas protons from the sample are stopped in the proton detector. The electronics associated with the guard and proton

detectors are arranged so that an event registered in both will not be counted as coming from the sample. This anticoincidence arrangement reduces significantly the background in the proton mode of the instrument.

Separate, 128-channel, pulse-height analyzers are used with the alpha and proton detectors. An output pulse from a detector is amplified and converted to a time-analog signal whose duration is proportional to the energy deposited in the detector. The outputs of the two alpha detectors are combined before this conversion; a separate mixer circuit is used for the four proton-detector outputs. A rate meter circuit is used to measure the frequency of events occurring in the guard (anticoincidence) detectors, but provides no information on the energy of such events.

In addition to the curium-242 sources, detectors, and associated electronics, the sensor head contains a platinum-resistance thermometer, a 5-W heater, and an electronic pulser. The pulser is used to calibrate the electronics of the instrument by introducing electrical pulses of two known magnitudes at the detector stages of the alpha and proton systems. This calibration mode is initiated by command from earth. Small amounts of

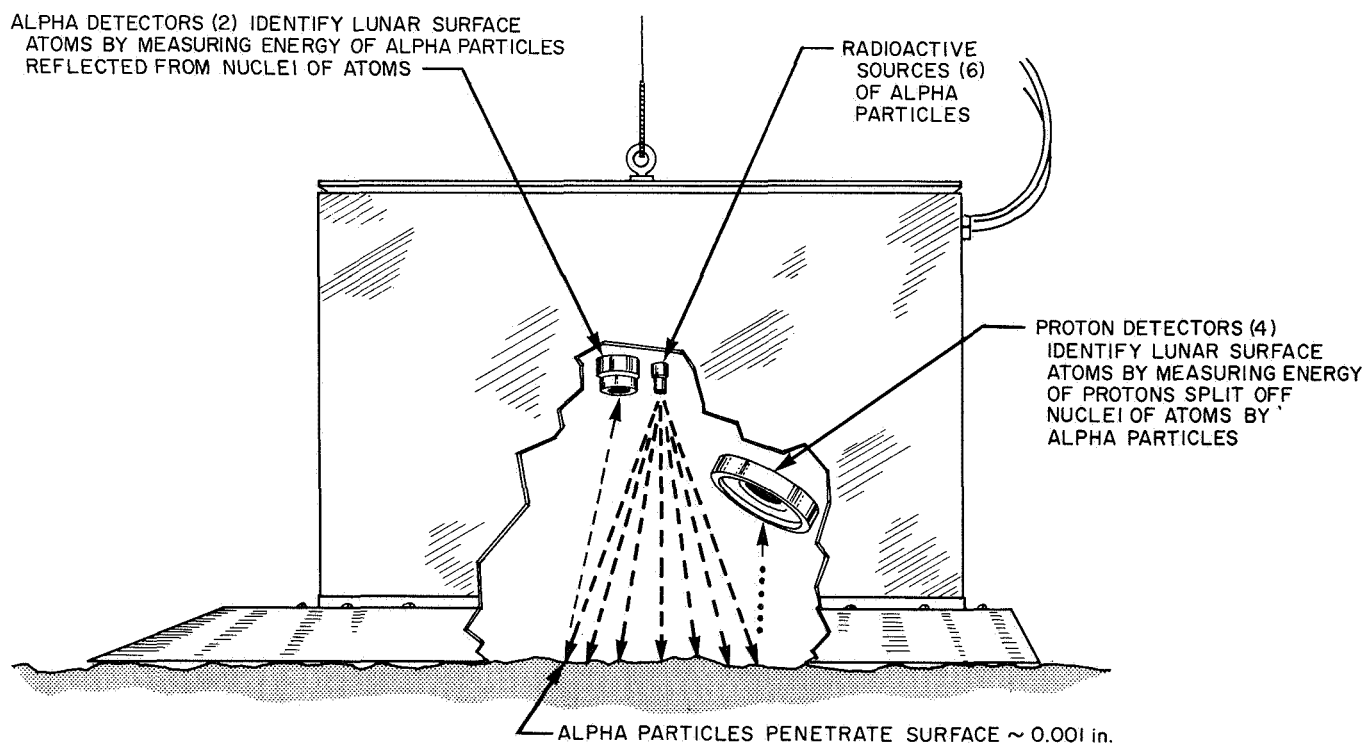


Fig. IV-54. Diagrammatic view of sensor head illustrating functional operation

alpha-radioactive einsteinium-254 are also used to calibrate the alpha and proton systems and, in addition, serve as real-time monitors. The einsteinium is located on the gold foil facing each proton detector and on the thin films mounted in front of the alpha detectors.

The external surfaces of the sensor head have been designed for passive thermal control. A second-surface mirror on top of the sensor head is used as a radiator to cool the sensitive components inside. The 5-W heater is used at low temperatures. The operating temperature range specified for the sensor head is -40 to $+122^{\circ}\text{F}$.

b. Digital electronics. The output of the sensor head is a signal (in time-analog form) that characterizes the energy of an event in either the scattered alpha or proton mode of the instrument. The signals from the sensor head are converted to 9-bit binary words by the digital electronics. Seven bits of each word identify which of the 128 channels represents the energy of the registered event. Two extra bits are added before transmission, one to identify the start of the word and one at the end of each word, as a parity check on transmission errors. Buffer registers provide temporary storage of the energy information for readout into the spacecraft telemetry system. The transmission rates are 2200 bits/sec for the alpha mode and 550 bits/sec for the proton mode. Measured events with energy greater than the range of the analyzers are routed to channel 126 (overflow channel).

The electronics package also contains power supplies and the logical electronic interfaces between the instrument and the spacecraft. For example, the output of an individual detector, together with its associated guard detector, can be blocked by command from earth. Also via the electronics unit, the temperature of the sensor head, as well as various monitoring voltages, can be transmitted to earth.

c. Electronic auxiliary. The required electrical interfaces between the sensor head, digital electronics and spacecraft circuits are provided by an electronic auxiliary that provides command decoding, signal processing, and power management. Basic spacecraft circuits interfacing directly with the sensor head and digital electronics are (1) the central signal processor, which provides signals at 2200 and 500 bits/sec for synchronization of instrument clocks, and (2) the engineering signal processor, which provides temperature-sensor excitation current and commutation of engineering data outputs.

The electronic auxiliary provides two data channels for the alpha scattering instrument. The separate alpha and proton channels are implemented using two subcarrier oscillators. Characteristics of these channels are defined in Table IV-21.

Table IV-21. Characteristics of alpha scattering instrument data channels

Characteristic	Alpha channel	Proton channel
Data input to electronic auxiliary	Digital (nonreturn to zero)	Digital (nonreturn to zero)
Input data rate	2200 bits/sec	550 bits/sec
Subcarrier oscillator center frequency	70,000 Hz	5400 Hz

The electronic auxiliary and the digital electronics are contained in Electronics Compartment C, which is attached to the upper part of the spaceframe. For passive control of temperatures at high sun angles the top of this compartment is painted white and the sides and bottom are insulated. A 10-W heater assembly, operated by means of the engineering signal processor, provides active thermal control at low temperatures. The operating temperature range specified for the electronic units in Compartment C is -4 to $+131^{\circ}\text{F}$.

d. Deployment mechanism/standard sample. The deployment mechanism provides stowage of the sensor head and deployment to the background position and to the lunar surface. The sensor head is mounted to the deployment mechanism by means of three support lugs on the bottom plate. Deployment mechanism clamps that engage these lugs are released during the deployment operation. Figure IV-55 illustrates the two-stage operation of the deployment mechanism. From the stowed position, the sensor head is first released on command to a position 22 in. above the nominal lunar surface by activation of an explosive-pin-puller device. From the background position, the sensor head is then lowered directly to the lunar surface by activation of another explosive-pin-puller device. The deployment velocity is controlled by an escapement.

A sample of known composition is attached to the platform on which the sensor head is mounted in the stowed position. This standard-sample assembly covers the circular opening in the bottom of the sensor head during spacecraft transit and landing to minimize entrance of

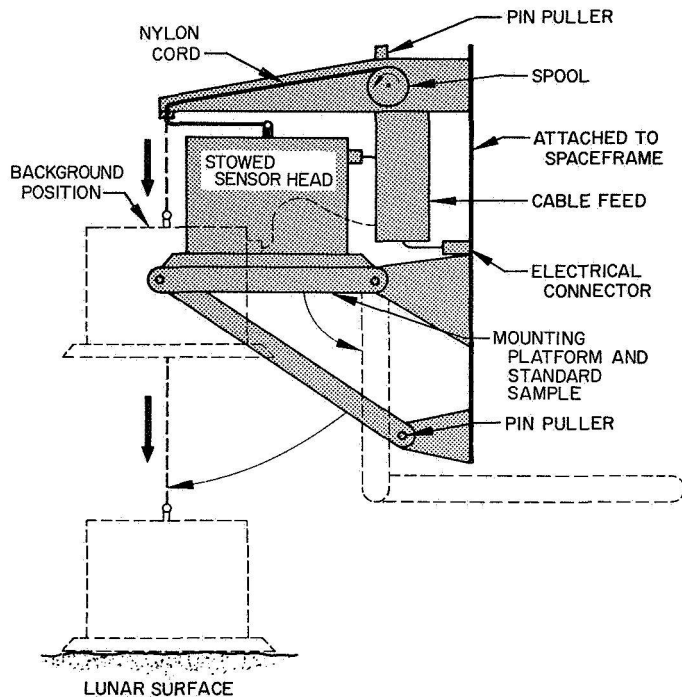


Fig. IV-55. ASI deployment mechanism

dust and light and to provide a means of assessing instrument performance shortly after the spacecraft lands on the moon. The standard sample and mounting platform move aside when the sensor head is deployed to the background position.

2. Alpha Scattering Instrument Data Handling

Two types of information relative to the alpha scattering experiment are transmitted from the spacecraft: engineering data and science data. The engineering measurements are used to monitor instrument voltages, temperatures, detector configuration, and background rates in the anticoincidence detectors. The seven parameters that are monitored are listed in Table IV-22.

The 9-bit digital words that characterize the energy of each of the analyzed alpha particles or protons comprise the science data. These data leave the instrument as separate alpha and proton bit streams and modulate separate subcarrier oscillators; they are then combined with the engineering data and transmitted by the spacecraft to earth. The composite signal from the spacecraft is recorded on magnetic tapes by an FR-1400 recorder at each DSIF station. These magnetic tapes, containing the raw data, comprise the prime source of alpha scattering information for use in postmission analysis.

Table IV-22. Engineering parameters telemetered from alpha scattering instrument

Telemetry channel	Parameter
AS-3	Sensor head temperature
AS-4	Compartment C (digital electronics temperature)
AS-5	Guard rate monitor
AS-6 (digital)	At least one alpha detector on
AS-7 (digital)	At least one proton detector on
AS-8	7-V monitor
AS-9	24-V monitor

For purposes of monitoring the experiment in real-time, the signal is separated at the DSIF station by discriminators and bit synchronizers into 2200-bits/sec alpha data and 550-bits/sec proton data. These reconstituted bit streams are presented to an on-site computer which establishes and maintains synchronization of the 9-bit data words and assembles, within its memory, four spectra of 128 channels each. The four spectra are: alpha parity-correct, alpha parity-incorrect, proton parity-correct, and proton parity-incorrect. In this manner, data is obtained at the stations in accumulations ranging in duration from 2 min during pulser calibration to a nominal 40 min during sample and background phases. The assembled spectra are transmitted via teletype to the SFOF for display and further computer processing.

Data analysis during the mission is performed so that proper control over the experiment may be exercised. The engineering data is simply displayed and compared with prelaunch measurements and predictions to assess the performance of the instrument and the functioning of commands.

The alpha and proton science data is also used to assess the performance of the instrument and is analyzed to determine the duration of the several operational phases. This science-data analysis is conducted in the SFOF using a 7094 computer program.

3. Alpha Scattering Instrument Performance

The *Surveyor VII* launch, transit, and landing operations proceeded normally. Alpha scattering instrument temperatures were monitored during transit to the moon, but the instrument was not activated prior to touchdown.

Analysis of the standard sample under lunar conditions verified that the ASI had arrived on the moon in satisfactory condition. Sharp breakpoints in the sample spectra showed that the high quality of the curium-242 sources had been preserved. The films covering the sources and alpha detectors had survived. The electronics, calibration pulser, and einsteinium sources performed properly as evidenced by the sharpness of calibration peaks and agreement with prelaunch data. The guard detector and anticoincidence system worked as designed; guard monitor voltage agreed well with predicted values.

The sensor head was released to the background position and data accumulation initiated. The data quality during this operational period was good except for a period of increased parity errors (possibly caused by high winds reported at the DSS 61 tracking receiver in Spain).

Because the amount of background data was considered adequate at this stage of the operation, a command to deploy the sensor head to the lunar surface was transmitted. During the *Surveyor V* and *VI* missions, when this command was transmitted, tracking-station personnel had reported that the rate of analyzed events had increased, indicating that the sensor head had descended properly to the lunar surface. This time, no apparent change in counting rate was observed. The deployment command was retransmitted; again, no increase in counting rate was observed. A 10-min accumulation of data verified that the instrument was still suspended above the lunar surface, and possibly had not moved at all.

When tracking operations were transferred to DSS 11, Goldstone, California, television pictures were taken to help diagnose the problem. The pictures showed that the sensor head was still suspended in the background position, but that a small retaining door (used to prevent premature deployment of the flat electronics cable) had opened correctly. This showed that the deployment command had been properly received by the spacecraft and that the squib-activated pin puller had operated. This information isolated the problem to the nylon suspension cord or its associated storage spool and escapement mechanism, affording hope that operation of one of the movable parts of the spacecraft would provide enough force to free the sensor head.

Although the surface sampler (with its versatility of movement and ability to reach the sensor head) offered the most promise of help, possible damage or entanglement of the surface sampler with the nylon cord had to

be considered. The first parts of the spacecraft to be moved, therefore, were the solar panel and planar array antenna. Vibrations induced in the spacecraft by these motions, however, were not sufficient to lower the instrument.

After initial checkout of the surface sampler, and after minimal lunar surface bearing tests had been performed, an attempt was made to free the sensor head by pressing down on the edge of its circular plate. Sufficient force could not be exerted to deploy the instrument, however, because of the manner in which it was free to rotate away from the force. Further attempts were postponed until the following day.

During the following Goldstone visibility period, the surface sampler was able to free the faulty deployment mechanism and push the sensor head to the lunar surface by wedging the sensor head against the spacecraft and then exerting a downward force (Fig. IV-56). The fact that the sensor head was finally deployed and in an acceptable position on the lunar surface was established by the measured rate of reflected alpha particles and by careful analysis of *Surveyor* television pictures.

The *Surveyor VII* mission was extremely productive from the chemical analysis viewpoint. Data was obtained from three positions of the ASI, each representing a different type of local sample: undisturbed local lunar surface, a lunar rock, and an extensively trenched area of the lunar surface. Figure IV-49 shows the location of the three samples relative to the spacecraft.

At the same time, the experiment was handicapped by time restrictions because of the delay in deploying the instrument to the lunar surface and the longer high-temperature period during the middle of the lunar day when the instrument was above its operating temperature. Because of the latitude of the landing site, shading of the instrument during this period by the solar panel and planar array (which had been very effective in the equatorial landing sites of *Surveyors V* and *VI*) was not possible. Shading by the surface sampler helped, but was less effective.

Because only a minimal amount of data on sample 3 could be obtained before sunset on the first lunar day, it was fortunate that the spacecraft and alpha scattering instrument survived the lunar night well enough so that useful data on this sample could be obtained during the second lunar day. A digital anomaly in the proton system prevented the accumulation of useful proton spectra. The

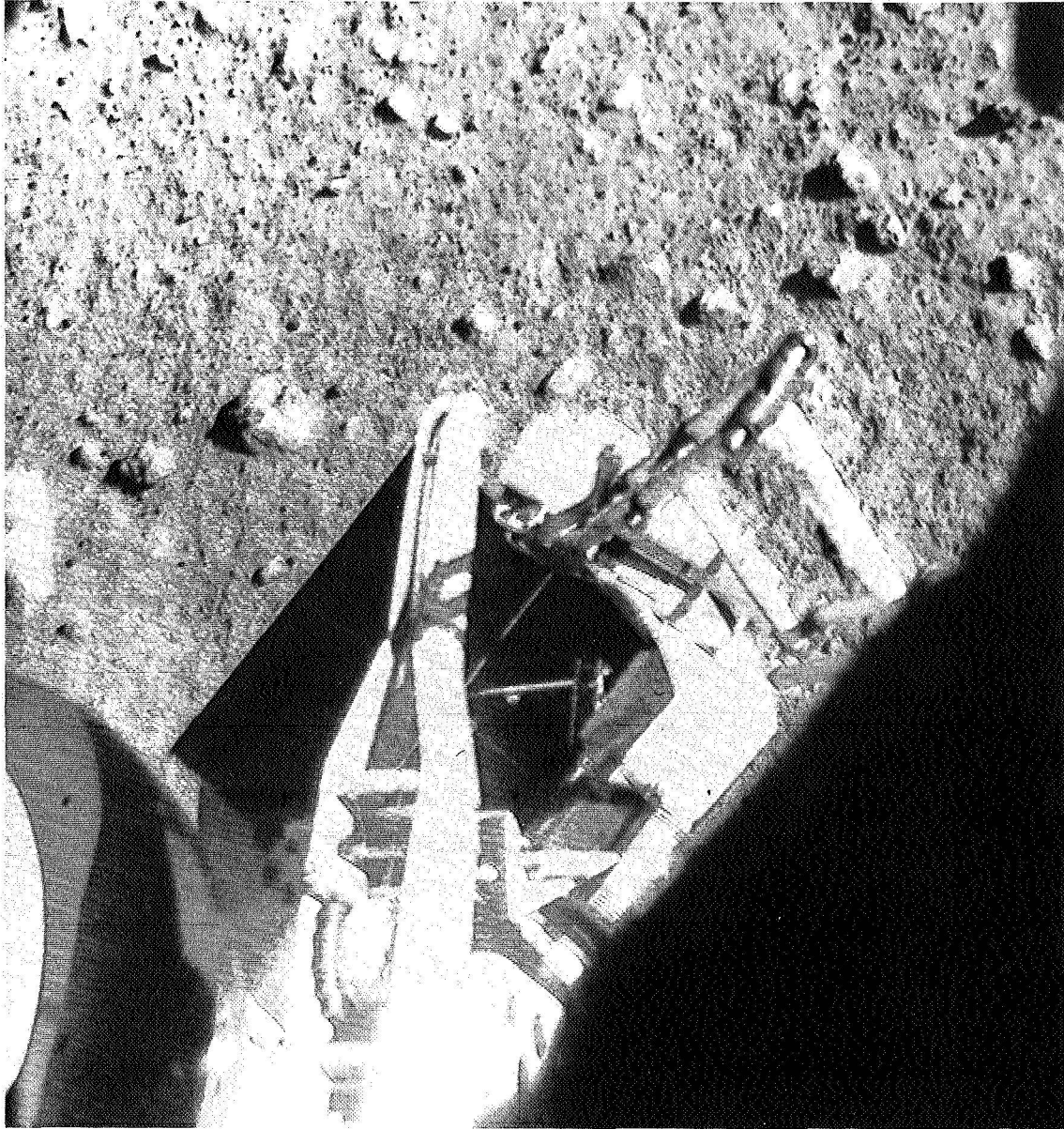


Fig. IV-56. SM/SS forcing the sensor head against the helium tank preparatory to applying downward force to free it (January 12, 1968, 06:57:30 GMT)

alpha system, however, performed nearly as well as during the first lunar day, and between February 13 and February 20, 1968, total accumulations of alpha spectra of 34.5 hr were received: the equivalent of approximately 20 hr of normal alpha data.

Table IV-23 is a summary of the science-data accumulation time on the *Surveyor VII* mission in each of the operational configurations based upon spectra assembled by the on-site computers and transmitted via teletype to the SFOF.

Preliminary scientific results of the *Surveyor VII* alpha scattering experiment are presented in Part II of this report.

Table IV-23. Data accumulation time summary

Operational configuration	Accumulation time, min
Transit	0
Standard sample	312
Background	720
Lunar surface	
Sample 1 (undisturbed soil)	1860
Sample 2 (a rock)	618
Sample 3 (disturbed soil)	402
First lunar day	3912 (65.2 hr)
Second lunar day (alpha data only)	
Sample 3 (disturbed soil)	2070 (34.5 hr)

V. Tracking and Data System

The Tracking and Data System (TDS) for the *Surveyor VII* mission included selected resources of the Air Force Eastern Test Range (AFETR), the Manned Space Flight Network (MSFN), the Deep Space Network (DSN) and the NASA Communications System (NASCOM). This section summarizes the mission preparation, flight support, and performance evaluation of each element of the TDS.

The TDS support for the *Surveyor VII* mission was considered good. The minor problems experienced by elements of the TDS did not affect the overall support. All requirements were met and in most cases exceeded.

A. Air Force Eastern Test Range

The AFETR performs TDS supporting functions for *Surveyor* missions during the countdown, launch, and near-earth phases of the flight. The *Surveyor* mission requirements for launch phase tracking and telemetry coverage are classified as follows, in accordance with their relative importance to successful mission accomplishment:

Class I requirements consist of the minimum essential needs to ensure accomplishment of

first-priority flight test objectives. These are mandatory requirements which, if not met, may result in a decision not to launch.

Class II requirements define the needs to accomplish all stated flight test objectives.

Class III requirements define the ultimate in desired support, and would enable the range user to achieve the flight test objectives earlier in the test program.

The AFETR configuration for the *Surveyor VII* mission is presented in Table V-1. The configuration is similar to the *Surveyor VI* configuration.

Figures V-1 and V-2 illustrate the planned coverage for *Surveyor VII* on launch day and the test support positions of the Range Instrumentation Ships (RIS) *Twin Falls* and *Sword Knot*. AFETR preparations for *Surveyor VII* consisted of routine testing of individual facilities, followed by several Operational Readiness Tests (ORT's). All *Surveyor VII* mission requirements were met by AFETR.

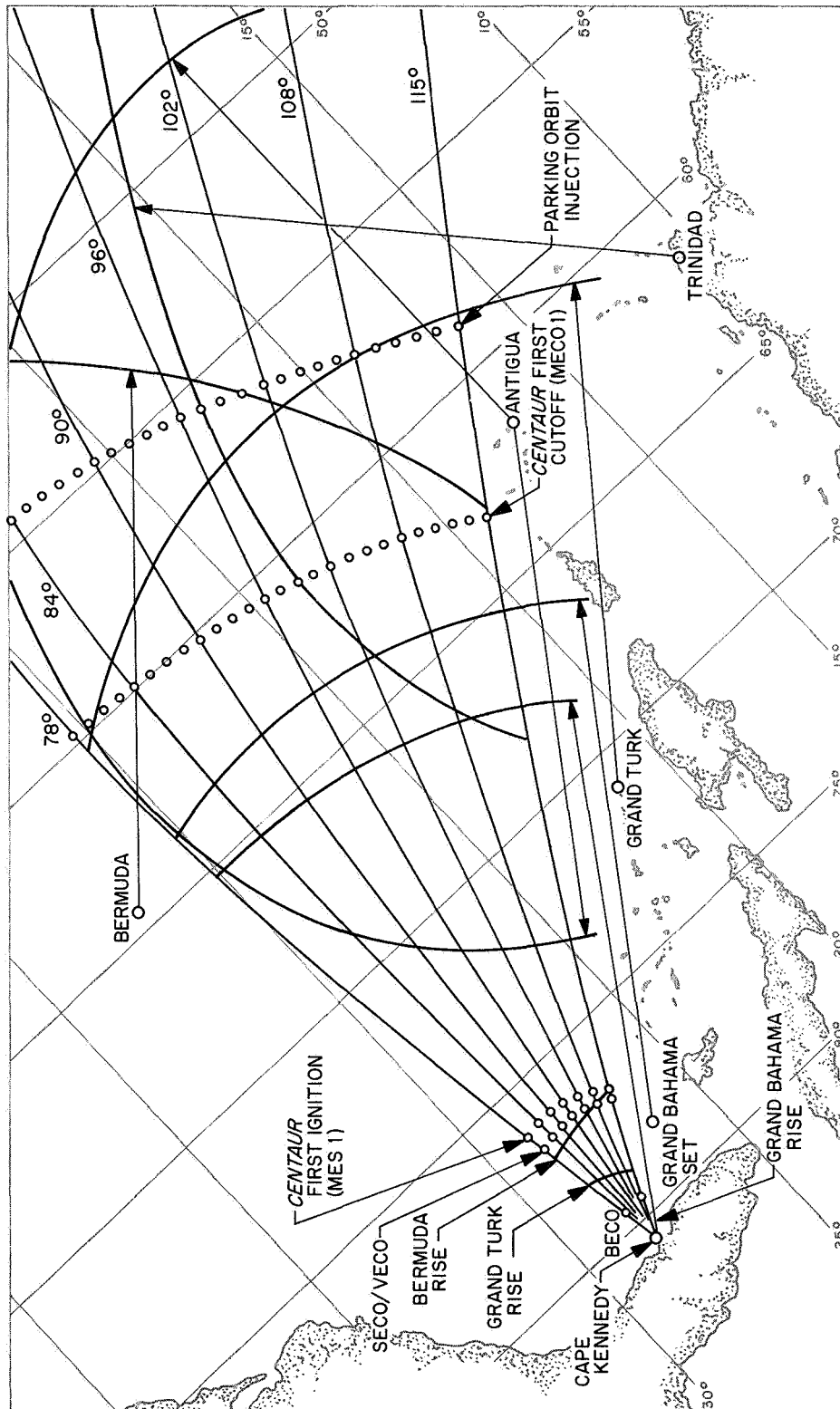


Fig. V-1. Planned up-range TDS coverage for the Surveyor VII mission

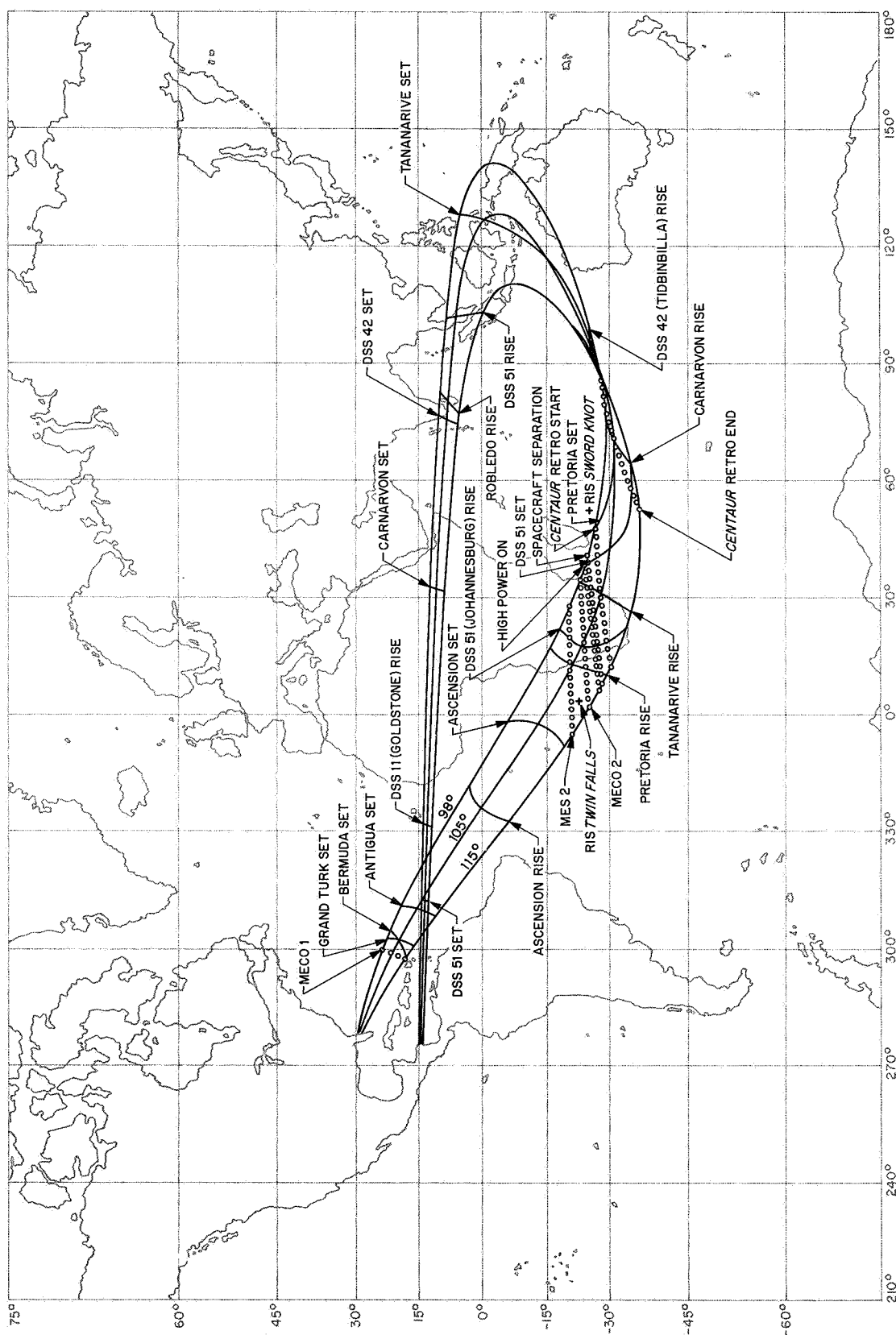


Fig. V-2. Planned near-earth TDS coverage for January 7, 1968

1. Metric Tracking Data

The AFETR tracks the C-band beacon of the *Centaur* stage to provide metric data. This data is required during intervals of time before and after separation of the spacecraft for use in calculating the *Centaur* orbit, which can be used as a close approximation of the postseparation spacecraft orbit. The *Centaur* orbit calculations are used to provide DSN acquisition information (in-flight predicts).

Estimated and actual radar coverages are shown in Fig. V-3. All Class I requirements were met, with the actual coverage equalling or exceeding the estimates in each instance. The land stations, Grand Bahama, Grand Turk, and Antigua, provided continuous coverage from liftoff to $L + 808$ sec; Ascension covered the interval from $L + 1268$ to $L + 1592$ sec; and the RIS *Twin Falls* and Pretoria provided coverage from $L + 1670$ to $L + 2342$ sec. A short dropout occurred as predicted during the Grand Turk interval. This was attributed to balance point shift.

2. Atlas/Centaur Telemetry (VHF)

To meet the Class I telemetry requirements, the AFETR must continuously receive and record *Atlas* telemetry (229.9-MHz link) from before liftoff until shortly after *Atlas/Centaur* separation, and *Centaur* telemetry (225.7-MHz link) until shortly after spacecraft separation. Thereafter, *Centaur* telemetry is to be recorded as station coverage permits, until completion of the *Centaur* retro maneuver.

Estimated and actual VHF telemetry coverages are shown in Fig. V-4. All requirements were met. Continuous and substantially redundant VHF telemetry data was received beginning with the countdown and through Antigua loss of signal (LOS), at $L + 826$ sec, and from $L + 1225$ to $L + 3261$ sec. Coverage was greater than predicted. The RIS *Twin Falls* retransmitted launch vehicle telemetry data in real-time. A noisy interval of data was noted around spacecraft separation. Pretoria was the only station in view at this particular time.

3. Surveyor Telemetry (S-Band)

The AFETR is required to receive, record and retransmit *Surveyor* S-band (2295-MHz) telemetry in real-time from spacecraft transmitter *high-power on* until 2 min after continuous view by DSIF stations begins.

The S-band telemetry resources assigned to meet this requirement are shown in Table V-1. All primary S-band systems were used on a limited commitment basis, since the *Centaur* vehicle is not roll-attitude-stabilized and the aspect angle cannot be predicted.

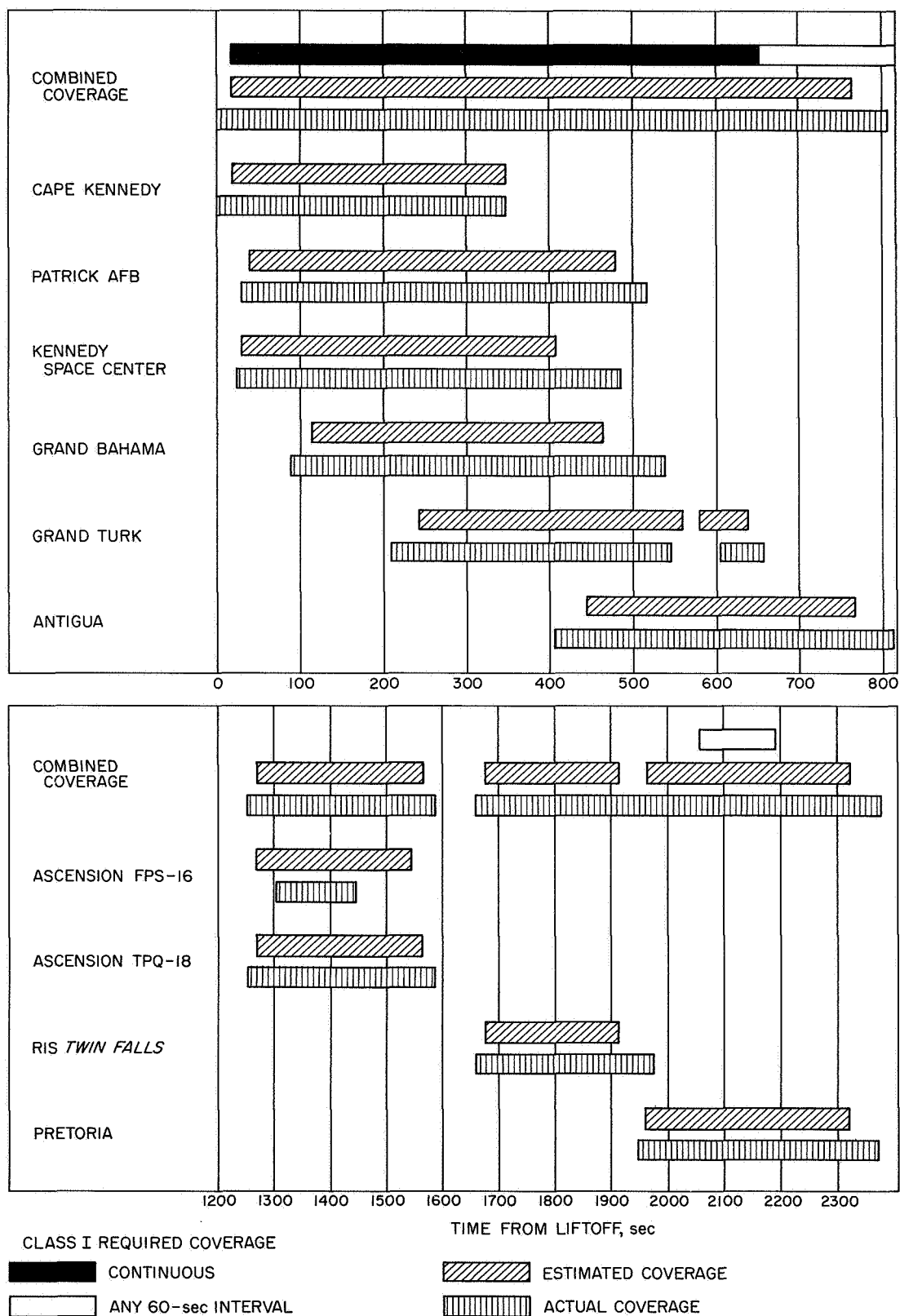
Table V-1. AFETR configuration for Surveyor VII mission

Station		C-band tracking		Telemetry	
Designation	Location	Capability	Antenna type	Capability	Antenna type
0	Patrick AFB	Beacon/skin	FPQ-6		
1	Cape Kennedy	Beacon/skin	FPS-16		
19	Kennedy Space Center, Merritt Island (Tel 4)	Beacon/skin	TPQ-18	VHF S-band	TAA-2A TAA-3A
3	Grand Bahama	Beacon	FPS-16	VHF	LH tri-helix
		Beacon/skin	TPQ-18	S-band	TAA-2
7	Grand Turk	Beacon/skin	TPQ-18		
91	Antigua	Beacon/skin	FPQ-6	VHF S-band	TLM-18 TAA-3A
12	Ascension	Beacon	FPS-16	VHF	TLM-18
		Beacon	TPQ-18	S-band	TAA-3A
UNI	RIS <i>Twin Falls</i>	Beacon	FPS-16	VHF S-band	Rantec TAA5-12
13	Pretoria	Beacon	MPS-25	VHF S-band	TLM-18 3-ft parabola
YAN	RIS <i>Sword Knot</i>			VHF S-band	TAA-1 TAA5-24

Estimated and actual S-band coverages are shown in Fig. V-5. Kennedy Space Center (Tel-4), Grand Bahama, and Antigua provided continuous coverage from liftoff to $L + 760$ sec. With the exception of a short gap between Ascension and the RIS *Twin Falls*, these two stations plus Pretoria and the RIS *Sword Knot* provided continuous coverage from $L + 1225$ to $L + 3709$ sec. The actual coverage from Tel-4 was about 100 sec short of the estimated coverage. This has been experienced on past launches, but has varied with the launch azimuth. Coverage from each of the remaining stations and ships exceeded the estimates.

4. Real-Time Telemetry Data

The AFETR retransmits *Surveyor* data (VHF or S-band) to DSS 71 and Building AO, Cape Kennedy, for



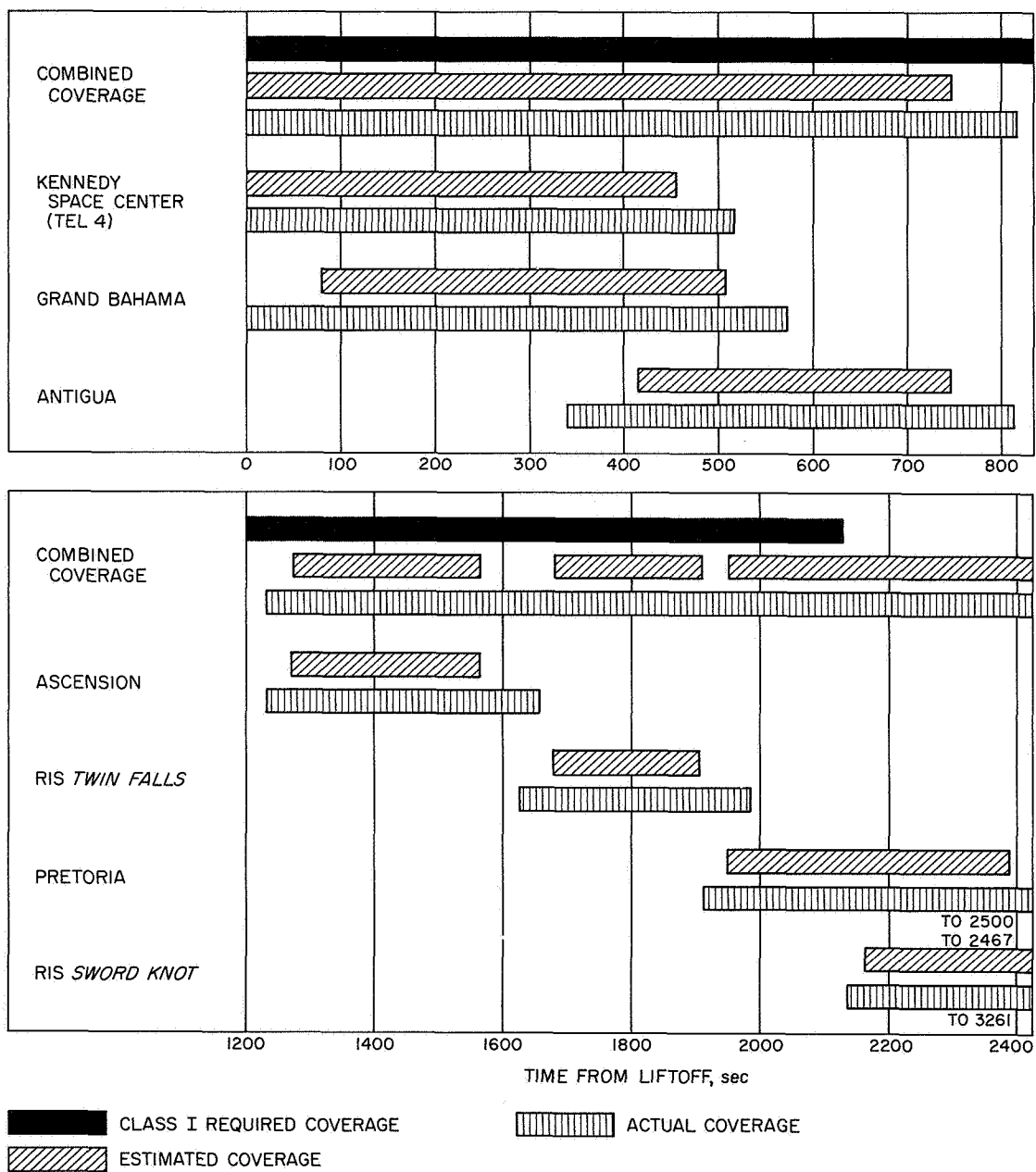


Fig. V-4. AFETR VHF telemetry coverage

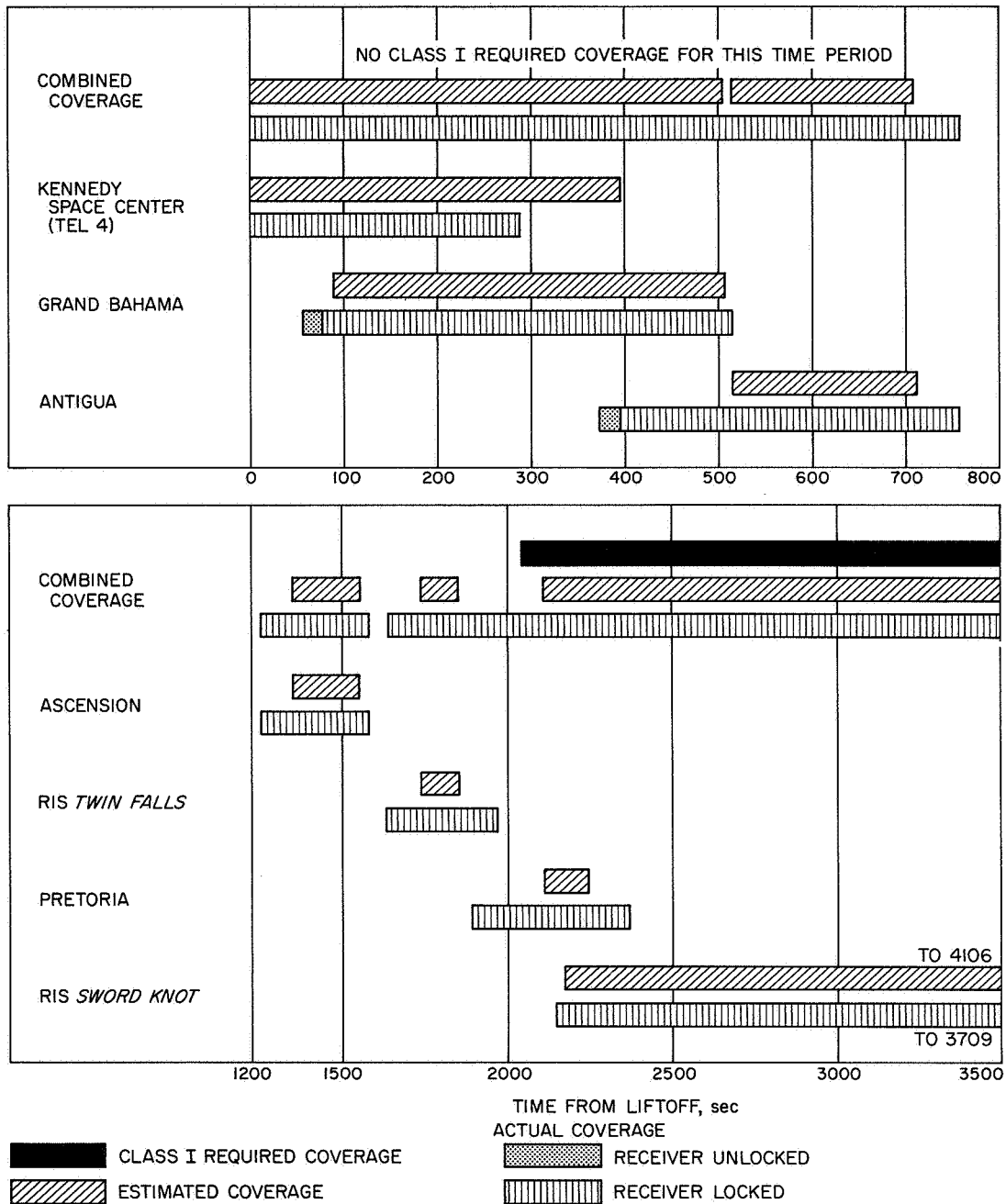


Fig. V-5. AFETR S-band telemetry coverage

display and for retransmission to the SFOF. In addition, down-range stations monitor specific channels and report events via voice communication. For the *Surveyor VII* mission, existing hardware and software facilities were utilized to meet the real-time data requirements.

All requirements were met. VHF telemetry data, including spacecraft data, was transmitted in real-time to the SFOF prior to spacecraft *high-power on*. Following *high-power on*, spacecraft S-band telemetry data was transmitted in real-time. The real-time data flow was of excellent quality. HF propagation conditions were such that the retransmission of data was not hampered by communication conditions. Mark Event times that were recorded and read out by AFETR and MSFN stations are shown in Table V-2.

5. Real Time Computer System (RTCS)

For the launch and near-earth phase of the mission, the RTCS provides trajectory computations based on tracking data and telemetered vehicle guidance data. The RTCS output includes:

- (1) The interrange vector (IRV), the standard orbital parameter message (SOPM), and orbital elements and injection conditions.
- (2) Predicts, look angles, and frequencies for acquisition use by down-range stations.
- (3) Injection conditions mapped to lunar encounter and I-matrices defining orbit determination accuracies for early trajectory evaluation prior to the highly refined orbits generated by the Flight Path Analysis and Command (FPAC) Group.

The RTCS provided all required support. A total of eight orbits were computed by the RTCS, including a parking orbit from Antigua data, a second and third parking orbit from *Centaur* guidance telemetry data, a theoretical transfer orbit using Antigua data plus nominal second-burn data, two actual preretro transfer orbits from Pretoria data, a postretro orbit using Carnarvon data and a spacecraft orbit from DSS 42 data. A problem was experienced with the 3100 computer used for reformatting the real-time radar data into the decimal format. About 2 min of Pretoria data was not reformatted. No other anomalies were encountered.

Table V-2. Atlas/Centaur Mark Event readouts

Mark Event	Time of Event (GMT)	Station reporting	Mark Event	Time of Event (GMT)	Station reporting
Liftoff	06:30:00.545	Cape Kennedy	14	07:02:21.300	Pretoria
1	06:32:33.100	Kennedy Space Center	15	07:04:15.500	Pretoria
2	06:32:36.080	Kennedy Space Center	16	07:04:36.700	Pretoria
3	06:33:18.050	Kennedy Space Center	17	07:04:44.700	Pretoria
4	06:33:47.600	Kennedy Space Center	18	07:05:00.000	Pretoria
5	06:34:09.200	Kennedy Space Center	19	Not reported	
	06:34:08.900	Bermuda	20	07:05:16.500	Pretoria
6	06:34:11.400	Kennedy Space Center	21	07:05:20.000	Pretoria
	06:34:11.500	Bermuda	22	07:06:30.900	Tananarive
7	06:34:22.120	Kennedy Space Center	23	Not reported	
	06:34:21.900	Bermuda	24	07:09:16.000	Tananarive
8	06:39:53.700	Antigua		07:09:15.700	RIS Sword Knot
	06:39:53.800	Bermuda		07:09:16.000	Pretoria
9	06:39:54.600	Antigua	25	07:13:26.800	Tananarive
	06:39:56.000	Bermuda		07:13:26.300	RIS Sword Knot
10	06:41:09.5			07:13:25.000	Carnarvon
11	06:41:11.100	Antigua	26	07:15:06.500	Tananarive
12	07:01:51.700			07:15:06.000	RIS Sword Knot
13	07:02:21.300	Pretoria		07:15:06.000	Carnarvon

B. Manned Space Flight Network

The MSFN, managed by GSFC, supported the *Surveyor VII* mission by performing the following functions:

- (1) Tracking the *Centaur* beacon (C-band).
- (2) Receiving and recording *Centaur*-link telemetry.
- (3) Receiving, recording, and retransmitting S-band telemetry to DSS 42 in real-time.
- (4) Providing real-time confirmation of certain Mark Events.
- (5) Providing computing support through the use of the GSFC Data Operations Branch.

The GSFC tracking and telemetry facilities and equipment used in support of *Surveyor VII* are listed in Table V-3. GSFC also supported the Operational Readiness Test (ORT) prior to launch.

Table V-3. GSFC network configuration

Location	Acquisition aid	VHF telemetry	S-band telemetry	C-band radar	SCAMA	Radar high-speed data	Real-time readouts
Bermuda	X	X		X	X	X	X
Tananarive	X	X		X	X		X
Carnarvon	X	X	X	X	X		X
GSFC					X	X	

1. Acquisition Aids

The MSFN stations are equipped with acquisition aids to track the vehicle and provide RF inputs to the telemetry receivers from AOS to LOS. Performance recorders are used to record AGC and angle errors for postmission analysis. The acquisition aid systems performed their required functions during the *Surveyor VII* mission.

2. Telemetry Data

The MSFN stations are also equipped to decommutate, receive and record telemetry. The telemetry requirements placed on the MSFN were:

- (1) Bermuda, Tananarive, and Carnarvon were to receive and record the *Centaur* 225.7-MHz link from AOS to LOS.

- (2) Bermuda was to receive and record the *Atlas* 229.9-MHz link from AOS to LOS.
- (3) *Centaur* Mark Event readouts were required from Bermuda, Tananarive, and Carnarvon in real-time or as near real-time as possible, after the vehicle was in view of the station.
- (4) Bermuda was to display range safety parameters on the *Atlas* and *Centaur* links.
- (5) Carnarvon was to receive, record, and retransmit S-band telemetry to DSS 42 in real-time.
- (6) All stations were to provide magnetic tape recordings, strip chart recordings, and Post-Launch Instrumentation Message (PLIM) data sheets.

The telemetry systems performed all required functions. Bermuda received and recorded range safety parameters and Mark Events 5 through 9. Tananarive reported Mark Events 22, 24, 25, and 26, and transmitted spacecraft separation and vibration data to Building AE. Tananarive experienced a serial decimal time problem which gave an erroneous day indication. The reason is unknown. Carnarvon reported Mark Events 25 and 26.

The predicted vs actual coverage is shown in Fig. V-6. As can be seen in Fig. V-6, the actual coverage for Tananarive and Carnarvon exceeds the estimates by a large amount. This is valid for Tananarive, because of equipment modifications which improved the range, but is unrealistic for Carnarvon. The latter part of Carnarvon's actual coverage did not provide usable data, and the station should have reported LOS earlier.

3. Metric Tracking Data (C-Band)

The radar requirements placed on the MSFN were:

- (1) Bermuda was to provide beacon tracking of the *Centaur* from AOS to LOS and range safety support to AFETR.
- (2) Bermuda was to provide real-time transmission of high-speed and low-speed radar data to GSFC and RTCS.
- (3) Tananarive and Carnarvon were to provide beacon tracking of the *Centaur* from AOS to LOS. (Tananarive's participation was on an engineering test basis.)
- (4) Tananarive and Carnarvon were to provide real-time transmission of low-speed radar data to GSFC and RTCS.

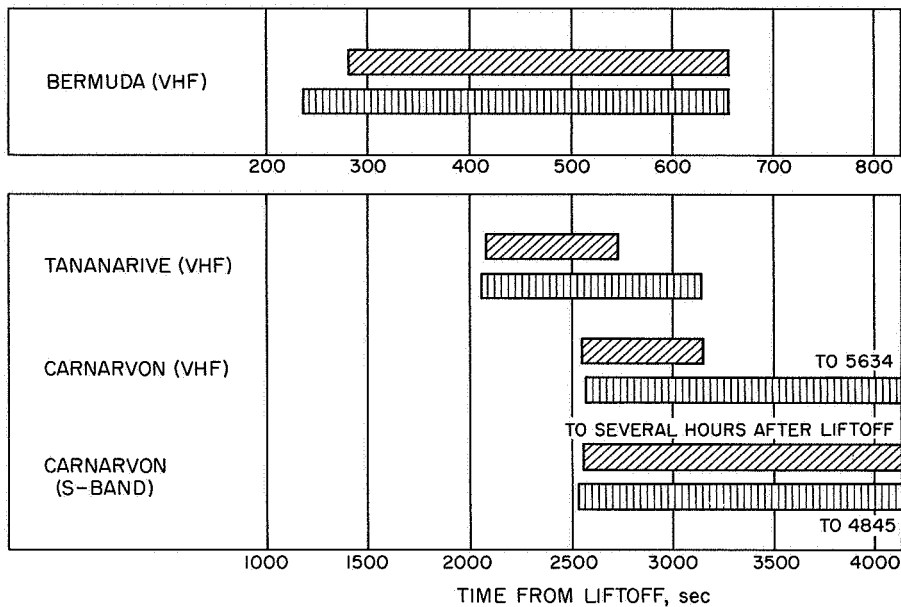




Fig. V-6. MSFN VHF and S-band telemetry coverage

 ESTIMATED COVERAGE
 ACTUAL COVERAGE

- (5) All stations were to provide magnetic tape recordings, strip chart recordings, and PLIM data sheets.

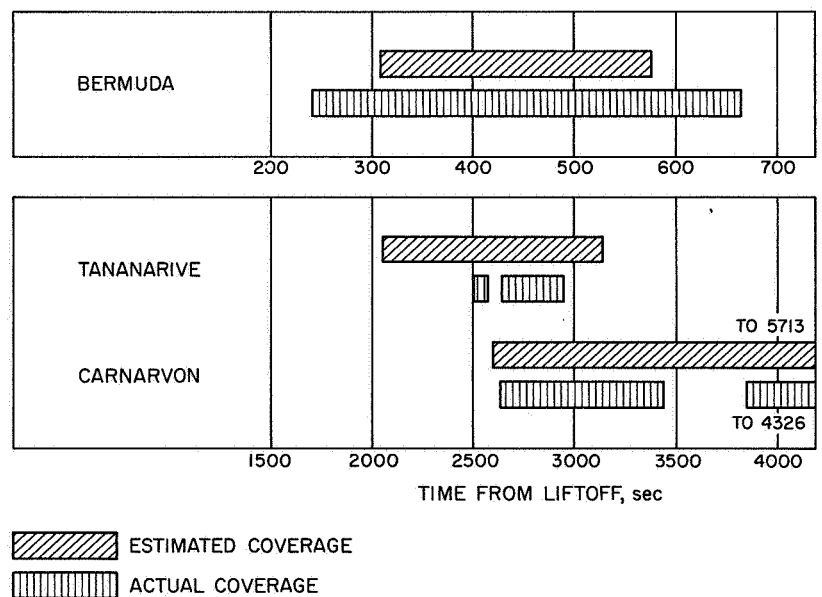
The predicted vs actual coverages are shown in Fig. V-7.


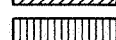
The Bermuda FPQ-6 radar achieved 426 sec of valid autotrack data, and the FPS-16 radar obtained 295 sec of passive track data.

Tananarive provided valid data during an overall coverage interval of 458 sec. However, 75 sec of data was lost during an unexplained dropout 1 min after their initial AOS.

Carnarvon experienced a 390-sec dropout during its tracking interval. The abrupt LOS was preceded by large signal variations. The initial tracking interval provided 822 sec of valid data; another 822 sec of data was obtained following the dropout.

Fig. V-7. MSFN C-band radar coverage



 ESTIMATED COVERAGE
 ACTUAL COVERAGE

Both Tananarive and Carnarvon acquired using look-angles from the RTCS.

4. Computer Support, Data Handling, and Ground Communications

The GSFC Data Operations Branch (DOB) was to provide computing support for the MSFN stations during the prelaunch, launch, and orbital phases of the mission. Computer requirements included providing MSFN station view periods for mission planning purposes, MSFN station nominal pointing data and real-time acquisition messages based on flight data, and postflight reformatting of magnetic tape recordings of the radar data received from AFETR and MSFN.

The prepass acquisition messages generated by the GSFC Data Operations Branch were in error. However, those transmitted during the pass were valid. All other support was provided as required.

C. Deep Space Network

The DSN supports *Surveyor* missions with the integrated facilities of the Deep Space Instrumentation Facility (DSIF), the Ground Communications Facility (GCF), and the Space Flight Operations Facility (SFOF).

The DSN provides a command and telemetry link with the spacecraft upon initial acquisition of spacecraft signals by a DSIF station, enabling the DSIF station to control the spacecraft and furnish range rate data, angular tracking data, and real-time telemetry data to the SFOF. Continuous tracking and control is then provided throughout the remainder of the mission by the prime DSIF stations designated to support each *Surveyor* mission.

Following the accumulation of sufficient tracking data by the SFOF, an orbit is determined that predicts the future path of the spacecraft. This data allows the computation of a midcourse maneuver to compensate for injection errors. The DSIF, under control of the MOS, commands the midcourse maneuver, after which engineering telemetry and tracking data is gathered and transmitted via the GCF to the SFOF, where the midcourse maneuver is evaluated and appropriate commands for the terminal maneuver are computed. After touchdown, DSIF stations command the spacecraft during lunar operations and receive engineering and scientific telemetry as well as video data.

1. The DSIF

The following Deep Space Stations were committed as prime stations for support of the *Surveyor VII* mission:

DSS 11, Goldstone Deep Space Communications Complex (DSCC), Barstow, California

DSS 42, Tidbinbilla, Australia, near Canberra

DSS 61, Robledo, Spain, near Madrid

In addition to the basic support provided by prime stations, the following support was provided for the *Surveyor VII* mission:

- (1) DSS 71 (Fig. V-8), Cape Kennedy, provided facilities for spacecraft/DSIF compatibility testing, and also received and recorded telemetry data after liftoff. In addition, DSS 71 used its Command and Data Handling Console (CDC) and Telemetry and Command Processor (TCP) computer to process AFETR range telemetry data for transmission to JPL.

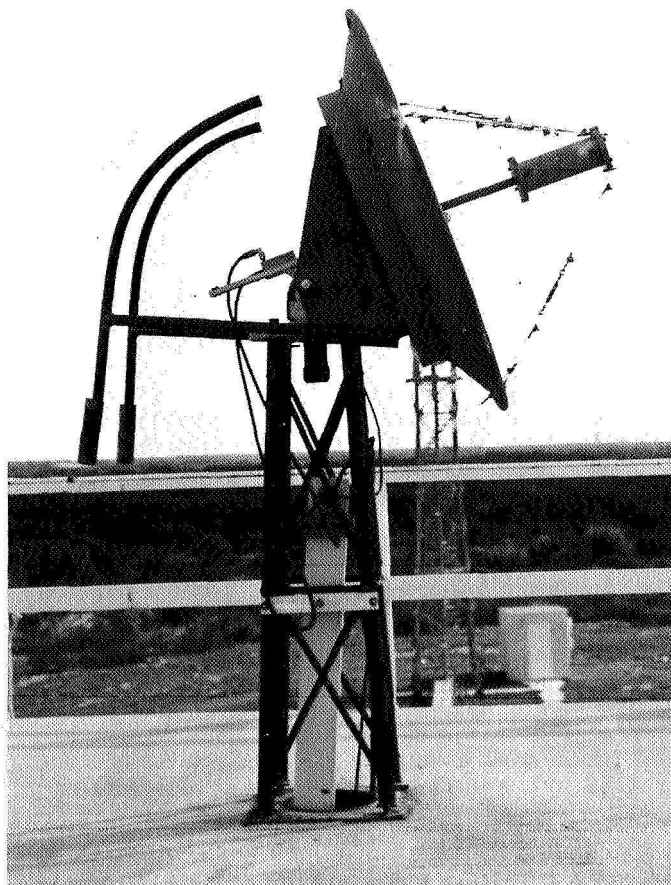


Fig. V-8. DSS 71 antenna, Cape Kennedy, Florida

- (2) DSS 14, Mars, Goldstone DSCC, Barstow, California, provided backup tracking and command support during midcourse and terminal maneuvers, using its 210-ft-diameter antenna. At touchdown, the baseband telemetry output of the DSS 14 prime receiver was transmitted to the SFOF.
- (3) DSS 51, Johannesburg, South Africa, provided tracking support during the transit phase.

For the January 7 launch date, DSS 42 was designated the initial two-way acquisition station as it met all the acquisition criteria of both the DSIF and the *Surveyor* Project.

The DSN was required to track the spacecraft and provide doppler and telemetry data as shown in Table V-4.

Table V-4. DSN tracking and telemetry data requirements

Coverage and sampling rate	Data required
Track spacecraft from separation to first midcourse at 1-min sample rate (from initial DSIF acquisition to $L + 1$ hr, the sample rate is 1 sample per 10 sec)	Doppler (two- and three-way), antenna pointing angles, and telemetry
Track spacecraft from first midcourse to touchdown at 1-min sample rate	Doppler (two- and three-way), antenna pointing angles, and telemetry
Track spacecraft during midcourse maneuver and terminal maneuver executions at 1-sec sample rate, and transmit data at 10-sec sample rate	Doppler (two- and three-way or one-way), antenna pointing angles, and telemetry
Track spacecraft from touchdown to end of mission at 1-min sample rate during 1 hr following 10-deg elevation rise, during 1 hr centered around maximum elevation, and during 1 hr prior to 10-deg elevation set for DSS 11, DSS 42, and 61	Doppler (two- and three-way) and telemetry

Data is handled by the prime DSIF stations as follows:

- (1) Tracking data, consisting of antenna pointing angles and doppler (radial velocity) data, is supplied in near-real-time via teletype to the SFOF and postflight in the form of punched paper tape. Two- and three-way doppler data is supplied full-time during transit, and also during lunar operations when requested by the *Surveyor* MOS. The two-way doppler function implies a transmit capability at the prime stations.
- (2) Spacecraft telemetry data is received and recorded on magnetic tape. Baseband telemetry data is supplied to the CDC for decommutation and real-time readout. The DSIF also performs precommunication processing of the decommutated data, using an on-site data processing (OSDP) computer. The data is then transmitted to the SFOF in near-real-time over high-speed data lines (HSDL).
- (3) Video data is received and recorded on magnetic tape. This data is sent to the CDC and, at DSS 11 only, to the spacecraft TV Ground Data Handling System (TV-GDHS, TV-11) for photographic recording. In addition, video data from DSS 11 is sent in real-time to the SFOF for magnetic and photographic recording by the TV-GDHS, TV-1. After lunar landing, the two DSS 11 receivers are used for different functions. One provides a signal to the CDC, the other to the TV-GDHS. (Signals for the latter system are the prime *Surveyor* Project requirement during this phase of a mission.)
- (4) Command transmission is another function provided by the DSIF. Approximately 280 commands are sent to the spacecraft during the nominal sequence from launch to touchdown. Confirmation of the commands sent is processed by the OSDP computer and transmitted by teletype to the SFOF.

The characteristics of the DSIF S-band tracking system with 85-ft antennas are shown in Table V-5. The maximum doppler tracking rate depends on the loop noise bandwidth. For phase error of less than 30 deg and strong signal (greater than -100 dbm), tracking rates are as follows:

Loop noise bandwidth, Hz	Maximum tracking rate, Hz/sec
12	100
48	920
152	5000

a. DSIF preparation testing. A spacecraft compatibility test, configuration verification tests, system readiness verification (SRV) tests, and an Operational Readiness Test (ORT) are conducted for each mission to verify that all prime stations, communication lines, and the SFOF are fully prepared to meet mission responsibility.

Owing to a high level of *Surveyor* V and VI activity prior to *Surveyor* VII launch, requirements for

Table V-5. Characteristics for S-band tracking systems

Antenna, tracking Type Mount Beamwidth ± 3 db Gain, receiving Gain, transmitting Feed Polarization Max. angle tracking rate ^a Max. angular acceleration Tracking accuracy (1σ)	85-ft parabolic Polar (HA-Dec) ~ 0.4 deg 53.0 db, $+1.0$, -0.5 51.0 db, $+1.0$, -0.5 Cassegrain LH ^b or RH circular 51 deg/min = 0.85 deg/sec 5.0 deg/sec/sec 0.14 deg	Transmitter Frequency (nominal) Frequency channel Power Tuning range Modulator Phase input impedance Input voltage Frequency response (3 db) Sensitivity at carrier output frequency Peak deviation Modulation deviation stability	2113 MHz 14b 10 kW, max ± 100 kHz $\geq 50 \Omega$ ≤ 2.5 V peak DC to 100 kHz 1.0 rad peak/V peak 2.5 rad peak $\pm 5\%$
Antenna, acquisition Type Gain, receiving Gain, transmitting Beamwidth ± 3 db Polarization	2 \times 2-ft horn 21.0 db ± 1.0 20.0 db ± 2.0 ~ 16 deg RH circular	Frequency, standard Stability, short-term (1σ) Stability, long-term (1σ)	Rubidium 1×10^{-11} 5×10^{-11}
Receiver Typical system temperature With paramp With maser Loop noise bandwidth threshold ($2B_{LO}$) Strong signal ($2B_{LO}$) Frequency (nominal) Frequency channel	S-band 270 $\pm 50^\circ$ K 55 $\pm 10^\circ$ K 12, 48 or 152 Hz +0, -10% 120, 255, or 550 Hz +0, -10% 2295 MHz 14a	Doppler accuracy at F_{rc} (1σ) Data transmission	0.2 Hz = 0.3 m/sec TTY and HSDL

^aBoth axes.

^bGoldstone only.

Surveyor VII prelaunch testing were reduced. No special alpha scattering instrument tests were conducted as extensive alpha scattering operations were performed, with all stations participating, during the second and fourth lunar day of *Surveyor V*.

The *Surveyor VII* spacecraft RF compatibility test verifying the compatibility of the spacecraft with the DSIF was conducted in December at DSS 71. One flight training test was conducted at DSS 11 during the last week in December. Also during December, a data-link engineering test was performed between Carnarvon and DSS 42 to verify the unified S-band, telemetry processing, and communication equipment interfaces.

A lunar video ORT and an RF verification test involving DSS 11 and the TV-GDHS were conducted during the last week in December.

DSIF configuration tests were performed. However, since data flow paths were verified by extended

Surveyor V and *VI* lunar operations, no system readiness verification tests were required.

At 48 hr before liftoff, DSS 11, 14, 42, 51, 61, and 71 participated in a single mission ORT. Selected portions of the sequence of events were followed during the ORT, using both standard and nonstandard procedures. An evaluation of station and net control support during the ORT indicated the readiness of the TDS to support the *Surveyor VII* mission.

b. DSIF flight support. The DSIF stations supported the *Surveyor VII* mission with a high level of performance. Continuous tracking and telemetry coverage was provided, except for minor outages, from 50 min after liftoff on January 7 until 3 earth-days after lunar sunset, which occurred on January 23.

A number of minor equipment anomalies and procedural problems occurred, but were readily corrected by station personnel without affecting the mission.

All of the DSIF prime stations reported "go" status during the countdown. All measured station parameters were within nominal performance specifications and, with the exception of circuits to DSS 51, all communications circuits were up. *Surveyor VII* was launched at 06:30:00 GMT on January 7, 1968, after the $T - 60$ -min hold was extended an additional 30 min to enable launch at a preferred azimuth of 102.9 deg.

Figure V-9 is a profile of the DSIF mission activity during the transit phase of the mission. This figure contains the periods each station tracked the spacecraft plotted against mission time from liftoff, and the number of commands transmitted by each DSS during each pass. (Also refer to the station view periods indicated in Fig. VII-2.)

One-way spacecraft signals were received by DSS 71 for 6 min and 3 sec after liftoff. Signal levels received

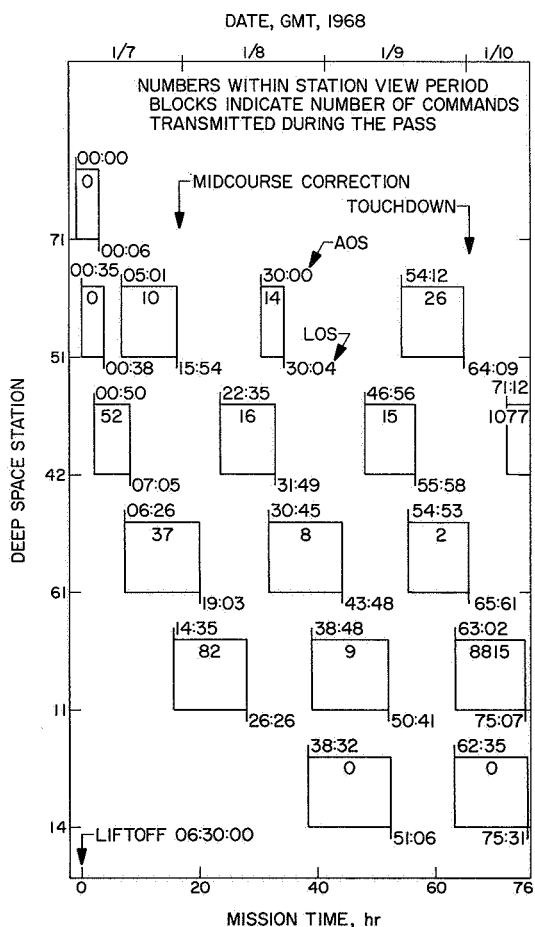


Fig. V-9. DSIF station view periods and command activity: transit phase

varied from approximately -68 dbm on the pad at liftoff to -158 dbm at loss of signal. DSS 71 also processed real-time AFETR telemetry with its CDC and on-site TCP computer.

DSS 51 acquired spacecraft signals 34 min after launch and tracked the spacecraft 3 min and 45 sec during the first pass. DSS 51 provided support during all three of its transit-view periods.

The initial two-way acquisition was achieved by DSS 42, 7 min and 58 sec after spacecraft rise over the station's horizon. Slightly over 8 min elapsed from the receipt of the first spacecraft signals until DSS 42 was prepared to command the spacecraft. Signal levels varied from approximately -128 dbm at first RF contact to -88 dbm at the time commanding began.

From the time of initial two-way acquisition by DSS 42 until approximately 40 min before spacecraft main retro ignition, DSIF stations tracked *Surveyor VII* in the two-way mode and, with minor exceptions, received high-quality doppler data. For *Surveyor VII*, all participating stations were equipped with doppler resolvers, which resulted in a reduction in the standard deviation of the doppler data by a factor of 4. However, this did not produce a significant decrease in the corresponding target uncertainties because, at doppler resolver levels, the main component of the target uncertainties was computer noise and not data noise.

The midcourse maneuver was successfully commanded by DSS 11 during its first pass. Two midcourse adjustments were scheduled, but orbit calculations indicated that the first midcourse performed the necessary adjustments; hence the second midcourse correction was not required. DSS 14 also provided support during the midcourse maneuver using its 210-ft antenna.

The spacecraft terminal maneuvers and retro descent were successfully commanded during the third DSS 11 pass. A smooth spacecraft touchdown in the targeted area was achieved with no loss of receiver lock.

The signal levels received at the DSIF stations during the transit phase are shown in Fig. V-10 and correspond very closely to the predicted levels. The predicted levels for the pre-star acquisition track are not given as the spacecraft was not roll-stabilized during this period. Therefore, the received signal level could vary over a wide range owing to variations in spacecraft antenna patterns. During star acquisition, midcourse correction,

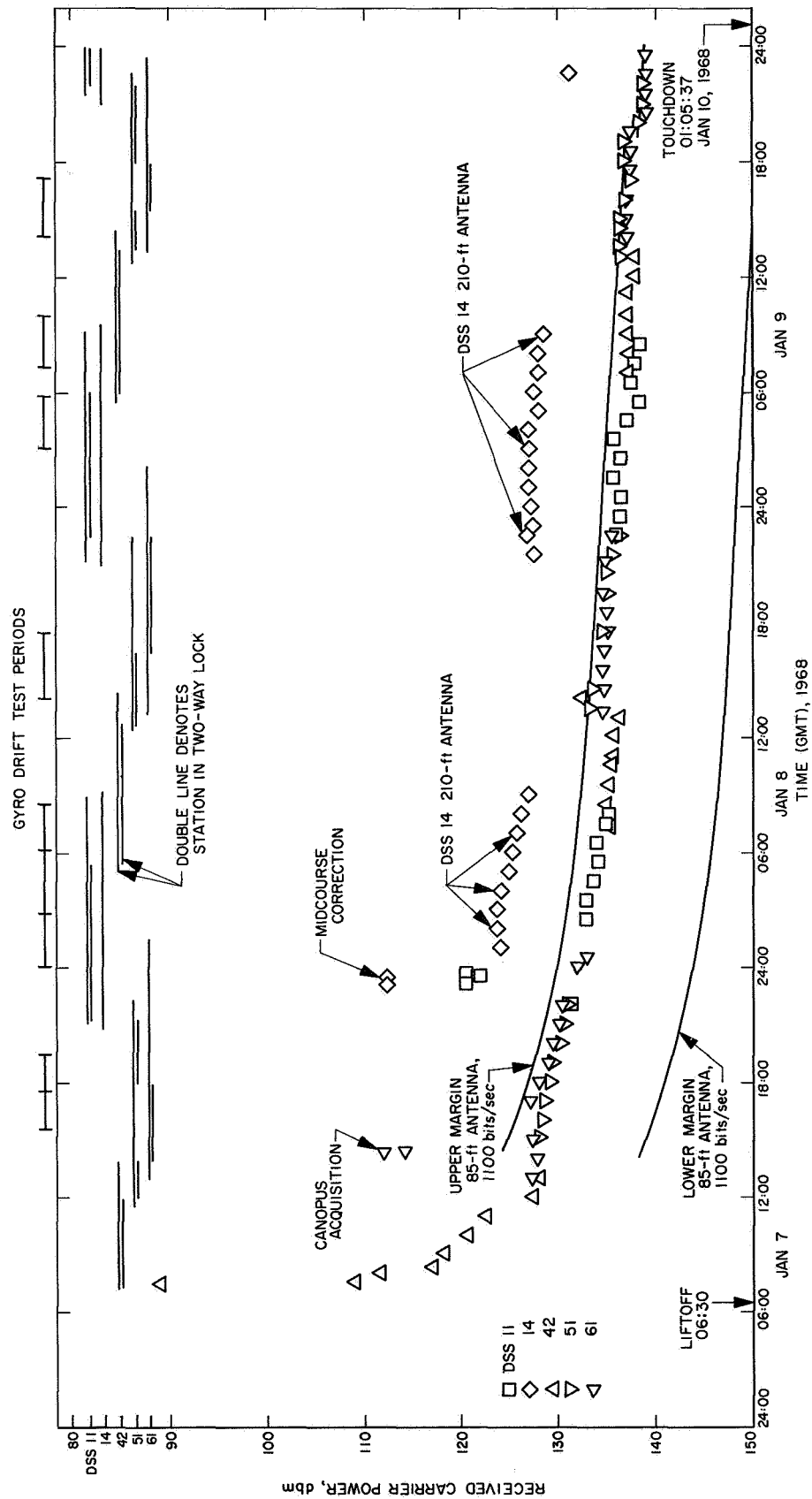


Fig. V-10. DSS received signal levels during transit

and retro maneuver, the spacecraft was in high-power mode, and the received data is 16.5 db above the low-power signal level. Data bit rate changes occurred within 2 db of the predicted thresholds. The periods during which gyro drift tests were conducted are shown at the top of the figure. The random gyro drift and subsequent antenna pattern variations produced a spread in the received signal level of ± 3 db.

At touchdown, the baseband telemetry output of the DSS 14 prime receiver was transmitted to the SFOF using the wideband microwave line. DSS 14 provided excellent support during all of its tracking periods.

Subsequent to the lunar landing, the DSIF provided 24-hr/day tracking coverage, with DSS 11, 42, and 61 providing postlanding mission operations support. Figure V-11 contains a summary of DSIF postlanding mission activity during the first lunar day until spacecraft shutdown approximately 80 hr after sunset. This figure contains, for each station pass: the period of tracking coverage, the number of commands transmitted, the number of TV pictures received by command, and the number of hours of alpha scattering data received.

During lunar operations several losses of up-link lock were experienced by both DSS 11 and 42, with a consequent loss of command capability. In each case, up-link was reacquired and commanding proceeded normally. A full investigation by the DSIF did not reveal the cause, as no evidence could be found of malfunctioning ground equipment.

Approximately 46 min after lunar touchdown, DSS 11 commanded and received 200-line TV pictures. On January 10, during the spacecraft's fourth pass over DSS 61, the alpha scattering instrument (ASI) was commanded to the background data position and received the first alpha scattering experiment data.

DSS 11 commanded the ASI to be lowered to the lunar surface during the spacecraft's fourth pass over DSS 11. However, the instrument failed to lower. During the fifth pass over DSS 11, the surface sampler was successfully commanded to push the ASI to the lunar surface.

Starting on January 13, the DSIF provided tracking support during a series of laser experiments. From January 15 through 17, the DSIF supported two unsuccessful attempts to revive *Surveyors I, III, V, and VI*.

For the remainder of the first lunar day, the DSIF provided spacecraft operations support by commanding soil sampler, alpha scattering experiment, and TV picture sequences, as well as receiving and recording spacecraft data.

Surveyor VII second lunar day operations were supported by the DSN using DSS 11, 42, 61, and 14. The DSN was committed to 24-hr/day support of *Surveyor VII* second lunar day activities.

DSS 61 commanded the initial revival attempt on February 12, 1968, to which *Surveyor VII* responded immediately. A parallel attempt to revive *Surveyors V and VI* was terminated following the quick response of *Surveyor VII*. DSS 61 received spacecraft engineering data assessing the spacecraft condition as good. Commands to position the spacecraft high-gain antenna and solar panel were successfully received and acted upon by the spacecraft.

Initial TV operation commands were sent during the *Surveyor VII* pass over DSS 11 on February 12, 1968. However, only one good 200-line TV picture was received. TV operations continued on February 13 during the DSS 11 view period, and 39 frames of good 200-line TV pictures were received. Performance tests, with DSS 11 commanding and DSS 14 receiving, indicated a camera failure in the TV 600-line mode. Also on this date, DSS 11 commanded operation of the alpha scattering and surface sampler instruments. The DSN received TV pictures which confirmed extension movement of the surface sampler. However, almost no proton data was received from the alpha scattering instrument. A critical spacecraft battery malfunction prevented scheduled science activities as high-power operation was not possible.

During a *Surveyor VII* standby period on February 15, the DSN supported an unsuccessful 1-hr attempt to revive *Surveyor VI*. Progressive deterioration of the *Surveyor VII* spacecraft power system late in the second lunar day prevented further positioning of the solar panels. By careful spacecraft power management, with DSS 14 tracking in parallel with DSS 11, it was possible to obtain alpha scattering data from February 16 through February 20. Subsequent experiments and tests with various *Surveyor VII* spacecraft configurations were supported by the DSN on February 20 and 21. During this period there were frequent losses of the spacecraft signal, one of which was prolonged.

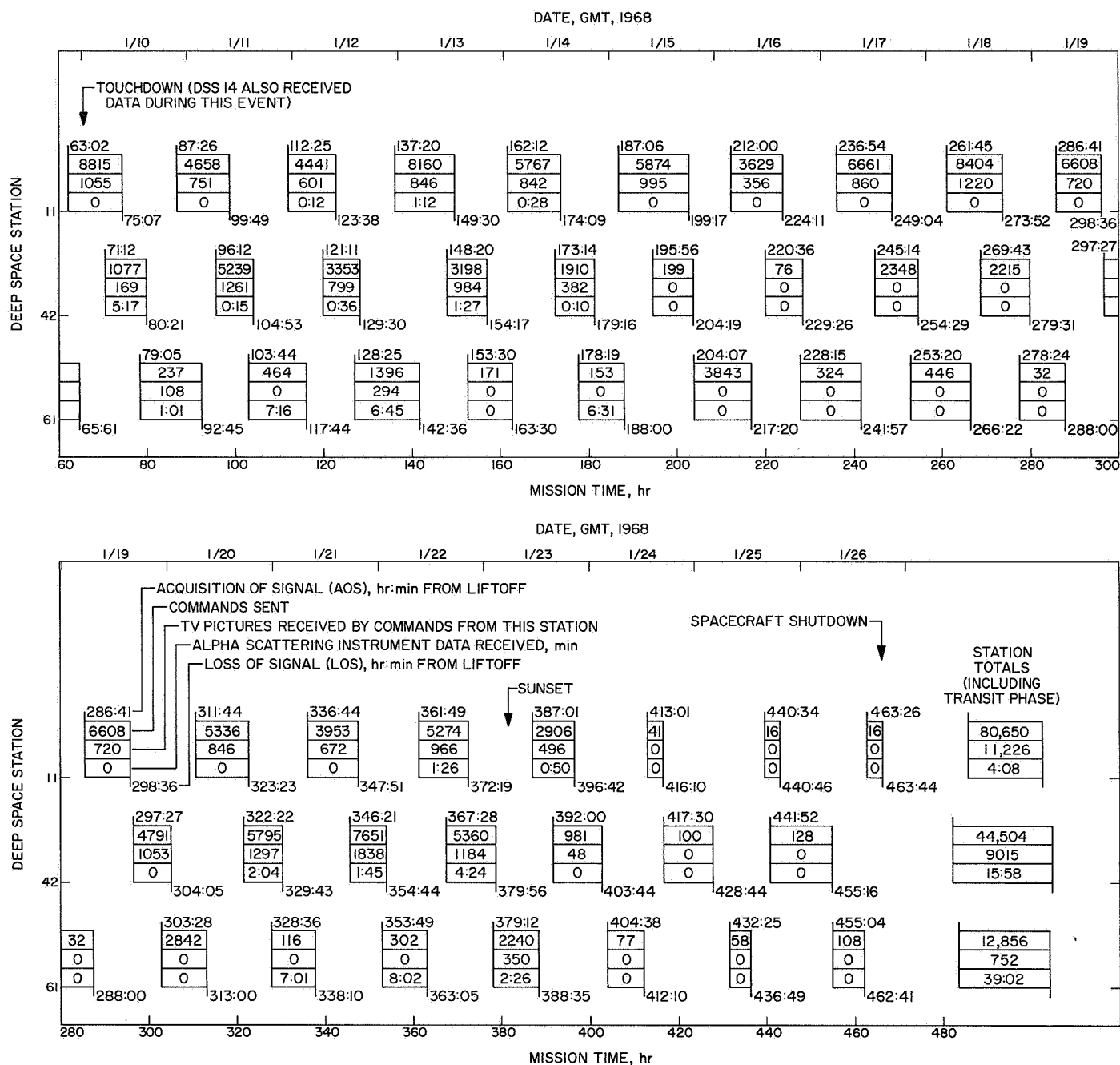


Fig. V-11. DSIF station tracking periods and reported command activity: postlanding (first lunar day)

On February 22, during spacecraft electrical load adjustment commands, the spacecraft signal was lost, and after all revival and search attempts were unsuccessful, DSN support of *Surveyor VII* second lunar day operations was terminated, 21½ hr prior to lunar sunset. A total of 34 hr of alpha scattering experiment operations were conducted during this second lunar day. DSN support of *Surveyor VII* second lunar day operations, and revival attempts of *Surveyors V* and *VI*, were considered excellent.

2. GCF/NASCOM

For *Surveyor* missions, the GCF transmits tracking, telemetry, and command data from the DSIF to the SFOF, and control and command functions from the SFOF to the DSIF by means of NASCOM facilities. The GCF also transmits simulated tracking data to the DSIF and video data and base-band telemetry from DSS 11, Goldstone DSCC, to the SFOF. The links involved in the system are shown in Fig. V-12. On the *Surveyor VII* mission all communication circuits between the DSIF and SFOF were automatically switched using a communication processor (CP).

The performance of the GCF/NASCOM facilities in support of the *Surveyor VII* mission was considered excellent, demonstrating a high degree of reliability.

a. Teletype circuits. Teletype (TTY) circuits (four available to prime stations) are used for transmitting tracking and telemetry data, commands, and administrative traffic. The *Surveyor VII* mission was supported through the Canberra, London, GSFC, and JPL communication processors.

At launch, the communications processor/data processing system interface could not be established but was restored 1 min after launch and caused no data loss. The CP proved very reliable during critical mission phases. Hardwire teletype circuits were available in the event of a CP failure. These circuits were checked out during pre-mission testing, but they were not needed during the transit phase of the flight because of the high reliability of the CP's during this period. During lunar operations the project did not elect to use the hardwire circuits because of the generally short duration of the CP outages which did occur. During lunar operations, Goddard and overseas CP's experienced many periodic outages, which did not, however, cause a serious loss of data.

Teletype communications through this system were considered excellent. During lunar operations there were 22 failures at Goddard, necessitating manual and automatic recoveries and substitution of some elements of the system. However, the effects of these failures were minimal. The Canberra CP experienced three failures and the London CP experienced five. These were all of short duration.

Utilization of the CP system, however, did not exempt DSS 51 from propagation-caused outages. Teletype communications during the *Surveyor VII* mission were still degraded because of this remaining problem.

The teletype circuits and the CP were exceptionally reliable, the weakest circuits (to DSS 51) showing approximately 97% reliability.

b. Voice circuits. The voice circuits are shared between the DSIF and the *Surveyor* Project for administrative control and commanding functions. The NASCOM voice circuits provided for the *Surveyor VII* mission performed well except for several minor outages.

The voice portion of the NASCOM network generally provides a higher reliability factor than the teletype, with the exception of the radio link between London and Pretoria. Similar to the DSS 51 teletype circuits, degraded propagation conditions caused the majority of voice failures to South Africa. The DSS 51 voice circuit was out at liftoff due to propagation, but was restored prior to DSIF acquisition. The rest of the NASCOM voice circuits encountered very little outage time and, when outages did occur, they were held to short durations by means of switching to alternate "make-good" circuits. Voice communications with the Goldstone stations were nearly optimum with no major problems encountered.

All voice circuits exhibited 99 to 100% reliability except DSS 51, the weakest circuit, which showed 95% reliability.

c. High-speed data lines (HSDL). One HSDL is provided to each prime site for telemetry data transmission to the SFOF in real-time. This part of the communications system performed well during both the prelaunch testing and mission phases.

The outbound sides of the lines were used during testing to transmit simulation data to the stations and

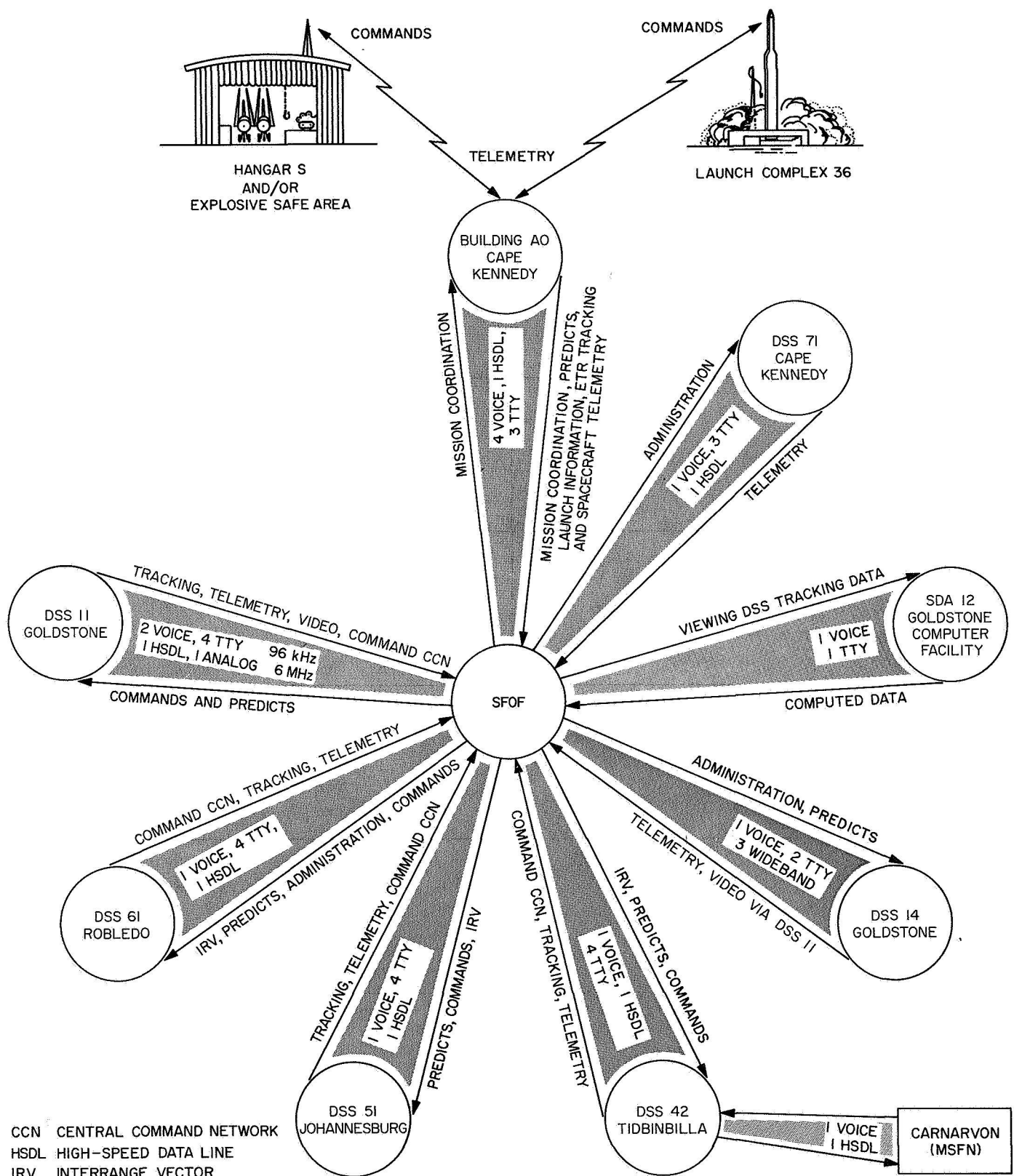


Fig. V-12. DSN/GCF communications links for the Surveyor VII mission

during the mission to backfeed various voice nets as required. During the mission, all HSDL exhibited from 99 to 100% reliability except DSS 51, which showed 91% reliability after an outage due to propagation during the initial short view period during the launch pass. Both NASCOM and Hallicrafter data sets (DSS 51 only) were employed for *Surveyor VII*, and no major problems were encountered at any of the DSN stations.

d. Wideband microwave system. The wideband microwave link between DSS 11, Goldstone DSCC, and the SFOF consists of one 6-MHz simplex (one-way) channel for video and one 96-kHz duplex (two-way) data channel.

Communications between JPL and Goldstone via the Western Union microwave system were almost 100% reliable in passing teletype, voice, and HSD. However, that portion of the microwave system that carries the 6-MHz video channels did experience one outage of 23 min during the *Surveyor VII* mission. This outage was due to a high "B" beam pilot tone, causing the beam switch to oscillate sooner than normal. Other system failures were minor and of short duration. Longer outages on the system were avoided by immediate switching to the backup land/line circuits.

3. DSN in SFOF

The DSN supports *Surveyor* missions by providing mission control facilities and performing special functions within the SFOF.

a. Data Processing System. The SFOF Data Processing System (DPS) performs the following functions for *Surveyor* missions:

- (1) Computation of acquisition predictions for DSIF stations (antenna pointing angles and receiver and transmitter frequencies).
- (2) Orbit determinations.
- (3) Maneuver computation and analysis.
- (4) On-line telemetry processing.
- (5) Command tape generation.
- (6) Simulated data generation (telemetry and tracking data for tests).

The DPS general configuration for the *Surveyor VII* mission is shown in Fig. V-13, and consists of two

PDP-7 computers in the telemetry processing station (TPS), two strings of IBM 7044/7094 computers in the Central Computing Complex (CCC), and a subset of the input/output (I/O) system.

Surveyor VII utilized a redesigned computer configuration in conjunction with a communication processing system which automatically switched teletype lines and allowed computer sharing in support of other concurrent space program missions. Its capabilities included switching, real-time monitoring, quick access message logging, and recall. Communication processor problems, although not significantly affecting the mission, did cause minor delays in providing SFOF user areas with incoming data.

The DPS performed in an excellent manner, with only minor hardware problems which did not detract from mission support. The two PDP-7 computers were used extensively to process high-speed telemetry data for the *Surveyor VII* mission. This processing consisted of decommutating and transferring the data to the 7044 computer via the 7288 data channels, generating a digital tape for non-real-time processing, and supplying digital-to-analog converters with discrete data parameters to drive analog recorders in both the spacecraft analysis area and the space science analysis area.

The IBM 7044/7094 computer string dual configuration successfully processed all high-speed data received from the TPS and all teletype data received from the communications center, as well as all input/output requests from the user areas.

The input/output system provides the capability for entering data control parameters into the 7044/7094 computers and also for displaying computed data in the user areas via the various display devices. The input/output system performed adequately; many minor problems were reported, but were resolved in real-time with only a minor loss of data.

b. DSN Intracommunications System (DSN/ICS). The DSN/ICS provides the capability of receiving, switching, and distributing all types of information required for spaceflight operations and data analysis to designated areas or users within the SFOF. The system includes facilities for handling all voice communications, closed circuit television, teletype, high-speed data, and data received over the microwave channels.

The DSN/ICS performed in an exceptional manner, with only minor anomalies.

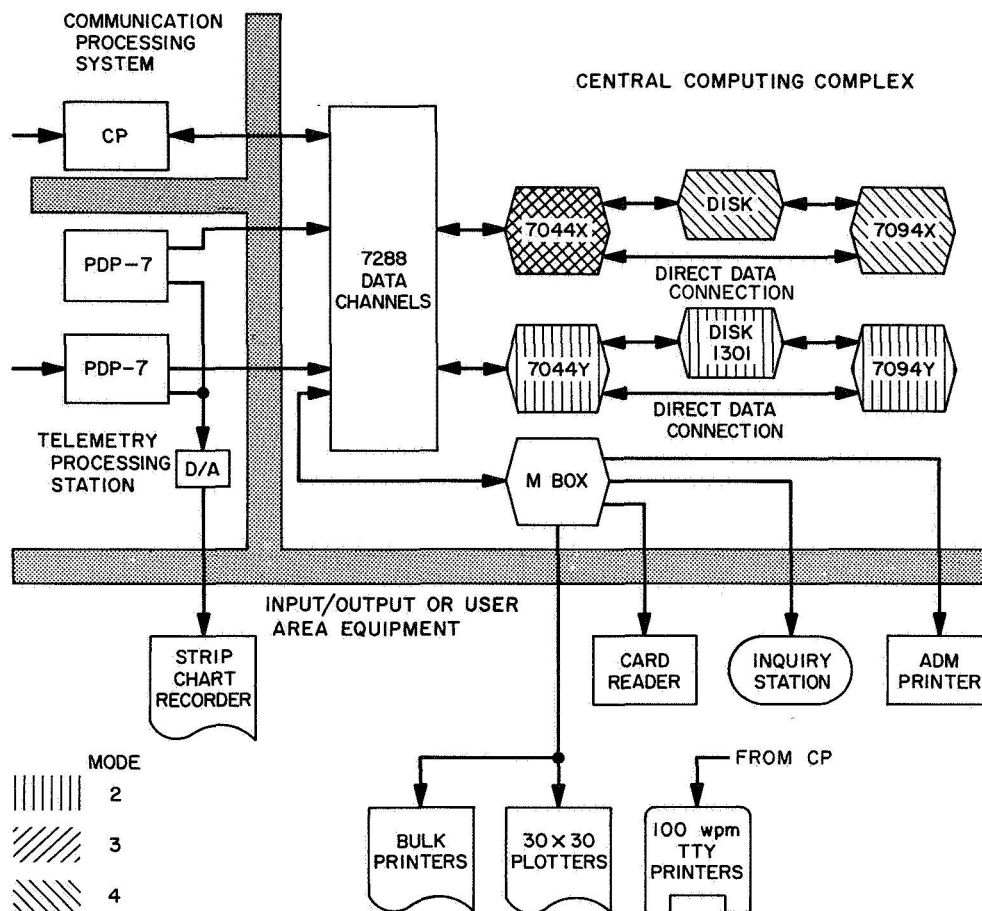


Fig. V-13. General configuration of SFOF Data Processing System

Both modem* types (NASCOM and Hallicrafters) were required during the *Surveyor VII* mission. NASCOM modems were used for sending high-speed data from all stations except DSS 51, and reliability was very high. DSS 51 used the Hallicrafters modems, which performed reliably, the only circuit problems being due to propagation. Minor problems occurred during launch, when several stations were active and modem switching was required within the SFOF in order for each station to perform data transfer tests.

The television communications subsystem experienced minor equipment problems that were resolved in real-time. During the launch phase there was a shortage of TV monitors used for viewing teletype lines.

*A modem (modulator-demodulator) is a device for converting a digital signal to a signal which is compatible with telephone line transmission (e.g., frequency-modulated tone).

4. DSN/AFETR Interface

The DSN/AFETR interface provides real-time data transmission capability for both VHF and S-band down-range telemetry from Building AO at Cape Kennedy to the SFOF. The nominal switchover time from VHF to S-band data is after the spacecraft S-band transmitter high-power turnon. Incoming AFETR telemetry is sent from TEL 4 simultaneously to Building AO and to DSS 71 for processing and transmission to JPL. The output of both stations is transmitted to the SFOF via the GCF/NASCOM. During the *Surveyor VII* mission, the TEL 4 to DSS 71 configuration was established as the prime link between the SFOF and AFETR to provide an interface similar to the data transmission links with prime DSIF stations. The previously used link between Building AO and SFOF, via Bell modems, was retained as backup.

In addition, two new satellite communications circuits were used from the Ascension Island station of AFETR

to provide improved reliability of communications from down range. These circuits were implemented by NASCOM in cooperation with AFETR. One voice/data grade circuit extended from AFETR Station 12 (Ascension) to JPL via GSFC. Model 202 high-speed data sets were used to transmit 550-bits/sec *Surveyor* telemetry data directly to JPL from Ascension and stations farther down range. Good data was received in the TPS via this circuit. However, it was not processed because of the high quality of the data coming in via the normal TEL 4/DSS 71 path. A second satellite circuit was used to transmit down-range metric data via teletype from Ascension to Cape Kennedy. This circuit was also checked out and provided good data.

In-flight spacecraft telemetry was received from the AFETR stations and relayed to the SFOF until approximately 40 min after liftoff. Both the prime DSS 71 and

the backup circuits at Building AO provided good data during the mission, but owing to the high quality of the DSS 71 data, the Building AO data was not processed. The backup system was also used during the ORT to provide simulated telemetry data from the SFOF to Building AO and performed well.

DSIF tracking data for early orbit determination was successfully backed to the Real Time Computer System at the AFETR.

The system for transmission of real-time telemetry data from the Carnarvon, Australia MSFN station to the SFOF via DSS 42 was again activated for *Surveyor VII*. This system performed very well, and good data was received in the SFOF from Carnarvon acquisition until DSS 42 switched over to processing their own data, a period of approximately 14 min.

VI. Mission Operations System

A. Functions and Organization

The basic functions of the Mission Operations System (MOS) are the following:

- (1) Continual assessment and evaluation of mission status and performance, utilizing the tracking and telemetry data received and processed.
- (2) Determination and implementation of appropriate command sequences required to maintain spacecraft control and to carry out desired spacecraft operations during transit and on the lunar surface.

The *Surveyor* command system philosophy introduces a major change in the concept of unmanned spacecraft control: virtually all in-flight and lunar operations of the spacecraft must be initiated from earth. In previous space missions, spacecraft were directed by a minimum of earth-based commands. Most in-flight functions of those spacecraft were automatically controlled by an on-board sequencer which stored preprogrammed instructions. These instructions were initiated by either an on-board timer or by single direct commands from earth. For example, during the *Ranger VIII* 67-hr mission, only 11 commands were sent to the spacecraft; whereas for a standard *Surveyor* mission, approximately 300 commands

are sent to the spacecraft during the transit phase, out of a command vocabulary of 201 different direct commands. For *Surveyor VII*, about 335 commands were sent during transit and about 150,000 commands were sent following touchdown.

Throughout the space flight operations of each *Surveyor* mission, the command link between earth and spacecraft is in continuous use, transmitting either fill-in or real commands every 0.5 sec. The *Surveyor* commands are controlled from the SFOF and are transmitted to the spacecraft by a DSIF station.

The equipment utilized to perform MOS functions falls into two categories: mission-independent and mission-dependent equipment. The former is composed chiefly of the *Surveyor* TDS equipment described in Section V. It is referred to as mission-independent because it is general purpose equipment which can be utilized by more than one NASA project when used with the appropriate project computer programs. Selected parts of this equipment have been assigned to perform the functions necessary to the *Surveyor* Project. The mission-dependent equipment (described in Section VI-B, following) consists of special equipment which has been installed at DSN facilities for specific functions peculiar to the project.

The *Surveyor* Project Manager, in his capacity as Mission Director, is in full charge of all mission operations. The Mission Director is aided by the Assistant Mission Director and a staff of mission advisors. During the mission, the MOS organization was as shown in Fig. VI-1.

Mission operations are under the immediate, primary control of the Space Flight Operations Director (SFOD) and supporting *Surveyor* personnel. Other members of the team are the TDS personnel who perform services for the *Surveyor* Project.

During space flight and lunar surface operations, all commands are issued by the SFOD or his specifically delegated authority. Three groups of specialists provide technical support to the SFOD in the flight path, spacecraft performance, and science areas.

1. Flight Path Analysis and Command Group

The Flight Path Analysis and Command (FPAC) Group handles those space flight functions that relate to the location of the spacecraft. The FPAC Director maintains control of the activities of the group and makes specific recommendations for maneuvers to the SFOD in accordance with the flight plan. In making these recommendations, the FPAC director relies on five subgroups of specialists within the FPAC Group.

- (1) The Trajectory (TRAJ) Group determines the nominal conditions of spacecraft injection and generates lunar encounter conditions based on injection conditions as reported by AFETR and computed from tracking data by the Orbit Determination Group. The actual trajectory determinations are made by computer.
- (2) The Tracking Data Analysis (TDA) Group makes a quantitative and descriptive evaluation of tracking data received from the DSIF stations. The TDA Group provides 24-hr/day monitoring of incoming tracking data. To perform these functions the TDA Group takes advantage of the Data Processing System (DPS) and of computer programs generated for their use. The TDA Group acts as direct liaison between the data users (the Orbit Determination Group) and the DSIF and provides predictions to the DSIF.
- (3) The Orbit Determination (OD) Group, during mission operations, determines the actual orbit of the spacecraft by processing the tracking data received

from the DSN tracking stations by way of the TDA Group. Also, statistics on various parameters are generated so that maneuver situations can be evaluated. The OD Group generates tracking predictions for the DSIF stations and recomputes the orbit of the spacecraft after maneuvers to determine the success of the maneuver.

- (4) The Maneuver Analysis (MA) Group is the subgroup of FPAC responsible for developing possible midcourse and terminal maneuvers for both standard and nonstandard missions in real-time during the actual flight. In addition, once the decision has been made as to what maneuver should be performed, the MA Group generates the proper spacecraft commands to effect these maneuvers. These commands are then relayed to the Spacecraft Performance Analysis and Command Group to be included with other spacecraft commands. Once the command message has been generated, the MA Group must verify that the calculated commands are correct.
- (5) The Computer Support (CS) Group acts in a service capacity to the other FPAC subgroups, and is responsible for ensuring that all computer programs used in space operations are fully checked out before mission operations begin and that optimum use is made of the Data Processing System facilities.

2. Spacecraft Performance Analysis and Command Group

The Spacecraft Performance Analysis and Command (SPAC) Group, operating under the SPAC Director, is basically responsible for the operation of the spacecraft itself. The SPAC Group is divided into four subgroups:

- (1) The Performance Analysis (PA) Group monitors incoming engineering data telemetered from the spacecraft, determines the status of the spacecraft, and maintains spacecraft status displays throughout the mission. The PA Group also determines the results of all commands sent to the spacecraft. In the event of a failure aboard the spacecraft, as indicated by telemetry data, the PA Group analyzes the cause and recommends appropriate nonstandard procedures.
- (2) The Command Preparation and Control (CPC) Group is basically responsible for preparing command sequences to be sent to the spacecraft. In so doing they provide inputs for computer programs

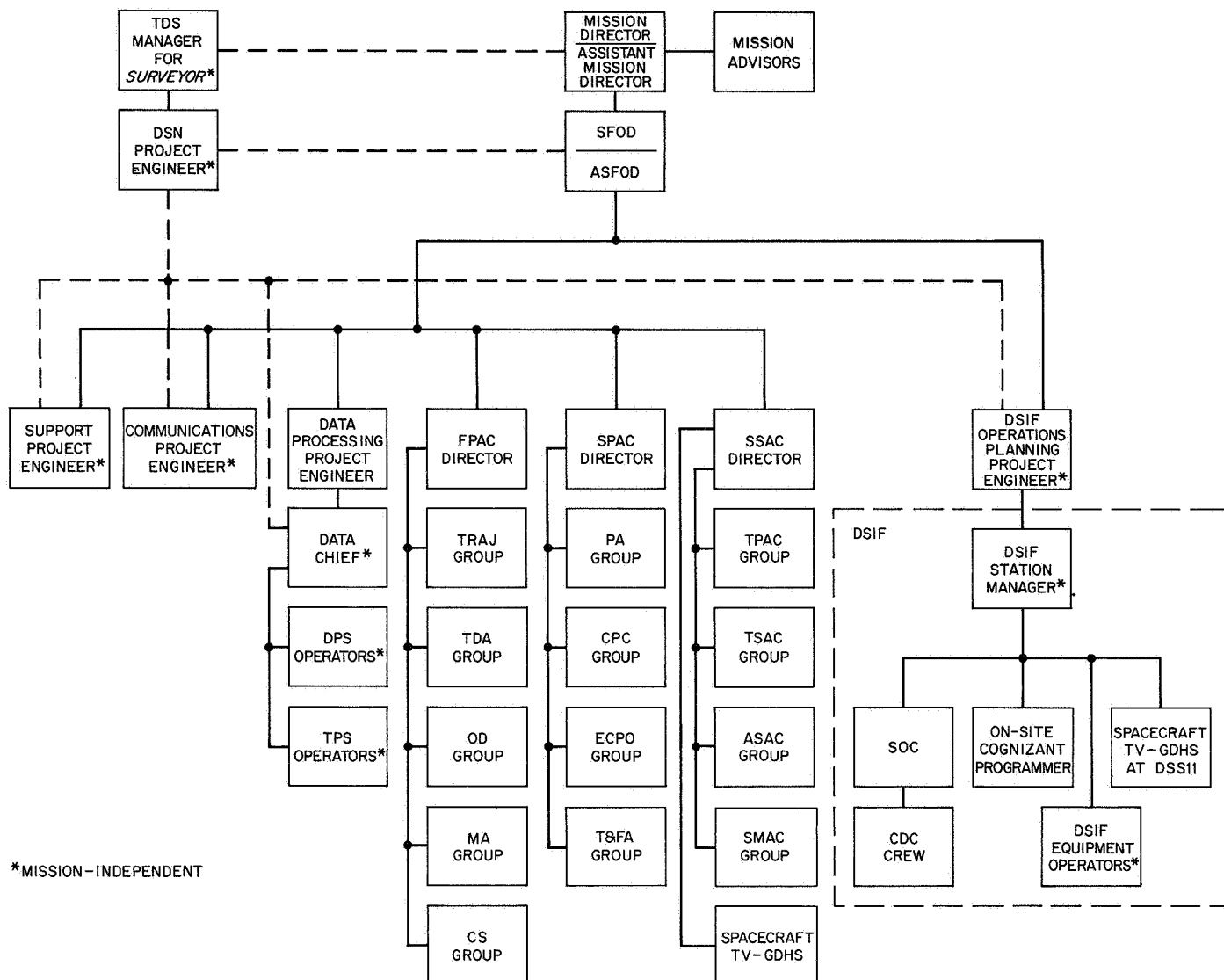


Fig. VI-1. Organization of the MOS during the Surveyor VII mission

used in generating the sequences, verify that the commands for the spacecraft have been correctly received at the DSS, and then ascertain that the commands have been correctly transmitted to the spacecraft. If nonstandard operations become necessary, the group also generates the required command sequences. The CPC Group controls the actual transmission of commands at the DSS by the Surveyor operations chief.

- (3) The Engineering Computer Program Operations (ECPO) Group includes the operators for the DPS input/output (I/O) console and related card punch, card reader, page printers, and plotters in the spacecraft performance analysis area (SPAA).

The ECPO Group handles all computing functions for the rest of the SPAC Group, including the maintenance of an up-to-date list of parameters for each program.

- (4) The Trend and Failure Analysis (T&FA) Group consists of spacecraft design and analysis specialists who provide in-depth, near-real-time spacecraft performance analysis (in contrast to the PA Group's real-time analysis). The group also manages the interface for the SCCF computer facility at Hughes Aircraft Company. The SCCF 1219 is used mainly for premission spacecraft ground testing but, during the mission, the T&FA Group is provided two data lines to the SCCF 1219 via the

TPS, which will accommodate telemetry rates up to 4400 bits/sec, and eight incoming lines terminating at seven teleprinters and one line printer in the SPAC area. The T&FA Group uses the system to process and display engineering data transmitted from the spacecraft. The group also includes draftsmen who perform wall chart plotting and maintain wall displays of spacecraft condition and performance.

3. Space Science Analysis and Command Group

The Space Science Analysis and Command (SSAC) Group performs those space flight functions related to the operation of the TV camera and science instruments. SSAC is divided into the following operating subgroups:

- (1) The Television Performance Analysis and Command (TPAC) Group analyzes the performance of the TV equipment and is responsible for generating standard and nonstandard command sequences for the survey TV camera.
- (2) The Television Science Analysis and Command (TSAC) Group analyzes and interprets the TV pictures for the purpose of ensuring that the mission objectives are being met. The TSAC Group is under the direction of the Project Scientist and performs the scientific analysis and evaluation of the TV pictures.
- (3) The Soil Mechanics Analysis and Command (SMAC) Group prepares and recommends the commands to be sent to the soil mechanics/surface sampler instrument (SM/SS), and is also responsible for operating the SM/SS and analyzing its performance.
- (4) The Alpha Scattering Analysis and Command (ASAC) Group prepares and recommends the commands to be sent to the alpha scattering instrument. This group is also responsible for conducting alpha scattering instrument operations during transit and lunar phases and for analyzing its performance.

The portion of the spacecraft TV Ground Data Handling System (TV-GDHS) in the SFOF provides direct support to the SSAC Group in the form of processed electrical video signals and finished photographic prints. The TV-GDHS operates as a service organization within the MOS structure. Documentation, system checkout, and quality control within the system are the responsibility of the TV-GDHS Operations Manager. During

operations support the TV-GDHS Operations Manager reports to the SSAC Director.

4. Data Processing Personnel

The use of the Data Processing System (DPS) by *Surveyor* is under the direction of the Assistant Space Flight Operations Director (ASFOD) for Computer Programming. His job is to direct the use of the DPS from the viewpoint of the MOS. He communicates directly with the Data Chief, who is in direct charge of DPS personnel and equipment. Included among these personnel are the I/O console operators throughout the SFOF, as well as the equipment operators in the DPS and Telemetry Processing Station (TPS) areas.

Computer programs are the means of selecting and combining the extensive data processing capabilities of electronic computers. By means of electronic data processing, the vast quantities of mission-produced data are assembled, identified, categorized, processed and displayed in the various areas of the SFOF where the data are used. Their most significant service to the MOS is providing knowledge in real-time of the current state of the spacecraft throughout the entire mission. This service is particularly important to engineers and scientists of the technical support groups since, by use of the computer programs, they can select, organize, compare and process current-status data urgently needed to form their time-critical recommendations to the SFOD. (See Section V-C-3 for a description of the DPS.)

5. Other Personnel

The Communications Project Engineer (PE) controls the operational communications personnel and equipment within the SFOF, as well as the DSN/GCS lines to the DSIF stations throughout the world.

The Support PE is responsible for ensuring the availability of all SFOF support functions, including air conditioning and electric power; for monitoring the display of *Surveyor* information on the Mission Status Board and throughout the facility; for directing the handling, distribution, and storage of data being derived from the mission; and for insuring that only those personnel necessary for mission operations are allowed to enter the operational areas.

The DSIF Operations Planning PE is in overall control of all DSIF stations; his post of duty is in the SFOF in Pasadena. At each station, there is a local DSIF station

manager, who is in charge of all aspects of his DSIF station and its operation during a mission. The *Surveyor* personnel located at each station report to the station manager.

B. Mission-Dependent Equipment

Mission-dependent equipment consists of special hardware provided exclusively for the *Surveyor* Project to support the Mission Operations System. Most of the equipment in this category is contained in the Command and Data Handling Consoles (CDC) and spacecraft Television Ground Data Handling System (TV-GDHS), which are described below.

1. Command and Data Handling Console

a. CDC equipment. The Command and Data Handling Console comprises that mission-dependent equipment located at the participating Deep Space Stations that is used to:

- (1) Generate command for control of the *Surveyor* spacecraft by modulation of the DSS transmitter.
- (2) Process and display telemetered spacecraft data and relay telemetry signals to the on-site data processor (OSDP) for transmission to the SFOF
- (3) Process, display, and record television pictures taken by the spacecraft.

The CDC consists of four major subsystems:

- (1) The command subsystem generates FM digital command signals from punched tape or manual inputs for the DSS transmitter and prints a permanent record of the command sent. The major units of the command subsystem, which can accommodate 1024 different commands, are the command generator, the command subcarrier oscillator, the punched tape reader, and the command printer. Outgoing commands are logged on magnetic tape by the DSS and are relayed to the SFOF.
- (2) The FM demodulator subsystem accepts the FM intermediate-frequency signal of the DSS receiver and derives from it a baseband signal. The baseband signal consists of either video data or a composite of engineering subcarrier signals. Depending upon the type of data constituting the baseband signal, the CDC processes the data in either the TV data subsystem or the telemetry data subsystem.

(3) The TV data subsystem receives video data from the FM demodulator and processes it for real-time display at the CDC and for 35-mm photographic recording. In addition, telemetered frame-identification data is displayed and photorecorded. A long-persistence-screen TV monitor is mounted in the CDC. The operator, when requested, can thus evaluate the picture and, upon the SFOF's direction, initiate corrective commands during lunar television surveys.

(4) The telemetry data subsystem of the CDC separates the various data channels from the baseband signal coming from either the FM demodulator or the DSS receiver phase-detected output and displays the desired data to the operators. Discriminators are provided for each subcarrier channel contained in the baseband signal. In the case of time-multiplied data, the output of each discriminator is sent to the pulse code modulation (PCM) decommutator and then relayed to both the OSDP computer for subsequent transmission to the SFOF and to meters for evaluation of spacecraft performance. In the case of continuous data transmissions, the output of the discriminator is sent to an oscillograph for recording and evaluation. Alpha scattering experiment data is demodulated like other telemetry data but, is allowed to accumulate for periods of time in a SDS 920 computer in order to form spectrum information, which is then relayed to SFOF via teletype circuits.

The CDC contains built-in test equipment to insure normal operations of its subsystems. A CDC tester, consisting of a spacecraft transponder with the necessary modulation and demodulation equipment, insures day-to-day compatibility of the CDC and DSIF stations.

b. CDC operations. Table VI-1 lists the CDC mission-dependent equipment provided for support of *Surveyor VII* at the DSIF stations. CDC's were located at DSS 11, 42, 51, 61, 71, and 72, and during the mission, CDC operations were conducted at each of these stations except DSS 72. Table VI-2 lists the total number of commands transmitted, number of TV frames commanded, and the minutes of alpha scattering data accumulated in the telemetry and command processor (TCP) at each station during the transit phase and through the first lunar day's activities.

- (1) DSS 11, Goldstone. The Pioneer station at Goldstone participated in 19 passes. Major mission

Table VI-1. CDC mission-dependent equipment support of Surveyor VII at DSIF stations

DSS 11, Goldstone	Prime station with command, telemetry, TV, and alpha scattering
DSS 42, Canberra	Prime station with command, telemetry, TV, and alpha scattering
DSS 51, Johannesburg	Prime station for telemetry during cislunar phase
DSS 61, Madrid	Prime station with command, telemetry, TV, and alpha scattering
DSS 71, Cape Kennedy	Station used for spacecraft compatibility tests and prelaunch and postlaunch telemetry data processing
DSS 14, Goldstone	Station configured for command backup and telemetry reception via both the DSS 11 CDC and SFOF; also used to record the terminal descent

Table VI-2. Reported Surveyor VII command, TV, and alpha scattering activity before shutdown for first lunar night

Station	Commands transmitted	TV frames commanded	Alpha scattering data accumulated in station TCP, min
DSS 11	81,650	9626	62
DSS 42	44,521	9015	242
DSS 51	50	0	0
DSS 61	12,860	752	2952
DSS 71	0	0	0
Totals	139,081	19,393	3256

events occurring at DSS 11 were midcourse maneuver, terminal descent and landing, and the laser experiment. This station's activity emphasized the commanding of TV pictures, although some alpha scattering data was also accumulated and engineering interrogations were performed. Of the total number of TV frames obtained, 49.7% was commanded from this station, but only 2% of the total alpha scattering data was accumulated by this station. Several equipment problems were experienced during the lunar operations, although none had any affect upon the mission. Problems were experienced with the paper tape reader, the command SCO, and an intermittent 35-mm film counter.

- (2) DSS 42, Canberra. Canberra participated in 19 passes. This station accomplished 46.5% of the TV

commanding and 7½% of the total alpha scattering data accumulated in the TCP. During the mission no CDC hardware problems occurred. A possible operational problem which occurred was a stuck filter wheel. This occurred during pass 15 due to an insufficient time lapse between command transmissions.

- (3) DSS 51, Johannesburg. DSS 51 participated in three passes during the transit phase and was not committed for use after touchdown. Initial decommutator lock lasted for only 4 min during the launch pass. There were no CDC, equipment, or operational problems.
- (4) DSS 61, Madrid. DSS 61 participated in 19 passes. Primary activity during the lunar phase consisted of engineering interrogations and alpha scattering data accumulations. Only 3.9% of the total TV activity was commanded, yet 91% of the total alpha scattering data was accumulated by this station. There were no CDC equipment or operational problems.
- (5) DSS 71, Cape Kennedy. DSS 71 support for Surveyor VII consisted of a DSIF Spacecraft Compatibility Test, an Operational Readiness Test, a spacecraft prelaunch countdown phase, and a post-launch phase lasting through approximately the first 40 min of the mission. During launch this station processed the data being received from the various AFETR tracking stations and then sent this data to the SFOF. As a backup, the DSS 71 receiver tracked the spacecraft from launch for nearly 5 min, and this data was available for transmittal to SFOF if necessary. There were no CDC equipment problems.
- (6) DSS 14, Goldstone. DSS 14 provided backup for DSS 11 during transit through touchdown. The output of the station's receiver is sent to the SFOF and to the DSS 11 CDC for processing at either location if necessary. The station's output was used during the terminal descent phase. The station also provides backup for command transmission using the DSS 11 CDC and the intersite microwave link.

2. Spacecraft Television Ground Data Handling System

The spacecraft Television Ground Data Handling System (TV-GDHS) was designed to record, on film, the television images received from Surveyor spacecraft. The principal guiding criterion was photometric and

photogrammetric accuracy with negligible loss of information. This system was also designed to provide display information for the conduct of mission operations, and the production of user products, such as archival negatives, prints, enlargements, duplicate negatives, and a digital tape of the TV ID information for use in production of the ID catalogs.

The system is in two parts, TV-11 at DSS 11, Goldstone, and TV-1 at the SFOF in Pasadena. At DSS 11 is an on-site data recovery (OSDR) subsystem and an on-site film recorder (OSFR) subsystem. These subsystems are duplicated in the media conversion data recovery (MCDR) subsystem, and in the media conversion film recorder (MCFR) subsystem at the SFOF. The portion of the system used in real-time at the SFOF is comprised of the MCDR, the MCFR, the media conversion computer, the video display and driver subsystem (VDDS), and the FR-700 and HW-7600 magnetic tape recorders. (An FR-1400 was available as backup.) A film processor, the strip contact printer, and the strip contact print processor are used in near-real-time. The photographic subsystem used in non-real-time is comprised of several enlargers, a copy camera, two film processors, a film chip file, other photographic equipment, and film storage areas.

a. TV-GDHS at DSS 11 (TV-11). Data for the TV-GDHS is injected into the system at the interface between the DSS 11 receiver and the OSDR. In both the 200-line and the 600-line modes, the OSDR provides to the film recorder subsystem: (1) the baseband video signal, (2) the horizontal sync signal, (3) the vertical frame gate, (4) the resynchronized raw ID telemetry information, and (5) the time code. In 200-line mode, the OSDR supplies a 500-kHz predetection signal to the DSS 11 FR-800 and FR-1400 magnetic tape recorders and to the SFOF via the microwave communication link. In 600-line mode, the OSDR provides: (1) a 4-MHz predetected signal to the DSS 11 FR-800 and to the SFOF via the microwave communication link, and (2) a baseband video signal to the DSS 11 FR-1400 magnetic tape recorder. In addition, the DSN provided an FR-900 recorder as backup to the FR-800 recorder.

The OSFR records the following on 70-mm film: the video image, the raw ID telemetry in bit form, the "human readable" time and record number, and an internally generated electric gray scale. The film is then sent to the SFOF for development.

b. TV systems at overseas DSIF stations. In addition to the TV systems at DSS 11, Stations 61, 42, and 51 provide some TV recording capability for *Surveyor* missions. As described in Section VI-B, Stations 61, 42, and 51 all have 35-mm film recording capability in the Command and Data Consoles. They also provide FR-1400 and FR-800 recordings of video data received. In addition, DSS 61 provided an FR-900 video recorder as a backup to the FR-800 recorder. The tapes and film from these stations are sent to TV-1 for processing and for evaluation.

c. TV-GDHS at the SFOF (TV-1). The signal presented to the microwave terminal at DSS 11 is transmitted to the SFOF, where it is distributed to the MCDR and to the VDDS. The MCDR processes the signal in the same manner as the OSDR. In addition, the MCDR passes the raw ID information to the media conversion computer, which converts the data to engineering units. This converted data is used by (1) the film recorder, where it is recorded as human readable ID, (2) the wall display board in the SSAC area, (3) the disc file where the film chip index file is kept, and (4) the history tape.

The VDDS produces the signals to drive the scan converter and the signals to drive the various display monitors and the paper camera in the SSAC area. Either the VDDS or the MCDR may be used to supply the signals recorded by the FR-700 and the HW-7600 video magnetic tape recorders in the same manner as the FR-800 and the FR-1400 recorders at DSS 11. The scan converter converts the slow scan information from the spacecraft to a standard RETMA television signal for use by the SFOF closed circuit television and the public TV broadcasting stations.

The MCFR records on two different films. Both films are wet-processed off line. One of the negatives is used to make strip contact prints which are delivered to the users. Additionally, this negative is used to make a master positive for the production of a duplicate negative for the JPL Public Information Office (PIO) and a preliminary duplicate negative for the science users. The negative is then cut into chips which are entered into the chip file where they are available for use in making additional contact prints and enlargements.

d. TV-GDHS performance. The system used for *Surveyor VII* was the same as the configuration employed during *Surveyor VI*. Operations in the TV-1 area ran comparatively smoothly and trouble free during the entire lunar day. Real-time spacecraft signals received

via the microwave link were of excellent quality, with the exception of a portion of one pass when channel switching problems occurred. The data that was lost was quickly recovered the following day from the FR-900 recording at the DSN. Minor equipment failures that occurred within the TV-1 area were corrected during real-time operations when feasible, and the loss of TV data was held to a minimum. Among those failures were:

- (1) The main clutch spring in film transport 1 broke but was rebuilt and installed by JPL machinists with minimum loss of film data transfer.
- (2) The video data simulator failed to operate in the framing mode, but the simulator at TV-11 was used as a backup and the countdown calibration schedules were met.
- (3) Normal wear to gear trains and drive belts in the photo processing equipment required replacement during real-time operations but did not affect the scheduled delivery of photo products.

Following is a summary of photo product output for the first lunar day operations.

Mosaics: 1134 prints, 648 negatives.

Photo enlargements: 5619 prints.

Strip contact prints: 560 rolls.

Master positive: 80 rolls.

Public Information Office duplicate negatives: 80 rolls.

Experimenters' data record: 80 rolls.

CDC film: 59 rolls.

Video tapes recorded at TV-1:

HW-7600 analog recorder: 90 each.

FR-1400 analog recorder: 26 each.

FR-700 video recorder: 68 each.

C. Mission Operations Chronology

Inasmuch as mission operations were carried out on an essentially continuous basis throughout the *Surveyor VII* mission, only the more significant and special events including nonstandard operations are described in this chronicle. Refer also to the sequence of mission events presented in Tables A-1 and A-2 of Appendix A.

1. Countdown and Launch Phase

The prelaunch countdown for *Surveyor VII* proceeded normally and smoothly with only minor ETR downrange equipment problems and temporary communications outages being reported. Launch time was rescheduled from 05:55 to 06:30 GMT in order to obtain improved down-range tracking coverage from the Range Instrumentation Ship (RIS) *Twin Falls*. The new launch time was established by extending the built-in hold at $T - 90$ min an additional 35 min. The countdown was resumed at 04:50 GMT.

At 06:13 GMT ($L - 17$ min), the generation of $T - 5$ min predictions for initial DSIF acquisition of the spacecraft was recommended by the FPAC Systems Data Analysis Group. Acquisition predictions are composed of time-tagged DSIF antenna pointing coordinates, doppler frequencies, and best-lock ground transmitter frequencies which are routinely supplied to the DSIF stations to ensure initial spacecraft acquisition and to assist in the station-to-station transfers of the spacecraft. The information is based on nominal launch azimuths and measurements of the spacecraft transmitter and transponder center frequencies with respect to temperature. The frequencies are measured before the mission to provide the stations with preflight information and again several times within the last 10 hr of the countdown. Although both preflight and $T - 5$ -min predictions are generated before the launch, the $T - 5$ -min predictions are based on the latest temperature/frequency measurement and the actual launch azimuth. For *Surveyor VII*, the $T - 5$ predictions were generated for DSS 51 (Johannesburg) and DSS 42 (Tidbinbilla) using corrected center frequencies supplied by SPAC, the predicted actual launch azimuth of 102.9 deg, and individual station parameters. A minor communications processor failure occurred approximately at liftoff, causing a 10-min delay in the computation and its subsequent transmission to the stations.

All systems reported "go" during the 10-min built-in hold at $T - 5$ min, and the count was resumed on schedule at 06:25 GMT. Liftoff ($L + 0$) occurred at 06:30:00.545 GMT, January 7, 1968, on the predicted launch azimuth of 102.914 deg. ETR Operations reported that all tracking stations were functioning without problems and all launch vehicle systems were "looking good" on telemetry. All telemetered launch phase events (Mark Events) occurred very close to the nominal times. Following a parking orbit coast phase of approximately 22 min, the *Centaur* main engines were ignited for a second burn of 1 min 55 sec. At separation, the spacecraft was injected

into a lunar transfer trajectory well within the required limits. With the exception of *Centaur/Surveyor* electrical disconnect (Mark 19), all preseparation events were confirmed in real-time from spacecraft telemetry. A description of launch vehicle performance and the flight sequence of events from launch through injection is contained in Section III.

Following separation from the *Centaur* at 07:05:16 GMT ($L + 00:35:16$), the spacecraft automatically executed the following maneuvers. Using the cold-gas attitude control jets, the flight control subsystem first nulled out the small rotational rates imparted to the spacecraft during the separation event, then initiated a roll-yaw maneuver sequence to acquire the sun. After a minus roll of 224 deg, and a plus yaw of 37 deg, sun acquisition and lock-on by the spacecraft sun sensors were completed at 07:14:30 GMT. Concurrent with sun acquisition, the antenna and solar panel positioner (A/SPP) stepping sequence was initiated to deploy the solar panel to its transit position. At 07:10:37 and 07:14:28 GMT, respectively, spacecraft telemetry signals confirmed that the solar panel and roll axis were positioned and locked. Having completed automatic solar panel deployment and sun acquisition, the spacecraft entered the initial coast phase with pitch and yaw axes controlled by tracking the sun and the roll axis inertially fixed.

2. DSIF and Canopus Acquisition Phase

Both DSS 51 (Johannesburg) and DSS 42 (Tidbinbilla) were receiving the $T - 5$ -min predictions by 06:45 GMT, approximately 10 min later than normal but still with an ample 35-min margin before the predicted spacecraft rise at DSS 42, the initial acquisition station. First DSIF contact with the spacecraft was accomplished on schedule by DSS 51. Using $T - 5$ -min predictions, the station acquired the spacecraft down-link frequency at 07:04:53 GMT, 35 min after liftoff, and tracked in one-way mode during the initial but very short (4-min) DSS 51 view period. Telemetry received during this time verified that spacecraft status was nominal and that solar panel deployment was in progress. Prior to DSS 42 acquisition, approximately 12 min of good one-way telemetry data was received by the MSFN tracking station at Carnarvon, Australia, and relayed to the SFOF via DSS 42.

Spacecraft rise at DSS 42 at 07:20:04 ($L + 00:50:04$) was indicated by $T - 5$ -min predictions. Initial RF contact and one-way lock was reported accomplished at 07:20:25 GMT, 21 sec later than predicted. After switching from the 16-deg beam of the acquisition antenna to

the 0.4-deg main antenna beam, the ground transmitter was turned on and the station reported the spacecraft receiver in phase lock at 07:27:12 GMT. At 07:28:02 GMT ($L + 00:58:01$), DSS 42 was receiving good two-way data and initial two-way acquisition was complete.

The first ground-commanded operations (Initial Spacecraft Operations) were initiated at 07:31:47 GMT to reconfigure the spacecraft from its automatically controlled launch-to-DSIF acquisition configuration to cruise mode. The command sequence includes (1) switching the transmitter from high power (10 W) to low power (100 mW), (2) turning off solar panel deployment logic, (3) securing the solar panel and roll axis locking pins, (4) consecutively interrogating telemetry commutator modes 1, 4, 2, 6, and 5, for an overall assessment of the spacecraft, and (5) changing the telemetry data rate from 550-bits/sec low modulation index to the 1100-bits/sec normal modulation index. Assessment of initial operations confirmed that spacecraft performance and all systems were normal. The commanding of *cruise mode on* was postponed, however, owing to the generation of a high star intensity signal by the Canopus sensor, indicating that the earth was still present in the sensor field of view. The flight control system was kept in sun mode, since commanding *cruise mode on* at this time would have caused the spacecraft to roll in response to the earth signal, resulting in an unnecessary expenditure of the nitrogen gas supply used for attitude control. It was also determined that Receiver A was successfully locked up to the ground transmitter and that the tuning procedure to capture Receiver A would not be required.

Initial spacecraft operations were completed at 07:49:56 GMT, with *Surveyor VII* configured in low power, coast phase commutator (mode 5), and transmitting at 1100 bits/sec. Telemetry and two-way tracking data were being received via Omnantenna B from Transmitter B operating in the transponder (two-way) mode. The spacecraft continued to coast normally in sun mode, with its pitch-yaw attitudes controlled by tracking the sun and with its roll attitude inertially fixed. (The spacecraft telemetry bit rate/mode profile for the complete transit portion of the mission is given in Fig. VI-2.)

The initial spacecraft orbit estimate generated at the SFOF by the FPAC Orbit Determination Group is customarily based on AFETR data and was completed at $L + 01:19$. Using range and angle data from Pretoria, this first estimate verified a very nominal launch and injection and predicted that the present orbit would achieve the basic objective of a lunar encounter without

a midcourse correction. The first spacecraft orbit estimate based entirely on DSN data was computed at $L + 01:50$, using approximately 17 min of DSS 42 doppler and angle data. This orbit solution again verified that a lunar encounter would be achieved without a midcourse correction, and that the correction required to achieve a landing at the desired aim point near the crater Tycho was well within the nominal midcourse correction capability. These first results continued to be confirmed as the second and third orbit computations based on DSN data were completed at $L + 02:49$ and $L + 03:55$, respectively. When sufficient "doppler only" orbit solutions became available as inputs to the preliminary midcourse computation, the first estimate of the required maneuver was initiated at 11:50 GMT ($L + 05:20$).

The preliminary midcourse conference was convened at 14:00 GMT ($L + 07:30$), shortly before the Canopus acquisition phase of the mission. In order to meet the landing accuracy goal of 10 km or less, the FPAC recommendation was to perform two midcourse corrections: the first at approximately 17 hr after launch and the second at 48 hr after launch. The execution of two maneuvers at the times chosen would allow (1) sufficient tracking time to accurately determine the initial trajectory, (2) sufficient tracking time after the first maneuver to accurately perform a second maneuver, and (3) performance of both corrections during the Goldstone view period. Based on the preliminary maneuver computation, execution of the first maneuver was recommended for 23:30 GMT, using a burn time of approximately 11 sec to achieve a landing at the desired aiming point 40.87° S and 11.37° W on the Tycho ejecta blanket. SPAC confirmed that all spacecraft subsystems were normal and that the maneuver requirements did not conflict with spacecraft operational constraints.

At approximately 10:48 GMT ($L + 04:18$), the SPAC completed its analysis of the star verification and acquisition sequence and recommended that the maneuver be performed in high power with Transmitter B on Omni-antenna B, one-way lock, and transmitting commutator mode 1 data at 4400 bits/sec. The star verification and acquisition sequence consists of two roll maneuvers. The first revolution provides an analog recording of the light intensity and relative roll angle of celestial bodies passing through the field of view of the Canopus sensor. This star map is then compared with preflight computations of star locations and intensity data. After positive identification of Canopus, the star is automatically acquired during the second roll. The premaneuver analysis indicated that a data loss of up to 60 sec could occur on Omni-

antenna B during the scan of the star Caph. No significant nulls were expected, and there was a high probability that the spacecraft would maintain up-link lock during the entire maneuver.

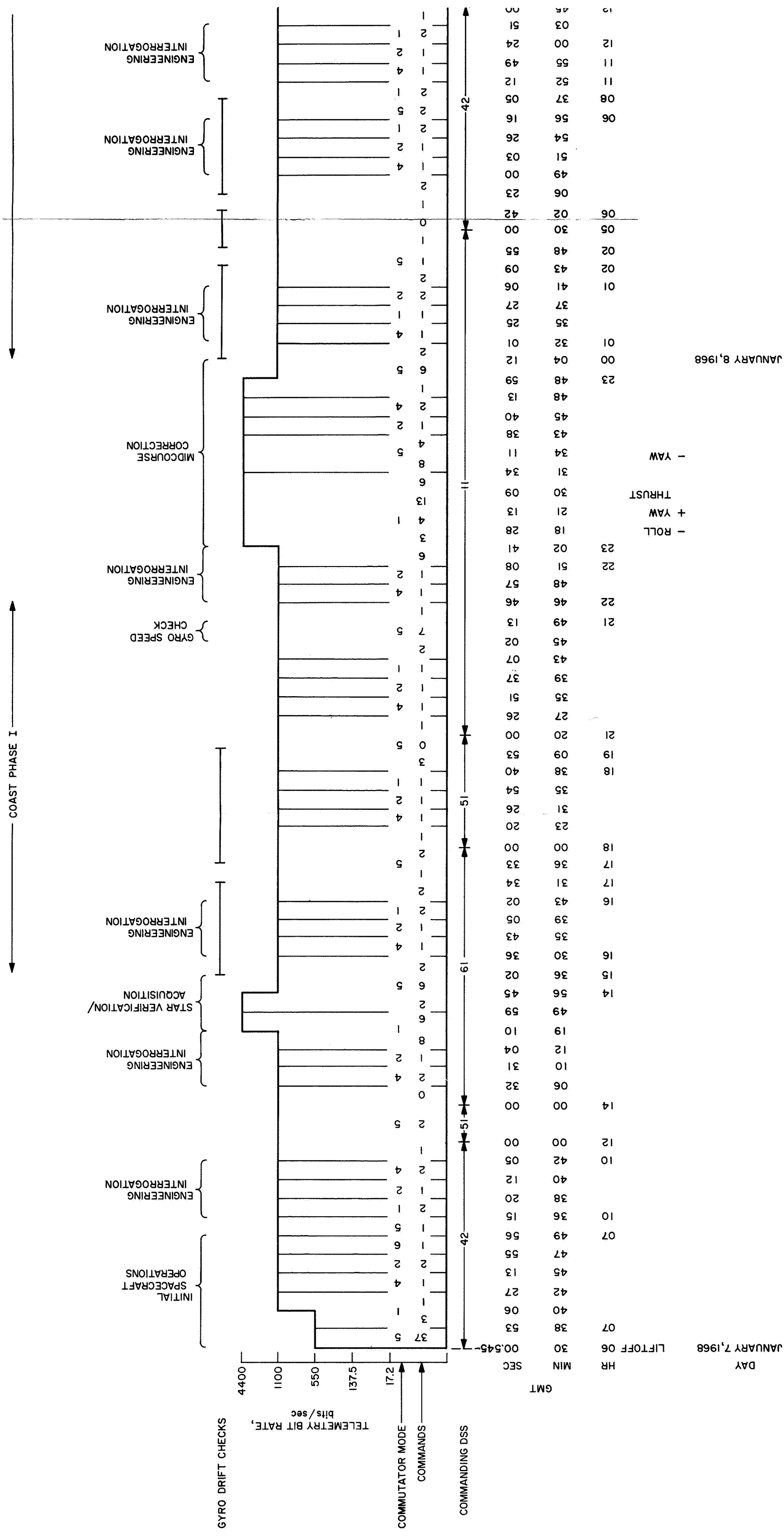
After completing an engineering interrogation at 14:12 GMT, the spacecraft was placed in the desired configuration for Canopus acquisition, and at 14:24:05 GMT, DSS 61 (Robledo) commanded the first roll maneuver. Rolling at $1/2$ deg/sec, the star intensity and angle signals indicated four clearly distinguishable stars plus two wide low-intensity signals and one wide high-intensity signal. After comparing the roll angle relationships of these signals with the previously calculated star map, the SPAC Flight Control Group was able to confirm that the spacecraft had sensed the presence of Alpha Canum Venaticorum, Mizar, the star groupings of Gamma Ursa Minoris/Kochab and Caph/Shedar/Zeta Cassiopeiae, the moon and earth, and, at 267 deg of roll, Canopus. During this first view of Canopus, the star lock-on signal nominally generated by the intensity of the Canopus signal was not produced. The sensed Canopus intensity proved much greater than expected, and above the upper threshold of the lock-on signal range. Consequently, preparations were made to perform a "manual" Canopus lock-on during the second roll.

The same light sources reappeared during the second revolution and, as the spacecraft approached its second view of Canopus, sun mode was commanded, manually stopping the roll maneuver as the star appeared in the sensor field of view. After the transients had settled, manual lock-on was commanded at 14:47:32 GMT ($L + 08:17:31$), ending the Canopus acquisition sequence. The maneuver had taken 25 min to complete as the spacecraft rolled through a total of 629 deg.

Following the star verification/acquisition sequence, Transponder B was commanded back on, and two-way tracking mode was reestablished at 14:51:04 GMT. Commutator mode 5 was commanded, the data rate was reduced from 4400 to 1100 bits/sec, and the transmitter returned to low power. With pitch and yaw attitudes controlled by tracking the sun and the roll attitude controlled by tracking Canopus, *Surveyor VII* was now in a known, fixed attitude, a precise position from which midcourse maneuvers could be computed and executed.

3. Pre-midcourse Coast Phase

During this phase, continuous engineering data was obtained at 1100-bits/sec data rate, and all activities were



conducted in low power. Approximately 50 min after Canopus lock-on, the first of two pre-midcourse gyro drift checks was initiated by commanding the spacecraft flight control attitude from celestial to inertial mode. In this attitude, the drift rate of all three axes is measured and the results supplied to FPAC so that planned attitude maneuvers can be compensated for drift as necessary. At 17:31:28 GMT, the first drift check was terminated by returning the spacecraft to celestial mode. The second check was initiated 6 min later.

During this period, the solar panel switch again tripped off to prevent overcharging the battery. This occurred four times during the flight and, as on the *Surveyor V* and *VI* missions, was considered normal. After allowing the battery to discharge for approximately 15 min, the switch was commanded back on.

Tracking data consistency checks and pre-midcourse orbit solutions continued to reduce the uncertainties in the initial trajectory toward Hipparchus and the unbraked, uncorrected target point. The orbit solution selected for final computation of midcourse parameters was completed at 20:25 GMT and contained all of the two-way doppler data up to midcourse minus 3 hr 49 min. The pre-midcourse attitude maneuver to orient the spacecraft in the desired direction for the velocity correction was selected from eight possible maneuver combinations for an $L \pm 16$ -hr midcourse. The one chosen was based on the best possible conditions for continuous high antenna gain, no antenna switching requirements, and maximum sun lock time. (Refer to Section VII for a full discussion of the midcourse correction.)

A gyro speed check was conducted at 21:45:07 GMT; the angular spin rates in roll, pitch, and yaw axes were measured and found to be exactly nominal at 50 Hz.

4. Midcourse Maneuver Phase

The midcourse maneuver sequence was initiated at 22:46:40 GMT ($L + 16:16:39$) with an engineering interrogation of commutator modes 4, 2, and 1. After confirmation that the spacecraft was in satisfactory condition for midcourse operations, Transmitter B was commanded to high power and the telemetry data rate was increased from 1100 to 4400 bits/sec. Beginning at 23:08:05 GMT ($L + 16:38:04$), the pre-midcourse attitude maneuvers consisting of a -3.1 -deg roll and a $+117.1$ -deg yaw were loaded and executed to align the spacecraft acceleration vector in the proper direction with the velocity vector for applying midcourse thrust. To increase point-

ing accuracy, each maneuver was delayed until the axis limit cycle was passing through a null. With the spacecraft positioned for thrusting, command sequences were sent to (1) turn on propulsion strain gage power, (2) turn on inertial mode, (3) turn off cyclic thermal loads, and (4) pressurize the vernier propulsion system. A midcourse thrust phase time of 11.35 sec was loaded into the flight control programmer magnitude register, and at 23:30:10 GMT ($L + 17:00:10$) the midcourse velocity correction was executed. All three engines ignited and burned smoothly for a total of 11.36 sec. The spacecraft remained stable throughout the thrusting period, achieving a constant acceleration of 0.1 g and a velocity change of 11.13 m/sec.

Following the midcourse velocity correction, the various power sources required for the thrusting phase were turned off, commutator mode 5 was selected, and the cyclic thermal loads were turned back on. A reverse yaw maneuver of 117.1 deg was commanded at 23:34:10 GMT, with sun acquisition indicated approximately 3.5 min later. The end of the yaw maneuver also brought Canopus into the star sensor field of view, making a post-midcourse roll maneuver unnecessary. Cruise mode was commanded on, returning the spacecraft flight control system to celestial mode followed by manual Canopus lock-on. An engineering interrogation in modes 2, 4, and 5 was conducted, followed by a reduction in the data rate to 1100 bits/sec. At 23:51:56 GMT, January 7, Transmitter B was returned to low power, ending the midcourse maneuver sequence after 49 min 56 sec of high-power operation.

5. Post-midcourse Coast Phase

Approximately 9 hr after the midcourse execution, the first post-midcourse orbit computations were completed. Orbit solutions were converging on an unbraked impact point approximately 3 km from the maneuver aiming point, disclosing that the execution of the maneuver had been exceptionally accurate. The second and third post-midcourse orbits were completed at approximately 11 and 21.5 hr after the maneuver and continued to confirm the extremely good results of the first post-midcourse orbit. At the second midcourse meeting held at 00:30 GMT, January 9, to discuss the planned second maneuver, FPAC advised that, without a second midcourse correction, the probability of landing in an undesirable rocky area within the target uncertainty ellipse was 11.5 percent. Performance of a second maneuver to land at the original target point would increase the probability of landing in the rocky area to 13.2 percent.

Since the present orbits were converging within an acceptable area, plans for the second maneuver were cancelled by the Mission Director. With essentially all terminal descent parameters having been fixed by the midcourse correction (i.e., burnout velocity, propellant margin, time of flight, etc.), only the terminal attitude maneuver remained to be selected. A roll-yaw-roll maneuver was recommended to satisfy telecommunications requirements and to achieve the desired landed attitude requested for optimum science activities. The recommended maneuver was accepted on a tentative basis to accommodate any changes warranted by subsequent orbit results.

Operations during the 48-hr coast phase II period were normal and followed the planned sequence of events with only minor deviations. Six three-axis gyro drift checks and one roll-axis-only check were performed between $L + 17:34:11$ and $L + 58:34:12$. Thirteen engineering interrogations were conducted between $L + 19:01:55$ and $L + 64:17:49$. Other operations included thermal control activities to maintain temperatures within nominal limits. A heater turn-on profile was established for Compartment A (battery warmup), the survey TV camera, and the alpha scattering instrument to insure that these temperatures would be within operating ranges at touchdown. Compartment A heater was turned on for approximately 8.7 hr, starting at 14:00:21 GMT, January 9, and ending at 22:44:04 GMT. The alpha scattering electronics (Compartment C) heater and the alpha scattering sensor head heater were turned on at 22:27:24 GMT and 22:32:00 GMT, respectively. The survey television electronics thermal control and vidicon temperature control were turned on at 18:19:46 GMT and 23:54:48 GMT, respectively.

There were no commanding problems as such during the coast phase II period. However, for the greater part of the coast phase, the earth vector to Omnantenna A was directly in line with the deep null region of the antenna gain pattern. After the midcourse maneuver, the antenna null caused the Receiver A signal level to at times fall not only below command threshold but also below the indexing* threshold. This made it necessary to do intentional indexing before commands were initiated in order to assure that Receiver B (and thus Omni-

antenna B) was selected for command processing. During preparation for the terminal sequence, spacecraft limit cycling caused Receiver A to index so frequently that it was necessary to repeat some commands. Indexing was not a problem during the terminal maneuver and descent phase since the earth vector to Omnantenna A was moved out of the null region after the spacecraft had rolled approximately 5 deg.

Completion of the fourth post-midcourse orbit produced little or no change in the extremely good results of the midcourse maneuver indicated by the earlier orbit determinations. With no need for a terminal maneuver conference, the meeting was cancelled by Mission Control, and operations proceeded based on the previously recommended terminal maneuver plan. Out of eight possible maneuver combinations that would properly position the spacecraft for the terminal descent, a standard roll-yaw-roll combination had been selected as the optimum for maintaining satisfactory up-link and down-link telecommunications performance during the terminal maneuver and terminal descent. The maneuver would be performed in high power with Transmitter B on Omnantenna B, in one-way lock, transmitting 1100-bits/sec data. The final roll orientation was also designed to meet science requirements for post-landing operations and would position the spacecraft in the most favorable attitude for TV operations with respect to the sun angle at touchdown.

By 16:30 GMT, final SPAC inputs to the terminal maneuver computation were ready for submittal to FPAC. These consisted of the telecommunications terminal maneuver analysis and finalized recommendations, retro motor burn time predictions, and gyro drift rate data. Based on a predicted retro motor bulk temperature of 53°F at retro ignition, an estimated retro motor burn time of 42.78 sec was submitted to FPAC. Analysis of the nine gyro drift checks performed during the transit phase disclosed a very nominal drift rate in all three axes amounting to a total offset of approximately 0.04 deg. Owing to the smallness of the error, no attempt was made to compensate the terminal maneuver for drift.

A touchdown strain gage turn-on criterion was also recommended based on an SPAC analysis of the received signal strength expected during terminal descent and touchdown. Strain gage signals are not commutated but supplied directly to the subcarrier oscillator and transmitted continuously during terminal descent and landing. The minimum signal strength turn-on criterion is

*The spacecraft is designed to automatically switch (index) receiver/decoders whenever the ground-transmitted signal strength falls below the command threshold level, or whenever there is an interruption in command modulation. The receivers can be intentionally indexed (switched) by sending a modulation interrupt command.

established to prevent degradation of the essential 1100-bits/sec engineering telemetry when the strain gage analog signals are added to the carrier.

The FPAC final terminal guidance computer run was completed at 22:49 GMT. Predicted times for automatic descent events, the delay time between AMR *mark* and vernier engine ignition, and the desired AMR backup command time were generated and delivered to SPAC for preparation of the terminal descent command message and its transmission to DSS 11. The final message was sent and the duplicate return message verified at 23:33 GMT, approximately 90 min before retro ignition.

Activities immediately preceding the terminal phase consisted of a preterminal engineering interrogation of modes 4, 2, and 1, followed by a final gyro speed check. Both up-link and down-link frequencies were checked, and frequency offsets were calculated to compensate for the very rapid doppler shift which would occur during the last 3.5 min of the flight as the spacecraft slowed from approximately 6100 mph at retro ignition to 3.5 mph just before touchdown. By 23:52 GMT, January 9, the frequency offsets were entered into the ground receiver and transmitter at DSS 11 and the station reported green for commanding. SPAC reported all spacecraft systems green and *Surveyor VII* was ready to enter the terminal descent phase.

6. Terminal Descent Phase

At 23:59 GMT, January 9, approximately 1 hr before retro ignition, the terminal descent phase was initiated with a final engineering interrogation. Transmitter B was commanded to high power and the data rate was increased to 1100 bits/sec. (Indexing of Receiver A at this time required that some commands be sent twice.) Transponder B was commanded off at 00:21:15 GMT, January 10, placing the spacecraft in one-way mode for the terminal sequence.

Starting at 00:22:56 GMT, 40 min before retro ignition, the terminal attitude maneuvers were consecutively loaded into the flight programmer and executed. The first two maneuvers, a plus roll of 80.5 deg and a plus yaw of 96.1 deg, positioned the retro motor thrust axis in alignment with the velocity vector. The third maneuver, a negative roll of 16.5 deg, established the desired landed orientation of the spacecraft. Applying the same technique used during midcourse, the execution of each maneuver was delayed until the axis limit cycle was

passing through a null. At the completion of the third maneuver, the DSS 11 received signal strength was -125.9 dbm, within the recommended strain gage turn-on criterion, and at 00:42:33 GMT, the touchdown strain gages were commanded on.

With the spacecraft now in the desired retro attitude, the final retro sequence operational configuration was commanded to control the terminal descent. The vernier engine thrust level was set at 200 lb and a retro delay time of 2.775 sec between the altitude *mark* (AMR *mark*) and vernier engine ignition was stored. Telemetry mode 6 was selected, and the retro sequence mode for ensuring that the automatic flight control sequence responds to the AMR mark was turned on. Cyclic thermal loads were turned off, and AMR power and thrust phase power were turned on. At 01:00:34 GMT, 1 min 47 sec before main retro motor ignition, the altitude marking radar was enabled, placing the remainder of the descent sequence under automatic control.

At 01:02:10 GMT* ($L + 66:32:11$) the spacecraft reached a slant-range altitude of 60 miles above the moon, and the AMR *mark* signal was automatically generated. The standard, precautionary AMR backup command reached the spacecraft 3.9 sec later. The vernier engines were ignited on schedule, followed by main retro ignition 1.1 sec later. RADVS was energized, increased to high power, and acquisition of the lunar surface by the doppler velocity sensor beams was successfully signalled seconds later. Main retro burnout occurred as predicted 43 sec after ignition, followed by ejection of the retro case. RADVS-controlled descent was initiated at 01:03:12 GMT, and a few seconds later the radar altimeter acquired the lunar surface. Under control of RADVS, *Surveyor VII* continued to decelerate smoothly. When the spacecraft intercepted the programmed descent contour, the vernier engine thrust level increased, beginning a constant deceleration descent. Reaching a 10-ft/sec velocity at an altitude of 50 ft, vernier thrust was again increased to produce a 5-ft/sec constant velocity. At an altitude of 14 ft above the lunar surface, the vernier engines were cut off. *Surveyor VII* now fell freely to the surface, increasing speed slightly before finally touching down on the lunar surface at 01:05:36.32 GMT ($L + 66:35:35.78$), January 10, 1968.

*Times for automatic descent events have been corrected for 1.297/sec radio transmission delay to show time of occurrence at the spacecraft. Refer to Section IV-A for a more complete description of the terminal descent sequence.

7. First Lunar Day

In the SPAC area at the SFOF, the first quick look at the incoming touchdown strain gage data indicated that *Surveyor VII* had landed normally. The analog recording showed all three legs touching down almost simultaneously, the order of impact being Leg 1, 3, and 2, respectively. Peak landing loads in the order of impact were estimated to be 1650, 1360, and 1840 lb, from which the nominal landing velocity was determined to be approximately 12 ft/sec. (See Table IV-8 for final data.) A preliminary analysis of both the strain gage data and touchdown gyro data indicated that *Surveyor VII* had landed evenly on a nearly flat surface with a tilt from the vertical of approximately 3 deg.

(Based on final postflight tracking data, the estimated landing coordinates are 40.86°S latitude and 11.53°W longitude, approximately 6.0 km from the in-flight aiming point. Correlation of the terrain features pictured by *Surveyor VII* with earlier *Lunar Orbiter* photographs places the landed location at 40.95°S latitude and 11.41°W longitude, or a miss of 1.69 km. Final *Surveyor VII* science results are presented in Part II of the Mission Report and are repeated here only in a mission operations relationship.)

SPAC specialists proceeded quickly to the postlanding power shutdown and assessment of essential spacecraft systems. In the next 5 min, the various power sources required for the terminal descent were commanded off, and an interrogation of telemetry modes 2 and 5 was initiated. During this time, fluctuations in the down-link received signal level and in the up-link signal received at the spacecraft were noted by DSS 11 and DSS 14. The down-link signal variation was on the order of ± 0.5 db and was present when transmitting over either omnidirectional antenna. Later, during transmission over the planar array after it had been stepped into orientation with the earth, the down-link signal variations disappeared. The up-link variations continued periodically throughout the lunar day. Subsequent investigation eliminated anomalous spacecraft behavior as the cause and attributed the problem to multipath reflections from the nearby lunar terrain.

Continuing with the postlanding checkout, SPAC reported that the spacecraft was responding as commanded and that an estimated 92.3 A-hr remained in the battery, ample to continue planned high-power operations before positioning the solar panel to supply battery

charge current. Commands normally sent at this time to lock the landing legs and dump the helium pressure supply for the vernier propulsion system were postponed, thus preserving the capability to perform an optional spacecraft hop experiment similar to the successful hop performed by *Surveyor VI*. Next, thermal control heaters for the vernier system, alpha scattering instrument and TV system were activated to protect against the extreme cold during the first hours of the lunar morning. After a preliminary checkout of the spacecraft radio, signal processor, and TV camera controls, SPAC was able to confirm that these essential systems were indeed operating normally. Because of the light landing loads experienced at touchdown, SPAC recommended skipping the initial checkout of the antenna and solar panel positioner in order to speed up the start of television operations. By 01:34 GMT, the spacecraft was configured for initial television operations in 200-line mode. Control of the spacecraft was transferred to SSAC, and at 01:45 GMT, 40 min after touchdown, the first TV picture was commanded and successfully received. The initial 200-line television sequence consisted of a wide-angle survey beginning with Footpad 3, then up and across the local horizon and down to Footpad 2. The purpose of the sequence is to quickly determine if any gross structural damage has been sustained and to provide information on the landed attitude of the spacecraft as well as the lunar location. Between 01:46 and 02:11 GMT, 14 good-quality pictures were received, revealing that *Surveyor VII* was structurally sound and had landed with close-to-nominal orientation on a rock-strewn landscape leading to a series of ridges and upland hills. A fairly prominent crater could be seen approximately 8 miles away to the northeast. The view of Footpad 3 showed that the pad had come precariously close to landing directly on top of an 8-in. rock.

Assured of a healthy spacecraft, control was returned to SPAC to reconfigure for 600-line, high-resolution television which requires the more lengthy A/SPP stepping operations to roughly align the high-gain planar array antenna with the earth and the solar panel with the sun. This initial, or gross positioning A/SPP sequence provides the increased signal strength for 600-line mode TV and the necessary power via the solar panel for continuing lunar operations. The sequence involves stepping the A/SPP to the predicted sun and earth positions which have been necessarily calculated for a vertical spacecraft that has retained the roll orientation established during the terminal maneuver. The greater the deviation from the predicted landed attitude, the more time required to

accomplish gross positioning. This in turn reduces the time remaining in the Goldstone postlanding view period and hastens the end of the real-time video display transmitted to the SFOF via the Television Ground Data Handling System (TV-GDHS). The real-time display capability is especially important since it permits science and television performance groups in the SFOF to evaluate the lunar subject in real-time and control camera performance accordingly. The photos obtained from these initial sequences are then used to direct the continuation of TV operations after transfer to DSS 42.

Because of the favorable landing, the sun and earth were found very close to their predicted positions, allowing the gross positioning sequence to be completed in a nominal 44 min (which left nearly 4.5 hr before the scheduled transfer to DSS 42). Because of the southerly location of the spacecraft, the acquisition could not be carried out without unlocking the elevation axis as well as the roll and solar axes. The elevation axis is preferably kept locked since this simplifies calculations for the other axes (see Fig. IV-10). The first 600-line high-resolution picture was initiated at 03:23 GMT with excellent results. Activities for the remainder of the DSS 11 view period consisted of a wide-angle 360-deg panorama, a special area survey, and periodic engineering interrogations scheduled roughly at 1.5- and 2-hr intervals. Telemetry indicated that the gradually rising sun had warmed the spacecraft sufficiently, and by 07:43 GMT nearly all thermal control heaters had been turned off. The spacecraft attitude determined from this first A/SPP data agreed favorably with the initial gross estimate based on touchdown gyro error and strain gage data.

At 08:00 GMT, control of the spacecraft was transferred to DSS 42. TV operations were continued but without benefit of the real-time video display at the SFOF. As pictures were received at the Australian station, the DSS 42 *Surveyor* Operations Chief (SOC-42) described the images over the voice line to the Television Science (TSAC) and Television Performance (TPAC) groups in the SFOF. With the DSS 11 pictures available for reference, the TSAC and TPAC groups consulted with SOC-42 and recommended camera changes as necessary. From 08:29 to 08:51 GMT, narrow-angle pictures of the earth were taken using various polarization filters and with very good results. Unlike previous *Surveyor* missions, earth viewing was possible throughout the lunar day. Numerous pictures of the earth and its cloud cover were taken, showing approximately 60% of the day-side of the earth during the best viewing opportu-

nity. Cloud pattern progress during the picture sequences was particularly notable.

At 09:05 GMT, television operations were halted to reconfigure the spacecraft for the beginning of alpha scattering operations. The instrument was commanded on in its stowed position for initial calibration and the start of approximately 5 hr of standard-sample data accumulations. (Refer to Section IV-K for a description of the alpha scattering instrument.) The incoming spectra received at the SFOF via teletype were monitored by the principal investigators, who confirmed that the instrument was operating properly. Concurrently during this period, the A/SPP "fine positioning" sequence was conducted by SPAC attitude determination specialists. Fine positioning of the solar panel to the sun and the planar array to the earth provides data for a more accurate determination of the spacecraft attitude. A precise determination of the spacecraft attitude and orientation on the lunar surface provides the basic information necessary for efficient thermal and power management of the spacecraft. Television operations are also dependent on accurate attitude information, since many TV sequences are conducted by command tapes which are designed to automatically position the camera relative to a vertical spacecraft. Manually conducted astronomical sightings are totally dependent on accurate knowledge of the spacecraft attitude. Planned for 3 hr, the sequence was completed in a little over 2 hr. Starting with a signal strength of 123.8 dbm, the planar array output at the end of the sequence measured -117.5 dbm, an improvement of 6.3 db. Based on a combination of fine positioning and touchdown gyro data, the spacecraft downhill tilt was calculated to be 3.09 deg toward lunar north. The spacecraft +X axis was located 22.25 deg counterclockwise from lunar east, placing Leg 1 south by east, Leg 2 roughly northwest, and Leg 3 west by north. (The final attitude determination, based on A/SPP data, TV fixes on Jupiter and the earth, FPAC orbit information, gyro data and *Lunar Orbiter* data, is illustrated in Fig. IV-9.)

At 14:15 GMT, approximately 30 min before the end of the DSS 42 view period, control of the spacecraft was transferred to DSS 61. By 15:30 GMT, a total of 5 hr 10 min of alpha scattering standard sample data had been accumulated and preparations were made to release the sensor head to its "background" position to detect and calibrate natural background radiation before deployment to the lunar surface. A commanded tape prepared at DSS 61 was used to routinely deploy the

sensor head to a position approximately 22 in. above the lunar surface and to monitor the operation on television. The tape provided a stop-motion TV sequence of the deployment which included approximately 100 pictures taken at 2.5-sec intervals of a slow, swinging motion developed by the head which had been observed during the *Surveyor VI* mission.

Toward the end of January 10, the general pattern of lunar operations for the remainder of the mission had been established. Under the direction of SSAC, TV sequences and other spacecraft activities requiring television support were alternated with alpha scattering operations, while periodic halts for engineering interrogations and tests provided SPAC with the continuous information necessary for thermal and power management of the spacecraft. The majority of the video sequences and video-supported experiments were reserved for the Goldstone view period. Alpha scattering accumulations and other activities not requiring TV support were generally scheduled for the DSS 42 and DSS 61 view periods. Coordination and scheduling of lunar activities were accomplished on a daily basis during regularly scheduled lunar operations planning meetings attended by all elements of the space flight operations team. Chaired by the Assistant Space Flight Operations Director for Lunar Operations, the meetings were convened shortly before the beginning of each Goldstone view period to brief mission personnel on the current status of the spacecraft and the accomplishments of the preceding 24 hr. Science and engineering requests for the upcoming 24 hr were then submitted and scheduled on a priority basis.

After accumulating 5 hr of background data, preparations were made for the final deployment of the alpha scattering sensor head to the lunar surface. DSS 61 reported that the TV survey of the area beneath the instrument still showed mostly shadows but that one small rock could be seen which might possibly cause interference. At 22:01 GMT, the command to deploy was sent. Television was not used to monitor the event since deployment to the surface could be confirmed by an increase in alpha and proton activity. But the incoming teletype data monitored during the next few minutes showed no characteristic increase in event rates. A second deployment command was transmitted, but the event rates continued to remain at the background level, indicating that the sensor head had not been deployed. A few minutes later, at 22:25 GMT, operations were momentarily halted for the transfer to DSS 11. The

spacecraft was configured for television and a series of pictures taken, showing the sensor head was indeed still in its background position. Views of the deployment mechanism disclosed that the explosive pin-puller which releases the head to the lunar surface had functioned properly, indicating that the spacecraft had received and acted on the deployment command. This evidence pointed toward a mechanical problem, most probably located in the escapement mechanism which controls the velocity of the release. What could be seen of the escapement, however, showed nothing unusual. Use of the SM/SS to assist the deployment was immediately considered, and planning was begun along that line. An attempt was first made to jar the head loose by stepping the A/SPP but without success. In order to keep other activities on schedule, it was decided to complete 4 hr of planned TV and surface sampler operations before making any further attempts.

Beginning at 07:23 GMT on January 11, SSAC specialists directed the lazy-tongs arm of the surface sampler out toward the sensor head and quickly discovered that the head was suspended too high to permit positioning the SM/SS scoop on top for a downward push. Using only limited force to prevent damaging the SM/SS, a series of experimental taps and pushes were exerted on the skirt extending around the bottom of the head in hopes that a downward nudge or a swinging motion might overcome the unknown obstruction. Close examination of TV photos seemed to indicate some downward movement was taking place, but after 80 min of trying, activities were terminated, with mostly indeterminate results. A crash effort was then organized to develop an effective deployment technique before the next Goldstone view period. Using operating models of the spacecraft located at the Hughes Payload System Laboratory and the JPL Science Evaluation Test Laboratory, the effort was directed toward devising a means to first lower the sensor head sufficiently to position the SM/SS scoop on top and then force it to the surface. While this effort was proceeding, scheduled TV sequences and additional accumulations of alpha scattering background data were performed during the DSS 42 and 61 view periods.

At the January 11 Lunar Operations Planning Meeting, the discussion centered on the delay caused by the deployment failure and its evident effect on the overall lunar operations plan. After evaluating the relative importance of the experiment, both project management and project scientists unanimously agreed that first scientific priority should be assigned to obtaining alpha

scattering data. TV and surface sampler experimenters accordingly arranged their activities to provide the requested time and assistance during the upcoming deployment attempt. At this time, since good pictures of the earth were obtainable, plans for a laser communications experiment were confirmed. Argon laser light transmitted from six astronomical observatories would be simultaneously beamed at the spacecraft, which would then be commanded to take pictures of the earth. The experiment would be scheduled as soon as all operational elements reported ready.

At the beginning of the DSS 11 view period, more pictures were taken of the escapement mechanism on a chance that the changing sun angle might have revealed the problem, but nothing unusual could be seen. The next 4 hr were devoted to surface sampler operations to insure obtaining some SM/SS data, since there was a definite possibility of damaging the instrument during the deployment attempt. Beginning at 05:48 GMT on January 12, the surface sampler scoop was first opened and then maneuvered into position on the sensor head skirt. The head was stabilized by moving it toward the spacecraft until the opposite side of the skirt was wedged against the helium tank. The scoop was then pressed down on the skirt, successfully lowering the head several inches and permitting the scoop to be positioned on top. The head was then gradually lowered to the surface with a series of "fine" pushes. The instrument was turned on but analysis of the received data indicated that the head was not yet fully on the surface. More pictures were taken, the head was given a final push, and the first good data sample was confirmed at 11:30 GMT, some 37 hr after the initial command to deploy the head had been sent.

The exact cause of the deployment failure is unknown, but a careful analysis of the TV picture record indicates that the deployment mechanism was near the threshold of movement and that relatively little force was required to move the sensor head downward.

As expected, the alpha scattering deployment failure had placed all scheduled lunar activities considerably behind time. Additionally, as on previous missions, rising spacecraft temperatures were beginning to affect operations. Unlike previous *Surveyors*, whose objectives were to explore *Apollo* landing sites at the lunar equator, the *Surveyor VII* landing site near the crater Tycho was located some 40 deg south of the lunar equator and presented a somewhat different thermal environment. Although prelaunch calculations indicated that surface temperatures at noon would be generally cooler in the Tycho

vicinity, 211°F as opposed to 261°F at the equator, these calculations were of necessity based on an ideal or "smooth" moon and did not account for local surface conditions, boulders, rocks, craters, slopes, etc., which could greatly affect spacecraft temperatures during the mid-morning to mid-afternoon periods. Also contributing to the uncertainty was the sun angle. During previous missions, the solar panel and planar array had been extensively used to keep temperatures within operating limits by shading thermally sensitive components and subsystems from direct solar illumination. But the combination of spacecraft orientation and the relatively low sun elevation (approximately 53 deg maximum at the Tycho latitude) would make it nearly impossible to provide shade for the scientific payload, particularly the alpha scattering sensor head, throughout most of the lunar day.

At the end of the DSS 11 view period, an initial 52 min of good alpha scattering lunar sample data had been accumulated. The DSS 42 view period was devoted almost exclusively to television, and by the middle of January 12 a TV duty cycle of 90 min on, 15 min off was required to keep the camera and TV electronics temperatures within operating limits. Alpha scattering operations were resumed after transfer to DSS 61, and a total of 5.5 hr of data was accumulated. The sensor head and alpha scattering electronics (Compartment C) temperatures were also rising but were not yet critical. The operational goal was to obtain 25 hr of noise-free lunar sample data before the sensor head and Compartment C temperatures reached their upper operational limits. With no A/SPP shading available, the surface sampler scoop was positioned to provide some shade for the sensor head at the conclusion of surface sampler operations. Because of higher operating temperature limits, the surface sampler mechanism temperature was the least critical. Mission activities were now directed toward obtaining as much scientific data as possible before rising temperatures forced a complete shutdown of the spacecraft during the lunar noon, which was predicted to occur on January 16 at 05:23 GMT.

Toward the end of January 12, propulsion specialists reported that the vernier propulsion system oxidizer relief valve had vented a total of eight times and that the fuel valve had vented once. Shading was required for the next 72 hr in order to preserve propulsion system capability for conducting a spacecraft hop. Attitude determination specialists reported that some A/SPP shading was possible and began preparing a series of A/SPP patterns that would provide shade for the valves while

leaving the planar array antenna pointed toward the earth. When stepping the A/SPP to produce a new shadow pattern, it was generally necessary to break earth lock with the planar array and operate the spacecraft transmitter via the omnidirectional antenna. By 22:00 GMT, SPAC was ready to reposition the A/SPP, but in order to prevent interference with alpha scattering operations then presently in progress, Mission Control directed that the repositioning be postponed until it could be performed on a noninterference basis with science activities.

DSS 11 television operations were resumed early on January 13. Camera temperatures soon limited operations to a 50% duty cycle of approximately 1 hr on, 1 hr off, causing some TV sequences to be cancelled or postponed. During the first cooldown period at 02:45 GMT, the A/SPP was repositioned to shade the propulsion system relief valves. A temperature assessment 2 hr later indicated that some shading of the TV camera had also been effected. To make use of the frequent TV cooldowns, alpha scattering operations were conducted during all three station view periods. Procedures were also modified to perform alpha scattering accumulations concurrently with engineering interrogations, but by 08:18 GMT, the sensor head reached above its maximum operating temperature of 122°F, and the instrument was turned off for cooling. Again, at 20:21 GMT during the DSS 61 view period, the instrument was shut down when the head temperature reached over its limit. Both times the SM/SS scoop was repositioned to adjust shading on the head, bringing temperatures back within operating limits after an 80-min wait.

During the January 13 Lunar Operations Planning Meeting, SPAC specialists reported that, since being shaded, the vernier propulsion system oxidizer relief valve had vented twice and the fuel valve once. Concern remained that increasing temperatures might prevent the valves from reseating properly, thus causing a total loss of system pressure and ending any chance of performing a vernier static firing or a spacecraft hop. At this time, project management directed that shading priorities be limited strictly to science components and that special efforts to shade the vernier propulsion system, even on a noninterference basis, be terminated.

Science operations on January 14 continued normally but with increasing intermittence as the temperatures of the unshaded science components continued to increase. TV operations were reduced to a 25% duty cycle. During cooldowns and dormant periods, camera temperatures

were eased somewhat by stepping the camera away from the sun to reduce solar absorption through the camera hood.

At 04:30 GMT, during the DSS 11 view, the first of four earth-moon laser communication experiments was conducted. This initial attempt involved four astronomical observatories located across the U.S., each equipped with an argon ion laser which was precisely aimed at the spacecraft. At a given signal, the lasers were turned on while the spacecraft took pictures of the earth. Results, however, were indeterminate. The experiment was repeated on January 19, 20, and 21, successful results being achieved on the latter two attempts. Pictures of the earth showed two adjacent pinpoints of light which could be identified as emanating from earth observatories at Table Mountain, California, and Kitt Peak, Arizona. The experiment was the first of its kind and produced the first known visual evidence of laser communication between the earth and another celestial body. The experiment verified that laser power output as low as 1 W can produce detectable light signals between the earth and the moon and provided an opportunity to exercise and evaluate different laser pointing techniques. Proof that the images recorded by the television camera were actually received laser beams and not vidicon blemishes was indicated by the geographical location of the light pinpoints on the television earth image. Proof confirmation was made by turning the laser on and off at a specific observatory, causing the pinpoints to appear and disappear at corresponding times in consecutive pictures, and stepping the camera one azimuthal step, causing the light image to shift accordingly with the earth image.

At 15:48 GMT, the camera failed to respond to some commands when the up-link signal was lost during a tape-operated TV sequence commanded by DSS 42. Although TV temperatures were near the upper limit, troubleshooting procedures could locate no spacecraft problems or ground transmitter difficulties. A normal up-link search recaptured the spacecraft receiver, and normal TV operations were resumed. The malfunction repeated itself on January 15 during DSS 11 TV operations. Subsequent investigation disclosed that the same TV command tape sequence had been in operation at both stations and that the difficulty had occurred at exactly the same point on each tape.

Alpha scattering operations were resumed immediately after transfer to DSS 61 on January 14. Although solar radiation was now holding the sensor head above its

122°F limit, project scientists continued to operate the instrument in hopes of obtaining the desired 25 hr of data before 07:00 GMT, January 15, the predicted time for Compartment C to reach its 140°F upper limit. The instrument was monitored closely as the sensor head temperature ranged between 137 and 144°F. One of the four proton detectors was turned off to help eliminate excessive heat-generated noise in the telemetry stream. The heat degradation continued to increase, however, and the instrument was turned off at 01:15 GMT, January 15, instead of the predicted 07:00 GMT. Approximately 6.5 hr of usable data had been obtained, increasing lunar sample time to 18.5 hr, but this was still short of the desired 25-hr total.

At approximately 22:45 GMT on January 14, during the DSS 61 view period, the center frequency of the Transmitter A wide-band voltage-controlled crystal oscillator drifted outside the tuning range of the ground receivers. The spacecraft had been operating continuously on Transmitter A since shortly after touchdown, and the drift had been watched closely since first being noted on January 12. After switching to Transmitter B, several frequency checks were performed and Transmitter B was found to be well within the tuning range.

On January 15, science activities were limited to 7- and 8-min periods of operation. Compartments A and B, however, containing the power, radio, and signal processing subsystems and the TV electronics auxiliary, were behaving better than expected. SPAC thermal specialists were able to report that current temperature trends indicated that a total spacecraft shutdown, which had been necessary during the lunar noon at the four *Surveyor* equatorial landing sites, would not be required. Compartment A had been shaded by the A/SPP without special effort. The critical battery temperature had peaked at 112°F, 3 deg below the 115°F maximum, and was now decreasing. Science component temperatures, however, were higher than expected and predictions were for a continued upward trend.

With science activities brought practically to a standstill, time was now available to perform some of the postponed engineering activities. An RF and signal processing test was performed during the DSS 42 view period, and at 00:30 and 04:30 GMT, January 16, attempts to revive *Surveyors I, III, V, and VI* were conducted. Both attempts were unsuccessful. Special telecommunications tests to analyze the up- and down-link signal fluctuations observed following touchdown were also conducted.

Science payload temperatures were monitored closely on January 16 and 17. With the spacecraft able to continue operating through the lunar noon, SPAC and SSAC specialists concentrated on developing operating techniques that would overcome or reduce science temperatures. A/SPP shading for either the alpha scattering sensor head or the surface sampler electronics auxiliary was still not possible and both temperatures continued rising. Thermal predictions for both instruments indicated that temperatures would not return within operating limits before January 20 or 21. Various alternatives, including using the surface sampler to relocate the head, were analyzed but found not significantly helpful. The surface sampler was operated only briefly on both days to adjust shading on the sensor head. Television operations were greatly improved, however, by stepping the A/SPP to provide a prolonged period of shade for the camera before the beginning of the DSS 11 view period. The camera was operated for an initial 40 min on January 16 and for 1 hr 35 min on January 18 before the first cooldown was required. After completing the TV schedule, the A/SPP was again stepped to shade the camera with a pattern that also included Compartment A and Compartment C. A special TV threshold test was also conducted to determine if usable TV could be received with the ground receiver locked on a planar antenna sidelobe. Results were not usable but, if successful, would have broadened A/SPP shading capabilities. In particular, the present unavoidable shading of Compartment A had caused compartment temperatures to drop too low. Thermal loads had to be turned on to bring temperatures up to desirable operating levels.

Although television activities had been significantly assisted during the lunar noon, the SM/SS and ASI temperatures remained out of reach. Lunar sunset was predicted to occur on January 23, making the time left to complete scheduled operations a critical factor. The plan for the ASI called for 8 more hours of data accumulations in its present position, after which the SM/SS would be used to move the sensor head to a new position, placing it over a rock. Obtaining as much alpha scattering data as possible on this first lunar day was a primary objective, since it was unlikely that the instrument would survive the lunar night. On both the *Surveyor V* and *VI* missions, the proton detectors located in the sensor head had been severely damaged by the extremely low night temperatures, and the data collected afterward had been of limited scientific value. At the Lunar Operations Planning Meeting on January 18, SSAC specialists were asked to evaluate the feasibility of relaxing the presently established thermal limits and to determine how long after

sunset the science payload could be operated before the low-temperature limits were reached. The performance history of the alpha scattering sensor head disclosed that definite risk was involved in operating above the present 122°F limit. Surface sampler specialists, however, expressed confidence in operating above present limits, reporting that a laboratory test version of the sampler had been successfully operated over a range of -40 to 212°F. On the low-temperature side, the electronics auxiliaries of both instruments, presently limited to -4°F, could be effectively operated at temperatures down to -40°F.

Except for television, operations on January 18 were minimal. Thermal predictions indicated that alpha scattering operations could be resumed, at the earliest, on January 21. The new temperature limits for the surface sampler would permit SM/SS operations to resume at the beginning of the DSS 11 view period on January 19. The A/SPP shadow pattern for the camera and Compartment C was still unavoidably shading Compartment A and causing temperatures to fall below the desired range. Loads were turned on to raise the compartment temperature and to reduce the battery charge current. Two-way doppler data was gathered by all three stations, and a spacecraft transmitter best-lock frequency test was performed by DSS 61. Also during January 18, SPAC thermal and power personnel evaluated the postsunset power consumption requirements for the spacecraft and the science payload. Predictions were made of the available operating time before the low-temperature operating limits would be reached, and a revised science operations plan was developed. With heaters on, the alpha scattering instrument was expected to remain at or above its -40°F operating limit indefinitely, depending upon available power. SM/SS operations would be limited to motor performance; the motor temperature would reach its -40°F limit 5.5 hr before the predicted lunar sunset. The television camera was expected to have a maximum 27 hr of life after sunset, depending on power consumption and operating mode.

An assessment of the vernier propulsion system on January 18 indicated that fuel and oxidizer pressures were gradually decreasing in accord with decreasing system temperatures. The last relief valve activity had been recorded at 09:00 GMT on January 16. The temperature of vernier engine 3, however, was 274°F, 54 deg above its operating limit. Almost since touchdown, either one or more of the vernier engines had been above the operating temperature limit, precluding any chance of firing

the engines, since A/SPP shading was not possible at the Tycho latitude. At 06:35 GMT on January 19, surface sampler operations were resumed with the electronics auxiliary temperature at 164°F, 6 deg above the previously specified limit. Television camera temperatures were well within limits after shading during the DSS 61 view period, and an initial 92 min of activity was accomplished before the first cooldown was required. A 50% duty cycle was maintained thereafter. As expected, surface sampler operations at the increased temperature went smoothly, and by the end of the DSS 11 activity, the surface sampler electronics auxiliary was back within its normal operating temperature range. During January 20, television temperatures remained within operating limits and TV sequences returned to a normal duty cycle. The alpha scattering sensor head temperature was reducing slowly but was still above its 122°F operating limit during the DSS 11 view period. Surface sampler operations at this time included preparations for moving the sensor head to its second site. The selected rock sample was outboard of the head's present position. The nature of the relocation presented some operational difficulties and 4 hr was allocated to make the move. Additionally, with thermal conditions predicted to be favorable for operating into the lunar night, the operations plan was expanded to include moving the sensor head to a third prepared location which would provide a data sample of subsurface soil. Concurrently during January 20, SPAC power and thermal specialists began preparations for lunar night. Lunar sunset was predicted to occur sometime between 06:00 and 09:30 GMT on January 23, during the DSS 61 view period. Best-lock frequency tests were scheduled for every 5-deg decrease in Compartment A temperature. Landing gear temperatures were analyzed and a time was tentatively established to lock the landing legs. Owing to the effects of extreme cold on the gas-filled shock absorbers, the legs must be locked to prevent collapse of the landing gear when the critical temperatures are reached. (During the *Surveyor V* mission, two landing legs sagged shortly after sunset, indicating that the squib-fired landing gear locks had malfunctioned.)

Television operations were continued during the DSS 42 view period. At 19:00 GMT, both the alpha scattering sensor head and Compartment C were finally within operating limits. The scheduled TV sequences were completed, and at 21:15 GMT the instrument was turned on. Analysis of the initial data accumulations confirmed that the instrument was operating normally, and approximately 2 hr 10 min of data was accumulated

before transfer to DSS 61. An additional 6 hr 40 min of data was accumulated during the DSS 61 view period, completing operations at the original site. After transfer to DSS 11 at 07:30 GMT on January 21, the spacecraft was reconfigured for television, and the surface sampler was activated to move the sensor head to its second site. As anticipated, the move required extensive trial-and-error manipulation and took all of the allotted 4 hr to complete. Analysis of the first data samples at the second site disclosed that the data return was approximately twice that of the first site. This was attributed to the increased surface area of the rock protruding into the sensor head. Scientists estimated that, with the increased data rate, only 11 hr of data would be needed at the second site, making it possible to move the sensor head to its third site during the next DSS 11 view period. Also on January 21, at 05:00 GMT, the first step of the lunar night survival plan was initiated when the Compartment A heater control was turned on to keep the battery temperature from falling below 100°F. Effectively, the survival plan had originally begun shortly after spacecraft touchdown with initial positioning of the solar panel and establishment of a battery charge rate that would leave a full charge in the battery at sunset. With the exception of the flight control system, virtually all spacecraft and science temperatures were now back within operating limits and continuing to move lower.

The solar panel was stepped to optimize the battery charge, and at 15:32 GMT the landing gear lock command was transmitted. A special engineering mechanisms auxiliary test was subsequently conducted to determine if adequate current flow had been available to fire the landing gear lock squibs. Telemetry data indicated that proper current flow was present in the circuit, but the only positive proof that the legs were locked would be spacecraft performance after sunset.

Early on January 22, the propulsion system oxidizer pressure began a series of fluctuations, which were determined to be the result of a small, gaseous oxidizer leak. Evidence of a fuel leak had been noted on January 20, when a rapid cooling of vernier engine 2 from 88 to 0°F occurred during one 4-hr period. The cooling was attributed to fuel vaporization at the fuel shutoff valve poppet. A simultaneous rise in fuel line temperature indicated flow to the engine from the fuel tank. Analysis of the fuel system afterward indicated a leakage rate of about 10 psi/hr. These beginning signs of deterioration of the propulsion system were not unexpected since similar failures had occurred on all previous *Surveyor* missions.

At 09:36 GMT on January 22, the solar panel was again stepped to adjust the battery charge, and additional thermal loads were turned on in Compartment A. At 09:51 the alpha scattering instrument was turned off in preparation for the move to the third site. Only 10 hr of data had been accumulated at the second site but, due to the increased data rate, the sample time was considered to be sufficient. The sensor head and Compartment C heaters were turned on and, at 10:01 GMT, the sensor head was successfully moved to its third site. The initial sample disclosed an intermediate data rate between the first and second sample rates. During the remainder of January 22, surface sampler, TV and alpha scattering operations continued on schedule while preparations were made for lunar night. Updated calculations had narrowed the predicted sunset time to between 08:00 and 09:30 GMT on January 23, but uncertainties in the local terrain made an exact prediction difficult. Therefore, sunset at the spacecraft would be officially determined by absence of sunlight on the camera. Science activities were scheduled to continue for approximately 35 hr after sunset. Based on temperature and power consumption predictions, the first 12 hr would be devoted to TV operations, including 1 hr of SM/SS trenching activity; the next 23 hr would be devoted to alpha scattering operations.

DSS 42 activities on January 22 consisted primarily of television commanding and included two shadow progression sequences, two earth surveys, and a number of command tapes. Transfer to DSS 61 occurred at 02:00 GMT, January 23. Alpha scattering operations were begun shortly before transfer and were interrupted only twice for shadow progression sequences. During the second shadow progression sequence at 05:30 GMT, the light decreased rapidly, indicating that lunar sunset was occurring much earlier than the 08:00 GMT prediction. DSS 61 switched quickly to specially prepared shadow progression command tapes designed to record the changing light effects now moving swiftly across the darkening scene.

Camera sunset (sunlight off the camera) occurred at 06:06 GMT, January 23. Solar panel sunset (zero solar panel output) occurred approximately 18 min later, at 06:24 GMT. Immediately after camera sunset, the camera was positioned to obtain pictures of the solar corona. Between 06:41 and 14:30 GMT, TV sequences of the sun's corona and various other sunset phenomena were alternated with engineering interrogations. Sunlit features on the eastern horizon, some 10 to 25 km away,

were observed for approximately 10 hr after sunset. At times, the glare caused by back-scatter from these features was strong enough to interfere with some of the corona sequences. Some very good pictures of the earth were recorded, and the planet Mercury was photographed.

Also at sunset, Phase II of the lunar night survival plan was put into operation and consisted of the following:

- (1) Battery consumption for postsunset science activities limited to approximately 50 A-hr.
- (2) After completing science activities, operations to consist of alternate standby and interrogation modes to allow compartment temperatures to drop as rapidly as possible. After stabilizing Compartment A and B temperatures near their lower operating limits, operations then to be extended as far into the lunar night as possible in order to minimize the severe cooling period between shutdown and sunrise on the second lunar day.
- (3) Interrogation times during the cooldown to be held to a minimum and to be performed every 4 hr during the first 48 hr, then at 12-hr intervals 48 to 96 hr after sunset, and, finally, once every 24 hr until the remaining battery charge is reduced to 45 A-hr.
- (4) Maintain battery at $+20^{\circ}\text{F}$ and Compartment B at -15 to -20°F after all Compartment A and B thermal switches have opened (effectively disconnecting the conduction paths from the interior of the compartment to the exterior).

Postsunset surface sampler operations were performed satisfactorily during two 35-min operating periods beginning at 07:52 and 12:41 GMT. Activities included trenching and a low-temperature motor torque experiment. Postsunset alpha scattering operations were activated at 13:00 GMT for an initial series of 15-min data accumulations. Temperatures decreased much more rapidly than predicted, however, and by 14:32 GMT the temperature of Compartment C had fallen 9 deg below the -40°F operating limit. Shortly afterward, a definite shift in the received data was noted, which made further operation impractical, and at 15:35 GMT, alpha scattering power and heater current were turned off, ending operations for the first lunar day. Approximately 50 min of postsunset data was obtained during the unexpectedly short operating period, limiting the total operating time

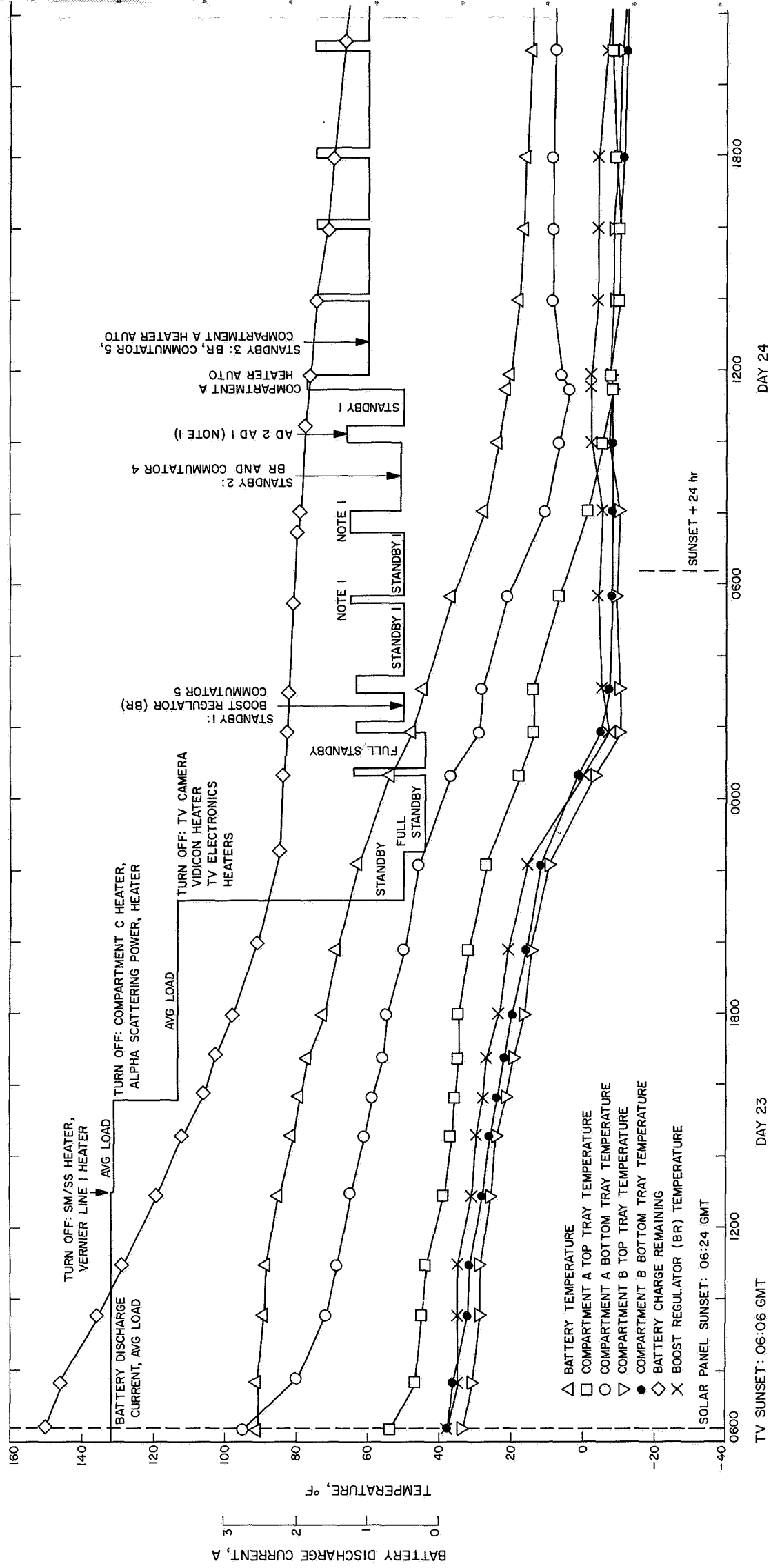
at the third site to 6 hr 49 min. Television sequences were resumed and continued periodically until 21:06 GMT, when TV operations were terminated. Approximately 800 pictures were obtained during the 15 hr of activity after lunar sunset. At 21:21 GMT, the solar panel and planar array were stepped to optimum positions for revival of the spacecraft on the second lunar day. The solar panel was positioned so that charging current would not be generated until 120 hr after sunrise, allowing sufficient time for the battery to warm to its thawing temperature of -40°F , at which point it will receive a charge.

Figure VI-3 shows several key performance parameters during lunar night operations. The data is plotted from shortly after sunset through final spacecraft shutdown.

For the remainder of January 23 and into January 24, the spacecraft was cycled approximately every 2 hr between engineering interrogations and standbys in accordance with the survival plan. Thermal specialists reported that Compartment A and B thermal switches (9 in Compartment A and 6 in Compartment B) were so far opening satisfactorily. At 19:00 GMT, January 23, one out of four telemetered switches in Compartment A and 2 out of 3 telemetered switches in Compartment B had opened. Compartment temperature performance indicated that nearly all of the untelemetered switches had opened. Operations on January 24 consisted of engineering interrogations, adjusting compartment thermal loads, and best-lock frequency checks. By 16:00 GMT, compartment temperatures had begun to level off. The battery discharge rate had been established at 1 A, and approximately 92 A-hr remained in the battery. On January 25, all thermal switches in Compartment B had opened, while two switches remained stuck closed in Compartment A. Compartment thermal loads were adjusted, and standby periods were lengthened to 3- and 4-hr periods. Engineering interrogations also disclosed that the propulsion system was undergoing further degradation. Telemetry indicated further propellant leaks and pressure sensor malfunctions and, by the end of January 25, all propulsion system pressures had decayed to zero.

At 08:06 GMT on January 26, the remaining battery power reached 47 A-hr. Thermal and power management activities were terminated and all nonessential loads were commanded off, placing *Surveyor VII* in full standby. Six interrogations were subsequently conducted on the hour to monitor the decreasing temperature rates.

1c



2c

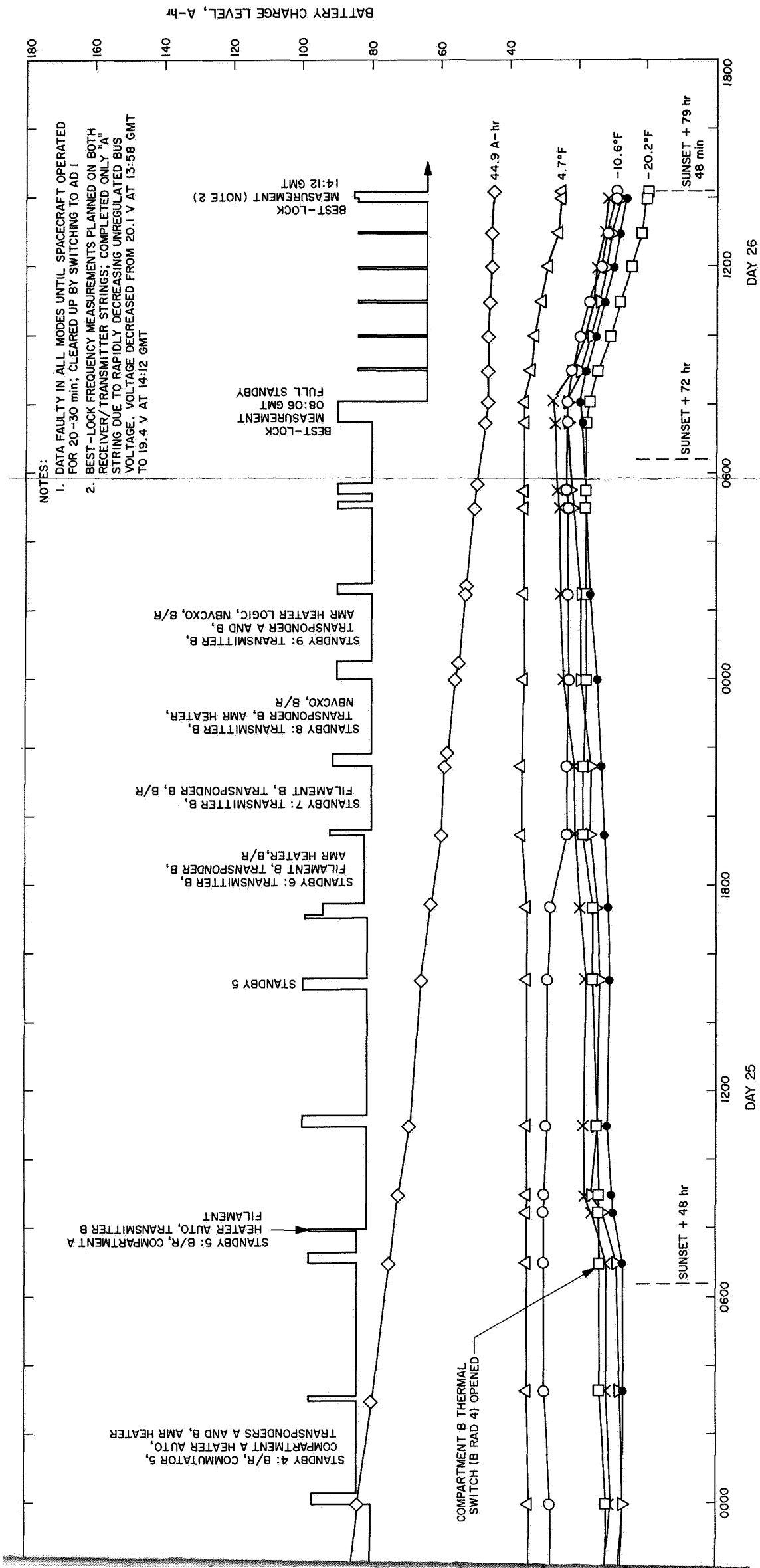


Fig. VI-3. Key spacecraft thermal and power parameters controlled during first lunar night operations before shutdown

During the sixth interrogation, a final best-lock frequency measurement of both receiver/transmitter combinations was initiated, but the rapidly decreasing voltage permitted only one measurement to be completed. Final shutdown was commanded at 14:12 GMT, terminating first lunar day operations 79 hr 48 min after sunset.

8. Second Lunar Day

Attempts to revive *Surveyor VII* on its second lunar day were initiated by DSS 61 at 19:00 GMT, February 12, approximately 132 hr after sunrise at the landing site. The spacecraft responded almost immediately to the first revival command, interrupting plans for a simultaneous attempt to revive *Surveyors V* and *VI*. The signal level was -123.3 dbm, and the initial engineering interrogation found all commutator modes accessible. Lunar noon at this time was approximately two earth days away, and rising temperatures were expected to be a problem almost immediately. The initial engineering assessment disclosed that all essential spacecraft systems were operating normally except for the power system. Battery temperature (45°F) and battery voltage (22 V) were approximately normal, but the battery manifold pressure (normally 15 psi) was reading under 2 psi, most probably due to a cracked or ruptured manifold. Landing Leg 1 had collapsed, giving the spacecraft an 8-deg tilt toward lunar south and away from the earth. All science temperatures were within operating limits except for the alpha scattering sensor head (139 vs 122°F) and the surface sampler electronics (169 vs 158°F). Power system specialists reported that the regulated output current was varying between zero and approximately 2 A, apparently in response to a short. A checkout of various power and heater systems was performed to locate the short, but the results were inconclusive. At 23:14 GMT, the spacecraft was configured for television, but attempts to operate in 600-line high-resolution mode were unsuccessful. Operation in 200-line mode was found to be normal, and six good-quality pictures were received. Subsequent tests located a failure in the 600-line mode horizontal sweep circuit. A check of the alpha scattering instrument disclosed that the proton system was inoperable. The alpha system appeared to be functioning normally although somewhat noisily due to already high sensor head temperature. Television operations were resumed at 03:30 GMT, February 13. After 30 min of activity, telemetry indicated that the battery temperature had risen significantly. At 06:15 GMT, after another period of television activity, the battery temperature was found to have risen to 117°F , 2 deg over its upper operating limit. The solar panel was stepped to reduce the charging cur-

rent, and the spacecraft was routinely commanded to stand by to allow the battery to cool. Coming out of the standby 2 hr and 17 min later, the battery temperature was found to have risen to 156°F , indicating a critical battery problem. The solar panel was stepped to shade Compartment A, but the temperature continued to rise, reaching 175°F at 11:00 GMT. Battery terminal voltage, normally 23 to 24 V, continued to drop during this time, reaching a low of 15.5 V. Battery survival was considered marginal. The solar panel was stepped to increase the charging rate and placed in the most desirable power-producing position in case the battery expired. The exact cause of the battery problem remained unknown but the severity of the symptoms pointed toward a large internal short.

Shortly after the charging current was increased, the battery temperature started downward and the battery terminal voltage started upward. These desirable trends continued for a while and then reversed again. The remainder of February 13 consisted of engineering interrogations and standby periods.

On January 14, a limited science effort was initiated during the DSS 11 view period. Television operations were begun at 03:14 GMT and 39 good-quality 200-line TV pictures were received. Views of Compartments A and B showed everything to be normal, at least on the outside. Pictures were taken of new, nearby surface areas revealed by the spacecraft tilt, and most of a stereo tape sequence was performed. The surface sampler was operated very briefly, responding to one extension command to confirm its survival through the lunar night. The battery continued to perform marginally during these operations, requiring recovery periods of approximately 10 min between each picture. Activities were terminated 10.5 hr later at 13:28 GMT, when battery voltage dropped just under 15 V. The spacecraft was placed in standby to rest until the next DSS 11 view period. During the standby, a 1-hr attempt to revive *Surveyor VI* was commanded without success.

On February 15, the chances for acquiring any more meaningful scientific data were evaluated against the extremely limited capability of the spacecraft. Since the battery had not yet responded to any of the attempts to arrest its deterioration, there was a strong chance of losing the spacecraft at any moment. Both project science and project management agreed that the alpha scattering instrument should continue with first scientific priority. Favorably, power requirements for the instrument were

low and could be met entirely by the solar panel, if necessary. The instrument could not be operated at this time, however, since temperatures were above operating limits due to the lunar noon. The decision by project management was to forego TV and SM/SS activities and to continue with attempts to preserve the spacecraft in favor of the alpha scattering experiment.

Operations during February 15 consisted of experimenting with spacecraft standby time periods and evaluating battery recovery characteristics in order to establish an optimum duty cycle. Battery temperature fluctuated during this time, reaching a high of 180°F early on January 16 before starting downward, and remaining unaffected by changes in the electrical load. The battery charge rate was also uncontrolled, fluctuating between 0.5 and 1.0 A owing to the internal shorting condition.

Toward the end of February 16, experimentation with the duty cycle began to produce some improvement. Fifteen-min standbys were found to provide a maximum battery charge (up to 20 V) with the least increase in battery temperature. The standbys were held to a minimum, however, leaving the spacecraft operating in order to stabilize the battery by balancing the discharge current against the solar panel charging current (essentially no charge, no discharge). The response was a favorable downward trend in temperature. The solar panel was successfully stepped to keep pace with the sun, increasing the current level to 2.97 A.

The battery continued its improving trend until approximately 04:00 GMT, February 17, when the battery output current began a series of fluctuations, indicating increased battery degradation. At 12:40 GMT, the spacecraft was placed in a 15-min standby. Coming out of the standby, A/SPP stepping commands were sent to update the solar panel. The spacecraft power system was unable to support the activity, causing the spacecraft to drop lock with the up-link signal. Contact was reestablished 7 min later, but subsequent attempts to step the solar panel during February 17 were also unsuccessful, con-

firmed that the battery was now unable to support any significant load. With the solar panel immobilized, current to operate the spacecraft would now gradually decrease. At 01:07 GMT, February 18, alpha scattering operations were resumed although the sensor head was still above operating limits. Estimates were that approximately two more earth days of operation were possible before the signal strength would fall below the instrument's minimum operating limit. The incoming alpha system data was still noisy but was expected to improve as the sensor head temperature decreased.

With the spacecraft now powered exclusively by the solar panel, operations continued satisfactorily during February 18 and 19. Various alpha scattering operational configurations were tried in attempts to optimize the received data. Battery temperature gradually decreased; charging current was still applied, but there was no indication of response. On February 19, solar panel current had decreased to 1.81 A. Various electrical configurations were energized to help regulate voltage distribution. The DSS 14 210-ft antenna was activated and tracked in parallel with DSS 11 during the Goldstone view period to help overcome the decreasing down-link signal strength. On January 20, power management tests were performed, resulting in frequent losses of lock. Experimental attempts to command 200-line television and the SM/SS also resulted in loss of lock. At 12:24 GMT, the carrier was again lost immediately after commanding a change in commutator modes. Search sequences were conducted by DSS 11 until 17:50 GMT, when project management ordered that all revival efforts be terminated. DSS 42 was given permission to continue revival attempts on its own, however, and succeeded in regaining the signal at 18:16 GMT. Operations were resumed, consisting primarily of power management to adjust spacecraft loads. At 00:24 GMT, January 21, the spacecraft was lost for the final time after another attempt to command on TV camera power. Revival attempts were continued until 06:48 GMT, when all search activities were ended, terminating the *Surveyor VII* mission.

VII. Flight Path and Events

Surveyor VII was injected first into a parking orbit and then into a lunar transfer trajectory which satisfied the targeting criteria with great accuracy. However, the targeting criteria specified a landing site in Hipparchus, whereas the desired landing site, which was selected subsequent to targeting, was located just north of the crater Tycho. The preflight mission design allocated 12 m/sec of the midcourse capability to achieve this landing site change (approximately 1200 km on the lunar surface) in flight. Actually, an 11.08-m/sec midcourse maneuver was executed at about $L + 17$ hr to achieve the site change and simultaneously compensate for the very small injection errors. It was expected that a second midcourse maneuver at about $L + 47$ hr would be required to achieve the desired landing accuracy of about 10 km, 3σ . However, because the orbit determination accuracy and execution accuracy of the first maneuver was phenomenally good, a second midcourse was not required. Soft landing occurred at 40.92°S latitude and 11.45°W longitude, only 1.69 km from the desired landing site.*

*Landing coordinates based on correlation of *Surveyor* and *Lunar Orbiter* pictures.

A. Prelaunch

Surveyor VI concluded the required direct support to the *Apollo* Program. Consequently, the prime objective of *Surveyor VII* was to obtain data at a site offering the greatest chemical diversity from the maria sites of all previous landings. Selection of the landing site which would be compatible with this objective, while providing an acceptable probability of soft landing, was a difficult and lengthy process. The selection had not yet been made at the time the launch vehicle targeting had to commence. Therefore, targeting was generated for landing sites in Hipparchus and Copernicus craters because these sites were prime candidates and also provided for reaching almost any other site within the communication and incidence angle constraints with a midcourse maneuver of less than 15 m/sec.

The landing site eventually selected for *Surveyor VII* was on the Tycho ejecta or flow blanket at 40.87°S latitude and 11.37°W longitude, north of the crater itself. Since Hipparchus was the closer of the targeted sites, the Hipparchus targeting was selected for the mission, resulting in a nominal midcourse requirement of about 13 m/sec. Furthermore, since the landing site was only

10 km in radius because of the extremely rough surrounding terrain and since the nominal midcourse was fairly large, it was expected that two midcourse maneuvers would be required in order to land within the site. Because maximum landing accuracy would normally be achieved by maximizing the time between the maneuvers, it was planned to execute the first maneuver as early as practicable during the first Goldstone view period and the second as late as practicable during the second Goldstone view period.

The unbraked design impact speed of 2660 m/sec was selected for *Surveyor VII* because it was virtually the maximum speed the spacecraft could tolerate, and therefore yielded the maximum achievable postlanding Goldstone visibility.

B. Launch Phase

The *Surveyor VII* spacecraft was launched from AFETR Launch Pad 36A at Cape Kennedy, Florida, January 7, 1968, using an *Atlas/Centaur* (AC-15) boost vehicle. Liftoff occurred on schedule at 06:30:00.545 GMT. Two seconds after liftoff, the launch vehicle began a 13-sec programmed roll that oriented the vehicle from a pad-aligned azimuth of 105 deg to a launch azimuth of 102.914 deg. At 15 sec, a programmed pitch maneuver was initiated which was completed at *Atlas* booster engine cutoff (BECO). Following booster section jettison, the remainder of the flight to injection was guided by the *Centaur* inertial guidance system. The *Centaur* first burn injected the vehicle into a parking orbit having a 90-nm apogee and 86-nm perigee. The spacecraft was in the earth's shadow during the first 20.3 min of flight, but left the shadow during parking orbit coast and remained in sunlight during the remainder of the flight. After a 22.4-min coast, the *Centaur* burned a second time to inject the *Surveyor VII* spacecraft into the desired lunar transfer trajectory. All event times for the launch phase were close to nominal. The launch phase sequence is discussed in greater detail in Section III, and actual event times for all phases of the mission are summarized in Table A-1 of Appendix A.

C. Pre-midcourse Cruise Phase

Separation of *Surveyor VII* from *Centaur* occurred at 07:05:16 GMT on January 7, 1968, at an approximate geocentric latitude and longitude of -24 and 26 deg, respectively. Automatic sun acquisition began about

1 min after separation and was completed after a maneuver of -224 deg roll and $+37$ deg yaw.

Predictions indicated *Surveyor VII* would rise over the DSS 42 horizon at $L + 00:50:05$. DSS 42 received good one-way data at predicted rise $+ 21$ sec and good two-way data at rise $+ 7$ min, 58 sec. This acceptable, but relatively slow, two-way acquisition time can be partially attributed to the comparatively slow ascent of the spacecraft above the horizon. Acquisition procedure prohibits turning on the transmitter prior to a 10-deg elevation over the local horizon. This can account for as much as 2 min in this type of acquisition. Taking this factor into consideration, the acquisition compares reasonably with past missions.

A plot of the *Centaur* and *Surveyor VII* trajectories, projected on the earth's equatorial plane, is provided in Fig. VII-1. The earth track traced by *Surveyor VII* appears in Fig. VII-2. Specific events such as sun and Canopus acquisition and rise and set times for DSIF stations are also noted.

Prior to Canopus acquisition, the spacecraft was rolled to generate a star map. Then Canopus was acquired at $L + 08:17$ with a net roll of 267 deg. In normal cruise mode, the spacecraft minus Z axis is aligned to the sun and the minus X axis to the projection of Canopus on the spacecraft X - Y plane.

From the time of two-way acquisition by DSS 42 until approximately 40 min before retro ignition, the DSN tracked the *Surveyor VII* spacecraft in the two-way mode and, with minor exceptions, returned extremely high-quality two-way doppler data. All four DSIF stations supporting *Surveyor VII* (DSS 11, 42, 51, and 61) provided usable data during the pre-midcourse phase of the flight. Two-way doppler was also obtained during the midcourse maneuver.

All participating DSIF stations were equipped with doppler resolvers, which resulted in a reduction in the standard deviation of the doppler data (60-sec samples) from a preresolver level of approximately 0.008 to about 0.002 Hz—a reduction by a factor of 4. This did not produce a significant decrease in orbit determination uncertainties because these uncertainties are dominated by other error sources. The only significant losses of good two-way doppler data occurred during the first passes over DSS 51 and DSS 11. DSS 51 lost approximately $\frac{1}{2}$ hr of good two-way doppler at the start of its

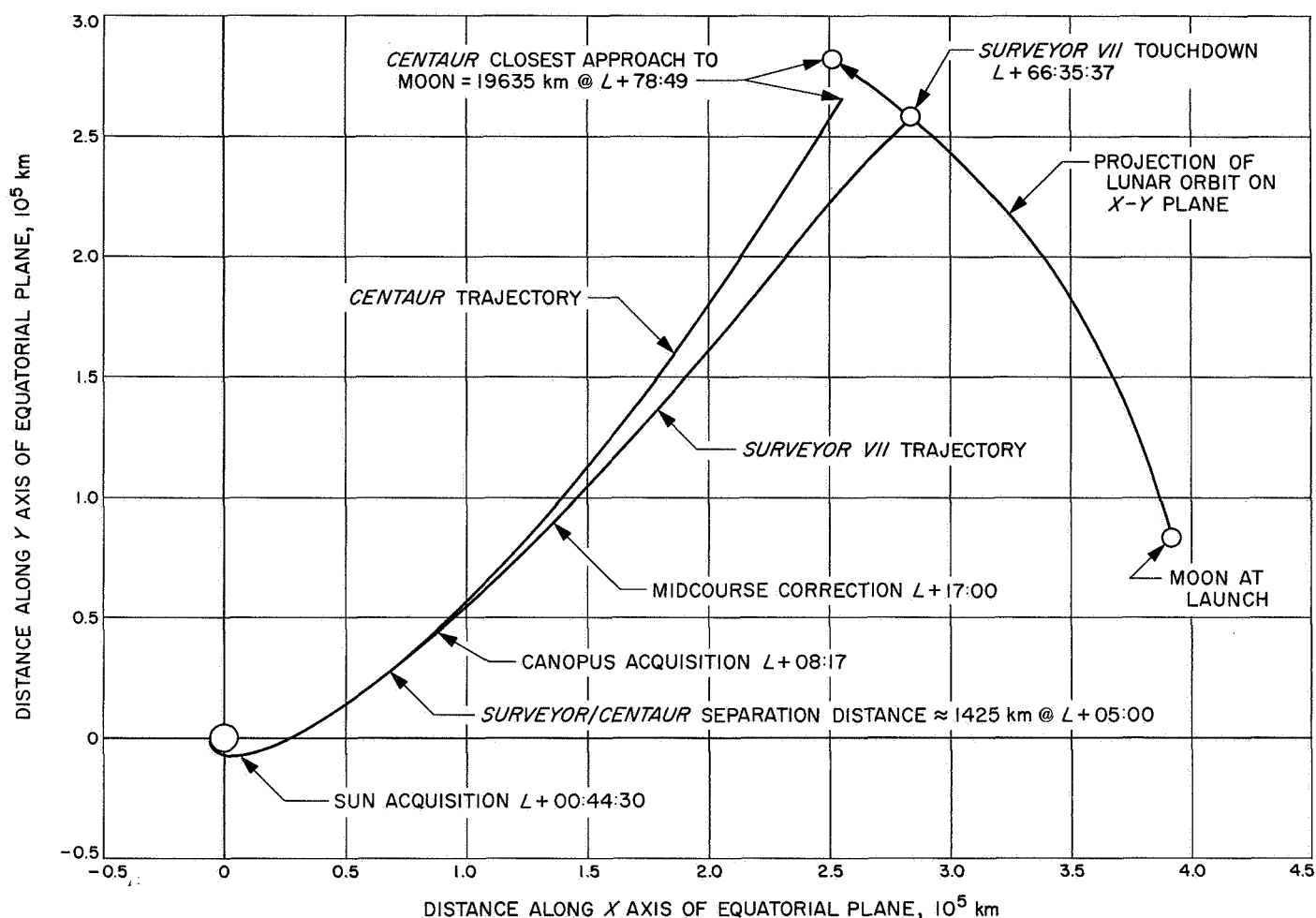


Fig. VII-1. Surveyor and Centaur trajectories in earth's equatorial plane

first pass because of a faulty frequency shifter unit; the problem was eliminated by replacing the unit. DSS 11 lost 30 min of doppler resolver data during the midcourse maneuver (although the basic two-way doppler data was not affected) because of a misadjusted potentiometer in the doppler resolver counter. The problem was eliminated by correctly adjusting the potentiometer. However, DSS 14 made the same error on its third pass. All two-way tracking data taken during the *Surveyor VII* mission was computer-monitored in near-real-time, resulting in the timely discovery of the doppler data problems at DSS 51 and DSS 11.

As shown in Fig. VII-3, the current best estimate of the uncorrected, unbraked impact point is in the central area of Hipparchus at selenographic coordinates of 6.05° S latitude and 5.39° E longitude. The target point was 4.95° S latitude and 3.88° E longitude. The two

points are approximately 77 km (48 miles) apart on the surface of the moon.

A few selected pre-midcourse orbit computations mapped to the moon are also shown in Fig. VII-3. The numerical data for these selected pre-midcourse computations are presented in Table VII-1. Included are the results of the orbit determinations from the Real Time Computer System (RTCS), Cape Kennedy, which were obtained at $L + 00:40$ and $L + 01:20$.

The customary initial SFOF orbit estimate based on AFETR data was computed for *Surveyor VII* using seven points of range and angle data from Pretoria. This estimate indicated a nominal launch, which would result in a lunar encounter without a midcourse correction. The first SFOF estimate of the spacecraft orbit (PROR YA), based on DSS data only, was obtained at $L + 01:50$,

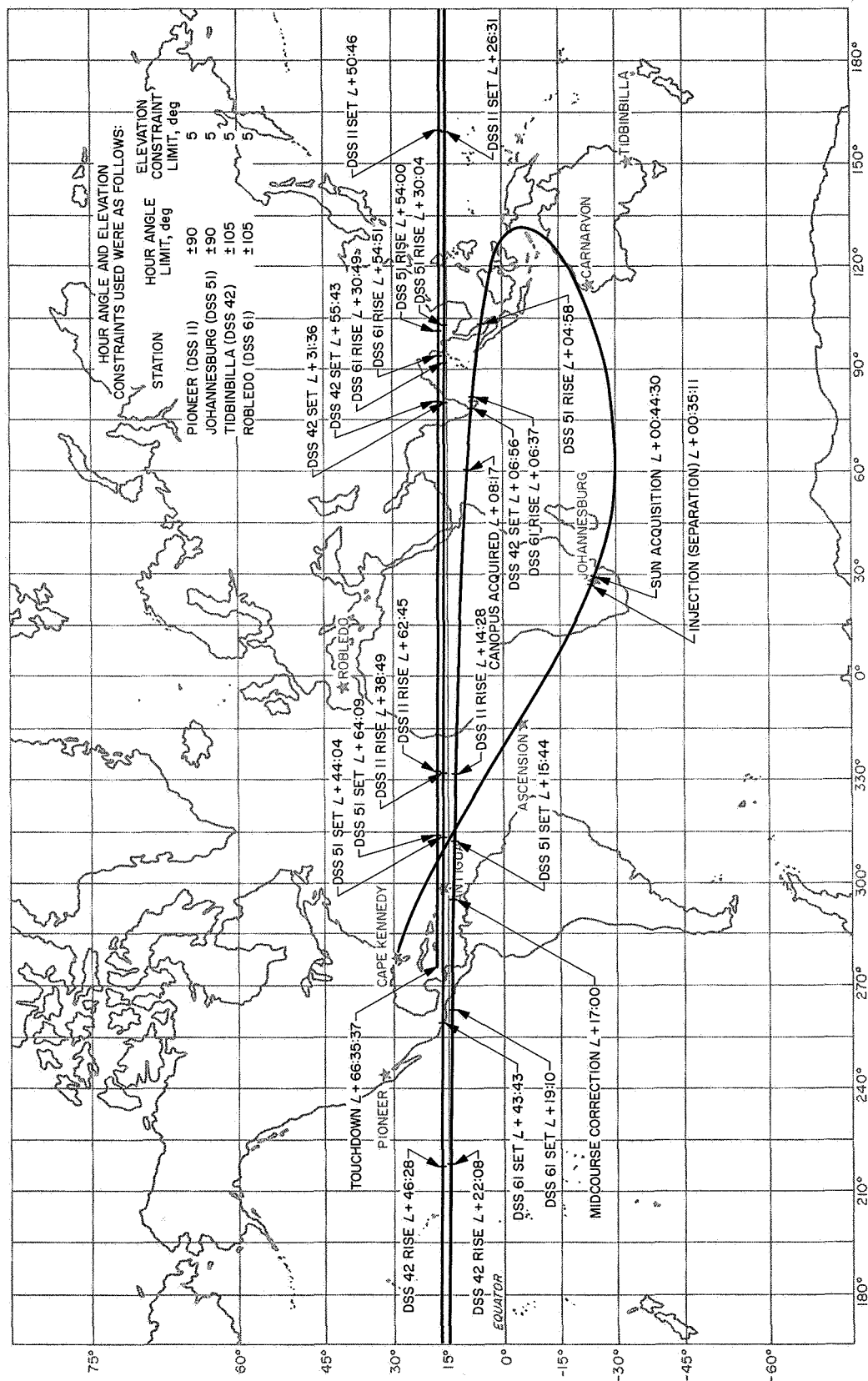


Fig. VII-2. Surveyor VII earth track

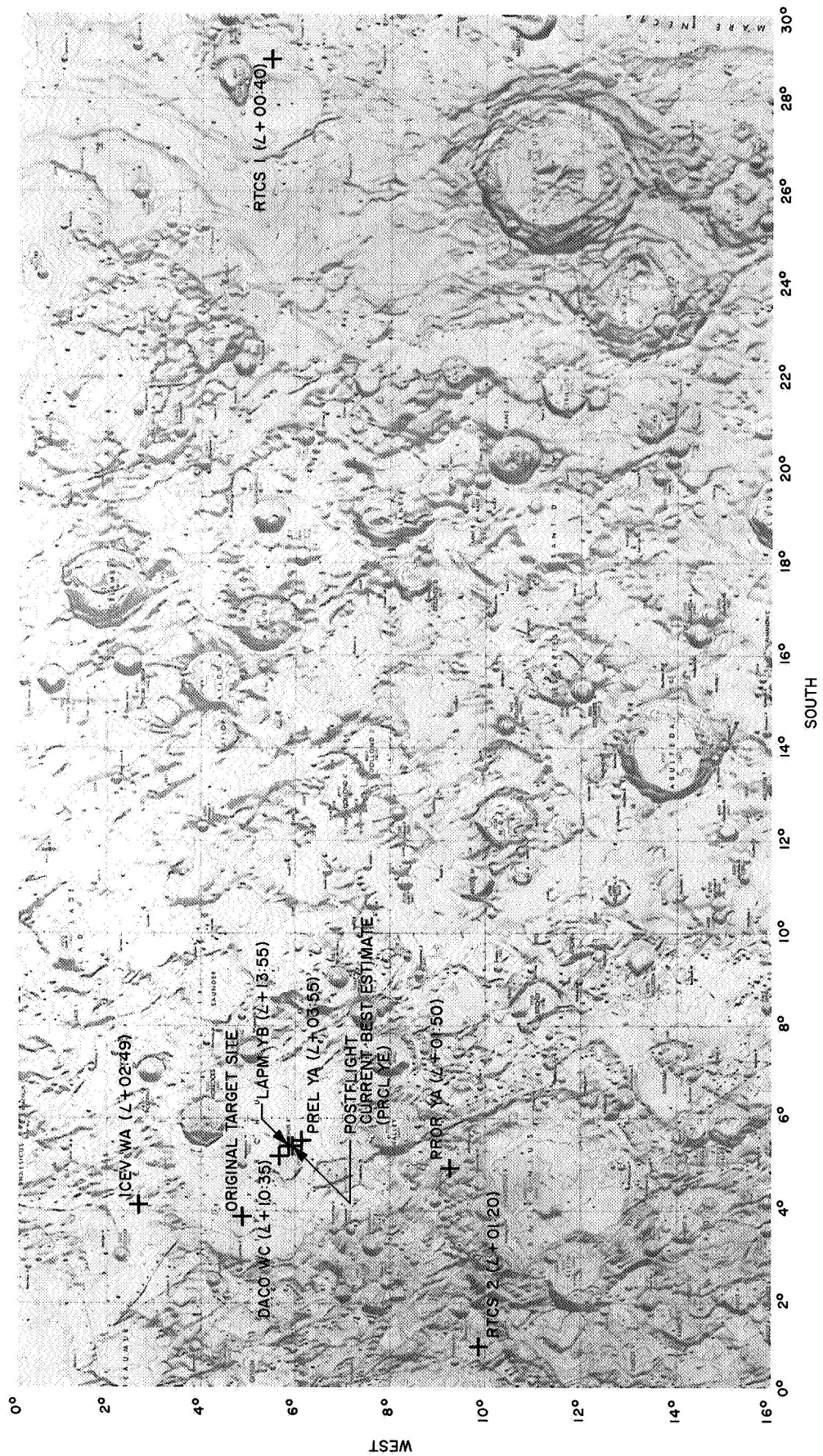


Fig. VII-3. Computed Surveyor VII pre-midcourse unbraked impact locations

Table VII-1. Surveyor VII encounter conditions based on selected pre-midcourse orbit determinations

Orbit identification	Time computation completed (from liftoff)	Target statistics										Unbraked impact conditions			Data used
		B, km	B • TT, km	B • RT, km	TL, hr	SMAA (1 σ), km	SMIA (1 σ), km	THETA, deg	σ_{π} IMPACT (1 σ), sec	PHIP 99, deg	SVFIX R (1 σ), m/sec	Lat, deg	Long, deg	GMT January 10, 1968	
RTCS 1	00:40	2947.30	2926.51	349.46	66.57							-5.789	28.814	01:39:48.4	AFETR (Pretoria) angular and range
SFOF-ETR	01:19	2040.01	1993.36	433.77	65.94	1625.89	125.54	178.00	3397.35	134.82	0.0101	-7.414	4.389	00:58:08.146	AFETR (Pretoria) angular and range
RTCS 2	01:20	1927.84	1847.37	551.16	65.18							-9.738	1.024	01:00:54.2	DSS 42 angular and two-way doppler
PROR YA	01:50	2077.98	2009.10	530.61	65.61	619.91	117.40	93.01	234.58	17.355	1.0245	-9.316	4.910	01:01:11.189	DSS 42 angular and two-way doppler
ICEV WA	02:49	2008.73	1999.05	196.91	65.65	84.33	63.17	133.19	16.862	1.783	0.6134	-2.755	4.109	01:03:16.218	DSS 42 angular and two-way doppler
PREL YA	03:55	2081.80	2048.16	372.79	65.64	1628.2	117.6	127.73	103.90	31.65	0.8495	-6.206	5.511	01:02:52.683	DSS 42 two-way doppler
DACO WC	10:35	2067.48	2037.30	352.00	65.64	21.954	4.516	120.68	2.1188	0.43761	0.6112	-5.798	5.212	01:02:54.784	DSS 42, 51, and 61 two-way doppler
NOMA YC	19:16	2078.19	2045.94	364.73	65.64	34.684	16.420	115.65	5.4599	0.74416	0.6114	-6.048	5.444	01:02:53.124	DSS 42, 51, and 61 two-way doppler
LAPM YB ^a	13:55	2075.45	2044.16	359.04	65.64	39.97	16.66	112.71	5.6303	0.81352	0.6115	-5.936	5.392	01:02:53.534	DSS 42, 51, and 61 two-way doppler
PRCL YE ^b	20:26	2076.17	2043.84	364.94	65.64	8.258	2.414	101.72	0.86785	0.1482	0.6111	-6.052	5.393	01:02:53.103	DSS 11, 42, 51, and 61 two-way doppler
^a Orbit used for midcourse computations. ^b Current best estimate. SMAA semimajor axis of 1 σ dispersion ellipse. SMIA semiminor axis of 1 σ dispersion ellipse. THETA orientation angle of 1 σ dispersion ellipse measured counter clockwise from TT axis B-plane. σ_{π} IMPACT 1 σ uncertainty in predicted unbraked impact time.															
PHIP 99 99% velocity vector pointing error. SVFIX 1 σ uncertainty in magnitude of velocity vector at unbraked impact. TL flight time from injection.															

based on approximately 17 min of two-way doppler and angle (HA-DEC) data from DSS 42. When mapped to the moon, this orbit solution indicated that the midcourse correction required to achieve encounter at the desired aim point near the crater Tycho was well within the nominal midcourse correction capability. These results were further verified by the second (ICEV) and third (PREL) orbit computations completed at $L + 02:49$ and $L + 03:55$, respectively.

When sufficient two-way doppler data had been received to compute a "doppler only" orbit solution, the angle data was deleted. This was first accomplished in the PREL YA orbit computation, which utilized approximately 2 hr and 8 min of two-way doppler data from DSS 42. Removing the angle data from the solution resulted in a change of approximately 45 km in B•TT and 174 km in B•RT* when the solution was mapped to lunar encounter, showing that the early angle data was biased with respect to the doppler data.

During the data consistency (DACO) and nominal maneuver (NOMA) orbit computation periods, 11 orbit solutions were computed with various combinations of two-way doppler data from DSS 42, 51, and 61. During this period, the first data from DSS 61 were received. It was first felt that either DSS 61 or DSS 51 data were biased. However, deleting either station from the orbit solution did not change the orbit estimate significantly. There is some problem with the pre-midcourse data which made it difficult to fit all the data together. However, isolation of this problem remains for postflight analysis.

In order to minimize the orbit determination (OD) uncertainties for the planned second midcourse maneuver, it was decided to perform the first maneuver as early as practical ($L + 17$ hr) during the first Goldstone view period. This forced the LAPM orbit solution back in time so that DSS 11 data was not used in the solution (LAPM YB) for the midcourse computations. The LAPM YB orbit solution was computed using all the two-way doppler data available up to 3 hr and 49 min before the midcourse. When mapped to the moon, this solution indicated an unbraked impact point at 5.936°S latitude and 5.392°E longitude. The last orbit solution (LAPM YC) computed during the LAPM orbit computa-

tion period was the first solution to utilize data from DSS 11, which seemed to be consistent with the other data.

For the current best estimate of the spacecraft pre-maneuver orbit (PRCL YE), all usable data from DSS 11, 42, 51, and 61, taken from initial DSS acquisition to the start of the midcourse maneuver, was employed.

D. Midcourse Maneuver Phase

The *Surveyor VII* midcourse correction, computed to enable the spacecraft to soft-land at the desired landing site of 40.87°S latitude and 11.37°W longitude was 11.08 m/sec. This correction was executed upon ground command at 23:30 GMT on January 7, 1968. The resulting soft-landing site is estimated (based on correlation of *Surveyor* and *Lunar Orbiter* pictures) to be at 40.92°S latitude and 11.45°W longitude, only 1.69 km from the desired site. Figure VII-4 shows the final aim point, the estimated soft-landing site, and the associated dispersions. The small ellipse is centered on the landing site based on orbit determination and represents the 3σ OD uncertainties in touchdown location based on the current best estimate of the postmaneuver orbit. The 99% midcourse dispersions are shown as an ellipse on the lunar surface with a semimajor axis of 75 km and a semiminor axis of 25 km, oriented 57 deg south of east. The unusually large size of this dispersion ellipse was due primarily to large uncertainties in the pre-midcourse orbit, which resulted from difficulties in fitting all the available data. However, since it was expected that a second midcourse would be required even for average first midcourse dispersions, the large dispersions were not of great concern except to the extent that they indicated the possibility of similar difficulties at the second midcourse.

The maximum midcourse correction capability, as a function of the unbraked impact speed, is shown in Fig. VII-5. Typical 3σ *Centaur* injection guidance dispersions and the effective lunar radius are also shown. The midcourse capability contours are in the conventional R-S-T coordinate system.

The maneuver execution time of 16.41 hr after injection was chosen to allow: (1) sufficient pre-midcourse tracking time to accurately determine the orbit, (2) sufficient post-midcourse tracking time to provide the required accuracy in the event a second midcourse was required, and (3) performance of the corrections during the Goldstone view period. Goldstone viewed

*Kisner, W. A., *A Method of Describing Miss Distances for Lunar and Interplanetary Trajectories*, External Publication 674, Jet Propulsion Laboratory, Pasadena, August 1, 1959.

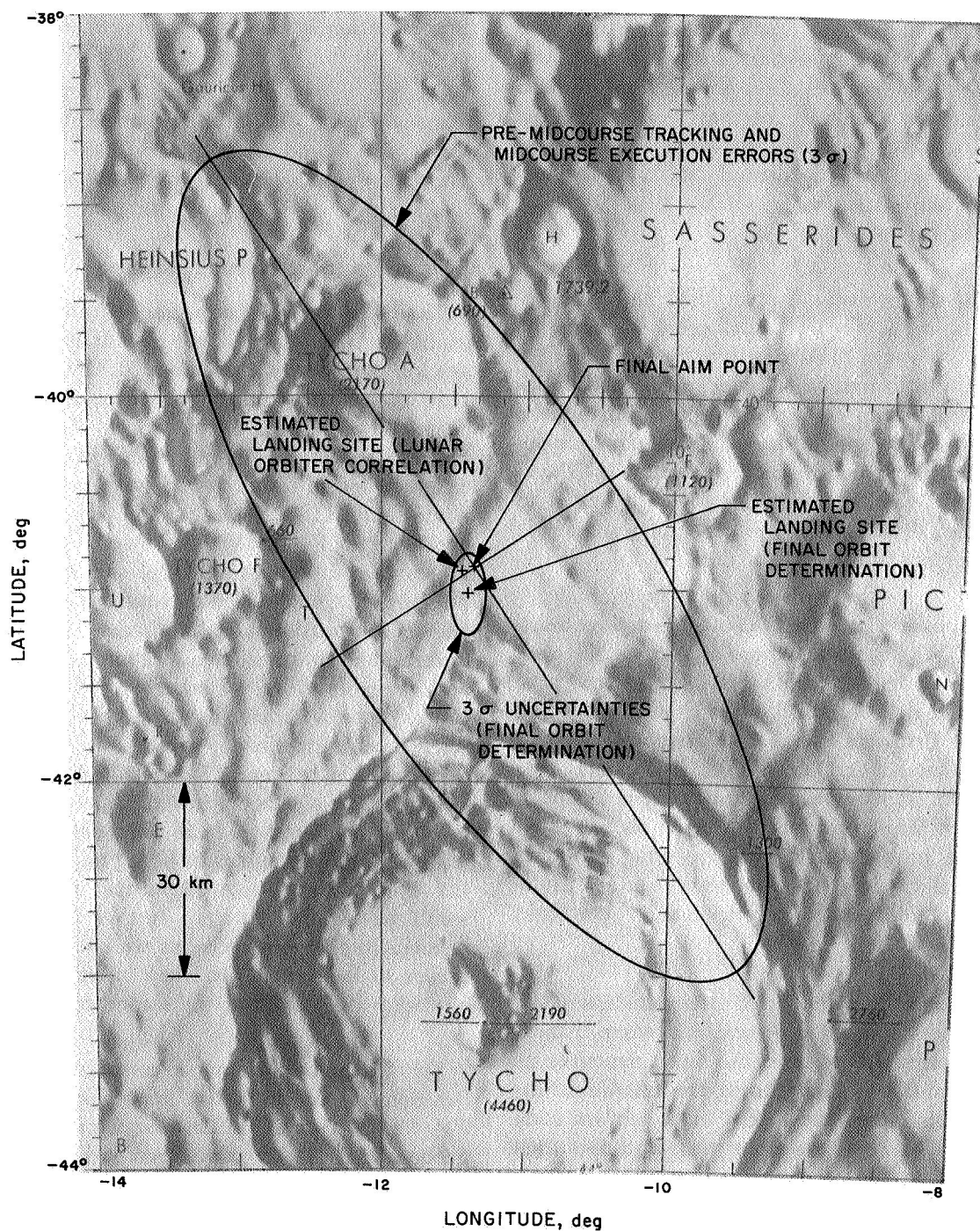


Fig. VII-4. Surveyor VII landing location

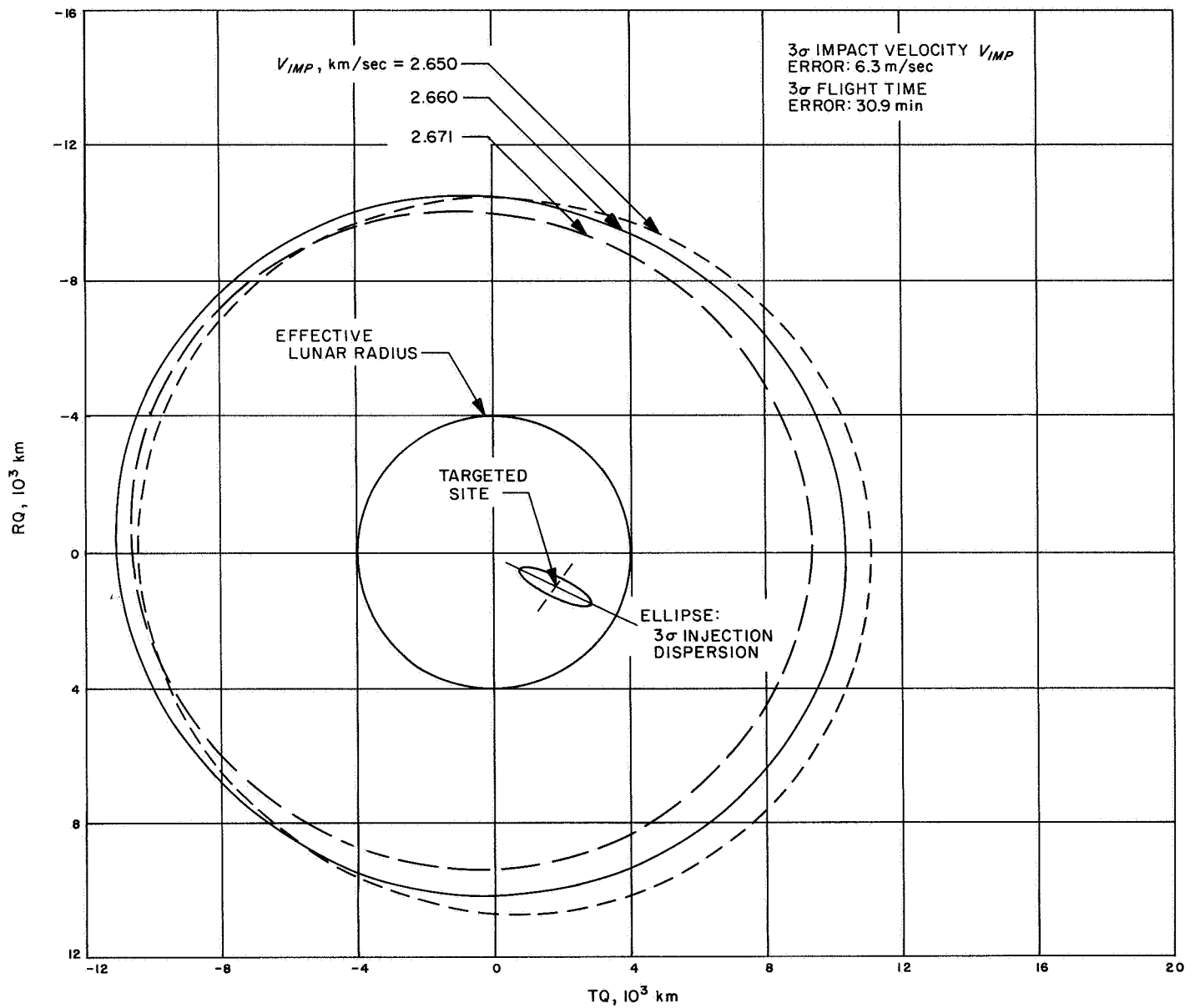


Fig. VII-5. Midcourse correction capability contours (for a correction 20 hr after injection)

Surveyor VII for about 32 min pre-midcourse and about 9.5 hr post-midcourse.

The required velocity component in the critical plane, to correct "miss only," was 11.05 m/sec. The noncritical direction component was +0.8 m/sec and was selected to minimize the maneuver timing error. By adjusting the noncritical direction component, the computed engine burn time was varied to coincide with an exact commandable quantity. The resulting total delta velocity was 11.08 m/sec. Figure VII-6 shows the possible flight times, burnout velocities, propellant margin, and landing site dispersions for the range of available noncritical component velocity corrections.

If the maneuver strategy had been to correct the trajectory at 20 hr after injection to the prelaunch target point in Hipparchus, then the "miss-only" correction would have been 0.463 m/sec. The corresponding "miss-plus-time-of-flight" correction would have been 1.18 m/sec. Both are remarkably small values.

The predicted results of the selected midcourse correction and other alternatives considered are given in Table VII-2. The possibility of not performing a midcourse correction was eliminated because of the prime objective to land in the Tycho blanket area. Execution

of a single midcourse correction approximately 47 hr after injection during the second Goldstone pass was precluded because the desired landing accuracy could not be achieved. Therefore, it was decided to execute a correction during the first Goldstone pass to be followed by a second correction, if necessary, during the second Goldstone pass. This was the nominal prelaunch mission plan.

Orbit determination estimates of the landing site following the first midcourse were closely clustered approximately 3 km from the midcourse aiming point. The uncertainties associated with these estimates indicated a 10% probability of landing in the very hazardous terrain surrounding the desired site. However, these uncertainties were judged to be overly conservative based on the extreme consistency of the orbit estimates. Furthermore, execution of a second correction presented a significant probability (~20%) of degrading the landing accuracy in addition to the risk associated with system reliability. Consequently, it was decided not to execute a second correction.

An analysis was made of eight pairs of pre-midcourse attitude rotations, any pair of which would have correctly oriented the spacecraft for the midcourse velocity correction. A combination of -3.20 deg roll and

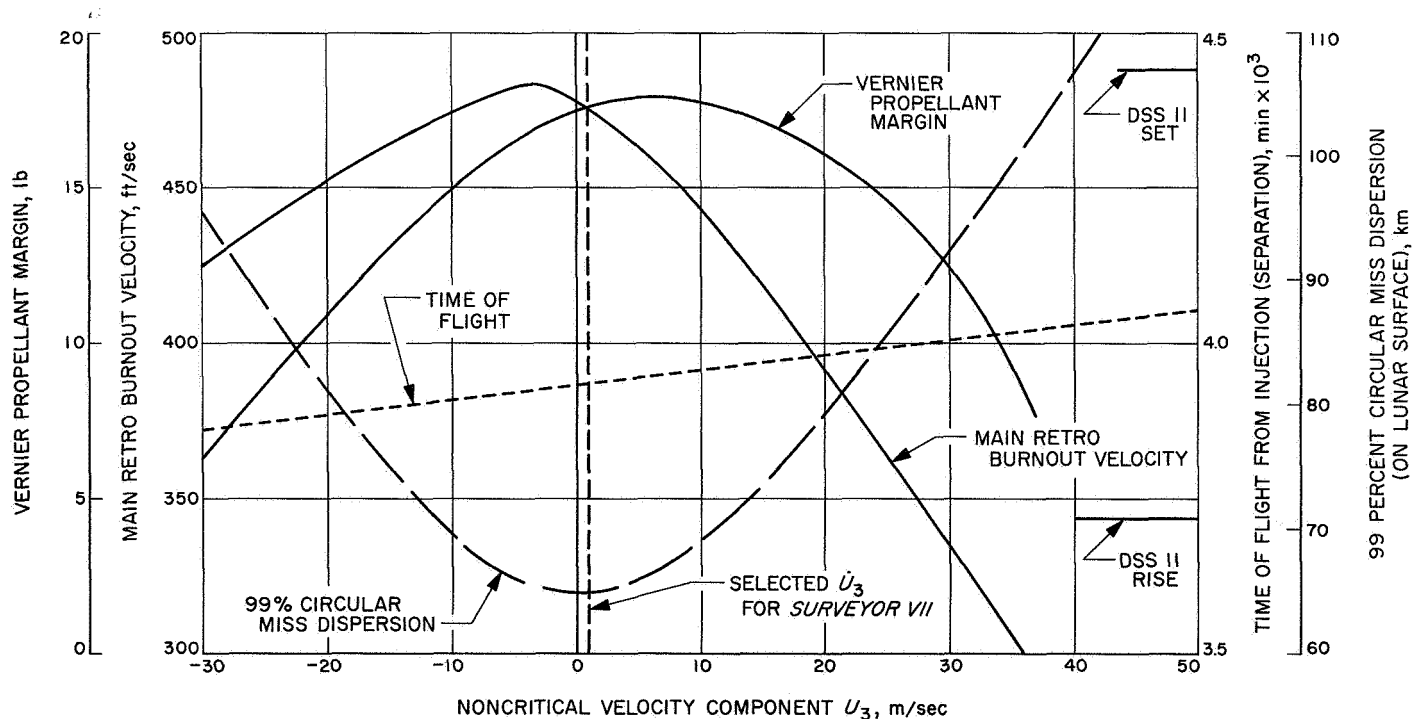


Fig. VII-6. Effect of noncritical component of midcourse velocity correction on terminal descent parameters

Table VII-2. Midcourse maneuver alternatives

Parameter	Midcourse selected with expectation of executing a second midcourse	Alternate considerations	
		No midcourse	One midcourse during second Goldstone pass
Midcourse parameters			
Velocity magnitude, m/sec	11.08		27.26
Critical component, m/sec	11.05		27.26
Noncritical component, m/sec	+0.8		0.0
Propellant required, lb	9.50		23.38
First rotation, roll, deg	-3.20		-5.13
Second rotation, yaw, deg	117.03		119.12
Engine burn time, sec	11.350		27.925
Landing site dispersions (midcourse mechanization plus tracking), 3σ			
Semimajor axis, km	75		17.8
Seminor axis, km	25		13.5
Ellipse inclination (positive from TQ toward RQ), deg	57		74
Terminal parameters			
Aim point			
Latitude, deg south	41.870	6.159	41.870
Longitude, deg east	348.630	5.434	348.630
Incidence angle, deg	35.9	32.6	36.3
Impact speed, m/sec	2660.6	2660.2	2660.3
Burnout velocity, ft/sec	477.2	525.8	362.3
Burnout altitude, ft	38736.4	40476.6	31387.4
Propellant margin, lb	24.5	29.2	22.4
Descent propellant, lb	139.8	144.7	128.1
Descent time, sec	192.5	193.1	181.6
First rotation, yaw, deg	80.5		81.3
Second rotation, pitch, deg	96.0		95.5
Third rotation, roll, deg	-16.5		-16.9
Ignition delay, sec	2.76		4.05

+117.03 deg yaw using Omniantenna B was chosen because it maximized the probability of mission success by providing maximum sun-lock time and continuous high antenna gain without requiring antenna switching. The selected attitude rotations were compensated to achieve

alignment of the actual thrust axis (determined prior to launch) with the desired midcourse vector. Compensations for gyro drift were not included in the final rotations since the drift rates were too small to contribute significantly to landing site error. However, the attitude rotations were initiated at limit-cycle nulls in order to reduce pointing errors.

E. Post-midcourse Cruise Phase

The results of a few selected post-midcourse orbit computations mapped to the moon are presented in Table VII-3. The first post-midcourse orbit computations were completed approximately 10 hr after the midcourse correction. For the final orbit computation (IPOM WF) during this period, approximately 5 hr and 38 min of DSS 11 data and 2 hr and 50 min of DSS 42 two-way doppler data was used. When the IPOM WF solution was mapped to target, it indicated an unbraked impact point of 41.079°S latitude and 348.697°E longitude, approximately 3.2 km from the midcourse aim point. The final terminal computations were based on the 5POM YD orbit solution.

Both pre- and post-midcourse injection and terminal conditions are presented in Table VII-4. It should be noted that the post-midcourse terminal conditions presented in Table VII-4 do not match the conditions shown in Table VII-3 very closely. This is due to use of estimated gas-jet perturbing forces in the orbit determination program to give a better fit of the data. The trajectory program used to generate the data of Table VII-4 cannot simulate these perturbations.

F. Terminal Phase

A terminal attitude maneuver consisting of +80.50 deg roll, +96.04 deg yaw, and -16.50 deg roll was selected using Omniantenna B. The selection of this combination was based on an assessment of all possible maneuvers to provide satisfactory telecommunication performance during the terminal maneuver and terminal descent phases.

Roll attitude of the spacecraft at main retro ignition was dictated by a determination to (1) maximize margins against RADVS beam rejects, (2) refrain from roll attitudes for which RADVS scintillation problems were possible, and (3) obtain a favorable touchdown orientation for postlanding operations. The final roll maneuver was selected so that, at touchdown, the projection of the sun

Table VII-3. Surveyor VII encounter conditions based on selected post-midcourse orbit determinations

Orbit identification	Time computation completed (from liftoff)	Target statistics								Unbraked impact conditions				Data used	
		B, km	B • TT, km	B • RT, km	TL, hr	SMAA (1 σ), km	SMIA (1 σ), km	THETA, deg	σ_T IMPACT (1 σ), sec	PHIP 99, deg	SVFIX R (1 σ), m/sec	Lat, deg	Long, deg		GMT January 10, 1968
1POM WF	26:17	2259.11	1033.92	2008.63	49.32	139.33	16.70	66.68	41.342	2.513	0.6251	-41.079	348.697	01:02:53.240	DSS 11 and 42 two-way doppler
2POM WA	27:10	2259.53	1034.42	2008.85	49.32	138.73	14.17	66.73	35.792	2.271	0.6215	-41.084	348.71	01:02:52.028	DSS 11 and 42 two-way doppler
3POM YD	33:55	2260.33	1036.92	2008.46	49.32	21.188	3.537	59.72	9.6952	0.4145	0.6115	-41.071	348.78	01:02:45.525	DSS 11, 42, 51, and 61 two-way doppler
4POM WB	40:51	2264.23	1036.02	2013.31	49.32	15.706	2.731	59.20	7.4480	0.31843	0.6113	-41.186	348.80	01:02:46.584	DSS 11, 42, 51, and 61 two-way doppler
4POM WD	43:09	2272.78	1041.74	2019.98	49.32	30.714	19.716	91.74	11.716	0.52075	0.6169	-41.34	349.02	01:02:48.422	DSS 11, 42, 51, and 61 two-way doppler
4POM YN	60:33	2265.91	1036.67	2014.86	49.32	7.414	2.054	74.63	2.6573	0.09508	0.6111	-41.222	348.83	01:02:46.578	DSS 11, 42, 51, and 61 two-way doppler
5POM YD ^a	63:09	2263.62	1036.74	2012.25	49.32	11.68	5.474	68.22	3.3393	0.14545	0.6118	-41.161	348.81	01:02:47.393	DSS 11, 42, 51, and 61 two-way doppler
FINAL WA	64.48	2265.97	1034.72	2015.93	5.720	1.8401	0.8584	88.71	0.72792	2.1032	0.6110	-41.249	348.79	01:02:48.315	DSS 11 and 51 two-way doppler
FINAL YC	65:20	2264.95	1034.49	2014.90	5.720	1.2657	0.6435	63.98	0.52028	0.02713	0.6110	-41.225	348.77	01:02:47.92	DSS 11 and 51 two-way doppler
FINAL WE	65:58	2264.77	1034.44	2014.73	5.720	1.1963	0.4738	55.37	0.48781	0.02591	0.6110	-41.221	348.77	01:02:47.888	DSS 11 and 51 two-way doppler
PTD - 1	Postlanding	2265.09	1034.81	2014.89	49.32	3.808	1.44	28.13	0.84805	0.06407	0.6112	-41.224	348.78	01:02:48.056	DSS 11, 42, 51 and 61 two-way doppler

^aOrbit used for terminal maneuver computations.
^bCurrent best estimate.

^aOrbit used for terminal maneuver computations.

^bCurrent best estimate.

Table VII-4. Injection and terminal conditions for pre- and post-midcourse trajectories

Pre-midcourse injection conditions, January 7, 1968, 07:27:00.000 GMT							
Coordinate system	Inertial Cartesian	X = 9448.6719 km	Y = -6127.0318 km	Z = -4457.8123 km	DX = 7.9198726 km/sec	DY = 1.4086439 km/sec	DZ = 0.10226823 km/sec
	Inertial spherical	RAD = 12111.565 km	DEC = -21.596172 deg	RA = 327.03843 deg	VI = 8.0448192 km/sec	PTI = 42.435593 deg	AZI = 67.639206 deg
	Earth-fixed spherical	RAD = 12111.565 km	LAT = -21.596173 deg	LON = 109.34894 deg	VE = 7.5083482 km/sec	PTE = 46.300454 deg	AZE = 64.186438 deg
	Orbital elements	C3 = -1.1024780 km ² /sec ²	ECC = 0.98189491	INC = 30.696195 deg	TA = 85.844692 deg	LAN = 8.8581949 deg	APF = 228.01784 deg
Pre-midcourse encounter conditions, January 10, 1968, 01:02:53.121 GMT							
Coordinate system	Selenocentric	RAD = 1736.5999 km	LAT = -6.0521469 deg	LON = 5.3931117 deg	VP = 2.6577089 km/sec	PTP = -57.571363 deg	AZP = 98.303678 deg
	Miss parameter earth equator	BTQ = 1761.5232 km	BRQ = 1098.8838 km	B = 2076.1767 km			
	Miss parameter moon equator	BTT = 2043.8528 km	BRT = 364.94286 km	B = 2076.1785 km			
Post-midcourse injection conditions, January 7, 1968, 23:45:00.000 GMT							
Coordinate system	Inertial Cartesian	X = 137530.65 km	Y = 91469.540 km	Z = 41087.171 km	DX = 1.2431288 km/sec	DY = 1.2850196 km/sec	DZ = 0.62826964 km/sec
	Inertial spherical	RAD = 170204.32 km	DEC = 13.969131 deg	RA = 33.627272 deg	VI = 1.8950903 km/sec	PTI = 77.029020 deg	AZI = 63.765732 deg
	Earth-fixed spherical	RAD = 170204.32 km	LAT = 13.969131 deg	LON = 290.76837 deg	VE = 1.1809685 km/sec	PTE = 89.965304 deg	AZE = 270.92365 deg
	Orbital elements	C3 = -1.0924297 km ² /sec ²	ECC = 0.98181463	INC = 29.487126 deg	TA = 160.02306 deg	LAN = 7.5294431 deg	APF = 229.34520 deg
Post-midcourse encounter conditions, January 10, 1968, 01:02:47.892 GMT							
Coordinate system	Selenocentric	RAD = 1736.5999 km	LAT = -41.230615 deg	LON = 348.84419 deg	VP = 2.6593373 km/sec	PTP = -54.085985 deg	AZP = 142.65023 deg
	Miss parameter earth equator	BTQ = 213.80258 km	BRQ = 2256.3335 km	B = 2266.4406 km			
	Miss parameter moon equator	BTT = 1037.0671 km	BRT = 2015.2543 km	B = 2266.4418 km			

in the spacecraft X-Y plane would be 15 deg from the plus X axis toward the plus Y axis.

The selected attitude rotations were compensated for a flight control sensor group deflection of 0.31 deg. Analysis indicated the net offset in the desired retro thrust direction due to the measured gyro drift rates would be approximately 0.04 deg. Hence no attempt was made to compensate for this small error. An attempt was made to initiate the rotations at limit-cycle nulls in an effort to further reduce the offset in the thrust direction.

The terminal attitude maneuver was initiated approximately 35 min prior to retro ignition with a 2- to 5-min delay between rotations.

A number of times were computed for transmitting backup commands for the terminal phase including (1) the backup AMR *mark*, (2) the emergency AMR *mark*, and (3) the start of the emergency terminal descent command tape. The computation of these command times was based on the final estimate of the unbraked impact time and the uncertainty associated with it. These values were obtained from the final pre-retro orbit determination generated 40 min prior to ignition. The uncertainty (orbit determination and manual implementation) associated with executing the AMR backup command was determined to be $[(0.70)^2 + (0.15)^2]^{1/2} = 0.715$ sec (1σ). Using this value and the amount of predicted vernier engine propellant available, a backup delay of 1.2 sec was specified. Known fixed delays such as the propagation delay, operator delay, and command generator and command decoder delays totaled 2.37 sec. Fixed delays were anticipated by executing the command early. In addition, because of a questionable situation with regard to determining the final unbraked impact time via orbit determination, a conservative bias of 1 sec was added to the backup transmission time. The final GMT for transmission of the AMR backup command, rounded off to the next second, was 01:02:12. This backup *mark* command should have arrived at the spacecraft approximately

3.1 sec after the AMR *mark*, which was predicted to occur at 01:02:11.06 GMT. Based on the actual data, the backup *mark* arrived 3.92 ± 0.15 sec after AMR *mark*, which is estimated to have occurred at 01:02:10.60 GMT.

The emergency AMR *mark* would have been employed if AMR *power on* and AMR *enable* were not confirmed, indicating that the AMR was inoperative. The emergency terminal descent command tape contains commands beginning with *vernier ignition*, and would have been started if the spacecraft flight control timer were known to be inoperative. The approach taken to determine the times to employ these backups is to define a new nominal main retro burnout altitude centered with respect to the programmed descent contour, predicted nominal burnout velocity, and the maximum burnout altitude for which the spacecraft has capability to soft-land with the available vernier propellant. In general, the new burnout altitude is greater than the nominal value, and this higher burnout altitude gives rise to the desire for earlier-than-nominal backup command times. For *Surveyor VII*, the computed emergency AMR *mark* time was 01:02:08 GMT, approximately 3 sec earlier than the predicted AMR *mark*. The time computed for start of the emergency terminal descent command tape was 01:02:12 GMT, about 1 sec after predicted AMR *mark*.

The terminal descent sequence is described in Section IV-A. Table A-1 of Appendix A gives terminal phase event times. Initial touchdown occurred at 01:05:36.32 GMT on January 10, 1968, at a mission time of $L + 66:35:35.78$.

G. Landing Site

Based upon final postflight orbit determination using data obtained in flight, the landing site of *Surveyor VII* was computed to be at 41.059°S latitude and 11.451°W longitude. This corresponds to a miss of 6.0 km. However, correlation of *Surveyor VII* and *Lunar Orbiter* pictures indicates *Surveyor VII* is located at 40.92°S and 11.45°W, corresponding to a miss of 1.69 km. These touchdown locations are illustrated in Fig. VII-4.

Appendix A
Surveyor VII Flight Events

Table A-1. Mission flight events

Event	Mark No.	Mission time (predicted)	Mission time (actual)	GMT (actual)
Liftoff to DSIF acquisition^a				
		January 7, 1968 (Day 7)		
Liftoff (2-in. rise)		L + 00:00:00.00	L + 00:00:00.00	06:30:00.545
Initiate roll program		L + 00:00:02.00	L + 00:00:02.0	06:30:02.5
Terminate roll, initiate pitch program		L + 00:00:15.00	L + 00:00:14.9	06:30:15.4
Mach 1			L + 00:01:04.5	06:31:05.0
Maximum aerodynamic loading			L + 00:01:18.5	06:31:19.0
Atlas booster engine cutoff (BECO)	1	L + 00:02:33.09	L + 00:02:32.40	06:32:32.95
Jettison booster package	2	L + 00:02:36.19	L + 00:02:35.48	06:32:36.03
Admit guidance steering		L + 00:02:41.09	L + 00:02:40.4	06:32:40.9
Jettison Centaur insulation panels	3	L + 00:03:18.09	L + 00:03:17.08	06:33:17.62
Start Centaur boost pumps		L + 00:03:35.09	L + 00:03:33.95	06:33:34.49
Jettison nose fairing	4	L + 00:03:48.09	L + 00:03:46.36	06:33:46.90
Atlas sustainer engine cutoff (SECO)	5	L + 00:04:08.88	L + 00:04:08.71	06:34:09.25
Atlas/Centaur separation	6	L + 00:04:10.88	L + 00:04:10.59	06:34:11.13
Prestart Centaur main engines (chilldown)		L + 00:04:12.38	L + 00:04:12.2	06:34:12.7
Centaur main engines start (MES 1)	7	L + 00:04:20.38	L + 00:04:20.19	06:34:20.74
Centaur main engines cutoff (MECO 1)	8	L + 00:09:41.05	L + 00:09:53.11	06:39:53.66
100-lb thrust on	9	L + 00:09:41.05	L + 00:09:53.13	06:39:53.68
Vehicle-destruct system safed by ground command			L + 00:10:10.9	06:40:11.4
100-lb thrust off	10	L + 00:10:57.05	L + 00:11:08.98	06:41:09.53
6-lb thrust on	11	L + 00:10:57.05	L + 00:11:09.00	06:41:09.55
100-lb thrust on	12	L + 00:31:34.71	L + 00:31:39.26	07:01:39.81
Start Centaur boost pumps		L + 00:31:46.71	L + 00:31:51.24	07:01:51.79
Prestart Centaur main engines (chilldown)		L + 00:31:57.71	L + 00:32:02.34	07:02:02.89
Centaur C1 main engine start (MES 2)	13	L + 00:32:14.71	L + 00:32:19.26	07:02:19.80
Centaur C2 main engine start (MES 2)	14	L + 00:32:14.71	L + 00:32:19.26	07:02:19.80
Centaur main engines cutoff (MECO 2)	15	L + 00:34:08.28	L + 00:34:14.93	07:04:15.47
Extend Surveyor landing legs command	16	L + 00:34:28.71	L + 00:34:32.85	07:04:33.40
Extend Surveyor omniantennas command	17	L + 00:34:39.21	L + 00:34:43.89	07:04:44.44
Surveyor transmitter high power on	18	L + 00:34:59.71	L + 00:34:59.5	07:05:00
Surveyor/Centaur electrical disconnect	19	L + 00:35:05.21	L + 00:35:10.00	07:05:10.54
Surveyor/Centaur separation (injection)	20	L + 00:35:10.71	L + 00:35:15.29	07:05:15.84
Surveyor solar panel unlocked to begin stepping				07:05:16
Start Centaur 180-deg turn	21	L + 00:35:15.71	L + 00:35:20.0	07:05:20.5
Start Centaur lateral thrust	22	L + 00:35:55.71	L + 00:36:00.3	07:06:00.8
Start Surveyor sun acquisition roll			L + 00:36:01	07:06:01
Cut off Centaur lateral thrust	23	L + 00:36:15.71	L + 00:36:20.3	07:06:20.8
Start Centaur tank blowdown (retro)	24	L + 00:39:10.71	L + 00:39:15.4	07:09:15.9

Table A-1 (contd)

Event	Mark No.	Mission time (predicted)	Mission time (actual)	GMT (actual)
Liftoff to DSIF acquisition (contd)				
		January 7, 1968 (Day 7)		
Solar panel locked for transit, start A/SPP roll axis stepping	25		L + 00:40:36	07:10:37
Cut off Centaur blowdown, 100-lb thrust on		L + 00:43:20.71	L + 00:43:25.32	07:13:25.87
Complete Surveyor roll, begin sun acquisition yaw turn			L + 00:43:33	07:13:34
A/SPP roll axis locked for transit			L + 00:44:27	07:14:28
Surveyor primary sun sensor lock-on			L + 00:44:29	07:14:30
Cut off Centaur electrical power, 100-lb thrust off	26	L + 00:45:00.71	L + 00:45:05.3	07:15:05.8
Initial acquisition and good two-way lock completed by DSS 42			L + 00:58:01	07:28:02
Initial spacecraft operations to Canopus acquisition			Mission time (actual)	GMT (actual)
Initial spacecraft operation				
1. Command Transmitter B from high to low power			L + 01:01:46	07:31:47
2. Command off A/D isolation amplifiers, solar panel deployment logic; Transmitter A to low power			L + 01:04:45	07:34:46
3. Command step solar panel minus and plus to seat solar panel lock pin			L + 01:06:13	07:36:14
4. Command step roll axis plus and minus to seat roll axis lock pin			L + 01:07:48	07:37:49
5. Command from telemetry mode 5 to telemetry mode 1 for interrogation at 550-bits/sec data rate			L + 01:08:44	07:38:45
6. Command on 1100-bits/sec data rate and interrogate telemetry modes 1, 4, 2, and 6 and return to mode 5			L + 01:10:04 to L + 01:19:55	07:40:05 to 07:49:56
Command on and interrogate telemetry modes 1, 2, and 4 and return to mode 5 at 1100-bits/sec data rate			L + 04:06:14 to L + 04:12:04	10:36:15 to 10:42:05
Command on solar panel switch ^b			L + 05:57:47, L + 06:16:01	12:27:48, 12:46:02
Command on and interrogate telemetry modes 4, 2, and 1 at 1100-bits/sec data rate			L + 07:36:31 to L + 07:42:03	14:06:32 to 14:12:04
Command modulation interrupt to capture Receiver B			L + 07:45:21	14:15:22
Star verification/acquisition				
1. Command Transmitter B from low to high power			L + 07:48:27	14:18:28
2. Command on 4400-bits/sec data rate			L + 07:19:09	14:19:10
3. Command off transponder power (establish one-way tracking mode)			L + 07:51:19	14:21:20
4. Command flight control preparation: manual delay mode, positive roll direction			L + 07:52:16	14:22:17
5. Command positive sun and roll for star verification (light sources successively detected by Canopus sensor: Alpha C Venaticorum, Mizar, Gamma U Minoris/Kochab, Caph/Shedar/Zeta Cassiopeiae, moon, Canopus, earth)			L + 07:54:04	14:24:05
6. Command on sun acquisition mode (to end roll in preparation for manual lock-on due to insufficient star lock-on signal)			L + 08:14:58	14:44:59
7. Command manual lock-on (Canopus acquisition complete)			L + 08:17:31	14:47:32
8. Command off telemetry mode 1 and command on coast phase telemetry mode 5 at 4400-bits/sec data rate			L + 08:19:58	14:49:59
9. Command on Transponder B (resume two-way tracking mode)			L + 08:21:03	14:51:04
10. Command on 1100-bits/sec data rate			L + 08:26:45	14:56:46
11. Command Transmitter B from high to low power			L + 08:27:55	14:57:56

Table A-1 (contd)

Event	Mission time (actual)	GMT (actual)
Pre-midcourse coast phase: coast phase I		
	January 7, 1968 (Day 7)	
Command on inertial mode (start first gyro drift check, all three axes, at 1100-bits/sec data rate)	L + 09:06:01	15:36:02
Command on and interrogate telemetry modes 4, 2, and 1 and return to mode 5 at 1100-bits/sec data rate	L + 10:00:31 to L + 10:13:01	16:30:32 to 16:43:02
Command on cruise mode and manual lock-on (end first gyro drift check)	L + 11:01:27	17:31:34
Command on inertial mode (start second gyro drift check, all three axes)	L + 11:06:32	17:36:33
Command on and interrogate telemetry modes 4, 2, and 1 and return to mode 5 at 1100-bits/sec data rate	L + 11:53:12 to L + 12:08:46	18:23:13 to 18:38:47
Command on cruise mode and manual lock-on (end second gyro drift check)	L + 12:39:42	19:09:53
Pre-midcourse interrogation and gyro speed check		
1. Command on and interrogate telemetry modes 4, 2, and 1 and return to mode 5 at 1100-bits/sec data rate	L + 14:57:18 to L + 15:13:13	21:27:19 to 21:43:14
2. Command on gyro speed signal processor and check angular rate of gyro spin in all three axes; command off gyro speed signal processor and resume coast phase telemetry mode 5	L + 15:15:06 to L + 15:19:12	21:45:07 to 21:49:13
Midcourse phase		
Command on and interrogate telemetry modes 4, 2, and 1 at 1100-bits/sec data rate	L + 16:16:39 to L + 16:21:07	22:46:40 to 22:51:08
Command Transmitter B from low to high power	L + 16:32:02	23:02:03
Command on 4400-bits/sec data rate	L + 16:32:40	23:02:41
Pre-midcourse attitude maneuver		
1. Store negative roll magnitude of 6.2 sec (−3.1 deg)	L + 16:38:04	23:08:05
2. Command negative roll execution	L + 16:48:27	23:18:28
3. Command positive yaw maneuver direction and store yaw magnitude of 234.2 sec (+117.1 deg)	L + 16:49:00	23:19:01
4. Command yaw execution	L + 16:51:12	23:21:13
Command on propulsion strain gage power, inertial mode, and reset programmer latch (Group IV outputs)	L + 16:56:49	23:26:50
Command off AMR temperature control and vernier fuel and oxidizer lines thermal controls; unlock vernier engine 1 and pressurize vernier system (helium)	L + 16:57:44	23:27:45
Midcourse correction		
1. Command on flight control thrust phase power	L + 16:58:38	23:28:39
2. Store midcourse thrust phase quantity of 11.35 sec for a velocity correction of 11.08 m/sec	L + 16:59:20	23:29:21
3. Command execution of midcourse velocity correction	L + 17:00:08	23:30:09
4. Command standard emergency terminate thrust	L + 17:00:22	23:30:23
5. Command off flight control thrust phase power, propulsion strain gage power, touchdown strain gage power	L + 17:00:42	23:30:43
6. Command on and interrogate telemetry mode 5 at 4400-bits/sec data rate	L + 17:01:38	23:31:39
7. Command on temperature controls for vernier propellant lines and AMR	L + 17:02:33	23:32:34

Table A-1 (contd)

Event	Mission time (actual)	GMT (actual)
Midcourse phase (contd)		
Post-midcourse attitude maneuver	January 7, 1968 (Day 7)	
	L + 17:03:29	23:33:30
	L + 17:04:10 to L + 17:08:04	23:34:11 to 23:38:05
	L + 17:10:38	23:40:39
	L + 17:13:31 to L + 17:18:12	23:43:32 to 23:48:13
	L + 17:18:58	23:48:59
	L + 17:21:18	23:51:19
Post-midcourse coast phase: coast phase II		
Command on inertial mode (start third gyro drift check, all three axes) Command on and interrogate telemetry modes 4, 2, and 1 and return to mode 5 at 1100-bits/sec data rate Command on cruise mode and manual lock-on (end third gyro drift check) Command on sun acquisition mode (start fourth gyro drift check, roll axis only) Command manual lock-on (end fourth gyro drift check) Command on inertial mode (start fifth gyro drift check, all three axes) Command on and interrogate telemetry modes 4, 2, and 1 and return to mode 5 at 1100-bits/sec data rate Command on cruise mode and manual lock-on (end fifth gyro drift check) Command on and interrogate telemetry modes 4, 2, and 1 and return to mode 5 at 1100-bits/sec data rate Command on inertial mode (start sixth gyro drift check, all three axes) Command on and interrogate telemetry modes 4, 2, and 1 and return to mode 5 at 1100-bits/sec data rate Command on cruise mode and manual lock-on (end sixth gyro drift check) Command on and interrogate telemetry modes 4, 2, and 1 and return to mode 5 at 1100-bits/sec data rate Command on vernier oxidizer tank 2 thermal control Command on and interrogate telemetry modes 4, 2, and 1 and return to mode 5 at 1100-bits/sec data rate	January 8, 1968 (Day 8)	
	L + 17:34:11	00:04:12
	L + 19:01:55 to L + 19:11:05	01:31:56 to 01:41:06
	L + 20:12:57	02:43:09
	L + 20:18:54	02:48:55
	L + 23:32:41	06:02:42
	L + 23:36:22	06:06:23
	L + 24:18:45 to L + 24:26:15	06:48:46 to 06:56:16
	L + 26:06:49	08:37:05
	L + 29:22:03 to L + 29:33:50	11:52:04 to 12:03:51
	L + 31:32:21	14:02:22
	L + 33:30:36 to L + 33:43:24	16:00:37 to 16:13:25
	L + 34:44:32	17:14:41
	L + 36:39:41 to L + 36:53:58	19:09:42 to 19:23:59
	L + 37:34:57	20:04:58
	L + 39:25:27 to L + 39:31:43	21:55:28 to 22:01:44
	January 9, 1968 (Day 9)	
	L + 42:49:28 to L + 42:56:18	01:19:29 to 01:26:19
	L + 44:35:44	03:05:45
	L + 47:04:23	05:34:34

Table A-1 (contd)

Event	Mission time (actual)	GMT (actual)
Post-midcourse coast phase: coast phase II (contd)		
	January 9, 1968 (Day 9)	
Command on and interrogate telemetry modes 4, 2, and 1 and return to mode 5 at 1100-bits/sec data rate	L + 47:41:35 to L + 47:49:15	06:11:36 to 06:19:16
Command on inertial mode (start eighth gyro drift check, all three axes)	L + 48:46:23	07:16:24
Command on cruise mode and manual lock-on (end eighth gyro drift check)	L + 51:18:32	09:48:39
Command on and interrogate telemetry modes 4, 2, and 1 and return to mode 5 at 1100-bits/sec data rate	L + 52:29:40 to L + 52:42:30	10:59:41 to 11:12:31
Command modulation interrupt	L + 55:19:42	13:49:43
Command modulation interrupt	L + 55:29:48	13:59:49
Command on inertial mode (start ninth gyro drift check, all three axes)	L + 55:30:05	14:00:06
Command on Compartment A heater	L + 55:30:20	14:00:21
Command on and interrogate telemetry modes 4, 2, and 1 and return to mode 5 at 1100-bits/sec data rate	L + 55:44:00 to L + 55:54:40	14:14:01 to 14:24:50
Command on cruise mode and manual lock-on (end ninth gyro drift check)	L + 58:34:12	17:04:25
Command on and interrogate telemetry modes 4, 2, and 1 and return to mode 5 at 1100-bits/sec data rate	L + 59:36:50 to L + 59:47:20	18:06:51 to 18:19:21
Command on survey TV electronics temperature control	L + 59:49:45	18:19:46
Command from 1100-bits/sec to 550-bits/sec data rate	L + 61:25:15	19:55:16
Command on and interrogate telemetry modes 4, 2, and 1 and return to mode 5 at 550-bits/sec data rate	L + 62:28:08 to L + 62:37:53	20:58:09 to 21:07:54
Command on Compartment C and alpha scattering instrument heaters	L + 63:57:23	22:27:24
Command off Compartment A heater	L + 64:14:03	22:44:04
Preterminal maneuver interrogation, gyro speed check and VCXO check		
1. Command on and interrogate telemetry modes 4, 2, and 1 and return to mode 5 at 550-bits/sec data rate	L + 64:17:49 to L + 64:28:07	22:47:50 to 22:58:08
2. Command on gyro speed signal processor and check angular rate of gyro spin in all three axes; command off gyro speed signal processor	L + 64:29:21 to L + 64:32:00	22:59:22 to 23:02:01
3. Command off transponder power to perform VCXO check; then command Transponder B back on	L + 64:34:25 to L + 64:36:07	23:04:26 to 23:06:08
Terminal maneuver and descent phase		
Command on survey camera vidicon temperature control	L + 65:24:47	23:54:48
Command on telemetry mode 6 (thrust phase commutator)	L + 65:29:10	23:59:11
	January 10, 1968 (Day 10)	
Command on telemetry mode 4	L + 65:31:17	00:01:18
Command on Transmitter B and high power (twice)	L + 65:35:54, L + 65:37:17	00:05:55, 00:07:18
Command from 550 bits/sec to 1100 bits/sec	L + 65:38:02	00:08:03
Presumming amplifiers off, phase summing amplifier B on	L + 65:38:41	00:08:42

Table A-1 (contd)

Event	GMT (predicted)	Mission time (actual)	GMT (actual)
Terminal maneuver and descent phase (contd)			
	January 10, 1968 (Day 10)		
Command on and interrogate telemetry mode 2 and return to mode 5 at 1100-bits/sec data rate (mode 5 commanded twice)		L + 65:39:12 to L + 65:41:32	00:09:13 to 00:11:33
Command on propulsion strain gage power, touchdown strain gage power, and data channels		L + 65:48:28	00:18:29
Command off transponder power (establish one-way tracking mode)		L + 65:51:14	00:21:15
Terminal maneuvers			
1. Command positive angle maneuver and store roll magnitude of 161.0 sec (+80.5 deg)		L + 65:52:55	00:22:56
2. Command sun and roll maneuver		L + 65:57:13	00:27:14
3. Store yaw magnitude of 192.2 sec (+96.1 deg)		L + 66:00:28	00:30:29
4. Command yaw execution, aligning retro motor thrust axis with velocity vector		L + 66:05:49	00:35:50
5. Command on inertial mode (to permit negative maneuver direction) and store roll magnitude of 33.0 sec (-16.5 deg)		L + 66:09:44	00:39:45
6. Command roll execution		L + 66:11:06	00:41:07
Command on presuming amplifier (touchdown strain gages on)		L + 66:12:32	00:42:33
Command reset nominal thrust bias (200-lb vernier thrust level)		L + 66:13:38	00:43:39
Store retro sequence delay quantity (2.775 sec between AMR mark and vernier engine ignition)		L + 66:15:09	00:45:10
Command on telemetry mode 6 (thrust phase commutator)		L + 66:20:09	00:50:10
Command reset programmer latch (group IV outputs)		L + 66:20:54	00:50:55
Command on retro sequence mode		L + 66:26:10	00:56:11
Command off vernier propulsion thermal controls, survey camera vidicon and electronics temperature controls, AMR temperature control, Compartment C temperature control, and alpha scattering heater power (cyclic thermal loads)		L + 66:26:25	00:56:26
Command on AMR power		L + 66:27:33	00:57:34
Command on thrust phase power		L + 66:28:33	00:58:34
Command AMR enable		L + 66:32:33	01:00:34
Terminal descent ^c			
1. AMR mark at 59.8 mile slant range from lunar surface; start delay quantity countdown	01:02:11.6	L + 66:32:10.1	01:02:10.6
2. Vernier engine ignition (197-lb thrust)	01:02:13.82	L + 66:32:12.9	01:02:13.4
3. Main retro motor ignition and AMR ejection	01:02:14.92	L + 66:32:14.0	01:02:14.5
4. RADVS power on for warmup		L + 66:32:14	01:02:15
5. RADVS high voltage on		L + 66:32:15	01:02:16
6. Reliable operate doppler velocity sensor (RODVS) signal, following acquisition of the lunar surface by RADVS beams 1, 2, and 3		L + 66:32:47	01:02:48
7. Main retro burnout (3.5-g level sensed by inertia switch)		L + 66:32:57.2	01:02:57.7
8. Vernier engines to high thrust level (279-lb thrust)		L + 66:33:07	01:03:08
9. Retro case eject signal		L + 66:33:09.2	01:03:09.7
10. Retro motor case ejection		L + 66:33:09.2	01:03:09.7
11. Start RADVS-controlled descent (vernier engine thrust decreased to approximately 115 lb to produce 0.9-lunar-g constant deceleration); retro sequence mode off		L + 66:33:11.3	01:03:11.8

Table A-1 (contd)

Event	GMT (predicted)	Mission time (actual)	GMT (actual)
Terminal maneuver and descent phase (contd)			
	January 10, 1968 (Day 10)		
12. <i>Reliable operate radar altimeter (RORA) signal, following acquisition of lunar surface by RADYS beam 4</i>		L + 66:33:15	01:03:16
13. <i>Programmed descent segment intercept and vernier thrust level increase to approximately 240 lb to begin constant deceleration descent segment down to 14-ft mark</i>		L + 66:34:01.5	01:04:01.7
14. <i>1000-ft mark: change RADYS flight-control-loop parameters</i>		L + 66:35:11.5	01:05:12.0
15. <i>10-ft/sec mark: 50-ft altitude; increase vernier thrust from approximately 230 to 250 lb to produce 5-ft/sec constant velocity; flight control from RADYS to gyros</i>		L + 66:35:28.4	01:05:28.9
16. <i>14-ft mark: cut off vernier engines (105-lb thrust)</i>		L + 66:35:34.5	01:05:35.0
17. <i>Touchdown (Footpad 1)</i>	01:05:26.35	L + 66:35:35.78	01:05:36.32 ^d
^a The predicted values were computed postflight utilizing actual launch azimuth, tanked propellant weights, and atmospheric data which depend on day and time of liftoff. ^b The solar panel switch is automatically tripped off by normal function of the battery charge regulator overvoltage protection circuit in response to high buss voltage. The switch was commanded back on a total of four times during the transit phase of the mission. ^c Automatically controlled sequence except for emergency AMR mark command sent from earth as a standard precautionary backup procedure. Actual times for terminal descent events have been corrected for 1.297-sec radio transmission delay to indicate time of occurrence at spacecraft. ^d Touchdown time of 01:05:37.61 is used elsewhere in this document and represents touchdown time as received and recorded at DSS 14.			

Table A-2. Lunar operations^a

Date, 1968	Engineering (SPAC or DSIF)	Science (SSAC)	
		Television and SM/SS	Alpha scattering instrument
First lunar day			
Jan 10	Postlanding power shutdown and abbreviated engineering assessment Initial gross positioning of solar panel and planar array (A/SPP) to acquire sun and earth for 600-line TV Solar panel and planar array (A/SPP) fine positioning for attitude determination Alpha scattering instrument (ASI) deployed to background by on-site command tape (DSS 61) ASI surface deployment malfunction	Initial survey: Pad 3 to Pad 2, 200-line mode, 14 pictures 360-deg W/A panorama, 600-line mode Special area and auxiliary mirror surveys N/A panorama: segments 1-5 Earth polarimetric survey ASI background deployment coverage (108 pictures) ASI surface deployment failure coverage SM/SS area survey Stereo mirror coverage	Data accumulation and calibration in stowed and background positions Deployment to lunar surface unsuccessful
Jan 11	A/SPP stepped in blocks of 10 steps in attempt to jar loose ASI SM/SS employed experimentally to help free ASI A/SPP stepped to reduce battery charge	ASI deployment attempt coverage SM/SS operation ASI deployment attempt coverage SM/SS bearing test Polarimetric survey Special area and magnets survey Auxiliary mirrors survey Omniantenna B photo target ASI deployment attempt coverage Star survey, earth, jupiter Focus ranging: azimuths -108, -126 deg 360-deg W/A panorama N/A panorama: segments 1-5 ASI deployment mechanism coverage N/A panorama: segment 4	Background data accumulation and calibration
Jan 12	ASI successfully deployed with aid of SM/SS Transmitter A wideband frequency check	Stereo mirror coverage SM/SS operation Survey: earth and one star ASI deployment attempt using SM/SS; instrument successfully deployed End stop coverage Focus ranging N/A panorama: segments 1, 2, 3, and 5	Background data accumulation and surface data accumulation and calibration at first surface position

Table A-2 (contd)

Date, 1968	Engineering (SPAC or DSIF)	Science (SSAC)	
		Television and SM/SS	Alpha scattering instrument
First lunar day (contd)			
Jan 13	A/SPP stepped to shade check and relief valves and TV camera	Polarimetric survey SM/SS area survey Stereo mirror coverage ASI deployment mechanism SM/SS operations Earth, star, and laser experiment; indeterminate results Special area and magnets survey Auxiliary mirrors survey N/A panorama: segments 2, 3, 4, 5, and 1	Data accumulation and calibration
Jan 14	A/SPP repositioned to peak planar array Wideband VCXO checks (3) Up-link lost momentarily during TV sequence Transmitter A and B frequency check; switched from Transmitter A to Transmitter B because of excessive wideband frequency drift	ASI on lunar surface N/A panorama: segments 3 and 2 SM/SS operations Laser experiment and earth survey SM/SS operations Particle viewing mirrors survey Polarimetric survey ASI mirror coverage 360-deg W/A panorama N/A panorama: segment 1	Data accumulation and calibration
Jan 15	A/SPP stepped to reduce battery charge current, and to shade check and relief valves Combined RF communications and signal processing tests performed A/SPP stepped to increase battery charge current	ASI auxiliary mirror and W/A coverage Polarimetric survey Special area survey Auxiliary mirrors survey 360-deg W/A panorama N/A panorama: segments 1, 4, and 5	Data accumulation; operations suspended due to excessive instrument temperatures
Jan 16	A/SPP positioned to shade TV camera and part of Compartment A at end of TV operations; communication via omniantenna at 550 bits/sec during shading; planar array repositioned on earth for TV and returned to shade camera at end of activity	Polarimetric survey Footpad 2 magnets N/A panorama: segment 2 Magnets and SM/SS rock surveys	No operations due to high temperatures

Table A-2 (contd)

Date, 1968	Engineering (SPAC or DSIF)	Science (SSAC)	
		Television and SM/SS	Alpha scattering instrument
First lunar day (contd)			
Jan 17	A/SPP stepped to position planar array on earth for TV; returned to shade camera at end of TV activity Various compartment loads energized to regulate battery charge rate Special telecommunications test (multipath experiment) A/SPP stepped to improve Compartment C shading, decrease Compartment A shading	Polarimetric survey Special area segments 2 and 3 SM/SS area survey ASI mirror, N/A survey N/A panorama: segments 4 and 5 SM/SS positioned to shade ASI	No operations due to high temperatures
Jan 18	Best lock frequency measurement A/SPP stepped to shade TV camera after TV activity Compartment A loads adjusted to regulate compartment temperature and battery charge current	Polarimetric survey, special rocks, and ASI head survey Special area survey Auxiliary mirrors survey Earth survey 360-deg W/A panorama Earth and polarimetric surveys Special rocks survey N/A panorama: segments 1, 2, 3, and 5 Particle viewing mirrors survey	No operations due to high temperatures
Jan 19	Best lock frequency measurement (2) Compartment A loads adjusted to regulate battery temperature A/SPP stepped to unshade TV camera and position planar array on earth; then stepped to shade camera at conclusion of TV activity	SM/SS operations Earth survey and laser experiment SM/SS operations and examination of SM/SS scoop magnet Polarimetric surveys (2) and rock polarimetry Stereo mirror coverage SM/SS area survey Special area and auxiliary mirror surveys N/A panorama: segments 1, 2, 3, and 5 360-deg W/A panorama	No operations due to high temperatures
Jan 20	A/SPP stepped to unshade TV camera and position planar array on earth Best lock frequency measurement Battery logic disabled to eliminate solar panel switch tripping	SM/SS operations (4) Earth surveys (2) and laser experiment (1); results successful Star survey, Sirius (2) SM/SS operations and magnet examination Magnet test with SM/SS SM/SS N/A segment Polarimetric survey and special rocks survey	Data accumulation and calibration

Table A-2 (contd)

Date, 1968	Engineering (SPAC or DSIF)	Science (SSAC)	
		Television and SM/SS	Alpha scattering instrument
First lunar day (contd)			
Jan 21	A/SPP stepped to reduce battery charge level prior to TV operations A/SPP repositioned to resume battery charge rate Landing gear lock command sent; indications positive Step solar panel plus to meet power requirements	Earth polarimetry Laser experiment SM/SS operations; ASI moved to second site (rock) Star survey, Sirius Polarimetric survey SM/SS area survey and ASI partial survey Focus ranging Special area survey Auxiliary mirrors N/A panorama: segments 1-5 360-deg W/A panorama	Data accumulation and calibration; instrument moved to surface position 2
Jan 22	Vernier engine 2 oxidizer leak noted Power computations revised to include TV start-frame commands Solar panel positioned for peak current Planar array positioned for peak signal (-117.5 dbm) ASI and Compartments A, B, and C heaters on	SM/SS operations; ASI moved to third site Polarimetric survey Special area survey Focus ranging Earth polarimetry (2) 360-deg W/A panorama N/A panorama: segments 3, 1, 2, 4, and 5 Shadow progression (2)	Data accumulation and calibration; instrument moved to surface position 3
Jan 23	Solar panel stepped to sun angle position for desired revival time on second lunar day Change in Leg 2 deflection noted; fuel and oxidizer leaks noted Engineering interrogations for power and thermal status limited to 7-min intervals Science payload heaters off; spacecraft to standby Best lock frequency measurement	Shadow progression sequences (3) and earth survey (1) Earth polarimetry (6) and star Sirius (1) (lunar sunset: 06:06:13 GMT) Solar corona and W/A horizon survey Horizon scans: segments 2 and 3 Solar corona survey SM/SS and view of Footpad 2 Eastern horizon surveys, segments 1, 2, and 3 (2) SM/SS operations; bearing strength tests Solar corona (30-min exposures), (8) Mercury photographed Eastern horizon surveys, segments 1, 2 Lunar polarimetry (2) (Camera secured at 21:07 GMT)	Data accumulation and calibration; instrument commanded off at 15:36 GMT due to rapidly decreasing instrument temperature

Table A-2 (contd)

Date, 1968	Engineering (SPAC or DSIF)	Science (SSAC)	
		Television and SM/SS	Alpha scattering instrument
First lunar day (contd)			
Jan 24	Periodic engineering interrogations for power and thermal assessment and compartment thermal load adjustments Best-lock frequency measurement		
Jan 25	Periodic engineering interrogations for power and thermal assessment and return to standby Compartment thermal load adjustments Best-lock frequency measurement		
Jan 26	Periodic engineering interrogations and best-lock frequency measurements (2) Final shutdown at 14:12 GMT, ending first lunar day		
Second lunar day			
Feb 12	Spacecraft revived on first attempt at 19:00 GMT A/SPP stepped for attitude determination and optimum battery charge Leg 1 deflection of 24.5 deg noted, indicating collapse of leg Low battery manifold pressure noted, indicating ruptured manifold	SM/SS above operating temperature limit 600-line mode TV inoperable	Instrument above operating temperature limit
Feb 13	Special power system tests to check for battery short 600-line TV low-power test with DSS 14 unsuccessful Narrowband and wideband configuration check-out Rising battery temperature noted A/SPP stepped to shade Compartment A, then repositioned to peak planar array on earth and solar panel to lead the sun Battery analysis indicates probable shorted cells	600-line mode TV attempt unsuccessful 200-line mode TV operable; 6 pictures received	
Feb 14	600-line TV low-power test unsuccessful Spacecraft placed in standby due to high battery temperature Solar panel stepped to lead the sun	200-line TV operations; 39 pictures received including new lunar surface revealed by spacecraft tilt SM/SS successfully commanded to extend arm	

Table A-2 (contd)

Date, 1968	Engineering (SPAC or DSIF)	Science (SSAC)	
		Television and SM/SS	Alpha scattering instrument
Second lunar day (contd)			
Feb 15	Spacecraft to standby mode, alternating with periodic interrogations to monitor battery performance		
Feb 16	Standby period experiments to improve battery performance; solar panel stepped to lead the sun; battery deterioration stabilized by operating spacecraft continuously		
Feb 17	Solar panel stepped; receivers out of lock; carrier search unsuccessful; spacecraft commanded to standby, then successfully revived Attempts to step solar panel unsuccessful; battery unable to support load due to continuing deterioration Compartment loads adjusted Periodic interrogations and standbys		
Feb 18	Solar panel stepping attempts (2) unsuccessful Special spacecraft power consumption vs charge current test Up-link and down-link lost for 2 min Various bit rates selected in attempts to improve intermittently bad alpha scattering data Spacecraft loads adjusted to regulate bus voltage Bit rate lowered to 550 bits/sec to assist locking up on engineering data; unsuccessful		Instrument turned on; alpha system data accumulation only; proton data unusable Instrument turned off for 6 min during load adjustment
Feb 19	7.35-kHz SCO turned off to assist locking up on alpha scattering data; locked up on 1100-bits/sec engineering data; alpha scattering accumulations alternated with engineering interrogations SM/SS power turned on to assist power management; spacecraft momentarily dropped lock with SM/SS command Spacecraft reconfigured from 550 to 1100 bits/sec with 7.35-kHz SCO		Alpha system data accumulations alternated with engineering interrogations

Table A-2 (contd)

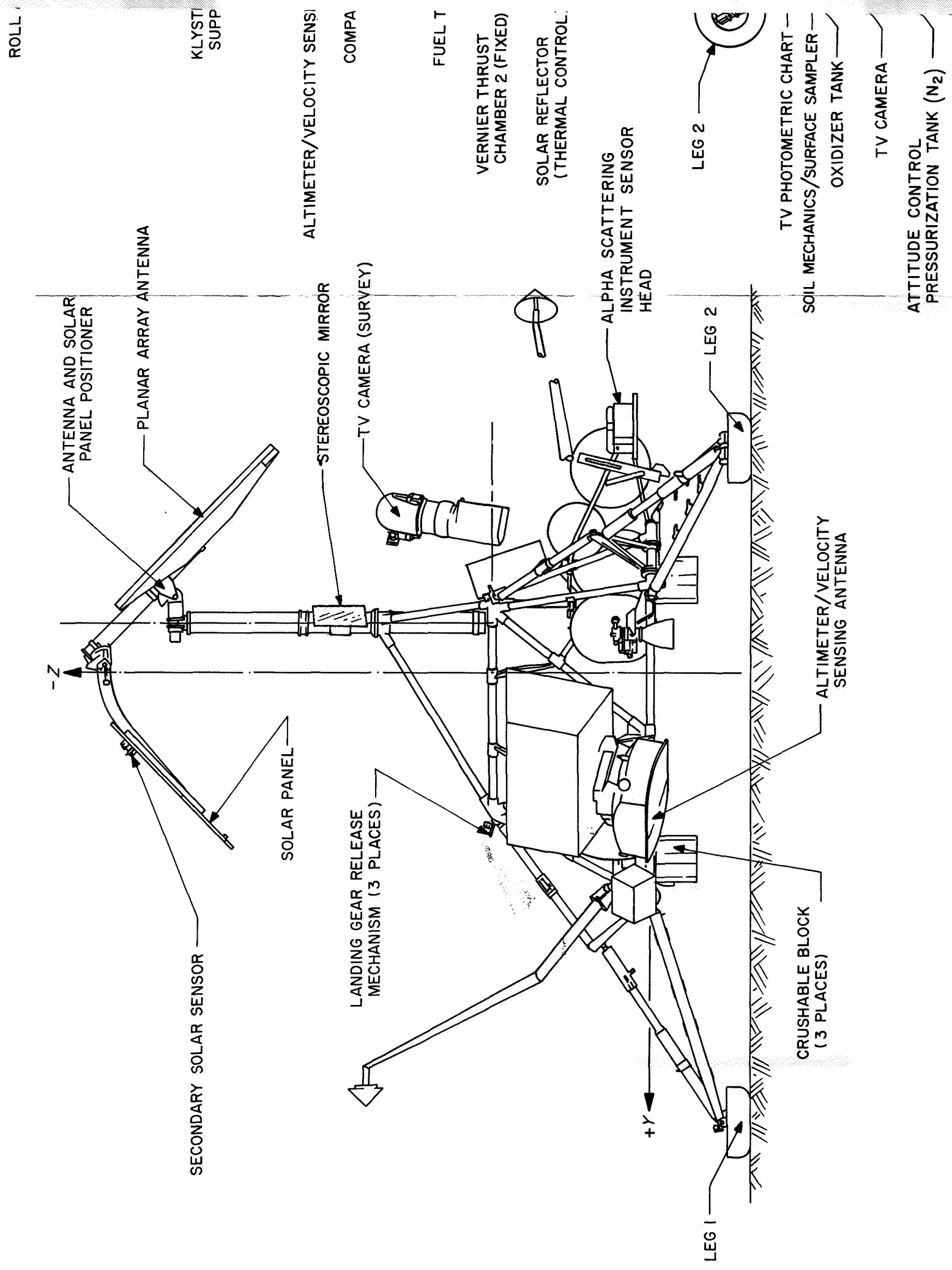
Day, 1968	Engineering (SPAC or DSIF)	Science (SSAC)	
		Television and SM/SS	Alpha scattering instrument
Second lunar day (contd)			
Feb 20	Engineering interrogations alternated with alpha scattering data accumulations and power management operations Unsuccessful attempt to improve signal strength with new ground tracking frequency Switch to Transmitter B, Omnantenna B successful TV attempt and load adjustments result in frequent loss of lock Various shutdown and turn-on sequences commanded during revival attempts	200-line-mode TV attempt unsuccessful SM/SS fine-stepping extension unsuccessful	Alpha system data accumulations alternated with engineering interrogations and TV attempt Instrument turned off at 11:50 GMT
Feb 21	Spacecraft recovered at 00:09 GMT after prolonged search. Receivers out of lock at 00:24 GMT when TV power commanded on. Mission terminated at 06:48 GMT when all search efforts were halted	200-line-mode TV attempt unsuccessful	

^aRoutine engineering interrogations are not listed. All television sequences are 600-line mode unless otherwise noted. Wide angle and narrow angle are abbreviated W/A and N/A, respectively. DSIF two-way doppler tracking and resolver doppler counting were performed throughout lunar operations.

Appendix B
Surveyor VII Spacecraft Configuration

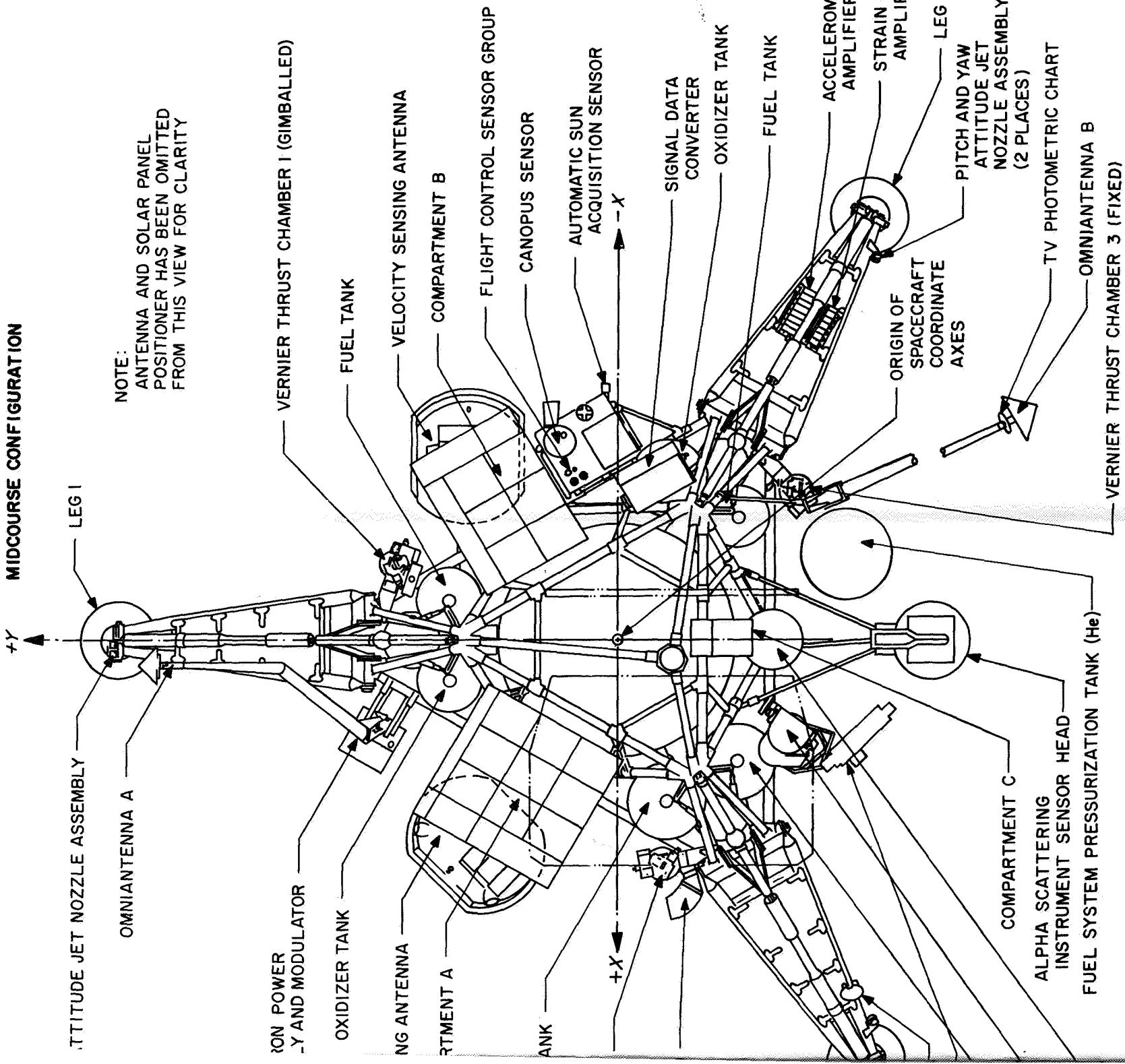
1d

POSTLANDING CONFIGURATION

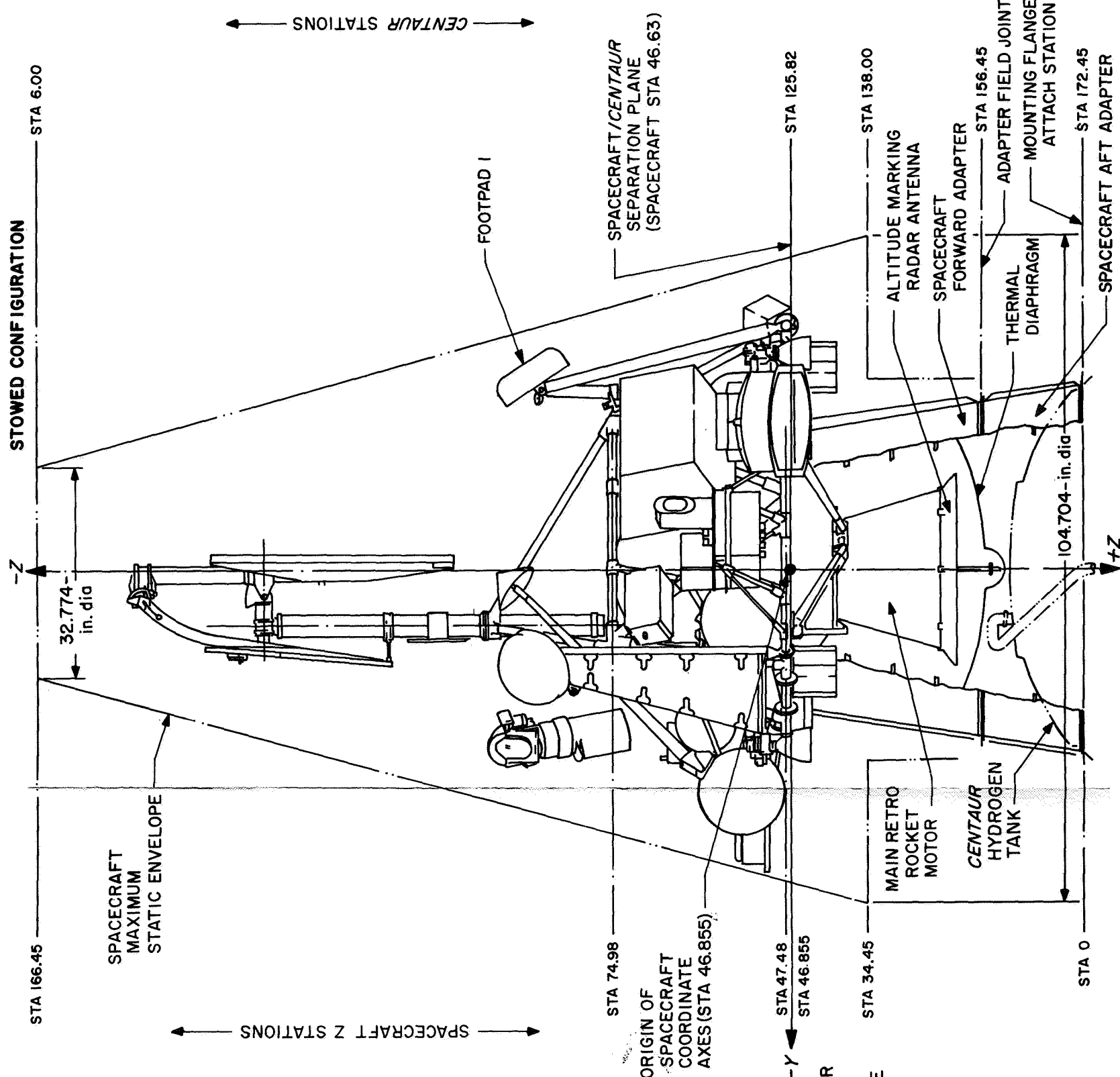


2d

MIDCOURSE CONFIGURATION



STOWED CONFIGURATION



Appendix C **Surveyor VII Spacecraft Data Content of Telemetry Modes**

ALPHA SCATTERING INSTRUMENT

CHAN	NAME	MODE 1 WORDS	MODE 2 WORDS	MODE 3 WORDS	MODE 4 WORDS	MODE C (5) WORDS	MODE T (6) WORDS
AS-3	SENSOR HEAD TEMP.						
AS-4	ELECTRONICS TEMP.						
AS-5	GUARD EVENT MONITOR				40		
AS-6	+7A VDC MONITOR				91		
AS-9					41		
RADIO AND COMMAND DECODING (DATA LINK)							
D-1	OWNI B TRANSMITTER POWER				1	87	
D-2	OWNI B TRANSMITTER POWER				1	117	
D-3	STATIC PHASE ERROR A	66			3,23,43,63,83	17	
D-8	STATIC PHASE ERROR B	39,78	81		13,33,53,73,93	27	
D-9	RECEIVER B AGC	39,78	55		17	33	81
D-10	RECEIVER B AGC	39,78	55		2	6	79
D-13	TRANSMITTER A TEMPERATURE		44		12	30	
D-14	TRANSMITTER B TEMPERATURE		44		12	30	
D-17	RECEIVER B AGC		13		15,35,55,75,95	41	
ELECTRICAL POWER							
EP-1	28V NON-ESSENTIAL VOLTAGE	90	90	48	27	59	69
EP-2	UNREGULATED BUS VOLTAGE	48	48		7,57	60	
EP-3	UNREGULATED OUTPUT CURRENT	22	22		51	9	
EP-6	BATTERY CHARGE CURRENT		69		49	45	
EP-7	BOOST REG DIFFERENCE CURRENT		72		47	45	
EP-9	SOLAR CELL ARRAY VOLTAGE	44	72		47	29	
EP-10	SOLAR CELL ARRAY VOLTAGE	39	59		39	67	
EP-11	SOLAR CELL ARRAY CURRENT	24	42		10	35	
EP-13	BOOST REGULATOR TEMPERATURE	42	82		42	20	20
EP-14	REGULATED OUTPUT CURRENT		49		42	39	
EP-17	RADAR AND SQUIR CURRENT		29		49	49	
EP-22	COMPARTMENT B HEATER CURRENT		21		29	93	
EP-30	BOOST REG. P-REG. VOLTAGE	64			78	35	
EP-34	BATTERY CHARGE REG. TEMP.					65	
EP-36	IRADIATED SOLAR CELL S.C. CURRENT					65	
EP-37	SOLAR CELL OPEN CRT. VOLTAGE	79	79		79	55	
EP-38	SOLAR CELL OPEN CRT. VOLTAGE	32	32		32	19	
EP-40	ELUSTRATED UNREGULATED CURRENT						
FLIGHT CONTROL							
FC-4	NITROGEN GAS PRESSURE	10,40				89	
FC-5	PRIM. SUN SENSOR PITCH ERROR	20,70				71	
FC-6	SECONDARY SUN SENSOR CELL A					99	
FC-7	SECONDARY SUN SENSOR CELL B					101	
FC-8	SECONDARY SUN SENSOR CELL C					105	
FC-9	SECONDARY SUN SENSOR CELL D					109	
FC-10	CANONOUS ERROR					115	
FC-12	STAR INTENSITY SIGNAL	7,27,47,67,87	11			1	6,36,66,96
FC-14	PITCH RATE ERROR	11,31,51,71,91	12			3	3,33,63,93
FC-15	PITCH RATE ERROR	16,46	18			1	17,47,77,107
FC-17	YAW GYRO ERROR	15,35,55,75,95	9,43			1	16,46,76,106
FC-23	THRUST CMD TO VERNIER ENG 1	16,46,76,106	2,52			1	16,46,76,106
FC-27	THRUST CMD TO VERNIER ENG 3	7,27,47,67,87	2,52			1	16,46,76,106
FC-32	RETRO ACCELEROMETER	7,27,47,67,87	2,52			1	16,46,76,106
FC-33	RADAR ALTITUDE RANGE SIGNAL		44			1	16,46,76,106
FC-35	DOPLER VELOCITY Vx		45,93			1	16,46,76,106
FC-40	DOPLER VELOCITY Vy		45,93			1	16,46,76,106
FC-41	ROLL ACTUATOR SIGNAL	1,21,41,61,81	3,53			1	16,46,76,106
FC-43	FLIGHT CONTROL E/U TEMP 1		41,91			1	16,46,76,106
FC-45	FLIGHT CONTROL E/U TEMP 2		41,91			1	16,46,76,106
FC-46	ROLL GYRO TEMPERATURE		60			1	16,46,76,106
FC-47	CANONOUS SENSOR TEMPERATURE		17			1	16,46,76,106
FC-49	PITCH PRECISION COMMAND		10			1	16,46,76,106
FC-50	PITCH PRECISION COMMAND		87			1	16,46,76,106
FC-51	YAW PRECISION COMMAND		20			1	16,46,76,106
FC-54	PITCH GYRO TEMPERATURE		80			1	16,46,76,106
FC-55	YAW GYRO TEMPERATURE		80			1	16,46,76,106
FC-70	ATTITUDE GAS JET 2 TEMP					1	16,46,76,106
FC-77	FLT. CONT. REFERENCE RETURN					1	16,46,76,106
MECHANISMS							
M-3	SOLAR PANEL POSITION		98			37	
M-5	ELEVATION AXIS POSITION		71			79	
M-6	ROLL AXIS POSITION		77			91	
M-7	PLANAR ARRAY TEMPERATURE		87			38	
M-8	PLANAR ARRAY TEMPERATURE		14			51	
M-12	ELEV. AXIS STEP. MOTOR TEMP.		64			106	
SPARE	(HIGH-ACC. TEMP)				80,90		

PROPULSION

CHAN	NAME	MODE 1 WORDS	MODE 2 WORDS	MODE 3 WORDS	MODE 4 WORDS	MODE C (5) WORDS	MODE T (6) WORDS
P-1	HELIUM PRESSURE	84	25			51	21
P-2	UPPER RETRO CASE TEMPERATURE	3	50			52	80
P-3	VERNIER FUEL TANK 2 TEMP.	2	68			52	
P-4	VERNIER FUEL TANK 3 TEMP.		86			70	70
P-5	VERNIER ENGINE 1 TEMPERATURE	26	52			90	90
P-6	VERNIER ENGINE 2 TEMPERATURE	52	80			100	100
P-7	VERNIER ENGINE 3 TEMPERATURE	80	80			50	60
P-8	VERNIER ENGINE 4 TEMPERATURE	46				28	
P-9	LOWER RETRO CASE TEMPERATURE		88			54	4
P-10	VERNIER FUEL TANK 3 TEMP.		70			92	2
P-11	VERNIER OXIDIZER TANK 1 TEMP.		84			86	
P-12	VERNIER OXIDIZER TANK 2 TEMP.				20		
P-13	VERNIER ENGINE 1 STRAIN GAGE	13, 33, 53, 73, 93	13	13			7, 37, 57
P-14	VERNIER ENGINE 2 STRAIN GAGE	14, 34, 54, 74, 94	14	14			11, 41, 71, 91
P-15	VERNIER ENGINE 3 STRAIN GAGE	8, 58	8	8			28, 88
P-16	VERNIER FUEL LINE #1 TEMP		78				
P-17	VERNIER FUEL LINE #2 TEMP		58				
P-18	VERNIER FUEL LINE #3 TEMP	86				84	
P-19	VERNIER FUEL LINE PRESSURE						
P-20							
P-21							
P-22							
P-23							
P-24							
P-25							
P-26							
RADAR							
R-2	RADVS-8 AMPLITUDE		26	26			4, 64
R-3	RADVS-D1 AMPLITUDE		38	38			14, 74
R-4	RADVS-D2 AMPLITUDE		36	36			34, 94
R-5	RADVS-D3 AMPLITUDE		46	46			
R-6	AWR ANTENNA TEMPERATURE		54	54			
R-7	AWR KLY. UNIT TEMP.		38	38		26	
R-8	RADVS KLY. UNIT TEMP.		36	36		10	
R-9	RADVS SIG. DATA CONVERT. TEMP.		62	62		22	
R-10	DOPPLER RADAR SENSOR TEMP.		94	94		76	
R-11	ALTITUDE RADAR SENSOR TEMP.		96	96		59	
R-12	ALTITUDE RADAR SENSOR TEMP.		33	33		24	
R-13	ALTITUDE MARKING RADAR AGC		71			43	
R-14	ALTITUDE MARKING RADAR AGC					89	
R-15	ALTITUDE MARKING RADAR AGC						
R-16	ALTITUDE MARKING RADAR AGC						
R-17	ALTITUDE MARKING RADAR AGC						
R-18	ALTITUDE MARKING RADAR AGC						
R-19	ALTITUDE MARKING RADAR AGC						
R-20	ALTITUDE MARKING RADAR AGC						
R-21	ALTITUDE MARKING RADAR AGC						
R-22	ALTITUDE MARKING RADAR AGC						
R-23	ALTITUDE MARKING RADAR AGC						
R-24	ALTITUDE MARKING RADAR AGC						
R-25	ALTITUDE MARKING RADAR AGC						
R-26	ALTITUDE MARKING RADAR AGC						
R-27	ALTITUDE MARKING RADAR AGC						
R-28	ALTITUDE MARKING RADAR AGC						
R-29	ALTITUDE MARKING RADAR AGC						
R-30	ALTITUDE MARKING RADAR AGC						
R-31	ALTITUDE MARKING RADAR AGC						
R-32	ALTITUDE MARKING RADAR AGC						
R-33	ALTITUDE MARKING RADAR AGC						
R-34	ALTITUDE MARKING RADAR AGC						
R-35	ALTITUDE MARKING RADAR AGC						
R-36	ALTITUDE MARKING RADAR AGC						
R-37	ALTITUDE MARKING RADAR AGC						
R-38	ALTITUDE MARKING RADAR AGC						
R-39	ALTITUDE MARKING RADAR AGC						
R-40	ALTITUDE MARKING RADAR AGC						
R-41	ALTITUDE MARKING RADAR AGC						
R-42	ALTITUDE MARKING RADAR AGC						
R-43	ALTITUDE MARKING RADAR AGC						
R-44	ALTITUDE MARKING RADAR AGC						
R-45	ALTITUDE MARKING RADAR AGC						
R-46	ALTITUDE MARKING RADAR AGC						
R-47	ALTITUDE MARKING RADAR AGC						
R-48	ALTITUDE MARKING RADAR AGC						
R-49	ALTITUDE MARKING RADAR AGC						
R-50	ALTITUDE MARKING RADAR AGC						
R-51	ALTITUDE MARKING RADAR AGC						
R-52	ALTITUDE MARKING RADAR AGC						
R-53	ALTITUDE MARKING RADAR AGC						
R-54	ALTITUDE MARKING RADAR AGC						
R-55	ALTITUDE MARKING RADAR AGC						
R-56	ALTITUDE MARKING RADAR AGC						
R-57	ALTITUDE MARKING RADAR AGC						
R-58	ALTITUDE MARKING RADAR AGC						
R-59	ALTITUDE MARKING RADAR AGC						
R-60	ALTITUDE MARKING RADAR AGC						
R-61	ALTITUDE MARKING RADAR AGC						
R-62	ALTITUDE MARKING RADAR AGC						
R-63	ALTITUDE MARKING RADAR AGC						
R-64	ALTITUDE MARKING RADAR AGC						
R-65	ALTITUDE MARKING RADAR AGC						
R-66	ALTITUDE MARKING RADAR AGC						
R-67	ALTITUDE MARKING RADAR AGC						
R-68	ALTITUDE MARKING RADAR AGC						
R-69	ALTITUDE MARKING RADAR AGC						
R-70	ALTITUDE MARKING RADAR AGC						
R-71	ALTITUDE MARKING RADAR AGC						
R-72	ALTITUDE MARKING RADAR AGC						
R-73	ALTITUDE MARKING RADAR AGC						
R-74	ALTITUDE MARKING RADAR AGC						
R-75	ALTITUDE MARKING RADAR AGC						
R-76	ALTITUDE MARKING RADAR AGC						
R-77	ALTITUDE MARKING RADAR AGC						
R-78	ALTITUDE MARKING RADAR AGC						
R-79	ALTITUDE MARKING RADAR AGC						
R-80	ALTITUDE MARKING RADAR AGC						
R-81	ALTITUDE MARKING RADAR AGC						
R-82	ALTITUDE MARKING RADAR AGC						
R-83	ALTITUDE MARKING RADAR AGC						
R-84	ALTITUDE MARKING RADAR AGC						
R-85	ALTITUDE MARKING RADAR AGC						
R-86	ALTITUDE MARKING RADAR AGC						
R-87	ALTITUDE MARKING RADAR AGC						
R-88	ALTITUDE MARKING RADAR AGC						
R-89	ALTITUDE MARKING RADAR AGC						
R-90	ALTITUDE MARKING RADAR AGC						
R-91	ALTITUDE MARKING RADAR AGC						
R-92	ALTITUDE MARKING RADAR AGC						
R-93	ALTITUDE MARKING RADAR AGC						
R-94	ALTITUDE MARKING RADAR AGC						
R-95	ALTITUDE MARKING RADAR AGC						
R-96	ALTITUDE MARKING RADAR AGC						
R-97	ALTITUDE MARKING RADAR AGC						
R-98	ALTITUDE MARKING RADAR AGC						
R-99	ALTITUDE MARKING RADAR AGC						
R-100	ALTITUDE MARKING RADAR AGC						
R-101	ALTITUDE MARKING RADAR AGC						
R-102	ALTITUDE MARKING RADAR AGC						
R-103	ALTITUDE MARKING RADAR AGC						
R-104	ALTITUDE MARKING RADAR AGC						
R-105	ALTITUDE MARKING RADAR AGC						
R-106	ALTITUDE MARKING RADAR AGC						
R-107	ALTITUDE MARKING RADAR AGC						
R-108	ALTITUDE MARKING RADAR AGC						
R-109	ALTITUDE MARKING RADAR AGC						
R-110	ALTITUDE MARKING RADAR AGC						
R-111	ALTITUDE MARKING RADAR AGC						
R-112	ALTITUDE MARKING RADAR AGC						
R-113	ALTITUDE MARKING RADAR AGC						
R-114	ALTITUDE MARKING RADAR AGC						
R-115	ALTITUDE MARKING RADAR AGC						
R-116	ALTITUDE MARKING RADAR AGC						
R-117	ALTITUDE MARKING RADAR AGC						
R-118	ALTITUDE MARKING RADAR AGC						
R-119	ALTITUDE MARKING RADAR AGC						
R-120	ALTITUDE MARKING RADAR AGC						
R-121	ALTITUDE MARKING RADAR AGC						
R-122	ALTITUDE MARKING RADAR AGC						
R-123	ALTITUDE MARKING RADAR AGC						
R-124	ALTITUDE MARKING RADAR AGC						
R-125	ALTITUDE MARKING RADAR AGC						
R-126	ALTITUDE MARKING RADAR AGC						
R-127	ALTITUDE MARKING RADAR AGC						
R-128	ALTITUDE MARKING RADAR AGC						
R-129	ALTITUDE MARKING RADAR AGC						
R-130	ALTITUDE MARKING RADAR AGC						
R-131	ALTITUDE MARKING RADAR AGC						
R-132	ALTITUDE MARKING RADAR AGC						
R-133	ALTITUDE MARKING RADAR AGC						
R-134	ALTITUDE MARKING RADAR AGC						
R-135	ALTITUDE MARKING RADAR AGC						
R-136	ALTITUDE MARKING RADAR AGC						
R-137	ALTITUDE MARKING RADAR AGC						
R-138	ALTITUDE MARKING RADAR AGC						
R-139	ALTITUDE MARKING RADAR AGC						
R-140	ALTITUDE MARKING RADAR AGC						
R-141	ALTITUDE MARKING RADAR AGC						
R-142	ALTITUDE MARKING RADAR AGC						
R-143	ALTITUDE MARKING RADAR AGC						
R-144	ALTITUDE MARKING RADAR AGC						
R-145	ALTITUDE MARKING RADAR AGC						
R-146	ALTITUDE MARKING RADAR AGC						
R-147	ALTITUDE MARKING RADAR AGC						
R-148	ALTITUDE MARKING RADAR AGC						
R-149	ALTITUDE MARKING RADAR AGC						
R-150	ALTITUDE MARKING RADAR AGC						
R-151	ALTITUDE MARKING RADAR AGC						
R-152	ALTITUDE MARKING RADAR AGC						
R-153	ALTITUDE MARKING RADAR AGC						
R-154	ALTITUDE MARKING RADAR AGC						
R-155	ALTITUDE MARKING RADAR AGC						
R-156	ALTITUDE MARKING RADAR AGC						
R-157	ALTITUDE MARKING RADAR AGC						
R-158	ALTITUDE MARKING RADAR AGC						
R-159	ALTITUDE MARKING RADAR AGC						
R-160	ALTITUDE MARKING RADAR AGC						
R-161	ALTITUDE MARKING RADAR AGC						
R-162	ALTITUDE MARKING RADAR AGC						
R-163	ALTITUDE MARKING RADAR AGC						
R-164	ALTITUDE MARKING RADAR AGC						
R-165	ALTITUDE MARKING RADAR AGC						
R-166	ALTITUDE MARKING RADAR AGC						
R-167	ALTITUDE MARKING RADAR AGC						
R-168	ALTITUDE MARKING RADAR AGC						
R-169	ALTITUDE MARKING RADAR AGC						
R-170	ALTITUDE MARKING RADAR AGC						
R-171	ALTITUDE MARKING RADAR AGC						
R-172	ALTITUDE MARKING RADAR AGC						
R-173	ALTITUDE MARKING RADAR AGC						
R-174	ALTITUDE MARKING RADAR AGC						
R-175	ALTITUDE MARKING RADAR AGC						
R-176	ALTITUDE MARKING RADAR AGC						
R-177	ALTITUDE MARKING RADAR AGC						
R-178	ALTITUDE MARKING RADAR AGC						
R-179	ALTITUDE MARKING RADAR AGC						
R-180	ALTITUDE MARKING RADAR AGC						
R-181	ALTITUDE MARKING RADAR AGC						
R-182	ALTITUDE MARKING RADAR AGC						
R-183	ALTITUDE MARKING RADAR AGC						
R-184	ALTITUDE MARKING RADAR AGC						
R-185	ALTITUDE MARKING RADAR AGC						
R-186	ALTITUDE MARKING RADAR AGC						
R-187	ALTITUDE MARKING RADAR AGC						
R-188	ALTITUDE MARKING RADAR AGC						
R-189	ALTITUDE MARKING RADAR AGC						
R-190	ALTITUDE MARKING RADAR AGC						
R-191	ALTITUDE MARKING RADAR AGC						
R-192	ALTITUDE MARKING RADAR AGC						
R-193	ALTITUDE MARKING RADAR AGC						
R-194	ALTITUDE MARKING RADAR AGC						
R-195	ALTITUDE MARKING RADAR AGC						
R-196	ALTITUDE MARKING RADAR AGC						
R-197	ALTITUDE MARKING RADAR AGC						
R-198	ALTITUDE MARKING RADAR AGC						
R-199	ALTITUDE MARKING RADAR AGC						
R-200	ALTITUDE MARKING RADAR AGC						
R-201	ALTITUDE MARKING RADAR AGC						
R-202	ALTITUDE MARKING RADAR AGC						
R-203	ALTITUDE MARKING RADAR AGC						
R-204	ALTITUDE MARKING RADAR AGC						
R-205	ALTITUDE MARKING RADAR AGC						
R-206	ALTITUDE MARKING RADAR AGC						
R-207	ALTITUDE MARKING RADAR AGC						
R-208	ALTITUDE MARKING RADAR AGC						
R-209	ALTITUDE MARKING RADAR AGC						
R-210	ALTITUDE MARKING RADAR AGC						
R-211	ALTITUDE MARKING RADAR AGC						
R-212	ALTITUDE MARKING RADAR AGC						
R-213	ALTITUDE MARKING RADAR AGC						
R-214	ALTITUDE MARKING RADAR AGC						
R-215	ALTITUDE MARKING RADAR AGC						
R-216	ALTITUDE MARKING RADAR AGC						
R-217	ALTITUDE MARKING RADAR AGC						
R-218	ALTITUDE MARKING RADAR AGC						
R-219							

COMMUTATED DIGITAL WORDS

β	β_{eff}	β_{eff}/β
0.00	0.00	0.00
0.05	0.05	1.00
0.10	0.10	1.00
0.15	0.15	1.00
0.20	0.20	1.00
0.25	0.25	1.00
0.30	0.30	1.00
0.35	0.35	1.00
0.40	0.40	1.00
0.45	0.45	1.00
0.50	0.50	1.00
0.55	0.55	1.00
0.60	0.60	1.00
0.65	0.65	1.00
0.70	0.70	1.00
0.75	0.75	1.00
0.80	0.80	1.00
0.85	0.85	1.00
0.90	0.90	1.00
0.95	0.95	1.00
1.00	1.00	1.00

DIGITAL WORDS	MODE 1	MODE 2	MODE 3	MODE 4	MODE C (5)	MODE T (6)
1	40	40	40	40	23	23
2	50	50	50	50	53	53
3	5, 25, 45, 65, 85	65	50	50	13, 43, 73, 103	13
4	5, 45, 85	5, 10, 15, 20, 25, 30, 35, 40, 45	50	50	2, 12, 22, 32, 42, 52, 62, 72, 82, 92, 102, 112	2
5	6	6	6	50	50	50
6	6	6	6	50	50	50
7	8	16	8	50	50	50
8	8	16	16	50	50	50
9	4	4	4	83	83	83
10	4	4	4	111	111	111
11	11	11	11	113	113	113
12	11	11	11	113	73	73
13	13	13	13	103	103	103
SYNC	(100)	(100)	(50)	(100)	118, 120	118, 120
SYNC COMP	(99)	(99)	(49)	(99)	119	119

CHAN	NAME	MODE 7 WORDS
TV-1	CAMERA NUMBER	2
TV-2	MIRROR AZIMUTH	3, 11
TV-3	MIRROR ELEVATION	7
TV-4	LOCAL SETTING	12
TV-5	LENS FOCAL SETTING	13
TV-6	LENS IRIS SETTING	13
TV-7	LENS IRIS SERVO ON	15
TV-8	FLUTTER SHUTTER ON	15
TV-9	FLUTTER SHUTTER TEMP.	18
TV-10	CAMERA ELECTRONICS TEMP.	4
TV-11	SHUTTER MODE (OPEN OR NORMAL)	4
TV-12	SHUTTER SPEED	6, 14
TV-13	MIRROR STEP FOCUS ON	14
TV-14	(BANKER WORD)	1

CHAN	NAME	SCO FREQ. (KC)	CARRIER MOD. MODE *
D-11, 15	COMMAND REJECT/ENABLE	2.3	PM
FC-1	ROLL GYRO SPEED	5.4	PM
FC-2	ROLL GYRO SPEED	5.4	PM
FC-3	YAW GYRO SPEED	70	PM
AS-1	ALPHA PARTICLE COUNT (2200 BPS)	1.3	PM
AS-2	PROTON COUNT (500 BPS)	1.4	PM
V-12	LEG 1 SHOCK ABSORBER STRAIN GAGE	1.7	PM
V-13	LEG 2 SHOCK ABSORBER STRAIN GAGE	1.7	PM
V-14	LEG 3 SHOCK ABSORBER STRAIN GAGE	1.96	PM
TV-14	COMPOSITE VIDEO	CARRIER	FM

BIT RATE (BPS)	SCS CENTER REQ. (KC)	CARRIER MODULATION
4400	33	FM OR PM
1100	7.35	FM OR PM
550	3.675	FM OR PM
330 (LOW MOD INDEX)	3.9	FM
137.5	.56	PM
4400 (NORMAL MODE TWD)	CARRIER	FM

*BRACKETED SCO'S TURNED ON BY A SINGLE COMMAND

Appendix D
***Surveyor VII* Spacecraft Temperature Histories**

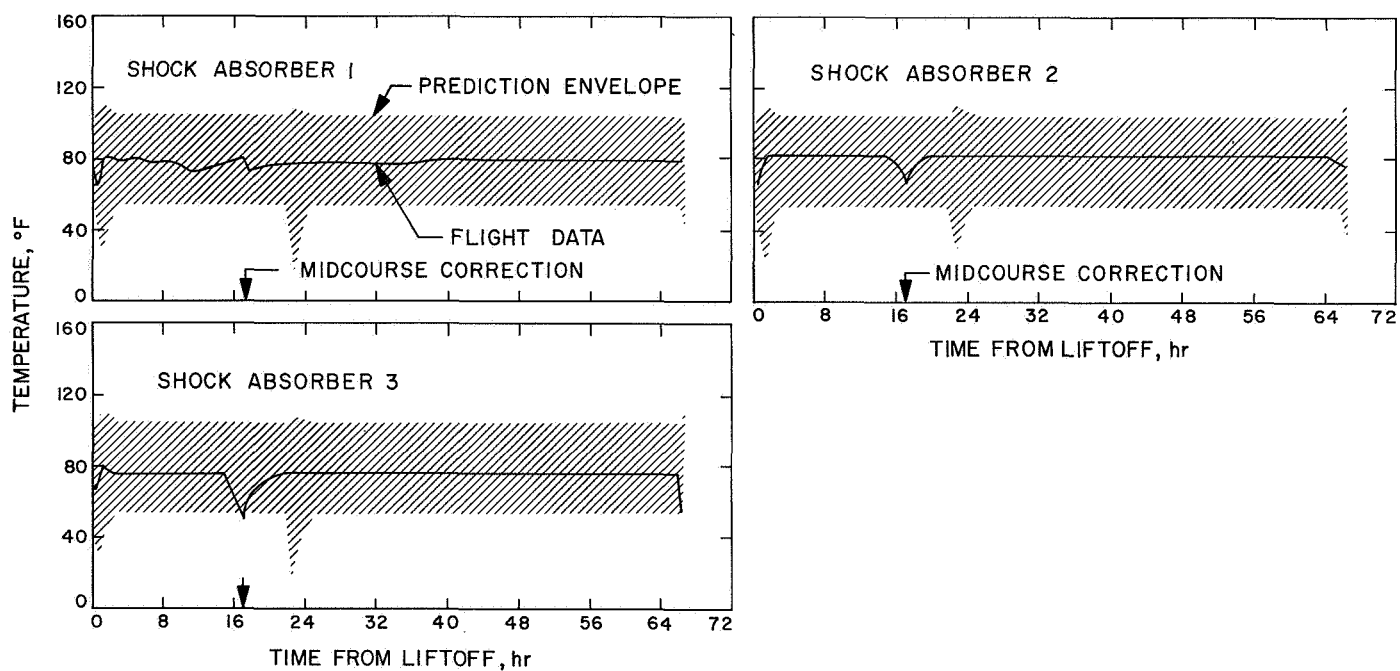


Fig. D-1. Landing gear transit temperatures

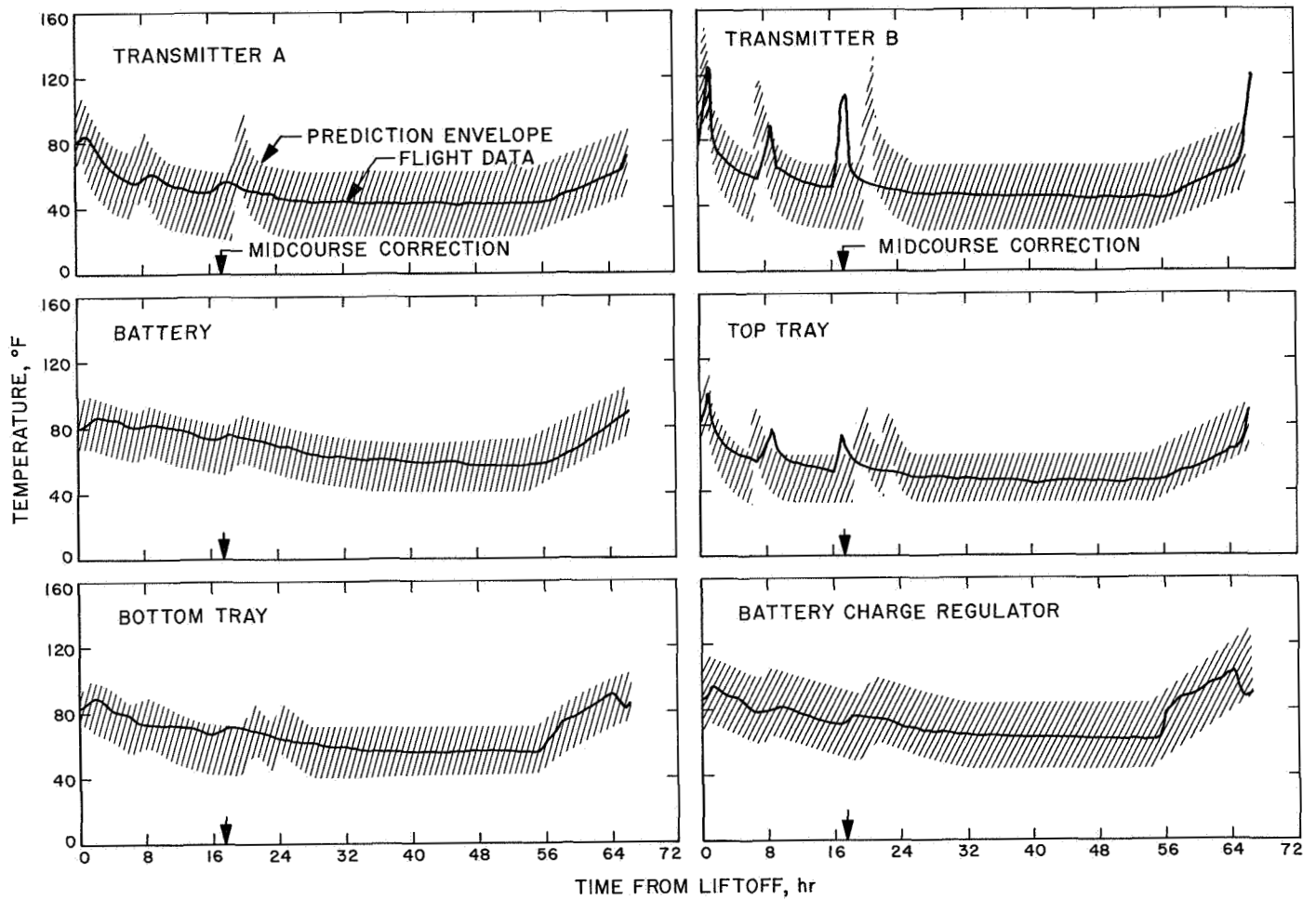


Fig. D-2. Compartment A transit temperatures

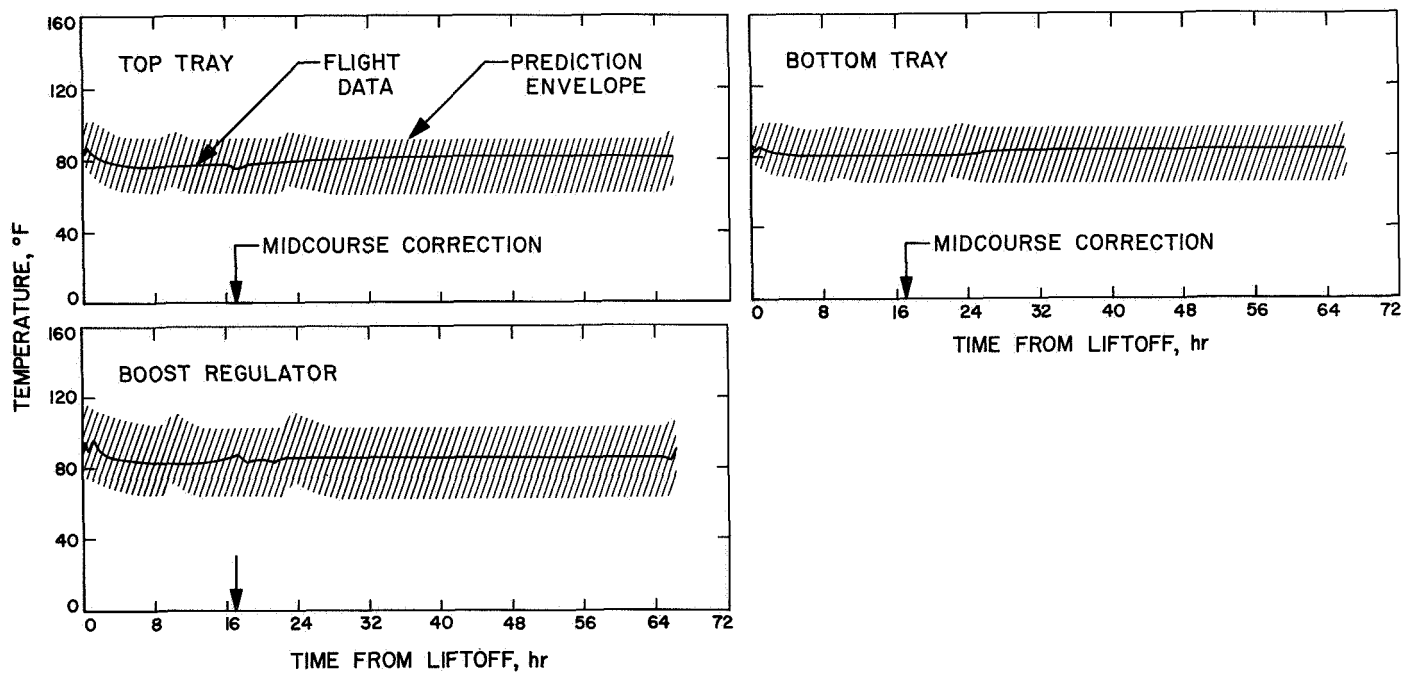


Fig. D-3. Compartment B transit temperatures

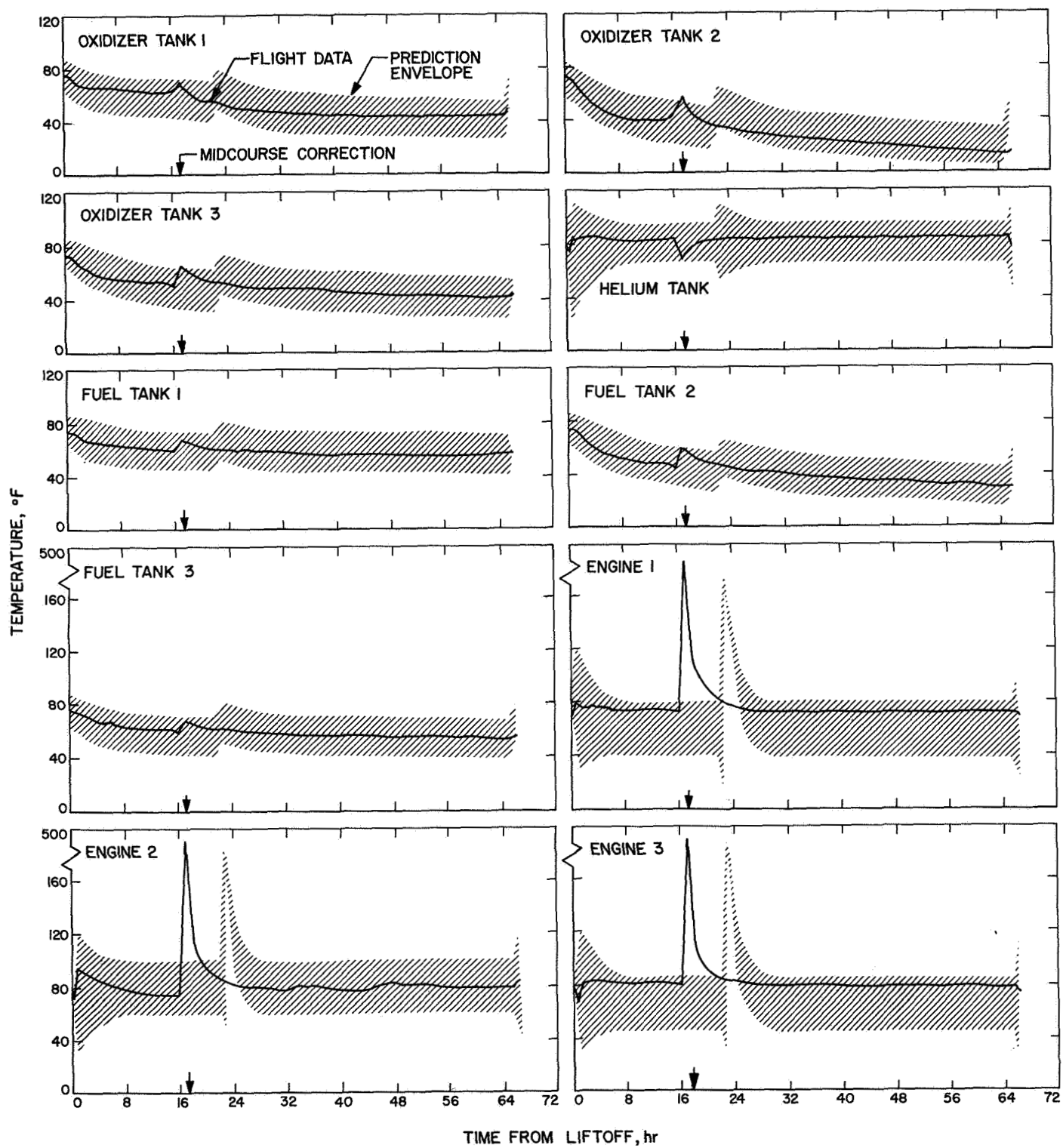


Fig. D-4. Vernier propulsion system transit temperatures

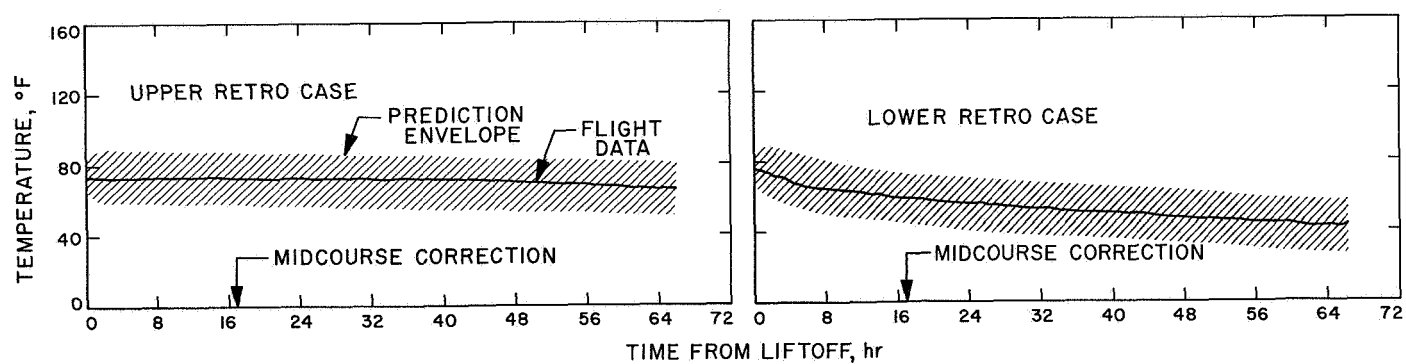


Fig. D-5. Main retro motor transit temperatures

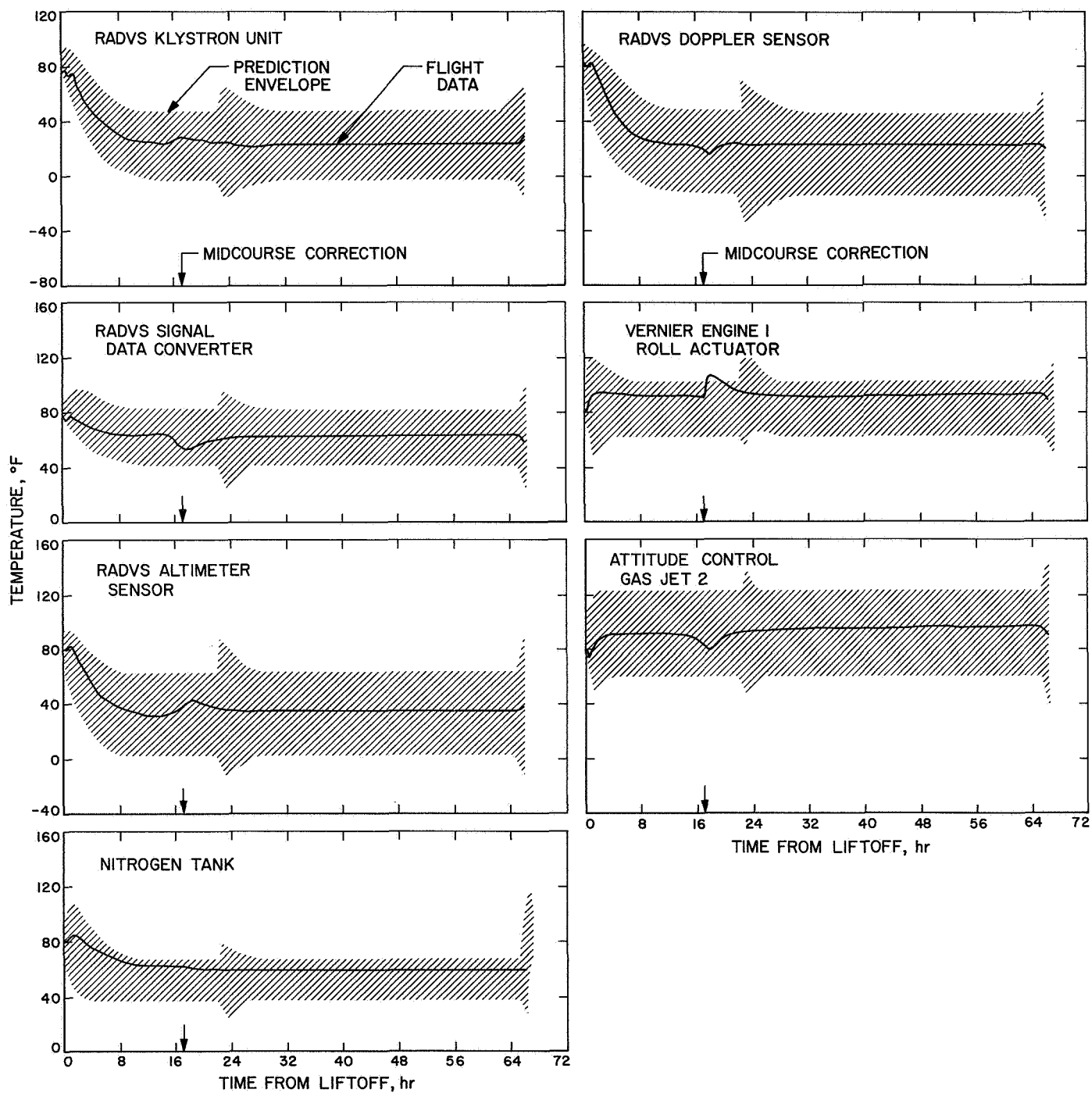


Fig. D-6. Radar and flight control transit temperatures

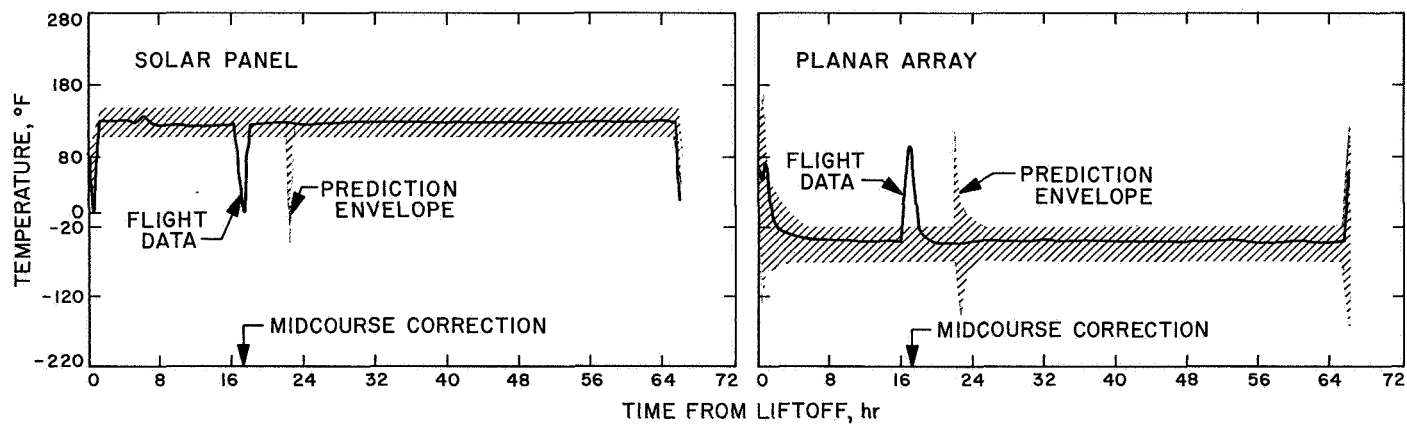


Fig. D-7. Solar panel and planar array transit temperatures

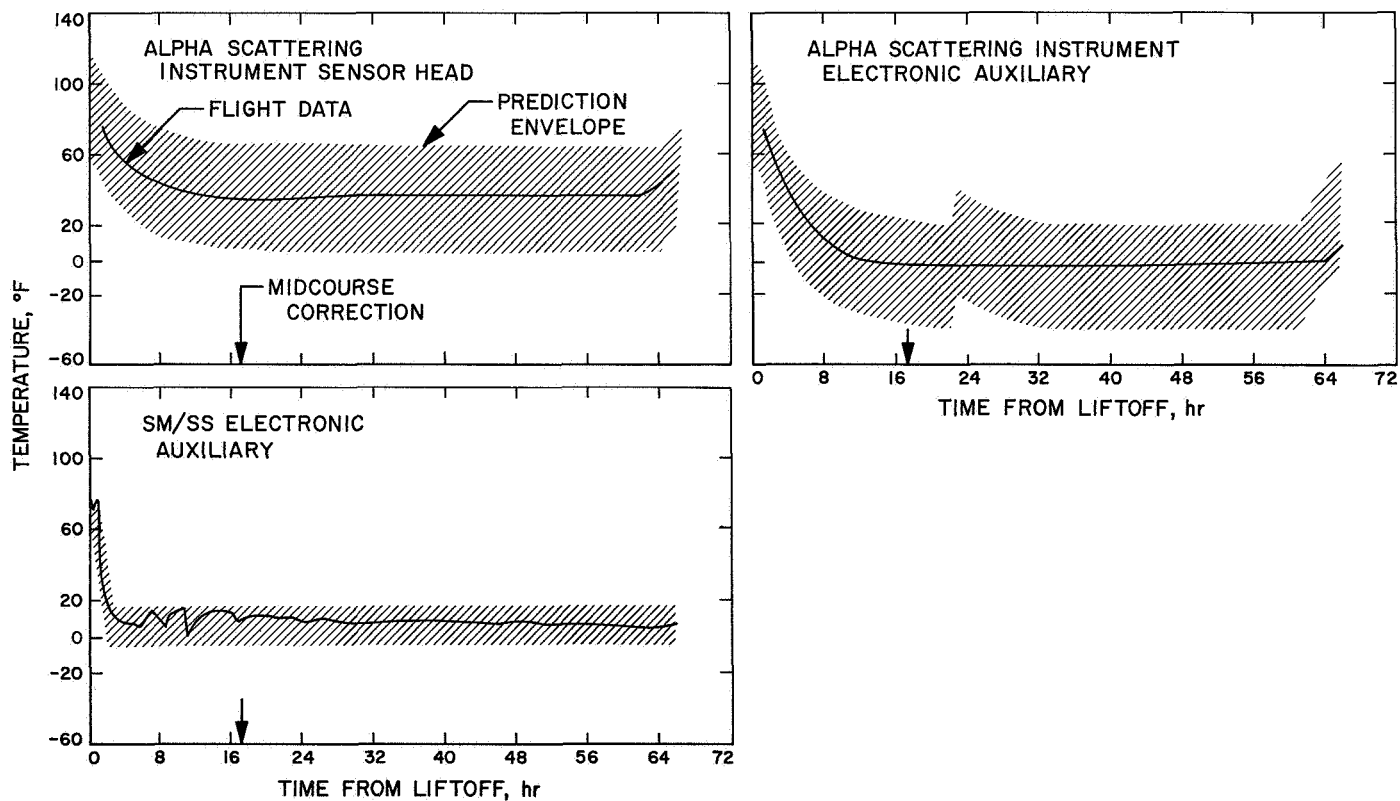


Fig. D-8. ASI and SM/SS transit temperatures

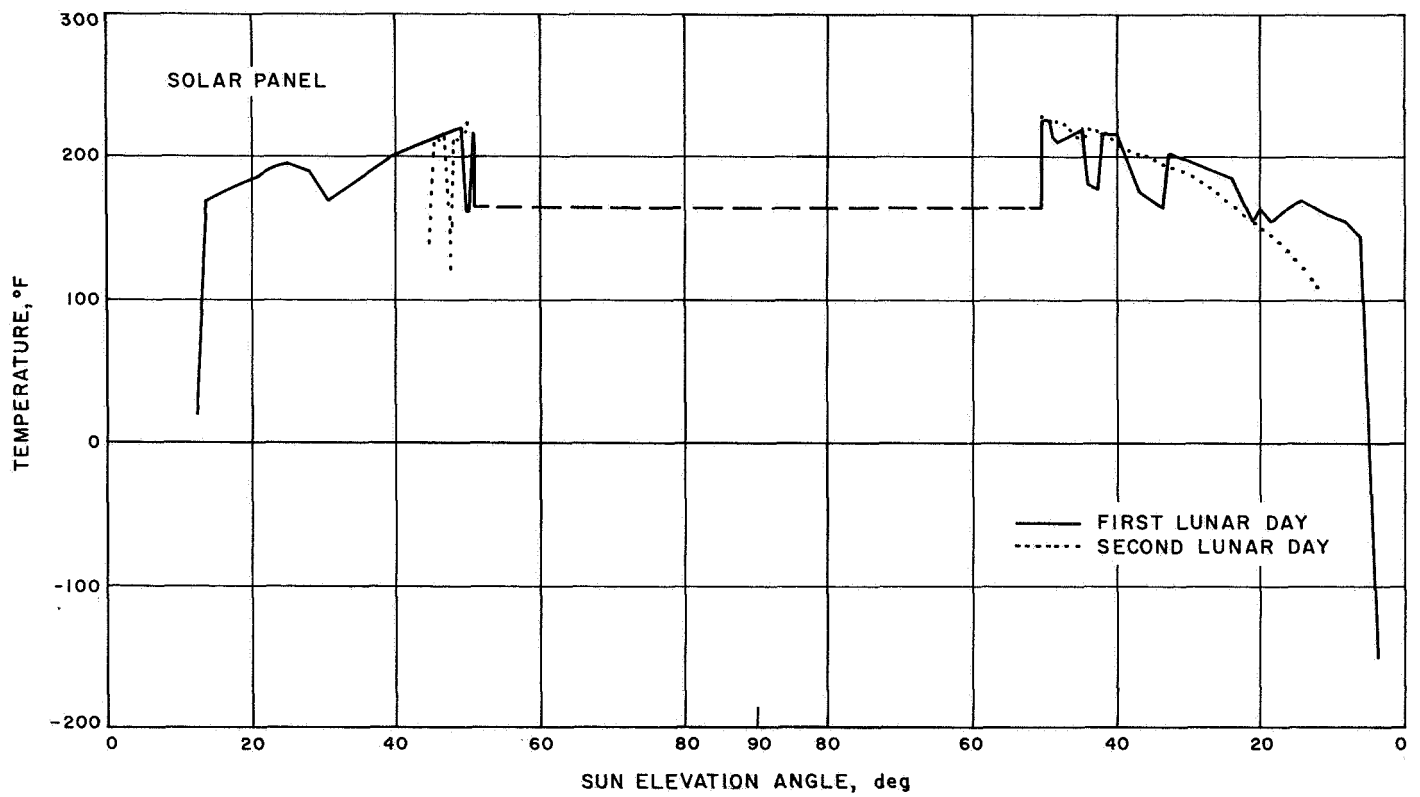


Fig. D-9. Electrical power subsystem postlanding temperatures

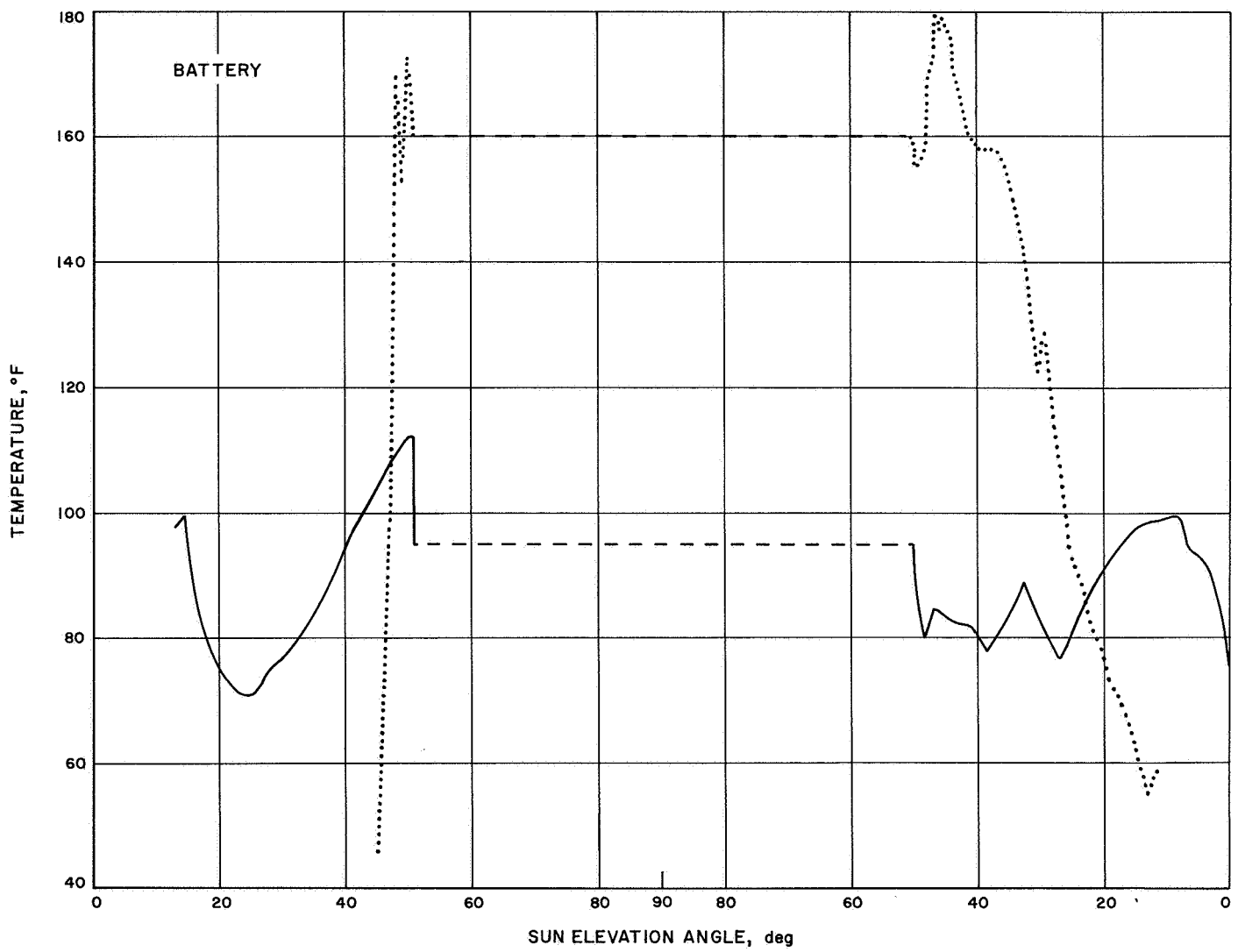


Fig. D-9 (contd)

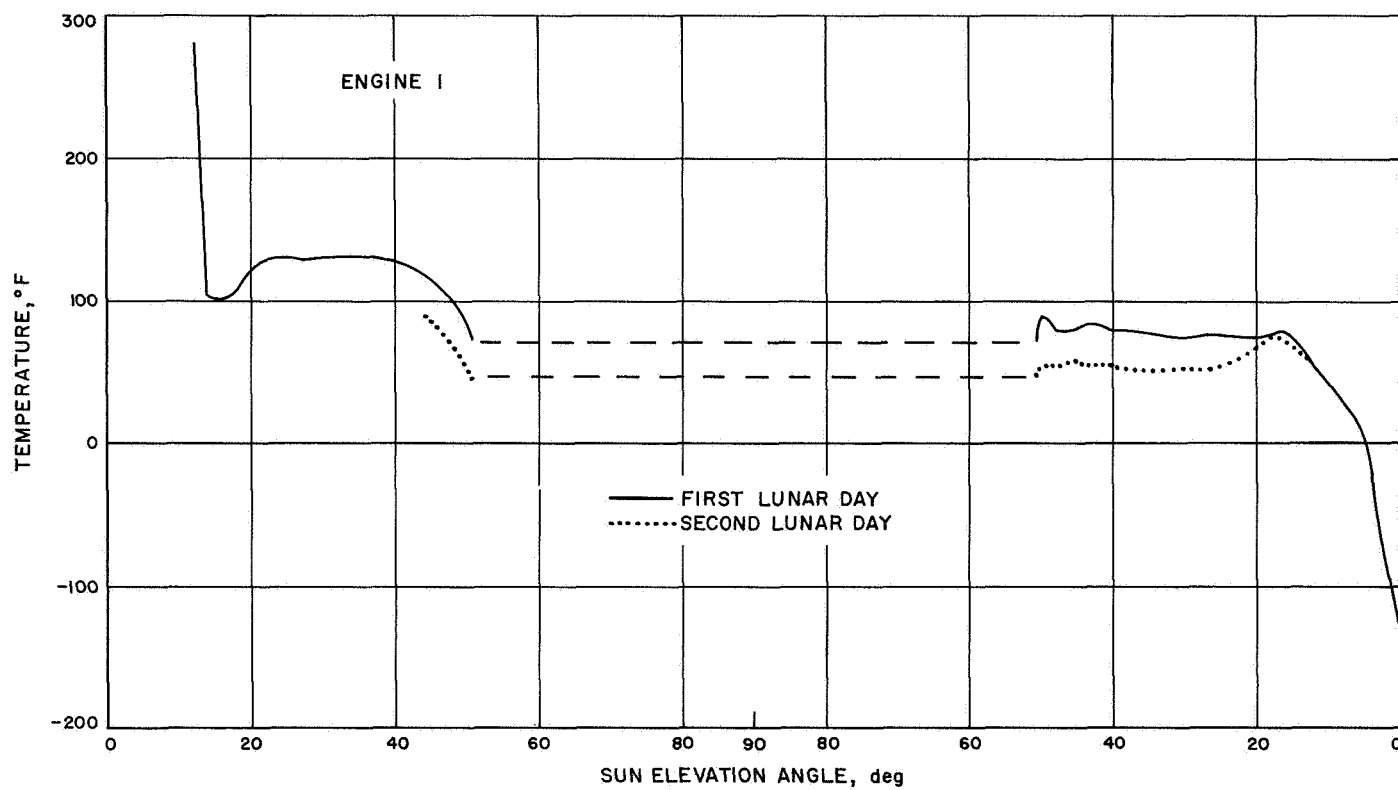


Fig. D-10. Vernier propulsion subsystem postlanding temperatures

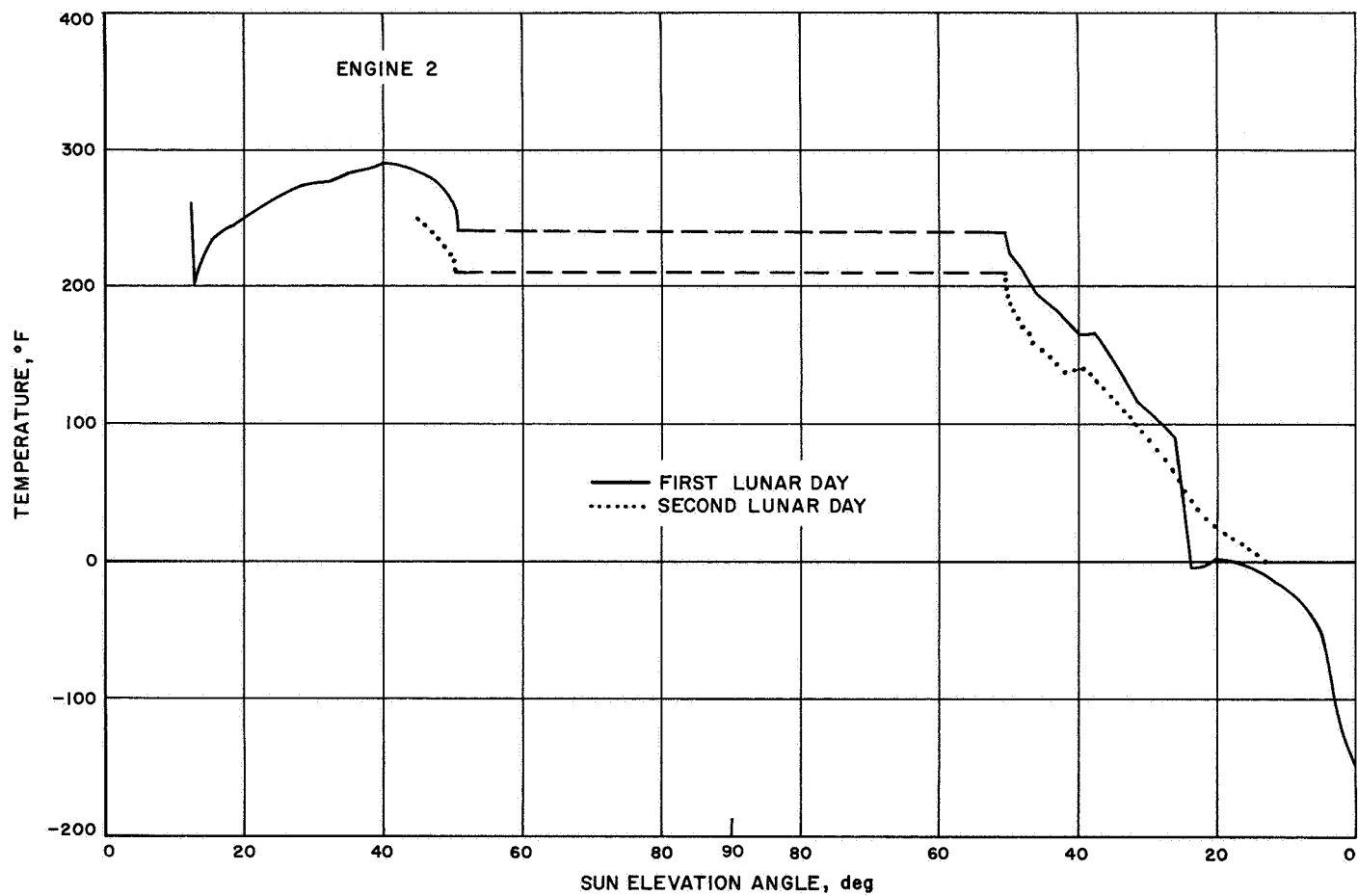


Fig. D-10 (contd)

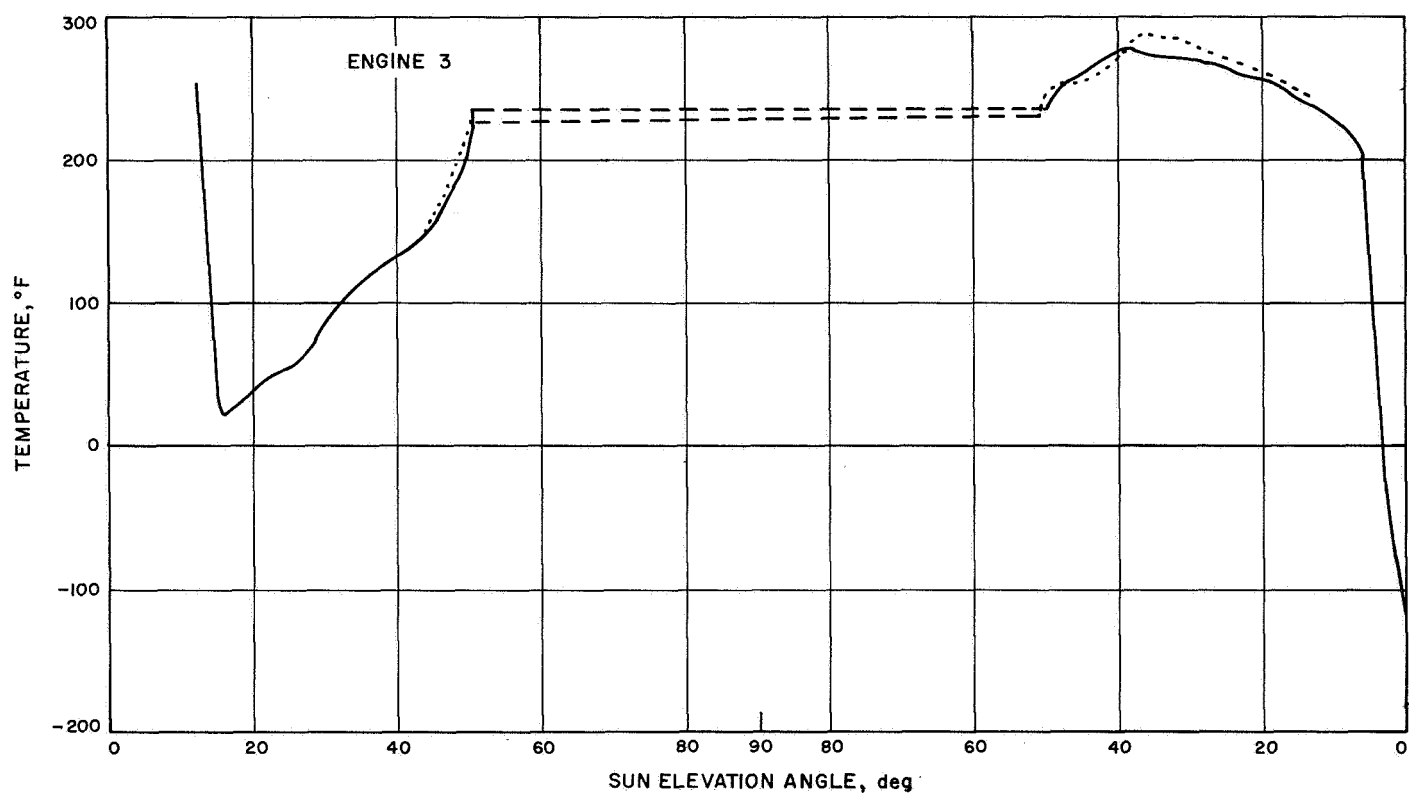


Fig. D-10 (contd)

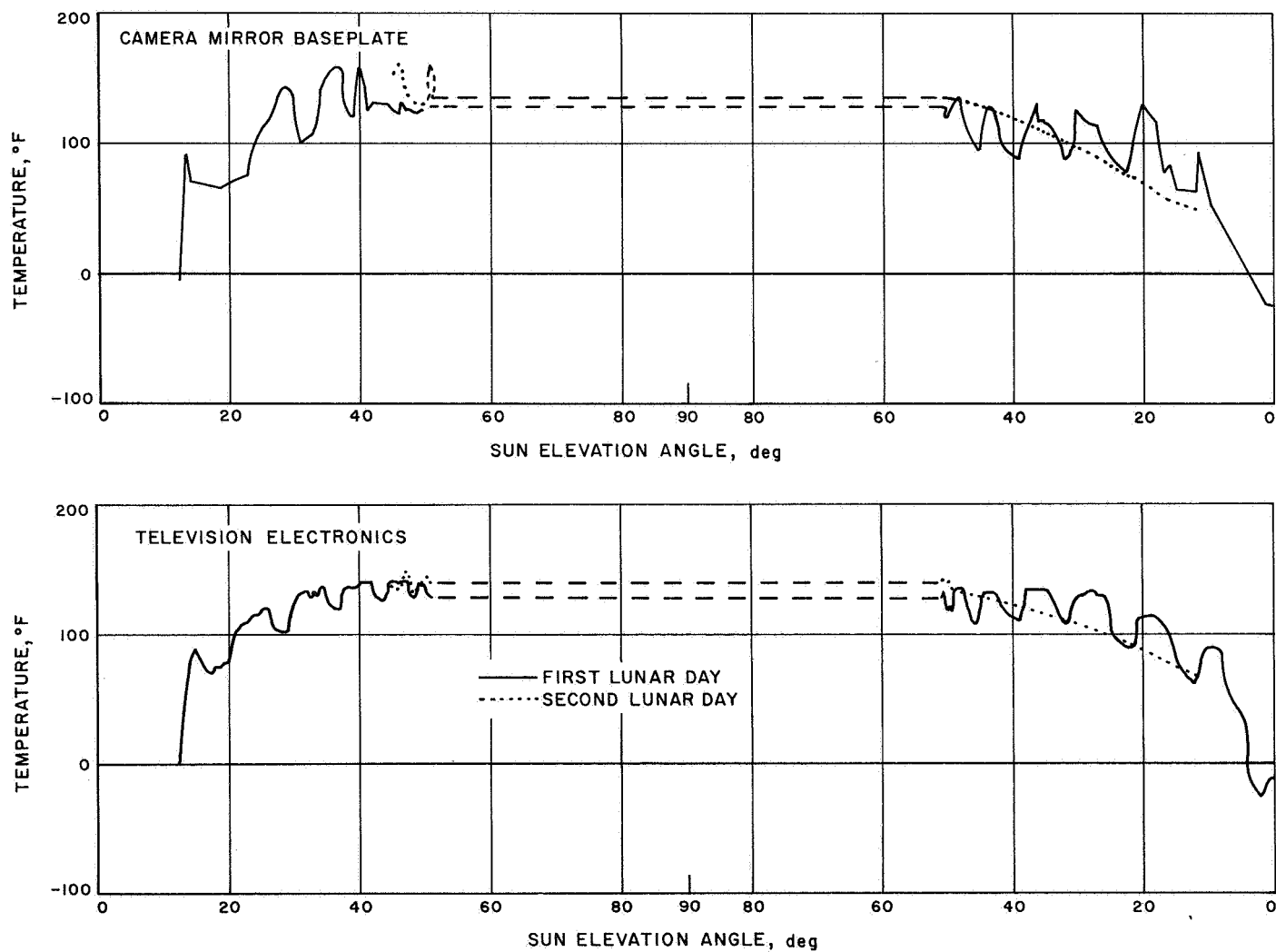


Fig. D-11. Scientific instruments, postlanding temperatures

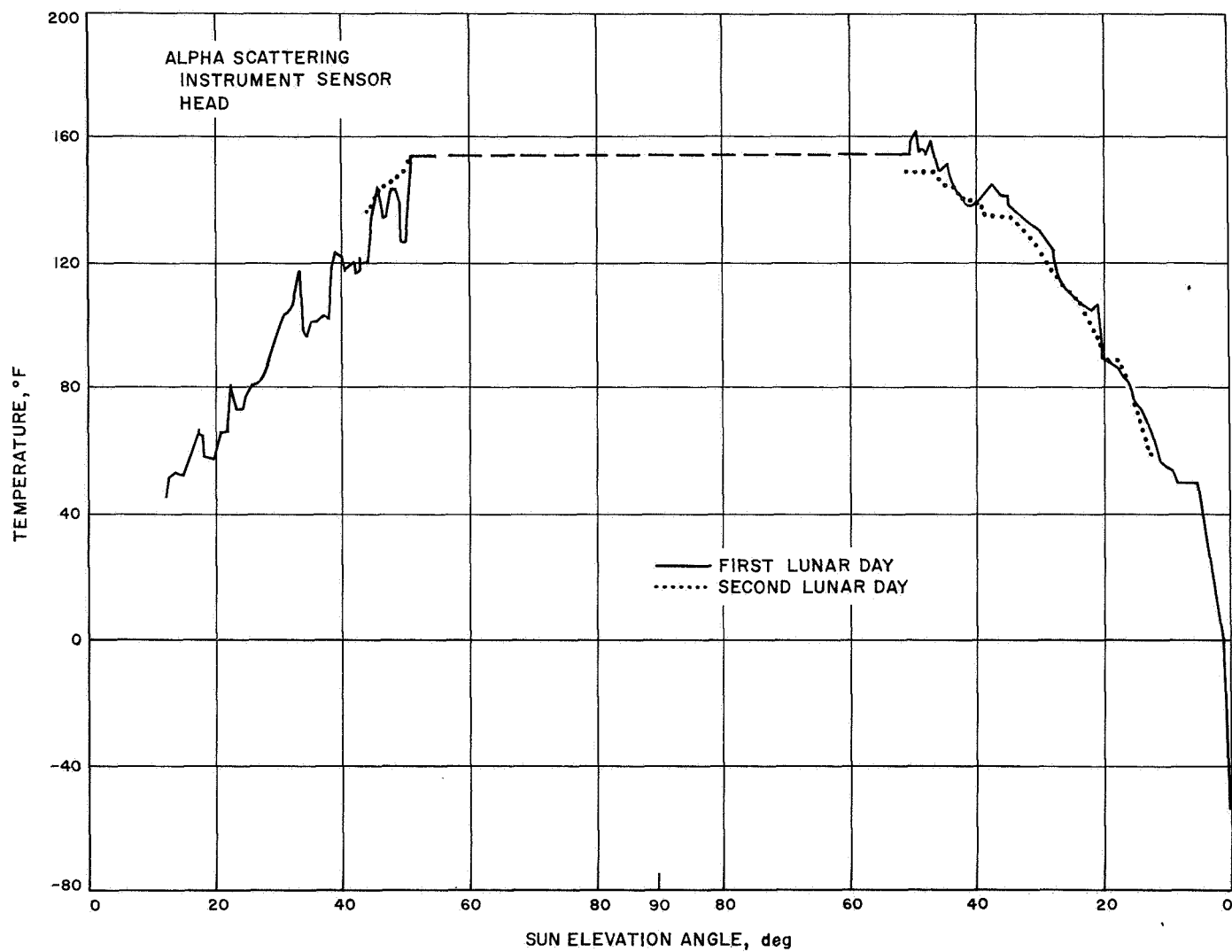


Fig. D-11 (contd)

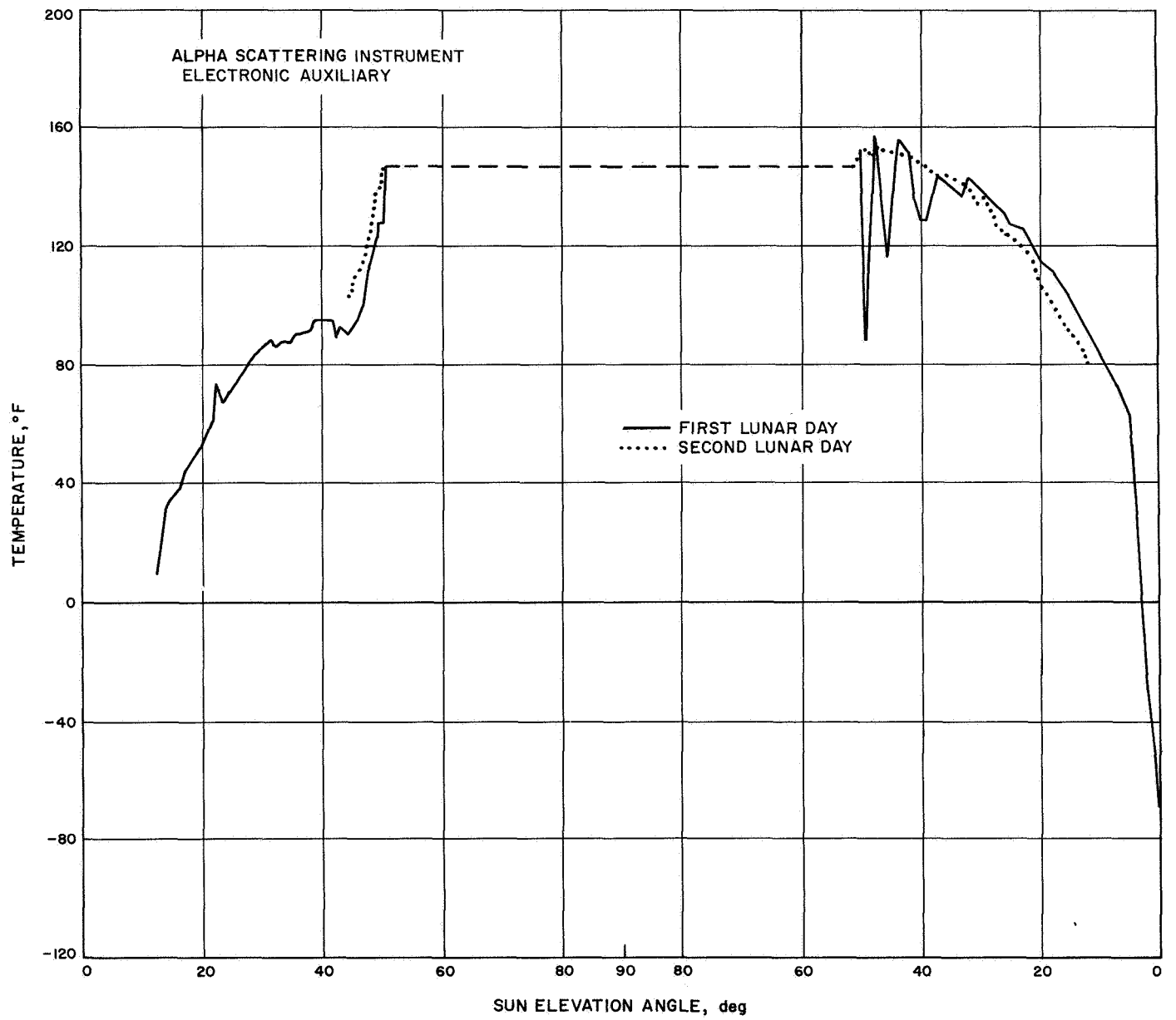


Fig. D-11 (contd)

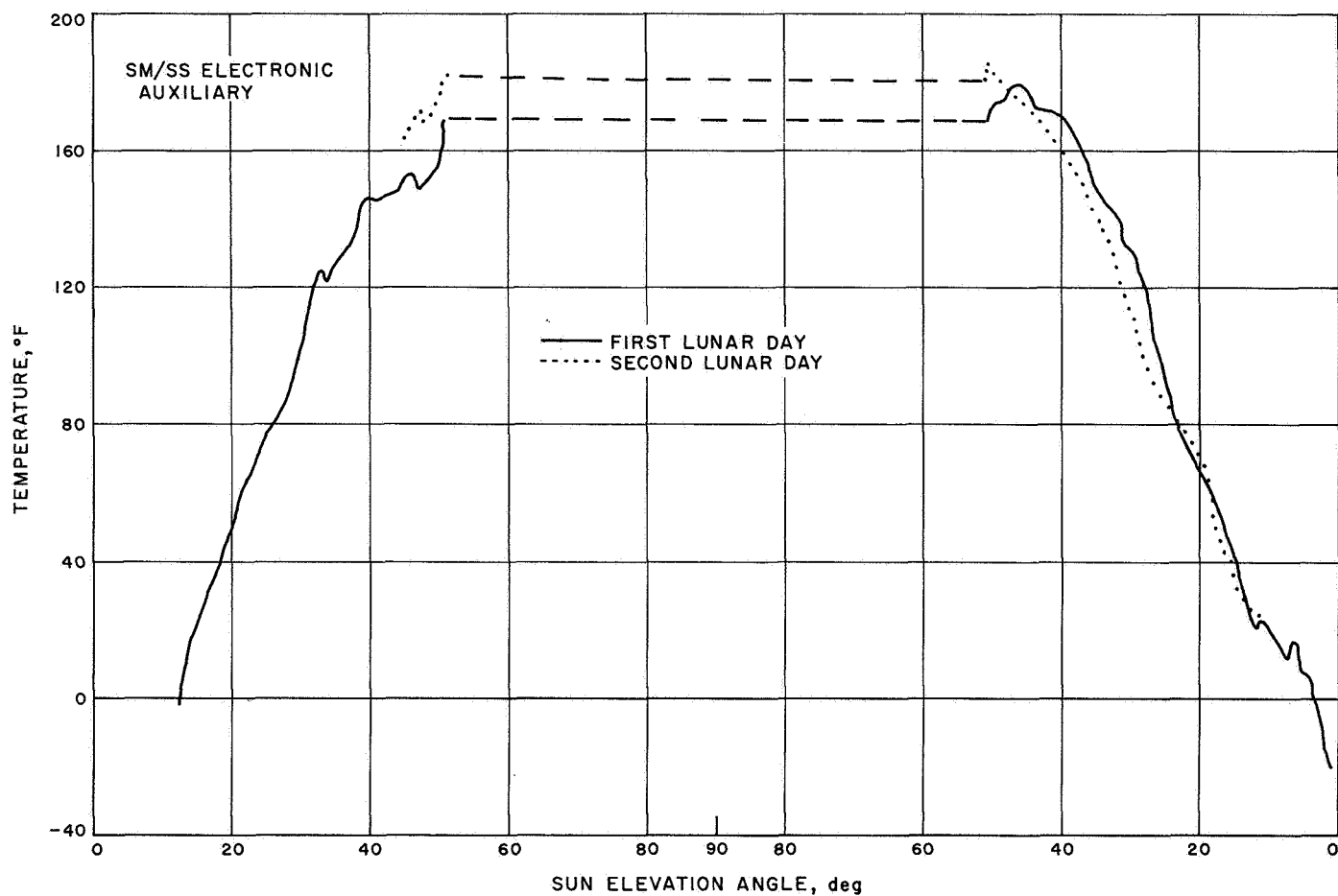


Fig. D-11 (contd)

Glossary

ABC	auxiliary battery control	DSCC	Deep Space Communications Complex
AC	<i>Atlas/Centaur</i>	DSIF	Deep Space Instrumentation Facility
A/D	analog-to-digital	DSS	Deep Space Station
ADC	analog-to-digital converter	DVS	doppler velocity sensor
AESP	auxiliary engineering signal processor	ECPO	Engineering Computer Program Operations (Group)
AFC	automatic frequency control	EM	electromagnetic
AFETR	Air Force Eastern Test Range	EMA	engineering mechanism auxiliary
AGE	aerospace ground equipment	ESF	Explosive Safe Facility
AMR	altitude marking radar	ESP	engineering signal processor
AOS	acquisition of signal	FACT	Flight Acceptance Composite Test
APC	automatic phase control	FC	flight control
ASAC	Alpha Scattering Analysis and Command (Group)	FCSG	Flight Control Sensor Group
ASI	alpha scattering instrument	FPAC	Flight Path Analysis and Command
A/SPP	antenna and solar panel positioner	FRB	Failure Review Board
BCD	binary coded decimal	FRT	fine resolution tracking
BCR	battery charge regulator	GCF	Ground Communications Facility
BECO	booster engine cutoff	GSE	ground support equipment
BIH	built-in hold	GSFC	Goddard Space Flight Center
BR	boost regulator	HSDL	high-speed data line
CCC	Central Computing Complex	ICS	Intracommunications System
CCN	Control Command Network	IF	intermediate frequency
CDC	command and data (handling) console	I/O	input/output
CDS	computer data system	IRIG	Inter-Range Instrumentation Group
CP	Command Preparation (Group)	IRV	interrange vector
CPC	Command Preparation and Control (Group)	ISCO	initial system checkout
CRODVS	conditional reliable operate doppler velocity sensor	J-FACT	Joint Flight Acceptance Composite Test
CRT	Composite Readiness Test	KPSM	klystron power supply modulator
CSP	central signal processor	KSC	Kennedy Space Center
CSTS	Combined Systems Test Stand	LOS	loss of signal
DC	direct command	MAG	Maneuver Analysis Group
DOD	Department of Defense	MCDR	media conversion data recovery (subsystem)
DPS	Data Processing System	MCFR	media conversion film recorder (subsystem)

Glossary (contd)

MECO	main engine cutoff	RODVS	reliable operate doppler velocity sensor
MES	main engine start	RORA	reliable operate radar altimeter
MOS	Mission Operations System	RTCS	Real Time Computer System, Cape Kennedy
MS	mission sequence	SCAMA	signaling, conferencing, and monitoring arrangement (voice circuits)
MSFN	Manned Space Flight Network	SCAT	Spacecraft Analysis Team
NASCOM	NASA World-Wide Communication Network	SCF	Spacecraft Checkout Facility
NBVCXO	narrow-band voltage-controlled crystal oscillator	SDC	signal data converter
OCR	optimum charge regulator	SECO	sustainer engine cutoff
ODG	Orbit Determination Group	SFOD	Space Flight Operations Director
ORT	Operational Readiness Test	SFOF	Space Flight Operations Facility
OSCP	on-site computer program	SMAC	Soil Mechanics Analysis and Command (Group)
OSDP	on-site data processing	SM/SS	soil mechanics/surface sampler
OSDR	on-site data recovery (subsystem)	SOCP	<i>Surveyor</i> on-site computer program
OSFR	on-site film recorder (subsystem)	SOPM	standard orbital parameter message
OTC	overload trip circuit	SOV	solenoid-operated valves
OVCS	operational voice communication system	SRT	System Readiness Test
PA	Performance Analysis (Group)	SPAC	Spacecraft Performance Analysis and Command (Group)
PAM	pulse-amplitude modulation	SSAC	Space Science Analysis and Command
PCM	pulse code modulation	SSD	subsystem decoder
PLIM	postlaunch instrumentation message	SSE	Standard Sequence of Events
PU	propellant utilization	STEA	system test equipment assembly
PUVEP	propellant utilization valve electronics package	STV	solar-thermal-vacuum
PVT	Performance Verification Tests	TC&HA	thermal control and heater assembly
QC	quantitative command	TCP	telemetry and command processor
RA	radar altimeter	TDA	Tracking Data Analysis (Group)
RADVS	radar altimeter doppler velocity sensor	TDM	time division multiplexer
RATAC	radar target acquisition (system)	TDS	Tracking and Data System
RETMA	Radio Electronics Television Manufacturing Association	T&DA	tracking and data acquisition
RFI	radio frequency interference	T&FA	Trend and Failure Analysis (Group)
RIS	range instrumentation ship	TelPAC	Television Performance Analysis and Command (Group)
		TPS	Telemetry Processing Station

Glossary (contd)

TSAC	Television Science Analysis and Command (Group)	VCXO	voltage-controlled crystal oscillator
TTY	teletype	VECO	vernier engine cutoff
TV-GDHS	TV Ground Data Handling System	VEV	vernier engine vibration (test)
		VPS	vernier propulsion system

Bibliography

Project and Mission

- Surveyor A-G Project Development Plan*, Project Document 13, Vol. 1. Jet Propulsion Laboratory, Pasadena, Calif., Jan. 3, 1966.
- Clarke, V. C., Jr., *Surveyor Project Objectives and Flight Objectives for Missions A Through D*, Project Document 34. Jet Propulsion Laboratory, Pasadena, Calif., Mar. 15, 1965.
- Willingham, D. E., *Lunar Surface Generation and Surveyor Landing Analysis*, Project Document 602-4. Jet Propulsion Laboratory, Pasadena, Calif., Mar. 25, 1967.
- Travers, E. S., *Surveyor G Mission Plan*, Project Document 602-66. Jet Propulsion Laboratory, Pasadena, Calif., Jan. 2, 1968.
- Surveyor I Mission Report. Part I. Mission Description and Performance*, Technical Report 32-1023. Jet Propulsion Laboratory, Pasadena, Calif., Aug. 31, 1966.
- Surveyor II Mission Report. Mission Description and Performance*, Technical Report 32-1086. Jet Propulsion Laboratory, Pasadena, Calif., Apr. 1, 1967.
- Surveyor III Mission Report. Part I. Mission Description and Performance*, Technical Report 32-1177. Jet Propulsion Laboratory, Pasadena, Calif., Sept. 1, 1967.
- Surveyor IV Mission Report. Part I. Mission Description and Performance*, Technical Report 32-1210. Jet Propulsion Laboratory, Pasadena, Calif., Jan. 1, 1968.
- Surveyor V Mission Report. Part I. Mission Description and Performance*, Technical Report 32-1246. Jet Propulsion Laboratory, Pasadena, Calif., Mar. 15, 1968.
- Surveyor VI Mission Report. Part I. Mission Description and Performance*, Technical Report 32-1262. Jet Propulsion Laboratory, Pasadena, Calif., Sept. 15, 1968.

Launch Operations

- Macomber, H. L., *Surveyor Launch Constraints Document*, Project Document 43, Rev. 1. Jet Propulsion Laboratory, Pasadena, Calif., Mar. 6, 1967.
- Travers, E. S., *Surveyor Launch Constraints, Mission G — January 1968 Launch Opportunity*, Project Document 43, Rev. 1, Addendum No. 7. Jet Propulsion Laboratory, Pasadena, Calif., Dec. 14, 1967.
- Centaur Unified Test Plan, AC-15/SC-7 Launch Operations and Flight Plan (Surveyor Mission G)*, Report AY62-0047, Section 8.15A. General Dynamics/Convair, San Diego, Calif., Dec. 15, 1967.
- Test Procedure Centaur/Surveyor Launch Countdown Operations, AC-15/SC-7 Launch (CTP-INT-0004N)*, Report AA63-0500-004-03N. General Dynamics/Convair, San Diego, Calif., Dec. 22, 1967.
- Atlas/Centaur-15 Surveyor-G, Operations Summary*, TR-601. Centaur Operations Branch, KSC/ULO, Cape Kennedy, Fla., Dec. 27, 1967.

Bibliography (contd)

Launch Operations (contd)

Barnum, P. W., *JPL/ETR Field Station Launch Operations Plan, Surveyor Missions E, F and G*, JPL/ETR Field Station Document 690-11. Jet Propulsion Laboratory, ETR Field Station, Cape Kennedy, Fla., Sept. 1, 1967.

Atlas/Centaur-15 Surveyor-7, Flash Flight Report, Report TR-608. Centaur Operations Branch, KSC/ULO, Cape Kennedy, Fla., Jan. 11, 1968.

Travers, E. S., *Surveyor VII Launch Phase Mission Analysis Report*, Technical Memorandum 312-877. Jet Propulsion Laboratory, Pasadena, Calif., Mar. 4, 1968.

Launch Vehicle System

Shaffer, J., Jr., *Surveyor Spacecraft/Atlas-Centaur Launch Vehicle Interface Requirements*, Project Document 1, Rev. 3. Jet Propulsion Laboratory, Pasadena, Calif., Sept. 1, 1967.

Atlas Space Launch Vehicle Systems Summary, Report GDC-BGJ67-001. General Dynamics/Convair, San Diego, Calif., Feb. 1967.

Centaur Systems Summary, Report GDC-BGJ 67-003. General Dynamics/Convair, San Diego, Calif., April 1967.

Centaur Technical Handbook, Convair Division, Report GDC-BPM64-001-2, Rev. C. General Dynamics/Convair, San Diego, Calif., Mar. 20, 1967.

Centaur Configuration, Performance and Weight Status Report, Report GDC-63-0495-51. General Dynamics/Convair, San Diego, Calif., Dec. 21, 1967.

Preliminary AC-15 Atlas-Centaur Flight Evaluation (by staff of Lewis Research Center, Cleveland, Ohio), NASA Technical Memorandum X-52411. NASA, Washington, D. C., 1968.

Atlas/Centaur AC-15 Flight Evaluation Report, GDC-BKF68-002. General Dynamics/Convair, San Diego, Calif., June 1, 1968.

Spacecraft System

Surveyor Spacecraft A-21 Functional Description, Document 239524 (HAC Pub. 70-93401), 3 Vols. Hughes Aircraft Co., El Segundo, Calif., Nov. 1, 1964 (with revision sheets).

Surveyor Spacecraft A-21 Model Description, Document 224847B. Hughes Aircraft Co., El Segundo, Calif., Mar. 1, 1965 (with revision sheets).

Surveyor Spacecraft Monthly Performance Assessment Report, SSD 68252-11. Hughes Aircraft Co., El Segundo, Calif., Sept. 21, 1967.

Surveyor VII Flight Performance Final Report, SSD 68189-7. Hughes Aircraft Co., El Segundo, Calif., Mar. 1968.

Tracking and Data Acquisition

Program Requirements No. 3400, Surveyor, Revision 15. Air Force Eastern Test Range, Patrick Air Force Base, Fla., Sept. 22, 1967.

Bibliography (contd)

Tracking and Data Acquisition (contd)

Operations Requirement No. 3400, Surveyor Launch, Revision 12. Air Force Eastern Test Range, Patrick Air Force Base, Fla., Nov. 17, 1967.

Operations Directive No. 3400, Surveyor Launch, Revision 3. Air Force Eastern Test Range, Patrick Air Force Base, Fla., Dec. 9, 1967.

Project Surveyor — Support Instrumentation Requirements Document, Rev. 6. prepared by JPL for NASA, Dec. 8, 1967.

Surveyor Project/Deep Space Network Interface Agreement, Engineering Planning Document 260, Rev. 4. Jet Propulsion Laboratory, Pasadena, Calif., Dec. 27, 1967.

DSIF Tracking Instruction Manual (TIM), For Surveyor Missions (4 volumes), Engineering Planning Document 391. Jet Propulsion Laboratory, Pasadena, Calif., and Hughes Aircraft Company, El Segundo, Calif., Dec. 1967 (with revision sheets for Mission G).

Elliott, C. F., *Report on Tracking and Data System, Near-Earth Phase for Surveyor*, JPL/ETR Field Station Document 690-21. Jet Propulsion Laboratory, ETR Field Station, Cape Kennedy, Fla., Mar. 6, 1968.

Network Operations Plan for the Surveyor G Mission, AC-15, NOP, Goddard Space Flight Center, Greenbelt, Md.

Surveyor G Deep Space Network Post-Flight Critique, Document No. 602-73. Jet Propulsion Laboratory, Pasadena, Calif., Mar. 15, 1968.

Mudgway, D. J., *A Review of Tracking and Data Acquisition System Support for Surveyors A - G*, Project Document 602-84. Jet Propulsion Laboratory, Pasadena, Calif., Apr. 1, 1968.

Mission Operations System

Surveyor Mission Operations System, Technical Memorandum 33-264. Jet Propulsion Laboratory, Pasadena, Calif., Apr. 4, 1966.

Space Flight Operations Plan — Surveyor Missions, Engineering Planning Document 180-S/MG. Jet Propulsion Laboratory, Pasadena, Calif., Dec. 14, 1967.

Goble, M. E., *Surveyor Lunar Operations Plan — Mission G*, Engineering Planning Document 486-MG (Project Document 602-1, Rev. 4). Jet Propulsion Laboratory, Pasadena, Calif., Dec. 22, 1967.

Surveyor Mission G Space Flight Operations Report, Report SSD 88016. Hughes Aircraft Company, El Segundo, Calif., Feb. 1968, and Addendum (Report SSD 88025), Mar. 1968.

Callan, R., *Space Flight Operations Memorandum — Surveyor VII*, Project Document 602-74. Jet Propulsion Laboratory, Pasadena, Calif., Mar. 1, 1968.

Bibliography (contd)

Flight Path

- Davids, L., Meredith, C., and Ribarich, J., *Midcourse and Terminal Guidance Operations Programs*, SSD 4051R. Hughes Aircraft Co., El Segundo, Calif., Apr. 1964.
- Cheng, R. K., Meredith, C. M., and Conrad, D. A., *Design Considerations for Surveyor Guidance*, IDC 2253.2/473. Hughes Aircraft Co., El Segundo, Calif., Oct. 15, 1965.
- Surveyor Spacecraft/Launch Vehicle Guidance and Trajectory Interface Schedule*, Project Document 14, Rev. 3. Jet Propulsion Laboratory, Pasadena, Calif., Nov. 30, 1966.
- Surveyor/Centaur Target Criteria — Surveyor Mission G*, Specification LS501488, Rev. A. Jet Propulsion Laboratory, Pasadena, Calif., Nov. 13, 1967, with Amendment 1, Dec. 14, 1967.
- Fisher, J. N., and Gillett, R. W., *Surveyor Parking Orbit Trajectory Characteristics*, SSD 68219R. Hughes Aircraft Co., El Segundo, Calif., Nov. 1966.
- Surveyor Station View Periods and Parking Orbit Trajectory Coordinates — Launch Dates January, February, March, 1968*, SSD 68242-4. Hughes Aircraft Company, El Segundo, Calif., Mar. 1967.
- Petzel, G. D., *Pre-Injection Trajectory Characteristics Report — AC-14*, GDC-BKM67-064. General Dynamics/Convair, San Diego, Calif., Sept. 1967.
- Dunn, H. S., *Surveyor Mission G Post-Injection Standard Trajectories*, SSD 68169-6 and Appendix A (SSD 78178). Hughes Aircraft Company, El Segundo, Calif., Dec. 1967.
- Gans, J. F., *Surveyor Mission G Final Preflight Maneuver Analysis Report*, SSD 68230-5. Hughes Aircraft Company, El Segundo, Calif., and Appendix A (SSD 78180), Dec. 1967, and Appendix Addendum (SSD 78180), Jan. 7, 1968.
- AC-15 Final Guidance Equations and Performance Analysis*, GDC-BKM67-086. General Dynamics/Convair, San Diego, Calif., Nov. 1967.
- O'Connell, H. P., *Firing Tables — AC-15, January 1968 Opportunity*, GDC-BKM67-083, and Appendix A. General Dynamics/Convair, San Diego, Calif., Dec. 5, 1967.
- Surveyor VII Flight Path Analysis and Command Operations Report*, SSD 88014. Hughes Aircraft Company, El Segundo, Calif., Jan. 25, 1968.
- Gross, D. E., *Range Safety and Range Planning Trajectory Data, Atlas/Centaur AC-15*, GDC-BKM67-082. General Dynamics/Convair, San Diego, Nov. 1967.